MTA DOKTORA PÁLYÁZAT
DOKTORI ÉRTEKEZÉS

SEJTFELSZÍNI RECEPTOROK ÉS JELÁTVITELI RENDSZEREK SZEREPE A SEJTPROLIFERÁCIÓ SZABÁLYOZÁSÁBAN

BÍRÓ TAMÁS

DEBRECENI EGYETEM
ORVOS- ÉS EGÉSZSÉGTUDOMÁNYI CENTRUM
ÁLTALÁNOS ORVOSTUDOMÁNYI KAR
ÉLETTANI INTÉZET

Debrecen
2010

TARTALOMJEGYZÉK

1. BEVEZETÉS

1.1. A jelátvitel szerepe a proliferáció és a differenciálódás szabályozásában

Az emberi szervezetben található szervek és szövetek folyamatos (gyakran élethosszig tartó) fejlődése, növekedése, valamint a sérülést követő átépülése-regenerációja a külső és belső környezethez való alkalmazkodás alapfeltétele. Ezen, az adott egyed mindenkori igényeit messzemenően figyelembe vevő mechanizmusok élettani működését az egyes sejtek osztódásának (sejtproliferáció); egyéni, az adott sejtre jellemző „specializált" fejlődésének (differenciálódás); valamint a sejtek élettartamának és túlélésének (programozott sejthalál, apoptózis) dinamikusan változó szabályozása teszi lehetővé (1,2).

A „finoman hangolt" proliferációs, differenciálódási és túlélési folyamatok működése során az egyes sejtek genetikai programja igen sokrétű kontroll alatt áll, melyben gyakorlatilag a szervezet valamennyi szabályozó rendszere résztvesz. A sejtek növekedésének regulációjában így, a teljesség igénye nélkül, kiemelkedő szereppel bírnak a közvetlen sejt-sejt és sejt-mátrix kapcsolatok; a humorális faktorok (pl. hormonok, citokinek, növekedési faktorok, vazoaktív ágensek, gyulladásos mediátorok) által létrehozott auto-, para- és endokrin intercelluláris kommunikációs hálózatok; a növekvő-differenciálódó sejteket ellátó neuronális végződések trofikus hatásai (pl. mitogén hatású neurohormonok és -peptidek felszabadítása révén), stb. (3,4).

A fenti „neuro-immuno-endokrin" rendszerek elsődleges hírvivői komplex, többlépcsős szignalizációs mechanizmusok aktivitását megváltoztatva szabályozzák a célsejtek növekedését (5,6). Ezen jelátviteli folyamatok magukba foglalják, többek között, különféle sejtfelszíni (metabotróp, ionotróp) és/vagy intracelluláris

(citoplazmatikus, nukleáris) receptorok aktiválódását; másodlagos hírvivő molekulák (pl. kalcium, ciklikus nukleotidok, lipidek) képződését; protein kináz és foszfatáz rendszerek aktivitásának módosulását; bizonyos gének kifejeződésének és átíródásának megváltozását, stb. (5,6). Mivel a különféle kommunikációs csatornákon keresztül befutó jelek szuperpozíciója, valamint az egymással számos szinten kapcsolódó jelátviteli útvonalak interferenciája határozza meg az adott sejt „sorsát" (proliferáció és/vagy differenciálódás és/vagy apoptózis), a folyamatsor megértéséhez elengedhetetlenül szükséges a sejtszinten zajló döntési mechanizmusokat befolyásoló szignalizációs útvonalak felderítése.

A jelátviteli rendszerek működésének patológiás módosulása mélyreható változásokat eredményezhet a sejtek proliferációs és differenciálódási folyamataiban, mely olyan súlyos következményekkel járhat, mint pl. a daganatos transzformáció, autoimmun betegségek kifejlődése vagy gyulladásos állapotok kialakulása (7). Ismervén ezen kórképek incidenciájának és főként mortalitásának riasztóan emelkedő adatait nem meglepő, hogy a fenti összefüggések is a transzmembrán és intracelluláris jelátviteli folyamatok aktivitását szabályozó molekulák tanulmányozására irányították a figyelmet.

1.2. A vizsgált jelátviteli rendszerek

Kísérleteinkben három jelátviteli rendszer szerepét vizsgáltuk az *in vitro* és *in vivo* sejtproliferáció szabályozásában.

1.2.1. A tranziens receptor potenciál vanilloid-1 (TRPV1) ioncsatorna

A TRPV1 egy jelentős Ca^{2+}-permeabilitással rendelkező nem-szelektív kationcsatorna, mely a „celluláris szenzorokként" működő TRP ioncsatornák

családjának egyik képviselője (8,9). A csatornát elsőként a csípőspaprikából izolált kapszaicin celluláris célmolekulájaként írták le („kapszaicin receptor”) a spinális hátsó gyöki és trigeminális szenzoros ganglionok kis méretű sejttesttel és C-típusú axonnal jellemezhető polimodális nociceptorain (10). Megállapították továbbá, hogy a szenzoros neuronokon kifejeződő receptor központi szerepet tölt be a fájdalomérzés és a neurogén gyulladás folyamataiban (11,12).

A TRPV1-et a kapszaicinen és a rokon vanilloid vegyületeken (pl. a resiniferatoxin) kívül többféle, a szervezetben képződő „endovanilloid” ágens is képes aktiválni és/vagy szenzitizálni. Ezek közül a TRPV1 legfontosabb endogén aktivátora a hőmérséklet emelkedése (>43°C) és a pH csökkenése (acidózis, <pH 5,5). Ezen hatások mellett számos, leginkább gyulladásos mediátornak tekinthető anyag (pl. bradikinin, ATP, arachidonsav-származékok, leukotriének, a lipid-peroxidáció termékei, az endogén kannabinoidként leírt anandamid, stb.) is képes a TRPV1 szenzitizációjára. Ezek a mediátorok részben direkt módon, részben saját (főként metabotróp) receptoraikhoz kötődve intracelluláris jelátviteli útvonalak (kinázok, intracelluláris hírvivők) módosítása révén szabályozzák a TRPV1 működését (9,11-14).

Főként saját (az Értekezésben bemutatott kísérleteket megalapozó) kutatásainknak köszönhetően kiderült ugyanakkor az is, hogy a TRPV1 számos nem-neuronális sejtféleségen is kifejeződik. Megállapítottuk, hogy a TRPV1 funkcionális formában expresszálódik emlős hízó- és gliasejteken, és olyan folyamatok szabályozásában vesz részt, mint pl. a sejtek proliferációja, differenciálódása, vazoaktív mediátortermelése és citokinfelszabadítása (15,16). Ezt követően más munkacsoportok is kimutatták a TRPV1 molekuláris jelenlétét, többek között, pl. epidermális keratinocitákon, a gasztrointesztinális és urogenitális traktus

számos sejtféleségén, a bronchusok epitéliumán és többféle mononukleáris sejten is (17-19). Kísérleteink megkezdésekor ugyanakkor felderítésre várt a TRPV1-kapcsolt szignalizáció funkcionális, a sejtek növekedését reguláló szerepének, valamint a molekula szabályozásának leírása, főként humán nem-neuronális sejtpopulációkon.

1.2.2. Az endokannabinoid rendszer (ECS)

Az elmúlt két évtizedben a *Cannabis sativa* növényben megtalálható talán legfontosabb anyag, a növény pszichoaktív hatását kifejtő Δ^9-tetra-hidro-kannabinol (Δ^9-THC) vizsgálata során kiderült, hogy a Δ^9-THC számos, az emberi szervezet által termelt endogén vegyület hatását „utánozza". Ezen lipid természetű endokannabinoid vegyületek, mint pl. az anandamid vagy a 2-arachidonoil-glicerol (2-AG), az őket felismerő receptorok, valamint az endokannabinoidat szintetizáló és lebontó enzimhálózat együttesen képezi az ECS-t (20-22).

Az endokannabinoidokat először a központi idegrendszerben, mint retrográd neurotranszmittereket, illetve neuromodulátorokat jellemezték. Megállapították, hogy ezen vegyületek – főként az 1-típusú, G-protein kapcsolt kannabinoid receptor (CB1), valamint több jelátviteli mechanizmus (pl. cAMP, kináz rendszerek) aktiválásán keresztül – központi szereppel bírnak pl. a tanulás (long-term potentiation), a memória és a viselkedési folyamatok szabályozásában. Ezzel szemben az ugyancsak G-protein kapcsolt CB2-t főként az immunrendszer sejtjein írták le, ahol a receptor aktivációja mélyreható változásokat eredményezett a gyulladásos és immunológia folyamatokban (23-26). Bebizonyosodott továbbá, hogy a fenti metabotróp receptorokon kívül számos egyéb molekula (így egyes TRP csatornák, mint pl. a TRPV1) is képes a kannabinoidok celluláris hatásainak közvetítésére (26).

Érdekes módon az elmúlt néhány év kutatásainak köszönhetően kiderült az is, hogy az ECS elemei (receptorok, enzimek) szinte minden perifériás szervben (így pl. szív, máj, izom, zsírszövet, stb.) megtalálhatóak (23,24). Kísérleteink megkezdésekor ugyanakkor nem volt ismert az, hogy a kutatásaink középpontjában álló (humán) bőrben hogyan működik az ECS, valamint, hogy szerepet játszik-e a folyamatos proliferációs-differenciálódási programmal jellemezhető sejtek növekedésének szabályozásában.

1.2.3. A protein kináz C (PKC) izoenzimek

A sejten belüli jelátvitel egyik központi molekuláris rendszere a PKC izoenzimcsalád (27). Ezen szerin-treonin kinázok csoportjában a mai napig 11 különböző PKC izoenzimet különböztettek meg, melyeket aktivációs mechanizmusaik és szerkezeti sajátságaik alapján 4 nagyobb csoportba sorolhatunk. A „klasszikus" csoportba (cPKC) a cPKCα, βI, βII és γ izoenzimek tartoznak, mely fehérjék aktiválódásukhoz diacil-glicerolt (DAG) és kalciumot igényelnek. A második csoportba a „novel" kalcium-független, de DAG-függő nPKCδ, ε, η és θ izoenzimek tartoznak. A harmadik csoportba az „atípusos" aPKCζ és λ/ι izoenzimek sorolhatók, melyek aktiválódásukhoz sem kalciumot, sem DAG-analóg forbol-észtert nem igényelnek. A negyedik csoportot egyetlen enzim a PKCμ (újabb nevén a PKD) alkotja, mely mind aktivációját, mind struktúráját tekintve rendhagyó izoformának tekinthető (28-30).

Szervezetünknek nincs olyan sejttípusa, amely ne rendelkezne valamely PKC izoformával, illetve izoformákkal. Fontos tény ugyanakkor, hogy nem mindegyik izoenzim található meg minden sejttípusban (28); azaz a PKC izoenzimek a szervezetben az adott szövetre, valamint sejtre jellemző megoszlást és mintázatot

hoznak létre. Ezen megoszlás gazdagságából fakad, hogy a PKC enzimek az élettani szabályozó folyamatok legszélesebb skáláját képesek befolyásolni. Alapvető és központi szereppel bírnak (a teljesség igénye nélkül) pl. a sejtek proliferációjának és differenciálódásának szabályozásában, a programozott sejthalál (apoptózis) folyamatsorában, meghatározott sejttípusok által termelt mediátorok (vazoaktív anyagok, növekedési faktorok, citokinek) szintézisében, ingerlékeny szövetek elektrofiziológiai jellegzetességeinek (csatorna-aktivitás, akciós potenciál kódolás, izomkontrakció) optimális kialakításában, a központi idegrendszer integritásának és működésének fenntartásában, a szervezet védekező mechanizmusaiban (fagocitózis, immunglobulin termelés), stb. (összefoglalva 31).

Az utóbbi időben egyre több bizonyíték szól amellett, hogy a PKC izoenzimek nemcsak szerkezeti, aktivációs és megoszlási heterogenitást mutatnak, hanem regulációjuk és biológiai szerepük is jelentősen különbözhet egymástól. Felmerült emellett az is, hogy egy adott sejtválasz (különös tekintettel a proliferáció, differenciálódás és regeneráció) kialakításában a különböző PKC izoformák nemcsak eltérő aktivitással vehetnek részt, de hatásuk gyakran ellentétesnek adódhat (31,32).

2. CÉLKITŰZÉSEK

2.1. A TRPV1 vizsgálata során először célul tűztük ki a receptor azonosítását a humán bőr epiteliális és mezenchimális sejtféleségein, valamint a bőr függelékein (szőrtüsző, faggyúmirigy). Ezt követően jellemezni kívántuk a TRPV1 funkcionális szerepét a különféle sejtek proliferációs, differenciálódási és apoptotikus folyamataiban, valamint a kapcsolódó immunológiai mechanizmusokban. Elemeztük

továbbá a TRPV1-aktiváció hatását a sejtek szekretoros működésére (lipidszintézis, citokin- és növekedési faktor termelés), valamint bizonyos, a sejtproliferáció és differenciálódás folyamataiban kulcsszerepet játszó gének expressziójára.

2.2. A TRPV1-mediált sejtválaszok szabályozásának elemzését is végrehajtottuk. Ennek során tanulmányozni kívántuk a sejtproliferáció és az apoptózis szabályozásában kulcsfontosságú $[Ca^{2+}]_i$ TRPV1-mediált változását, valamint a funkcionális ioncsatorna szubcelluláris lokalizációját. Emellett vizsgáltuk a sejtnövekedés egyik legfontosabb molekulacsaládjának, a neurotrofinoknak a TRPV1 működésére gyakorolt hatását, valamint új TRPV1-en ható agonistákat is azonosítottunk.

2.3. A TRPV1 vizsgálatához hasonlóan elemezni kívántuk az ECS szabályozó szerepét a humán bőrfüggelékek különféle sejtjeinek növekedésében, differenciálódási folyamataiban, túlélésében, valamint mediátortermelésében.

2.4. Többféle sejtes rendszert alkalmazva emellett tanulmányoztuk a PKC izoformák kifejeződésének változását a sejtek proliferációs és differenciáltsági állapotának függvényében. Vizsgáltuk továbbá a PKC rendszer farmakológiai befolyásolásának (PKC aktivátorok és gátlók) hatását a sejtfolyamatokra. Ezen túlmenően molekuláris biológiai módszerekkel megváltoztatott PKC mintázatú sejteket hoztunk létre, majd – a különféle sejtes modellrendszerekben észlelt megfigyeléseinket összehasonlítva – izoformaspecifikus válaszokat kívántunk azonosítani.

2.5. Végezetül számos, megváltozott proliferációs állapottal jellemezhető humán megbetegedésben (daganatok, autoimmun betegségek) elemeztük a PKC izoformamintázat, valamint a TRPV1 és a CB receptorok kifejeződésének esetleges módosulásait.

3. AZ ELVÉGZETT VIZSGÁLATOK, MÓDSZEREK

(A **római számok** a Értekezés alapjául szolgáló közlemények sorszámát jelölik;
A közlemények listája a 6. fejezetben található)

3.1. Az alkalmazott modellrendszerek

A proliferáció, a differenciálódás, a sejthalál, valamint ezek patológiás megváltozásainak (pl. tumorgenezis és progresszió) vizsgálatára számos sejtes rendszer található az irodalomban, melyek jól jellemzik a fenti folyamatok jellegzetességeit. Kutatásaink során olyan, főként humán rendszereket fejlesztettünk és alkalmaztunk, melyek (i) sejtjeire az egész életen át tartó folyamatos proliferáció, differenciálódás és regeneráció jellemző; (ii) egymást jól kiegészítve lehetőséget teremtenek a proliferáció és differenciálódás mechanizmusait szabályozó rendszerek főbb aspektusainak széleskörű tanulmányozására; valamint (iii) mind fiziológiailag, mind farmakológiailag, mind klinikailag releváns módon modellezik az *in vivo* folyamatokat.

3.1.1. Sejtes in vitro rendszerek

Kutatásaink túlnyomó többségét primer sejttenyészeteken (vázizom, szőrtüsző-eredetű keratinocita, monocita-eredetű dendritikus sejtek) (**II,V,XI,XII**); primer szervkultúrán (izolált szőrtüsző) (**II,IX**); immortalizált és daganatos sejtvonalakon (SZ95 humán faggyúmirigy-eredetű szebocita, HaCaT humán epidermális keratinocita, Cal27 humán nyelv laphámkarcinóma, MonoMac-6 humán monoblasztos leukémia, C2C12 egér mioblaszt) (**I,IV,X-XVII**); valamint egészséges önkéntesekből és betegekből származó primer sejteken (T-limfocita, monocita) (**XX)** és szövetmintákon (bőr, szőrtüsző, daganatok) (**I,II,IV,IX,X,XVII-XIX**) hajtottuk végre. Emellett számos homológ és heterológ expressziós rendszert hoztunk létre, melynek

sejtjeiben az adott jelátviteli molekulákat vagy túltermeltettük (rekombináns overexpresszió); vagy a vizsgálni kívánt fehérje kifejeződését RNS interferencia (siRNS) technika alkalmazásával „lecsendesítettük” (**IV,VI-VIII,X,XIII,XV,XVI**).

3.1.2. In vivo állatkísérletek

Az *in vivo* proliferáció (tumorgenezis) tanulmányozása során a molekuláris biológiai technikákkal módosított sejteket Severe Combined Immunodeficiency (SCID) egerekbe injektáltuk, majd szövettani és immunhisztokémiai módszerekkel elemeztük a kifejlődött daganatok jellegzetességeit (**XV**). Vadtípusú, valamint TRPV1-knockout (KO) egerekben emellett tanulmányoztuk az *in vivo* szőrnövekedés folyamatát (**III**).

3.2. A jelátviteli molekulák azonosítása

A vizsgált molekulák fehérje szintű kimutatására immunhisztokémia/citokémia (konfokális mikroszkópiával) (**I-VI,IX-XV,XVII,XVIII)**, Western blot (**I,II,IV-VII,X-XX**) és áramlásos citometria (**II,IV,V,X,XV,XVI,XX**) technikákat alkalmaztunk, míg a sejtalkotókat mRNS szinten konvencionális RT-PCR és kvantitatív „real-time” Q-PCR technikák (**I,II,IV,V,IX,X,XVII,XVII**) segítségével azonosítottuk. Az endokannabinoidok termelődését tömegspektroszkópiával (**VII,X**) mutattuk ki.

3.3. Funkcionális vizsgálatok

A sejtproliferációt növekedési görbék (**II,IX,XI-XIII**), immunhisztokémia/ citokémia (Ki67) (**II,XI,XV**), valamint kolorimetriás (MTT, BrdU) és fluorimetriás (CyQuant) assay-k segítségével (**II,IV,V,X,XIII-XVII**); a differenciálódást különféle markerek fehérje és génszintű kimutatásával (**II,IV,V,X-XV**); az apoptózist

immunhisztokémia (TUNEL) (**II,IX**), áramlásos citometria (Annexin-V) (**II,IV,X**) és fluorimetriás (Annexin-V, $DiIC_1(5)$ mitokondriális membránpotenciál-érzékeny jelölés) technikákkal (**IV,X**); a nekrotikus sejthalált áramlásos citometria (propidium-jodid) (**II,IV,X**) és fluorimetriás (SYTOX Green festődés, glükóz-6-foszfát-dehidrogenáz felszabadulás) (**IV,X**) módszerekkel; a kinázok aktiválódását radioaktív assay-k és Western blot metódusokkal (**X,XIII,XV**); míg a sejtek mediátortermelését ELISA (**IV,X**) és radioaktív vizsgálatokkal (**XVI**) határoztuk meg. A TRPV1 aktivációját követően az intracelluláris kalciumkoncentráció ($[Ca^{2+}]_i$) változásait fluorimetriás mérésekkel (**II,V-VIII,XIV**) tanulmányoztuk.

4. EREDETI TUDOMÁNYOS EREDMÉNYEK

(A **római számok** a Értekezés alapjául szolgáló közlemények sorszámát jelölik;
A közlemények listája a 6. fejezetben található)

Az alább bemutatandó eredeti tudományos eredményeket szolgáltató kísérletek túlnyomó többségét a Debreceni Egyetem, Orvos- és Egészségtudományi Centrum (DE OEC) Élettani Intézetében, az általam vezetett Sejt- és Molekuláris Élettani Laboratóriumban végeztük. Tudományos munkánkat számos hazai, valamint külföldi klinikai (pl. DE OEC Bőrklinika és III. Belklinika; Dept. Dermatology, Univ. Lübeck, Németország) és elméleti (pl. DE OEC Biokémiai és Immunológiai Intézet; National Cancer Institute, NIH, USA) kollaborációs partner segítette, mely kapcsolatok a saját tudományos munkánkat jól kiegészítő kísérletes megközelítések együttes alkalmazását tették lehetővé. Projektjeink kivitelezésének anyagi feltételeit a Laboratórium munkatársai által elnyert nagyszámú hazai (pl. OTKA, ETT) és nemzetközi (pl. EU Keretprogramok) kutatási támogatás biztosította.

4.1. A nem-neuronális sejteken újonnan leírt TRPV1 funkcionális szerepe a sejtproliferáció szabályozásában

4.1.1. A TRPV1 vizsgálata során az irodalomban elsőként sikerrel azonosítottuk a receptor *in situ* kifejeződését a humán bőr számos neuroektodermális (epidermális keratinociták, verejtékmirigyek) és mezenchimális (Langerhans-sejtek, hízósejtek, simaizom) sejttípusán, valamint a bőrfüggelékek különféle sejtpopulációin (szőrtüsző keratinocitái, faggyúmirigyek szebocitái) (**I,II**).

4.1.2. Humán izolált szőrtüsző szervkultúra modellrendszert alkalmazva bebizonyítottuk továbbá, hogy a TRPV1 aktiválása az agonista kapszaicinnel specifikus (azaz TRPV1 antagonistákkal teljes mértékben felfüggeszthető) és dózisfüggő módon gátolta a hajszál hossznövekedését, csökkentette a szőrtüsző bulbáris keratinocitáinak proliferációját, fokozta ezen sejtek apoptózisát, valamint a korai katagén (regressziós) stádiumra jellemző morfológiai jegyek kialakulását váltotta ki. Humán szőrtüsző-eredetű tenyésztett külső gyökérhüvely (ORS) keratinocitákon, valamint humán immortalizált epidermális HaCaT keratinocitákon emellett kimutattuk, hogy a TRPV1 aktiválása, a $[Ca^{2+}]_i$ receptor-függő növekedésén keresztül, gátolta a sejtek proliferációját és apoptózist indukált. Megállapítottuk továbbá, hogy a kapszaicin mélyreható változásokat okozott a hajciklus szabályozásában résztvevő számos molekula (citokinek, növekedési faktorok) termelődésében. Azaz, a TRPV1 aktiválása csökkentette a hajciklus pozitív regulátoraként ismert hepatic growth factor, insulin-like growth factor-I (IGF-I) és scattered factor kifejeződését, míg a szőrnövekedést gátló transforming growth factor-β_2 és interleukin-1β (IL-1β) expressziója emelkedett kapszaicin hatására (**II**).

4.1.3. A TRPV1 ioncsatorna sejt-, illetve szőrnövekedést szabályozó lehetséges szerepét TRPV1-KO egérmodellben is vizsgáltuk. Kvantitatív hisztomorfometria

módszert alkalmazva megállapítottuk, hogy a TRPV1-et nem expresszáló állatok szőrtüszőinek anagén-katagén transzformációja jelentős késést mutat a vadtípusú állatokban mértekhez képest (**III**). Mivel ezen adataink jó összhangban voltak a humán szőrtüsző szervkultúrán mértekkel (lásd **II**), eredményeink a TRPV1 központi szerepét valószínűsítik a haj- és szőrnövekedés *in vivo* és *in vitro* növekedésének gátlásában.

4.1.4. A humán pilosebaceous egység másik tagján (faggyúmirigyek) is vizsgáltuk a TRPV1 működését, humán faggyúmirigy-eredetű immortalizált SZ95 szebocitákat alkalmazva. A humán faggyúmirigy *in situ* vizsgálatához hasonlóan (lásd **I**), az SZ95 szebocitákon is igazoltuk a TRPV1 (fehérje és génszintű) jelenlétét. Kimutattuk továbbá, hogy a TRPV1 agonista kapszaicin jelentősen és dózisfüggő módon gátolta a szebociták bazális és arachidonsav indukálta lipidtermelését, mely hatás egyaránt kivédhetőnek bizonyult a TRPV1 specifikus gátlószer iodo-resiniferatoxin alkalmazásával, az ioncsatona siRNS-mediált „csendesítésével", valamint az extracelluláris kalciumkoncentráció ($[Ca^{2+}]_e$) csökkentésével. Génszintű (mRNS) vizsgálataink során emellett bebizonyosodott, hogy a szebocitákon kifejeződő TRPV1 aktivációja megváltoztatta a lipidanyagcsere szabályozásában szerepet játszó transzkripciós faktorok (pl. peroxiszóma proliferátor-aktivált receptor [PPAR] izoformák) expresszióját és egyes citokinek (pl. IL-1β) termelését (**IV**). Mindezen eredmények a TRPV1-kapcsolt szignalizáció gátló hatására utalnak a szebociták differenciálódásának (faggyútermelés) szabályozásában.

4.1.5. Humán monocita-eredetű dendritikus sejteken, az irodalomban elsőként, szintén kimutattuk a Ca^{2+}-csatornaként funkcionáló TRPV1 jelenlétét. Megállapítottuk továbbá, hogy a kapszaicin (a TRPV1 specifikus aktiválásán keresztül) gátolta a dendritikus sejt irányú differenciálódást, az éretlen dendritikus sejtekre jellemző

markerek (pl. DC-SIGN, CD11c, HLA-DR) kifejeződését, valamint a sejtek fagocitotikus aktivitását. A TRPV1 aktivációja emellett jelentősen gátolta a dendritikus sejtek pro-inflammatórikus citokinekkel kiváltott érését és aktivációját; lecsökkentette számos dendritikus sejt érési marker (pl. CD83, CCR7) és ko-aktivációs molekula (pl. CD40, CD80, CD86) kifejeződését, valamint egyes gyulladásos citokinek (pl. IL-6, IL-12) termelését; miközben fokozta az anti-inflammatórikus IL-10 szintjét (**V**). Mindezen adataink azt sugallják, hogy a dendritikus sejteken megtalálható TRPV1-kapcsolt szignalizációs útvonal gyulladásgátló hatással rendelkezik.

4.1.6. Vizsgáltuk továbbá a TRPV1 ioncsatorna molekuláris szabályozását is különféle, a rekombináns TRPV1-et kifejező heterológ expressziós rendszereket újonnan létrehozva. Ezen sejtes modellekben kimutattuk, hogy a TRPV1 vanilloid vegyületek (kapszaicin, resiniferatoxin) iránt mutatott érzékenysége, valamint ezen agonisták által beindított sejtválaszok (excitáció, $[Ca^{2+}]_i$-növekmény, deszenzitizáció, sejthalál) jellegzetességei jelentős mértékben függnek az adott expressziós rendszer (tranziens, stabil, indukálható) tulajdonságaitól, valamint az $[Ca^{2+}]_e$-tól. Kísérleteink során bebizonyosodott továbbá, hogy a funkcionális, kalciumpermeabilis csatornaként működő TRPV1 nemcsak a sejtfelszíni, hanem intracelluláris kalciumraktárként szereplő kompartmentek (pl. endoplazmatikus retikulum) membránjába is beépülhet (**VI**).

4.1.7. A heterológ rendszerek emellett lehetőséget teremtettek új, a TRPV1 működését befolyásoló molekulák azonosítására is. Megállapítottuk, hogy a sejt-szöveti fejlődés, proliferáció és regeneráció szabályozásában központi szereppel bíró neurotrofinok – az általunk vizsgált nerve growth factor, brain-derived neurotrophic factor, valamint a neurotrophin-3 és -4 – mindegyike képes a TRPV1

működésének fokozására, azaz a receptor szenzitizációjára (**VII**). Bebizonyosodott továbbá, hogy a orvosi gyakorlatban széleskörűen alkalmazott fájdalomcsillapító tramadol a TRPV1 agonistájaként is működik, hiszen a klinikai terápiás dózistartománnyal jól korreláló koncentrációkban megemelte a TRPV1-et kifejező sejtek $[Ca^{2+}]_i$-ját, mely hatás a TRPV1 antagonista kapszazepin adagolásával kivédhető volt (**VIII**).

4.2. Az ECS szerepe a humán bőrfüggelékek növekedésének és differenciálódásának szabályozásában

4.2.1. A pilosebaceous egység tagjain, hasonlóan a TRPV1 fent bemutatott jellemzéséhez, vizsgáltuk az ECS funkcionális szerepét is. Az irodalomban elsőként mutattuk ki, hogy humán szőrtüszőben jelentős mértékben termelődnek endokannabinoidok (anandamid, 2-AG). Humán szőrtüsző szervkultúrát alkalmazva megállapítottuk továbbá, hogy az anandamid (valamint a növényi kannabinoid Δ^9-THC) dózisfüggő módon gátolta a hajszál elongációját és a szőrtüsző keratinocitáinak proliferációját, ugyanakkor apoptózist és katagén regressziót indukált a szőrtüszőben. Bebizonyosodott az is, hogy az anandamid fenti hatásait a szőrtüszőben főként az ORS keratinocitákon (a CB receptorok közül kizárólagosan) kifejeződő CB1 közvetítette. Végezetül kimutattuk, hogy – habár az anandamid számos sejten aktiválhatja a TRPV1-et – ezen hatásai függetlenek a TRPV1-aktiváció teljes mértékben megegyező (fentebb részletezett, lásd **II**) következményeitől. Mindezen adatok szinergista, a szőrnövekedést gátló TRPV1- és CB1-mediált szignalizációs folyamatok jelenlétére utalnak a humán szőrtüszőben (**IX**).

4.2.2. A humán faggyúmirigyet vizsgálva megállapítottuk, hogy a tenyésztett SZ95 szebociták ugyancsak jelentős mennyiségben termelnek endokannabinoidokat (anandamid, 2-AG). Kimutattuk azt is, hogy az endokannabinoidok a sejteken kifejeződő CB2 stimulálása, valamint egy komplex intracelluláris jelátviteli mechanizmus beindítása révén (pl. p42/44 Erk-1/2 mitogén-aktivált protein kinázok [MAPK] aktiválása, PPAR izoformák és célgénjeik átíródásának fokozása) jelentősen fokozták a szebociták zsírtermelését. siRNS technika alkalmazásával emellett bebizonyosodott, hogy a fenti mechanizmus „konstitutíven aktív"; azaz a faggyúmirigyben termelődő endokannabinoidok folyamatos jelenléte és autokrin-parakrin hatása szükséges a szebociták bazális (normál) zsírtermelésének fenntartásához (**X**).

4.3. A PKC izoenzimek specifikus, egymással gyakran ellentétes, valamint sejttípus-függő szerepe a proliferáció és differenciálódás szabályozásában

4.3.1. A PKC izoenzimek sejtproliferációban betöltött szerepének vizsgálata során először kimutattuk, hogy a primer humán tenyésztett vázizomsejtek jellegzetes PKC izoformamintázattal rendelkeznek; bennük a cPKCα és γ; a nPKCδ, η és θ; valamint az aPKCζ jelenléte volt tetten érhető. Megállapítottuk továbbá, hogy a különféle izoenzimek szubcelluláris lokalizációjának mintázata, valamint expressziójának szintje az *in vitro* vázizomsejt proliferáció, fúzió és differenciálódás különböző stádiumaiban eltérően változott (**XI**).

4.3.2. Ugyanezen sejtes rendszert alkalmazva megállapítottuk továbbá, hogy az „univerzális" PKC aktivátor, DAG-analóg forbol-12-mirisztát-13-acetát (PMA) dózisfüggő módon gátolta a vázizomsejtek növekedését és differenciálódását. Konfokális mikroszkópia alkalmazásával bebizonyosodott emellett, hogy a PMA

jelentősen módosította egyes PKC izoformák szubcelluláris lokalizációját: a nPKCη PMA adagolásakor a citoplazmából a magmembránba és a magba helyeződött át; a nPKCθ a citoplazmából a magba és feltehetően a nukleoluszba transzlokálódott; míg a cPKCγ a magból részlegesen a citoplazmába került át. Mivel a PKC izoformák transzlokációja aktiválódásuk jeleként értelmezhető, eredményeink a fenti izoformák szerepét valószínűsítik a PMA vázizomsejt-növekedést gátló celluláris hatásainak kifejlődésében (**XII**).

4.3.3. Különféle vázizomsejteken vizsgáltuk továbbá a PKC izoformák lehetséges szerepét az egyik leghatásosabb szöveti növekedési faktor, az IGF-I mitogén hatásának kialakulásában. Primer humán tenyésztett vázizomsejteken megállapítottuk, hogy a nPKCδ izoforma kizárólagos szereppel bír az IGF-I vázizomsejt proliferációt és differenciálódást serkentő hatásának kifejlődésében (a MAPK és Akt/foszfatidil-inozitol 3-kináz rendszerek ugyanakkor nem vesznek részt a folyamatban). Egér rabdomióma eredetű immortalizált C2C12 sejvonalon ugyanakkor kimutattuk, hogy a nPKCδ-specifikus aktivitás központi szerepe mellett a MAPK útvonal is résztvesz az IGF-I hatásainak kialakításában. Bebizonyosodott az is, hogy C2C12 mioblasztokon a nPKCδ a MAPK útvonal „upstream" regulátoraként viselkedik, azaz megelőző aktivációja szükséges a MAPK rendszer aktivitásának fokozódásához. Mivel (i) a nPKCδ konstitutíven aktív formájának overexpressziója C2C12 mioblasztokban teljes mértékben "utánozta" az IGF-I hatását; valamint (ii) a nPKCδ kináz (domináns) negatív mutánsát kifejező sejtek nem reagáltak az IGF-I adagolására, eredményeink a nPKCδ központi szerepét bizonyítják az IGF-I hatásainak kialakulásában vázizomsejteken (**XIII**).

4.3.4. A vázizom vizsgálatával párhuzamosan elemeztük a folyamatos regenerációs aktivitást mutató humán bőr keratinocitáinak PKC rendszerét, humán

immortalizált HaCaT epidermális keratinocita modellt felhasználva. Hasonlóan a vázizomsejtekben tapasztaltakhoz megállapítottuk, hogy a HaCaT keratinociták is jellegzetes PKC izoformamintázattal rendelkeznek (cPKCα és β; nPKCδ, ε és η; aPKCζ), mely jelentős mértékben változott a sejtek proliferációja és a nagy sejtdenzitás indukálta keratinocita differenciálódás során. Bebizonyosodott az is, hogy az általános PKC aktivátor PMA, eltérő módon hatva az egyes izoformákra, gátolta a HaCaT keratinociták proliferációját, valamint terminális differenciálódást indukált (**XIV**).

4.3.5. Ezt követően olyan HaCaT keratinocitákat állítottunk elő, melyek egyes PKC izoformák konstitutíven aktív formáját fejezték ki. Ezen sejtek *in vitro* vizsgálata során kimutattuk, hogy a cPKCα és a nPKCδ izoformák overexpressziója jelentősen lecsökkentette a sejtproliferációt, ugyanakkor pozitív hatást gyakorolt a differenciálódásra és a sejtek apoptózisára. Ezzel ellentétben, a cPKCβ és a nPKCε aktivitása fokozta a sejtek növekedését, ugyanakkor gátolta a differenciálódást és a programozott sejthalált. Az *in vivo* proliferáció (tumorgenezis) tanulmányozása során a rekombináns technikákkal módosított HaCaT keratinocitákat immunhiányos (SCID) egerekbe injektáltuk, majd szövettani és immunhisztokémiai módszerekkel elemeztük a kifejlődött daganatok jellegzetességeit. Jó összhangban a sejttenyészetekben kapott adatokkal megállapítottuk, hogy a cPKCβ és a nPKCε overexpressziója megnövelte, míg a cPKCα és a nPKCδ fokozott aktivitása lecsökkentette a HaCaT keratinociták *in vivo* növekedési potenciálját. Mindezen adataink az egyes PKC izoenzimek specifikus, ugyanakkor egymással ellentétes szerepére utalnak a humán epidermális keratinociták növekedésének, differenciálódásának és túlélésének szabályozásában (**XV**).

4.3.6. Végezetül monoblasztos leukémia modellben (MonoMac-6 sejtek) vizsgáltuk a PKC izoenzimek szerepét. Megállapítottuk, hogy két legnagyobb mennyiségben expresszálódó izoforma, a cPKCβ és a nPKCδ serkenti a sejtek proliferációját, valamint arachidonsav termelését. Bebizonyosodott továbbá, hogy a cPKCβ és a nPKCδ „downstream" célmolekulák (kalcium-independens foszfolipáz A_2, DAG-lipáz) aktiválásán keresztül fejtik ki hatásaikat. Kimutattuk azt is, hogy a cPKCα kisebb mértékben fejeződik ki a sejtekben, valamint, hogy – a fenti két izoenzimmel ellentétes funkciót ellátva – gátolja a MonoMac-6 sejtek proliferációját és arachidonsav termelését (**XVI**).

4.4. A jelátviteli molekulák kifejeződése és funkciója jelentősen módosul egyes humán megbetegedésekben

4.4.1. Humán betegségek vizsgálata során először különféle daganatokban vizsgáltuk a fenti jelátviteli molekulák kifejeződését. A TRPV1 vizsgálata során megállapítottuk, hogy az ioncsatorna fehérje és génszintű kifejeződése (mely igen alacsonynak bizonyult az egészséges nyelv epitéliumában) drámaian fokozódott a humán nyelv prekancerózus elváltozásában (leukoplakia), valamint nyelv laphámkarcinómában. Bebizonyosodott ugyanakkor, hogy a megemelkedett TRPV1 expresszió mértéke nem korrelált a primer tumorok malignitásának (hisztopatológiai grádus) fokával (**XVII**).

4.4.2. A fentiekhez hasonlóan a humán prosztata megbetegedéseiben is vizsgáltuk TRPV1, valamint a CB1 kifejeződését. Megállapítottuk, hogy mindkét molekula (fehérje és mRNS szintű) expressziója jelentősen fokozódott humán prosztatakarcinómában (PCC). Kimutattuk ugyanakkor, hogy míg a megemelkedett TRPV1 szint jó korrelációt mutatott a PCC növekvő grádusával (azaz a malignitás

fokával), addig a CB1 esetében hasonló jelenséget nem tapasztaltunk. Bebizonyosodott az is, hogy a CB1 expressziója nagymértékben megnövekedett benignus prosztata hiperpláziában, míg a TRPV1 szintje nem változott az egészséges kontrollhoz képest (**XVIII**). Mindezen adatok arra utalnak, hogy a TRPV1 és CB1 molekulák meghatározó szereppel bírhatnak a humán prosztata daganatos elváltozásainak kialakulásában.

4.4.3. A PKC izoformák kifejeződésében bekövetkező esetleges módosulásokat először tranzicionális sejtes húgyhólyagkarcinómában vizsgáltuk. Megállapítottuk, hogy az egészséges uroepitéliumban általunk leírt PKC izoformamintázat (cPKCα és β; nPKCδ és ε; aPKCζ) szignifikánsan változott a primer tumorok grádusának függvényében. Kimutattuk, hogy a cPKCβ és a nPKCδ szintje (mely izoformák jelentős mértékben kifejeződtek a kontroll hólyagban) folyamatosan csökkent a grádus növekedésével párhuzamosan. Ezzel ellentétben a cPKCα, a nPKCε és az aPKCζ expressziója a daganatok grádusával párhuzamosan emelkedett, azaz a legmagasabb szintű kifejeződést a legrosszabb prognózisú tumorokban tapasztaltuk. Mindezen adatok azt sugallják, hogy a PKC rendszer egyes izoformái (feltehetően egymással ellentétes) szereppel bírnak a húgyhólyagkarcinóma patogenezisében (**XIX**).

4.4.4. A PKC izoformák szintjét különböző autoimmun betegségekben szenvedők perifériás vér mononukleáris sejtjeiben is tanulmányoztuk. Az irodalomban elsőként mutattuk ki, hogy szisztémás lupus erythematosusos (SLE) betegek csökkent proliferációs kapacitással jellemezhető T-limfocitáiban a cPKCβ; a nPKCδ, ε és η; valamint az aPKCζ expressziója, míg az SLE-s betegek monocitáiban a nPKCδ és ε, valamint az aPKCζ szintje jelentős mértékben lecsökkent az egészséges önkéntesek sejtjeiben mértekhez képest. Bebizonyítottuk azt is, hogy mind a klinikai javulást

eredményező *in vivo*, mind az *in vitro* kortikoszteroid kezelés (különböző mértékben ugyan, de) a legtöbb PKC izoforma expresszióját az egészséges kontrollhoz közeli értékre emelte („normalizálta"). Leírtuk emellett, hogy ezen változások kizárólag az SLE-s betegek esetében mutathatóak ki, hiszen Sjögren-szindrómás és Kevert Kötőszöveti Betegségben (MCTD) szenvedők sejtjeiben a PKC izoformák kifejeződése nem változott a kontrollhoz viszonyítva (**XX**).

5. AZ EREDMÉNYEK HASZNOSÍTHATÓSÁGA

Kísérleteink számos, a klinikai, farmakológiai és biotechnológiai gyakorlatban közvetlenül hasznosítható új eredményt szolgáltattak, melyekről több összefoglaló publikációban is beszámoltunk (az Értekezéshez csatolva: **XXI**, **XXII**). Ezek közül az alábbiakat emeljük ki:

5.1. TRPV1 agonisták és CB2 antagonisták (akár kombinált) alkalmazása, valamint az endokannabinoidok termelődését gátló ágensek (pl. a szintetizáló enzimek inhibitorainak) adagolása sikerrel kecsegtet a faggyúmirigy patológiásan fokozott zsírtermelésével jellemezhető kórképek (pl. acne vulgaris) terápiájában. Ezen logikát követve a TRPV1 antagonisták, CB2 agonisták, illetve az endokannabinoidok szintézisét fokozó anyagok (pl. a lebontó enzimek gátlószereinek) adagolása jó hatékonyságú lehet a száraz bőr (és a hozzá kapcsolódó másodlagos kórképek, mint pl. a viszketés) kozmetológiai és dermatológiai kezelésében. Mivel a faggyúmirigy könnyen „hozzáférhető" a bőrön

alkalmazott hatóanyagok számára, ezen vegyületek nagy valószínűséggel helyileg (pl. krém formájában) is adagolhatók lesznek.

5.2. A szőrtüszőben kifejeződő TRPV1 és CB1 aktiválása terápiás értékű lehet fokozott szőrnövekedéssel járó kórképekben (pl. hipertrichózis), míg TRPV1 és CB1 antagonisták a csökkent hajnövekedéssel és/vagy fokozott hajhullással jellemezhető betegségek (pl. az alopécia különböző formái, effluvium) kezelésében lehetnek alkalmazhatók.

5.3. Mivel a TRPV1 aktiválása jelentősen lecsökkentette a humán epidermális keratinociták növekedését, felmerül a TRPV1 agonistáinak alkalmazása a humán bőr hiperproliferatív megbetegedéseinek (pl. pikkelysömör) kezelésében is.

5.4. A daganatos megbetegedések nagy százalékát kitevő bőrgyógyászati tumorokban hatékony beavatkozás lehet továbbá a keratinociták fokozott proliferációját indukáló cPKCβ és nPKCε izoformák aktivitásának csökkentése szelektív inhibitorok alkalmazásával. Másik, az előzőeket akár kiegészítő terápiás alternatívaként olyan szerek alkalmazása is sikerrel kecsegtet, melyek a sejtproliferációt gátló (és a sejtek differenciálódását elősegítő) nPKCδ és cPKCα izoenzimek aktivitásának fokozásán keresztül fejtik ki hatásukat.

5.5. A fenti gondolatmenetet követve természetes és szintetikus TRPV1 és CB1 agonisták ugyancsak új támadáspontú daganatellenes szerekként szerepelhetnek a jövőben pl. a bőr, a prosztata és a nyelv benignus és malignus elváltozásaiban.

5.6. A humán dendritikus sejteken tapasztaltak fényében végezetül felmerül a TRPV1 aktivitását fokozó szerek potenciális gyulladásgátló hatásának kiaknázása is.

6. AZ ÉRTEKEZÉS ALAPJÁUL SZOLGÁLÓ KÖZLEMÉNYEK

(Tematikus sorrendben, az Értekezésben bemutatottaknak megfelelően)

I Bodó E., Kovács I., Telek A., Varga A., Paus R, Kovács L. and **Bíró T.** (2004): Vanilloid Receptor-1 is Widely Expressed on Various Epithelial and Mesenchymal Cell Types of Human Skin. J. Invest. Dermatol. 123(2):410-413; IF: 4,238

II Bodó E., **Bíró T.**[#], Telek A., Czifra G., Griger Z., Tóth I.B., Mescalchin A., Ito T., Bettermann A., Kovács L. és Paus R. (2005): A "Hot" New Twist to Hair Biology – Involvement of Vanilloid Receptor-1 (VR1/TRPV1) Signaling in Human Hair Growth Control. Am. J. Pathol. 166(4):985-998; IF: 5,796 ([#]megosztott elsőszerzőség)

III **Bíró T.**, Bodó E., Telek A., Géczy T., Tychsen B., Kovács L. és Paus R. (2006): Hair Cycle Control by Vanilloid Receptor-1 (TRPV1): Evidence from TRPV1 Knockout Mice. J. Invest. Dermatol. 126:1909-1912; IF: 4,535

IV Tóth I.B., Géczy T., Griger Z., Dózsa A., Seltmann H., Kovács L., Nagy L., Zouboulis C.C., Paus R. és **Bíró T.** (2009): Transient Receptor Potential Vanilloid-1 Signaling as a Regulator of Human Sebocyte Biology. J. Invest. Dermatol. 129(2):329-339 IF: 5,251

V Tóth I.B., Benkő S., Szöllősi A.G., Kovács L., Rajnavölgyi É. és **Bíró T.** (2009): Transient Receptor Potential Vanilloid-1 Signaling Inhibits Differentiation and Activation of Human Dendritic Cells. FEBS Lett. 583(10):1619-1624; IF: 3,264

VI Lázár J., Szabó T., Kovács L., Blumberg P.M. és **Bíró T.** (2003): Distinct Features of Recombinant Vanilloid Receptor-1 Expressed in Various Expression Systems. Cell. Mol. Life Sci. 60(10):2228-2240; IF: 4,995

VII Lázár J., Szabó T., Marincsák R., Kovács L., Blumberg P.M. és **Bíró T.** (2004): Sensitization of Recombinant Vanilloid Receptor-1 by Various Neurotrophic Factors. Life Sci. 75(2):153-163; IF: 2,158

VIII Marincsák R., Tóth I.B., Czifra G., Szabó T., Kovács L. és **Bíró T.** (2008): The Analgesic Drug Tramadol Acts as an Agonist of the Transient Receptor Potential Vanilloid-1 (TRPV1). Anesth. Analg. 106(6):1890-1896; IF: 2,590

IX Telek A., **Bíró T.**[#], Bodó E., Tóth I.B., Borbíró I., Kovács L., Kunos G. és Paus R. (2007): Inhibition of Human Hair Follicle Growth by Endo- and Exocannabinoids. FASEB J. 21(13):3534-3541; IF: 6,791 ([#]megosztott elsőszerzőség)

X Dobrosi N., Tóth I.B., Nagy G., Dózsa A., Géczy T., Nagy L., Zouboulis C.C., Paus R., Kovács L. és **Bíró T.** (2008): Endocannabinoids Enhance Lipid Synthesis and Apoptosis in Human Sebocytes via Cannabinoid Receptor-2-Mediated Signaling. FASEB J. 22(10):3685-3695; IF: 7,049

XI Boczán J., Boros S., Mechler F., Kovács L. és **Bíró T.** (2000): Differential Expressions of Protein Kinase C Isozymes During Proliferation and Differentiation of Human Skeletal Muscle Cells in vitro. Acta Neuropathol. 99(2):96-104; IF: 2,446

XII Boczán J., **Bíró T.**, Czifra G., Lázár J., Papp H., Bárdos H., Ádány R., Mechler F. és Kovács L. (2001): Phorbol Ester Treatment Inhibits Proliferation and Differentiation of Cultured Human Skeletal Muscle Satellite Cells by Differentially Acting on Protein Kinase C Isoforms. Acta Neuropathol. 102:55-62; IF: 2,165

XIII Czifra G., Tóth I.B., Marincsák R., Juhász I., Kovács I., Ács P., Kovács L., Blumberg P.M. és **Bíró T.** (2006): Insulin-like Growth Factor-I-Coupled Mitogenic Signaling in Primary Cultured Human Skeletal Muscle Cells and in C2C12 Myoblasts. A Central Role of Protein Kinase Cδ. Cell. Signal. 18:1461-1472; IF: 4,887

XIV Papp H., Czifra G., Lázár J., Boczán J., Gönczi M., Csernoch L., Kovács L. és **Bíró T.** (2003): Protein Kinase C Isozymes Regulate Proliferation and High Cell Density-Mediated Differentiation of HaCaT Keratinocytes. Exp. Dermatol. 12:811-824; IF: 2,040

XV Papp H., Czifra G., Bodó E., Lázár J., Kovács I., Aleksza M., Juhász I., Ács P., Sipka S., Kovács L., Blumberg P.M. és **Bíró T.** (2004): Opposite Roles of Protein Kinase C Isoforms in Proliferation, Differentiation, Apoptosis, and Tumorigenicity of Human HaCaT Keratinocytes. Cell. Mol. Life Sci. 61(9):1095-1105; IF: 4,812

XVI Griger Z., Páyer E., Kovács I., Tóth I.B., Kovács L., Sipka S. és **Bíró T.** (2007) Protein Kinase Cβ and δ Isoenzymes Promote Arachidonic Acid Production and Proliferation of MonoMac-6 Cells. J. Mol. Med. 85:1031-1042; IF: 4,820

XVII Marincsák R., Tóth I.B., Czifra G., Márton I., Rédl P., Tar I., Tóth L., Kovács L. és **Bíró T.** (2009): Increased Expression of TRPV1 in Squamous Cell Carcinoma of the Human Tongue. Oral Dis. 15:328-335; IF: 2,087

XVIII Czifra G., Varga A., Nyeste K., Marincsák R., Tóth I.B., Kovács I., Kovács L. és **Bíró T.** (2009): Increased Expression of Cannabinoid Receptor-1 and Transient Receptor Potential Vanilloid-1 (TRPV1) in Human Prostate Carcinoma. J. Cancer Res. Clin. 135(4):207-214; IF: 2,217

XIX Varga A., Czifra G., Tállai B., Németh T., Kovács I., Kovács L. és **Bíró T.** (2004): Tumor Grade-Dependent Alterations in the Protein Kinase C Isoform Pattern in Urinary Bladder Carcinomas. Eur. Urol. 46(4):462-465; IF: 2,651

XX **Bíró T.**, Griger Z., Kiss E., Papp H., Aleksza M., Kovács I., Zeher M., Bodolay E., Csépány T., Szűcs K., Gergely P., Kovács L., Szegedi G. és Sipka S. (2004): Abnormal Cell-Specific Expressions of Certain Protein Kinase C Isoenzymes in Peripheral Mononuclear Cells of Patients with Systemic Lupus Erythematosus. Effect of Corticosteroid Application. Scand. J. Immunol. 60(4):421-428; IF: 1,912

XXI Paus R., Schmelz M., **Bíró T.** és Steinhoff M. (2006): Frontiers in Pruritus Research: Scratching the Brain for More Effective Itch Therapy. J. Clin. Invest. 116(5):1174-1186; IF: 15,754

XXII **Bíró T.**, Tóth I.B., Haskó G., Paus R. és Pacher P. (2009): The Endocannabinoid System of the Skin in Health and Disease: Novel Perspectives and Therapeutic Opportunities. Trends Pharmacol. Sci. 30(8):411-420; IF: 9,34

7. SCIENTOMETRIA

7.1. Általános adatok

7.1.1. In extenso közlemények (teljes pályafutás)

a. A közlemények száma: 69
    i. Ebből első és utolsószerzős: 34
b. A közlemények összesített impakt faktora: 289,085
c. A közleményekre kapott független citációk száma: 927
d. Hirsch-index: 21

7.1.2. In extenso közlemények (Ph.D. fokozat megszerzése óta)

a. A közlemények száma: 60
    i. Ebből első és utolsószerzős: 29
b. A közlemények összesített impakt faktora: 243,449
c. A közleményekre kapott független citációk száma: 571
d. Hirsch-index: 16

7.2. Az Értekezés alapjául szolgáló közleményekre vonatkozó adatok

a. Közlemények száma: 22
    i. Ebből első és utolsószerzős: 20
b. A közlemények összesített impakt faktora: 101,798

8. KÖSZÖNETNYÍLVÁNÍTÁS

Mindenek előtt mentoromnak, Dr. Kovács László akadémikus úrnak, a DE OEC Élettani Intézet korábbi igazgatójának mondok köszönetet, aki pályám kezdetétől fogva felbecsülhetetlen értékű szakmai, baráti és néha atyai támogatásával lehetővé tette számomra, hogy az Intézet hasznos tagja lehessek.

Köszönöm továbbá Dr. Csernoch László professzor úrnak, a DE OEC Élettani Intézet jelenlegi igazgatójának, hogy lehetővé tette tudományos munkám minél magasabb szintű kivitelezését.

Köszönöm emellett közvetlen munkatársaimnak, hogy a kísérletes munka néha igen göröngyös útján – a korántsem könnyű természetemből fakadó viharok ellenére – mellettem álltak, valamint, hogy szorgalmukkal és hozzáértésükkel segítették munkámat.

Hálával tartozom szerzőtársaimnak, hazai elméleti és klinikus kollégáimnak, valamint külföldi kollaborációs partnereimnek (külön kiemelve Ralf Paus és Peter M. Blumberg professzorokat), hogy ötleteikkel és javaslataikkal folyamatosan segítették tevékenységemet.

Köszönöm továbbá az Élettani Intézet valamennyi munkatársának, hogy baráti légkört teremtve hozzájárultak kutatásaim sikeréhez.

Hálával gondolok végezetül családomra, akik tudományos pályafutásom során folyamatosan biztosították a szükséges támogatást és a lelki hátteret. Külön köszönöm csodálatos feleségem és gyermekeim áldozatos odaadását és határtalan türelmét. Nélkülük nem lehetnék az, ami vagyok.

9. AZ ÉRTEKEZÉSBEN IDÉZETT KÖZLEMÉNYEK

1. Evan et al. (2001) *Nature* **411**, 342-8
2. Raff (1992) *Nature* **356**, 397-400
3. Roosterman et al. (2006) *Physiol. Rev.* **86***,* 1309-79
4. Paus et al. (2006) *Trends. Immunol.* **27***,* 32-9
5. Hunter (2000) *Cell* **100**, 113-27
6. Premont et al. (2007) *Annu. Rev. Physiol.* **69**, 511-34
7. Brown (2005) *Nat. Rev. Cancer.* **5**, 231-7
8. Clapham (2003) *Nature* **426***,* 517-24
9. Nilius et al. (2007) *Physiol. Rev.* **87***,* 165-217
10. Caterina et al. (1997) *Nature* **389***,* 816-24
11. Caterina et al. (2001) *Annu. Rev. Neurosci.* **24***,* 487-517
12. Szallasi et al. (1999) *Pharmacol. Rev.* **51***,* 159-212
13. Prescott et al. (2003) *Science* **300***,* 1284-88
14. Di Marzo et al. (2002) *Curr. Opin. Neurobiol.* **12***,* 372-79
15. Bíró et al. (1998) *Blood* **91***,* 1332-40
16. Bíró et al. (1998) *Brain. Res. Mol. Brain. Res.* **56***,* 89-98
17. Inoue et al. (2002) *Biochem. Biophys. Res. Commun.* **291***,* 124-9
18. Birder et al. (2001) *Proc. Natl. Acad. Sci. USA* **98***,* 13396-401
19. Amantini et al. (2004) *Cell. Death. Differ.* **11***,* 1342-56
20. Mechoulam et al. (1998) *Eur. J. Pharmacol.* **359**, 1-18
21. Howlett et al. (2002) *Pharmacol. Rev.* **54**, 161-202
22. Di Marzo (2008) *Rev. Physiol. Biochem. Pharmacol.* **160**, 1-24
23. Pacher et al. (2006) *Pharmacol. Rev.* **58**, 389-462
24. Di Marzo (2008) *Nat. Rev. Drug Discov.* **7**, 438-55
25. Pertwee (2005) *Handb. Exp. Pharmacol.* 1-51
26. Howlett (2005) *Handb. Exp. Pharmacol.* 53-79
27. Nishizuka (1992) *Science* **258**, 607-14
28. Reyland (2009) *Front. Biosci.* **14**, 2386-99
29. Roffey et al. (2009) *Curr. Opin. Cell Biol.* **21**, 268-79
30. Rosse et al. (2010) *Nat. Rev. Mol. Cell. Biol.* **11**, 103-12
31. Decker (ed) (2003) *Protein Kinase C, Oxford Press, New York*
32. Kazanietz et al. (2007) *Nat. Rev. Cancer.* **7**, 281-94

10. FÜGGELÉK

Az Értekezés alapjául szolgáló közlemények másolatai

I.

Vanilloid Receptor-1 (VR1) is Widely Expressed on Various Epithelial and Mesenchymal Cell Types of Human Skin

To the Editor:

A subset of sensory neurons can be defined by their susceptibility to capsaicin and related vanilloids (Szallasi and Blumberg, 1999). The molecular target of these agents is the vanilloid receptor-1 (VR1), which functions as a calcium-permeable non-specific cation channel (Caterina *et al*, 1997). This receptor can also be activated by heat and acidosis, and by endogenous "endovanilloids" such as arachidonic acid derivatives and eicosanoids (Di Marzo *et al*, 2002). Therefore, VR1 was suggested as a key integrator molecule of various nociceptive stimuli.

In addition to its presence on sensory neurons, functional VR1s have also been identified on various non-neuronal cell types *in vitro*. We have previously shown that activation of VR1 in mast cells (Bíró *et al*, 1998b) and glial cells (Bíró *et al*, 1998a), similar to findings by others on bronchial (Veronesi *et al*, 1999) and uroepithelial cells (Birder *et al*, 2001), resulted in the onset of a variety of cellular processes such as changes in proliferation, apoptosis, differentiation, and cytokine release.

Very recently, a functional VR1 was also identified on human epidermal keratinocytes (NHEK, Denda *et al*, 2001; Inoue *et al*, 2002; Southall *et al*, 2003). It is not clear, however, whether VR1 is also expressed in normal human skin in addition to sensory neurons and keratinocytes. Therefore, in this study, our goal was to characterize VR1 immunoreactivity on epithelial and mesenchymal cells of normal human skin *in situ*.

Normal skin samples (n = 7; trunk, back), obtained during plastic surgery, were used as either frozen or formaldehyde-fixed sections embedded in paraffin (3–5 μm thickness in both cases). To detect VR1, a streptavidin–biotin-complex (SABC) three-step immunohistochemical technique (DAKO, Hamburg, Germany) was employed. Inhibition of endogenous peroxidase activity was performed using 0.5% H_2O_2 in 100% methanol. Non-specific binding of the antibodies was blocked by 2% bovine serum albumin (BSA, Sigma, St Louis, Missouri) in phosphate-buffered saline (pH 7.6). Sections were first incubated with an anti-VR1 goat primary antibody against the N-terminus of VR1 (1:20 dilution, Santa Cruz, Santa Cruz, California), then with a biotin-coupled anti-goat secondary antibody (1:500, DAKO), and, finally, with streptavidin conjugated with horseradish peroxidase (1:400, DAKO). To reveal the peroxidase activity, DAB (Vector, Burlingame, California) or VIP SK-4600 (Vector) was employed as chromogenes. Tissue samples were finally slightly counterstained with hematoxylin Gill I (Surgipath Europe, Peterborough, UK) and mounted with Aquatex (Merck, Vienna, Austria).

In control experiments, the specificity of VR1 staining was assessed by (1) omitting the primary antibody or by incubating the sections with the VR1 antibody pre-absorbed with a synthetic blocking peptide (Santa Cruz) (Fig 1*G*); (2) using another antibody against the C-terminus of VR1 (Santa Cruz), which resulted in an identical staining pattern (data not shown); and (3) performing VR1 immunostaining on frozen skin sections from wild-type C57BL/6J and VR1 knock-out (VR1/KO) B6.129S4-Trpv1 mice (The Jackson Laboratory, Bar Harbor, Maine) (Fig 1*J, K*). In this latter case, a fluorescein-isothiocyanate (FITC)-conjugated secondary antibody was used for visualization. Frozen sections of rat spinal cord were used as positive tissue controls (Fig 1*H, I*).

For double immunohistochemistry, frozen skin sections were first labeled to detect VR1 as described above and then were again blocked using 2% BSA. To detect mast cells or dendritic cells, sections were incubated with either a monoclonal mouse anti-human mast cell tryptase antibody (1:50, DAKO) or with a monoclonal mouse anti-CD1a (a dendritic cell-specific marker) antibody (1:20, Novocastra, Newcastle upon Tyne, UK), then with biotin-conjugated anti-mouse secondary antibody (1:500, DAKO), and, finally, with alkaline phosphatase-conjugated streptavidine (1:50 dilution, DAKO). Endogenous alkaline phosphatase activity was blocked using Levamisole (Sigma), and Fast blue BB (Sigma) was applied as a chromogene.

To detect VR1 mRNA expression, skin homogenates were pulverized in liquid N_2. Total RNA was then isolated using TRIzol (Invitrogen, Paisley, UK) and was reverse transcribed strictly following the procedure described before (Southall *et al*, 2003). PCR amplification was performed using human VR1-specific primers: sense, 5′-ctcctacaacagcctgtac-3′; antisense, 5′-aaggcccagtgttgacagtg-3′ (RT-PCR).

To detect VR1 protein expression, skin homogenates (60–80 μg protein) were subjected to SDS-PAGE as described before (Lázár *et al*, 2003). VR1 expression was determined by immunoblotting using the above goat anti-VR1 antibody, a horseradish peroxidase-conjugate rabbit anti-goat secondary antibody (BioRad, Wien, Austria), and enhanced chemiluminescence (Amersham, Little Chalfont, England). For the RT-PCR and western blot analyses, cultured NHEK and HaCaT keratinocytes were used as VR1-expressing positive controls (Denda *et al*, 2001; Southall *et al*, 2003). The study was approved by the

Abbreviations: VR1, vanilloid receptor-1; VR1-ir, VR1 immunoreactivity

Institutional Research Ethics Committee and adhered to Declaration of Helsinki guidelines.

Since we are currently investigating in detail VR1 expression and function in human hair biology in a separate study, hair follicle VR1 immunoreactivity patters were ignored in this manuscript (Bodó *et al*, manuscript in preparation).

Using immunolabeling on paraffin-embedded human skin samples, specific VR1 immunoreactivity (VR1-ir) was identified on several cell types of human skin (Table I). The specificity of VR1-ir was approved by using various positive and negative controls (Fig 1*G–I*), including skin sections of VR1/KO mice in which there was a complete lack of VR1-ir (Fig 1*J, K*). With respect to the epidermis, confirming previous data (Denda *et al*, 2001), VR1 was expressed in the epidermal keratinocytes. The VR1-ir pattern, however, was inhomogeneous; i.e., whereas a rather strong cytoplasmic and nuclear VR1-ir was detected in the basal and spinous layers, much weaker signals were found in the suprabasal layers (Fig 1*A*). Of great novelty, VR1 was also expressed in CD1a-positive epidermal Langerhans cells (Fig 1*B*). Epidermal melanocytes, instead, were negative for VR1 (data not shown).

In addition to sensory nerve fibers (which also served as positive controls, Fig 1*C*), we demonstrated VR1-ir, for the first time, on various cells populations of the dermis. A strong VR1-ir was observed on sebocytes (Fig 1*D*) and sweat gland epithelium (Fig 1*E*), on endothelial and smooth muscle cells of skin blood vessels (Fig 1*C–F*), on smooth muscles (Fig 1*D*), and on tryptase-positive dermal mast cells (Fig 1*F*). Connective tissue fibroblasts showed no VR1-ir (Fig 1*C*). There was no difference in the VR1 expression pattern of skin samples of different patients or of different body sites (data not shown). Finally, the presence of VR1 in human skin, both at the mRNA and protein levels, was also demonstrated using Western blotting (Fig 1*L*) and RT-PCR (Fig 1*M*).

The complex functional roles of VR1 signaling in human skin biology and pathology now await dissection and clarification. One straightforward possibility is that VR1, functioning as a calcium-permeable channel (Caterina *et al*, 1997; Szallasi and Blumberg, 1999), upon activation, leads to an increase in intracellular calcium concentration ($[Ca^{2+}]_i$) and hence may initiate calcium-mediated processes. Such calcium-coupled mechanisms were described for urinary epithelial cells (nitric oxide release) (Birder *et al*, 2001), glial cells (proliferation, differentiation, apoptosis) (Bíró *et al*, 1998a), and mast cells and epidermal keratinocytes (pro-inflammatory mediator release) (Bíró *et al*, 1998b; Southall *et al*, 2003). In addition, since most skin cell functions are strongly affected by $[Ca^{2+}]_i$ (Hennings *et al*, 1980; Bikle and Pillai, 1993; Vicanova *et al*, 1998), VR1 may possess a significant role, e.g., in the regulation of keratinocyte differentiation and proliferation. This is supported by our demonstration that the expression of VR1

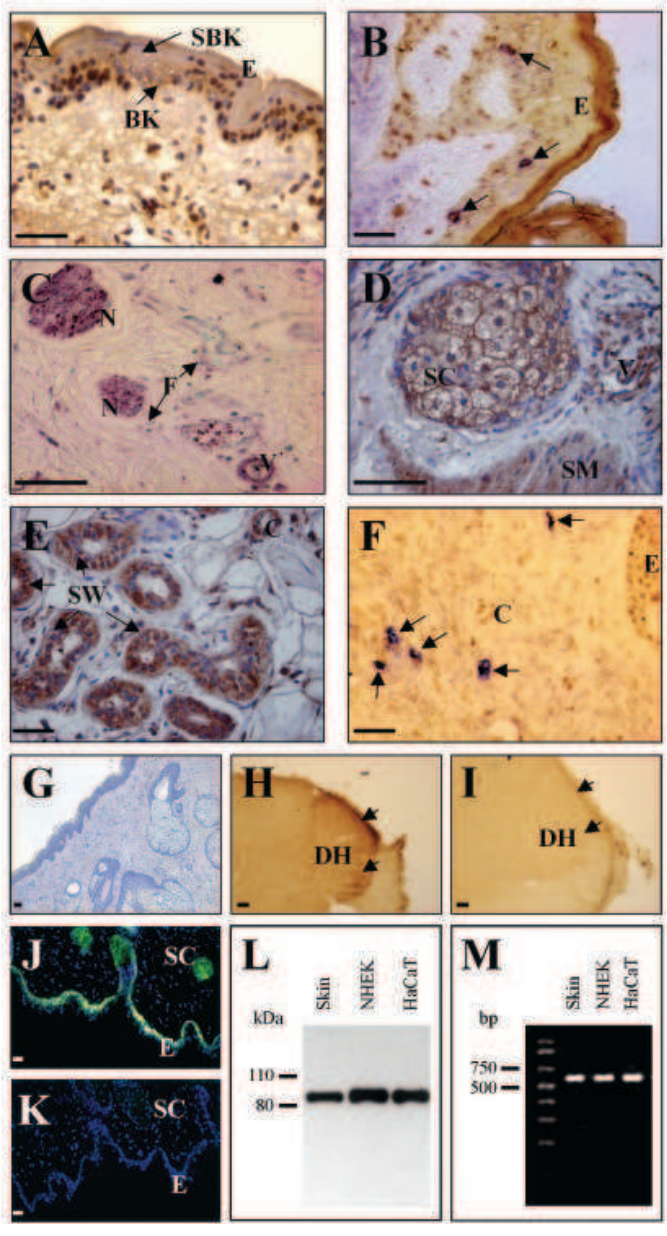

Figure 1
VR1 immunoreactivity and protein and mRNA expression on human skin. (*A*) Immunoreactivity for VR1 (VR1-ir) on epidermal keratinocytes. Note the stronger staining observed on basal (BK) than on suprabasal (SBK) keratinocytes (E, epidermis). (*B*) Co-localization of VR1 (brown) and CD1a (blue) on Langerhans cells (arrow) of the epidermis (E), as revealed by double immunolabeling. (*C*) VR1-ir on nerve fibers (N) and endothelium and smooth muscle cells of dermal blood vessels (V). Note the lack of VR-ir on dermal fibroblasts (F, *arrows*). (*D*) VR1-ir on sebocytes (SC), endothelial and smooth muscle cells of blood vessels (V), and on smooth muscle of dermis (SM). (*E*) VR1 expression on sweat gland epithelium (SW, *arrows*) (C, capillary). (*F*) Co-localization of VR1 (brown) and mast cell-specific tryptase (blue) on dermal mast cells (*arrows*) (E, epidermis; C, capillary). (*G*) Negative control. Specificity of staining was assessed by incubating skin sections with the VR1 antibody pre-absorbed with a synthetic blocking peptide. (*H*) Positive control. VR1-ir (*arrows*), as observed on the dorsal horn (DH) of rat spinal cord. (*I*) Negative control. Lack of VR1-ir (*arrows*) on dorsal horn (DH) of rat spinal cord when stained with the VR1 antibody pre-absorbed with a synthetic blocking peptide. (*J, K*) VR1-ir on skin of wild type C57BL/6J (*J*) and VR1/KO (*K*) mice (an FITC-conjugated secondary antibody was used for visualization). E, epidermis; SC, sebocytes. (*A, C, D, E, G*). Paraffin-embedded sections. (*B, F, H, I–K*) Frozen sections. In most cases, DAB was used to develop VR1-ir, except for *C*, where VIP SK-4600 was applied as a chromogene; and *C*, where VIP SK-4600 was applied as a chromogene. Original magnifications, *A–F*: × 400; *G*: × 40; × *H–K*: × 100. (*L*) Western blot analysis of VR1 protein expression (approximately 90 kDa) in human skin homogenates and in NHEK and HaCaT keratinocytes. (*M*) RT-PCR analysis of VR1 mRNA expression (predicted size of approximately 680 base pairs, bp) in human skin homogenates and in NHEK and HaCaT keratinocytes.

Table I. Vanilloid receptor-1 (VR1) immunoreactivity (VR1-ir) on various cell types of human skin

Cell	Type	VR1-ir
Epidermis		
Basal keratinocytes	E	+ + +
Suprabasal keratinocytes	M	+
Melanocytes	M	–
Langerhans cells	M	+ +
Dermis		
Mast cells	M	+ +
Sweat gland epithelium	E	+ + +
Sebocytes	E	+ + +
Endothelial cells	M	+ +
Smooth muscle cells	M	+ + +
Connective tissue fibroblasts	M	–

Intensity of VR1-ir: –, no; +, weak; + +, medium; + + +, strong.
E, neuroectodermal; M, mesenchymal.

among epidermal keratinocytes appeared to be linked to their distinct differentiation status (Fig 1*A*). In fact, activation of VR1 by capsaicin in cultured HaCaT keratinocytes results in a concentration-dependent inhibition of proliferation (Bíró *et al*, unpublished observations).

Our findings may possess even therapeutic significance. The VR1 agonist capsaicin was previously described to act exclusively indirectly on non-neuronal cells of skin via the release of various neuropeptides from sensory neurons (Bíró *et al*, 1998b; Szallasi and Blumberg, 1999; Townley *et al*, 2002). This study, however, clearly argues for that activators of VR1 signaling can directly target cutaneous structures other than sensory neurons. Therefore, the "dual" activation of VR1 by exogenous capsaicin or "endovanilloids" on neuronal and non-neuronal cell types of the skin likely results in the simultaneous release of neuropeptides from sensory axons and of other mediators (e.g., histamine, pro-inflammatory cytokines) from keratinocytes, mast cells, or endothelial cells. This could activate a complex, multi-directional signaling cascade augmenting the action of the VR1 agonist. No wonder, therefore, that capsaicin application was found to be most effective in the treatment of chiefly histamine-dependent and/or neurogenic pruritic skin disorders (Greaves and Wall, 1996; Bíró *et al*, 1997; Ständer *et al*, 2001, 2003).

In conclusion, in this study, we presented evidence that VR1-ir is expressed not only on epidermal keratinocytes of normal human skin (Denda *et al*, 2001) but also by neuroectodermal and mesenchymal cell types such as Langerhans cells, sebocytes, sweat gland epithelium, endothelial and smooth muscle cells of skin blood vessels, and mast cells. This widespread, but certainly not ubiquitous, VR1 protein expression pattern suggests multiple, previously unappreciated additional functions for VR1-mediated signaling, well beyond nociception.

Enikő Bodó,*† Ilona Kovács,‡ Andrea Telek,*† Attila Varga,§ Ralf Paus,† László Kovács,* and Tamás Bíró*

*Department of Physiology and Cell Physiology Research Group of the Hungarian Academy of Sciences, Debrecen, Hungary; †Department of Dermatology, University Hospital Hamburg-Eppendorf, University of Hamburg, Hamburg, Germany; ‡Department of Pathology, Kenézy Hospital, Debrecen, Hungary; §Department of Urology, University of Debrecen, Medical and Health Science Center, Research Center for Molecular Medicine, Debrecen, Hungary

This work was supported by Hungarian research grants: OTKA F035036, NKFP 00088/2001, OMFB 00200/2002, and ETT 365/2003. Tamás Bíró is a recipient of the György Békésy Postdoctoral Scholarship of the Hungarian Ministry of Education.

DOI: 10.1111/j.0022-202X.2004.23209.x

Manuscript received January 12, 2004; revised March 3, 2003; accepted for publication March 19, 2004

Address correspondence to: Tamás Bíró, MD, PhD, Department of Physiology, Medical and Health Science Center, Research Center for Molecular Medicine, University of Debrecen, Nagyerdei krt. 98, PO Box 22, H-4012 Debrecen, Hungary. Email: biro@phys.dote.hu

Note added in proof: During the revision process of this manuscript, we were intrigued to learn that a similar study was performed by Ständer *et al* (2004), confirming our findings presented above.

References

Bikle DD, Pillai S: Vitamin D, calcium, and epidermal differentiation. Endocr Rev 14:3–19, 1993

Birder LA, Kanai AJ, de Groat WC, *et al*: Vanilloid receptor expression suggests a sensory role for urinary bladder epithelial cells. Proc Natl Acad Sci USA 98:13396–13401, 2001

Bíró T, Ács G, Ács P, Modarres S, Blumberg PM: Recent advances in understanding of vanilloid receptors: A therapeutic target for treatment of pain and inflammation in skin. J Investig Dermatol Symp Proc 2:56–60, 1997

Bíró T, Brodie C, Modarres S, Lewin NE, Ács P, Blumberg PM: Specific vanilloid responses in C6 rat glioma cells. Mol Brain Res 56:89–98, 1998a

Bíró T, Maurer M, Modarres S, *et al*: Characterization of functional vanilloid receptors expressed by mast cells. Blood 91:1332–1340, 1998b

Bodó E, Bíró T, Telek A, *et al*: A "hot" new twist to hair biology—Involvement of vanilloid receptor-1 (VR1) signaling in human hair growth control (manuscript in preparation).

Caterina MJ, Schumacher MA, Tominaga M, Rosen TA, Levine JD, Julius D: The capsaicin receptor: A heat-activated ion channel in the pain pathway. Nature 389:816–824, 1997

Denda M, Fuziwara S, Inoue K, Denda S, Akamatsu H, Tomitaka A, Matsunaga K: Immunoreactivity of VR1 on epidermal keratinocyte of human skin. Biochem Biophys Res Commun 285:1250–1252, 2001

Di Marzo V, Blumberg PM, Szallasi A: Endovanilloid signaling in pain. Curr Opin Neurobiol 12:372–379, 2002

Greaves MW, Wall PD: Pathophysiology of itching. Lancet 348:938–940, 1996

Hennings H, Michael D, Cheng C, Steinert P, Holbrook K, Yuspa SH: Calcium regulation of growth and differentiation of mouse epidermal cells in culture. Cell 19:245–254, 1980

Inoue K, Koizumi S, Fuziwara S, Denda S, Inoue K, Denda M: Functional vanilloid receptors in cultured normal human epidermal keratinocytes. Biochem Biophys Res Commun 291:124–129, 2002

Lázár J, Szabó T, Kovács L, Blumberg PM, Bíró T: Distinct features of recombinant vanilloid receptor-1 expressed in various expression systems. Cell Mol Life Sci 60:2228–2240, 2003

Southall MD, Li T, Gharibova LS, Pei Y, Nicol GD, Travers JB: Activation of epidermal vanilloid receptor-1 induces release of proinflammatory mediators in human keratinocytes. J Pharmacol Exp Ther 304:217–222, 2003

Ständer S, Luger T, Metze D: Treatment of prurigo nodularis with topical capsaicin. J Am Acad Dermatol 44:471–478, 2001

Ständer S, Moormann C, Schumacher M, *et al*: Expression of vanilloid receptor subtype 1 in cutaneous sensory fibers, mast cells, and epithelial cells of appendage structures. Exp Dermatol 13:129–139, 2004

Ständer S, Steinhoff M, Schmelz M, Weisshaar E, Metze D, Luger T: Neurophysiology of pruritus: Cutaneous elicitation of itch. Arch Dermatol 139:1463–1470, 2003

Szallasi A, Blumberg PM: Vanilloid (Capsaicin) receptors and mechanisms. Pharmacol Rev 51:159–212, 1999

Townley SL, Grimbaldeston MA, Ferguson I, *et al*: Nerve growth factor, neuropeptides, and mast cells in ultraviolet-B-induced systemic suppression of contact hypersensitivity responses in mice. J Invest Dermatol 118:396–401, 2002

Veronesi B, Oortgiesen M, Carter JD, Devlin RB: Particulate matter initiates inflammatory cytokine release by activation of capsaicin and acid receptors in a human bronchial epithelial cell line. Toxicol Appl Pharmacol 154:106–115, 1999

Vicanova J, Boelsma E, Mommaas AM, *et al*: Normalization of epidermal calcium distribution profile in reconstructed human epidermis is related to improvement of terminal differentiation and stratum corneum barrier formation. J Invest Dermatol 111:97–106, 1998

II.

American Journal of Pathology, Vol. 166, No. 4, April 2005

Epithelial and Mesenchymal Cell Biology

A Hot New Twist to Hair Biology

Involvement of Vanilloid Receptor-1 (VR1/TRPV1) Signaling in Human Hair Growth Control

Enikő Bodó,*† Tamás Bíró,*‡ Andrea Telek,*† Gabriella Czifra,* Zoltán Griger,* Balázs I. Tóth,* Alessandra Mescalchin,§ Taisuke Ito,† Albrecht Bettermann,† László Kovács,*‡ and Ralf Paus†

From the Department of Physiology and the Cell Physiology Research Group of the Hungarian Academy of Sciences,‡ University of Debrecen, Medical and Health Science Center, Research Center for Molecular Medicine, Debrecen, Hungary; the Department of Dermatology,† University Hospital Hamburg-Eppendorf, University of Hamburg, Hamburg, Germany; and Cutech Srl,§ Venice, Italy*

The vanilloid receptor-1 (VR1, or transient receptor potential vanilloid-1 receptor, TRPV1) is activated by capsaicin, the key ingredient of hot peppers. TRPV1 was originally described on sensory neurons as a central integrator of various nociceptive stimuli. However, several human skin cell populations are also now recognized to express TRPV1, but with unknown function. Exploiting the human hair follicle (HF) as a prototypic epithelial-mesenchymal interaction system, we have characterized the HF expression of TRPV1 *in situ* and have examined TRPV1 signaling in organ-cultured human scalp HF and outer root sheath (ORS) keratinocytes *in vitro*. TRPV1 immunoreactivity was confined to distinct epithelial compartments of the human HF, mainly to the ORS and hair matrix. In organ culture, TRPV1 activation by capsaicin resulted in a dose-dependent and TRPV1-specific inhibition of hair shaft elongation, suppression of proliferation, induction of apoptosis, premature HF regression (catagen), and up-regulation of intrafollicular transforming growth factor-β_2. Cultured human ORS keratinocytes also expressed functional TRPV1, whose stimulation inhibited proliferation, induced apoptosis, elevated intracellular calcium concentration, up-regulated known endogenous hair growth inhibitors (interleukin-1β, transforming growth factor-β_2), and down-regulated known hair growth promoters (hepatocyte growth factor, insulin-like growth factor-I, stem cell factor). These findings strongly support TRPV1 as a significant novel player in human hair growth control, underscore the physiological importance of TRPV1 in human skin beyond nociception, and identify TRPV1 as a promising, novel target for pharmacological manipulations of epithelial growth disorders. *(Am J Pathol 2005, 166:985–998)*

The tingling or burning sensation that comes along with the consumption of hot peppers arises from capsaicin.[1] The molecular target of this agent is the vanilloid (capsaicin) receptor-1 (VR1/TRPV1), which functions as a calcium-permeable nonspecific cation channel.[1,2] In addition to capsaicin, as the best-investigated (exogenous) TRPV1 ligand, this receptor can also be activated and/or sensitized by endogenous endovanilloids such as heat, acidosis, arachidonic acid derivatives, lipid peroxidation metabolites, and endocannabinoids (such as anandamide), suggesting that TRPV1 operates as a central integrator molecule of various nociceptive stimuli.[3,4] In fact, a subset of sensory neurons can be defined by their exquisite susceptibility to neuropeptide-depletion and ultimately induction of neuronal degeneration by capsaicin and other vanilloids such as resiniferatoxin (RTX).[1,5] Clinically, this has long been exploited for the management of numerous chronic pain (such as postherpetic neuralgia) and pruritic syndromes.[6]

However, beginning with our discovery that mast cells also express functional TRPV1,[7] we and others have

Supported in part by grants from the Deutsche Forschungsgemeinschaft (Pa 345/11-1 to R.P.), Cutech Srl (to R.P.), Hungarian research grants (OTKA F035036, OTKA TS040773, NKFP 00088/2001, OMFB 00200/2002, ETT 365/2003 to T.B.), the European Union (Erasmus fellowship to E.B.), the Hungarian Ministry of Education (György Békésy postdoctoral scholarship to T.B.), and NATO (science fellowship to T.B.).

E.B. and T.B. contributed equally to this work.

Accepted for publication December 2, 2004.

Address reprint requests to Tamás Bíró, M.D., Ph.D., Department of Physiology, University of Debrecen, MHSC, 4012 Debrecen, Nagyerdei krt. 98., PO Box 22, Hungary. E-mail: biro@phys.dote.hu.

subsequently described that TRPV1 expression is much more widespread than previously thought suggesting that TRPV1 functions are not limited to sensory ones. It is now recognized that the activation of TRPV1 on several neuroectoderm- or mesoderm-derived cell populations, such as mast cells,[7] glial cells,[8] bronchial epithelial cells,[9] uroepithelial cells,[10] and keratinocytes[11–13] *in vitro* results in changes in proliferation, apoptosis, differentiation, and/or cytokine release. Most recently, we and others[14,15] found by immunohistology that human skin and its appendages prominently express TRPV1 immunoreactivity (TRPV1-ir) *in vivo* not only on sensory nerve fibers, but also in the epidermis, hair follicle (HF), sebaceous gland, and several dermal cell populations. Although this supports the concept that the functional roles of TRPV1 in human skin biology reach well beyond nociception, the full range of the functional properties of TRPV1 signaling in cutaneous physiology and pathology remains to be explored and defined.

Because human HF prominently express TRPV1-ir,[14,15] and because the HF represents a prototypic, easily manipulated and abundantly available neuroectodermal-mesodermal interaction system that allows to exemplarily dissect the effects of test agents on well-defined epithelial, neural crest-derived, and mesenchymal cell functions under physiologically relevant conditions,[16–20] we chose to explore TRPV1 expression and functions in this microcosmic tissue interaction system *in situ* and in HF organ culture.[21]

Specifically, we wished to characterize the expression of TRPV1 in human HFs *in situ* to assess the effects of TRPV1 stimulation on hair shaft elongation, pigmentation, HF keratinocyte proliferation, and apoptosis as well as on HF cycling and the expression patterns of selected major hair growth-regulatory genes in organ-cultured (ie, denervated) human scalp HFs *in vitro*. This was complemented with studies on the effect of capsaicin on cultured human outer root sheath (ORS) and HaCaT keratinocytes. With the help of these studies in a physiologically and clinically highly relevant human model system, we hoped to obtain new hot insight into the functional role of TRPV1 signaling in epithelial-mesenchymal interactions, as an essential basis for the design of novel therapeutic strategies in the management of clinically relevant epithelial growth disorders via the pharmacological targeting of TRPV1.

Materials and Methods

Isolation and Maintenance of HFs

The study was approved by the Institutional Research Ethics Committee and adhered to Declaration of Helsinki guidelines. Human anagen HFs were isolated from skin obtained from females undergoing face-lift surgery.[21] Isolated HFs were maintained in 24-multiwell plates in supplemented Williams E medium (Biochrom, Cambridge, UK) supplemented with 2 mmol/L L-glutamine (Invitrogen, Paisley, UK), 10 ng/ml hydrocortisone (Sigma-Aldrich, Taufkirchen, Germany), 10 μg/ml insulin (Sigma), and antibiotics. Length measurements were performed on individual HFs using a light microscope with an eyepiece measuring graticule.

ORS and HaCaT Keratinocyte Cultures

Anagen HFs were digested using trypsin to obtain ORS keratinocytes.[22] Similarly, human dermal fibroblasts (HDFs) were obtained from de-epidermized dermis using enzymatic digestion. ORS cultures were kept on feeder layer of mitomycin-treated HDFs[23] in a 1:3 mixture of Ham's F12 (Biochrom) and in serum-free medium (SFM, Invitrogen) supplemented with 0.1 nmol/L cholera toxin, 5 μg/ml insulin, 0.4 μg/ml hydrocortisone, 2.43 μg/ml adenine, 2 nmol/L triiodothyronine, 10 ng/ml epidermal growth factor, 1 mmol/L ascorbyl-2-phosphate, and antibiotics (all from Sigma). HaCaT keratinocytes were cultured in Dulbecco's modified Eagle's medium (Sigma) supplemented with 10% fetal calf serum (Sigma), 2 mmol/L L-glutamine, and antibiotics.

Histology

Cryostat sections (8 μm thick) of scalp skin and cultured HFs were fixed in acetone, air-dried, and processed for histochemistry. Hematoxylin and eosin (H&E, Sigma) staining was used for studying HF morphology whereas melanin pigment was visualized by the Masson-Fontana histochemistry.[24]

Immunohistochemistry and Immunocytochemistry

For the detection of TRPV1 in human skin, a peroxidase-anti-peroxidase technique (Linaris, Wertheim, Germany), using diaminobenzidine as a chromogen, was used.[25] After incubation with a polyclonal goat anti-TRPV1 antibody (1:40; Santa Cruz Biotechnology, Santa Cruz, CA), sections were stained with biotinylated multilink swine anti-goat/mouse/rabbit IgG (1:200; DAKO, Glostrup, Denmark) as secondary antibody and then with an avidin-biotin kit (Linaris). As negative controls, the appropriate TRPV1 antibody was either omitted from the procedure or was preincubated with a synthetic blocking peptide (Santa Cruz). In addition, similarly to as we described before,[14] the specificity of TRPV1 staining was also measured on tissues recognized to be TRPV1-positive (rat spinal cord) or TRPV1-negative (spinal cord and skin samples from TRPV1 knockout mice) (data not shown).

For the detection of TRPV1 on isolated HFs, two complementary techniques, the tyramide-substrate amplification (TSA)[26,27] and the alkaline-phosphatase (AP) activity-based[25,28] methods were used. For the TSA technique, sections were first incubated by the TRPV1 antibody (1:400), then with biotinylated multilink swine anti-goat/mouse/rabbit IgG (1:200), and finally with streptavidin-horseradish peroxidase (TSA kit; Perkin-Elmer, Boston, MA) followed by an application of tetramethyl-rhodamine isothiocyanate-

tyramide (1:50, TSA kit). Sections were counterstained by 4,6-diamidino-2-phenylindole (DAPI) (1 μg/ml; Boehringer Mannheim, Mannheim, Germany) for visualization of cell nuclei. For the AP-based method, after staining with the TRPV1-antibody (1:40) and the biotinylated multilink swine anti-goat/mouse/rabbit IgG (1:200), sections were labeled by a streptavidin-AP conjugate (1% reagent mixture; Vector Laboratories, Burlingame, CA). Immunoreactions were finally visualized using Fast Red (Sigma) and the sections were counterstained by hematoxylin (Sigma). The intensity of TRPV1-ir was measured at four previously defined reference areas of interest of the distal ORS layers at a 0 to 255 U/pixel intensity range using the Image Pro Plus 4.5.0 software (Media Cybernetics, Silver Spring, MD), and the average TRPV1-ir was calculated (n = 20 to 30 HFs in each group). For the detection of TRPV1 in ORS keratinocytes, acetone-fixed cells were incubated with the TRPV1-antibody (1:40) and then a fluorescein isothiocyanate (FITC)-conjugated secondary antibody (1:400, Vector) was used to visualize the immunosignal.

To evaluate apoptotic cells in co-localization with a proliferation marker Ki-67, a Ki-67/TUNEL (terminal dUTP nick-end labeling) double-staining method was used.[29,30] Cryostat sections were fixed in formalin, ethanol, and acetic acid and labeled with a digoxigenin-deoxyUTP (ApopTag Fluorescein In Situ Apoptosis detection kit; Intergen, Purchase, NY) in the presence of terminal deoxynucleotidyl transferase (TdT), followed by incubation with a mouse anti-Ki-67 antiserum (DAKO). TUNEL+ cells were visualized by an anti-digoxigenin FITC-conjugated antibody (ApopTag kit), whereas Ki-67 was detected by a rhodamine-labeled goat anti-mouse antibody (Jackson ImmunoResearch, West Grove, PA). Negative controls were performed by omitting TdT and the Ki-67 antibody.

For simultaneous immunodetection of TRPV1 and NKI/beteb, a sensitive marker of skin melanocytes,[31] acetone-fixed cryostat sections were incubated with a goat anti-TRPV1 antibody (1:40) and then with a rhodamine-labeled rabbit anti-goat IgG (1:200, Jackson ImmunoResearch). Samples were then stained with a mouse anti-NKI/beteb antibody (1:20; Cell Systems, St. Katharinen, Germany) and finally with a FITC-conjugated goat anti-mouse secondary antibody (1:200, Jackson ImmunoResearch).

Staining for transforming growth factor (TGF)-β_2 was performed with a rabbit anti-TGF-β_2 antibody (1:50, Santa Cruz)[32] followed by a FITC-labeled goat anti-rabbit antibody (1:200, Jackson ImmunoResearch). Filaggrin immunostaining was performed using a rabbit anti-filaggrin antibody (1:100; Covance, Richmond, CA) and a FITC-labeled goat anti-rabbit secondary antibody (1:200, Jackson ImmunoResearch). The mean fluorescence intensity of TGF-β_2 and filaggrin was measured at four previously defined reference areas of interest in the hair matrix of the hair bulb (for TGF-β_2) or in the isthmus region (for filaggrin) using the Image Pro Plus 4.5.0 software (Media Cybernetics), and the average values were calculated (n = 20 to 30 HFs in each group).

Quantitative Real-Time PCR (Q-PCR)

Q-PCR was performed on an ABI Prism 7000 sequence detection system (Applied Biosystems, Foster City, CA) by using the 5′ nuclease assay. Total RNA was isolated using either TRIzol (for cell cultures, Invitrogen) or the RNA easy kit (for HFs; Qiagen, Hilden, Germany). Three μg of total RNA were then reverse-transcribed into cDNA by using 15 U of AMV reverse transcriptase (RT) (Promega, Madison, WI) and 0.025 μg/μl random primers (Promega). PCR amplification was performed by using the TaqMan primers and probes (assay ID, Hs00218912_m1 for human TRPV1; assay ID, Rn00583117_m1 for rat TRPV1) using the TaqMan universal PCR master mix protocol (Applied Biosystems). As internal controls, transcripts of glyceraldehyde 3-phosphate dehydrogenase (GAPDH) were determined (assay ID, Hs99999905_m1 for human GAPDH; assay ID, Rn00576699_m1 for rat GAPDH).

Semiquantitative RT-PCR

The expression of mRNA for TGF-β_2 in cultured HFs (15 per group) was determined by semiquantitive RT-PCR.[33] The total RNA was extracted using the RNA easy kit (Qiagen) and then was reverse-transcribed with random primers and RT provided in the First Strand cDNA Synthesis kit for RT-PCR (Boehringer). Subsequent PCR amplification [94°C for 5 minutes; 30 cycles of 94°C for 30 seconds, 57°C (TGF-β_2) or 55°C (β-actin) for 60 seconds, 72°C for 60 seconds; 72°C for 10 minutes] was performed on the UNO-Thermoblock (Biometra, Göttingen, Germany) with the following primers (all from Sigma): TGF-β_2, 5′-ATC CCG CCC ACT TTC TAC AGA C-3′ and 5′-CAT CCA AAG CAC GCT TCT TCC-3′ (GenBank accession number, Y00083); β-actin, 5′-CGA CAA CGG CTC CGG CAT GTG C-3′ and 5′-CGT CAC CGG AGT CCA TCA CGA TGC-3′ (GenBank accession number, NM001101). The PCR products were visualized on a 2% agarose gel with ethidium bromide and the photographed bands were quantified by an Image Pro Plus 4.5.0 software (Media Cybernetics).

Western Blotting

To determine the expression of TRPV1 in cultured cells, the Western blot technique was applied.[34] Cells were harvested in homogenization buffer [20 mmol/L Tris-Cl, pH 7.4, 5 mmol/L EGTA, 1 mmol/L 4-(2-aminoethyl)benzenesulfonyl fluoride, 20 μmol/L leupeptin, all from Sigma] and the protein content of samples was measured by a modified BCA protein assay (Pierce, Rockford, IL). The samples were subjected to sodium dodecyl sulfate-polyacrylamide gel electrophoresis (8% gels were loaded with 20 to 30 μg protein per lane), transferred to nitrocellulose membranes (Bio-Rad, Vienna, Austria), and then probed with the above anti-TRPV1 antibody (1:100). A horseradish peroxidase-conjugated rabbit anti-goat IgG antibody (1:1000, Bio-Rad) was used as a secondary antibody, and the immunoreactive bands were visualized by enhanced chemiluminescence (Amersham, Little

Chalfont, UK) on light-sensitive films (AGFA, Brussels, Belgium).

Calcium Measurement

Changes in intracellular calcium concentration ($[Ca^{2+}]_i$) on TRPV1 activation were detected as described before.[34] Cells were cultured on coverslips and a calcium-sensitive probe fura-2 AM (5 μmol/L; Molecular Probes, Eugene, OR) was introduced into the intracellular space (1 hour at 37°C). The coverslips, containing the fura-2-loaded cells, were then placed on the stage of an inverted fluorescence microscope (Diaphot; Nikon, Tokyo, Japan). Excitation was alternated between 340 and 380 nm using a dual-wavelength monochromator (Deltascan; Photon Technology Int., New Brunswick, NJ). The emission was monitored at 510 nm with a photomultiplier at an acquisition rate of 10 Hz per ratio, and the fluorescence ratio (F_{340}:F_{380}) values were determined. Cells were continuously washed by Tyrode's solution (in mmol/L, 137 NaCl, 5.4 KCl, 0.5 $MgCl_2$, 1.8 $CaCl_2$, 11.8 Hepes-NaOH, 1 g/L glucose, pH 7.4, all from Sigma) using a slow background perfusion system, whereas the agents investigated were applied through a rapid perfusion system positioned in close proximity to the cell measured.

Proliferation Assay

Proliferation was measured by a colorimetric bromodeoxyuridine (BrdU) assay kit (Boehringer).[8] Cells were plated in 96-well multititer plates (for the HaCaT cells, 5000 cells/well; for the ORS keratinocytes, 10,000 cells/well layered on 5000 cells/well mitomycin-treated HDFs) in quadruplicates and 4 hours later were treated with various compounds for 72 hours. Cells were then incubated with 10 μmol/L BrdU for 4 hours, and the cellular incorporation of BrdU was determined colorimetrically according to the manufacturer's protocol. During the proliferation experiments, the following media were used (see above for detailed compositions): low-Ca SFM (low Ca^{2+} concentration, 0.4 mmol/L); high-Ca SFM (Ca^{2+} concentration was set to 2 mmol/L using $CaCl_2$).

Flow Cytometry

The effect of TRPV1 activation on cellular proliferation, differentiation, apoptosis, and the expressions of various regulators of HF growth and development were assessed by flow cytometry. Control and capsaicin-treated ORS keratinocytes were immunostained with the following primary antibodies: Ki67 (mouse, 1:100; DAKO), proliferating cell nuclear antigen (mouse, 1:50; Novocastra, Newcastle on Tyne, UK), filaggrin (rabbit, 1:100; Covance), cytokeratin-14 (CK-14, mouse, 1:20; Novocastra), CK-17 (mouse, 1:20; Novocastra), involucrin (mouse, 1:50; Sigma), insulin-like growth factor-I (rabbit, 1:100; Santa Cruz), hepatic growth factor (1:20, rabbit; Santa Cruz), c-kit/stem cell factor (SCF, mouse, 1:50; Santa Cruz), TGF-β_2 (mouse, 1:50; Santa Cruz), interferon-γ (IFN-γ) (goat, 1:20; Santa Cruz), interleukin (IL)-1β (goat, 1:50; Santa Cruz), tumor necrosis factor-α (rabbit, 1:20; BD Pharmingen, San Diego, CA), and fibroblast growth factor-5 (goat, 1:20; Santa Cruz). FITC-conjugated appropriate secondary antibodies (1:100, Vector) were then applied and, after fixation, cells were analyzed by a flow cytometer (EPICS XL-4; Coulter, Miami, FL). After isotype control calibration, the immunopositive signals were determined (at least 50,000 cells per antigen) and expressed as the percentage of total cell number. For the detection of apoptosis, cells were incubated with a FITC-conjugated annexin-V antibody (Sigma) and analyzed similarly.

Statistical Analysis

When applicable, data were analyzed using a two-tailed unpaired *t*-test and $P < 0.05$ values were regarded as significant differences.

Results and Discussion

Human Scalp HFs Express TRPV1 Mainly in the ORS and in the Hair Matrix

Recent reports suggest the expression of TRPV1 on human epidermal keratinocytes.[11–15] However, given the substantial differences between epidermal and HF keratinocytes[17,18,35] and the multiple changes in their gene expression patterns that keratinocytes are known to undergo after being placed in culture, we began by characterizing TRPV1 expression in the human HF *in vivo*, using full-thickness normal scalp skin obtained during routine plastic surgery.

As revealed by immunohistochemistry, TRPV1-ir in human scalp HFs in anagen VI stage of the hair cycle[17,18] was restricted to the follicle epithelium, where it was most prominent in the ORS and less pronounced in the hair matrix (Figure 1A). This specific (as assessed by numerous positive and negative controls, see Materials and Methods section; Figure 1A, inset)[14] and marked TRPV1-ir was comparably high to that previously seen on

Figure 1. TRPV1-ir on human skin and cultured human HFs. **A:** TRPV1-ir (with diaminobenzidine as a chromogen) on inner root sheath, ORS, and matrix (MK) keratinocytes (DP). **Inset**, negative control of TRPV1 staining. **B:** Negative control of TRPV1 staining. TSA (**C**, **D**) and AP (**E**, **F**) TRPV1-ir on cultured anagen (**C**, **E**) and catagen (IFN-γ-induced; **D**, **F**) human HFs. **G/1**, **G/2:** Double-fluorescence immunolabeling of TRPV1+ (red, **G/1**) and NKI/beteb+ (green, **G/2**) cells in the human cultured HFs. Note the lack of co-localization of TRPV1-ir on HF melanocytes. Nuclei were counterstained by DAPI (blue fluorescence in **B–D**; also in **G**, but not shown for clarity). **H:** Q-PCR analysis of TRPV1 expression in the human HF. Data of TRPV1 expression were normalized to the expression of GAPDH of the same sample and are expressed as relative mRNA amounts as a function of startup cDNA (relative amount of 1 was defined as the detection threshold). NTC, nontemplate (negative) control; TRPV1/C6 and TRPV1/CHO, C6 and CHO cells stably expressing the recombinant rat TRPV1 (positive controls). Values are mean ± SEM of three independent determinations. Original magnifications: ×100 (**A**), ×200 (**B–G**).

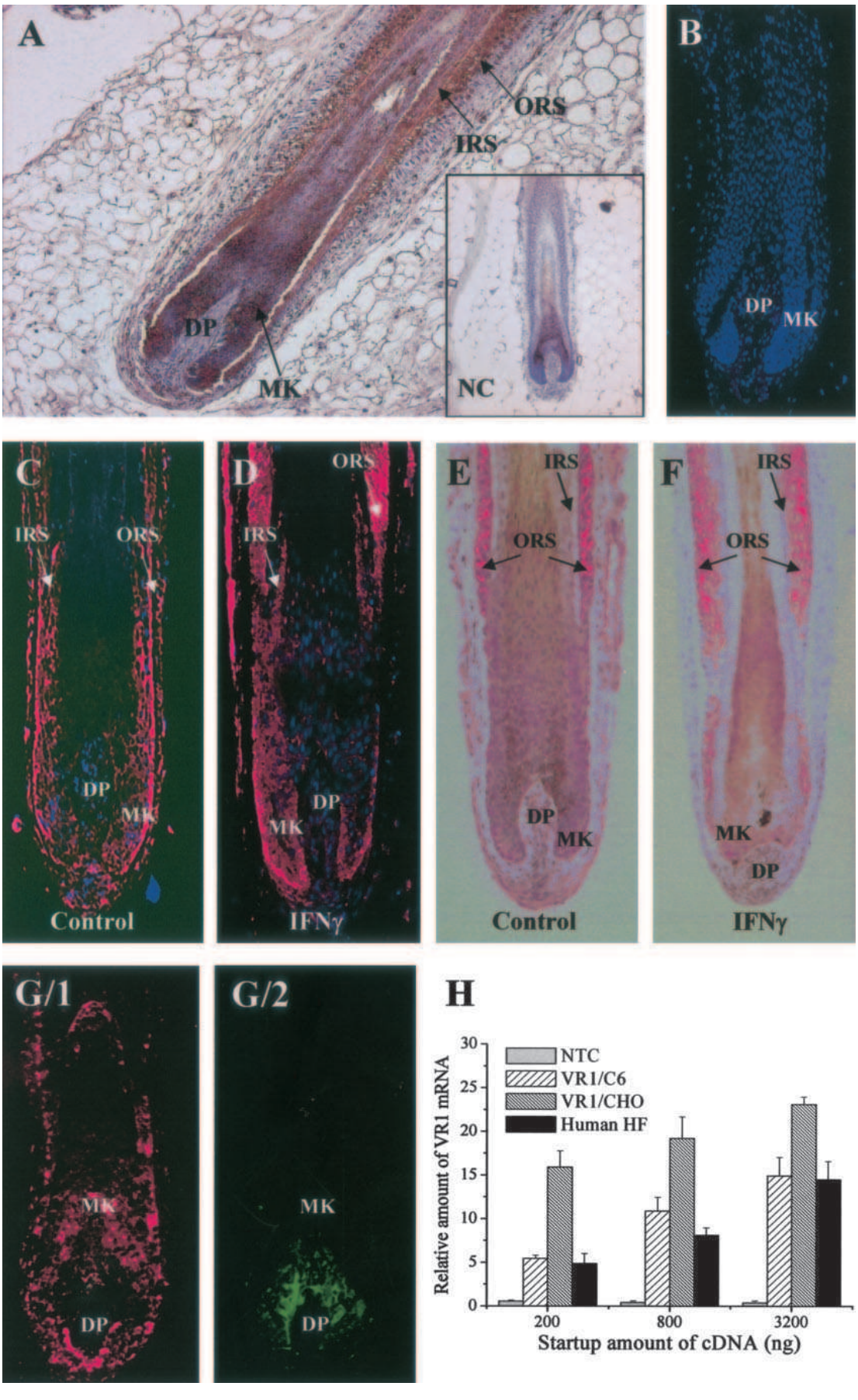
A
ORS
IRS
DP
MK
NC
B
DP
MK
C
IRS
ORS
DP
MK
Control
D
ORS
IRS
DP
MK
IFNγ
E
IRS
ORS
DP
MK
Control
F
IRS
ORS
MK
DP
IFNγ
G/1
MK
DP
G/2
MK
DP
H
NTC
VR1/C6
VR1/CHO
Human HF
Relative amount of VR1 mRNA
0
5
10
15
20
25
30
200
800
3200
Startup amount of cDNA (ng)

epidermal keratinocytes of human skin.[14] TRPV1-ir, however, was absent from the inductive, specialized HF mesenchyme, the fibroblasts of the dermal papilla (DP) (Figure 1A). An identical expression pattern of TRPV1-ir, as assessed by complementary TSA and AP techniques, was found on anagen VI HFs cultivated in organ cultures (Figure 1, C and E); ie, most intense signals were localized to the ORS and matrix keratinocytes and (yet much less intensively) to inner root sheath keratinocytes.

It has long been appreciated in the field that organ-cultured human HFs usually do not achieve more than early catagen development, before the follicle begins to degenerate.[21,36] However, using IFN-γ as the strongest *in vitro* catagen inducer for human scalp HFs described so far, we have recently even been able induce mid-catagen stages.[27,37] Using these results, it was intriguing to observe that TRPV1 expression significantly increased on cultured HFs (especially on the ORS keratinocytes) that were experimentally induced to undergo the early to mid stages of HF involution (catagen) phase by 1000 IU/ml IFN-γ (Figure 1, D and F) (catagen I/II was evident by light microscopy evaluation of morphological signs, up-regulation of TUNEL+ and down-regulation of Ki67+ keratinocytes of the hair matrix, along with termination of melanogenesis in the HF pigmentary unit, see below and in Stenn and Paus[18] and Müller-Röver et al[38]). Image analysis revealed that the mean staining intensity of TRPV1 was by 32.3 ± 6.8% (mean ± SEM, $P < 0.05$, $n =$ 20 to 30 HFs in each group) higher in the IFN-γ-treated (hence catagen I/II) HFs than in the control (anagen) ones (data not shown) suggesting that the expression of TRPV1 in these cells is in fact regulated by the cycling machinery of the HF.

To clarify whether some of the TRPV1-ir in the hair matrix reflected TRPV1 expression by the specialized melanocytes of the HF pigmentary unit,[39] double-immunolabeling was performed with antibodies against TRPV1 and NKI/beteb, a very sensitive melanocyte marker (Figure 1G).[31] Using this method, we found no co-localization of the two immunosignals suggesting that HF melanocytes, similar to our previous demonstration on human epidermal melanocytes *in situ*,[14] also failed to express TRPV1. Therefore, both the mesoderm-derived DP fibroblast, and the neural crest-derived HF melanocytes did not express TRPV1 immunoreactivity.

To control whether intraepithelial TRPV1-ir corresponded to the presence of TRPV1 transcripts, RNA was rapidly extracted from freshly microdissected proximal human HF in the anagen VI stage of the hair cycle[17–19] and subjected to Q-PCR. As shown in Figure 1H, mRNA transcripts for TRPV1 were unambiguously identified in normal human scalp HFs. Remarkably, the HFs expressed TRPV1 at very high levels, which were comparable to those of the two positive controls; ie, Chinese hamster ovary (CHO) and C6 cells recombinantly overexpressing the rat TRPV1.[34] Therefore, *in vivo* the human HF epithelium indeed transcribes the TRPV1 gene at high levels, similarly to other nonneuronal epithelial and mesenchymal cell types.[7–14]

TRPV1 Stimulation Inhibits Hair Shaft Elongation and Hair Matrix Keratinocyte Proliferation

To explore the functional consequences of TRPV1 stimulation *in vitro* under as physiological conditions as pos-

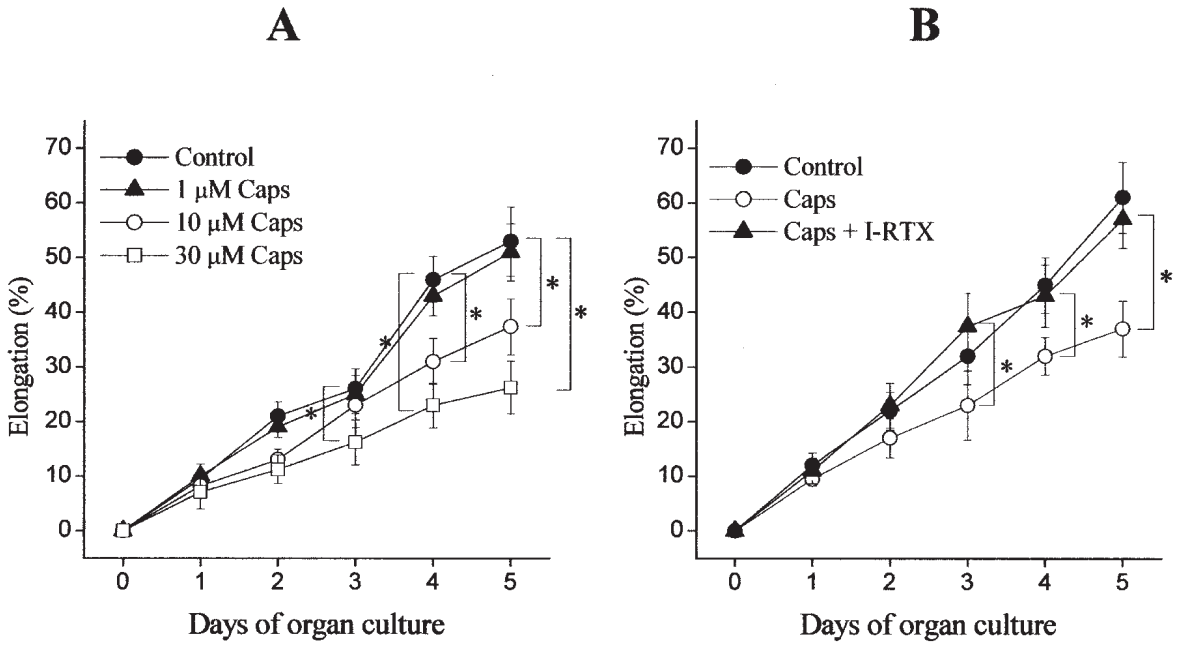

Figure 2. The activation of TRPV1 inhibits HF elongation. **A:** Cultured HFs (18 per group) were treated with either the vehicle (DMSO, control) or with various concentrations of capsaicin (Caps) for the time indicated. **B:** Cultures were treated with the vehicle (control), 10 μmol/L capsaicin (Caps), or 10 μmol/L capsaicin and 100 nmol/L iodo-RTX (Caps + I-RTX). Length measurements were made on individual HFs using a light microscope with an eyepiece measuring graticule. All data were compared with those of the control group, and analyzed by two-tailed unpaired *t*-test. Results are expressed as mean ± SD. *, Significant ($P < 0.05$) differences. Two to three additional experiments yielded similar results.

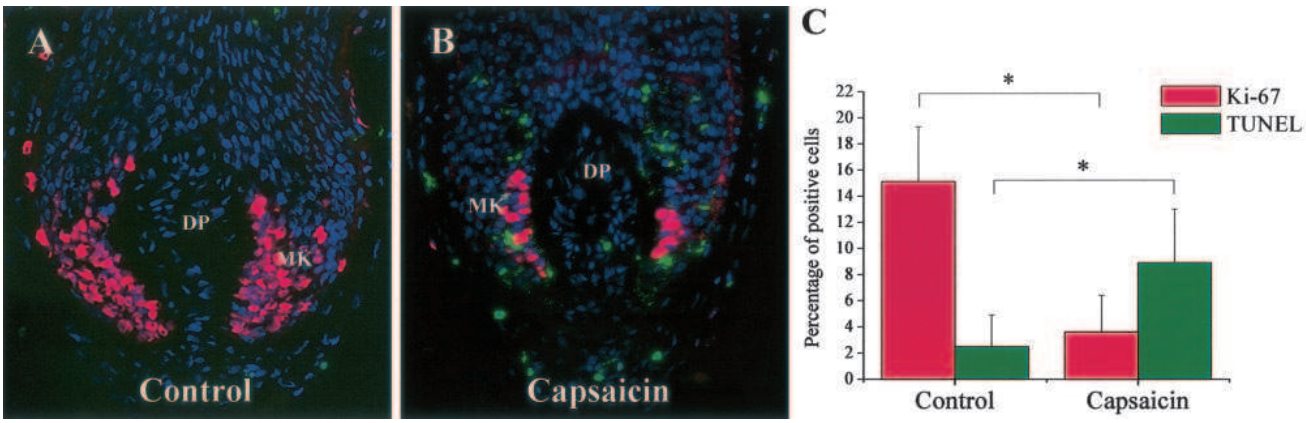

Figure 3. The activation of TRPV1 inhibits proliferation and induces apoptosis in cultured HFs. Co-immunolabeling of proliferating (Ki-67+, red fluorescence) and apoptotic (TUNEL+, green fluorescence) cells on control (**A**) and capsaicin-treated (10 μmol/L for 5 days, **B**) cultured HFs. Nuclei were counterstained by DAPI (blue fluorescence). MK, matrix keratinocytes. **C:** Statistical analysis of number of Ki-67 and TUNEL+ cells as compared to the number of DAPI+ cells on several HFs per group. Data are expressed as mean ± SD. *, Significant ($P < 0.05$) differences. Original magnifications, ×400.

sible, microdissected, organ-cultured normal anagen VI scalp HFs were exposed to the prototypic, most extensively studied, and clinically used TRPV1 agonist, capsaicin (0.1 to 30 μmol/L).[1,5,6,15] Capsaicin significantly inhibited hair shaft elongation in a time- and dose-dependent manner (Figure 2A), as an indication of hair growth-inhibitory properties of TRPV1 signaling. Hair growth inhibition by capsaicin was further confirmed by the finding that treatment of cultured HFs by capsaicin for 5 days significantly decreased the number of Ki67+ keratinocytes in the anagen hair bulb (Figure 3).

The inhibitory effect of capsaicin on hair shaft elongation was completely abolished by the specific TRPV1 antagonist iodo-resiniferatoxin (I-RTX, 100 nmol/L),[40] demonstrating a TRPV1 specificity of the observed hair growth-inhibitory effect of capsaicin (Figure 2B). The antagonist alone only exerted a minor, statistically insignificant modulation of HF elongation (data not shown).

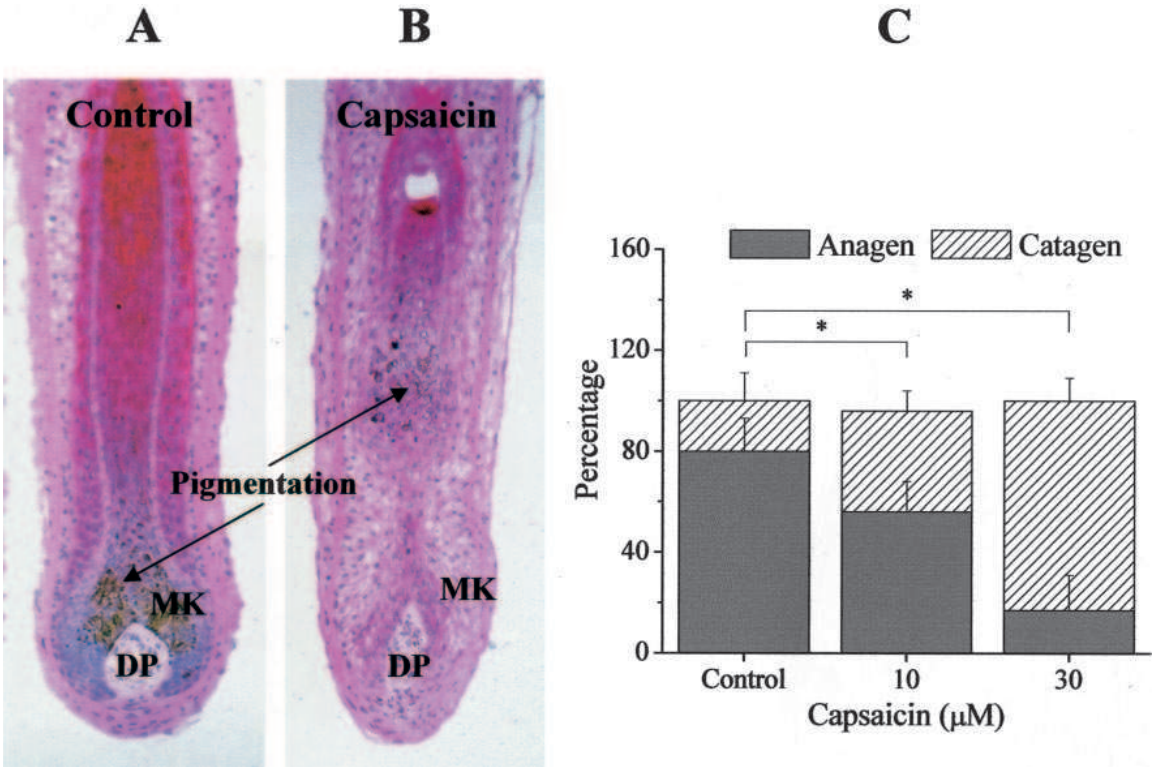

Figure 4. The activation of TRPV1 induces catagen transformation in cultured HFs. Cultured HFs were treated with either the vehicle (**A**) or with 10 μmol/L capsaicin for 5 days (**B**), then processed for H&E staining, and the percentage of HFs in anagen or catagen state, according to previously well-defined criteria (narrower hair bulb and depigmentation in catagen HFs), was determined (**C**). MK, matrix keratinocytes. Results are expressed as mean ± SEM. *, Significant ($P < 0.05$) differences. Two to three additional experiments yielded similar results. Original magnifications, ×100.

These data unambiguously argue for the functional expression of TRPV1 in human organ-cultured scalp HFs.

TRPV1 Stimulation Up-Regulates HF Keratinocyte Apoptosis and Induces Premature Catagen Onset in Vitro

These findings were further supported by the observation that the number of TUNEL+ keratinocytes in the hair bulb significantly increased after capsaicin stimulation, suggesting the induction of apoptosis by TRPV1 stimulation (Figure 3). This inhibition of proliferation and stimulation of apoptosis by TRPV1 signaling in normal epithelial cells of the human HF *in situ* are perfectly in line with previous reports on the proliferation-inhibitory and apoptosis-stimulatory effects of TRPV1 activation for example in glial cells,[8] and in airway[9,41] and breast epithelial cells[42] *in vitro*.

Using quantitative histomorphometry of H&E-staining section of HFs and analyzing such staining based on well-defined morphological criteria,[18,38] we next assessed the effect of the TRPV1 agonist on HF cycling *in vitro*, namely on the anagen-catagen transition, which is characterized by massive up-regulation of keratinocyte apoptosis and down-regulation of keratinocyte proliferation in the anagen hair bulb.[18,38,43] As shown in Figure 4, capsaicin stimulated the onset of catagen transformation of the HF; whereas at day 0, most of the HFs (~80%) were in the anagen VI phase, after 5 days of treatment with 10 to 30 μmol/L capsaicin, ~50 to 80% of the HFs had entered catagen (Figure 4C). It should be noted, however, that capsaicin was primarily capable of inducing only early catagen stages, and that we very rarely found that HF regression *in vitro* had progressed into late stages of the catagen transformation after application of the TRPV1 agonist.

Characteristically, the onset of catagen is accompanied by an interruption of all pigmentary activity of HF melanocytes and by a gradual depigmentation of the lower HF,[18,39] which was also evident in capsaicin-treated HFs (Figure 4, A and B). However, we were interested in learning whether TRPV1 activation affected pigmentation on HFs, which were not yet transformed to catagen. Since the first visible signs of catagen induction were seen at days 3 to 4 of capsaicin treatment, in the next experiments, the application of the TRPV1 agonist was terminated at day 3. Using Masson-Fontana histochemistry, we found that the activation of TRPV1 by capsaicin did not modify the pigmentation (data not shown), which was in accordance with our finding that the melanocytes of the HF pigmentary unit do not express TRPV1 (Figure 1F).

Terminal Differentiation of Human HF Keratinocytes in Situ *Appears To Be Independent of TRPV1 Stimulation*

Next, we investigated whether capsaicin also affected differentiation in the HF epithelium. Therefore, the expres-

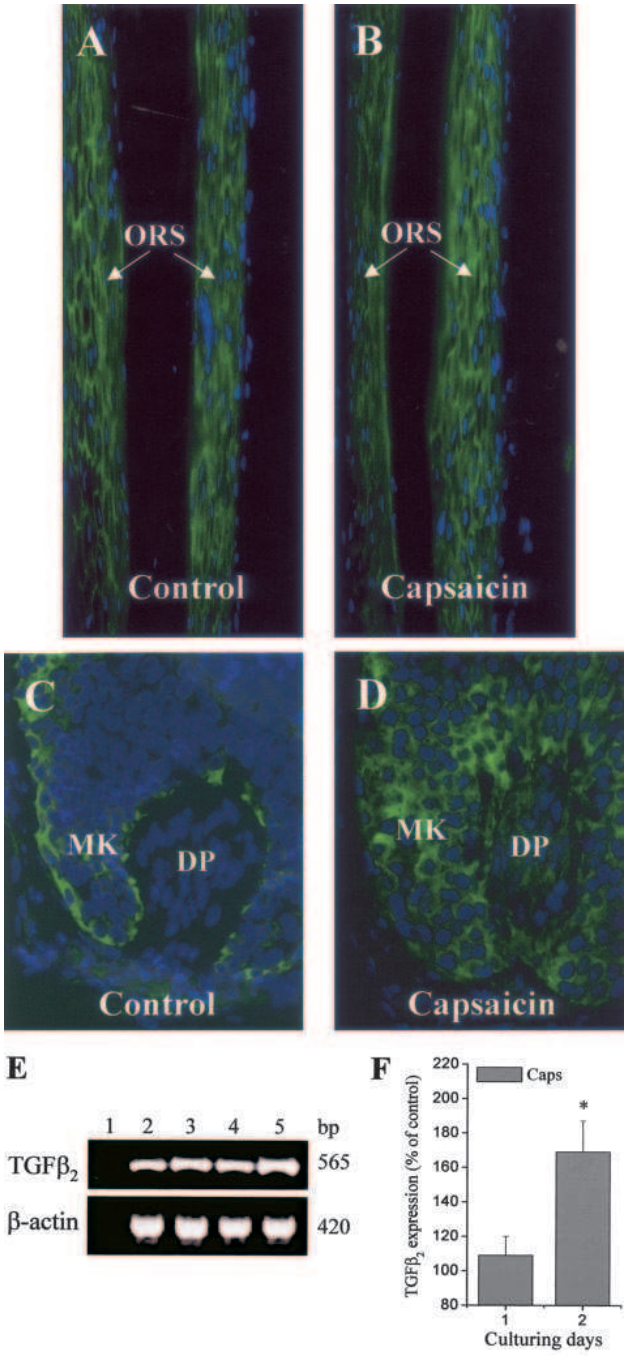

Figure 5. The activation of TRPV1 does not affect terminal differentiation but up-regulates TGF-β_2 expression in cultured HFs. Fluorescence immunolabeling of differentiation marker filaggrin on control (**A**) and capsaicin-treated (10 μmol/L for 3 days, **B**) HFs (the isthmus region exhibiting the most intense staining is shown). Note the lack of effect of capsaicin on filaggrin expression (see text for statistics). Fluorescence immunolabeling of TGF-β_2 on control (**C**) and capsaicin-treated (10 μmol/L for 2 days, **D**) HFs. MK, matrix keratinocytes. Note the up-regulation of TGF-β_2 by capsaicin (see text for statistics). Nuclei were counterstained by DAPI (blue fluorescence). **E:** RT-PCR analysis of TGF-β_2 (and β-actin, used as an internal control) mRNA expression in cultured HFs. **Lane 1**, reaction without template (negative control); **lane 2**, control at day 1; **lane 3**, 10 μmol/L capsaicin treated at day 1; **lane 4**, control at day 2; **lane 5**, 10 μmol/L capsaicin treated at day 2. bp, predicted product sizes. **F:** mRNA of transcripts were quantified by densitometry and the values of TGF-β_2 were normalized to those of β-actin. Data of the capsaicin-treated groups, obtained in three independent experiments, are expressed as mean ± SEM values as a percentage of the daily matched control samples regarded as 100%. *, Significant ($P < 0.05$) differences. Original magnifications: ×100 (**A**, **B**); ×400 (**C**, **D**).

Table 1. Effect of Capsaicin Treatment on the Expressions of Different Markers on ORS Keratinocytes

Marker	Capsaicin (% of control)
Proliferation	
Ki-67	73.8 ± 7* (↓)
PCNA (proliferating cell nuclear antigen)	71.6 ± 9* (↓)
Apoptosis	
Annexin-V	143 ± 8* (↑)
Differentiation	
CK-14 (cytokeratin-14)	94.2 ± 11
CK-17 (cytokeratin-17)	98.3 ± 6
Filaggrin	102.3 ± 8
Involucrin	95.1 ± 13
Hair growth-promoting factors	
HGF (hepatic growth factor)	63.5 ± 81* (↓)
IGF-I (insulin-like growth factor-I)	53 ± 9* (↓)
SCF (c-kit/stem cell factor)	74.9 ± 6* (↓)
Hair growth-inhibitory factors	
FGF-5 (fibroblast growth factor-5)	95 ± 5
IFN-γ (interferon-γ)	91.3 ± 9
IL-1β (interleukin-1β)	143.7 ± 5* (↑)
TGF-β_2 (transforming growth factor-β_2)	128.6 ± 6* (↑)
TNF-α (tumor necrosis factor-α)	98.6 ± 4

Flow cytometry analyses were performed, as described under Materials and Methods, on control and capsaicin-treated (10 μmol/L for 2 days in high-Ca^{2+} SFM) ORS keratinocytes, and values of the treated samples were normalized as percentage of the control regarded as 100%. Data are expressed as mean ± SEM of three determinations.

*Significant ($P < 0.05$) alterations.

sion of the keratinocyte differentiation marker filaggrin[44] was studied. As before, cultured HFs were treated with capsaicin only for 3 days, and then immunohistochemistry was performed to detect filaggrin expression. As seen Figure 5, A and B, vanilloid application modified filaggrin expression only insignificantly: the mean fluorescence intensity values in the isthmus region were 76.8 ± 6.3 for the control and 80.3 ± 4.8 for the capsaicin-treated HFs (mean ± SEM, $P > 0.5$, $n = 20$ to 30 HFs in each group, data not shown). These data suggest that, in contrast to its effect on HF elongation (Figure 2), proliferation (Figure 3), cycling (Figure 4), and apoptosis (Figure 3), capsaicin, similarly to its *in vitro* action on cultured ORS keratinocytes (see below and Table 1), does not affect *in situ* differentiation of HF keratinocyte in a major way. Our findings, therefore, indicate that the hair growth-inhibitory effects of TRPV1 stimulation are chiefly based on a stimulation of hair matrix keratinocyte apoptosis and on inhibiting proliferation (Figure 3) of these cells. These results were in contrast with our previous findings on glial cells[8] where the growth-inhibitory effect of capsaicin was accompanied by the modification of differentiation, suggesting that the characteristics of TRPV1 signaling show strong cell-type dependence (see also Concluding Remarks section).

The Hair Growth-Inhibitory Effects of TRPV1 Signaling May in Part Be Mediated via TGF-β_2

The capsaicin-induced changes on cultured HFs were very similar to those described for TGF-β_2, a well-known inhibitor of hair shaft elongation and inducer of both apoptosis and catagen in human HFs.[21,29,45] Therefore, we investigated a possible involvement of TGF-β_2 in the hair growth-inhibitory effect of TRPV1 stimulation. Capsaicin treatment for 2 to 3 days indeed markedly up-regulated the HF expression of TGF-β_2, both at the protein (as revealed by immunohistochemistry, Figure 5, C and D) (at day 2, the mean fluorescence intensity values in the hair bulb region of the capsaicin-treated HFs were by 132.8 ± 13% higher than the control ones; mean ± SEM, $P < 0.001$, $n = 20$ to 30 HFs in each group, data not shown) and the mRNA level (as assessed by RT-PCR; Figure 5, E and F). In addition, co-culture of anagen HFs with capsaicin and TGF-β_2-neutralizing antibodies partially abrogated the capsaicin-induced inhibition of hair shaft elongation (35.2 ± 6% suppression of the effect of capsaicin to inhibit hair shaft elongation; mean ± SEM, $P < 0.05$, $n = 6$, data not shown). These findings, ie, TRPV1 activation up-regulated the level of TGF-β_2 in HFs that were not yet induced to transform to catagen and TGF-β_2-neutralizing antibodies partially abrogated the TRPV1-mediated effects indicate that at least some of the hair growth-inhibitory effects of TRPV1 signaling in epithelial biology may be indirectly mediated by stimulation of the expression and secretion of TGF-β_2. The activation of TRPV1 very often results in the release of various cytokines and growth modulatory agents (eg, interleukins, prostaglandins) on numerous cell types such as mast cells,[7] bronchial epithelial cells,[9] and keratinocytes.[13] However, according to our knowledge, this is the first demonstration of the link between the TRPV1 and TGF-β_2 signaling mechanisms. We should emphasize, however, the TRPV1-mediated alterations in organ-cultured human anagen VI HFs may indeed recruit other signaling pathways in addition to TGF-β2 and signaling via its cognate receptor (see also Concluding Remarks section).

Human Cultured ORS Keratinocytes, but Not DP Fibroblasts, Express TRPV1

To double-check and further analyze the data obtained with intact, microdissected anagen HFs, primary cultures of human ORS keratinocytes were used, whereas HaCaT keratinocytes were used as positive controls, since the latter have previously been reported to express functional TRPV1.[13] By immunocytochemistry (Figure 6A) and Western blotting (Figure 6B), we were able to present the first evidence that the TRPV1 protein is indeed expressed in normal ORS keratinocytes, and this at a level comparable to that of HaCaT keratinocytes (Figure 6B). Using Q-PCR, we could also detect TRPV1 mRNA transcripts in ORS keratinocytes and, as expected,[11–13] in HaCaT cells and normal human epidermal keratinocytes (Figure 6C). In perfect agreement with our findings obtained with cultured HFs (Figure 1) and on human skin *in situ*,[14] TRPV1 was undetectable in cultured HDFs, neither at the protein (Figure 6B) nor at the mRNA (Figure 6C) level.

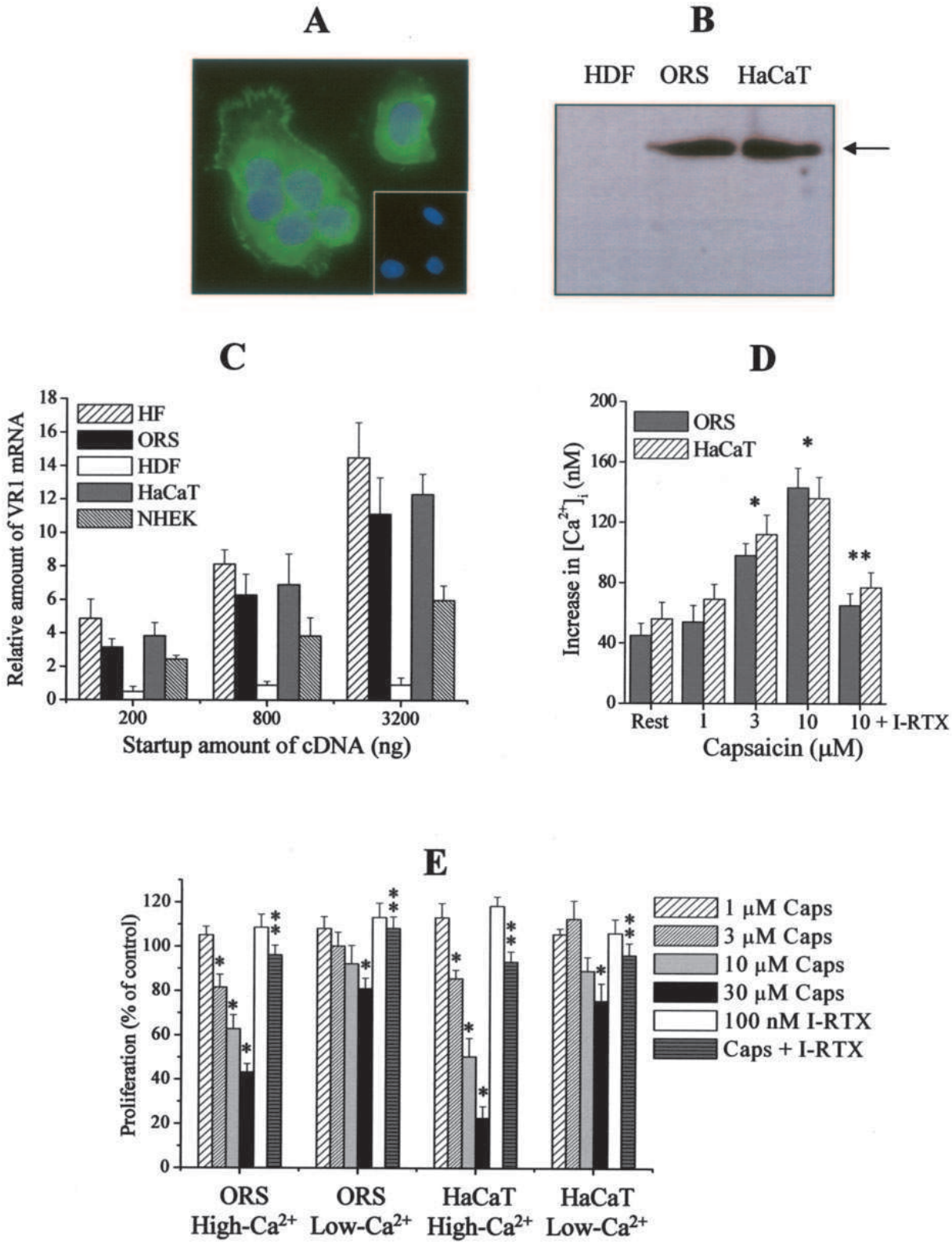
A
B
HDF
ORS
HaCaT
C
D
HF
ORS
HDF
HaCaT
NHEK
Relative amount of VR1 mRNA
Startup amount of cDNA (ng)
200
800
3200
Increase in [Ca2+]i (nM)
Rest
1
3
10
10 + I-RTX
Capsaicin (μM)
E
Proliferation (% of control)
1 μM Caps
3 μM Caps
10 μM Caps
30 μM Caps
100 nM I-RTX
Caps + I-RTX
ORS High-Ca2+
ORS Low-Ca2+
HaCaT High-Ca2+
HaCaT Low-Ca2+

TRPV1 Stimulation Inhibits the Proliferation, Elevates $[Ca^{2+}]_i$, and Induces Apoptosis in Cultured ORS and HaCaT Keratinocytes

On sensory neurons and several nonneuronal cell types (including HaCaT cells), TRPV1 functions as a Ca^{2+}-permeable cation channel.[1,2,5,7–9,12,13] Hence, we also tested whether the application of capsaicin affects the intracellular Ca^{2+} homeostasis in ORS keratinocytes. As revealed by optical Ca^{2+} imaging, capsaicin dose-dependently increased $[Ca^{2+}]_i$ in ORS keratinocytes (similarly to HaCaT cells) in Tyrode's solution containing 1.8 mmol/L Ca^{2+} (Figure 6D). In contrast, the TRPV1 antagonist I-RTX prevented the $[Ca^{2+}]_i$-increasing action of capsaicin, demonstrating that this is a TRPV1-mediated event. It is important to note that none of the studied concentrations of capsaicin was able to significantly modify $[Ca^{2+}]_i$ of ORS or HaCaT keratinocytes *in vitro* when calcium was removed from the Tyrode's solution (data not shown). This supports the concept that the capsaicin-induced elevation in $[Ca^{2+}]_i$ originated chiefly from the extracellular space via TRPV1.

We also measured the effect of TRPV1 activation on ORS and HaCaT keratinocyte proliferation using BrdU enzyme-linked immunosorbent assays. In addition, because TRPV1-induced cellular events on sensory neurons (eg, excitation, desensitization, and neurotoxicity) and on nonneuronal cell types (eg, cytokine release) are chiefly initiated by the influx of Ca^{2+} via TRPV1,[1,2,5,7–9,13] we also investigated the extracellular Ca^{2+} dependence of TRPV1 activation (this was impossible to measure in the case of organ-cultured HFs that did not grow and eventually died in low-Ca^{2+} solutions, data not shown). As seen in (Figure 6E), in high-Ca^{2+} (2 mmol/L) SFM, capsaicin dose-dependently inhibited proliferation of ORS and HaCaT keratinocytes which effect was prevented by I-RTX. However, as a marked contrast, the TRPV1 agonist exerted a much less growth-inhibitory effect in low-Ca^{2+} (0.4 mmol/L) SFM. These data strongly argued for that the TRPV1-evoked cellular responses in cultured keratinocytes (and presumably in cultured HFs) are mediated by the concomitant elevation of $[Ca^{2+}]_i$.

These assays were complemented with a wide-spectrum flow cytometry analysis of alterations in the levels of selected proliferation and apoptosis markers on capsaicin treatment of cultured ORS keratinocytes (Table 1). Consistent with the above findings (Figures 3 and 6), capsaicin (10 μmol/L for 2 days in high-Ca^{2+} SFM) significantly suppressed the expression of Ki67 and proliferating cell nuclear antigen also suggesting inhibition of proliferation. Moreover, the TRPV1 agonist elevated the number of annexin-V+ cells reflecting stimulation of apoptosis (similarly to that seen in the HF, Figure 3). However, also similarly to data obtained with the cultured HFs (Figure 5, A and B), capsaicin did not modify the expression of numerous differentiation markers (Table 1).[45–47] These data indicate that the activation of TRPV1 signaling both on organ-cultured HFs and on primary ORS keratinocytes results in the inhibition of proliferation and induction of apoptosis, with an insignificant effect on the process of differentiation.

TRPV1 Stimulation in ORS Keratinocytes Down-Regulates the Expression of Hair Growth-Stimulatory Factors but Up-Regulates the Expression of Hair Growth Inhibitors

Finally, we investigated whether and how TRPV1 stimulation by capsaicin application altered the protein expressions of various cytokines and growth factors that are well appreciated to positively or negatively regulate HF growth (Table 1). Flow cytometry analysis revealed that vanilloid treatment significantly down-regulated the ORS keratinocyte expressions of key promoters of HF growth such as hepatocyte growth factor,[18,30,48] insulin-like growth factor-I,[18,49] and stem cell factor.[18,50] In contrast, capsaicin up-regulated the levels of IL-1β and TGF-β_2, well-known potent hair growth inhibitors[18,21,29,45,51] whereas the expressions of other hair growth inhibitory agents such as fibroblast growth factor-5, IFN-γ, and tumor necrosis factor-α[18,27,52,53] were not affected.

Concluding Remarks

Taken together, the data reported here introduce vanilloid receptors as significant new players in human hair growth control, with TRPV1-mediated signaling exerting profound effects on HF keratinocyte proliferation and apoptosis, and directly and/or indirectly manipulating a number of well-recognized hair growth modulators. This underscores that the physiological functions of TRPV1 and its elusive endogenous ligands, in human skin and likely other mammalian tissues as well, far extend beyond sensory neuron-coupled nociception. Thus TRPV1 joins the group of other receptors (eg, nicotinic and muscarinic

Figure 6. Identification of TRPV1 in cultured ORS and HaCaT keratinocytes, the activation of which elevates $[Ca^{2+}]_i$ and inhibits proliferation. **A:** TRPV1-ir (green fluorescence) in cultured ORS keratinocytes. Nuclei were counterstained by DAPI (blue fluorescence). **Inset**, negative control of TRPV1 staining. **B:** Western blot analysis of TRPV1 expression on cell lysates of ORS and HaCaT keratinocytes, and of HDFs. **Arrow** indicates predicted molecule size (95 kd). **C:** Q-PCR analysis of TRPV1 expression in cultured cells and in the human HFs (for the human HFs, data are identical to those shown in Figure 1H). Data of TRPV1 expression were normalized to the expression of GAPDH of the same sample and are expressed as relative mRNA amounts as a function of startup cDNA (relative amount of 1 was defined as the detection threshold). NHEK, normal human epidermal keratinocytes. Values are mean ± SEM of three independent determinations. **D:** Fura-2 AM-loaded cells were challenged with various concentrations of capsaicin or with 10 μmol/L capsaicin and 100 nmol/L iodo-RTX (I-RTX) together in Tyrode's solution containing 1.8 mmol/L calcium, and $[Ca^{2+}]_i$ was determined as described in Materials and Methods. Data are expressed as mean ± SEM obtained on 15 to 20 cells per group. *, Significant ($P < 0.05$) differences compared to the resting $[Ca^{2+}]_i$. **, Significant ($P < 0.05$) effect of I-RTX to prevent the action of 10 μmol/L capsaicin to increase $[Ca^{2+}]_i$. **E:** A BrdU proliferation assay. Cells were plated in 96-well multititer plates in quadruplicates and were treated with various concentrations of capsaicin (Caps) or with 30 μmol/L capsaicin and 100 nmol/L iodo-RTX (I-RTX) together for 72 hours. For determining the extracellular calcium dependence, experiments were performed in low-Ca^{2+} SFM (0.4 mmol/L) and high-Ca^{2+} SFM (2 mmol/L). Data are expressed as mean ± SEM as a percentage of the matched control values regarded as 100%. *, Significant ($P < 0.05$) differences compared to control (vehicle-treated) proliferation. **, Significant ($P < 0.05$) effect of I-RTX to prevent the action of 30 μmol/L capsaicin to inhibit proliferation. Original magnification, ×630 (**A**).

acetylcholine receptors, tachykinin, or glutamate receptors) that were originally described as neuron-specific signal transducers, but later were identified to be functionally active on numerous nonneuronal cell types, including those present in human skin and its appendages.[54–56]

The concept that TRPV1 signaling targets previously unappreciated cellular mechanisms is supported by most recent preliminary data that we have obtained in a pilot MicroArray assay (using a commercially available focus chip that contains 1300 genes with recognized relevance in investigative dermatology). Namely, capsaicin treatment (10 μmol/L for 2 days) of organ-cultured human scalp HFs resulted in the induction of such genes of agents inhibiting HF growth as insulin-like growth factor-I-binding protein-3,[57] growth/differentiation factor-15/macrophage inhibitory cytokine-1/placental TGF-β,[58] and activin βA,[59] whereas TRPV1 activation down-regulated the gene expression of matrix GLA-protein precursor (MGP) that is an inhibitor of bone morphogenic protein-2/TGF-β signaling in the HF.[59] Although these preliminary results remain to be repeated and confirmed by Q-PCR, they already point to an even wider spectrum of direct or indirect target genes of TRPV1 signaling that is apparent from the current study.

Interestingly, although the cellular actions affected by TRPV1 activation showed clear calcium dependence (ie, capsaicin was much less effective in inhibiting ORS keratinocyte proliferation in low-Ca^{2+} SFM, Figure 6E), capsaicin did not significantly affect terminal differentiation of cultured ORS keratinocytes, a process that is also dependent on extracellular [Ca^{2+}] in the skin.[60] These data might be explained by several arguments, such as: 1) the induction of catagen and, therefore, the processes of apoptosis (along with the inhibition of proliferation) were initiated earlier by the activation of TRPV1 than possible alterations in expression of differentiation markers; 2) the high calcium concentration of the culturing medium (close to 2 mmol/L), that was required to maintain the HF in organ-culture, alone induced increased expression of the differentiation markers filaggrin (Figure 5A); hence, the TRPV1-mediated calcium influx was unable to further modify (presumably increase) this elevated level (Figure 5B); 3) the effect of capsaicin of various cellular mechanisms possesses a strong dose and cell-type dependence, as reflected by differential action, eg, on stimulation of cytokine release (in keratinocytes, IL-8;[13] in mast cells, IL-4 but not tumor necrosis factor-α[7]), cell death (apoptosis at small concentrations in thymocytes;[61] apoptosis in glial cells,[8] and in airway[9,41] and breast epithelial cells;[42] necrotic cell death[1] in neurons and, at high doses, on thymocytes[61]), and, as revealed by current findings, on differentiation (modification of differentiation on glial cells[8] but not of ORS keratinocytes, Figure 5); 4) finally, given that capsaicin treatment up-regulates the expression of hair growth inhibitors (such as TGF-β_2 and IL-1β) whereas down-modulates the levels of the hair growth stimulators hepatocyte growth factor, insulin-like growth factor-I, and stem cell factor (Figure 5, Table 1), it appears that TRPV1 stimulation results in a complex alterations of the cytokine network of human HFs, the net effects of which eventually coalesce in the cellular HF changes described in Figures 2 to 6.

The well-defined, close physical association of TRPV1-expressing sensory nerve fibers with the TRPV1-expressing ORS keratinocytes of the HF,[62,63] along with other TRPV1-positive nonneuronal cell types such as, eg, mast cells and Langerhans cells,[7,14,15] invite an intriguing hypothesis with potential therapeutic implication. Namely, the dual activation of TRPV1 by exogenous capsaicin or endovanilloids (such as eicosanoids and prostaglandins that are also found in the HF[64]) on neuronal and nonneuronal cell types of the skin likely results in the simultaneous release of neuropeptides from sensory axons and of other mediators (eg, histamine, proinflammatory cytokines) from HF cells, presumably from ORS keratinocytes. Given the recognized hair growth-modulatory properties of such sensory neuron-derived neuropeptides as substance P and calcitonin gene-related peptides[16,65,66] and the involvement of TRPV1-expressing mast cells[7,14] in hair growth,[67,68] this could activate complex, multidirectional signaling cascades including augmentation of the action of the TRPV1 agonists and mast cell degranulation both via TRPV1 and certain neuropeptide receptors such as NK1. The activation of such complex cascades may also explain why TRPV1 stimulation by capsaicin, under defined circumstances (various applied concentrations, telogen versus anagen HF stages, species differences), can even stimulate hair growth in mice,[65] ie, can induce anagen in telogen HF *in vivo* (note that in the current *in vitro* study the hair growth-inhibitory effects of capsaicin were seen on human scalp HFs that exhibited maximal growth activity, ie, anagen VI). Furthermore, preliminary observations from our currently ongoing studies in TRPV1 knockout mice[14] (such as alterations in HF cycling, effects on HF keratinocytes proliferation and perifollicular mast cells) appears to be also consistent with the concept that TRPV1 signaling is indeed a key molecular mechanism in hair biology (Bodó and colleagues, study in progress).

Taken together, the current study not only gives a hot new twist to human hair growth control by introducing TRPV1 signaling as a potent, physiologically relevant hair growth-inhibitory force that may be clinically exploited, eg, for the treatment of unwanted hair growth (hirsutism) by the topical application of TRPV1 agonists, and of hair loss (effluvium, alopecia) by administering TRPV1 antagonists. Our study also highlights that TRPV1 signaling is a major, newly recognized player in epithelial biology in general—both by its direct effect on epithelial tissues (eg, epidermal and ORS keratinocytes) and its complex indirect effects on neuroectodermal-mesenchymal interaction (eg, via the modification of neuropeptide release from sensory skin nerves and of skin mast cell activation). This invites one to systemically explore in future studies how the anti-proliferative TRPV1 signaling can be manipulated in a clinically desired manner by endogenous and exogenous ligands in the management of hyperproliferative epithelial growth disorders of the skin (eg, psoriasis, actinic keratosis, keratoacanthoma, and squamous cell carcinoma) and elsewhere. Therefore, clinicians who apply agents that activate and/or sensitize TRPV1 (eg, cap-

saicin or resiniferatoxin[1,5,6,14,15,69]) now need to take the above into account.

Acknowledgments

We thank S. Wegerich, G. Pilnitz-Stolze, and M. Dietrich for technical assistance; Dr. B. Gerstmayer (Memorec Biotec GmbH, Cologne, Germany) for performance of the MicroArray assay; and P. Pertile (Cutech Srl, Venice, Italy) for continuous consultation.

References

1. Szallasi A, Blumberg PM: Vanilloid (capsaicin) receptors and mechanisms. Pharmacol Rev 1999, 51:159–212
2. Caterina MJ, Schumacher MA, Tominaga M, Rosen TA, Levine JD, Julius D: The capsaicin receptor: a heat-activated ion channel in the pain pathway. Nature 1997, 389:816–824
3. Ugawa S, Ueda T, Ishida Y, Nishigaki M, Shibata Y, Shimada S: Amiloride-blockable acid-sensing ion channels are leading acid sensors expressed in human nociceptors. J Clin Invest 2002, 110:1185–1190
4. Di Marzo V, Blumberg PM, Szallasi A: Endovanilloid signaling in pain. Curr Opin Neurobiol 2002, 12:372–379
5. Karai L, Brown DC, Mannes AJ, Connelly ST, Brown J, Gandal M, Wellisch OM, Neubert JK, Olah Z, Iadarola MJ: Deletion of vanilloid receptor 1-expressing primary afferent neurons for pain control. J Clin Invest 2004, 113:1344–1352
6. Bíró T, Ács G, Ács P, Modarres S, Blumberg PM: Recent advances in understanding of vanilloid receptors: a therapeutic target for treatment of pain and inflammation in skin. J Invest Dermatol Symp Proc 1997, 2:56–60
7. Bíró T, Maurer M, Modarres S, Lewin NE, Brodie C, Ács G, Ács P, Paus R, Blumberg PM: Characterization of functional vanilloid receptors expressed by mast cells. Blood 1998, 91:1332–1340
8. Bíró T, Brodie C, Modarres S, Lewin NE, Ács P, Blumberg PM: Specific vanilloid responses in C6 rat glioma cells. Mol Brain Res 1998, 56:89–98
9. Veronesi B, Oortgiesen M, Carter JD, Devlin RB: Particulate matter initiates inflammatory cytokine release by activation of capsaicin and acid receptors in a human bronchial epithelial cell line. Toxicol Appl Pharmacol 1999, 154:106–115
10. Birder LA, Kanai AJ, de Groat WC, Kiss S, Nealen ML, Burke NE, Dineley KE, Watkins S, Reynolds IJ, Caterina MJ: Vanilloid receptor expression suggests a sensory role for urinary bladder epithelial cells. Proc Natl Acad Sci USA 2001, 98:13396–13401
11. Denda M, Fuziwara S, Inoue K, Denda S, Akamatsu H, Tomitaka A, Matsunaga H: Immunoreactivity of TRPV1 on epidermal keratinocyte of human skin. Biochem Biophys Res Commun 2001, 285:1250–1252
12. Inoue K, Koizumi S, Fuziwara S, Denda S, Inoue K, Denda M: Functional vanilloid receptors in cultured normal human epidermal keratinocytes. Biochem Biophys Res Commun 2002, 291:124–129
13. Southall MD, Li T, Gharibova LS, Pei Y, Nicol GD, Travers JB: Activation of epidermal vanilloid receptor-1 induces release of proinflammatory mediators in human keratinocytes. J Pharmacol Exp Ther 2003, 30:217–222
14. Bodó E, Kovács I, Telek A, Varga A, Paus R, Kovács L, Bíró T: Vanilloid receptor-1 is widely expressed on various epithelial and mesenchymal cell types of human skin. J Invest Dermatol 2004, 123:410–413
15. Ständer S, Moormann C, Schumacher M, Buddenkotte J, Artuc M, Shpacovitch V, Brzoska T, Lippert U, Henz BM, Luger TA, Metze D, Steinhoff M: Expression of vanilloid receptor subtype 1 in cutaneous sensory fibers, mast cells, and epithelial cells of appendage structures. Exp Dermatol 2004, 13:129–139
16. Paus R, Peters EM, Eichmüller S, Botchkarev VA: Neural mechanisms of hair growth control. J Invest Dermatol Symp Proc 1997, 2:61–68
17. Paus R, Cotsarelis G: The biology of hair follicles. N Engl J Med 1999, 341:491–497
18. Stenn KS, Paus R: Controls of hair follicle cycling. Physiol Rev 2001, 81:449–494
19. Cotsarelis G, Millar SE: Towards a molecular understanding of hair loss and its treatment. Trends Mol Med 2001, 7:293–301
20. Botchkarev VA, Botchkareva NV, Peters EM, Paus R: Epithelial growth control by neurotrophins: leads and lessons from the hair follicle. Prog Brain Res 2004, 146:493–513
21. Philpott MP, Green MR, Kealey T: Human hair growth in vitro. J Cell Sci 1990, 3:463–471
22. Limat A, Noser F: Serial cultivation of single keratinocytes from the outer root sheath of human scalp hair follicles. J Invest Dermatol 1986, 87:485–488
23. Limat A, Hunziker T, Biollat C, Bayreuther K, Noser F: Post-mitotic human dermal fibroblasts efficiently support the growth of human follicular keratinocytes. J Invest Dermatol 1989, 92:758–762
24. Barbosa AJ, Castro LP, Margarida A, Nogueira MF: A simple and economical modification of the Masson-Fontana method for staining melanin granules and enterochromaffin cells. Stain Technol 1984, 59:193–196
25. Paus R, van der Veen C, Eichmüller S, Kopp T, Hagen E, Müller-Röver S, Hofmann U: Generation and cyclic remodeling of the hair follicle immune system in mice. J Invest Dermatol 1998, 111:7–18
26. Botchkarev VA, Botchkareva NV, Albers KM, Chen LH, Welker P, Paus R: A role for p75 neurotrophin receptor in the control of apoptosis-driven hair follicle regression. FASEB J 2000, 14:1931–1942
27. Ito T, Ito N, Bettermann A, Tokura Y, Takigawa M, Paus R: Collapse and restoration of MHC class-I-dependent immune privilege: exploiting the human hair follicle as a model. Am J Pathol 2004, 164:623–634
28. Panteleyev AA, Botchkareva NV, Sundberg JP, Christiano AM, Paus R: The role of the hairless (hr) gene in the regulation of hair follicle catagen transformation. Am J Pathol 1999, 155:159–171
29. Foitzik K, Lindner G, Müller-Röver S, Maurer M, Botchkareva N, Botchkarev V, Handjiski B, Metz M, Hibino T, Soma T, Dotto GP, Paus R: Control of murine hair follicle regression (catagen) by TGF-beta1 in vivo. FASEB J 2000, 14:752–760
30. Lindner G, Menrad A, Gharadi E, Merlino G, Welkes P, Handjinski B, Roloff B, Paus R: Involvement of hepatocyte growth factor/scatter factor and met receptor signaling in hair follicle morphogenesis and cycling. FASEB J 2000, 14:319–332
31. Vennegoor C, Hageman P, Van Nouhuijs H, Ruiter DJ, Calafat J, Ringens PJ, Rumke P: A monoclonal antibody specific for cells of the melanocyte lineage. Am J Pathol 1988, 130:179–192
32. Botchkareva NV, Botchkarev VA, Chen LH, Lindner G, Paus R: A role for p75 neurotrophin receptor in the control of hair follicle morphogenesis. Dev Biol 1999, 216:135–153
33. Kjellman C, Olofsson SP, Hansson O, Von Schantz T, Lindvall M, Nilsson I, Salford LG, Sjogren HO, Widegren B: Expression of TGF-beta isoforms, TGF-beta receptors, and SMAD molecules at different stages of human glioma. Int J Cancer 2000, 89:251–258
34. Lázár J, Szabó T, Kovács L, Blumberg PM, Bíró T: Distinct features of recombinant rat vanilloid receptor-1 expressed in various expression systems. Cell Mol Life Sci 2003, 60:2228–2240
35. Panteleyev AA, Jahoda CA, Christiano AM: Hair follicle predetermination. J Cell Sci 2001, 114:3419–3431
36. Philpott MP, Sanders DA, Kealey T: Whole hair follicle organ culture. Dermatol Clin 1996, 14:595–608
37. Ito T, Ito N, Saathoff M, Bettermann A, Takigawa M, Paus R: IFN-γ is a potent inducer of catagen-like changes in cultured human anagen hair follicles. Br J Dermatol (in press)
38. Müller-Röver S, Handjiski B, van der Veen C, Eichmüller S, Foitzik K, McKay IA, Stenn KS, Paus R: A comprehensive guide for the accurate classification of murine hair follicles in distinct hair cycle stages. J Invest Dermatol 2001, 117:3–15
39. Tobin DJ, Paus R: Graying: gerontobiology of the hair follicle pigmentary unit. Exp Gerontol 2001, 36:29–54
40. Wahl P, Foged C, Tullin S, Thomsen C: Iodo-resiniferatoxin, a new potent vanilloid receptor antagonist. Mol Pharmacol 2001, 59:9–15
41. Agopyan N, Head J, Yu S, Simon SA: TRPV1 receptors mediate particulate matter-induced apoptosis. Am J Physiol 2004, 286:L563–L572
42. Kang HJ, Soh Y, Kim MS, Lee EJ, Surh YJ, Kim HR, Kim SH, Moon A: Roles of JNK-1 and p38 in selective induction of apoptosis by capsaicin in ras-transformed human breast epithelial cells. Int J Cancer 2003, 103:475–482

43. Lindner G, Botchkarev VA, Botchkareva NV, Ling G, van der Veen C, Paus R: Analysis of apoptosis during hair follicle regression (catagen). Am J Pathol 1997, 151:1601–1617
44. Lenoir MC, Bernard BA, Pautrat G, Darmon M, Shroot B: Outer root sheath cells of human hair follicle are able to regenerate a fully differentiated epidermis in vitro. Dev Biol 1988, 130:610–620
45. Soma T, Tsuji Y, Hibino T: Involvement of transforming growth factor-beta2 in catagen induction during the human hair cycle. J Invest Dermatol 2002, 118:993–997
46. Langbein L, Rogers MA, Winter H, Praetzel S, Beckhaus U, Rackwitz HR, Schweizer J: The catalog of human hair keratins. I. Expression of the nine type I members in the hair follicle J Biol Chem 1999, 28:19874–19884
47. Langbein L, Rogers MA, Winter H, Praetzel S, Schweizer J: The catalog of human hair keratins. II. Expression of the six type II members in the hair follicle and the combined catalog of human type I and II keratins. J Biol Chem 2001, 37:35123–35132
48. Shimaoka S, Tsuboi R, Jindo T, Imai R, Takamori K, Rubin JS, Ogawa H: Hepatocyte growth factor/scatter factor expressed in follicular papilla cells stimulates human hair growth in vitro. J Cell Physiol 1995, 165:333–338
49. Philpott MP, Sanders DA, Kealey T: Effects of insulin and insulin-like growth factors on cultured human hair follicles: IGF-I at physiologic concentrations is an important regulator of hair follicle growth in vitro. J Invest Dermatol 1994, 102:857–861
50. Peters EM, Maurer M, Botchkarev VA, Jensen K, Welker P, Scott GA, Paus R: Kit is expressed by epithelial cells in vivo. J Invest Dermatol 2003, 121:976–984
51. Hoffmann R, Eicheler W, Wenzel E, Happle R: Interleukin-1beta-induced inhibition of hair growth in vitro is mediated by cyclic AMP. J Invest Dermatol 1997, 108:40–42
52. Hebert JM, Rosenquist T, Gotz J, Martin GR: FGF5 as a regulator of the hair growth cycle: evidence from targeted and spontaneous mutations. Cell 1994, 78:1017–1025
53. Paus R, Ito N, Takigawa M, Ito T: The hair follicle and immune privilege. J Invest Dermatol Symp Proc 2003, 8:188–194
54. Nguyen VT, Ndoye A, Hall LL, Zia S, Arredondo J, Chernyavsky AI, Kist DA, Zelickson BD, Lawry MA, Grando SA: Programmed cell death of keratinocytes culminates in apoptotic secretion of a humectant upon secretagogue action of acetylcholine. J Cell Sci 2001, 114:1189–1204
55. Kanda N, Watanabe S: Substance P enhances the production of interferon-induced protein of 10 kDa by human keratinocytes in synergy with interferon-gamma. J Invest Dermatol 2002, 119:1290–1297
56. Genever PG, Maxfield SJ, Kennovin GD, Maltman J, Bowgen CJ, Raxworthy MJ, Skerry TM: Evidence for a novel glutamate-mediated signaling pathway in keratinocytes. J Invest Dermatol 1999, 112:337–342
57. Hembree JR, Harmon CS, Nevins TD, Eckert RL: Regulation of human dermal papilla cell production of insulin-like growth factor binding protein-3 by retinoic acid, glucocorticoids, and insulin-like growth factor-1. J Cell Physiol 1996, 167:556–561
58. Welsh JB, Sapinoso LM, Kern SG, Brown DA, Liu T, Bauskin AR, Ward RL, Hawkins NJ, Quinn DI, Russell PJ, Sutherland RL, Breit SN, Moskaluk LA, Frierson Jr HF, Hampton GM: Large-scale delineation of secreted protein biomarkers overexpressed in cancer tissue and serum. Proc Natl Acad Sci USA 2003, 100:3410–3415
59. Nakamura M, Matzuk MM, Gerstmayer B, Bosio A, Lauster R, Miyachi Y, Werner S, Paus R: Control of pelage hair follicle development and cycling by complex interactions between follistatin and activin. FASEB J 2003, 17:497–499
60. Bikle DD, Ratnam A, Mauro T, Harris J, Pillai S: Changes in calcium responsiveness and handling during keratinocyte differentiation. Potential role of the calcium receptor. J Clin Invest 1996, 97:1085–1093
61. Amantini C, Mosca M, Luccarini R, Perfumi M, Morrone S, Piccoli M, Santoni G: Distinct thymocyte subsets express the vanillioid receptor VR1 that mediates capsaicin-induced apoptotic cell death. Cell Death Differ 2004, 11:1342–1356
62. Kaidoh T, Inoue T: Intercellular junctions between palisade nerve endings and outer root sheath cells of rat vellus hairs. J Comp Neurol 2000, 420:419–427
63. Peters EM, Botchkarev VA, Müller-Röver S, Moll I, Rice FL, Paus R: Developmental timing of hair follicle and dorsal skin innervation in mice. J Comp Neurol 2002, 448:28–52
64. Müller-Decker K, Leder C, Neumann M, Neufang G, Bayerl C, Schweizer J, Marks F, Fürstenberger G: Expression of cyclooxygenase isozymes during morphogenesis and cycling of pelage hair follicles in mouse skin: precocious onset of the first catagen phase and alopecia upon cyclooxygenase-2 overexpression. J Invest Dermatol 2003, 121:661–668
65. Paus R, Heinzelmann T, Schultz KD, Furkert J, Fechner K, Czarnetzki BM: Hair growth induction by substance P. Lab Invest 1994, 71:134–140
66. Peters EM, Botchkarev VA, Botchkareva NV, Tobin DJ, Paus R: Hair-cycle-associated remodeling of the peptidergic innervation of murine skin, and hair growth modulation by neuropeptides. J Invest Dermatol 2001, 116:236–245
67. Paus R, Maurer M, Slominski A, Czarnetzki BM: Mast cell involvement in murine hair growth. Dev Biol 1994, 163:230–240
68. Maurer M, Fischer E, Handjiski B, von Stebut E, Algermissen B, Bavandi A, Paus R: Activated skin mast cells are involved in murine hair follicle regression (catagen). Lab Invest 1997, 77:319–332
69. Stander S, Luger T, Metze D: Treatment of prurigo nodularis with topical capsaicin. J Am Acad Dermatol 2001, 44:471–478

III.

Hair Cycle Control by Vanilloid Receptor-1 (TRPV1): Evidence from TRPV1 Knockout Mice

Journal of Investigative Dermatology (2006) **126,** 1909–1912. doi:10.1038/sj.jid.5700321; published online 27 April 2006

TO THE EDITOR

The vanilloid receptor-1 (or transient receptor potential-1, TRPV1) is a Ca^{2+}-permeable cation channel that be stimulated by capsaicin, the pungent ingredient of chili peppers (Caterina *et al.*, 1997; Szallasi and Blumberg, 1999). TRPV1 was first described on capsaicin-sensitive nociceptive neurons that respond to various painful stimuli (Di Marzo *et al.*, 2002). Therefore, TRPV1 is recognized as a central integrator of noxious stimuli (Tominaga et al., 1998).

There is increasing appreciation, however, that functions of TRPV1 signaling extend far beyond the sensory nervous system (Bíró *et al.*, 1998a, b; Veronesi *et al.*, 1999; Birder *et al.*, 2001). In the skin, human epidermal and hair follicle keratinocytes, mast cells, and Langerhans cells are prominently positive for TRPV1 (Denda *et al.*, 2001; Inoue *et al.*, 2002; Ständer *et al.*, 2004; Bodó *et al.*, 2004, 2005) and TRPV1 agonists have been shown to modulate mast cell (Bíró *et al.*, 1998b) and keratinocyte functions (Inoue *et al.*, 2002; Southall *et al.*, 2003). In addition, we have recently provided the first evidence that TRPV1 signaling is indeed physiologically important in normal human skin *in situ*, by presenting that TRPV1 activation promotes hair follicle regression (catagen) and hair matrix keratinocyte apoptosis, whereas it inhibits hair matrix keratinocyte proliferation and retards hair shaft elongation *in vitro* (Bodó *et al.*, 2005).

Given the unsurpassed instructiveness of mouse models for hair research (Nakamura *et al.*, 2001; Stenn and Paus, 2001), we now wish to examine whether (1) the expression of TRPV1 changes during the murine hair cycle and (2) the deletion of functional TRPV1 has any effect on hair follicle cycling *in vivo*.

A tissue bank was prepared from adolescent back skin of female C57BL/6 mice in which hair follicle cycling had been induced by depilation (Paus *et al.*, 1994, Maurer *et al.*, 1997; Müller-Röver *et al.*, 2001). This was used for immunohistological detection of hair cycle-associated differences in TRPV1 expression. The functional role of TRPV1 signaling was addressed by quantitative histomorphometry of spontaneous, experimentally unmanipulated hair follicle cycling during the first murine hair cycle (P19–P45), comparing TRPV1 knockout B6.129S4-Trpv1 mice (Jackson Laboratory, Bar Harbor, MA) and their age-matched littermates. Cryostat sections of back skin (at least three animals each per time point) processed for histology; hematoxylin–eosin-stained sections were counted and hair follicles were morphologically assigned to their respective hair cycle stages.

For the detection of TRPV1 immunoreactivity, the tyramide-amplification (TSA, Ito *et al.*, 2004) and a peroxidase-based ABC technique (Paus *et al.*, 1998) were performed. Sections were first incubated with a primary rabbit anti-TRPV1 antibody (H-150, sc-20813; Santa Cruz BT, Santa Cruz, CA) (1:500 in TNB buffer for TSA, Perkin Elmer, Boston, MA and 1:50 in TBS for ABC), with biotinylated multilink swine anti-goat/mouse/rabbit IgG (DAKO, Glostrup, Denmark, 1:200 in TNB), and then by a streptavidin–horseradish peroxidase (1:100 in TNB for TSA; avidin–biotin peroxidase for ABC, Linaris, Wertheim, Germany). Finally, we applied fluorescein isothiocyanate-tyramide (1:50 in Amplification Diluent, TSA kit), or diamino-benzidine (Linaris), respectively and then sections were counterstained. The employed positive (mouse spinal cord) and negative controls (the primary antibody was omitted or sections were preincubated with a specific blocking peptide; spinal cord and skin of Trpv-$1^{-/-}$ mice) unambiguously argued the specificity and sensitivity of the immunoreactivity patterns. (Note that the TRPV1 positivity on sebaceous glands is a false-positive result as negative controls as well as sebaceous gland of Trpv-$1^{-/-}$ mice skin showed immunosignals.) The study was approved by the Institutional Research Ethics Committee.

Similar to human epidermis, adolescent wild-type C57BL/6 mouse skin showed strong TRPV1 immunreactivity (IR) on (mostly basal) epidermal keratinocytes (Figure 1a). In addition, also similarly to our previous human data, in the hair follicle, TRPV1-IR was exclusively restricted to the epithelial compartments (note the TRPV1-negativity of the dermal papilla during all hair cycle phases). Analysis of depilation-induced hair follicle cycling in these mice, however, revealed discrete, but important and statistically significant changes in the observed specific IR patterns corresponding to TRPV1 protein expression (Figure 1a–q).

Intriguingly, the strongest IR signal was detected on keratinocytes of the epithelial strand of the regressing catagen follicle (Figure 1o–p) and of the secondary hair germ of telogen hair follicles (Figure 1c, d, m and n). With the exception of an asymmetric, disc-like region in the anagen VI hair matrix (Figure 1i and k), the most highly proliferating cell populations in the hair follicle epithelium showed a slightly reduced intensity of TRPV1-IR (Figure

Abbreviations: IR, immunoreactivity; TRPV1, receptor potential-1

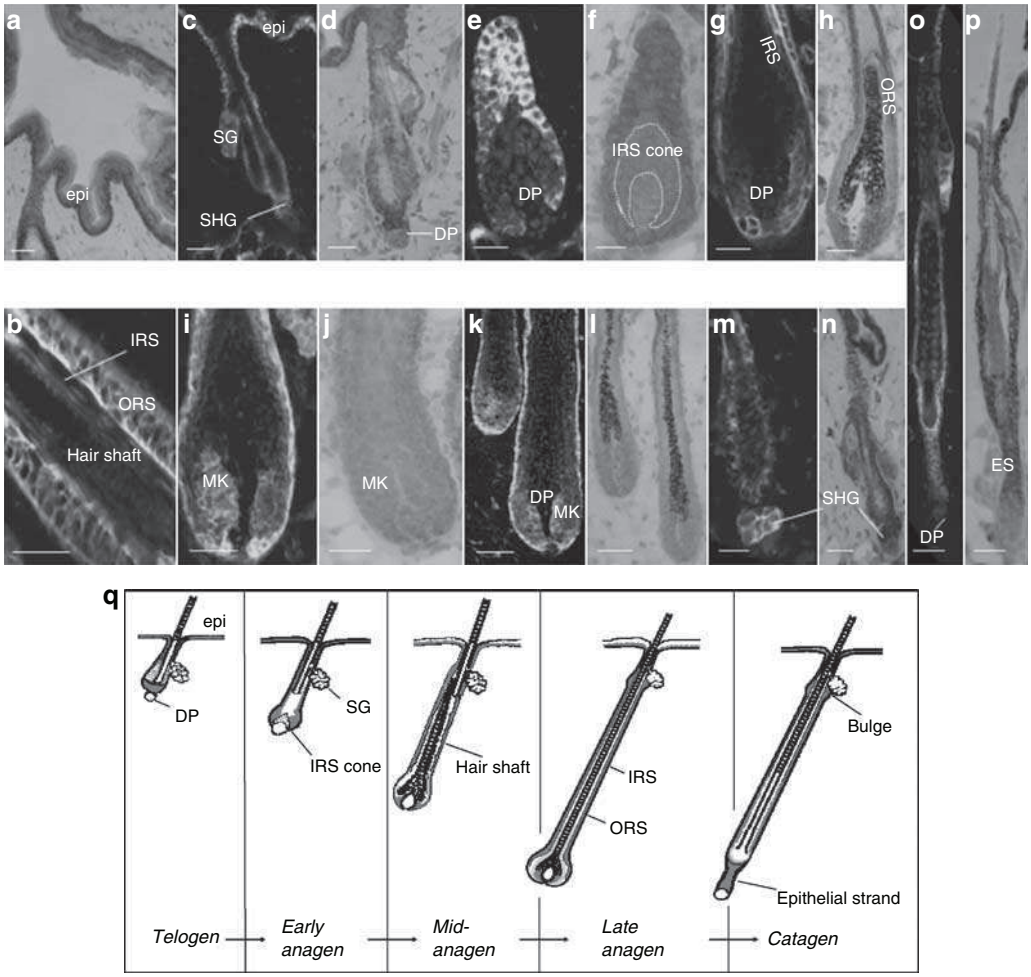

Figure 1. TRPV1 expression throughout the murine hair follicle cycle. (**a**) TRPV1-IR on (mostly basal) epidermal keratinocytes. (epi: epidermis) (**b**) Strong TRPV1-IR on outer root sheath (ORS) keratinocytes, but lack of expression on inner root sheath (IRS) keratinocytes and hair shaft of mature anagen follicles. (**c–p**) TRPV1-IR during depilation-induced hair cycle: (**c,d** and **m,n**) Telogen follicles: the most intensive TRPV1 signal was found on the secondary hair germ (SHG). No TRPV1-IR on dermal papilla (DP). Note that the TRPV1-IR of sebaceous glands (SG) is a non-specific signal. (**e,f**) Early anagen follicles: most intensive TRPV1 expression on ORS, moderate reactivity on IRS. (**g,h**) Mid-anagen follicles, (**i–l**) Late-anagen follicles: TRPV1-IR on ORS and on the asymmetric, disc-shaped field of matrix keratinocytes (MK). (**o,p**) Strongest IR on keratinocytes of the epithelial strand (ES) of the regressing catagen follicle. (**q**) Schematic illustration of TRPV1-IR during the cycle. (**a, d, f, h, j, l, n, p**) Peroxidase-based ABC method with DAB substrate; (**b, c, e, g, i, k, m, o**) TSA technique with fluorescein isothiocyanate labeling.

1i-l). The inner root sheath and the distal, precortical hair matrix also showed only strongly reduced TRPV1-IR (Figure 1b, e–l).

As TRPV1 activation by capsaicin caused hair follicle regression (anagen–catagen transition) in human hair follicle organ culture (Bodó *et al.*, 2005), spontaneous hair follicle-cycling was compared between age-matched TRPV1 wild-type and knockout mice by quantitative histomorphometry. The skin of Trpv-1$^{-/-}$ mice showed no obvious macroscopic or microscopic abnormalities compared to age-matched wild-type control. However, on day 19, Trpv-1$^{-/-}$ mice exhibited a significant delay in the first spontaneous transition of their hair follicles from morphogenesis stage 8 (which is often confused with ''the first anagen'', see Paus *et al.*, 1999) compared to wild-type littermates (Figure 2). This catagen retardation was independently confirmed by cumulative hair cycle score (Maurer *et al.*, 1997; Peters *et al.*, 2004) (383 ± 16 vs 267 ± 26 in wild-type and Trpv-1$^{-/-}$ mice, respectively; mean $\pm$ SEM, $P < 0.05$). Likewise, subsequent telogen development (P25) was slightly but significantly retarded (hair scores of 449 ± 9 vs 412 ± 3 in wild-type and Trpv-1$^{-/-}$ mice, respectively; mean $\pm$ SEM, $P < 0.05$) in the absence of functional TRPV1 signaling (Figure 2). Instead, the first spontaneous anagen development (Figure 2, P32) and subsequent hair follicle cycling (Figure 2, P45) were not significantly different between Trpv-1-competent and -deficient mice. This suggests that, in murine back skin pelage hair follicles, TRPV1-mediated signaling is important for modulating the transition from the final stages of hair follicle morphogenesis to that of cycling skin appendage, whereas signaling via this receptor looses functional importance once hair follicle cycling has been initiated.

In summary, we present here the first evidence that, very similar to human

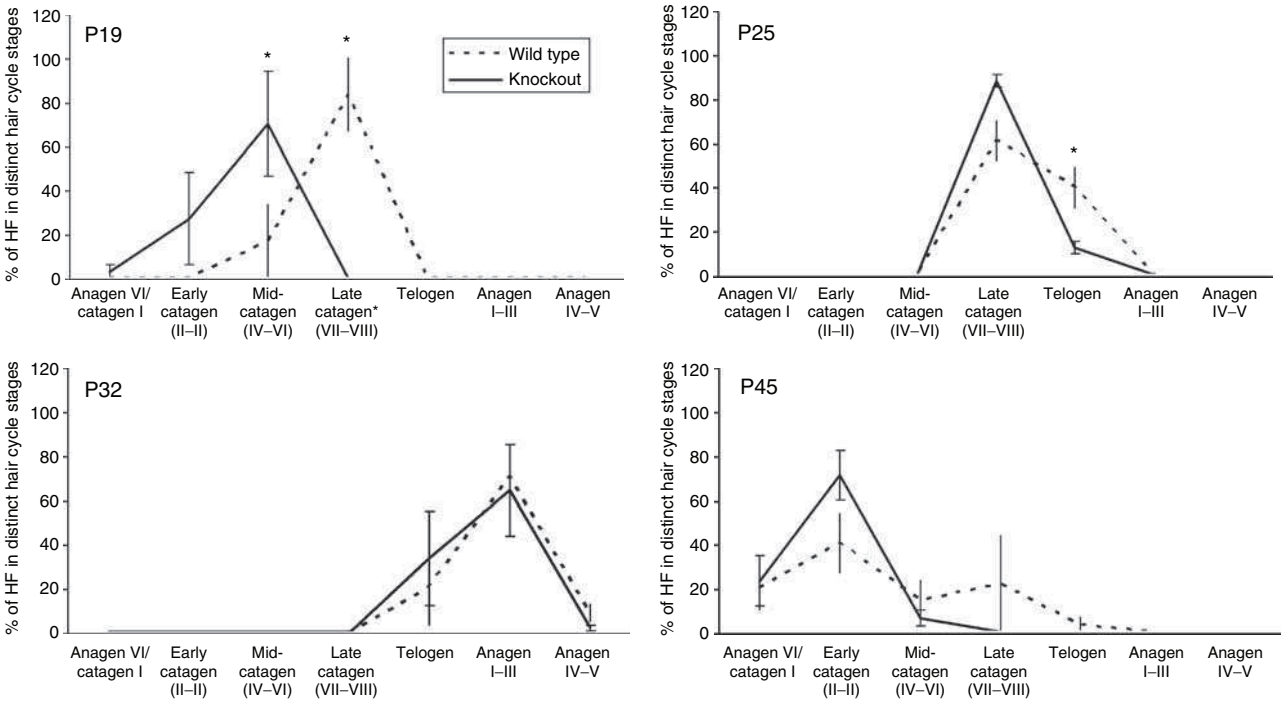

Figure 2. Retarded catagen development in TRPV1 knockout mice. Spontaneous hair follicle-cycling was compared between age-matched wild-type and TRPV1 knockout mice by quantitative histomorphometry. Trpv-1$^{-/-}$ mice showed a significant delay in the cycling at P19 (catagen development) and 25 (telogen development) compared to wild-type littermates. Data are expressed as mean ± SEM, whereas * mark significant ($P<0.05$) differences.

skin, murine skin expresses TRPV1 well outside of sensory nerves, namely in defined epithelial regions of the epidermis and hair follicle. The reported murine hair cycle analyses not only reveal hair cycle-dependent differences in the expression of TRPV1, but – by showing that the absence of TRPV1 is associated with a subtle yet significant delay in the spontaneous involution of hair follicles (catagen-telogen transition) – might also argue for that these receptors are indeed functional. Although one can also assume that the lack of TRPV1 in other cell types (i.e., besides keratinocytes) might also contribute to the observed hair cycle changes, the presented novel results (besides supporting our previous findings in human hair follicles, Bodó *et al.*, 2005) suggest that TRPV1 exerts much more widespread functions in mammalian skin and hair follicle biology than previously thought, which extend across species barriers and may include the inhibition of hair follicle keratinocyte proliferation.

CONFLICT OF INTEREST

The authors state no conflict of interest.

ACKNOWLEDGMENTS

This work was supported in part by a grant from DFG to RP (Pa 345/6-4) and by Hungarian research grants (NKFP 1A/008/04, OTKA T049231, OTKA K63153, RET 06/2004, ETT 365/2003) to TB. EB was recipient of an Erasmus student fellowship. The authors are grateful to S. Wegerich and G. Pilnitz-Stolze for excellent technical assistance and Dr Franziska Conrad for helpful advice.

Tamás Bíró[1,2,4], Enikõ Bodó[1,3,4], Andrea Telek[1,2], Tamás Géczy[1], Birte Tychsen[3], László Kovács[1,2] and Ralf Paus[3]

[1]Department of Physiology, University of Debrecen, Medical and Health Science Center, Research Center for Molecular Medicine, Debrecen, Hungary; [2]Cell Physiology Research Group of the Hungarian Academy of Sciences, University of Debrecen, Medical and Health Science Center, Research Center for Molecular Medicine, Debrecen, Hungary and [3]Department of Dermatology, University Hospital Schleswig-Holstein, Campus Lübeck, Lübeck, Germany. E-mail: biro@phys.dote.hu
[4]These authors contributed equally to this work.

REFERENCES

Birder LA, Kanai AJ, de Groat WC, Kiss S, Nealen ML, Berke NE *et al.* (2001) Vanilloid receptor expression suggests a sensory role for urinary bladder epithelial cells. *Proc Natl Acad Sci USA* 98:1339–401

Bíró T, Brodie C, Modarres S, Lewin NE, Ács P, Blumberg PM (1998a) Specific vanilloid responses in C6 rat glioma cells. *Mol Brain Res* 56:89–98

Bíró T, Maurer M, Modarres S, Lewin NE, Brodie C, Ács G *et al.* (1998b) Characterization of functional vanilloid receptors expressed by mast cells. *Blood* 91:1332–40

Bodó E, Kovács I, Telek A, Varga A, Paus R, Kovács L *et al.* (2004) Vanilloid receptor-1 is widely expressed on various epithelial and mesenchymal cell types of human skin. *J Invest Dermatol* 123:410–3

Bodó E, Bíró T, Telek A, Czifra G, Telek A, Tóth BI *et al.* (2005) A hot new twist to hair biology – Involvement of vanilloid receptor-1 (VR1/TRPV1) signalling in human hair growth control. *Am J Pathol* 166:985–98

Caterina MJ, Schumacher MA, Tominaga M, Rosen TA, Levine JD, Julius D (1997) The capsaicin receptor: a heat-activated ion channel in the pain pathway. *Nature* 389:816–24

Denda M, Fuziwara S, Inoue K, Denda S, Akamatsu H, Tomitaka A *et al.* (2001) Immunreactivity of VR1 on epidermal keratinocyte of human skin. *Biochem Biophys Res Commun* 285:1250–2

Di Marzo V, Blumberg PM, Szallasi A (2002) Endovanilloid signaling in pain. *Curr Opin Neurobiol* 12:372–9

Inoue K, Koizumi S, Fuziwara S, Denda S, Inoue K, Denda M (2002) Functional vanilloid

receptors in cultured normal human epidermal keratinocytes. *Biochem Biophys Res Commun* 291:124–9

Ito T, Ito N, Bettermann A, Tokura Y, Takigawa M, Paus R (2004) Collapse and restoration of MHC class-I dependent immune privilege: exploiting the human hair follicle as a model. *Am J Pathol* 164:623–34

Maurer M, Fischer E, Handjinski B, Von Stebut E, Algermissen B, Bavandi A *et al.* (1997) Activated skin mast cells are involved in murine hair follicle regression (catagen). *Lab Invest* 77:319–32

Müller-Röver S, Handjiski B, Van der Veen C, Eichmüller S, Foitzik K, McKay IA *et al.* (2001) A comprehensive guide for the accurate classification of murine hair follicles in distinct hair cycle stages. *J Invest Dermatol* 117:3–15

Nakamura M, Sundberg JP, Paus R (2001) Mutant laboratory mice with abnormalities in hair follicle morphogenesis, cycling, and/or structure: annotated tables. *Exp Dermatol* 10: 369–90

Paus R, Hoffmann U, Eichmüller S, Czarnetzki BM (1994) Distribution and changing density of gamma-delta T cells in murine skin during the induced hair cycle. *Br J Dermatol* 130: 281–9

Paus R, van der Veen C, Eichmüller S, Kopp T, Hagen E, Müller-Röver S *et al.* (1998) Generation and cyclic remodeling of the hair follicle immune system in mice. *J Invest Dermatol* 111:7–18

Paus R, Müller-Röver S, Van der Veen C, Maurer M, Eichmüller S, Ling G *et al.* (1999) A comprehensive guide for the recognition and classification of distinct stages of hair follicle morphogenesis. *J Invest Dermatol* 113:523–32

Peters EMJ, Handjiski B, Kuhlmei A, Hagen E, Bielas H, Braun A *et al.* (2004) Neurogenic inflammation in stress-induced termination of murine hair growth is promoted by nerve growth factor. *Am J Pathol* 165:259–71

Southall MD, Li T, Gharibova LS, Pei Y, Nicol GD, Travers JB (2003) Activation of epidermal vanilloid receptor-1 induces release of proinflammatory mediators in human keratinocytes. *J Pharmacol Exp Ther* 304:217–22

Stenn KS, Paus R (2001) Controls of hair follicle cycling. *Phys Rev* 81:449–94

Ständer S, Moormann C, Schumacher M, Buddenkotte J, Artuc M, Shpacovitch V *et al.* (2004) Expression of vanilloid receptor subtype 1 in cutaneous sensory fibers, mast cells, and epithelial cells of appendage structures. *Exp Dermatol* 13:129–39

Szallasi A, Blumberg PM (1999) Vanilloid (Capsaicin) receptors and mechanisms. *Pharmacol Rev* 51:159–212

Tominaga M, Caterina MJ, Malmberg AB, Rosen TA, Gilbert H, Skinner K *et al.* (1998) The cloned capsaicin receptor integrates multiple pain-producing stimuli. *Neuron* 21:531–43

Veronesi B, Oortgiesen M, Carter JD, Devlin RB (1999) Particulate matter initiates inflammatory cytokine release by activation of capsaicin and acid receptors in a human bronchial epithelial cell line. *Toxicol Appl Pharmacol* 154:106–15

Novel Keratin 14 Mutations in Patients with Severe Recessive Epidermolysis Bullosa Simplex

Journal of Investigative Dermatology (2006) **126,** 1912–1914. doi:10.1038/sj.jid.5700312; published online 13 April 2006

TO THE EDITOR

Epidermolysis bullosa simplex (EBS) is the most common subtype, accounting for one-half of all epidermolysis bullosa cases (Pfendner *et al.*, 2005). It is clinically characterized by nonscarring blisters of the skin caused by little or no trauma, and morphologically by intraepidermal blistering. The major subtypes of EBS result from mutations in either the keratin 5 (*KRT5*) or keratin 14 (*KRT14*) gene, whereas mutations in the gene for plectin (*PLEC1*) cause the rare forms, EBS with muscular dystrophy and EBS Ogna. The clinical spectrum of EBS ranges from mild blistering of the hands and feet (EBS Weber–Cockayne) to more generalized blistering (EBS Koebner, EBS Dowling-Meara, and EBS with mottled pigmentation). EBS, similarly to most of the keratin disorders identified in humans, is caused by dominant missense mutations; however, patients with recessive EBS due to keratin mutations have been reported, representing about 5% of all EBS mutations (Porter and Lane, 2003).

In this study, we investigated two unrelated patients with severe neonatal blistering, both offspring of consanguineous, unaffected parents of Turkish (patient 1), respectively German (patient 2) origin. Indirect immunofluorescence (IIF) of the skin cryosections was performed as described (Hammami-Hauasli *et al.*, 1998) with monoclonal antibodies anti-human keratin 5 (clone D5/16 B4, Dako, Hamburg, Germany) and keratin 14 (clone LL002, BioGenex, San Ramon, CA). Genomic DNA was extracted from peripheral blood samples collected from patients and their unaffected parents using the Qiagen Blood DNA Kit (Qiagen, Hilden, Germany). Long-range polymerase chain reaction amplification of the *KRT14* gene was performed as described (Wood *et al.*, 2003) and direct sequencing in both directions was performed, using primers as published by Schuilenga-Hut *et al.* (2003) and an ABI prism 3100 automated sequencer (ABI, Darmstadt, Germany). The study was conducted according to the Declaration of Helsinki Principles**,** and the participants gave their written informed consent. The medical committee of the University of Freiburg approved all described studies.

Patient 1, a 2-year-old boy, showed blistering predominantly on hands and feet since birth (Figure 1a). In the course of the disease, bullae became rarer, occurred mechanically induced also on the head and trunk and healed without scarring. Patient 2, aged 1 year, showed at birth extensive blistering of the hands and feet (Figure 1b) and suffered from congenital pneumonia. Oral

Abbreviations: EBS, epidermolysis bullosa simplex; IIF, indirect Immunofluorescence; KRT, keratin

IV.

Transient Receptor Potential Vanilloid-1 Signaling as a Regulator of Human Sebocyte Biology

Balázs I. Tóth[1,2], Tamás Géczy[1], Zoltán Griger[1], Anikó Dózsa[3], Holger Seltmann[4,5,6], László Kovács[1,2], László Nagy[3], Christos C. Zouboulis[4,5,6,7], Ralf Paus[8] and Tamás Bíró[1,2]

Transient receptor potential vanilloid-1 (TRPV1), originally described as a central integrator of nociception, is expressed on human epidermal and hair follicle keratinocytes and is involved in regulation of cell growth and death. In human pilosebaceous units, we had shown that TRPV1 stimulation inhibits hair shaft elongation and matrix keratinocyte proliferation, and induces premature hair follicle regression and keratinocyte apoptosis. In the current study, we have explored the role of TRPV1-mediated signaling in sebaceous gland (SG) biology, using a human sebocyte cell culture model (SZ95 sebocytes). Demonstrating that human skin SG *in situ* and SZ95 sebocytes *in vitro* express TRPV1, we show that the prototypic TRPV1 agonist, capsaicin, selectively inhibits basal and arachidonic acid-induced lipid synthesis in a dose-, time-, and extracellular calcium-dependent and a TRPV1-specific manner. Low-dose capsaicin stimulates cellular proliferation via TRPV1, whereas higher concentrations inhibit sebocyte growth and induce cell death independent of TRPV1. Moreover, capsaicin suppresses the expression of genes involved in lipid homeostasis and of selected proinflammatory cytokines. Collectively, these findings support the concept that TRPV1 signaling is a significant, previously unreported player in human sebocyte biology and identify TRPV1 as a promising target in the clinical management of inflammatory SG disorders (for example, acne vulgaris).

Journal of Investigative Dermatology (2009) **129,** 329–339; doi:10.1038/jid.2008.258; published online 4 September 2008

INTRODUCTION

Capsaicin (8-methyl-*N*-vanillyl-6-nonenamide) is the pungent ingredient of hot chili peppers (Jancsó, 1960; Szolcsányi, 1977). When applied topically to the skin, it initiates a classical ''multiple response'' of pain, desensitization, neurogenic inflammation, and neurotoxicity (reviewed in Holzer, 1991; Szállási and Blumberg, 1999). These actions of capsaicin establish the basis for its therapeutic application; indeed, capsaicin is widely used in the therapy of several dermatoses, such as neuropathies, psoriasis, pruritus, and prurigo nodularis (reviewed in Biró *et al.*, 2005; Paus *et al.*, 2006, Steinhoff *et al.*, 2006).

The above effects previously were exclusively attributed to the action of capsaicin on nociceptive sensory neurons expressing transient receptor potential vanilloid-1 (TRPV1), the molecular target of capsaicin (Caterina *et al.*, 1997; Tominaga *et al.*, 1998). The activation of this nonselective, calcium (Ca)-permeable channel on the nociceptors first results in action potential firing and initiation of pain sensation (Bevan *et al.*, 1993). In addition, TRPV1-mediated signaling also induces neuropeptide release (Szolcsányi, 1977; Holzer, 1991; Szállási and Blumberg, 1999) which, in turn, initiates vasodilation, flare, and edema (characteristic signs of neurogenic inflammation; Geppetti and Holzer, 1996). Finally, prolonged application of capsaicin evokes desensitization and/or degeneration of sensory afferents leading to cessation of pain sensation (reviewed in Holzer, 1991; Szállási and Blumberg, 1999).

Recent reports, however, have unambiguously identified the presence of TRPV1 on numerous non-neuronal cell types as well. We and others have found that functional TRPV1 is expressed, for example, on mast cells, dendritic cells, and both epidermal and hair follicle keratinocytes *in situ* (Bíró *et al.*, 1998; Birder *et al.*, 2001; Ost *et al.*, 2002; Lazzeri *et al.*, 2004; Ständer *et al.*, 2004; Bodó *et al.*, 2004, 2005; Li

[1]*Department of Physiology, Medical and Health Science Center, Research Center for Molecular Medicine, University of Debrecen, Debrecen, Hungary;* [2]*Cell Physiology Research Group of the Hungarian Academy of Sciences, Medical and Health Science Center, Research Center for Molecular Medicine, University of Debrecen, Debrecen, Hungary;* [3]*Department of Biochemistry and Molecular Biology, Medical and Health Science Center, Research Center for Molecular Medicine, University of Debrecen, Debrecen, Hungary;* [4]*Department of Dermatology, Dessau Medical Center, Dessau, Germany;* [5]*Department of Venereology, Dessau Medical Center, Dessau, Germany;* [6]*Department of Allergology and Immunology, Dessau Medical Center, Dessau, Germany;* [7]*Laboratory of Biogerontology, Dermato-Pharmacology and Dermato-Endocrinology, Institute of Clinical Pharmacology and Toxicology, Charité University of Berlin, Campus Benjamin Franklin, Berlin, Germany and* [8]*Department of Dermatology, University Hospital Schleswig-Holstein, University of Lübeck, Lübeck, Germany*

Correspondence: Dr Tamás Bíró, Department of Physiology, Medical and Health Science Center, Research Center for Molecular Medicine, University of Debrecen, Nagyerdei krt. 98. PO Box 22,Debrecen 4032, Hungary, E-mail: biro@phys.dote.hu

Abbreviations: AA, arachidonic acid; Ca, calcium; G6PD, glucose-6-phophate-dehydrogenase; I-RTX, iodo-resiniferatoxin; PPAR, peroxisome proliferator-activated receptor; Q-PCR, quantitative real-time PCR; RNAi, RNA interference; SG, sebaceous gland; TRPV1, transient receptor potential vanilloid-1

Received 4 December 2007; revised 14 April 2008; accepted 20 June 2008; published online 4 September 2008

et al., 2007). Studying organ-cultured human hair follicles and cultured epidermal HaCaT keratinocytes, we have shown that TRPV1 activation by capsaicin results in a TRPV1-specific inhibition of hair growth and proliferation, and induction of apoptosis and catagen (Bodó *et al.*, 2005). These findings make it mandatory to carefully consider the multiple direct, growth-modulatory actions of capsaicin on non-neuronal cell populations in human skin (Biró *et al.*, 2005; Paus *et al.*, 2006; Steinhoff *et al.*, 2006).

Given the instructiveness of pilosebaceous units for exploring nonclassical functions of TRPV1-mediated signaling in human skin biology (Bodó *et al.*, 2005), it is interesting to note that TRPV1 immunoreactivity is also found in the human sebaceous gland (SG; Bodó *et al.*, 2004). Moreover, reportedly differentiated (mature) sebocytes show a higher level of TRPV1 immunoreactivity *in situ* than less differentiated ones (Ständer *et al.*, 2004), suggesting a potential role of TRPV1 in the control of sebocyte proliferation and/or differentiation. However, the biological effects of TRPV1 agonists on the proliferation, differentiation, and apoptosis of sebocytes (which differentiate from outer root sheath hair follicle keratinocytes (Thody and Shuster, 1989; Wróbel *et al.*, 2003)) remain to be dissected. Sebocytes, engage in holocrine (sebum) secretion, are major site of hormone synthesis and metabolism in human skin (Zouboulis *et al.*, 2005; Alestas *et al.*, 2006; Zhang *et al.*, 2006), and express numerous receptor-coupled pathways that were originally described chiefly on neurons (Zouboulis *et al.*, 2002; Zouboulis and Bohm, 2004).

Human sebocytes, therefore, provide a highly instructive research tool for exploring nonclassical TRPV1 functions, which promises additional sets of information that perfectly complement those obtainable with human hair follicle. In the current study, we have therefore investigated the effects of capsaicin on SZ95 sebocytes—a human SG-derived immortalized cell line that possesses striking functional similarities to those of primary human sebocytes (Zouboulis *et al.*, 1999)—and have dissected the corresponding role of TRPV1 signaling.

RESULTS

TRPV1 is expressed on human SG *in situ* and on human SZ95 sebocytes

Using immunohistochemistry, confirming our previous findings (Bodó *et al.*, 2004), we first have shown that human SG epithelial cells indeed express TRPV1 *in situ* (Figure 1a and b). Moreover, we also found (similar to earlier reports; Ständer *et al.*, 2004) that TRPV1-specific immunosignals were more prominent on the more differentiated (matured) SG cells (Figure 1b).

We then measured the existence of TRPV1 on SZ95 sebocytes. Using various immunocytochemical methods, western blotting, and quantitative ''real-time'' PCR (Q-PCR), we here provide evidence that SZ95 cells also express TRPV1 on the gene and protein level (Figure 1c–f). Interestingly, similar to cultured normal human epidermal and human immortalized HaCaT keratinocytes (Denda *et al.*, 2001; Bodó *et al.*, 2004, 2005), the TRPV1-specific immunoreactivity was inhomogeneous in the cell culture (Figure 1c and d), possibly because the proliferation and differentiation status of the cells affect the actual expression level of TRPV1. This hypothesis was supported by the observation that the level of TRPV1-specific mRNA transcripts and of TRPV1 protein markedly increased in parallel with the culturing time, with TRPV1 being highest in the more ''older'' (hence possibly more differentiated) cultures (Figure 1e and f).

Capsaicin selectively inhibits basal and arachidonic acid-induced lipid synthesis of SZ95 sebocytes

One of the main hallmarks of sebocyte differentiation is the synthesis of various lipids, among which neutral lipids form a major part (Rosenfield, 1989; Thody and Shuster, 1989; Doran *et al.*, 1991, Zouboulis *et al.*, 1998). Therefore, we investigated the effect of capsaicin on the lipid content of cultured SZ95 sebocytes. Nile red staining-based quantitative fluorometric imaging plate reader (FLIPR) measurement revealed that capsaicin treatment (up to 48 hours) significantly inhibited basal synthesis of both neutral and polar lipids in a dose-dependent fashion (Figure 2a). Importantly, flow cytometry analysis showed that this effect of capsaicin was not accompanied by changes in sebocyte size or granulation (Figure 3a) the increase of which comprises further characteristics of sebocyte differentiation (Rosenfield 1989; Thody and Shuster, 1989; Zouboulis *et al.*, 1998; Sato *et al.*, 2001). Moreover, capsaicin did not induce cell death of any form (apoptosis, necrosis); namely, application of capsaicin did not significantly alter the viable cell number (3-(4,5-dimethylthiazol-2-yl)-2,5-diphenyltetrazolium bromide (MTT)-based colorimetric proliferation assay) and, did not induce necrotic (glucose-6-phophate-dehydrogenase (G6PD) release assay) or apoptotic cell death (fluorimetric measurement of the mitochondrial membrane potential, flow cytometry analysis of the number of Annexin-V/propidium iodide-positive cells; Figures 2b–d, 3b).

These data suggest that TPRV1 stimulation by capsaicin selectively modulates sebocyte lipid synthesis. As we have previously shown (Wróbel *et al.*, 2003; Alestas *et al.*, 2006), one of the most effective inducers of lipid synthesis in SZ95 sebocytes is arachidonic acid (AA). Therefore, we were also interested in whether or not capsaicin also affects AA-induced lipid formation. Capsaicin markedly and dose dependently counteracted the well-recognized effect of 50 μM AA to dramatically induce (chiefly neutral) lipid accumulation in SZ95 sebocytes (Figure 4a and b).

Our previous studies have also shown that the effect of AA to promote lipid synthesis in SZ95 sebocytes was accompanied by the induction of sebocyte apoptosis (Wróbel *et al.*, 2003). Therefore, we also investigated the action of capsaicin on the AA-induced apoptotic process. As expected, AA elevated the number of apoptotic cells (Annexin-V/propidium iodide) and suppressed the mitochondrial membrane potential (Figures 3b and 4c). In contrast to its effect on AA-stimulated lipid accumulation, capsaicin was unable to prevent the apoptosis-inducing action of AA (Figure 4c). This suggests that TRPV1 stimulation specifically targeted sebocyte lipid synthesis (Figure 4b) (note that AA did not cause necrotic cell death, Figure 4d).

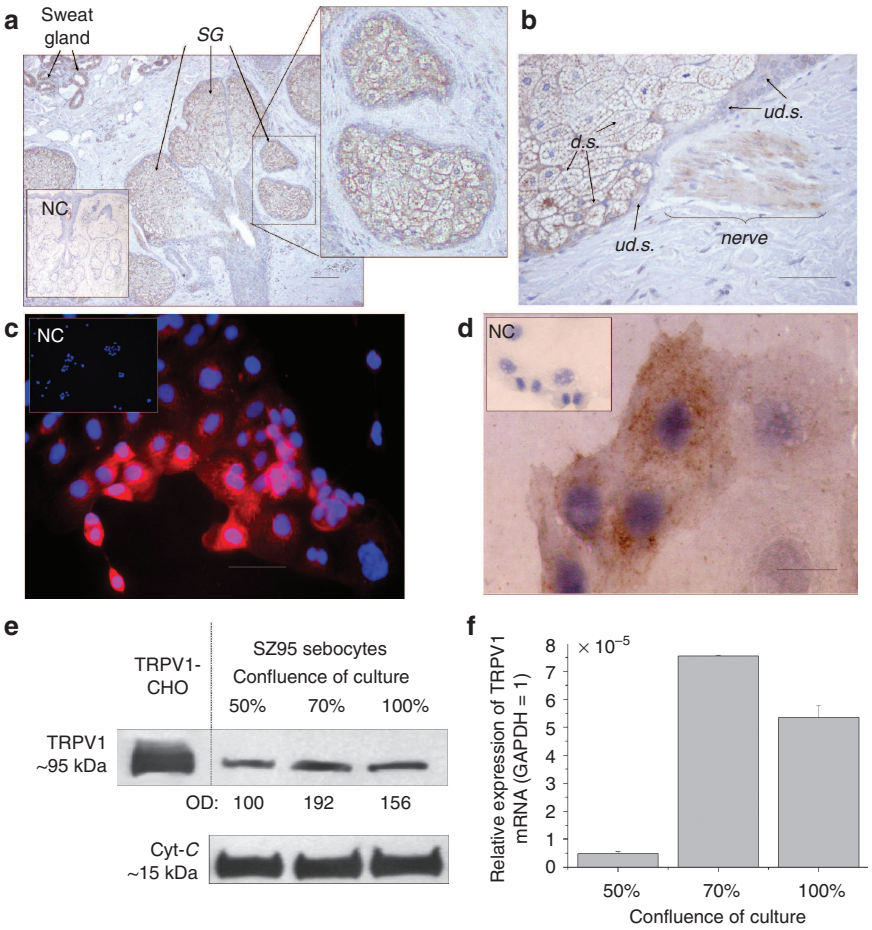

Figure 1. TRPV1 is expressed on human sebaceous gland *in situ* and on cultured human SZ95 sebocytes. (**a**, **b**) TRPV1-specific immunoreactivity (ir), as revealed by a streptavidine-biotin-complex technique, on human sebaceous gland (SG) epithelial cells *in situ*. Note that the membrane-localized TRPV1-ir is stronger on the central differentiated (d.s.) than on peripheral undifferentiated (ud.s.) sebaceous cells. As an ''internal positive control'', TRPV1-ir on a cutaneous nerve fiber is shown. NC, preabsorption negative control. (**c**, **d**) TRPV1-ir as determined by immunofluorescence (Texas red, **c**) or light microscopy (diaminobenzydine, **d**) labeling in SZ95 sebocytes. Nuclei were counterstained by DAPI (blue fluorescence, **c**) or hematoxylin (**d**). NC, preabsorption negative control. Scale bars = 200 μm (**a**), 100 μm (**b**), 60 μm (**c**), 30 μm (**d**). (**e**) Western blot analysis. TRPV1 expression was determined on cell lysates of SZ95 sebocytes harvested at various confluences. For positive controls, CHO cells overexpressing human TRPV1 were employed. Equal loading was assessed by determining expression of cytochrome *C* (Cyt-*C*). In each sample, the amount of TRPV1 was quantitated by densitometry and normalized to those of Cyt-*C* (normalized optical density, OD, values are indicated); OD value of the ''50% confluence'' sample was defined as 100%. (**f**) Q-PCR analysis of TRPV1 expression on cell lysates of SZ95 sebocytes harvested at various confluences. Data of TRPV1 expression were normalized to the level of GAPDH of the same sample and are expressed as mean ± SEM of three independent determinations. Three additional experiments yielded similar results.

The effect of capsaicin to inhibit lipid synthesis is mediated by TRPV1

On most TRPV1-expressing cell types, this receptor functions as a Ca-permeable channel (Bevan *et al.*, 1993; Caterina *et al.*, 1997; Bíró *et al.*, 1998; Birder *et al.*, 2001; Inoue *et al.*, 2002; Bodó *et al.*, 2005). Therefore, we next investigated the role of Ca in the TRPV1-mediated effects on SZ95 sebocytes. As seen in Figure 5a and b, the activity of the TRPV1 agonist to suppress basal and highly elevated, AA-induced lipid accumulation was almost completely abrogated by lowering the extracellular Ca concentration ($[Ca^{2+}]_e$) of the culturing medium (to 0.25 mM), Although changes in $[Ca^{2+}]_e$ may affect multiple cell signaling pathways, these findings proposed that the actions of capsaicin are mediated by TRPV1-specific $[Ca^{2+}]_i$ elevations.

To further investigate the issue of specificity, we then measured the effect of a specific TRPV1 antagonist, iodo-resiniferatoxin (I-RTX; Wahl *et al.*, 2001). This TRPV1 antagonist abrogated the effect of capsaicin to inhibit basal and AA-induced lipid accumulation in SZ95 cells (Figure 5c).

The TRPV1 specificity of the effect of capsaicin was further assessed by RNA interference (RNAi). Western blot and Q-PCR analysis revealed that the expression of TRPV1 was significantly ''knocked-down'' by both RNAi probes at day 2 after transfection (Figure 5d and e) and remained suppressed also on day 3 (data not shown). Scrambled RNAi probes possessed no effects on the expression of TRPV1, indicating the specificity of the procedure. Similar to the actions of I-RTX, RNAi-mediated knockdown of TRPV1 resulted in the loss of effect of capsaicin to inhibit basal and AA-evoked lipid synthesis (Figure 5f).

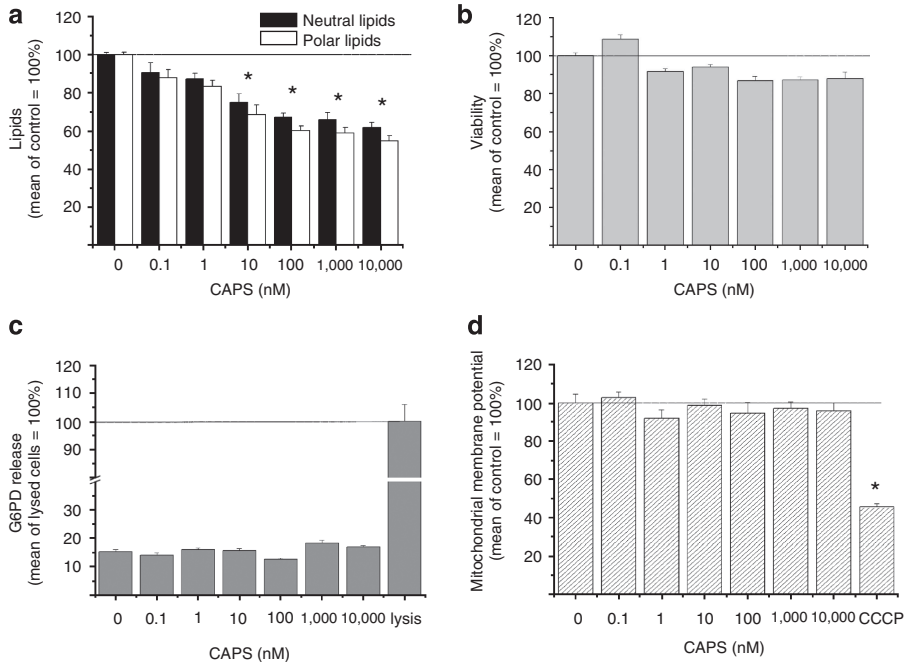

Figure 2. Capsaicin inhibits basal lipid synthesis of SZ95 sebocytes without affecting cell viability. Cells (20,000 cells per well) were cultured in 96-well black-well/clear-bottom plates in quadruplicates and were treated with various concentrations of capsaicin (CAPS) for 24 hours. (**a**) Quantitative measurement of intracellular lipids as assessed by Nile red labeling followed by FLIPR measurement. (**b**) Determination of viable cell number by colorimetric MTT assay. (**c**) Quantitative measurement of necrotic cell death by FLIPR-based G6PD release assay. (**d**) Quantitative measurement of apoptotic cell death by FLIPR-based $DiIC_1(5)$ assay reflecting mitochondrial membrane potential. Data (mean ± SEM) are expressed as a percentage of the mean value (defined as 100%) of the vehicle-treated control group (**a**, **b**, **d**) or of maximal G6PD release (induced by Triton X-100, lysis) (**c**). For positive control, that is, to induce apoptosis (and decrease mitochondrial membrane potential), 50 μM *m*-chlorophenylhydrazone (CCCP) was employed (**d**). *Significant ($P<0.05$) differences compared to the vehicle-treated control groups. Three additional experiments yielded similar results.

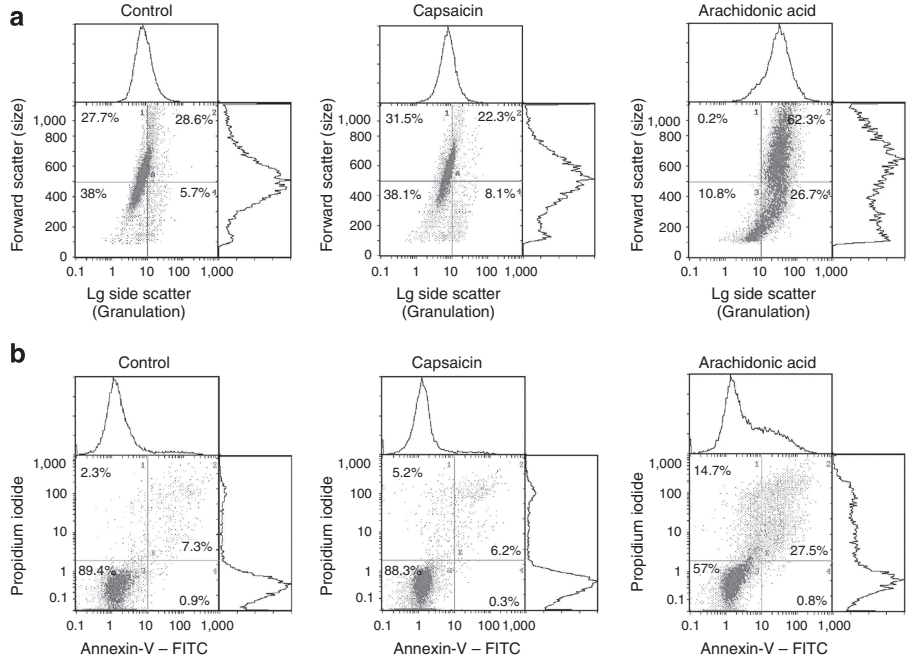

Figure 3. Unlike arachidonic acid, capsaicin does not affect size and granulation of SZ95 sebocytes, and does not induce apoptosis. (**a**) Phenotypic characterization of SZ95 sebocytes. Cells were treated by 10 μM capsaicin or 10 μM arachidonic acid (or vehicle, control) for 24 hours. Flow cytometry analysis was then performed to determine forward scatter (size) and side scatter (granulation) values. (**b**) Measurement of apoptosis. Following the above treatment, cells were harvested, stained with an Annexin-V-FITC and propidium iodide kit, and fluorescence intensity values were detected by flow cytometry. Three additional experiments yielded similar results.

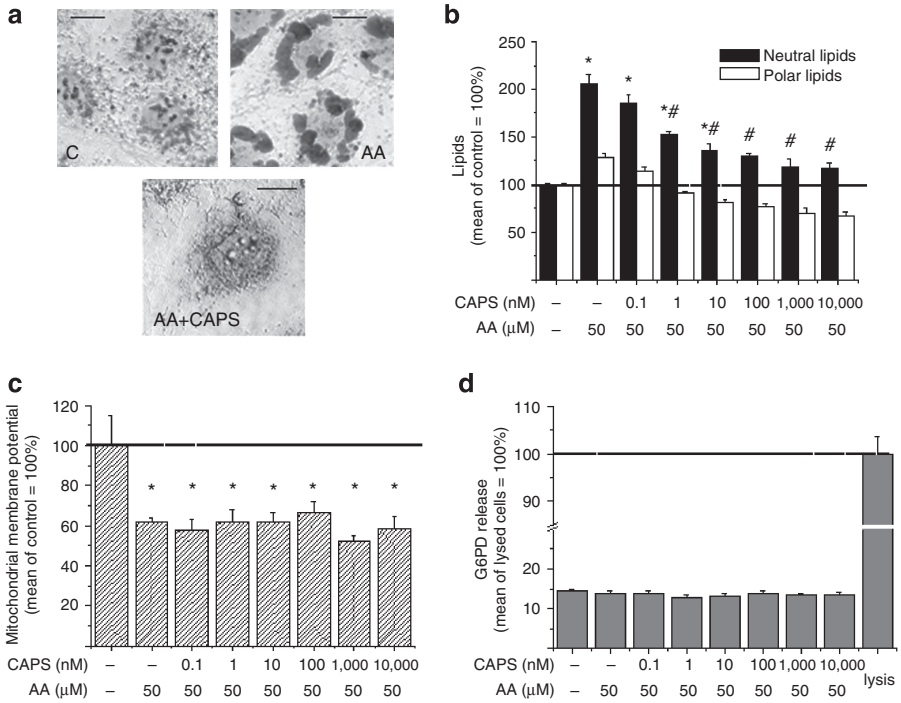

Figure 4. Capsaicin inhibits arachidonic acid-induced lipid synthesis, but not apoptosis, of SZ95 sebocytes. (**a**) Semiquantitative detection of sebaceous lipids. Cells were treated with 50 μM arachidonic acid (AA) or with 50 μM AA + 10 μM capsaicin (CAPS) for 24 hours and lipids were labeled by Oil red O solution (nuclei were counterstained with hematoxylin). Scale bars = 10 μM. (**b–d**) Cells (20,000 cells per well) were cultured in 96-well black-well/clear-bottom plates in quadruplicates and were treated with combinations of various concentrations of CAPS and 50 μM AA for 24 hours. (**b**) Quantitative measurement of intracellular lipids as assessed by Nile red labeling followed by FLIPR measurement. (**c**) Quantitative measurement of apoptotic cell death by FLIPR-based $DiIC_1(5)$ assay. (**d**) Quantitative measurement of necrotic cell death by FLIPR-based G6PD release assay. Data (mean ± SEM) are expressed as a percentage of the mean value (defined as 100%) of the vehicle-treated control group (**b**, **c**) or of maximal G6PD release (induced by Triton X-100, lysis) (**c**). *Significant ($P<0.05$) differences compared to the vehicle-treated control groups (**b**, **c**) whereas # marks the significant ($P<0.05$) differences compared to the 50 μM AA-treated control group (ie without CAPS, **b**). Three additional experiments yielded similar results.

Intriguingly, we also found that I-RTX (Figure 5c) as well as RNAi-mediated silencing of TRPV1 (Figure 5f) moderately (yet significantly) augmented the stimulatory effect of AA on lipid synthesis. Collectively, these findings suggest that the action of capsaicin was specifically mediated by TRPV1 and, furthermore, that TRPV1 may also act as an endogenous receptor channel to inhibit lipid formation of SZ95 sebocytes.

Prolonged application of capsaicin induces a biphasic alteration in cellular proliferation of SZ95 sebocytes, partly via the activation of TRPV1

Previously, we had found that capsaicin, when applied for 3–5 days, markedly inhibits the proliferation of human keratinocytes in a TRPV1-dependent fashion (Bodó *et al.*, 2005). Therefore, we also investigated the effect of long-term capsaicin application on the proliferation of SZ95 sebocytes. For this experiment, the serum content of the culture medium was decreased to 3% so as to be able to investigate both possible growth-promoting and -inhibitory actions (under these culture conditions, the SZ95 sebocytes fully survived but exhibited only an insignificant growth rate, Figure 6a).

Up to day 3, capsaicin (applied at concentrations as high as 30 μM) did not significantly alter the growth of SZ95 cells (Figure 6a). However, from day 3, higher doses (1–30 μM) of capsaicin significantly reduced the number of viable cells (Figure 6b), most probably due to the induction of necrotic cell death (SYTOX green assay; Figure 6c). However, of great importance, low doses (0.01–100 nM) of capsaicin significantly increased the viable cell number, presumably due to the stimulation of proliferation (Figure 6a and b).

We also tested whether the above, biphasic action of capsaicin on cell growth was mediated by TRPV1. First, we repeated the above experiments in low-Ca (0.25 mM) medium. As seen in Figure 6d, suppression of the $[Ca^{2+}]_e$ fully abrogated the growth-promoting effect of low capsaicin doses. In contrast, this intervention did not modify the growth-inhibitory and cytotoxic effect of (high concentrations of) the vanilloid. In good accord with these findings, the TRPV1 antagonist I-RTX completely prevented the growth-promoting action of low capsaicin concentrations (Figure 6d). However, the TRPV1 antagonist was unable to modify the effect of high capsaicin doses. These findings suggest that the growth-promoting effect of low capsaicin doses was indeed mediated by TRPV1, whereas the growth-inhibitory action of the high-dose vanilloid appeared to be receptor independent.

Capsaicin differentially alters expressions of genes involved in the regulation of lipid synthesis and of proinflammatory cytokines

Capsaicin treatment of human skin keratinocytes significantly alters the gene expression profile and the cytokine production of treated cells (Bíró *et al.*, 1998; Southall *et al.*, 2003; Bodó

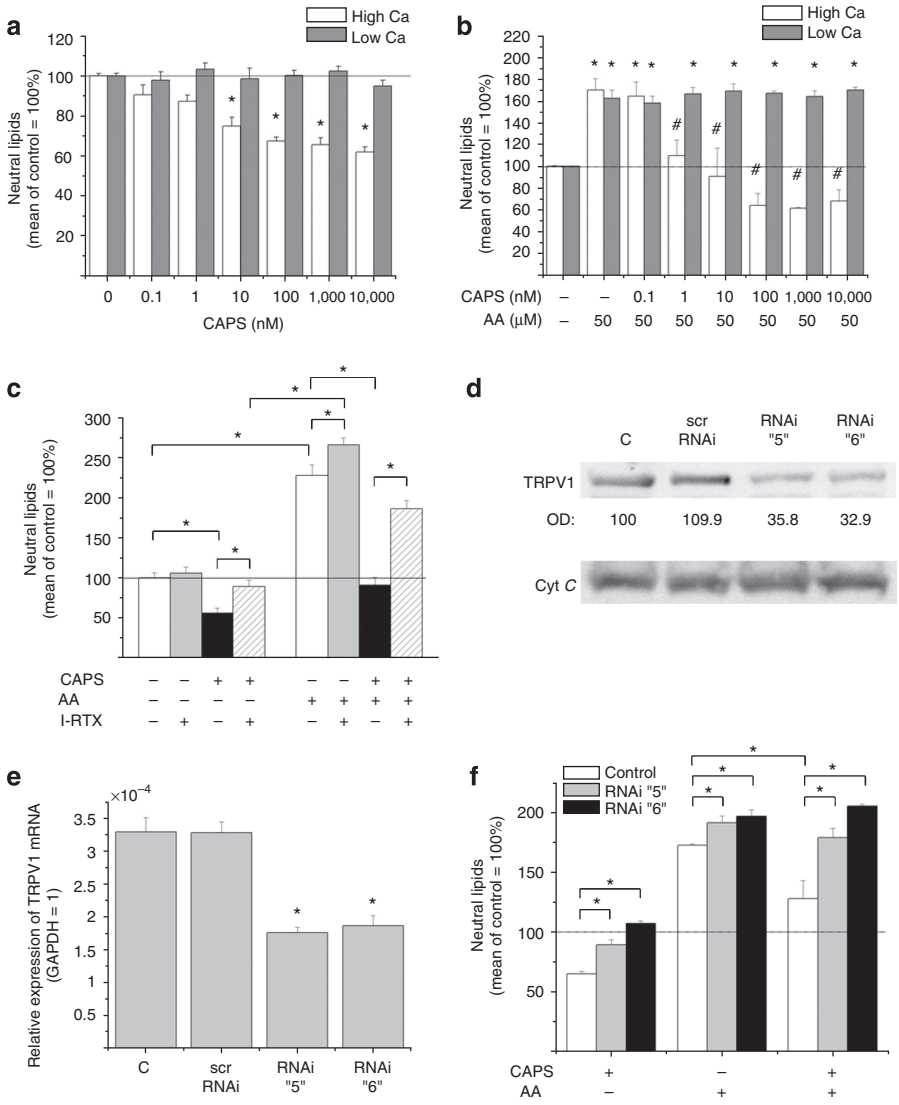

Figure 5. The effect of capsaicin to inhibit basal and arachidonic acid-induced lipid synthesis is mediated by TRPV1 and is dependent on extracellular calcium. (**a**–**c**) Quantitative measurement of intracellular lipids (following 24 hours treatment) as assessed by Nile red labeling followed by FLIPR measurement. Cells were treated for 24 hours with: (**a**) various concentrations capsaicin (CAPS) in high-Ca (2 mM) and low-Ca (0.25 mM) media; (**b**) combinations of various concentrations of CAPS and 50 μM arachidonic acid (AA) in high- and low-Ca media; (**c**) various combinations of 10 μM CAPS, 50 μM AA, and 50 nM iodo-resiniferatoxin (I-RTX) in high-Ca medium. Data (mean ± SEM) are expressed as a percentage of the mean value (defined as 100%) of the vehicle-treated control group. * Marks significant ($P<0.05$) differences compared to the vehicle-treated control groups (**a**, **b**) or between the indicated groups (**c**) whereas # marks the significant ($P<0.05$) differences compared to the 50 μM AA-treated control group (ie without CAPS, **b**). Three additional experiments yielded similar results. (**d** and **e**) Two RNAi probes against TRPV1 (indicated by numbers), as well as scrambled RNAi probes (scr), were introduced to SZ95 sebocytes (C, transfection reagent-treated control group). To evaluate the efficacy of this intervention, at days 1–3 after transfection, cells were subjected to western blot and Q-PCR analysis. (**d**) Representative western blot at day 2 after transfection. In each sample, the amount of TRPV1 was quantitated by densitometry and normalized to those of a housekeeping molecule (Cyt-*C*) (normalized optical density, OD, values are indicated), and expressed as the percentage of the OD value of the C group regarded as 100%. (**e**) Expression of TRPV1 after RNAi was also assessed by Q-PCR (panel represents data at day 2). Values of TRPV1 expression were normalized to the level of GAPDH of the same sample and are expressed as mean ± SEM of three independent determinations. *Significant ($P<0.05$) differences compared to the C group. (**f**) At day 2 after transfection, cells were treated with the indicated combinations of 10 μM CAPS and 50 μM AA for 24 hours. Intracellular lipids were then quantitatively measured by Nile red labeling followed by FLIPR measurement. Data (mean ± SEM) are expressed as a percentage of the mean value (defined as 100%) of the C group. *Significant ($P<0.05$) differences Two additional experiments yielded similar results.

et al., 2005). Therefore, we also investigated this phenomenon in SZ95 cells, concentrating on selected genes recognized to be involved in the stimulation of lipid synthesis in SZ95 sebocytes (Rosenfield *et al.*, 1999; Chen *et al.*, 2003; Trivedi *et al.*, 2006; see detailed description in Table 1 and in ''Discussion''). This was complemented by analyses of selected proinflammatory cytokines that had previously been found to be expressed by these cells (Alestas *et al.*, 2006).

As assessed by Q-PCR, the capsaicin-induced transcriptional modulation of lipid synthesis-related genes involved was markedly time dependent (Table 1). However, after 24 hours treatment (that is, the time-point at which lipid

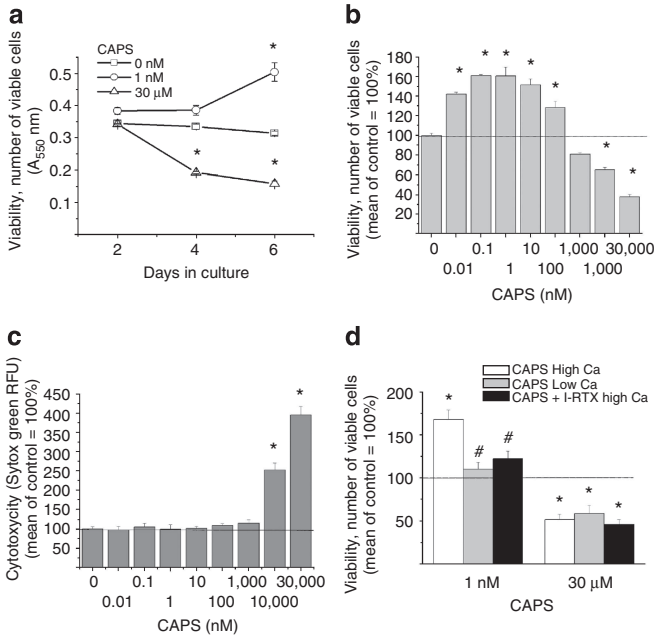

Figure 6. Prolonged application of capsaicin exerts a biphasic effect on cellular proliferation and viability of SZ95 sebocytes. (**a**) Cells (40,000 cells per well) were cultured in low serum (3%) medium in quadruplicates, treated with various concentrations of capsaicin (CAPS) for the time indicated, and the viable cell number was determined by colorimetric MTT assay. (**b**) Concentration dependence of the effect of CAPS on the viable cell number at day 6 (MTT assay). (**c**) Concentration dependence of the effect of CAPS on necrotic cell death at day 6 as assessed by quantitative FLIPR-based SYTOX green assay. (**d**) Cells were treated with various concentrations of CAPS in high-Ca (2 mM) and low-Ca (0.25 mM) media as well as combinations of various concentrations of CAPS and 50 nM iodo-resiniferatoxin (I-RTX), and MTT assay was performed at day 6. Data (mean ± SEM) are expressed as a percentage of the mean value (defined as 100%) of the vehicle-treated control group. *Significant ($P<0.05$) differences compared to the vehicle-treated control groups (**a**–**d**) whereas # marks the significant ($P<0.05$) differences compared to the 1 nM CAPS-treated control group in high-Ca medium (**d**). Three additional experiments yielded similar results.

Table 1. Effect of capsaicin treatment on gene expression of transcription factors known as stimulators of lipid synthesis (A) and on production of proinflammatory cytokines (B) in SZ95 sebocytes

	Capsaicin, 6 h (% of control)	Capsaicin, 24 h (% of control)
(A) Gene expression		
PPARα	87 ± 17	**63 ± 14**[1]
PPARγ	95 ± 11	**58 ± 16**[1]
PPARδ	123 ± 19	**51 ± 11**[1]
RXRα	103 ± 11	**54 ± 14**[1]
RXRβ	**34 ± 13**[1]	**69 ± 9**[1]
(B) Cytokine release		
IL-1β	NA	**27 ± 9**[1]
IL-6	NA	95 ± 13
TNFα	NA	106 ± 21

NA, not applicable; PPAR, peroxisome proliferator-activated receptor; RXR, retinoid X receptor; TNF, tumor necrosis factor-α.
Cells were treated with either vehicle or with 1 μM capsaicin for the times indicated. (A) Cells were then harvested and gene expression of members of the PPAR and RXR nuclear transcription factor families was determined by Q-PCR. (B) In another experimental setup, supernatants were collected, and amounts of the released IL-1β, IL-6, and TNFα were determined using specific OptEIA kits. In both cases, values of the capsaicin-treated samples were normalized as percentage of the control regarded as 100 %. Data are expressed as mean ± SEM of four independent determinations.
[1]Marks significant ($P<0.05$) differences compared to the vehicle-treated control groups.

synthesis was strongly suppressed, see above), capsaicin significantly reduced the expression of all genes that are recognized as stimulators of lipid synthesis. Interestingly, among the three proinflammatory cytokines investigated, vanilloid treatment selectively and markedly decreased the level of IL-1β (more than 70%) without affecting that of IL-6 and tumor necrosis factor-α (Table 1). These findings suggest that TRPV1-mediated-signaling pathway(s) modulate sebocyte biology also by regulating key genes of lipid synthesis and by impacting on the cytokine network of human SZ95 sebocytes.

DISCUSSION

The functional data reported here introduce TRPV1 as a significant new player in human sebocyte biology, with TRPV1-mediated signaling exerting profound, dose-dependent effects on sebocyte lipid synthesis, proliferation, cell death, gene expression, and cytokine production. Along with previous findings of our laboratories on human keratinocytes (Bodó *et al.*, 2005), this underscores the concept that TRPV1 signaling targets previously unappreciated, nonclassical mechanisms in human skin. This, in turn, suggests that the physiological functions of TRPV1 and its elusive endogenous ligands in human skin far extend beyond that of sensory neuron-coupled nociception.

Most of the actions of capsaicin studied here appeared to be mediated by TRPV1-coupled signaling. This is supported by (1) TRPV1 expression on the gene and protein level in human SZ95 sebocytes (Figure 1); (2) the inhibitory action of capsaicin on basal and AA-induced lipid synthesis (Figures 2a, 4a, b, 5a and b); (3) the effect of the TRPV1-antagonist I-RTX (Figures 5c and 6d) and the RNAi-mediated silencing of TRPV1 (Figure 5d–f). That the effects of capsaicin to inhibit lipid formation and promote cell growth were also inhibited by reducing $[Ca^{2+}]_e$ (Figures 5b and 6d) further suggests that these actions were executed by a TRPV1-mediated Ca influx—similar to what has been described for various neuronal and non-neuronal cell populations, including human keratinocytes (Bevan *et al.*, 1993; Caterina *et al.*, 1997; Bíró *et al.*, 1998; Birder *et al.*, 2001; Inoue *et al.*, 2002; Bodó *et al.*, 2005).

In addition, we also observed that capsaicin, when administered for longer durations at high concentrations, significantly inhibited proliferation and induced cell death (Figure 6), again similar to effects seen on epidermal HaCaT and hair follicle-derived keratinocytes (Bodó *et al.*,

2005). However, these effects were not modified by the TRPV1 antagonist I-RTX or by manipulating $[Ca^{2+}]_e$ (Figure 6d) suggesting a TRPV1-independent mode of action. These findings were in contrast to our previous results on various keratinocytes where the growth inhibitory action of capsaicin was mediated by TRPV1 (Bodó *et al.*, 2005). It appears, therefore, that although functional TRPV1-mediated signaling does exist on numerous cell populations of the human skin, its cellular ''consequences'' (especially in relation to regulation of cell growth) are markedly cell-type dependent.

Members of the peroxisome proliferator-activated receptor (PPAR) (Desvergne and Wahli, 1999; Kersten *et al.*, 2000) and the retinoid X receptor nuclear transcription factor families (Keller *et al.*, 1993, Berger and Moller, 2002) are recognized as key regulators of lipid homeostasis (Gregoire *et al.*, 1998; Chawla *et al.*, 2001; Nagy and Szanto, 2005, Szatmari *et al.*, 2007). With respect to sebocyte biology, PPAR ligands stimulate lipid synthesis both in animal models (Rosenfield *et al.*, 1999) and on cultured human immortalized SZ95 and SEB-1 sebocytes that express distinct PPARs (Chen *et al.*, 2003; Alestas *et al.*, 2006; Trivedi *et al.*, 2006). Therefore, our observation that capsaicin treatment downregulated the transcription of all PPARs and retinoid X receptors investigated here (Table 1) suggests that the suppression of lipid synthesis upon activation of TRPV1- and Ca-coupled signaling is mediated by decreasing the activity of the transcription factors. Consequently, these exciting data invite further, more extensive (most desirably MicroArray) experiments to define changes in the global gene expression profile in sebocytes upon vanilloid treatment (we have successfully employed this approach to identify previously unknown target genes of TRPV1 signaling in cultured human hair follicles, Bodó *et al.*, 2005).

Further intriguing results were obtained when we measured the effect of capsaicin on the action of AA, one of the key stimulators of lipid synthesis and inducer of apoptosis in sebocytes (Wróbel *et al.*, 2003; Alestas *et al.*, 2006). Previous studies have identified AA and certain of its derivatives (for example, leukotrienes) as potent endogenous ligands of TRPV1 (Hwang *et al.*, 2000; Di Marzo *et al.*, 2002). However, as shown here by several complementary assays, AA and capsaicin turned out to act in an opposite manner with respect to their modulation of sebocyte lipid synthesis (Figures 2a, 4a and b). Moreover, capsaicin treatment markedly abrogated the AA-induced lipid formation in a TRPV1- and $[Ca^{2+}]_e$-dependent manners (Figures 4a, b, 5). As AA and its metabolites also operate as potent activators for various PPARs (Devchand *et al.*, 1996; Desvergne and Wahli, 1999), it is conceivable that the inhibitory action of TRPV1 on the effect of AA is mediated (at least in part) by the capsaicin-induced downregulation of most of PPAR genes stimulating lipid formation. Furthermore, if we also take into consideration that the TRPV1 antagonist I-RTX alone as well as the RNAi-mediated silencing of TRPV1 significantly augmented AA-stimulated lipid synthesis (Figure 5c and f), TRPV1 signaling here surfaces as a previously unreported, endogenously active receptor-channel mechanism that keeps both constitutive and induced sebocyte lipid synthesis in check. (Evidently, the *in vivo* relevance of this proposal should be extensively investigated in the near future).

Besides stimulating lipid synthesis, AA and its derivatives also augment sebocyte production of a wide-array of proinflammatory cytokines (Alestas *et al.*, 2006). Therefore, the overall cellular modifications induced by AA strikingly resemble those seen in acne vulgaris, a common, multi-factorial pilosebaceous inflammatory skin disease in which lipid synthesis of sebocytes are pathologically increased (reviewed in Zouboulis *et al.*, 1998; Zouboulis, 2004; Zouboulis *et al.*, 2005). Therefore, our previously unreported findings that capsaicin (1) inhibits AA-induced lipid synthesis; (2) downregulates nuclear transcription factors that stimulate lipid accumulation; and (3) suppresses proinflammatory cytokine production (Table 1) raise the question whether insufficient TRPV1-mediated signaling contributes to acne pathogenesis (for example, by causing excess lipid production and by failing to suppresses local proinflammatory cytokine production).

Along these lines, our study will hopefully inspire one to systemically explore in future studies how certain vanilloids and the related TRPV1 signaling can be manipulated in a clinically desired manner by endogenous and/or exogenous ligands in the management of acne (and possibly other relevant sebaceous gland diseases). In these putative trials, on the one hand, prolonged stimulation of neuronal TRPV1 by, for example, topically administered capsaicin may result in the depletion of the neuropeptide content of the sensory afferents—among which substance P was shown to promote lipid synthesis of sebocytes (Toyoda and Morohashi, 2001) and was implicated in acne pathogenesis (Zouboulis, 2004)—hence indirectly suspending pathological lipid accumulation. On the other hand, as described in the current study, the additional ''chronic'' activation of TRPV1 signaling on sebocytes may directly inhibit synthesis of lipids and proinflammatory cytokines. Therefore, when applied topically, vanilloids may ''kill two birds with one stone'' to fight acne.

MATERIALS AND METHODS

Cell culturing

Human immortalized SZ95 sebocytes (Zouboulis *et al.*, 1999) were cultured in Sebomed basal medium (Biochrom, Berlin, Germany) supplemented with 10% fetal bovine serum (Invitrogen, Paisley, UK), 1 mM $CaCl_2$, 5 ng ml^{-1} human epidermal growth factor (Sigma-Aldrich, St. Louis, MO), 50 U ml^{-1} penicillin and 50 μg ml^{-1} streptomycin (both from Biogal, Debrecen, Hungary). The final Ca concentration of the medium was approximately 2 mM (high-Ca medium). The low-Ca Sebomed medium was prepared to set the Ca concentration to 0.25 mM.

Phenotypic characterization

Phenotypic characterization of SZ95 sebocytes was performed using flow cytometry by determining the forward scatter (size) and side scatter (granulation) values by a Coulter Epics XL (Beckman Coulter, Fullerton, CA) flow cytometer (Bodó *et al.*, 2005).

Determination of intracellular lipids

For semiquantitative detection of sebaceous lipids, cells were cultured on glass coverslips and treated with various compounds

for 24–48 hours. Cells were fixed in 4% paraformaldehyde, washed in 60% isopropanol (both Sigma-Aldrich), and stained in freshly prepared Oil red O solution (in 60% isopropanol; Sigma-Aldrich). Nuclei were counterstained with Mayer's hematoxylin (Sigma-Aldrich) and coverslips were mounted in mounting medium (DAKO, Glostrup, Denmark; Wróbel *et al.*, 2003).

For quantitative measurement of lipid content, cells (20,000 cells per well) were cultured in 96-well black-well/clear-bottom plates (Greiner Bio-One, Frickenhausen, Germany) in quadruplicates and were treated with compounds for 24–48 hours. Subsequently, supernatants were discarded and 100 µl of a 1 µg ml^{-1} Nile red (Sigma-Aldrich) solution in phosphate-buffered saline was added to each well. Fluorescence was measured on a Molecular Devices FlexStation^{384} II FLIPR (Molecular Devices, San Francisco, CA). Results are expressed as percentages of the relative fluorescence units in comparison with the controls using 485 nm excitation and 565 nm emission wavelengths for neutral lipids, and 540 nm excitation and 620 nm emission wavelengths for polar lipids (Alestas *et al.*, 2006).

Determination of viable cell numbers

The number of viable cells was determined by measuring the conversion of the tetrazolium salt MTT (Sigma-Aldrich) to formazan by mitochondrial dehydrogenases. Cells were plated in 96-well multi-titer plates (20,000 or 40,000 cells per well density) in quadruplicates and were cultured for 1–6 days. Cells were then incubated with 0.5 mg ml^{-1} MTT for 2 hours, and concentration of formazan crystals was determined colorimetrically according to the manufacturer's protocol (Bodó *et al.*, 2005).

Determination of apoptosis

A decrease in the mitochondrial membrane potential is one of the earliest markers of apoptosis (Green and Reed, 1998; Susin *et al.*, 1998). Mitochondrial membrane potential of SZ95 sebocytes was determined using a MitoProbe DiIC$_1$(5) Assay Kit (Invitrogen). Cells (20,000 cells per well) were cultured in 96-well black-well/clear-bottom plates (Greiner Bio-One) in quadruplicates and were treated with various compounds for the time indicated. After removal of supernatants, cells were incubated for 30 minutes with DiIC$_1$(5) working solution (30 µl per well) and the fluorescence of DiIC$_1$(5) was measured at 630 nm excitation and 670 nm emission wavelengths using the above FLIPR.

In addition, further apoptosis events were also assessed by flow cytometry according to our previous reports (Bodó *et al.*, 2005) In brief, following treatment with various agents cells were harvested and stained with an Annexin-V-FITC/Propidium Iodide Apoptosis Kit (Sigma-Aldrich) following the manufacturer's protocol. Fluorescence intensity was measured by a Coulter Epics XL (Beckman Coulter) flow cytometer.

Determination of cytotoxicity (necrosis)

Necrotic cell death was determined by measuring the G6PD release (G6PD Release Assay Kit, Invitrogen). The enzyme activity was detected by a two-step enzymatic process that leads to the reduction of resazurin into red-fluorescent resorufin. Cells (20,000 cells per well) were cultured in 96-well black-well/clear-bottom plates (Greiner Bio-One) in quadruplicates and treated with various compounds for 24 hours. A 2 × reaction medium was then prepared according to the manufacturer's protocol and added to the wells in 1:1 dilution. The fluorescence emission of resorufin was monitored by the FLIPR device at 545 excitation and 590 emission wavelengths. Results are presented as the percentage of the maximal G6PD release induced by detergent lysis of cells using undiluted Triton X-100 (Sigma-Aldrich).

As the activity of the G6PD released from necrotic cells decreases over 24 hours, the cytotoxic effect of long-term capsaicin treatment was determined by SYTOX Green staining (Invitrogen). The dye is able to penetrate (and then bind to the nucleic acids) only to necrotic cells with ruptured plasma membranes, whereas healthy cells with intact surface membranes show negligible SYTOX Green staining. Cells were cultured in 96-well black-well/clear-bottom plates (Greiner Bio-One) and treated with capsaicin up to 6 days. Supernatants were then discarded and the cells were incubated with 1 µM SYTOX Green solution. Fluorescence of SYTOX Green was measured at 490 nm excitation and 520 nm emission wavelengths using FLIPR.

Determination of cytokine release

Cells were treated in triplicates with capsaicin for 24 hours, supernatants were collected, and the released amount of IL-1β, IL-6, and tumor necrosis factor-α were determined using OptEIA kits (BD Pharmingen, Franklin Lakes, NJ) according to the manufacturer's protocol. Cytokine amount were expressed as percentage of the vehicle-treated control samples (Bíró *et al.*, 1998).

RNA interference

SZ95 sebocytes were seeded in six-well culture plates in medium lacking antibiotics. At 50–70% confluence, medium was replaced by serum-free OptiMEM (Invitrogen) and then cells were transfected with two TRPV1-specific Stealth RNAi oligonucleotides (ID, HSS111305 for no. ''5'', HSS111306 for no. ''6'', Invitrogen; 40 nM) using Lipofectamine 2000 transfection reagent (Invitrogen). For controls, RNAi Negative Control Duplexes (scrambled RNAi, Invitrogen) were employed. The efficacy of small-interfering RNA-driven ''knockdown'' was daily evaluated by Q-PCR and western blotting for 3 days (Griger *et al.*, 2007).

RNA isolation, reverse transcription, quantitative real-time PCR

Quantitative real-time PCR was performed on an ABI Prism 7000 sequence detection system (Applied Biosystems, Foster City, CA) using the 5′ nuclease assay as detailed in our previous report (Bodó *et al.*, 2005). Total RNA was isolated using TRIzol (Invitrogen) and then 3 µg of total RNA were reverse transcribed into cDNA by using 15 U of AMV reverse transcriptase (Promega, Madison, WI) and 0.025 µg µl^{-1} random primers (Promega). PCR amplification was performed by using the TaqMan primers and probes (assay ID, Hs00218912_m1 for human *TRPV1*) and the TaqMan universal PCR master mix protocol (Applied Biosystems). As internal controls, transcripts of glyceraldehyde 3-phosphate dehydrogenase were determined (assay ID, Hs99999905_m1 for human *glyceraldehyde 3-phosphate dehydrogenase*).

To detect the expression of genes involved in the regulation of lipid synthesis, individually designed TaqMan primers and probes were used: forward primer GATGACAGCGACTTGGCAA, reverse primer CTTCAATGGGCTTCACATTCA, and probe FAM-CAAACCT GGGCGGTCTCCACTGAG-TAMRA for human *PPARγ*; forward

primer AGCATCCTCACCGGCAAAG, reverse primer CCACAATGT CTCGATGTCGTG, and probe FAM-CAGCCACACGGCGCCCTT TG-TAMRA for human *PPARδ*; forward primer CATTACGGAGTC CACGCGT, reverse primer ACCAGCTTGAGTCGAATCGTT, and probe FAM-CAAACCTGGGCGGTCTCCACTGAG-TAMRA for human *PPARα*; forward primer GGCCTACTGCAAGCACAAGTA, reverse primer CAGGCGGAGCAAGAGCTTA, and probe FAM-CGAACC TTCCCGGCTGCTCTG-TAMRA for *human retinoid X receptor-α*; and a predesigned assay for *human retinoid X receptor-β* (Applied Biosystems, assay ID:Hs00232774_m1). As internal controls, transcripts of human *cyclophyllin* were determined (forward primer ACGGCGAGCCCTTGG, reverse primer TTTCTGCTGTCTTTGGGA CCT, and probe FAM-CGCGTCTCCTTTGAGCTGTTTGCA-TAMRA).

Immunohistochemistry

The study was approved by the Institutional Research Ethics Committee and adhered to Declaration of Helsinki guidelines. Normal skin samples ($n=5$; trunk, back), obtained during plastic surgery, were used as formaldehyde-fixed sections embedded in paraffin (3–5 μm thickness; Bodó *et al.*, 2004). To detect TRPV1, a streptavidine-biotin-complex three-step immunohistochemical technique (DAKO) was employed. Sections were first incubated with an anti-TRPV1 goat primary antibody against the *N* terminus of TRPV1 (1:50 dilution, Santa Cruz, Santa Cruz, CA), then with a biotin-coupled anti-goat secondary antibody (1:500, DAKO), and, finally, with streptavidine conjugated with horseradish peroxidase (1:400, DAKO). To reveal the peroxidase activity, DAB (Vector Laboratories, Burlingame, CA) was employed as a chromogene. Tissue samples were finally slightly counterstained with hematoxylin (Sigma-Aldrich) and mounted in aqueous mounting medium (DAKO).

In control experiments, specificity of TRPV1 staining was assessed by (1) omitting the primary antibody or by incubating the sections with the TRPV1 antibody preabsorbed with a synthetic blocking peptide (Santa Cruz; Figure 1a); (2) using another antibody against the C terminus of TRPV1 (Santa Cruz) that resulted in an identical staining pattern (data not shown); and (3) performing TRPV1 immunostaining on frozen skin sections from wild-type C57BL/6J and TRPV1 knockout B6.129S4-Trpv1 mice (The Jackson Laboratory, Bar Harbor, MA, data not shown; Bíró *et al.*, 2006). For positive controls, immunostaining on sections of rat spinal cord (data not shown; Bodó *et al.*, 2004) and on cutaneous nerves (''internal positive control'') was employed (Figure 1b).

Immunocytochemistry

SZ95 sebocytes, seeded and cultured on sterile coverslips in 24-well plates, were fixed in acetone, permeabilized by 0.1% Triton X-100 (Sigma-Aldrich), and then incubated with the anti-TRPV1 primary antibody (dilution 1:50). For fluorescence staining, slides were then incubated with Texas red-conjugated secondary antibodies (dilution 1:200, Vector Laboratories) and the nuclei were visualized using 46-diamidino-2-phenyl indole (Vector Laboratories). For light microscopy, after staining with the primary antibody, slides were incubated by an EnVision horseradish peroxidase-polymer-conjugated secondary antibody (DAKO) and developed by diaminobenzydine (DAKO). Nuclei were visualized using hematoxylin (Sigma-Aldrich) and mounted in aqueous mounting medium (DAKO). As negative controls, the appropriate TRPV1 antibody was either omitted from the procedure or was preincubated with a synthetic blocking peptide (Santa Cruz; Figure 1c and d; Bodó *et al.*, 2005).

Western blotting

To determine the expression of TRPV1 in SZ95 cells, the western blot technique was applied (Bíró *et al.*, 1998; Bodó *et al.*, 2004, 2005). Cell lysates were subjected to SDS–PAGE (8% gels were loaded with 60 μg protein per lane), transferred to BioBond nitrocellulose membranes (Whatman, Maidstone, UK), and then probed with the above anti-TRPV1 antibody (1:100). A horseradish peroxidase-conjugated rabbit anti-goat IgG antibody (1:1,000, Bio-Rad, Hercules CA) was used as a secondary antibody, and the immunoreactive bands were visualized by a SuperSignal West Pico Chemiluminescent Substrate enhanced chemiluminescence kit (Pierce, Rockford, IL) using LAS-3000 Intelligent Dark Box (Fuji, Tokyo, Japan). To assess equal loading, membranes were reprobed with an anti-cytochrome *C* antibody (1:50, Santa Cruz) and visualized as described above.

Statistical analysis

When applicable, data were analyzed using a two-tailed unpaired *t*-test and $P<0.05$ values were regarded as significant differences.

CONFLICT OF INTEREST

The authors state no conflict of financial interests.

ACKNOWLEDGMENTS

This work was supported in part by Hungarian Research Grants: OTKA T049231, OTKA K63153, ETT 480/2006, ETT 482/2006, RET 06/2004, and by Deutsche Forschungsgemeinschaft to RP. The SZ95 sebaceous gland cell line is protected by the patents and patent applications EP1151082, DE59913210D, AU200019804, US2002034820, CA2360762, CN1344314T, JP2002535984, IL144683D, PL350191, HU0200048, AT319813T, DK1151082T, and KR31762.

REFERENCES

Alestas T, Ganceviciene R, Fimmel S, Müller-Decker K, Zouboulis CC (2006) Enzymes involved in the biosynthesis of leukotriene B4 and prostaglandin E2 are active in sebaceous glands. *J Mol Med* 84:75–84

Berger J, Moller DE (2002) The mechanisms of action of PPARs. *Annu Rev Med* 53:409–35

Bevan SJ, Docherty RJ, Wood J (1993) Cellular mechanisms of the action of capsaicin. In: *Capsaicin in the Study of Pain* (Wood J, ed). Academic Press: New York, 27–44

Birder LA, Kanai AJ, de Groat WC, Kiss S, Nealen ML, Burke NE *et al.* (2001) Vanilloid receptor expression suggests a sensory role for urinary bladder epithelial cells. *Proc Natl Acad Sci USA* 98:13396–401

Bíró T, Bodó E, Telek A, Géczy T, Tychsen B, Kovács L *et al.* (2006) Hair cycle control by vanilloid receptor-1 (TRPV1): evidence from TRPV1 knockout mice. *J Invest Dermatol* 126:1909–12

Biró T, Ko MC, Bromm B, Wei ET, Bigliardi P, Siebenhaar F *et al.* (2005) How best to fight that nasty itch—from new insights into the neuroimmunological, neuroendocrine, and neurophysiological bases of pruritus to novel therapeutic approaches. *Exp Dermatol* 14:225–40

Bíró T, Maurer M, Modarres S, Lewin NE, Brodie C, Acs G *et al.* (1998) Characterization of functional vanilloid receptors expressed by mast cells. *Blood* 91:1332–40

Bodó E, Biró T, Telek A, Czifra G, Griger Z, Toth BI *et al.* (2005) A hot new twist to hair biology: involvement of vanilloid receptor-1 (VR1/TRPV1) signaling in human hair growth control. *Am J Pathol* 166:985–98

Bodó E, Kovács I, Telek A, Varga A, Paus R, Kovács L *et al.* (2004) Vanilloid receptor-1 (VR1) is widely expressed on various epithelial and mesenchymal cell types of human skin. *J Invest Dermatol* 123:410–3

Caterina MJ, Schumacher MA, Tominaga M, Rosen TA, Levine JD, Julius D (1997) The capsaicin-receptor: a heat-activated ion channel in the pain pathway. *Nature* 389:816–24

Chawla A, Barak Y, Nagy L, Liao D, Tontonoz P, Evans RM (2001) PPAR-gamma dependent and independent effects on macrophage-gene expression in lipid metabolism and inflammation. *Nat Med* 7:48–52

Chen W, Yang CC, Sheu HM, Seltmann H, Zouboulis CC (2003) Expression of peroxisome proliferator-activated receptor and CCAAT/enhancer binding protein transcription factors in cultured human sebocytes. *J Invest Dermatol* 121:441–7

Denda M, Fuziwara S, Inoue K, Denda S, Akamatsu H, Tomitaka A *et al.* (2001) Immunoreactivity of VR1 on epidermal keratinocyte of human skin. *Biochem Biophys Res Commun* 285:1250–2

Desvergne B, Wahli W (1999) Peroxisome proliferator-activated receptors: nuclear control of metabolism. *Endocr Rev* 20:649–88

Devchand PR, Keller H, Peters JM, Vazquez M, Gonzalez FJ, Wahli W (1996) The PPARalpha-leukotriene B4 pathway to inflammation control. *Nature* 384:39–43

Di Marzo V, Blumberg PM, Szállási Á (2002) Endovanilloid signaling in pain. *Curr Opin Neurobiol* 12:372–9

Doran TI, Baff R, Jacobs P, Pacia E (1991) Characterization of human sebaceous cells *in vitro*. *J Invest Dermatol* 96:341–8

Geppetti P, Holzer P (eds) (1996) *Neurogenic Inflammation*. CRC press: Boca Raton pp 324

Green DR, Reed JC (1998) Mitochondria and apoptosis. *Science* 281: 1309–1312

Gregoire FM, Smas CM, Sul HS (1998) Understanding adipocyte differentiation. *Physiol Rev* 78:783–809

Griger Z, Páyer E, Kovács I, Tóth IB, Kovács L, Sipka S *et al.* (2007) Protein kinase C-beta and -delta isoenzymes promote arachidonic acid production and proliferation of MonoMac-6 cells. *J Mol Med* 85: 1031–1042

Holzer P (1991) Capsaicin: cellular targets, mechanisms of action, and selectivity for thin sensory neurons. *Pharmacol Rev* 43:143–200

Hwang SW, Cho H, Kwak J, Lee SY, Kang CJ, Jung J *et al.* (2000) Direct activation of capsaicin receptors by products of lipoxygenases: endogenous capsaicin-like substances. *Proc Natl Acad Sci USA* 97: 6155–60

Inoue K, Koizumi S, Fuziwara S, Denda S, Inoue K, Denda M (2002) Functional vanilloid receptors in cultured normal human epidermal keratinocytes. *Biochem Biophys Res Commun* 291:124–9

Jancsó N (1960) Role of the nerve terminals in the mechanism of inflammatory reactions. *Bull Millard Fillmore Hosp* 7:53–77

Keller H, Dreyer C, Medin J, Mahfoudi A, Ozato K, Wahli W (1993) Fatty acids and retinoids control lipid metabolism through activation of peroxisome proliferator-activated receptor-retinoid X receptor heterodimers. *Proc Natl Acad Sci USA* 90:2160–4

Kersten S, Desvergne B, Wahli W (2000) Roles of PPARs in health and disease. *Nature* 405:421–4

Lazzeri M, Vannucchi MG, Zardo C, Spinelli M, Beneforti P, Turini D *et al.* (2004) Immunohistochemical evidence of vanilloid receptor 1 in normal human urinary bladder. *Eur Urol* 46:792–8

Li WH, Lee YM, Kim JY, Kang S, Kim S, Kim KH *et al.* (2007) Transient receptor potential vanilloid-1 mediates heat-shock-induced matrix metalloproteinase-1 expression in human epidermal keratinocytes. *J Invest Dermatol* 127:2328–35

Nagy L, Szanto A (2005) Roles for lipid-activated transcription factors in atherosclerosis. *Mol Nutr Food Res* 49:1072–4

Ost D, Roskams T, Van Der Aa F, De Ridder D (2002) Topography of the vanilloid receptor in the human bladder: more than just the nerve fibers. *J Urol* 168:293–7

Paus R, Schmelz M, Bíró T, Steinhoff M (2006) Frontiers in pruritus research: scratching the brain for more effective itch therapy. *J Clin Invest* 116:1174–86

Rosenfield RL (1989) Relationship of sebaceous cell stage to growth in culture. *J Invest Dermatol* 92:751–4

Rosenfield RL, Kentsis A, Deplewski D, Ciletti N (1999) Rat preputial sebocyte differentiation involves peroxisome proliferator-activated receptors. *J Invest Dermatol* 112:226–32

Sato T, Imai N, Akimoto N, Sakiguchi T, Kitamura K, Ito A (2001) Epidermal growth factor and 1alpha,25-dihydroxyvitamin D3 suppress lipogenesis in hamster sebaceous gland cells *in vitro*. *J Invest Dermatol* 117:965–70

Southall MD, Li T, Gharibova LS, Pei Y, Nicol GD, Travers JB (2003) Activation of epidermal vanilloid receptor-1 induces release of proinflammatory mediators in human keratinocytes. *J Pharmacol Exp Ther* 304:217–22

Ständer S, Moormann C, Schumacher M, Buddenkotte J, Artuc M, Shpacovitch V *et al.* (2004) Expression of vanilloid receptor subtype 1 in cutaneous sensory nerve fibers, mast cells, and epithelial cells of appendage structures. *Exp Dermatol* 13:129–39

Steinhoff M, Bienenstock J, Schmelz M, Maurer M, Wei E, Bíró T (2006) Neurophysiological, neuroimmunological, and neuroendocrine basis of pruritus. *J Invest Dermatol* 126:1705–18

Susin SA, Zamzami N, Kroemer G (1998) Mitochondria as regulators of apoptosis: doubt no more. *Biochem Biophys Acta* 1366:151–65

Szállási Á, Blumberg PM (1999) Vanilloid (capsaicin) receptors and mechanisms. *Pharmacol Rev* 51:159–212

Szatmari I, Torocsik D, Agostini M, Nagy T, Gurnell M, Barta E *et al.* (2007) PPAR{gamma} regulates the function of human dendritic cells primarily by altering lipid metabolism. *Blood* 110:3271–80

Szolcsányi J (1977) A pharmacological approach to elucidation of the role of different nerve fibres and receptor endings in mediation of pain. *J Physiol (Paris)* 73:251–9

Thody AJ, Shuster S (1989) Control and function of sebaceous glands. *Physiol Rev* 69:383–416

Tominaga M, Caterina MJ, Malmberg AB, Rosen TA, Gilbert H (1998) The cloned capsaicin receptor integrates multiple pain-producing stimuli. *Neuron* 21:1–20

Toyoda M, Morohashi M (2001) Pathogenesis of acne. *Med Electron Microsc* 34:29–40

Trivedi NR, Cong Z, Nelson AM, Albert AJ, Rosamilia LL, Sivarajah S *et al.* (2006) Peroxisome proliferator-activated receptors increase human sebum production. *J Invest Dermatol* 126:2002–9

Wahl P, Foged C, Tullin S, Thomsen C (2001) Iodo-resiniferatoxin, a new potent vanilloid receptor antagonist. *Mol Pharmacol* 59:9–15

Wróbel A, Seltmann H, Fimmel S, Muller-Decker K, Tsukada M, Bogdanoff B *et al.* (2003) Differentiation and apoptosis in human immortalized sebocytes. *J Invest Dermatol* 120:175–81

Zhang Q, Seltmann H, Zouboulis CC, Konger RL (2006) Involvement of PPARgamma in oxidative stress-mediated prostaglandin E(2) production in SZ95 human sebaceous gland cells. *J Invest Dermatol* 126:42–8

Zouboulis CC (2004) Acne and sebaceous gland function. *Clin Dermatol* 22:360–6

Zouboulis CC, Bohm M (2004) Neuroendocrine regulation of sebocytes—a pathogenetic link between stress and acne. *Exp Dermatol* 13(Suppl 4):31–5

Zouboulis CC, Eady A, Philpott M, Goldsmith LA, Orfanos C, Cunliffe WC *et al.* (2005) What is the pathogenesis of acne? *Exp Dermatol* 14:143–52

Zouboulis CC, Seltmann H, Hiroi N, Chen W, Young M, Oeff M *et al.* (2002) Corticotropin-releasing hormone: an autocrine hormone that promotes lipogenesis in human sebocytes. *Proc Natl Acad Sci USA* 99:7148–53

Zouboulis CC, Seltmann H, Neitzel H, Orfanos CE (1999) Establishment and characterization of an immortalized human sebaceous gland cell line (SZ95). *J Invest Dermatol* 113:1011–20

Zouboulis CC, Xia L, Akamatsu H, Seltmann H, Fritsch M, Hornemann S *et al.* (1998) The human sebocyte culture model provides new insights into development and management of seborrhoea and acne. *Dermatology* 196:21–31

V.

FEBS Letters 583 (2009) 1619–1624

FEBS Letters

journal homepage: www.FEBSLetters.org

Transient receptor potential vanilloid-1 signaling inhibits differentiation and activation of human dendritic cells

Balázs I. Tóth [a,1], Szilvia Benkő [b,1], Attila G. Szöllősi [a], László Kovács [a], Éva Rajnavölgyi [b], Tamás Bíró [a,*]

[a] Department of Physiology, University of Debrecen, Medical and Health Science Center, Research Center for Molecular Medicine, 4032 Debrecen, Nagyerdei krt. 98, P.O. Box 22, Hungary
[b] Department of Immunology, University of Debrecen, Medical and Health Science Center, Research Center for Molecular Medicine, 4032 Debrecen, Hungary

ARTICLE INFO

Article history:
Received 8 January 2009
Revised 31 March 2009
Accepted 20 April 2009
Available online 4 May 2009

Edited by Bing Sun

Keywords:
Transient receptor potential vanilloid-1
Human dendritic cell
Differentiation
Cytokine release
Anti-inflammatory

ABSTRACT

The goal of the current study was to investigate the expression of transient receptor potential vanilloid-1 (TRPV1) on human in vitro differentiated monocyte-derived dendritic cells (DCs) and to dissect the corresponding role of TRPV1-signaling in DC-specific functions. TRPV1 expression was identified both at the protein and gene levels in human DCs. Moreover, the prototypic TRPV1 agonist capsaicin specifically (i.e. via TRPV1) and dose-dependently inhibited cytokine-induced DC differentiation, phagocytosis of bacteria, activation of DCs, and pro-inflammatory cytokine secretion. These data introduce TRPV1-coupled signaling as a novel player in human monocyte-derived DC biology with anti-inflammatory actions.

1. Introduction

Capsaicin, the pungent ingredient of the hot chili peppers, induces a "multiple response" of pain, desensitization, neurotoxicity, and neurogenic inflammation [1]. These effects were exclusively attributed to the action of capsaicin on nociceptive sensory neurons expressing transient receptor potential vanilloid-1 (TRPV1, the "capsaicin receptor"), a non-selective, calcium-permeable ion channel [2]. Via activation of TRPV1, capsaicin was shown to induce neuropeptide release from the sensory afferents, which in turn, initiates vasodilation, flare, and edema [1].

However, several workgroups have also shown that TRPV1-coupled cellular mechanisms not only initiate neurogenic responses but the receptor may also mediate protective anti-inflammatory processes in certain inflammatory/allergic animal models [3,4]. Moreover, emerging recent evidence also suggest that TRPV1 is expressed in various non-neuronal cell types as well, including those involved in inflammation. Indeed, TRPV1 and capsaicin-induced signaling mechanisms were described on polymorphonuclear leukocytes, mast cells, and macrophages [5–7], and were shown to be involved both in pro-inflammatory (e.g. stimulation of the synthesis and release of a wide array of cytokines and growth factors) [5,8] as well as anti-inflammatory (e.g. inhibition of NO synthase, inactivation of NF-κB) [6,9,10] cellular responses.

Dendritic cells (DCs) represent a subset of professional antigen-presenting cells which are able to capture and process antigens, secrete cytokines and, following activation, migrate to lymph nodes and activate various lymphocyte subsets. Hence, DCs act as central players in the orchestration of tolerogenic and inflammatory immune responses [11,12].

Intriguingly, we possess limited and rather controversial data on the expression and function of TRPV1 on DCs. Using mouse bone-marrow derived DCs, Basu and Srivastava [13] have shown that the activation of TRPV1 induces maturation and activation of DCs, which results in the engagement of various immune functions. Conversely, others [14] were unable to detect the molecular or functional expression of TRPV1 on these cell types.

With respect to *human* DCs, we have identified TRPV1 on Langerhans cells of the human skin in situ [15]. However, we lack data on the functional existence of TRPV1 on human DCs. Therefore, in the current study, we have investigated the effects of capsaicin on human in vitro cultured monocyte-derived DCs, and have dissected the corresponding role of TRPV1-signaling in DC functions.

* Corresponding author. Fax: +36 52 432 289.
E-mail address: biro@phys.dote.hu (T. Bíró).
[1] BIT and SzB contributed equally to this work.

0014-5793/$36.00
doi:10.1016/j.febslet.2009.04.031

2. Materials and methods

2.1. DC cultures

Monocytes were isolated from buffy coats by immunomagnetic cell separation using anti-CD14-conjugated microbeads (Miltenyi Biotech, Bergisch Gladbach, Germany) [16]. To induce the differentiation of immature DCs (iDCs), monocytes were cultured in AIMV medium (Invitrogen, Paisley, UK) supplemented with 80 ng/ml GM-CSF and 100 ng/ml IL-4 (both from Peprotech, London, UK). At day 2, the same amount of GM-CSF and IL-4 was added and the cells were cultured for another 3 days. To generate matured DCs (mDCs), iDCs were activated for 24 h with a "pro-inflammatory cytokine cocktail" containing 80 ng/ml GM-CSF, 10 ng/ml TNF-α, 5 ng/ml IL-1β, 20 ng/ml IL-6 (all from Peprotech), and 1 μg/ml PGE_2 (Sigma–Aldrich, St. Louis, MO).

2.2. Flow cytometry

Phenotypic characterization of DCs was performed by flow cytometry using different fluorochrome-conjugated antibodies: CD83-FITC and CD14-PE (Beckman Coulter, Hialeah, FL); CD209/DC-SIGN-FITC (BD Pharmingen, San Diego, CA); CCR7-PE (R&D Systems, Minneapolis, MN) as described before [16] by a FACSCalibur flow cytometer (BD Biosciences Immunocytometry Systems, Franklin Lakes, NJ).

2.3. Immunocytochemistry

Acetone-fixed DCs were immunolabeled using a rabbit anti-TRPV1 primary antibody (1:200, Sigma–Aldrich) and a FITC-conjugated secondary antibody (1:200, Vector Laboratories, Burlingame, CA) as described before [17].

2.4. Western blotting

To determine the expression of TRPV1 in DCs at various stages of differentiation, the Western blot technique was applied as we have described before [5,15,17,18].

2.5. Ca^{2+}-imaging

The functionality of TRPV1 as a Ca^{2+}-permeable channel was assessed by fura-2-based Ca^{2+}-imaging as described in our earlier reports [19] using a dual wavelength monochromator system (Deltascan, Photon Technology International, New Brunswick, NJ).

2.6. Determination of viable cell numbers

The number of viable cells was determined by using the MTT based colorimetric EZ4U proliferation assay (Biomedica, Vienna, Austria) as described before [17–19].

2.7. Determination of apoptosis

A decrease in the mitochondrial membrane potential is one of the earliest signs of apoptosis. To assess the process mitochondrial membrane potential of DCs was determined by a Fluorescence Image Plate Reader (FLIPR, FlexStation^{384} II, Molecular Devices, San Francisco, CA) platform using a MitoProbe $DiIC_1(5)$ Assay Kit (Invitrogen) as described before [17,18].

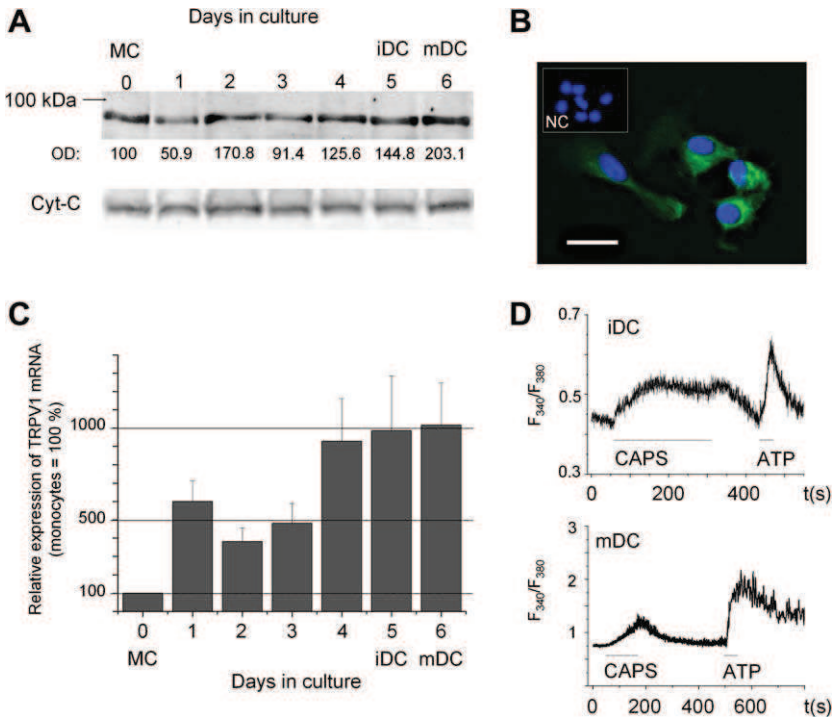

Fig. 1. TRPV1 is expressed on human monocyte-derived DCs. (A) Western blot analysis of TRPV1 on monocytes (MC), iDCs, and mDCs. Equal loading was assessed by determining expression of cytochrome C (Cyt-C). In each sample, the amount of TRPV1 was quantitated by densitometry and normalized to those of Cyt-C (normalized optical density values, OD). (B) TRPV1-immunoreactivity on iDCs as determined by immunofluorescence (FITC, green). Nuclei were counterstained by DAPI (blue). Inset, pre-absorption negative control (NC). Bar, 20 μm. (C) Q-PCR analysis of TRPV1 expression. Data of TRPV1 expression were normalized to the level of GAPDH of the same sample and are expressed as mean ± S.E.M. (n = 3–7). (D) Ca^{2+}-imaging on fura 2-loaded iDCs and mDCs. Fluorescence ratio (F_{340}/F_{380}) values of excitations at 340 and 380 nm wavelengths were recorded. The figure is a representative of multiple determinations and shows the effect of 1 μM capsaicin and 180 μM ATP (used as a positive control).

2.8. Determination of cytotoxicity (necrosis)

As described before [17,18], necrotic cell death was determined by assessing Sytox Green staining (Invitrogen) which dye is able to penetrate (and then bind to the nucleic acids) only the necrotic cells with ruptured plasma membranes.

2.9. Determination of phagocytotic activity

Phagocytosis was measured by the uptake of FITC-labeled *Escherichia coli* bioparticles by the DCs using a Vybrant™ Phagocytosis Assay Kit (Invitrogen) following the manufacturer's protocol. The fluorescence intensity values were measured by FLIPR.

2.10. Quantitative real-time PCR (Q-PCR)

RNA was isolated from cells using TRIzol (Invitrogen) and Q-PCR was performed on an ABI Prism 7000 sequence detection system (Applied Biosystems, Foster City, CA) using TaqMan primers and probes as described before [17–19].

2.11. ELISA

The production of various cytokines was assessed by specific ELISA kits (BD Pharmingen) as described before [16,17].

2.12. Statistical analysis

When applicable, data were analyzed using a two-tailed un-paired *t*-test and $P < 0.05$ values were regarded as significant differences.

3. Results and discussion

3.1. TRPV1-signaling inhibits DC differentiation

First, we measured the existence of TRPV1 on monocyte-derived DCs. Using complementary techniques, here we provide the first evidence that both human peripheral blood monocytes as well iDCs (and mDCs, see further details below) express TRPV1 at the gene and protein levels (Fig. 1A–C). The existence of TRPV1 was further verified by Ca^{2+}-imaging revealing that this Ca^{2+}-permeable channel is indeed functional on iDCs and mDCs (Fig. 1D). Of further importance, we also found that TRPV1 expression dramatically increased during the cytokine-induced in vitro differentiation of monocytes to iDCs (Fig. 1A and C). It appears, therefore, that human monocyte-derived DCs now "join" the emerging group of various non-neuronal *human* cell populations (including inflammatory and immune cells) on which the expression of functional TRPV1 was unambiguously identified [5,13,15,17,19].

We then investigated the effect of the functional TRPV1 agonist capsaicin. Long-term application (for 5 days from day 0) of capsaicin (even up to extremely high 50 μM concentration, data not shown) did not induce the in vitro differentiation of human peripheral monocytes to iDCs as monitored by DC-SIGN expression (Fig. 2A and B). Likewise, capsaicin did not significantly alter the viable cell number nor did it induce cell death of any form (Fig. 2C). These data were in a marked contrast to those seen on sensory neurons and on most of the TRPV1-expressing non-neuronal cells where capsaicin induced a massive, mostly Ca^{2+}-dependent cytotoxicity [1–3,17,19]. Apparently, the Ca^{2+}-handling

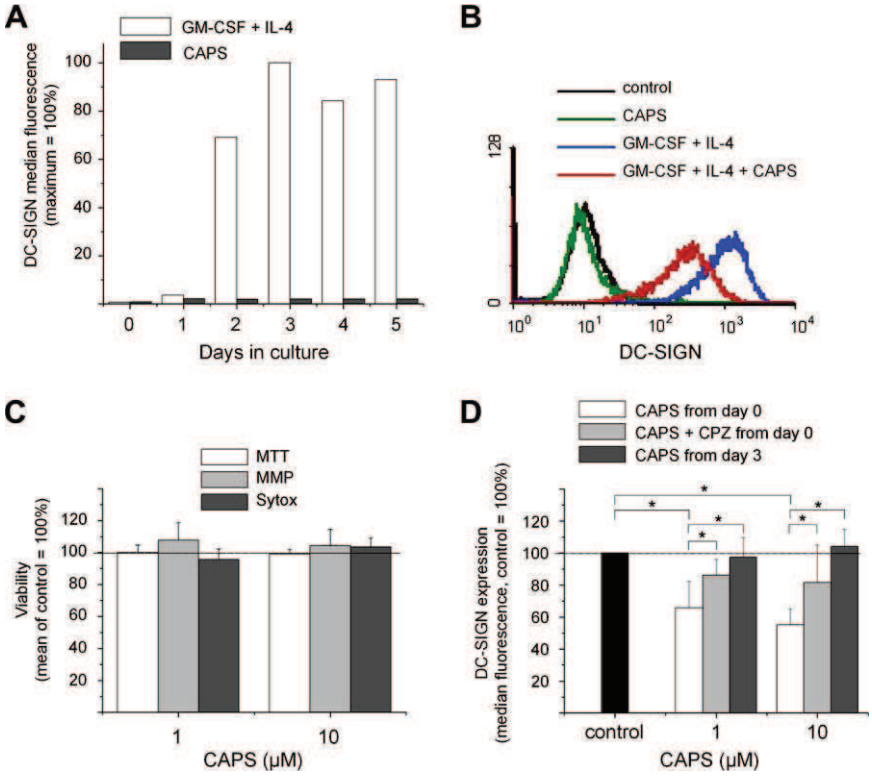

Fig. 2. Capsaicin inhibits differentiation of iDCs. (A) Flow cytometry analysis of DC-SIGN expression on monocytes and differentiating iDCs tested daily during differentiation. Median fluorescence of the maximal intensity was defined as 100%. Panel shows the effect of 10 μM capsaicin (CAPS) and 80 ng/ml GM-CSF + 100 ng/ml IL-4 on a representative donor. Three-five additional experiments yielded similar results. (B) Flow cytometry analysis of DC-SIGN expression at day 5 of differentiation. The figure is a representative of multiple determinations on independent donors. (C) FLIPR assays assessing viability (MTT), apoptosis (mitochondrial membrane potential, MMP) and necrosis (Sytox green accumulation) at day 5 of differentiation. Data represent mean ± S.E.M. of four independent determinations and values of iDCs without capsaicin were defined as 100%. (D) Flow cytometry analysis of DC-SIGN expression on iDCs differentiated by cytokines in the presence of capsaicin (CAPS) from day 0 or 3, and of 5 μM capsazepine (CPZ). Data represent mean ± S.E.M. of three independent experiments and values of iDCs without capsaicin were defined as 100%. $^{*}P < 0.05$.

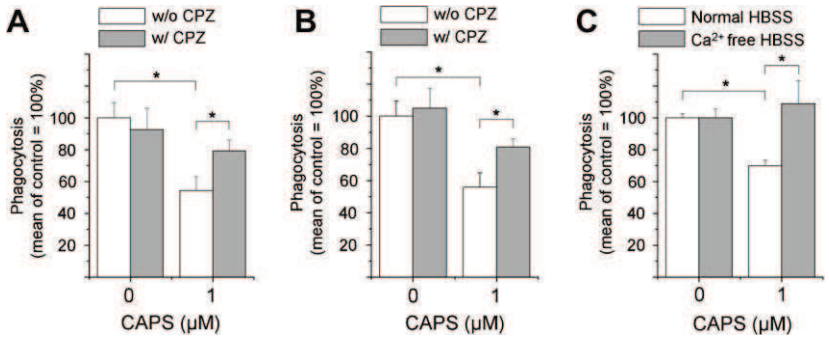

Fig. 3. Capsaicin inhibits phagocytosis of iDCs. (A) Phagocytotic activity of iDCs differentiated for 5 days by cytokines in the presence of capsaicin (CAPS) and 5 μM capsazepine (CPZ) applied daily. (B) Phagocytotic activity of iDCs treated with CAPS and CPZ for 2 h at day 5. (C) Effect of CAPS on phagocytotic activity of iDCs in normal (1.2 mM Ca^{2+}) and Ca^{2+} free Hank's Balanced Salt Solution (HBSS). In each panel, data represent mean ± S.E.M. of four independent determinations and mean values of the untreated groups were defined as 100%. $^{*}P < 0.05$.

mechanisms of the DCs are sufficient to "eliminate" the unwanted cellular effects of the TRPV1-mediated Ca^{2+}-influx.

However, of great importance, capsaicin markedly inhibited the cytokine-induced (IL-4 and GM-CSF) differentiation of iDCs (expressions of DC-SIGN, CD11c, HLA-DR) (Fig. 2B and D, Supplementary Fig. S1). This effect was most probably mediated by TRPV1 since the antagonist capsazepine (5 μM) [20] effectively prevented the action of capsaicin to suppress DC-SIGN expression (Fig. 2D). Of further importance, these effects of capsaicin were only observed when TRPV1 stimulation was employed daily from day 0 of

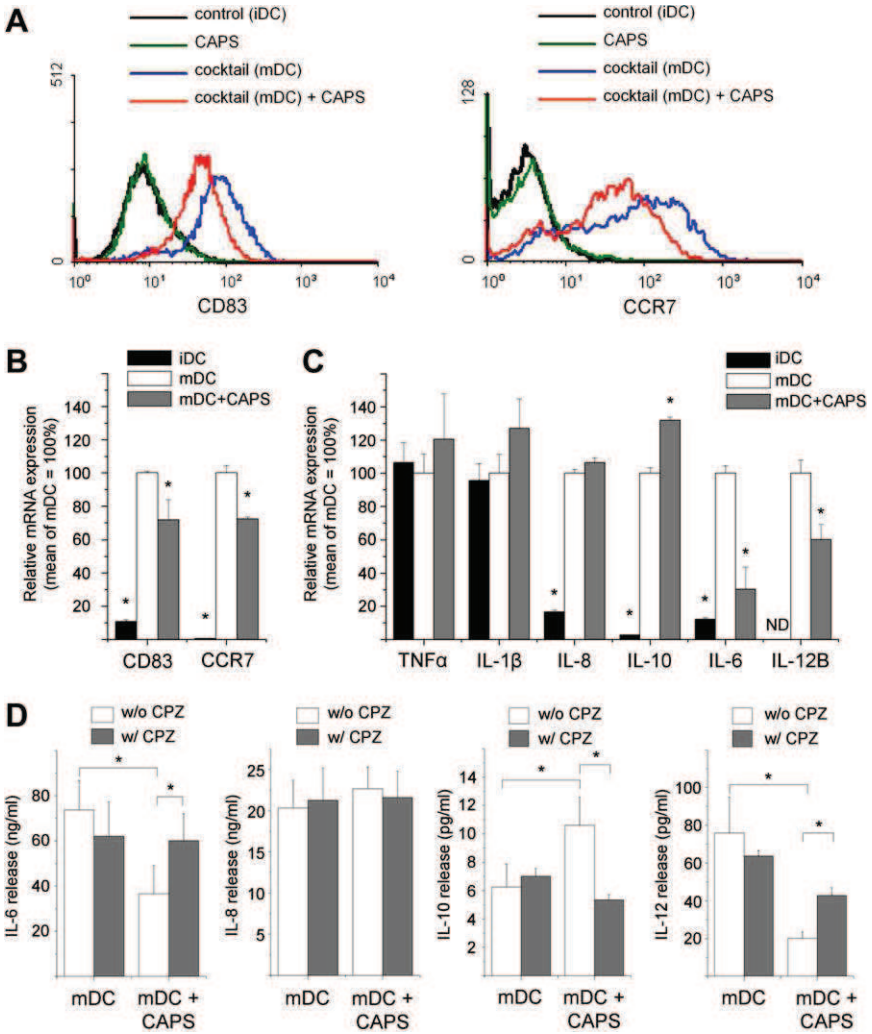

Fig. 4. Capsaicin inhibits maturation, activation, and migration of mDCs iDCs were treated for 24 h by a "pro-inflammatory cytokine cocktail" (to induce mDCs), 1 μM capsaicin (CAPS), 5 μM capsazepine (CPZ), or combination. (A) Flow cytometry analysis of CD83 and CCR7 maturation markers on DCs. (B and C) Q-PCR analysis of CD83 and CCR7 (B) and selected cytokines (C). Data were normalized to the level of GAPDH of the same sample and are expressed as mean ± S.E.M. of three independent determinations. Expressions on mDCs were defined as 100%. ND, not detectable. (D) Secretion of selected cytokines measured by ELISA. Data represent mean ± S.E.M. of three independent determinations. $^{*}P < 0.05$.

culturing; in fact, when applied from day 3, the TRPV1 agonist was ineffective in modifying the differentiation of iDCs (Fig. 2D). This latter finding suggests that the specific TRPV1-signaling interferes with the early events of DC differentiation; hence, when monocytes are already committed to the DC lineage, the activation of the existing TRPV1 cannot impede the process.

Another characteristic of iDCs is the capability of phagocytosis [11,12,16]; hence, we also investigated the involvement of TRPV1-signaling in this process. As assessed by *E. coli*-FITC internalization FLIPR analysis, in those cells which were treated by IL-4 and GM-CSF in the presence of capsaicin from day 0 for 5 days (i.e. during the "regular" iDC differentiation process), the phagocytotic activity was significantly suppressed (Fig. 3A). In addition, we also found that the co-application of capsazepine prevented the action of prolonged capsaicin administration to suppress phagocytosis (Fig. 3A) again arguing for the TRPV1-specificity of the effect of capsaicin.

We then measured the effect of "acute" application of capsaicin on the phagocytosis of the iDCs. As seen in Fig. 3B and C, as short as 2 h capsaicin treatment significantly inhibited the phagocytotic activity. Moreover, we also found that both capsazepine as well as the suppression of extracellular Ca^{2+}-concentration abrogated this effect, again suggesting that (i) the capsaicin-induced inhibition of phagocytosis was mediated by TRPV1; and (ii) TRPV1 indeed functions as a Ca^{2+}-permeable channel on iDCs.

3.2. TRPV1-signaling inhibits DC activation and maturation

As seen in Fig. 1, the expression of TRPV1 found on iDCs remained substantially high when the maturation of iDCs to mDCs was induced by a "pro-inflammatory cytokine cocktail" applied for 24 h. Therefore, we also assessed the role of TRPV1 in the maturation and activation of iDCs. In contrast to results obtained with mouse DCs [13], capsaicin alone (i.e. without a "pro-inflammatory cytokine cocktail") failed to induce the maturation of iDCs to mDCs as measured by assessing the expression of the mDC markers CD83 and CCR7 [11,12,16] (Fig. 4A). Likewise, capsaicin did not promote the release of selected pro-inflammatory cytokines (data not shown), an indicator of activation of DCs [11,12,16].

Intriguingly, the "pro-inflammatory cytokine cocktail" induced overexpression of CD83 and CCR7 (as well as their highly elevated mRNA transcript level) was significantly suppressed by capsaicin in a TRPV1-specific manner (Fig. 4A and B). Likewise, capsaicin also decreased the expression of HLA-DR as well as other co-stimulatory molecules (CD40, CD80, and CD86) induced by the pro-inflammatory cocktail (Supplementary Fig. S2). Moreover, capsaicin, via TRPV1, significantly yet differentially inhibited the action of the "cocktail" to stimulate the production and release of selected cytokines (Fig. 4C and D). Namely, capsaicin did not affect the highly elevated synthesis of the pro-inflammatory IL-8 whilst it effectively inhibited the production and release of IL-6 and IL-12 of mDCs. Intriguingly, capsaicin further stimulated the synthesis and release of the rather anti-inflammatory IL-10. It appears, therefore, that TRPV1-mediated signaling, similar to findings on other cell types [5,17], differentially affects the cytokine profile of the cells.

3.3. Concluding remarks

Collectively, the above data introduce TRPV1 as a novel player in human monocyte-derived DC biology. Moreover, our findings obtained on in vitro cultured cells suggest that the functional TRPV1 expressed on DCs exhibits anti-inflammatory properties since it inhibited the differentiation, maturation, phagocytosis, and (selected) pro-inflammatory cytokine production of the DCs. Further studies are therefore warranted to define the putative cross-talk between the sensory neuron- and the DC-localized TRPV1-coupled signaling mechanisms in the regulation of the immune-inflammatory responses of a given tissue. Likewise, it should also be explored (most preferably in clinical trials) how and to what extent the DC-localized TRPV1-mediated cellular actions are involved in (or can be engaged to) the in vivo anti-inflammatory effects of TRPV1-acting agents.

Acknowledgments

This work was supported in part by Hungarian Research Grants: OTKA T049231, OTKA K63153, ETT 480/2006, ETT 482/2006, and RET 06/2004. Tamás Bíró is a recipient of the János Bolyai Research Scholarship of the Hungarian Academy of Sciences.

Appendix A. Supplementary data

Supplementary data associated with this article can be found, in the online version, at doi:10.1016/j.febslet.2009.04.031.

References

[1] Szallasi, A. and Blumberg, P.M. (1999) Vanilloid (Capsaicin) receptors and mechanisms. Pharmacol. Rev. 51, 159–212.
[2] Caterina, M.J., Schumacher, M.A., Tominaga, M., Rosen, T.A., Levine, J.D. and Julius, D. (1997) The capsaicin receptor: a heat-activated ion channel in the pain pathway. Nature 389, 816–824.
[3] Szolcsányi, J. (2004) Forty years in capsaicin research for sensory pharmacology and physiology. Neuropeptides 38, 377–384.
[4] Bánvölgyi, A., Pálinkás, L., Berki, T., Clark, N., Grant, A.D., Helyes, Z., Pozsgai, G., Szolcsányi, J., Brain, S.D. and Pintér, E. (2005) Evidence for a novel protective role of the vanilloid TRPV1 receptor in a cutaneous contact allergic dermatitis model. J. Neuroimmunol. 169, 86–96.
[5] Bíró, T., Maurer, M., Modarres, S., Lewin, N.E., Brodie, C., Ács, G., Ács, P., Paus, R. and Blumberg, P.M. (1998) Characterization of functional vanilloid receptors expressed by mast cells. Blood 91, 1332–1340.
[6] Chen, C.W., Lee, S.T., Wu, W.T., Fu, W.M., Ho, F.M. and Lin, W.W. (2003) Signal transduction for inhibition of inducible nitric oxide synthase and cyclooxygenase-2 induction by capsaicin and related analogs in macrophages. Br. J. Pharmacol. 140, 1077–1087.
[7] Wang, J.P., Tseng, C.S., Sun, S.P., Chen, Y.S., Tsai, C.R. and Hsu, M.F. (2005) Capsaicin stimulates the non-store-operated Ca^{2+} entry but inhibits the store-operated Ca^{2+} entry in neutrophils. Toxicol. Appl. Pharmacol. 209, 134–144.
[8] Southall, M.D., Li, T., Gharibova, L.S., Pei, Y., Nicol, G.D. and Travers, J.B. (2003) Activation of epidermal vanilloid receptor-1 induces release of proinflammatory mediators in human keratinocytes. J. Pharmacol. Exp. Ther. 304, 217–222.
[9] Sancho, R., Lucena, C., Macho, A., Calzado, M.A., Blanco-Molina, M., Minassi, A., Appendino, G. and Munoz, E. (2002) Immunosuppressive activity of capsaicinoids: capsiate derived from sweet peppers inhibits NF-κB activation and is a potent antiinflammatory compound in vivo. Eur. J. Immunol. 32, 1753–1763.
[10] Kim, C.S., Kawada, T., Kim, B.S., Han, I.S., Choe, S.Y., Kurata, T. and Yu, R. (2003) Capsaicin exhibits anti-inflammatory property by inhibiting IkB-a degradation in LPS-stimulated peritoneal macrophages. Cell. Signal. 15, 299–306.
[11] Banchereau, J. and Steinman, R.M. (1998) Dendritic cells and the control of immunity. Nature 392, 245–252.
[12] Shortman, K. and Liu, Y.J. (2002) Mouse and human dendritic cell subtypes. Nat. Rev. Immunol. 2, 151–161.
[13] Basu, S. and Srivastava, P. (2005) Immunological role of neuronal receptor vanilloid receptor 1 expressed on dendritic cells. Proc. Natl. Acad. Sci. USA 102, 5120–5125.
[14] O'Connell, P.J., Pingle, S.C. and Ahern, G.P. (2005) Dendritic cells do not transduce inflammatory stimuli via the capsaicin receptor TRPV1. FEBS Lett. 579, 5135–5139.
[15] Bodó, E., Kovács, I., Telek, A., Varga, A., Paus, R., Kovács, L. and Bíró, T. (2004) Vanilloid receptor-1 (VR1) is widely expressed on various epithelial and mesenchymal cell types of human skin. J. Invest. Dermatol. 123, 410–413.
[16] Gogolák, P., Réthi, B., Szatmári, I., Lányi, Á., Dezső, B., Nagy, L. and Rajnavölgyi, É. (2007) Differentiation of CD1a− and CD1a+ monocyte-derived dendritic cells is biased by lipid environment and PPARgamma. Blood 109, 643–652.
[17] Tóth, B.I., Géczy, T., Griger, Z., Dózsa, A., Seltmann, H., Kovács, L., Nagy, L., Zouboulis, C.C., Paus, R. and Bíró, T. (2008). Transient receptor potential vanilloid-1 signaling as a regulator of human sebocyte biology, J. Invest. Dermatol. Epub ahead, doi: 10.1038/jid.2008.258.
[18] Dobrosi, N., Tóth, B.I., Nagy, G., Dózsa, A., Géczy, T., Nagy, L., Zouboulis, C.C., Paus, R., Kovács, L. and Bíró, T. (2008) Endocannabinoids enhance lipid synthesis and apoptosis of human sebocytes via cannabinoid receptor-2-mediated signaling. FASEB J. 22, 3685–3695.

[19] Bodó, E., Bíró, T., Telek, A., Czifra, G., Griger, Z., Tóth, B.I., Mescalchin, A., Ito, T., Bettermann, A., Kovács, L. and Paus, R. (2005) A hot new twist to hair biology: involvement of vanilloid receptor-1 (VR1/TRPV1) signaling in human hair growth control. Am. J. Pathol. 166, 985–998.

[20] Bevan, S., Hothi, S., Hughes, G., James, I.F., Rang, H.P., Shah, K., Walpole, C.S. and Yeats, J.C. (1992) Capsazepine: a competitive antagonist of the sensory neurone excitant capsaicin. Br. J. Pharmacol. 107, 544–552.

VI.

CMLS, Cell. Mol. Life Sci. 60 (2003) 2228–2240
1420-682X/03/102228-13
DOI 10.1007/s00018-003-3230-5

CMLS Cellular and Molecular Life Sciences

Research Article

Distinct features of recombinant rat vanilloid receptor-1 expressed in various expression systems

J. Lázár [a], T. Szabó [b], L. Kovács [a], P. M. Blumberg [b] and T. Bíró [a,*]

[a] Department of Physiology and Cell Physiology Research Group of the Hungarian Academy of Sciences, Research Center for Molecular Medicine, University of Debrecen, Medical and Health Science Center, Medical School, Nagyerdei Krt. 98, P.O. Box 22, 4012 Debrecen (Hungary), Fax: +36 52 432 289, e-mail: biro@phys.dote.hu
[b] Molecular Mechanism of Tumor Promotion Section, Laboratory of Cellular Carcinogenesis and Tumor Promotion, National Cancer Institute, National Institutes of Health, Bethesda, Maryland (USA)

Received 16 June 2003; received after revision 26 July 2003; accepted 31 July 2003

Abstract. In this study, we expressed rat vanilloid receptor 1 (VR1) in various heterologous expression systems using different VR1-encoding vectors, and examined how the VR1 agonists capsaicin and resiniferatoxin affected intracellular calcium. Our results clearly show that the magnitude and kinetics of response as well as the extent of tachyphylaxis differ markedly between systems. Using green fluorescent protein-tagged VR1, we show that much of the VR1 is localized to intracellular membranes. Consistent with this localization, VR1 agonists are able to liberate calcium from intracellular stores in the absence of extracellular calcium. As with other parameters of response, the three expression systems differ in the degree to which, in the absence of extracellular calcium, capsaicin and resiniferatoxin can liberate calcium from the intracellular stores. Our findings emphasize the influence of the expression system on characteristics of the response of VR1 to its ligands and the need for caution in extrapolating such results to other settings.

Key words. Vanilloid receptor 1; capsaicin; resiniferatoxin; heterologous expression system; calcium.

A distinct subpopulation of primary sensory neurons possesses a marked sensitivity to capsaicin [1, 2], the major pungent ingredient of hot peppers, and to other vanilloids [e.g., resiniferatoxin (RTX) isolated from the latex of *Euphorbia resinifera*] [3], which act via the stimulation of vanilloid receptors (VRs) [2, 4, 5]. The molecular description of the first VR on sensory neurons (VR1) [6], consistent with results obtained from previous electrophysiological and pharmacological studies [2, 5], revealed that the sensory neuron VR1 functions as a nonspecific, calcium-permeable cation channel.

The activation of VR1 on sensory neurons by vanilloids results in ionic (mostly calcium and sodium) influx, an increase in intracellular calcium concentration ($[Ca^{2+}]_i$), and a subsequent desensitization of the response resulting in tachyphylaxis [2, 5]. In the analysis of these rather complex phenomena, one of the key issues, in addition to the heterogeneity of action of different vanilloids [2, 7], was to describe the dependence of the processes on extracellular calcium concentration ($[Ca^{2+}]_e$). The patch-clamp technique showed unambiguously that the vanilloid-induced membrane currents are only minimally affected by $[Ca^{2+}]_e$ [8–10]. In contrast, in most cellular preparations, the processes of desensitization/tachyphylaxis showed a marked dependence on the availability of calcium in the medium [9, 11, 12].

However, the dependence of the increase in $[Ca^{2+}]_i$ on $[Ca^{2+}]_e$ remains unclear. Several groups have reported that VR1 is exclusively expressed on the surface membrane of sensory neurons and that vanilloids are capable

* Corresponding author.
J. Lázár and T. Szabó participated equally to this work.

of increasing $[Ca^{2+}]_i$ only in the presence of extracellular calcium [13–15]. In contrast, other findings have suggested that VR1 could functionally be expressed not only in the plasma membrane but also in intracellular membranes (e.g., in the membrane of the endoplasmic reticulum, ER) of the neurons; hence, the VR1-mediated cellular responses may also be initiated in the absence of extracellular calcium [16–18].

Molecular characterization of VR1 stimulated multiple efforts to describe how VR1 functions as an ionic channel in cells. Various heterologous expression systems for VR1 have been used to describe molecular and pharmacological features of the receptor channel and cellular mechanisms initiated by the activation of VR1, and also to provide tools for VR1-targeted drug design in pain therapy.

Results obtained in these systems, however, did not resolve the issue of the calcium dependence of $[Ca^{2+}]_i$ responses and, moreover, provided conflicting data both on the localization of VR1 in cells and on the effect of various vanilloids. The ability of capsaicin to increase $[Ca^{2+}]_i$ was reported to be totally dependent on $[Ca^{2+}]_e$ in VR1-expressing Chinese hamster ovary (CHO) [15] and in human embryonic kidney (HEK) 293 cells [6, 19]. In contrast, using cos-7 cells expressing the enhanced green fluorescent protein (eGFP)-tagged VR1 (VR1eGFP), we have previously shown [16, 17] that the application of RTX initiated a calcium rise and disruption of various intracellular organelles (ER and nuclear membranes). We have also described that VR1eGFP was localized in the surface membrane and, unexpectedly, also in the membrane of the ER, a finding that was also supported by others [20].

In this study, therefore, our goal was to investigate and compare the functional properties of VR1 expressed in various heterologous systems using similar technical approaches. We employed the previously mentioned transient expression system in which a GFP-tagged VR1 was transiently expressed in cos-7 cells [16, 17], an inducible expression system in which the level of VR1 was controlled by a tetracycline-regulated repressor protein in CHO cells [21–23], and a stable expression system in which a VR1-encoding ε-tagged plasmid [16] was stably expressed in C6 rat glioma cells. In these cells, we compared the effects of capsaicin and RTX on calcium homeostasis and cellular integrity in calcium-containing and calcium-free solutions to describe the relative contributions of the surface membrane and (the possible) ER-localized VR1s in the establishment of the vanilloid-induced cellular effects, and to analyze vanilloid actions. We conclude that several crucial functional features of VR1 expressed in various systems are different from one another, which suggests a need for careful selection of the given expression system and for caution in interpreting and comparing data obtained in such systems to results with primary sensory neurons.

Materials and methods

Construction of heterologous expression systems for rat VR1

For the transient expression system, cos-7 cells were transfected with 1–2 µg VR1eGFP plasmid or with the control empty vector by the LipofectAMINE (Life Technologies, Gaithersburg, Md.) transfection reagent, using the protocol suggested by the manufacturer (VR1eGFP/cos-7 cells). The plasmid was constructed as described in our previous report [16]. Briefly, VR1-specific mRNA was obtained from rat dorsal root ganglion using RT-PCR, and was cloned to the multiple cloning site of the pEGFP-N3 vector (Clontech, Palo Alto, Calif.) using various restriction enzymes. Transfected cells, cultured for 48 h in Dulbecco's modified Eagle's medium (DMEM; Sigma, St. Louis, Mo.) supplemented with 10% fetal calf serum (FCS), 2 mM glutamine, and antibiotics (all from Sigma) at 35 °C to avoid temperature-induced activation of the VR1 [6, 16], were used for calcium imaging.

The inducible expression system was generated as reported previously [23]. Briefly, cDNA of the rat VR1 was subcloned into pUHG102-3 (Clontech) and was tranfected into CHO cells carrying the pTet Off Regulator plasmid (Clontech) (VR1/CHO cells). In these cells, expression of the pUHG plasmid (hence VR1) is repressed in the presence of tetracycline and is expressed upon removal of the antibiotic. Therefore, cells were routinely cultured in Ham F-12 medium (supplemented with 10% FCS, 2 mM glutamine, and antibiotics, all from Sigma) which contained 1 µg/ml tetracycline (Sigma). Before calcium imaging, cells were seeded on glass coverslips and were switched to tetracycline-free Ham F-12 medium and cultured at 35 °C for the time indicated (usually for 48 h, see below). To evaluate the efficacy of the induction of VR1 expression, Western blot analysis was performed (see below).

For the stable expression system, a previously constructed metallothionein promoter-based pεMTH vector [24] encoding the cDNA of the rat VR1 was used [16]. This vector (2–4 µg cDNA) was transfected into C6 rat glioma cells growing in six-well tissue culture dishes (VR1/C6 cells). Cells were then selected in 10% FCS-supplemented DMEM containing 750 µg/ml G418 (geneticin; Life Technologies) for 12–18 days; then, single colonies were isolated. VR1-overexpressing cells were cultured in supplemented DMEM containing 500 µg/ml G418 at 35 °C. The efficacy of recombinant overexpression in several clones was monitored by Western blotting (see below).

Western blotting

In the cases of the inducible and stable expression systems, the expression of VR1 was evaluated by Western blotting [25]. Cells were harvested in homogenization buffer, subjected to SDS-PAGE according to Laemmli [26] and trans-

ferred to nitrocellulose membranes (BioRad, Vienna, Austria). Membranes were then probed with a goat anti-VR1 primary antibody (Santa Cruz, Santa Cruz, Calif.). A peroxidase-conjugated rabbit anti-goat IgG antibody (Bio-Rad) was used as the secondary antibody, and the immunoreactive bands were visualized by an ECL Western blotting detection kit (Amersham, Little Chalfont, UK) on light-sensitive film (AGFA, Brussels, Belgium).

Representative results of the expression of VR1 in the inducible and stable expression systems are seen in figure 1. Western blot analyses were performed on VR1/CHO cells harvested 0, 12, 24, and 48 h after induction, i.e., after withdrawing the tetracycline from the culturing medium. As seen in figure 1A, the expression of VR1 increased with time after tetracycline removal; therefore, cells after 48 h were used for calcium imaging. In addition, Western blot measurement was also performed on VR1/C6 cells and on C6 cells transfected with the empty pεMTH vector. As seen in Figure 1B, VR1 expression was several times higher in the three representative overexpressing clones than in control C6 cells.

Calcium imaging and analysis

Changes in intracellular calcium concentration ($[Ca^{2+}]_i$) were detected as described in our earlier reports [25, 27]. A calcium-sensitive probe was introduced into the intracellular space by incubating the cells with 5 µM fura-2 AM for 1 h at 37 °C. Before each measurement, the cells were kept at room temperature (22–24 °C) in normal Tyrode's solution (in mM: 137 NaCl, 5.4 KCl, 0.5 $MgCl_2$, 1.8 $CaCl_2$, 11.8 Hepes-NaOH, 1 g/l glucose, pH 7.4) for half an hour to allow homogeneous distribution of the dye. The coverslips, containing the fura-2-loaded cells, were then placed on the stage of an inverted fluorescence microscope (Diaphot;, Nikon, Tokyo, Japan). In the case of the transient expression system, single cells expressing the VR1eGFP fusion protein in cos-7 cells were selected by eGFP green fluorescence illuminating the cells at 488 nm wavelength. For calcium imaging, excitation was altered between 340 and 380 nm using a dual wavelength monochromator (Deltascan; Photon Technology International, New Brunswick, N. J.). The emission was monitored at 510 nm with a photomultiplier at an acquisition rate of 10 Hz per ratio. $[Ca^{2+}]_i$ levels were calculated according to the method of Grynkiewicz et al. [28] from the ratio ($R=F_{340}/F_{380}$) of the fluorescence intensities measured with excitation wavelengths of 340 (F_{340}) and 380 nm (F_{380}) as described earlier [28] ($K_d=76$ nM, $R_{min}=0.42$, $R_{max}=8.6$, $F380_{[0]}/F380_{[Ca]}=15.3$).

Cells were continuously washed by either normal or calcium-free Tyrode's solution (in the latter case, the $CaCl_2$ was substituted by 1 mM EGTA) using a slow background perfusion system, whereas the agents investigated (capsaicin from Sigma; RTX and capsazepine from Alexis, San Diego, Calif.) were applied through a rapid perfusion system positioned in close proximity to the cell measured. All compounds were applied until the maximal response was elicited.

Analyses of the $[Ca^{2+}]_i$ transients were performed by a PTI analysis program developed by us which measures maximal amplitude of the transient (above the baseline $[Ca^{2+}]_i$ level, in nM), the time to peak value (TTP, time interval between the start of the application of the drug and the peak of the elevation, in s), and the rate of rise value (ROR, slope of the ascending phase measured between the onset and peak of the transient, in nM/s). All data are expressed as the mean ± SE.

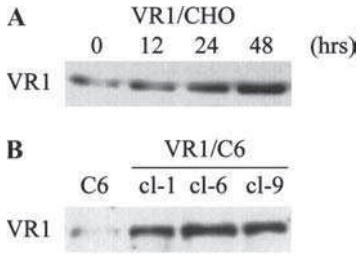

Figure 1. Determination of efficacy of VR1 expression in VR1/CHO and VR1/C6 cells. Cells were harvested in lysis buffer, similar amounts of proteins were subjected to SDS-PAGE, and Western immunoblotting was performed using a goat antibody against VR1 as described in Materials and methods. (*A*) VR1/CHO cells were induced to express VR1 by change to medium without tetracycline, and were subjected to Western blot analysis 0, 12, 24, and 48 h after induction. (*B*) VR1 expression was determined in empty vector transfected C6 cells (C6) and in three individual VR1/C6 clones (cl) with high VR1 levels.

Real-time confocal microscopy

Cos-7 cells were plated on glass coverslips and transfected with 1–2 µg VR1eGFP plasmid and, after 48 h in culture, were analyzed with an MRC-1024 Bio-Rad confocal microscope, as described before [16, 17]. To study the two- and three-dimensional distribution of fluorescent signals, each x-y plane was scanned over 1 s at 30-s intervals and at 0.2-µm increments in the z axis mode.

Results

In the VR1eGFP/cos-7 cell transient expression system, capsaicin induced cellular responses more effectively in 1.8 mM extracellular calcium solution

First, we investigated the effect of capsaicin on the intracellular calcium homeostasis of cells in calcium-free and calcium-containing extracellular solutions. Control (the empty pEGFP vector-transfected) cos-7 cells never responded to capsaicin with any type of increase in $[Ca^{2+}]_i$ whether in calcium-free or in 1.8 mM $[Ca^{2+}]_e$ solutions (data not shown). In contrast, as seen in figure 2, capsaicin at 1 µM was able to increase $[Ca^{2+}]_i$ of VR1eGFP/cos-7 cells both in 1.8 and 0 mM $[Ca^{2+}]_e$ solu-

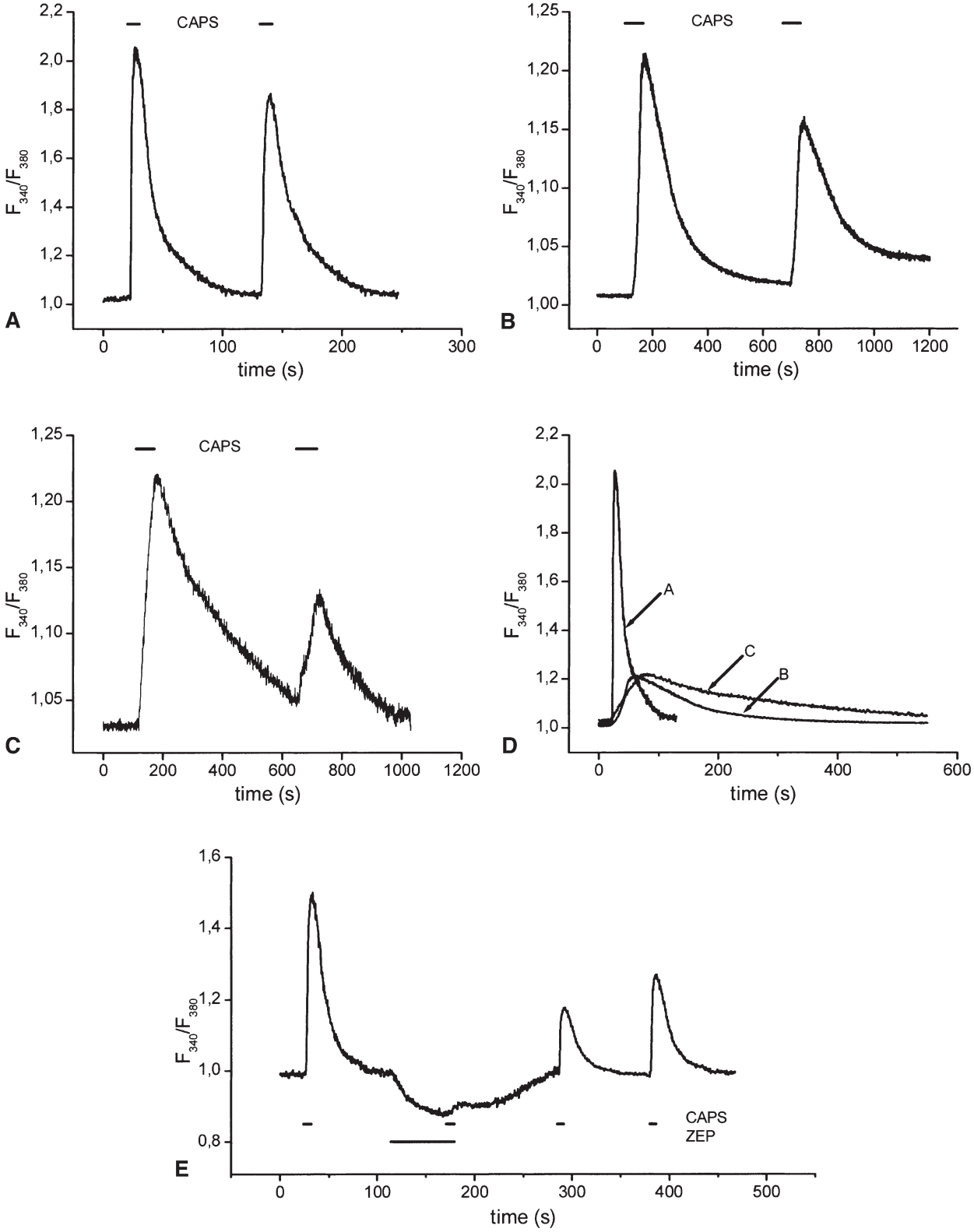

Figure 2. Effect of capsaicin on $[Ca^{2+}]_i$ in VR1eGFP/cos-7 cells. Cells growing on glass coverslips were loaded with 5 µM fura 2-AM and fluorescence ratio (F_{340}/F_{380}) values of excitations at 340- and 380-nm wavelengths were recorded at an acquisition rate of 10 Hz per ratio. The effects of 1 µM capsaicin (CAPS) were measured in 1.8 mM $[Ca^{2+}]_e$ (*A*, *B*) and in calcium-free (*C*) solutions. For better comparison of various parameters of the capsaicin-induced transients in different solutions, the first $[Ca^{2+}]_i$ elevations in A–C (indicated by arrows) are shown using the same time and ratio scales (*D*). The ability of 5 µM capsazepine (ZEP) to significantly yet reversibly inhibit the action of capsaicin in 1.8 mM $[Ca^{2+}]_e$ medium is also shown (*E*). Representative results of multiple determinations are summarized in table 1.

Table 1. Summary of various parameters of $[Ca^{2+}]_i$ transients induced by capsaicin and RTX in VR1eGFP/cos-7 cells.

	Capsaicin (1 µM)			RTX (1 nM)		
	1.8 mM Ca^{2+}		0 mM Ca^{2+}	1.8 mM Ca^{2+}	0 mM Ca^{2+}	
Responding cells (%)	79		46	42	48	
Transient type	fast (69%)	slow (31%)	slow (100%)	slow (100%)	fast (32%)	slow (68%)
Amplitude (nM)	124 ± 29	31 ± 11	28.6 ± 6	68 ± 16	65 ± 22	44 ± 14
Time to peak (TTP, s)	14.9 ± 1	63 ± 10	66 ± 11	133 ± 23	15.7 ± 3	166 ± 21
Rate of rise (ROR, nM/s)	16.6 ± 5	1.1 ± 1	0.4 ± 0.1	1.9 ± 1	7.1 ± 3	0.36 ± 0.2
Tachyphylaxis (% decrease)	24 ±11	40.8±8	44 ±12	100	41 ±11	100
Averaged tachyphylaxis (%)	27.3 ± 9		N/A	N/A	79 ± 13	

Parameters shown in the table were determined as described in Materials and methods. All values are expressed as the mean ± SE of several determinations. N/A, not applicable.

tions. However, there were significant differences in the proportion of responding cells and in the characteristics of the different transients for cells in the different extracellular solutions.

In 1.8 mM $[Ca^{2+}]_e$, 79% of the VR1eGFP/cos-7 cells (n = 42/53) responded with a significant increase in $[Ca^{2+}]_i$ upon capsaicin treatment (table 1). These transients, based on their various kinetic parameters (listed in table 1) could be classified into two groups. In the first group ('fast' transient, fig. 2A, D), the signals were recorded in 69% (n = 29/42) of the capsaicin-responding cells. Among these 'fast' $[Ca^{2+}]_i$ elevations, 66% of the transients (n = 19/29) returned to baseline after the termination of capsaicin application, whereas 3 % (n = 10/29) of the transients showed minimal return (less than 30% decline compared to the maximal level). For the group displaying transients which returned to baseline, we were able to investigate the effect of repeated capsaicin application and to measure the decrease in the amplitude of the transients (i.e., tachyphylaxis). Statistical analyses revealed that, upon repeated capsaicin treatment, the second transients had 24 ± 11% (mean ± SE) less amplitude compared to the maximal value of the first $[Ca^{2+}]_i$ elevation.

In the second group ('slow' transients), the signals were recorded on 31% (n = 13/42) of the capsaicin-responding VR1eGFP/cos-7 cells (fig. 2B, D). The transients had a much reduced maximum amplitude and a slower response (table 1). Similar to the 'fast' transients, approximately two-thirds (62%, n = 8/13) of the 'slow' $[Ca^{2+}]_i$ elevations returned to the baseline. However, within the 'slow' group, we observed a more pronounced tachyphylaxis upon repeated capsaicin application (40.8 ± 8% decrease in amplitude of the second transient compared to the first one; mean ± SE).

We also measured the specificity of the capsaicin response using capsazepine, a competitive antagonist of capsaicin for VR1. As seen in figure 2E, 5 µM capsazepine markedly yet reversibly inhibited the capsaicin-induced $[Ca^{2+}]_i$ responses. Statistical analyses showed that, in contrast to the 27.3 ± 9% average tachyphylaxis on VR1eGFP/cos-7 cells showing any type of responses to capsaicin (table 1), capsazepine decreased the amplitude of the second capsaicin-evoked $[Ca^{2+}]_i$ transient by 91.6 ± 4% (mean ± SE, n = 15) when compared to the peak value of the first elevation induced by capsaicin.

In calcium-free solution, capsaicin was able to evoke $[Ca^{2+}]_i$ transients in only 46% of the VR1eGFP/cos-7 cells (n = 25/54) (table 1). Furthermore, also in contrast to our findings with VR1eGFP/cos-7 cells in 1.8 mM $[Ca^{2+}]_e$, all of these transients were characterized as 'slow' and small (fig. 2C, D, table 1). Although most of the transients (84%, n = 21/25) returned to the baseline after cessation of vanilloid treatment, repeated application of capsaicin resulted in a significant decline in the maximal amplitude (44.5 ± 13% decrease compared to the peak of the first capsaicin-induced transient, mean ± SE).

We have previously shown [16] that the stimulation of VR1eGFP-expressing cos-7 cells by RTX results in specific morphological changes in various intracellular membrane structures. Therefore, using the eGFP-tag to provide a visual measure of cellular events, we also investigated the differences and similarities between the actions of capsaicin in calcium-free and calcium-containing solutions at the level of intracellular organelles by real-time confocal microscopy. As seen in figure 3, similar to the calcium imaging data, there were marked differences in the actions of capsaicin depending on the presence of $[Ca^{2+}]_e$. For VR1eGFP/cos-7 cells in calcium-containing solution (fig. 3, upper row), 1 µM capsaicin effectively induced the vesiculation and disruption of intracellular membrane elements, i.e., ER and nuclear membrane disruption, within 5–10 min (as was expected, the kinetics of vanilloid-induced changes in cell integrity were much slower, in the minute range, than those of the calcium responses, in the second range) [16]. In contrast, in calcium-free solution (fig. 3, middle row), capsaicin induced much less pronounced intracellular alterations. Although disorganization of the ER was prominent, the appearance of charac-

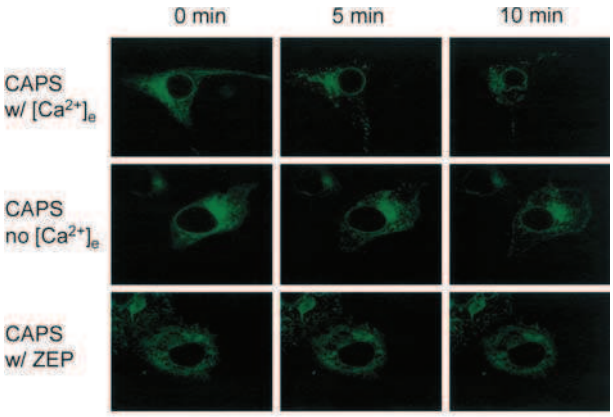

Figure 3. Effect of capsaicin on cellular membrane organization in VR1eGFP/cos-7 cells. Single VR1eGFP/cos-7 cells were identified by their green fluorescence using a confocal microscope. Images were obtained in the z axis mode as described in Materials and methods, and selected time points are represented in the figure. Application of 1 µM capsaicin (CAPS) was initiated at 0 min and was continued throughout the experiment. The action of capsaicin was investigated in 1.8 mM $[Ca^{2+}]_e$ (upper row) and in calcium-free (middle row) solutions, whereas the inhibitory effect of 5 min preincubation with 5 µM capsazepine (ZEP) in 1.8 mM $[Ca^{2+}]_e$ medium is shown in the lower row. Note the more pronounced effect of capsaicin in calcium-containing solution. Representative results of several determinations yielding similar results.

teristic nuclear blebs representing disruption of the nuclear membrane was rare. Preincubation of the VR1eGFP/cos-7 cells with 5 µM capsazepine for 10 min (which alone did not cause any modification of cellular integrity, data not shown) effectively inhibited the cellular changes induced by 1 µM capsaicin (fig. 3, lower row). In addition, capsaicin caused no measurable morphological changes in control cos-7 cells transfected with the empty pEGFP vector (data not shown). Consistent with the calcium imaging data, these findings strongly suggest that the actions of capsaicin on VR1eGFP/cos-7 cells are markedly dependent on the presence of extracellular calcium.

In the VR1eGFP/cos-7 transient expression system, RTX induced cellular responses with very similar potencies in 1.8 and 0 mM $[Ca^{2+}]_e$ solutions

We next investigated the cellular actions of an ultrapotent vanilloid agonist, RTX, on $[Ca^{2+}]_i$ homeostasis and morphological characteristics. As seen in figure 4, 1 nM RTX, like capsaicin, increased $[Ca^{2+}]_i$ both for cells in 0 and 1.8 mM $[Ca^{2+}]_e$ solutions. However, there were significant differences in the RTX-induced transients both as a function of the extracellular calcium and compared to the characteristics of the corresponding capsaicin-induced responses.

For VR1eGFP/cos-7 cells, in 1.8 mM $[Ca^{2+}]_e$ solution, RTX was able to evoke $[Ca^{2+}]_i$ transients in 42% of the cells examined (n = 27/64). However, in contrast to the data obtained with capsaicin (seen in fig. 2), all of these RTX-evoked transients could be classified as 'slow' (fig. 4A, D, table 1). Although 52% (n = 14/27) of the transients returned to the baseline after RTX application, none of the cells showed a $[Ca^{2+}]_i$ response after repeated RTX administration, reflecting maximal tachyphylaxis.

For VR1eGFP/cos-7 cells in calcium-free solution, like those in 1.8 mM $[Ca^{2+}]_e$, RTX was able to evoke $[Ca^{2+}]_i$ transients in approximately half (48%) of the cells examined (n = 33/69). These transients could be classified into two groups based on kinetic analysis (table 1). In the first group ('fast' transients, fig. 4B, D), the signals were recorded on 33% of the RTX-responding cells (n = 11/33) (table 1). On those cells which responded with $[Ca^{2+}]_i$ responses returning to baseline (55% of the 'fast' transients, n = 6/11), repeated application of RTX resulted in a marked tachyphylaxis (40 ± 11% decrease in the peak amplitude compared to that of the first elevation, mean ± SE).

In the second group ('slow' transients, fig. 4C, D), the signals were recorded on 67% of the RTX responding cells (n = 22/33) (table 1). Interestingly enough, although most (82%, n = 18/22) of the 'slow' transients returned to the baseline after the termination of the RTX application, none of the cells showing such $[Ca^{2+}]_i$ signals responded to repeated RTX administration, suggesting maximal tachyphylaxis.

To obtain more data about the possible functional role of the VR1eGFP fusion protein on intracellular calcium stores, we also determined the effect of emptying the intracellular calcium stores on the RTX-induced responses using thapsigargin (TG), an inhibitor of the ER Ca-ATPase molecule [29]. Since the RTX-induced transients in calcium-free solution exerted a marked tachyphylaxis (79.2 ± 13% averaged tachyphylaxis on cells showing any type of responses to RTX, mean ± SE, see table 1), we were unable to measure the effect of TG on repeated RTX-induced transients. Therefore, we investigated the amplitude of the first RTX-evoked transients under control and TG-treated (50 nM, 5 min) conditions and statistically compared the two populations. Whereas 48% of the cells responded with any type of transient $[Ca^{2+}]_i$ elevations to RTX in control calcium-free solution (with an averaged amplitude of 57.4 ± 14 nM, mean ± SE), we could detect only minimal (averaged amplitude of 3.6 ± 2 nM, mean ± SE, n = 20) responses on cells preincubated with TG. We can conclude, therefore, that the emptying of the ER calcium content resulted in a marked (approximately 93%) inhibition of the RTX-induced $[Ca^{2+}]_i$ transients in calcium-free solution.

We also investigated the effect of RTX on morphological characteristics of VR1eGFP-expressing cos-7 cells. As seen in figure 5 (upper and middle rows), 1 nM RTX was able to induce disruption of intracellular membrane components with similar efficiencies in calcium-free and normal solutions (in marked contrast to the more pronounced action of capsaicin in 1.8 mM $[Ca^{2+}]_e$, see fig. 3). How-

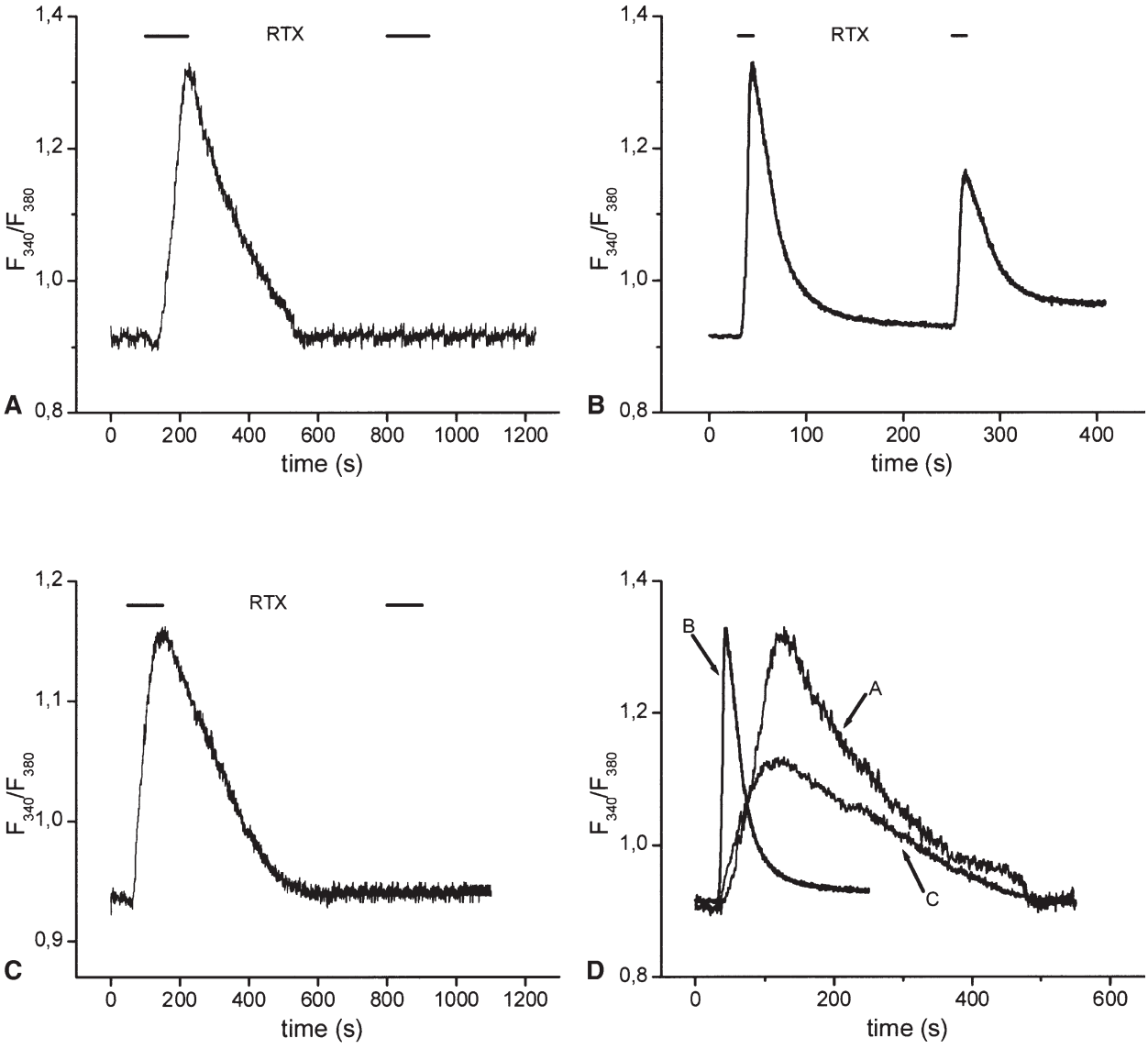

Figure 4. Effect of RTX on $[Ca^{2+}]_i$ in VR1eGFP/cos-7 cells. Cells growing on glass coverslips were loaded with 5 μM fura 2-AM and fluorescence ratio (F_{340}/F_{380}) values of excitations at 340- and 380-nm wavelengths were recorded at an acquisition rate of 10 Hz per ratio. The effects of 1 nM RTX were measured in 1.8 mM $[Ca^{2+}]_e$ (*A*) and in calcium-free (*B*, *C*) solutions. For better comparison of various parameters of the RTX-induced transients in different solutions, the first $[Ca^{2+}]_i$ elevations in panels A–C (indicated by arrows) are also shown using the same time and ratio scales (*D*). Representative results of several determinations are summarized in table 1.

ever, the action of RTX was much slower than that of capsaicin (maximal effects were seen after 15–20 min). Furthermore, we also found that the preincubation of the cells for 5 min with 50 nM TG (hence the emptying of intracellular calcium stores) largely but not completely prevented the disorganization of the intracellular membrane structures induced by RTX (fig. 5, lower row) (the partial extent of this blockade can possibly be explained by the effect of TG alone on $[Ca^{2+}]_i$ [30]). Like capsaicin, RTX was also ineffective on control empty vector-transfected cos-7 cells (data not shown). Consistent with the calcium imaging results, these data again strongly argue for the incorporation of the VR1eGFP into intracellular calcium store structures of cos-7 cells and its functional activity. Furthermore, our findings suggest that the effects of RTX on the VR1eGFP/cos-7 cells are much less dependent on the presence of extracellular calcium than seen in the case of capsaicin.

In the inducible VR1/CHO expression system, RTX but not capsaicin was ineffective when extracellular calcium was removed

In VR1/CHO cells in calcium-containing solution, 1 μM capsaicin induced $[Ca^{2+}]_i$ transients in 66% of cells (n = 66/100) and all of the evoked transients were characterized as 'fast' ones (fig. 6A, D, table 2). In striking con-

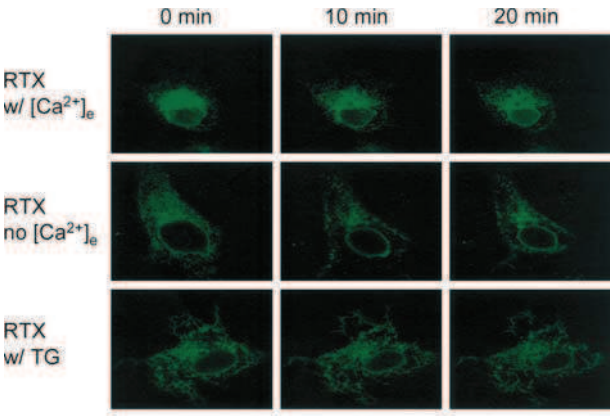

Figure 5. Effect of RTX on cellular membrane organization in VR1eGFP/cos-7 cells. Single VR1eGFP/cos-7 cells were identified by their green fluorescence using a confocal microscope. Images were obtained in the z axis mode as described in Materials and methods and selected time points are represented in the figure. Application of 1 nM RTX was initiated at 0 min and was continued throughout the experiment. The action of RTX was investigated in 1.8 mM $[Ca^{2+}]_e$ (upper row) and in calcium-free (middle row) solutions, whereas the partial inhibitory effect of 5-min preincubation with 50 nM thapsigargin (TG) in calcium-free medium is shown in the lower row. Note the similarly pronounced effects of RTX in both solutions. Representative results of several determinations yielding similar results.

trast, in calcium-free solution, only 25% of the VR1/CHO cells (n = 15/60) responded to capsaicin (table 2) and all of these responses were rather small and 'slow' (fig. 6B, D). In both solutions, most of the capsaicin transients (> 80%) completely returned to baseline (fig. 6A, B); hence, the effect of repeated applications of capsaicin could also be measured. However, in marked contrast to the behavior of VR1eGFP/cos-7 cells (see figs. 2, 4), repeated capsaicin application did not result in tachyphylaxis of the VR1/CHO cells (table 2) in either solution. Instead, especially in 1.8 mM $[Ca^{2+}]_e$ solution, the second application of capsaicin resulted in even higher Ca responses (table 2).

Interestingly (and also contrary to our findings in the VR1eGFP/cos-7 cell transient expression system; see fig. 4, table 1), in the VR1/CHO inducible expression system, 1 nM RTX was completely ineffective in calcium-free solution (table 2). Moreover, even in 1.8 mM $[Ca^{2+}]_e$ solution, only 16% of the cells (n = 8/50) responded to RTX with, in all cases, 'slow' $[Ca^{2+}]_i$ elevations (fig. 6C, D). In addition, we were unable to measure the effect of repeated RTX administration since the $[Ca^{2+}]_i$ levels never returned even close to baseline after the first RTX application.

The VR1 competitive antagonist capsazepine effectively blocked the action of capsaicin and RTX in both solutions. Namely, 2-min preincubation of cells with 5 μM capsazepine completely prevented the effect of the subsequent addition of capsaicin (the reversible action of the inhibitor in calcium-containing solution is seen in fig. 6E). Since the effect of a second application of RTX could not be measured in VR1/CHO cells, we determined the maximal amplitude of the RTX-induced responses in control and capsazepine-pretreated cells. Whereas in control cells, RTX initiated transients with an averaged maximum amplitude of 47 ± 19 nM (mean ± SE, table 2), the vanilloid was able to affect $[Ca^{2+}]_i$ only insignificantly in capsazepine-pretreated cells (3.8 ± 3 nM increase, mean ± SE, n = 8).

In the VR1/C6 stable expression system, both capsaicin and RTX were effective only in calcium-containing extracellular solution

In VR1/C6 cells measured in calcium-containing solution, the effect of capsaicin was very similar to that seen in VR1/CHO cells under similar conditions (table 3). Namely, all of the cells investigated (n = 99) responded to 1 μM capsaicin application with significant and 'fast' $[Ca^{2+}]_i$ transients (fig. 7A, C, table 3) which returned to baseline after cessation of capsaicin administration. Also similar to the VR1/CHO cells, the VR1/C6 cells never showed any tachyphylaxis upon repeated capsaicin application (table 3). However, in marked contrast to data obtained in the VR1/CHO inducible system, in the VR1/C6 cells, capsaicin was unable to evoke any significant change of $[Ca^{2+}]_i$ in calcium-free solution (n = 56).

The characterization of the effect of RTX in the VR1/C6 cells resulted in strikingly similar data to those obtained in the VR1/CHO inducible system (table 3). Namely, 1 nM RTX was only effective in calcium-containing solution and only in a much smaller portion of the cells than capsaicin (28%, n = 19/68). In addition, all of the RTX-evoked transients were small and 'slow' ones (fig. 7B, C, table 3). As seen in figure 7B, as was expected, the repeated application of RTX resulted in no further change in $[Ca^{2+}]_i$. However, since these transients only partially (if at all) returned toward the baseline after the first RTX application, we were unable to properly and, most importantly, statistically measure the phenomenon of tachyphylaxis.

The effect of capsazepine was tested in this system as well. A 2-min preincubation of the cells with 5 μM capsazepine, as in the inducible system, completely yet reversibly abolished the effect of capsaicin (fig. 7D). Since the effect of a second application of RTX could not be measured in these cells, we determined the maximal amplitude of the RTX-induced responses in control and capsazepine-pretreated cells. Whereas in VR1/C6 cells (not treated with the inhibitor), RTX was able to induce Ca response transients with an averaged maximum amplitude of 29.2 ± 4 nM (mean ± SE, table 3), the RTX was completely ineffective after capsazepine pretreatment (n = 10).

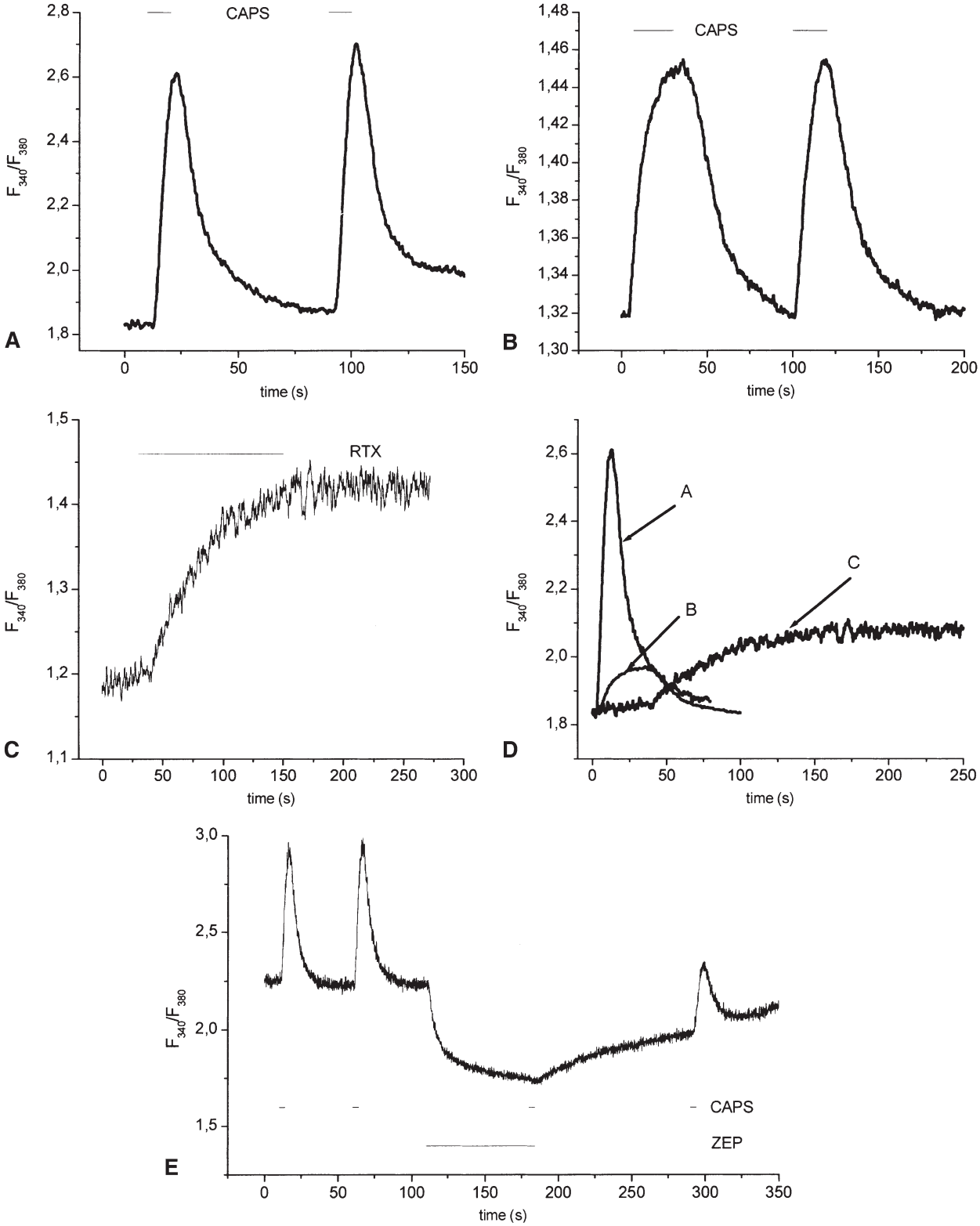

Figure 6. Effects of capsaicin and RTX on $[Ca^{2+}]_i$ in VR1/CHO cells. Cells growing on glass coverslips were loaded with 5 µM fura 2-AM and fluorescence ratio (F_{340}/F_{380}) values of excitations at 340- and 380-nm wavelengths were recorded at an acquisition rate of 10 Hz per ratio. The effects of 1 µM capsaicin (CAPS) in 1.8 mM $[Ca^{2+}]_e$ (*A*) and in calcium-free (*B*) solutions, and the effect of 1 nM RTX in 1.8 mM $[Ca^{2+}]_e$ medium (*C*) are represented. For better comparison of various parameters of the capsaicin- and RTX-induced transients in different solutions, the first $[Ca^{2+}]_i$ elevations *A*–*C* (indicated by arrows) are also shown using the same time and ratio scales (*D*). The effect of 5 µM capsazepine (ZEP) to significantly yet reversibly inhibit the action of capsaicin in 1.8 mM $[Ca^{2+}]_e$ medium is shown in *E*. Representative results of several determinations are summarized in table 2.

Table 2. Summary of various parameters of $[Ca^{2+}]_i$ transients induced by capsaicin and RTX in VR1/CHO cells.

	Capsaicin (1 µM)		RTX (1 nM)
	1.8 mM Ca^{2+}	0 mM Ca^{2+}	1.8 mM Ca^{2+}
Responding cells (%)	66	25	16
Transient type	fast (100%)	slow (100%)	slow (100%)
Amplitude (nM)	183 ± 29	28 ± 4	47 ± 19
Time to peak (TTP, s)	12.9 ± 3	49 ± 14	144 ± 28
Rate of rise (ROR, nM/s)	59 ± 12	7.5 ± 1	3.5 ± 1
Tachyphylaxis (% decrease)	–23 ± 13*	4.5 ± 6	N/A

Parameters shown in the table were determined as described in Materials and methods. RTX was ineffective in 0 mM $[Ca^{2+}]_e$ solution. The negative tachyphylaxis, represented by the asterisk, reflects an increase in the amplitude of the second transient evoked by capsaicin compared to the first one (see text for further details). All values are expressed as the mean ± SE of several determinations. N/A, not applicable.

Table 3. Summary of various parameters of $[Ca^{2+}]_i$ transients induced by capsaicin and RTX in VR1/C6 cells.

	Capsaicin (1 µM)	RTX (1 nM)
	1.8 mM Ca^{2+}	1.8 mM Ca^{2+}
Responding cells (%)	100	28
Transient type	fast (100%)	slow (100%)
Amplitude (nM)	117 ± 19	29.2 ± 4
Time to peak (TTP, s)	12.1 ± 8	75 ± 13
Rate of rise (ROR, nM/s)	25.7 ± 5	7.3 ± 2
Tachyphylaxis (% decrease)	–9.5 ± 5*	N/A

Parameters shown in the table were determined as described in Materials and methods. Capsaicin and RTX were both ineffective in 0 mM $[Ca^{2+}]_e$ solution. The negative tachyphylaxis, represented by the asterisk, reflects an increase in the amplitude of the second transient evoked by capsaicin compared to the first one (see text for further details). All values are expressed as the mean ± SE of several determinations. N/A, not applicable.

In the VR1eGFP/cos-7 cell transient and the VR1/CHO inducible expression systems, the membrane-incorporated VR1 may be partially open in resting cells

Comparison of different characteristics of control and VR1-expressing cells in 1.8 mM $[Ca^{2+}]_e$ solution revealed another interesting phenomenon. Namely, in the VR1eGFP/cos-7 cell transient and the VR1/CHO inducible expression systems, but not in the VR1/C6 stable expression system, the VR1 channel at the surface membrane may be partially open. We found that the resting $[Ca^{2+}]_i$ of empty eGFP vector-transfected cos-7 cells (n = 15) was 60.2 ± 5 nM, whereas this value in VR1eGFP/cos-7 cells (n = 53) was 148 ± 24 nM (all values are the mean ± SE). Similarly, the resting $[Ca^{2+}]_i$ in VR1/CHO cells was much higher (185 ± 29 nM, mean ± SE, n = 100) than that of the control CHO cells (76 ± 15 nM, mean ± SE, n = 25). However, in the VR1/C6 stable expression system, we did not detect such differences among the resting $[Ca^{2+}]_i$ of control and VR1/C6 cells; in control cells, the resting $[Ca^{2+}]_i$ was 46 ± 5 nM (mean ± SE, n = 17) whereas in VR1-expressing cells, it was 52.2 ± 8 nM (mean ± SE, n = 99).

The involvement of VR1 in the elevated resting $[Ca^{2+}]_i$ of the VR1eGFP/cos-7 cells and the VR1/CHO cells was supported by analyzing the effect of capsazepine. As seen in figure 2E and figure 6E, 5 µM capsazepine, beside inhibiting the action of 1 µM capsaicin, was alone able to markedly decrease the resting $[Ca^{2+}]_i$ in the VR1eGFP/cos-7 cell transient expression system and in the VR1/CHO inducible system. Statistical analysis revealed that this decline was 78 ± 13 nM (mean ± SE, n = 15) in VR1GFP/cos-7 cells and 110 ± 13 nM (mean ± SE, n = 8) in VR1/CHO cells. In marked contrast, similar pretreatment of VR1/C6 cells with the inhibitor resulted in an only 7.8 ± 2 nM (mean ± SE, n = 17) decrease in resting $[Ca^{2+}]_i$ (fig. 7D), yet effectively inhibited the action of capsaicin. Finally, 2-min incubation of control (empty vector-transfected) cos-7, CHO, or C6 cells by 5 µM capsazepine never caused more than a 10 nM decrease in resting $[Ca^{2+}]_i$ (data not shown).

Discussion

In the current study, our goal was to compare the functional characteristics of recombinant rat VR1 expressed in different (transient, inducible, stable) systems. Our results clearly demonstrate that the vanilloid sensitivity and extracellular calcium dependence of VR1-mediated $[Ca^{2+}]_i$ responses are markedly different in the various systems.

Similar to previous results [16, 17], here we showed that the GFP-tagged VR1 expressed in cos-7 cells was localized both to surface membrane and to intracellular (calcium store) structures (figs. 3, 5). The intracellular VR1 was functional (figs. 2, 4) in that both capsaicin and RTX were able to increase $[Ca^{2+}]_i$ and initiate subcellular disorganization even in the absence of $[Ca^{2+}]_e$, and that emptying of intracellular calcium stores by TG interfered

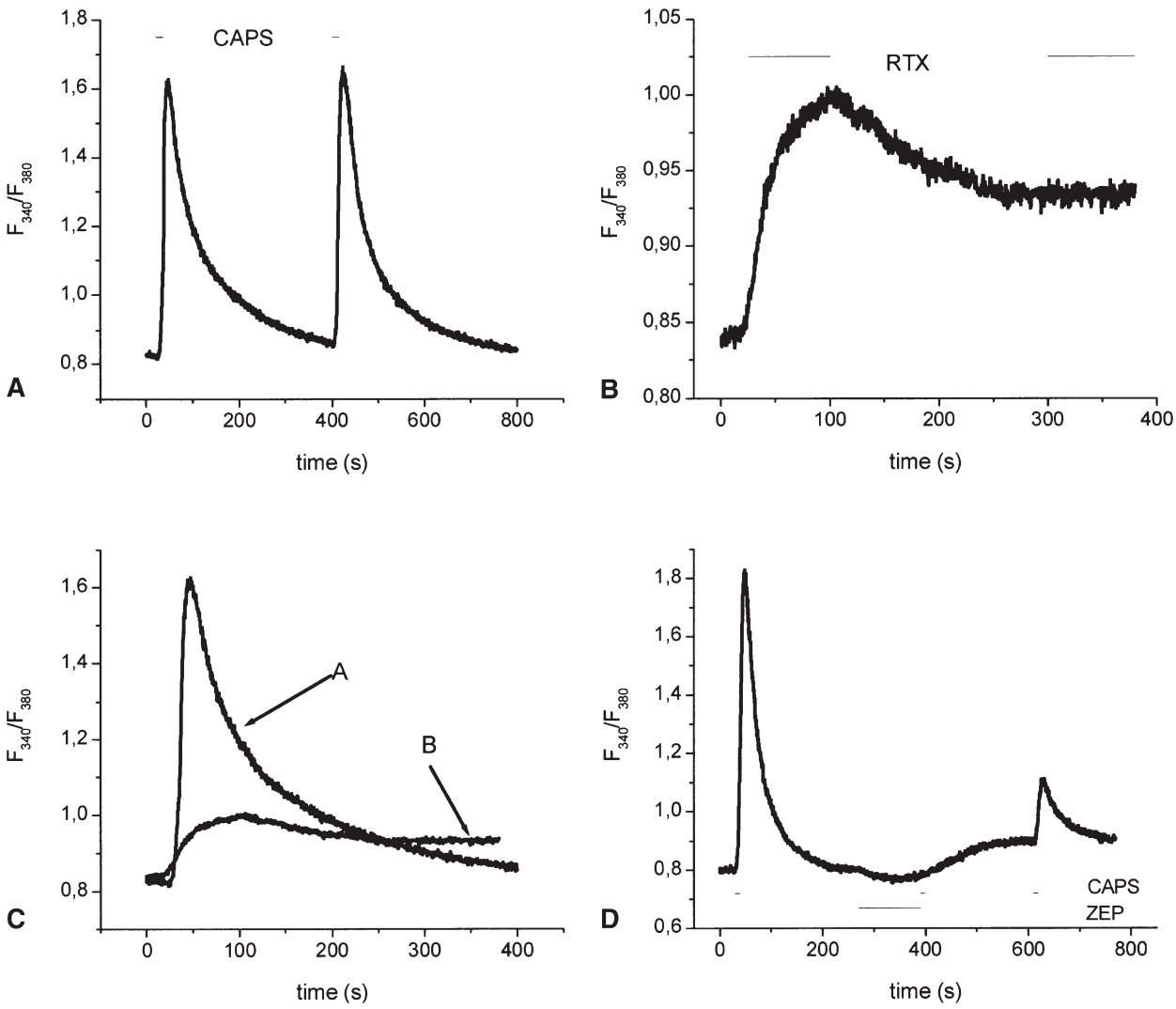

Figure 7. Effects of capsaicin and RTX on $[Ca^{2+}]_i$ in VR1/C6 cells. Cells growing on glass coverslips were loaded with 5 µM fura 2-AM and fluorescence ratio (F_{340}/F_{380}) values of excitations at 340- and 380-nm wavelengths were recorded at an acquisition rate of 10 Hz per ratio. The effects of 1 µM capsaicin (CAPS) (*A*) and 1 nM RTX (*B*) in 1.8 mM $[Ca^{2+}]_e$ solution are represented. For better comparison of various parameters of the capsaicin- and RTX-induced transients, the first $[Ca^{2+}]_i$ elevations in *A* and *B* (indicated by arrows) are shown using the same time and ratio scales (*C*). The effect of 5 μM capsazepine (ZEP) to significantly yet reversibly inhibit the action of capsaicin in 1.8 mM $[Ca^{2+}]_e$ medium is shown in *D*. Representative results of several determinations are summarized in table 3.

with these actions. There were, however, marked differences in the effectiveness of the two vanilloids to affect intracellular calcium depending on the calcium content of the medium. Whereas the action of capsaicin strongly depended on the $[Ca^{2+}]_e$, RTX was equally effective in calcium-containing and -free solutions. These data were in good accordance with recent data on human recombinant VR1 expressed in HEK 293 cells [31], where RTX but not capsaicin was able to increase intracellular calcium in calcium-free medium (see also below).

In the VR1eGFP/cos-7 cells, we observed a remarkable heterogeneity among the vanilloid-induced transients, i.e., both fast and slow transients were recorded for capsaicin in high calcium and for RTX in calcium-free solutions (table 1). Since these phenomena were exclusively seen in the VR1eGFP/cos-7 transient expression system, one explanation is that, due to the transient nature and variable degree of transfection of the VR1eGFP/cos-7 cells, the level of VR1 in the individual cells could be heterogenous, allowing the same vanilloid on different cells having different VR1 expression levels to cause different calcium responses. This hypothesis is consistent with previous molecular biological and functional data that VR1, both in sensory neurons and in recombinant systems, is expressed in various multimeric structures [21] which may result in heterogeneous responses to the same vanilloid [32].

Among the three systems we studied, the most homogenous vanilloid induced responses were observed in the sta-

ble (VR1/C6) system. In these cells, similar to findings in sensory neurons [13–15], capsaicin and RTX were effective only in calcium containing extracellular medium (fig. 7, table 3). In addition, the capsaicin- or RTX-evoked responses were characteristically very similar in all of the cells examined, i.e., capsaicin evoked fast whereas RTX induced slow $[Ca^{2+}]_i$ elevations, also reflecting well the previously described difference in pharmacokinetics of the two vanilloids [2, 33]. These data suggest that the expression of VR1 in VR1/C6 cells is well controlled by the recombinant vector and uniform circumstances can be obtained for VR1 characterization.

The vanilloid-evoked calcium responses in the inducible system (VR1/CHO cells) were generally very similar to those obtained in VR1/C6. In 1.8 mM $[Ca^{2+}]_e$ solution, both capsaicin and RTX induced uniform, fast and slow calcium responses, respectively. However, there were also differences between the inducible and stable expression systems. Namely, in VR1/CHO cells, capsaicin (but not RTX) was able to induce calcium transients even in calcium-free solution. However, under such conditions, capsaicin was effective in only a much lower percentage of the cells examined (25% compared to 66% in high calcium solution; table 2) and, furthermore, the capsaicin-evoked responses were much slower and smaller than seen in calcium-containing medium. Naturally, further experiments are needed to unambiguously clarify the putative localization of some portion of expressed VR1s to intracellular membrane structures (due to the nature of commercially available antibodies against VR1, which were developed to target intracellular domains of VR1, permeabilization of cells is required for immunocytochemistry and this may affect the localization). However, our data, consistent with recent findings by Tóth et al. [22] that TG pretreatment of VR1/CHO cells completely abolished the capsaicin-induced $[Ca^{2+}]_i$ elevations, strongly argue for additional (yet much less than seen in VR1eGF/cos-7 cells) intracellular incorporation of functional VR1 in this system.

A major 'unexpected' result, both in the VR1/C6 and VR1/CHO cell systems when compared to previously described data in sensory neurons [reviewed in ref. 2] was the complete lack of tachyphylaxis after repeated capsaicin applications under our conditions (figs. 6, 7, tables 2, 3). Since the complex mechanism of tachyphylaxis in sensory neurons [1, 2, 11, 12] may also involve the decrease in VR1 density upon repeated or prolonged vanilloid administration [2], we suppose that the stable or relatively stable nature of these expression systems may contribute to the lack of tachyphylaxis. In addition, since the sophisticated calcium handling and signal transduction (kinase, phosphatase) systems described in the host cells [34, 35] are distinct from those of the sensory neurons, the regulation of VR1 by such systems could be markedly different. Nevertheless, the phenomenon that repeated applications of capsaicin result in almost identical calcium responses in VR1/C6 and VR1/CHO cells may even possess an attractive feature for pharmacological studies characterizing inhibitory or sensitizing actions of agents on VR1.

Capsaicin and RTX, although their actions are qualitatively similar, have distinct spectra of action, resulting in differences in their relative potencies for different responses [1, 2]. RTX is generally regarded as an ultrapotent analog of capsaicin; however, there are some responses where it shows only slightly greater potency or, in contrast to the action of capsaicin, ineffectiveness. This latter phenomenon seems to be true for the inducible and stable recombinant expression systems; namely, in VR1/CHO and VR1/C6 cells, RTX was able to evoke only small and slow transients and, of great importance, in a markedly lower percentage of cells than did capsaicin (tables 2, 3). These findings were in good accord with previously published data that the relative potency of capsaicin was much greater on VR1 ectopically expressed in HEK 293 cells than on the native channel in sensory neurons [36], whereas RTX was more potent in activating VR1 in cultured neurons than in the recombinant expression system [37].

Naturally, identifying those factors that may contribute to differences (subcellular localization, calcium dependence, vanilloid sensitivity) seen in the various expression systems is of great importance. Based on both our presented data and the literature, the characteristics of the recombinant vector [16–18, 20, 38], the functional features (e.g., calcium handling) of the host cells [6, 8, 16, 17, 19, 38]; the type of expression (i.e., transient or stable) [10], the level of glycosylation and heterogenous stochiometry [21, 38], and the sensitivities of the methods to record the calcium signals may all contribute to the distinct properties of the systems. The importance of the techniques used for analysis is emphasized by the fact that most authors who either described calcium-dependent [13–15] or -independent [16–18] VR1-mediated responses and, in addition, exclusive surface membrane or simultaneous surface and intracellular membrane localizations, found very similar patterns on sensory neurons expressing the native VR1. In any case, although the relative contributions of different parameters to define VR1 functional characteristics in heterologous expression systems remain to be clearly established, our findings strongly argue for the influence of the heterologous expression system on the determination of VR1 cellular functions and suggest caution in extrapolating such findings to other systems such as primary sensory neurons.

Acknowledgement. The authors are indebted to Ms. I. Varga for helpful technical assistance. This work was supported by Hungarian research grants: OTKA T030246, OTKA F035036, NKFP 00088/2001, OMFB 00200/2002. Tamás Bíró is a recipient of the György Békéssy Postdoctoral Scholarship of the Hungarian Ministry of Education.

1 Holzer P. (1991) Capsaicin: cellular targets, mechanisms of action, and selectivity for thin sensory neurons. Pharmacol. Rev. **43:** 143–200
2 Szállási Á. and Blumberg P. M. (1999) Vanilloid (capsaicin) receptors and mechanisms. Pharmacol. Rev. **51:** 159–211
3 Hergenhahn M., Adolph W. and Hecker E. (1975) Resiniferatoxin and other esters of novel polyfunctional diterpenes from *Euphorbia* resinifera and unispina. Tetrahedron Lett. **19:** 1595–1598
4 Szállási Á. and Blumberg P. M. (1989) Resiniferatoxin, a phorbol-related diterpene, acts as an ultrapotent analog of capsaicin, the irritant constituent in red pepper. Neuroscience **30:** 515–520
5 Caterina M. J. and Julius D. (2001) The vanilloid receptor: a molecular gateway to the pain pathway. Annu. Rev. Neurosci. **24:** 487–517
6 Caterina M. J., Schumacher M. A., Tominaga M., Rosen T. A., Levine J. D. and Julius D. (1997) The capsaicin receptor: a heat-activated ion channel in the pain pathway. Nature **389:** 816–824
7 Ács G., Bíró T., Ács P., Modarres S. and Blumberg P. M. (1997) Differential activation and desensitization of sensory neurons by resiniferatoxin. J. Neurosci. **17:** 5622–5628
8 Tominaga M., Caterina M. J., Malmberg A. B., Rosen T. A., Gilbert H., Skinner K. et al. (1998) The cloned capsaicin receptor integrates multiple pain-producing stimuli. Neuron **21:** 531–543
9 Koplas P. A., Rosenberg R. L. and Oxford G. D. (1997) The role of calcium in the desensitization of capsaicin responses in rat dorsal root ganglion neurons. J. Neurosci. **17:** 3525–3537
10 Vellani V., Mapplebeck S., Moriondo A., Davis J. B. and McNaughton P. A. (2001) Protein kinase C activation potentiates gating of the vanilloid receptor VR1 by capsaicin, protons, heat and anandamide. J. Physiol. **534:** 813–825
11 Docherty R. J., Yeats J. C., Bevan S. and Bodekke H. W. G. M. (1996) Inhibition of calcineurin inhibits the desensitization of capsaicin-evoked currents in cultured dorsal root ganglion neurons from adult rats. Pflügers Arch. **431:** 828–837
12 Liu L. and Simon S. (1998) The influence of removing extracellular Ca^{2+} in the tachyphylaxis responses to capsaicin, zingerone and olvanil in rat trigeminal ganglion neurons. Brain Res. **809:** 246–262
13 Cholewinski A., Burgess G. M. and Bevan S. (1993) The role of calcium in capsaicin-induced desensitization in rat cultured dorsal root ganglion neurons. Neuroscience **55:** 1015–1023
14 García-Hirschfeld J., López-Briones L. G., Belmonte C. and Valdeolmillos M. (1995) Intracellular free calcium responses to protons and capsaicin in cultured trigeminal neurons. Neuroscience **67:** 235–243
15 Savidge J. R., Ranashinghe S. P. and Rang H. P. (2001) Comparison of intracellular calcium signals evoked by heat and capsaicin in cultured rat dorsal root ganglion neurons and in a cell line expressing the rat vanilloid receptor, VR1. Neuroscience **102:** 177–184
16 Oláh Z., Szabó T., Karai L., Hough C., Fields R. D., Caudle R. M. et al. (2001) Ligand-induced dynamic membrane changes and cell deletion conferred by vanilloid receptor 1. J. Biol. Chem. **276:** 11021–11030
17 Oláh Z., Karai L. and Iadarola M. J. (2001) Anandamide activates vanilloid receptor 1 (VR1) at acidic pH in dorsal root ganglia neurons and cells ectopically expressing VR1. J. Biol. Chem. **276:** 31163–31170
18 Eun S. Y., Jung S. J., Park Y. K., Kwak J., Kim S. J. and Kim J. (2001) Effects of capsaicin on Ca^{2+} release from the intracellular Ca^{2+} stores in the dorsal root ganglion cells of adult rats. Biochem. Biophys. Res. Commun. **285:** 1114–1120
19 Jerman J. C., Brough S. J., Prinjha R., Harries M. H., Davis J. B., Smart D. (2000) Characterization using FLIPR of rat vanilloid receptor (rVR1) pharmacology. Br. J. Pharmacol. **130:** 916–922
20 Wisnoskey B. J., Sinkins W. G. and Schilling W. P. (2003) Activation of vanilloid receptor type I (TRPV1 channel) in the endoplasmic reticulum fails to activate store-operated Ca^{2+} entry. Biochem. J. **372:** 517–528
21 Kedei N., Szabó T., Lile J. D., Treanor J. J., Oláh Z., Iadarola M. J. et al. (2001) Analysis of the native quaternary structure of vanilloid receptor 1. J. Biol. Chem. **276:** 28613–28619
22 Tóth A., Kedei N., Szabó T., Wang Y. and Blumberg P. M. (2002) Thapsigargin binds to and inhibits the cloned vanilloid receptor-1. Biochem. Biophys. Res. Commun. **293:** 777–782
23 Szállási Á., Szabó T., Bíró T., Modarres S., Blumberg P. M., Krause J. E. et al. (1999) Resiniferatoxin-type phorboid vanilloids display capsaicin-like selectivity at native vanilloid receptors on rat DRG neurons and at the cloned vanilloid receptor VR1. Br. J. Pharmacol. **128:** 428–434
24 Oláh Z., Lehel C., Jakab G. and Anderson W. B. (1994) A cloning and epsilon-epitope-tagging insert for the expression of polymerase chain reaction-generated cDNA fragments in *Escherichia* coli and mammalian cells. Anal. Biochem. **221:** 94–102
25 Papp H., Czifra G., Lázár J., Boczán J., Gönczi M., Csernoch L. et al. (2003) Protein kinase C isozymes regulate proliferation and high cell density-mediated differentiation of HaCaT keratinocytes. Exp. Dermatol. **12:** 1–14
26 Laemmli U. K. (1970) Cleavage of structural proteins during the assembly of the head of bacteriophage T4. Nature **227:** 680–685
27 Bíró T., Szabó I., Hunyadi J., Kovács L. and Csernoch L. (1998) Distinct sub-populations in HaCaT cells as revealed by the characteristics of intracellular calcium release induced by phosphoinositide-coupled agonists. Arch. Dermatol. Res. **290:** 270–276
28 Grynkiewicz G., Poenie M. and Tsien R. Y. (1985) A new generation of Ca^{2+} indicators with greatly improved fluorescence properties. J. Biol. Chem. **260:** 340–350
29 Thastrup O. (1990) Role of Ca2(+)-ATPases in regulation of cellular Ca2+ signalling, as studied with the selective microsomal Ca2(+)-ATPase inhibitor, thapsigargin. Agents Actions **29:** 8–15
30 Thastrup O., Foder B. and Scharff O. (1987) The calcium mobilizing tumor promoting agent, thapsigargin elevates the platelet cytoplasmic free calcium concentration to a higher steady state level: a possible mechanism of action for the tumor promotion. Biochem. Biophys. Res. Commun. **142:** 654–660
31 Marshall I. C., Owen D. E., Cripps T. V., Davis J. B., McNulty S. and Smart D. (2003) Activation of vanilloid receptor 1 by resiniferatoxin mobilizes calcium from inositol 1,4,5-trisphosphate-sensitive stores. Br. J. Pharmacol. **138:** 172–176
32 Liu L. and Simon S.A. (1996) Capsaicin-induced currents with distinct desensitization and Ca^{2+} dependence in rat trigeminal ganglion cells. J. Neurophysiol. **75:** 1503–1514
33 Maggi C. A., Patacchini R., Tramontana M., Amann R., Giuliani S. and Santicioli P. (1990) Similarities and differences in the action of resiniferatoxin and capsaicin on central and peripheral endings of primary sensory neurons. Neuroscience **37:** 531–539
34 Brismar T. (1995) Physiology of transformed glial cells. Glia **15:** 231–243
35 Verkhratsky A. and Kettenmann H. (1996) Calcium signaling in glial cells. Trends Neurosci. **19:** 346–352
36 Szállási Á., Blumberg P. M., Annicelli L. L., Krause J. E. and Cortright D. N. (1999) The cloned rat vanilloid receptor VR1 mediates both R-type binding and C-type calcium response in dorsal root ganglion neurons. Mol. Pharmacol. **56:** 581–587
37 Shin J. S., Wang M. H., Hwang S. W., Cho H., Cho S. Y. and Kwon M. J. (2001) Differences in sensitivity of vanilloid receptor 1 transfected to human embryonic kidney cells and capsaicin-activated channels in cultured rat dorsal root ganglion neurons to capsaicin receptor agonists. Neurosci. Lett. **299:** 135–139
38 Jahnel R., Dreger M., Gillen C., Bender O., Kurreck J. and Hucho F. (2001) Biochemical characterization of the vanilloid receptor 1 expressed in a dorsal root ganglia derived cell line. Eur. J. Biochem. **268:** 5489–5496

VII.

Available online at www.sciencedirect.com
SCIENCE DIRECT®
Life Sciences 75 (2004) 153–163
Life Sciences
www.elsevier.com/locate/lifescie

Sensitization of recombinant vanilloid receptor-1 by various neurotrophic factors

József Lázár[a], Tamás Szabó[b], Rita Marincsák[a], László Kovács[a], Peter M. Blumberg[c], Tamás Bíró[a,*]

[a] *Department of Physiology and Cell Physiology Research Group of the Hungarian Academy of Sciences, H-4012 Debrecen, Nagyerdei krt. 98. P.O. Box 22, Debrecen, Hungary*
[b] *Department of Pediatrics, Research Center for Molecular Medicine, Medical and Health Science Center, University of Debrecen, Debrecen, Hungary*
[c] *Molecular Mechanism of Tumor Promotion Section, Laboratory for Cellular Carcinogenesis and Tumor Promotion, National Cancer Institute, National Institutes of Health, Bethesda, MD, USA*

Received 12 September 2003; accepted 10 November 2003

Abstract

The vanilloid receptor (VR1) is a central integrator molecule of nociceptive stimuli. In this study, we have measured the effects of various neurotrophins (nerve growth factor, brain-derived neurotrophic factor, neurotrophin-3, and -4) on recombinant rat VR1-mediated intracellular calcium rise in response to capsaicin in VR1/C6 cells. Our results clearly show that all neurotrophins sensitize the VR1 to capsaicin. Furthermore, using K252a, an inhibitor of tyrosine kinases, we present that actions of neurotrophins are mediated by the trk (A, B, C) receptors expressed in these cells. These data argue for the putative roles of neurotrophins in inducing inflammatory (thermal) hyperalgesia via VR1.

Keywords: Vanilloid receptor-1; Neurotrophins; Sensitization; Calcium; Heterologous expression system

Introduction

The vanilloid receptor (VR1) is a ligand-gated cation channel localized mainly in a subset of sensory (nociceptive) neurons (Caterina et al., 1997; Caterina and Julius, 2001). The receptor can be activated by vanilloids such as capsaicin and its ultrapotent analog, resiniferatoxin (Szallasi and Blumberg, 1999;

* Corresponding author. Tel.: +36-52-416-634; fax: +36-52-432-289.
E-mail address: biro@phys.dote.hu (T. Bíró).

0024-3205/$ - see front matter © 2004 Elsevier Inc. All rights reserved.
doi:10.1016/j.lfs.2003.11.023

Caterina and Julius, 2001). Besides such exogenous factors, endogenous stimuli such as low-threshold heat, acidosis, bradykinin, eicosanoids, and other arachidonic acid derivatives (Caterina and Julius, 2001; Di Marzo et al., 2002) may also act on VR1. The effect of these ''endovanilloids'' may represent either a direct activation of the receptor or indirect sensitization of VR1 subsequent to modulation of various intracellular signaling pathways (Di Marzo et al., 2002). The process of sensitization, by decreasing the heat-threshold of VR1, therefore, may have a key role in initiating inflammatory (thermal) hyperalgesia (Caterina et al., 2000).

The neurotrophins (e.g., nerve growth factor, NGF; brain-derived growth factor, BDNF; neurotrophin-3, -4, NT3, NT4) are trophic factors critical in embryonic development, differentiation, survival and regeneration (Snider, 1994; Lewin and Barde, 1996) of various nerve cell types, including VR1-expressing sensory neurons (Kirstein and Farinas, 2002). Moreover, the in vivo and in vitro functional properties of such nociceptive neurons strongly depend on the presence of neurotrophins, particularly NGF (Winter et al., 1988; Crowley et al., 1994; Winston et al., 2001).

Recently, NGF was suggested to exert an acute effect on nociceptive sensory neurons in addition to its trophic effect (Shu and Mendell, 1999a). It was postulated that NGF, either indirectly (via the degranulation of mast cells) (Mazurek et al., 1986; Shu and Mendell, 1999a) or directly (via binding to its tyrosine kinase receptors which are expressed in such neurons) (McMahon et al., 1994) was able to sensitize the VR1-mediated cellular responses, e.g., increase the sensitivity of VR1 to capsaicin (Shu and Mendell, 1999b; Shu et al., 1999; Chuang et al., 2001). Levels of NGF are increased in inflamed tissues (Weskamp and Otten, 1987), and this effect may contribute to the role of neurotrophin(s) in inflammatory hyperalgesia (Shu and Mendell, 1999a; Chuang et al., 2001; Di Marzo et al., 2002).

Since only a few papers have explored the direct action of neurotrophins on VR1-expressing (native or recombinant) cells, in this study we sought to describe the effect of various neurotrophins on VR1-mediated calcium responses to capsaicin in a heterologous expression system stably expressing the rat VR1.

Materials and methods

Establishment of VR1/C6 cells stably expressing the rat VR1

A previously constructed metallothionein promoter-based pεMTH vector (2–4 μg cDNA) (Oláh et al., 1994) encoding the cDNA of the rat VR1 was used (Oláh et al., 2001; Lázár et al., 2003) to transfect C6 rat glioma cells growing in 6-well tissue culture dishes (VR1/C6 cells) by the LipofectAMINE (Invitrogen, Paisley, UK) transfection reagent, using the protocol suggested by the manufacturer. Cells were then selected in Dulbecco's Modified Eagle's Medium (DMEM) (Sigma, St. Louis, MO, USA) supplemented with 10 % fetal bovine serum (FBS) (Invitrogen), 2 mM/L-glutamine, 50 U/ml penicillin, 50 μg/ml streptomycin, 1,25 μg/ml fungison (Biogal, Debrecen, Hungary), and 750 μg/ml G418 (Geneticin) (Invitrogen) for 12–18 days; then, single colonies were isolated. VR1 overexpressing cells were cultured in supplemented DMEM containing 500 μg/ml G418 at 35 °C to avoid temperature-induced activation of the VR1 (Oláh et al., 2001; Lázár et al., 2003). The efficacy of stable transfection and expression was monitored by Western blotting (see detailed protocol below). As seen in Fig. 1A, control (empty vector transfected) C6 cells expressed the VR1 protein at a low level, as was expected

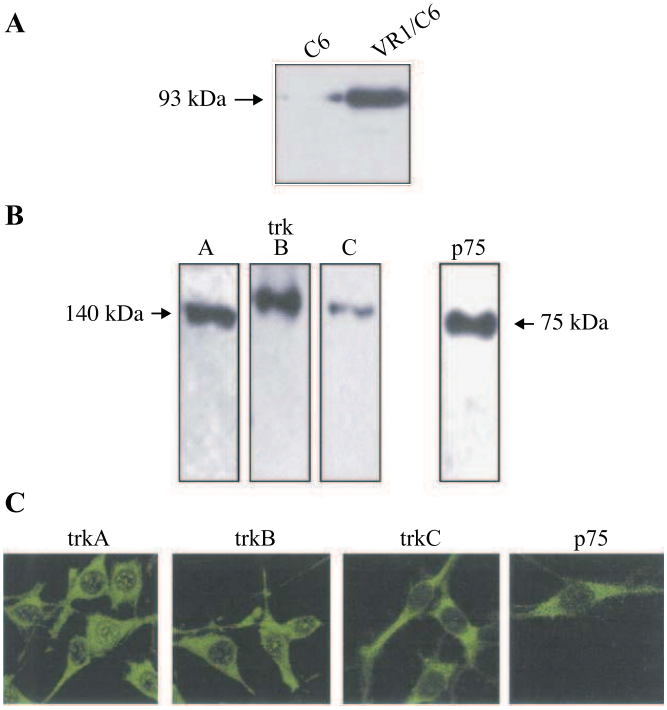

Fig. 1. Expression of VR1 and neurotrophin receptors in VR1/C6 cells. A: Control (empty vector transfected) C6 and VR1/C6 cells were harvested in lysis buffer, similar amounts of proteins were subjected to SDS-PAGE, and Western immunoblotting was performed using a goat anti-VR1 antibody as described under "Materials and methods". Note the several-fold higher expression of VR1 in VR1/C6 cells. B: A similar Western blot analysis, using rabbit antibodies, was performed on VR1/C6 cells to determine the expressions of trk (A, B, C) and p75 receptors. C: The expression of neurotrophin receptors was also determined by immunocytochemistry. VR1/C6 cells were fixed in acetone, then permeabilized and stained with rabbit antibodies against trk and p75 receptors. Immunofluorescence labeling was employed using a FITC-conjugated secondary antibody. Magnification, 630 ×. All figures are representatives of at least three determinations with similar results.

based on our previous findings (Bíró et al., 1998a). However, the levels of VR1 expression in the VR1-pεMTH stably transfected cells were much higher than in the control cells.

Western (immuno) blotting

Cells were washed with ice-cold phosphate-buffered saline (PBS), harvested in homogenization buffer (20 mM TRIS-Cl, pH 7.4, 5 mM EGTA, 1 mM 4-(2-aminoethyl)benzenesulfonyl fluoride, 20 μM leupeptin, all from Sigma) and disrupted by sonication on ice. The protein content of samples was measured by a modified BCA protein assay (Pierce, Rockford, IL, USA). Total cell lysates were mixed with SDS-PAGE sample buffer and boiled for 10 min at 100 °C. The samples were subjected to SDS-PAGE as described previously (Papp et al., 2003) (8% gels were loaded with 20–30 μg protein per lane) and transferred to nitrocellulose membranes (BioRad, Wien, Austria). Membranes were then blocked with 5% dry milk in PBS and probed overnight at 4 °C with rabbit primary antibodies (usually at 1:200 dilution) against trk A, B, and C, and against p75 (Santa Cruz, Santa Cruz, CA, USA) or with a goat primary antibody against the VR1 (1:100 dilution, Santa Cruz). Peroxidase-conjugated goat anti-rabbit (for the neurotrophin receptors) or rabbit anti-goat (for the VR1) IgG antibodies (1:1000 dilution, 1 hr,

room temperature, BioRad) were used as the secondary antibodies, and the immunoreactive bands were visualized by an ECL Western blotting detection kit (Amersham, Little Chalfont, England) on light sensitive film (AGFA, Brussels, Belgium).

Immunocytochemistry

VR1/C6 cells, growing on 25 mm glass coverslips, were washed 4 times in PBS and were fixed with ice-cold acetone for 5 min. Cells were then permeabilized and blocked with a blocking solution (0.6 % Triton X-100, 1 % bovine serum albumin in PBS, pH 7.4, both from Sigma) for 30 min at room temperature and were incubated with the appropriate primary antibodies (against the different neurotrophin receptors) at a dilution of 1:50 in blocking solution for 2 hrs. A fluorescein-isothiocyanate (FITC)-conjugated anti-rabbit goat IgG (Vector Laboratories, Burlingame, CA, USA) was used as second antibody at a dilution of 1:400 in PBS for 1 hr at room temperature. Samples were covered with a Vectashield mounting media (Vector Laboratories) and the fluorescent signals were visualized using a fluorescent microscope (Zeiss, Oberkochen, Germany).

Intracellular calcium measurements

Changes in intracellular calcium concentration ($[Ca^{2+}]_i$) were detected as described in our earlier reports (Bíró et al., 1998b; Papp et al., 2003). VR1/C6 cells were cultured on 25-mm glass coverslips and a calcium sensitive probe was introduced into the intracellular space by incubating the cells with 5 μM fura 2-AM (Molecular Probes, Eugene, OR, USA) for 1 hr at 37 °C. Before each measurement, the cells were kept at room temperature (22–24 °C) in normal Tyrode's solution (in mM; 137 NaCl, 5.4 KCl, 0.5 $MgCl_2$, 1.8 $CaCl_2$, 11.8 Hepes-NaOH, 1 g/l glucose, pH 7.4, all from Sigma) for 30 min to allow homogeneous distribution of the dye. The coverslips, containing the fura-2 loaded cells, were then placed on the stage of an inverted fluorescence microscope (Diaphot, Nikon, Tokyo, Japan). Excitation was altered between 340 and 380 nm using a dual wavelength monochromator (Deltascan, Photon Technology International, New Brunswick, NJ, USA). The emission was monitored at 510 nm with a photomultiplier at an acquisition rate of 10 Hz per ratio, and the fluorescence ratio (F_{340}/F_{380}) values were determined.

Cells were continuously washed by Tyrode's solution using a slow background perfusion system, whereas the agents investigated (capsaicin was form Sigma; NGF, BDNF, NT3, and NT4 were from Promega, Madison, WI, USA; K252a was from Calbiochem, San Diego, CA, USA) were applied through a rapid perfusion system positioned in close proximity to the cell measured. In initial experiments, varying concentrations of neurotrophins were tested and saturating doses resulting in maximal responses were selected for the subsequent experiments (these concentrations were in good accord with those used by other groups, Shu and Mendell, 1999a,b; Chuang et al., 2001).

Results and discussion

First, we examined neurotrophin receptor expression in the rVR1/C6 glioma cells. As was revealed by Western blotting (Fig. 1B), all of the high-affinity neurotrophin receptors, namely the trkA, B, C, as well as the low-affinity receptor p75 are expressed in the cells. Immunocytochemistry experiments

corroborated these observations (Fig. 1C). These findings confirm previous data (using mainly RT-PCR) that all members of the neurotrophin receptor family are expressed in C6 cells (Hutton et al., 1992; Kumar and de Vellis, 1996). Furthermore, these results demonstrate that the stable VR1 expression did not change the neurotrophin receptor pattern of C6 cells.

As we reported elsewhere (Lázár et al., 2003), repeated, short (5–20 s) applications of 1 μM capsaicin to VR1/C6 cells resulted in fast intracellular Ca-transients, the amplitude of which decrease insignificantly upon repetition (Fig. 2). This lack of tachyphylaxis makes the VR1/C6 cells a convenient system to objectively study the sensitizing effects of agents on VR1.

Control (empty vector transfected) C6 cells never responded to such a short (5–20 s) capsaicin challenge with changes in the $[Ca^{2+}]_i$. We were able to detect slowly developing and not transient $[Ca^{2+}]_i$ increases with very moderate amplitudes only after 2–10 min of the continuous presence of capsaicin (data not shown). These elevated $[Ca^{2+}]_i$ levels only approached the baseline (but never returned to it completely) tens of minutes after removal of the VR1 agonist. This finding was not unexpected since in our previous report (Bíró et al., 1998a,b) we predicted that the VR1 density in C6 cells was approximately 10 % of that seen in sensory neurons. Since in the VR1/C6 cells, which expressed 5–10 fold higher VR1 levels (Fig. 1A), 5–20 sec capsaicin application was sufficient to initiate maximal response, we believe that the endogenous VR1 expressed in the C6 cells did not contribute appreciably to the VR1-mediated $[Ca^{2+}]_i$ responses presented in this study.

The following protocol was used to investigate the effect of various neurotrophins on VR1 function. First, two Ca-transients (control transients) were evoked by repeated administration of 1 μM capsaicin (for clarity, only the second transients are shown in Figs. 3 and 4), then the cells were incubated for 2–5 min with the given neurotrophin, and, finally, another Ca-transient was induced by capsaicin (test transient). To reveal the effect of neurotrophins on the capsaicin-evoked responses, the amplitudes of the second control and the test Ca-transients were compared. The amplitude of each

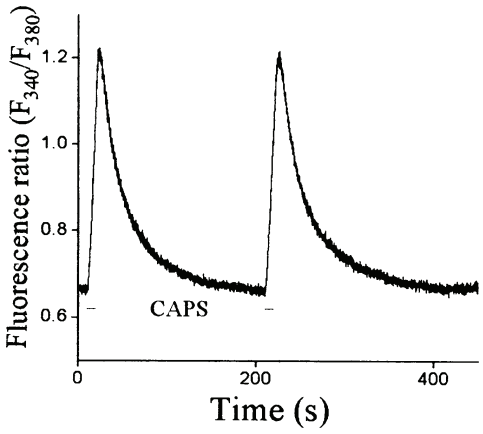

Fig. 2. Effect of repeated capsaicin application on the intracellular calcium level in VR1/C6 cells. VR1/C6 cells growing on glass coverslips were loaded with 5 μM fura 2-AM and fluorescence ratio (F_{340}/F_{380}) values of excitations at 340 and 380 nm wavelengths were recorded at an acquisition rate of 10 Hz per ratio. The effects of repeated, short (5–20 sec) application of 1 μM capsaicin (CAPS) were measured in Tyrode's solution. Note the lack of tachyphylaxis upon repeated capsaicin treatment. Results are representative of multiple determinations.

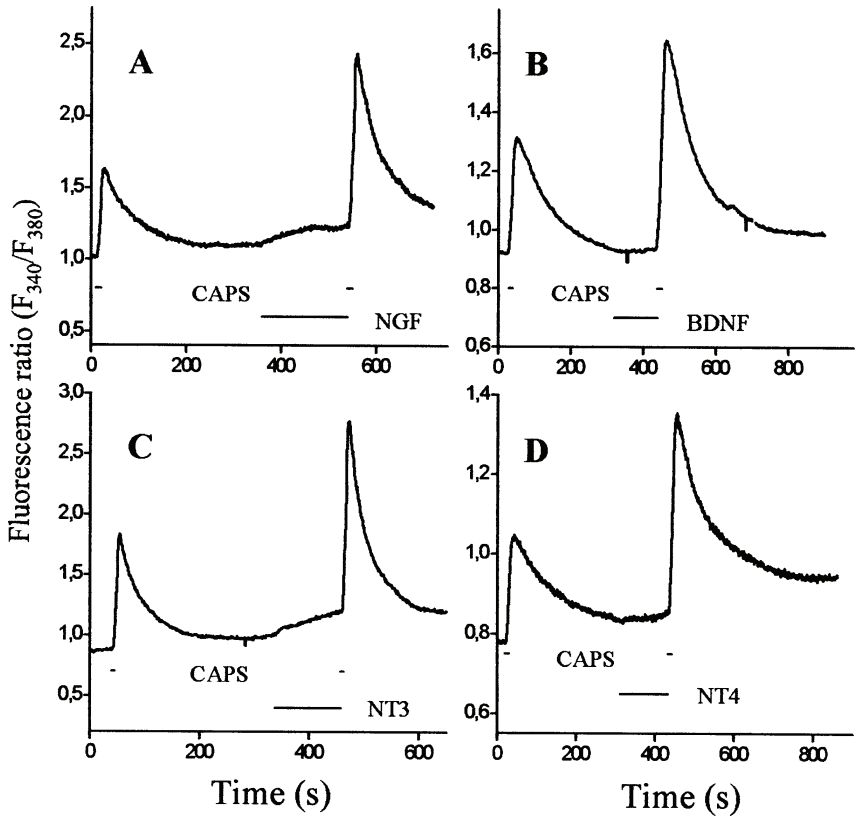

Fig. 3. Effects of neurotrophins on capsaicin-induced calcium elevations in VR1/C6 cells. Fura 2-AM-loaded VR1/C6 cells were fist challenged twice by short (5–20 sec) applications of 1 μM capsaicin (CAPS) (for clarity, only the second capsaicin-induced Ca-transients are shown in the Figure). Cells were then treated (for 2–5 min) by A: 100 ng/ml nerve growth factor (NGF); B: 50 ng/ml brain-derived neurotrophic factor (BDNF); C: 50 ng/ml neutotrophin-3 (NT3); D: 50 ng/ml neutotrophin-3 (NT4). At the end of the neurotrophin treatment, cells were again challenged by 1 μM capsaicin. Note the marked sensitizing effect of all of the neurotrophins. Results are representative of several determinations (see text for statistical analysis).

transient was calculated as a difference between the baseline Ca level (measured at the time of the initiation of the capsaicin application) and the maximum of the Ca elevation. This type of comparison made it possible to exclude from the analysis the effect of alterations in $[Ca^{2+}]_i$ during pre-incubation (see below).

All of the examined neurotrophins significantly, yet differentially, increased the amplitude of the test capsaicin-induced transients (Fig. 3). Statistical analysis of data obtained on multiple cells revealed that, when the amplitude of the control capsaicin-induced transient was regarded as 100%, the increase in the amplitude of the test transient was 83 ± 17 % (n = 28) in the case of 100 ng/ml NGF treatment; 104 ± 19 % (n = 14) in the case of 50 ng/ml BDNF application; 71 ± 16 % in the case of 50 ng/ml NT3 administration (n = 15); and 68 ± 11 % (n = 16) in the case of NT4 treatment (all values, mean ± SEM). These findings indicate that the recombinant rat VR1 can be sensitized by neurotrophins. In addition, they show that NGF, BDNF and NT4, in parallel with their actions on primary sensory neurons to sensitize the capsaicin-induced membrane currents (Shu and Mendell, 1999b; Shu et al., 1999; Chuang et al., 2001), are able to potentiate the VR1-mediated calcium

responses. Finally, these results demonstrate for the first time that NT3 exerts a sensitizing effect on the action of capsaicin on VR1.

In these studies, maximally effective concentrations of the neurotrophins were applied. These concentrations correspond to those described by other groups analyzing the action of neurotrophins on VR1 (Shu and Mendell, 1999a,b; Chuang et al., 2001). It should be noted that the concentrations are higher than the concentrations typically described in whole tissues, but direct comparison is difficult, because neurotrophins may be released in vivo by cells (e.g., keratinocytes, mast cells, and glial cells) (Acheson et al., 1991; Lewin and Barde, 1996; Botchkarev et al., 1999) that are in direct contact with sensory neurons (Wiesner-Menzel et al., 1999; Kettenmann, 1996; Botchkarev et al., 1997).

The various neurotrophins may exert their cellular effect via different membrane receptors (Kaplan and Miller, 1997; Huang and Reichardt, 2003). However, whereas all of the neurotrophins possess very similar sensitivities to the low-affinity p75 receptor, NGF binds mostly to trkA, BDNF and NT4 to trkB, and NT3 to the trkC receptor (Kaplan and Miller, 1997; Huang and Reichardt, 2003). Since all of these receptors are expressed in VR1/C6 cells (Fig. 1) and, moreover, since all of the examined neurotrophins caused sensitization of the VR1 (Fig. 3), we determined whether the actions of neurotrophins were mediated by the Trk or the p75 receptors. We applied K252a, the inhibitor of the tyrosine kinase pathway (Knusel and Hefti, 1992). In these experiments, the 2–5 min pre-incubation of the VR1/C6 cells with various neurotrophins (before the test capsaicin administration) was preceded by a 2–5 min treatment with 50 nM K252a (which was continued in parallel with the application of the given neurotrophin). As seen in Fig. 4, K252a completely prevented the VR1 sensitizing action of all of the neurotrophins. Statistical analysis on numerous cells revealed that, in the presence of the tyrosine kinase inhibitor, the amplitudes of the test Ca transients after neurotrophin treatment were not significantly different from those of the control ones: in the case of 100 ng/ml NGF treatment, the test Ca rise was 7 $\pm$ 5 % less than control (n = 13); in the case of 50 ng/ml BDNF application, 8 $\pm$ 6 % more than control (n = 8); in the case of NT3 administration, 6 $\pm$ 4 % less than control (n = 11); and in the case of NT4 treatment, 2 $\pm$ 5 % less than control (n = 9) (all values, mean $\pm$ SEM). These findings indicate that sensitizing effects of neurotrophins are mediated by the trk receptors, i.e., trkA for NGF, trkB for BDNF and NT4, and, of great novelty, trkC for NT3. In primary capsaicin-sensitive sensory neurons, which do co-express trkA and B but do not express trkC (McMahon et al., 1994), NGF and NT4 were effective in sensitizing the action of capsaicin on membrane currents whereas NT3 was not (Shu and Mendell, 1999b; Shu et al., 1999). The lack of crucial involvement of p75 receptor-mediated pathway in the response is also suggested by the observation that NGF was able to induce hyperalgesia in p75 knockout mice, which do express trk receptors (Bergmann et al., 1998).

Most of the neurotrophins caused a slow increase in the resting $[Ca^{2+}]_i$ level during the 2–5 min pre-incubation period in a significant portion (approximately 40 %) of the cells investigated. This effect was much less and slower than that of capsaicin and was in good agreement with previously published data on the effect of neurotrophins on various neuronal preparations (Marmigere et al., 2001; Lamb and Bielefeldt, 2003). However, of great importance, as revealed by statistical comparison of findings on cells where neurotrophins did or did not cause elevations of resting calcium level (data not shown), and, furthermore, as seen in Fig. 3, the presence, absence, or the degree of this slow calcium rise did not influence the sensitization effect of neurotrophins on VR1. In addition, K252a was unable to prevent the neurotrophin-induced slow calcium rise (Fig. 4). Instead, the inhibitor itself (similarly to the action of the neurotrophins in Fig. 3 and Fig. 4) also caused an elevation in the resting calcium level. Although the exact mechanism by which K252a alone raised intracellular calcium is still to be determined, it seems

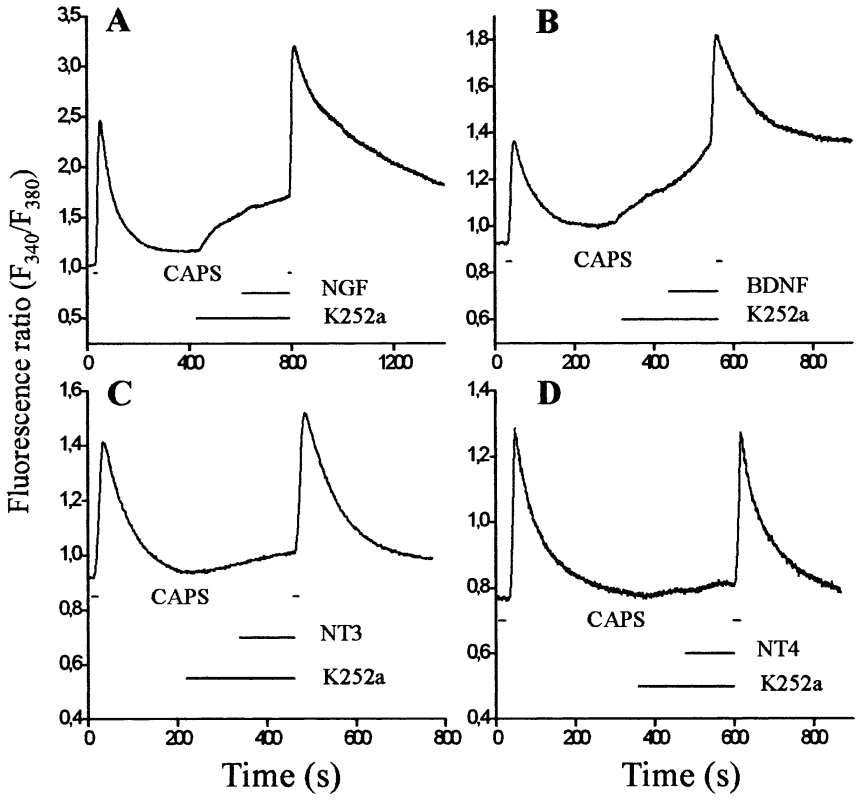

Fig. 4. Effects of neurotrophins on capsaicin-induced calcium elevations in the presence of the tyrosine kinase inhibitor K252a in VR1/C6 cells. Fura 2-AM-loaded VR1/C6 cells were fist challenged twice by short (5–20 sec) applications of 1 μM capsaicin (CAPS) (for clarity, only the second capsaicin-induced Ca-transients are shown in the Figure). Cells were then pretreated (for 2–5 min) by 50 nM K252a and then (for 2–5 min) by A: 100 ng/ml nerve growth factor (NGF); B: 50 ng/ml brain-derived neurotrophic factor (BDNF); C: 50 ng/ml neutotrophin-3 (NT3); D: 50 ng/ml neutotrophin-3 (NT4). K252a administration was continued during neurotrophin application. At the end of this protocol, cells were again challenged by 1 μM capsaicin. Note the lack of sensitizing effects of the neurotrophins in the presence of K252a. Results are representative of several determinations (see text for statistical analysis).

that the sensitizing effects of neurotrophins on VR1 and the inhibitory action of K252a to prevent such responses are independent on their actions on resting calcium.

Conclusions

In summary we can conclude that various neurotrophins are all capable of sensitizing the recombinant VR1-mediated intracellular calcium response to the action of capsaicin. Furthermore, we have also shown that the sensitization process may occur via either trk receptors (i.e., A, B, or C) suggesting a common intracellular mechanisms related to the activation of the trk receptor. Since all trk receptors may alter the activity of the phospholipase Cγ (PLCγ) (Kaplan and Miller, 1997; Huang and Reichardt, 2003), the most probable mechanism of VR1 sensitization by the neurotrophins is the one that suggested by Chuang et al. (2001) claiming that the cleavage of phosphatidylinositol-4,5-bisphosphate (PIP_2) by receptor-coupled PLCγ activation releases the VR1 from the tonic allosteric inhibition by PIP_2 and

hence decreases the agonist threshold of the receptor. In addition, the previously described PLC-mediated activation of certain protein kinase C isoforms (Premkumar and Ahern, 2000) and/or the cyclic AMP — protein kinase A system (De Petrocellis et al., 2001; Shu and Mendell, 2001; Bhave et al., 2002) have also been implicated in the sensitization of VR1. Therefore, neurotrophins, investigated in this study, may all participate in the development of inflammatory (thermal) hyperalgesia.

Acknowledgements

The authors are indebted to Ms. Ibolya Varga for helpful technical assistance. This work was supported by Hungarian research grants: OTKA F035036, NKFP 00088/2001, OMFB 00200/2002. Tamás Bíró is a recipient of the György Békésy Postdoctoral Scholarship of the Hungarian Ministry of Education.

References

Acheson, A., Barker, P.A., Alderson, R.F., Miller, F.D., Murphy, R.A., 1991. Detection of brain-derived neurotrophic factor-like activity in fibroblasts and Schwann cells: Inhibition by antibodies to NGF. Neuron 7, 265–275.

Bergmann, I., Reiter, R., Toyka, K.V., Koltzenburg, M., 1998. Nerve growth factor evokes hyperalgesia in mice lacking the low-affinity neurotrophin receptor p75. Neuroscience Letters 255 (2), 87–90.

Bhave, G., Zhu, W., Wang, H., Brasier, D.J., Oxford, G.S., Gereau IV, R.W. 2002. cAMP-dependent protein kinase regulates desensitization of the capsaicin receptor (VR1) by direct phosphorylation. Neuron 35 (4), 721–731.

Bíró, T., Brodie, C., Modarres, S., Lewin, N.E., Ács, P., Blumberg, P.M., 1998a. Specific vanilloid responses in C6 rat glioma cells. Brain Research and Molecular Brain Research 56 (1–2), 89–98.

Bíró, T., Szabó, I., Hunyadi, J., Kovács, L., Csernoch, L., 1998b. Distinct sub-populations in HaCaT cells as revealed by the characteristics of intracellular calcium release induced by phosphoinositide-coupled agonists. Archives of Dermatological Research 290 (5), 270–276.

Botchkarev, V.A., Eichmuller, S., Peters, E.M.J., Pietsch, P., Johansson, O., Maurer, M., Paus, R., 1997. A simple immunfluorescence technique for simultaneous visualization of mast cells and nerve fibers reveals selectivity and hair cycle — dependent changes in mast cell — nerve fiber contacts in murine skin. Archives in Dermatological Research 289, 292–302.

Botchkarev, V.A., Metz, M., Botchkareva, N.V., Welker, P., Lommatzch, M., Renz, M., Paus, R., 1999. Brain-derived neurotrophic factor, neurotrophin-3, and neurotrophin-4 act as ‘‘epitheliotrophins’’ in murine skin. Laboratory Investigation 76, 557–572.

Caterina, J.M., Schumacher, M.A., Tominaga, M., Rosen, T.A., Levine, J.D., Julius, D., 1997. The capsaicin-receptor: a heat-activated ion channel in the pain pathway. Nature 389, 816–824.

Caterina, M.J., Leffler, A., Malmberg, A.B., Martin, W.J., Trafton, J., Petersen-Zeitz, K.R., Koltzenburg, M., Basbaum, A.I., Julius, D., 2000. Impaired nociception and pain sensation in mice lacking the capsaicin receptor. Science 288 (5464), 306–313.

Caterina, J.M., Julius, D., 2001. The vanilloid receptor: A molecular gateway to the pain pathway. Annual Review of Neuroscience 24, 487–517.

Chuang, H., Prescott, E.D., Kong, H., Shields, S., Jordt, S.E., Basbaum, A.I., Chao, M.V., Julius, D., 2001. Bradykinin and nerve growth factor release the capsaicin receptor from PtdIns(4,5)P2-mediated inhibition. Nature 411 (6840), 957–962.

Crowley, C., Spencer, S.D., Nishimura, M.C., Chen, K.S., Pitts-Meek, S., Armanini, M.P., Ling, L.H., McMahon, S.B., Schelton, D.L., Levinson, A.D., Philips, H.S., 1994. Mice lacking nerve growth factor display perinatal loss of sensory and sympathetic neurons yet develop basal forebrain cholinergic neurons. Cell 76 (6), 1001–1011.

De Petrocellis, L., Harrison, S., Bisogno, T., Tognetto, M., Brandi, I., Smith, G.D., Creminon, C., Davis, J.B., Geppetti, P., Di Marzo, V., 2001. The vanilloid receptor (VR1)-mediated effects of anandamide are potently enhanced by the cAMP-dependent protein kinase. Journal of Neurochemistry 77 (6), 1660–1663.

Di Marzo, V., Blumberg, P.M., Szallasi, A., 2002. Endovanilloid signaling in pain. Current Opinion in Neurobiology 12 (4), 372–379.

Huang, E.J., Reichardt, L.F., 2003. TRK receptors: Roles in neuronal signal transduction. Annual Review of Biochemistry 72, 609–642.

Hutton, L.A., de Vellis, J., Perez-Polo, J.R., 1992. Expression of p75NGFR TrkA, and TrkB mRNA in rat C6 glioma and type I astrocyte cultures. Journal of Neuroscience Research 32, 363–375.

Kaplan, D.R., Miller, F.D., 1997. Signal transduction by the neurotrophin receptors. Current Opinion in Cell Biology 9 (2), 213–221.

Kettenmann, H., 1996. Beyond the neuronal circuitry. Trends in Neuroscience 19, 305–306.

Kirstein, M., Farinas, I., 2002. Sensing life: regulation of sensory neuron survival by neurotrophins. Cellular and Molecular Life Sciences 59 (11), 1787–1802.

Knusel, B., Hefti, F., 1992. K-252 compounds: modulators of neurotrophin signal transduction. Journal of Neurochemistry 59 (6), 1987–1996.

Kumar, S., de Vellis, J., 1996. Neurotrophin activates signal transduction in oligodendroglial cells: expression of functional TrkC receptor isoforms. Journal of Neuroscience Research 44 (5), 490–498.

Lamb, K., Bielefeldt, K., 2003. Rapid effects of neurotrophic factors on calcium homeostasis in rat visceral afferent neurons. Neuroscience Letters 336 (1), 9–12.

Lázár, J., Szabó, T., Kovács, L., Blumberg, P.M., Bíró, T., 2003. Distinct features of recombinant rat vanilloid receptor-1 (rVR1) when expressed in various heterologous expression systems. Cellular and Molecular Life Sciences 60 (10), 2228–2240.

Lewin, G.R., Barde, Y.-A., 1996. Physiology of the neurotrophins. Annual Review of Neuroscience 19, 289–317.

Marmigere, F., Choby, C., Rage, F., Richard, S., Tapia-Arancibia, L., 2001. Rapid stimulatory effects of brain-derived neurotrophic factor and neurotrophin-3 on somatostatin release and intracellular calcium rise in primary hypothalamic cell cultures. Neuroendocrinology 74 (1), 43–54.

Mazurek, N., Weskamp, G., Erne, P., Otten, U., 1986. Nerve growth factor induces mast cell degranulation without changing intracellular calcium levels. FEBS Letters 198 (2), 315–320.

McMahon, S.B., Armanini, M.P., Ling, L.H., Phillips, H.S., 1994. Expression and coexpression of Trk receptors in subpopulations of adult primary sensory neurons projecting to identified peripheral targets. Neuron 12, 1161–1171.

Oláh, Z., Lehel, C., Jakab, G., Anderson, W.B., 1994. A cloning and epsilon-epitope-tagging insert for the expression of polymerase chain reaction-generated cDNA fragments in Escherichia coli and mammalian cells. Analytical Biochemistry 221, 94–102.

Oláh, Z., Szabó, T., Karai, L., Hough, C., Fields, R.D., Caudle, R.M., Blumberg, P.M., Iadarola, M.J., 2001. Ligand-induced dynamic membrane changes and cell deletion conferred by vanilloid receptor 1. Journal of Biological Chemistry 276, 11021–11030.

Papp, H., Czifra, G., Lázár, J., Boczán, J., Gönczi, M., Csernoch, L., Kovács, L., Bíró, T., 2003. Protein kinase C isozymes regulate proliferation and high cell density-mediated differentiation of HaCaT keratinocytes. Experimental Dermatology 12, 811–824.

Premkumar, L.S., Ahern, G.P., 2000. Induction of vanilloid receptor channel activity by protein kinase C. Nature 408 (6815), 985–990.

Shu, X.Q., Mendell, L.M., 1999a. Neurotrophins and hyperalgesia. Proceedings of the National Academy of Sciences USA 96, 7693–7696.

Shu, X.Q., Mendell, L.M., 1999b. Nerve growth factor acutely sensitizes the response of adult rat sensory neurons to capsaicin. Neuroscience Letters 274 (3), 159–162.

Shu, X.Q., Mendell, L.M., 2001. Acute sensitization by NGF of the response of small-diameter sensory neurons to capsaicin. Journal of Neurophysiology 86, 2931–2938.

Shu, X.Q., Llinas, A., Mendell, L.M., 1999. Effects of trkB and trkC neurotrophin receptor agonists on thermal nociception: a behavioral and electrophysiological study. Pain 80 (3), 463–470.

Snider, W.D., 1994. Functions of the neurotrophins during nervous system development: what the knockouts are teaching us. Cell 77, 627–638.

Szallasi, A., Blumberg, P.M., 1999. Vanilloid (capsaicin) receptors and mechanisms. Pharmacological Reviews 51 (2), 150–211.

Wiesner-Menzel, L., Schulz, B., Vakilzadeh, F., Czarnetzki, B.M., 1999. Electron microscopical evidence for a direct contact between nerve fibres and mast cells. Acta Dermatologica et Venereologica 61 (6), 465–469.

Weskamp, G., Otten, U., 1987. An enzyme-linked immunoassay for nerve growth factor (NGF): a tool for studying regulatory mechanisms involved in NGF production in brain and in peripheral tissues. Journal of Neurochemistry 48 (6), 1779–1786.

Winston, J., Toma, H., Shenoy, M., Pasricha, P.J., 2001. Nerve growth factor regulates VR-1 mRNA levels in cultures of adult dorsal root ganglion neurons. Pain 89 (2–3), 181–186.

Winter, J., Forbes, C., Sternberg, J., Lindsay, R.M., 1988. Nerve growth factor (NGF) regulates adult rat cultured dorsal root ganglion neuron responses to capsaicin. Neuron 1, 973–981.

VIII.

The Analgesic Drug, Tramadol, Acts as an Agonist of the Transient Receptor Potential Vanilloid-1

Rita Marincsák, MD*

Balázs I. Tóth, MSc*†

Gabriella Czifra, PhD*

Tamás Szabó, MD, PhD‡

László Kovács, MD, PhD*†

Tamás Bíró, MD, PhD*†

BACKGROUND: Tramadol is an effective analgesic substance widely used in medical practice. Its therapeutic action have been mainly attributed to the activation of μ-opioid receptors as well as to the inhibition of neurotransmitter reuptake mechanisms and various voltage- and ligand-gated ion channels of the nociceptive system. As transient receptor potential vanilloid-1 (TRPV1, "the capsaicin receptor") has been shown to function as a central integrator molecule of pain sensation, our aim in the current study was to define the involvement of TRPV1 in the complex mechanism of action of tramadol.

METHODS: To achieve these goals, we used single-cell Ca-imaging as well as fluorescent image plate reader assays on Chinese hamster ovary (CHO) cells heterologously over-expressing TRPV1.

RESULTS: We found that (1) tramadol, similar to the well-known TRPV1 agonist, capsaicin, significantly increased $[Ca^{2+}]_i$ of TRPV1-CHO cells in a concentration-dependent fashion; (2) its effect was reversibly prevented by the TRPV1 antagonist capsazepine; (3) repeated application of tramadol resulted in marked tachyphylaxis; and (4) tramadol did not modify $[Ca^{2+}]_i$ in control (empty vector expressing) CHO cells.

CONCLUSIONS: Collectively, these findings strongly support the intriguing and novel concept that tramadol acts as an agonist of TRPV1. Considering that activation of TRPV1 on sensory neurons is followed by a local release of vasoactive neuropeptides and a marked desensitization of the afferent fibers (hence termination of pain sensation), our findings may equally explain both the desired analgesic as well as the often-seen, yet "unexpected," local side effects (e.g., initiation of burning pain and erythema) of tramadol.

(Anesth Analg 2008;106:1890–6)

Transient receptor potential vanilloid-1 (TRPV1) is a nonselective calcium-permeable cation channel, which was originally described on nociceptive sensory afferents as a central integrator of pain sensation.[1,2] TRPV1 can be activated and/or sensitized by certain exogenous agonists, such as capsaicin, a main pungent ingredient of hot chili peppers, or its ultrapotent analog, resiniferatoxin, and numerous endogenous substances, such as heat, protons, bradykinin, lipid peroxidation products, etc.[3,4] The activation of TRPV1 results in depolarization of the sensory afferents, firing of action potentials and, hence, the onset of pain.[1,5] Therefore, the molecule may serve as an attractive analgesic pharmacological target.[6,7]

Of great importance, several reports also suggest that certain analgesics and/or anesthetics, besides their previously appreciated target molecules, may also act on TRPV1. However, their action was very controversially documented by different groups. Namely, in cells heterologously expressing TRPV1, several local anesthetics, such as lidocaine, prilocaine, and procaine, were shown to inhibit the capsaicin-induced increase of intracellular calcium concentration ($[Ca^{2+}]_i$) in a concentration-dependent manner.[8] In contrast, on cultured TRPV1-expressing nociceptive neurons, tetracaine, another local anesthetic, was shown to enhance the membrane current induced by capsaicin.[9] In the above study, Hirota et al. have also found that the effect of capsaicin was not modified by a wide array of IV general anesthetics (such as thiopental, ketamine, propofol). However, in the same expression system, other researchers have shown that propofol acts as a potent agonist of the receptor.[10]

Tramadol is an effective analgesic substance widely used in medical practice.[11,12] Its therapeutic action was mainly attributed to the activation of μ-opioid receptors[11,13,14] and to the inhibition of serotonin and norepinephrine reuptake by the synaptosomes.[15,16]

From the *Department of Physiology, †Cell Physiology Research Group of the Hungarian Academy of Sciences, and ‡Department of Pediatrics, University of Debrecen, Medical and Health Science Center, Research Center for Molecular Medicine, Debrecen, Hungary.

Accepted for publication February 15, 2008.

Supported by Hungarian research grants: OTKA T49231, OTKA K63153, ETT 480/2006, ETT 482/2006.

Address correspondence and reprint requests to Tamás Bíró, MD, PhD, Department of Physiology, University of Debrecen, Medical and Health Science Center, Research Center for Molecular Medicine, 4032 Debrecen, Nagyerdei krt. 98. PO Box 22, Hungary. Address e-mail to biro@phys.dote.hu.

DOI: 10.1213/ane.0b013e318172fefc

Interestingly, however, on various cultured neuronal cell populations, tramadol was also shown to inhibit the activity of voltage-dependent Na^+ channels,[17] delayed rectifier K^+ channels[18] as well as γ-aminobutyric acid type A and *N*-methyl-D-aspartate ionotropic receptors.[19] These data strongly argue for a more complex mechanism of tramadol's action.

Of further importance, data from numerous *in vivo* studies also suggest that tramadol may also exert a local anesthetic-like effect.[20–23] In light of the above findings, in the current study, we aimed to investigate the effect of tramadol on one of the key molecules of nociception, i.e., TRPV1. Here, we report that tramadol, intriguingly, acts as an agonist of TRPV1.

METHODS

Expression System, Cell Culturing

The expression system was generated as we reported previously.[24-26] Briefly, cDNA of the rat TRPV1 was subcloned into pUHG102-3 (Clontech, Palo Alto, CA) and was transfected into Chinese hamster ovary (CHO) cells carrying the pTet Off Regulator plasmid (Clontech) (TRPV1-CHO cells). In these cells, expression of the pUHG plasmid (hence TRPV1) is repressed in the presence of tetracycline and is expressed upon removal of the antibiotic. Therefore, cells were routinely cultured in Ham F-12 medium (supplemented with 10% fetal calf serum, and antibiotics, all from Sigma St. Louis, MO), which contained 500 μg/mL G418 (Geneticin) (Invitrogen, Paisley, UK), and 1 μg/mL tetracycline (Sigma). Before calcium imaging, cells were seeded on 25-mm glass coverslips or 96-well plates and were switched to tetracycline-free Ham F-12 medium. Cells were then cultured at 34.5°C rigorously for 48 h to induce similar TRPV1 expression levels in the different experiments. To evaluate the efficacy and homogeneity of the induction of TRPV1 expression, Western blot analysis was performed as described in our previous report[25] (data not shown).

Measurements of $[Ca^{2+}]_i$ Using Single Cell Ca Imaging

Changes in $[Ca^{2+}]_i$ were detected as described in our earlier reports.[24,25] TRPV1-CHO cells were cultured on 25-mm glass coverslips and a calcium-sensitive probe was introduced into the intracellular space by incubating the cells with 2 μM fura-2 AM (Invitrogen) for 1 h at 37°C. Before each measurement, the cells were kept at room temperature (22°C–24°C) in normal Tyrode's solution (137 mM NaCl, 5.4 mM KCl, 0.5 mM $MgCl_2$, 1.8 mM $CaCl_2$, 11.8 mM HEPES-NaOH, 1 g/L glucose, pH 7.4, all from Sigma) for 30 min to allow de-esterification of the fluorophore. The coverslips, containing the fura-2-loaded cells, were then placed on the stage of an inverted fluorescence microscope (Diaphot, Nikon, Tokyo, Japan). Excitation was altered between 340 and 380 nm using a dual wavelength monochromator (Deltascan, Photon Technology International, New Brunswick, NJ). The emission was monitored at 510 nm with a photomultiplier at an acquisition rate of 10 Hz per ratio, and the fluorescence ratio (F_{340}/F_{380}) values were determined. Cells were continuously washed by Tyrode's solution using a slow background perfusion system, whereas the agents investigated (capsaicin and tramadol were from Sigma; capsazepine from Alexis, San Diego, CA) were applied through a rapid perfusion system positioned in close proximity to the cell measured. In initial experiments, varying concentrations of tramadol were tested and saturating concentrations resulting in maximal responses were selected for the subsequent experiments. Analyses of the $[Ca^{2+}]_i$ transients were performed by a PTI analysis program developed by us, which measures (1) maximal amplitude of the transient above the baseline (in fluorescence ratio, F_{340}/F_{380}); (2) the time to peak value (time interval between the start of the application of the drug and the maximal value of the increase, in s); and (3) the rate of rise value (slope of the ascending phase measured between the onset and peak of the transient, in ratio per second). All data are expressed as the mean ± SEM.

Microfluorimetric Measurements of $[Ca^{2+}]_i$

Cells were seeded in 96-well black-well/clear-bottom plates (Greiner Bio-One, Frickenhausen, Germany) at a density of 40,000 cells per well in Ham F-12 medium, supplemented as above, and cultured at 34.5°C for 48 h. The cells were then incubated with Ham F-12 medium containing the cytoplasmic calcium indicator 2 μM Fluo-4 AM (Invitrogen) at 34.5°C for 40 min. The cells were washed four times with and finally cultured in Hank's solution (136.8 mM NaCl, 5.4 mM KCl, 0.34 mM Na_2HPO_4, 0.44 mM KH_2PO_4, 0.81 mM $MgSO_4$, 1.26 mM $CaCl_2$, 5.56 mM glucose, 4.17 mM $NaHCO_3$, pH 7.2, all from Sigma) containing 1% bovine serum albumin (Sigma) and 2.5 mM Probenecid (Sigma) for 30 min at 34.5°C. The plates were then placed to a FlexStation II^{384} fluorimetric image plate reader (FLIPR, Molecular Devices, Sunnyvale, CA) and changes in $[Ca^{2+}]_i$ (reflected by changes fluorescence; lEX = 494 nm, lEM = 516 nm) induced by various concentrations of the drugs were recorded in each well (during the measurement, cells in a given well were exposed to only one given concentration of the agent). When calculating dose–response curves, data were fitted to the Hill equation

$$B/B_{max} = [X]^n/([EC50]^n + [X]^n)$$

where B is the actual fluorescence value, B_{max} is the theoretical maximum of B, X is the ligand in question (tramadol), and n is the Hill coefficient. Experiments were performed in quadruplets and the averaged data (as well as SEM) were used in the calculations.

Statistical Analysis

Data were analyzed using a Student's *t*-test, and $P < 0.05$ values were regarded as significant differences.

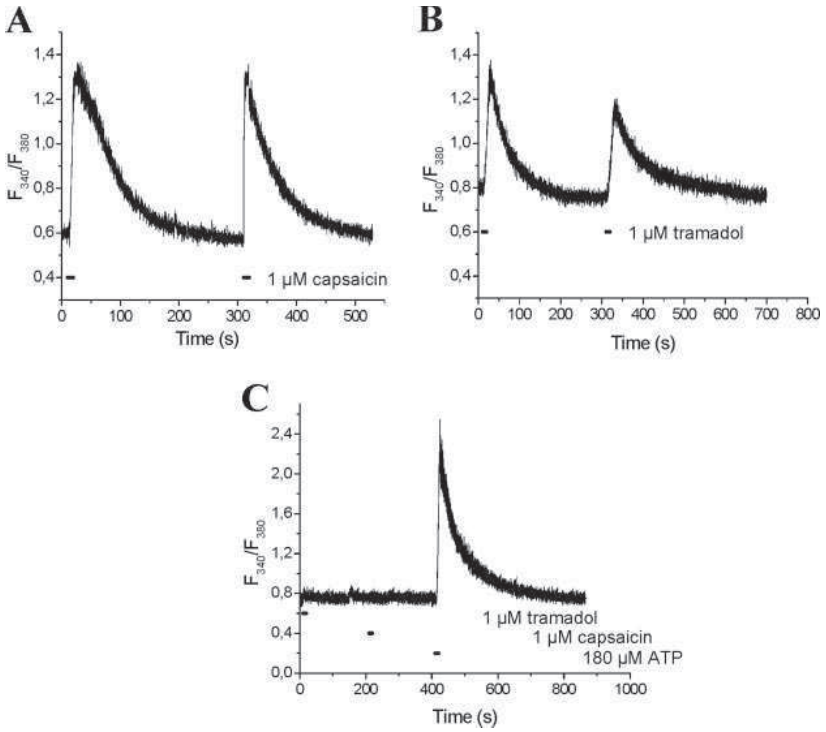

Figure 1. Effect of capsaicin and tramadol on $[Ca^{2+}]_i$ in TRPV1-CHO cells. Cells growing on glass coverslips were loaded with 2 μM fura 2-AM and fluorescence ratio (F_{340}/F_{380}) values of excitations at 340 and 380 nm wavelengths were recorded at an acquisition rate of 10 Hz per ratio. A and B represent the effect of 1 μM capsaicin and 1 μM tramadol, respectively, on TRPV1-CHO cells. (C) In contrast to ATP (used as a positive control), capsaicin and tramadol were unable to modify $[Ca^{2+}]_i$ on empty-vector expressing CHO cells. Results are representative of multiple determinations.

Table 1. Summary of Various Variables of $[Ca^{2+}]_i$ Transients Induced by Capsaicin and Tramadol on TRPV1-CHO Cells

	Capsaicin (1 μM)	Tramadol (1 μM)
Responding cells (%)	76 (n = 54/71)	72 (n = 41/57)
Amplitude (ratio)	1.5 ± 0.1	1.2 ± 0.1 (P = 0.029)
Time to peak (s)	14.5 ± 1.1	20.9 ± 1.2 (P = 0.0002)
Rate of rise (ratio/s)	0.49 ± 0.05	0.27 ± 0.04 (P = 0.001)
Tachyphylaxis of the 2nd transient (% of the 1st transient)	105 ± 9%	63.4 ± 5.4 (P = 0.00005)
Tachyphylaxis of the 3rd transient (% of the 2nd transient)	98 ± 6%	46.3 ± 3.8 (P = 0.000004)

Variables shown in the table were determined as described in Methods. All values are expressed as the mean ± SEM of several determinations. Significant differences (P values) were determined between the two groups using t-test.

RESULTS

Tramadol Induces Transient Increase of $[Ca^{2+}]_i$ in TRPV1-CHO Cells

We first investigated the effect of capsaicin on TRPV1-CHO cells. Confirming previous results,[25] 1 μM capsaicin induced a transient increase in $[Ca^{2+}]_i$, which, upon repeated applications (in a 300-s long interval), showed no tachyphylaxis (Fig. 1A, Table 1). This effect was mediated by TRPV1 since capsaicin was unable to modify $[Ca^{2+}]_i$ on empty-vector expressing CHO cells (in contrast to adenosine triphosphate which increased $[Ca^{2+}]_i$ on 73% of the cells investigated, n = 11) (Fig. 1C) and since the TRPV1 antagonist capsazepine (5 μM) effectively abrogated the action of capsaicin on TRPV1-CHO cells (data not shown).[25]

We then intended to investigate the effect of tramadol on the capsaicin-evoked $[Ca^{2+}]_i$ transients. However, intriguingly, we observed that 1 μM tramadol alone induced a transient increase in $[Ca^{2+}]_i$ (Fig. 1B), which, again similarly to the action of capsaicin, was not observed on CHO cells lacking TRPV1 (Fig. 1C). These data strongly suggest that tramadol, surprisingly, rather acted as a TRPV1 agonist in our system.

The Tramadol-Induced $[Ca^{2+}]_i$ Increases Are Distinct from Those Evoked by Capsaicin and Exhibit Profound Tachyphylaxis upon Repeated Applications

To further assess this issue, we have characterized the effect of tramadol on a large number of TRPV1-CHO cells (Table 1). Similar to capsaicin, 1 μM tramadol was able to induce transient increases in $[Ca^{2+}]_i$ in 72% of the TRPV1-CHO cells investigated (n = 41 of 57) (the threshold was minimum 10% increase in the fluorescence ratio within 60 s after the start of the application of the drug). These transients were characterized by medium amplitudes (1.2 ± 0.1 increase in the fluorescence ratio), time to peak values of 20.9 ± 1.2 s, and rate of rise values of 0.27 ± 0.04 ratio per second (all data expressed as mean ± SEM). Although these variables were comparable to those observed with the application of 1 μM capsaicin (Table 1 and Ref. 25), the maximal amplitude and rate of increase values were significantly smaller (P = 0.029 and 0.001, respectively), whereas the time to peak values were significantly greater (P = 0.0002) in the case of the tramadol-induced responses (Table 1). In addition, we found that a similar fraction of transients (76% with capsaicin, 79% with tramadol) returned to the baseline value after the cessation of administration of the drugs (data not shown).

The most striking difference was found when we compared the phenomenon of tachyphylaxis. As we

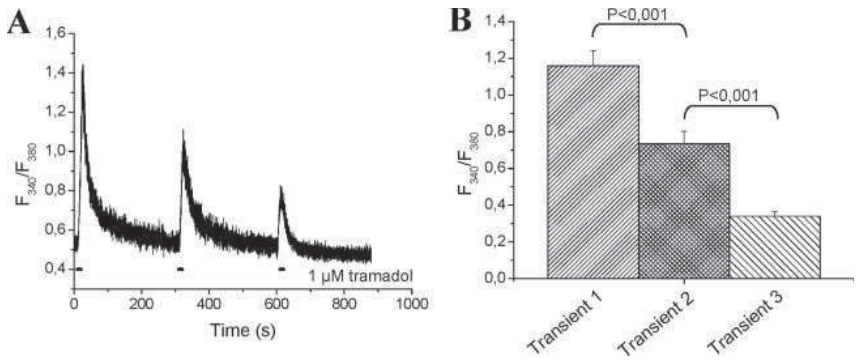

Figure 2. Effect of repeated application of capsaicin and tramadol on $[Ca^{2+}]_i$ in TRPV1-CHO cells. TRPV1-CHO cells growing on glass coverslips were loaded with 2 μM fura 2-AM. and fluorescence ratio (F_{340}/F_{380}) values were recorded. (A) Effect of repeated administration of short (10 s) 1 μM tramadol "pulses" at 300 s intervals. (B) Statistical analysis of F_{340}/F_{380} values upon repeated tramadol applications (as described under panel A). All values are expressed as the mean ± SEM of several determinations (n = 41). Significant differences (P values) were determined by t-test.

have previous shown[25] (and also confirmed in the current study, Fig. 1A), in TRPV1-CHO cells, the repeated application of 1 μM capsaicin resulted in an insignificant decrease in the amplitude of the subsequent $[Ca^{2+}]_i$ transients. In contrast, upon the repeated administration of 1 μM tramadol (in 300 s intervals), the amplitude of the second $[Ca^{2+}]_i$ transient was 63.4% ± 5.4% (mean ± SEM, n = 41) of the first (control) one (P = 0.0003), whereas the amplitude of the third $[Ca^{2+}]_i$ transient was 46.3% ± 3.8% (mean ± SEM, n = 41) of the second one (P = 0.000004) (Figs. 1B, 2A and B, Table 1).

The Effect of Tramadol to Increase $[Ca^{2+}]_i$ Is Mediated by TRPV1

To further assess the TRPV1-specificity of the tramadol-induced $[Ca^{2+}]_i$ responses, we also investigated the effect of the TRPV1 antagonist capsazepine (Fig. 3). In these experiments, due to the above tachyphylaxis, the following protocol was used. First, three consecutive 10 s-long 1 μM tramadol "pulses" were administered, but now in 600 s intervals. The rate of tramadol-induced tachyphylaxis on numerous cells was then determined. This relatively long interadministration period was chosen since (1) as was shown above (Figs. 1 and 2), it took approximately 200–300 s for the tramadol-induced $[Ca^{2+}]_i$ transients to return to the baseline, and (2) we intended to measure the effect of a 300 s-long capsazepine application. Statistical analysis has shown that, under these conditions, the amplitude of the second $[Ca^{2+}]_i$ tramadol-evoked transient was 76.6% ± 7.8% (mean ± SEM, n = 10) of the first (control) one (P = 0.001), whereas the amplitude of the third $[Ca^{2+}]_i$ transient was 78.2% ± 8.4% (mean ± SEM, n = 10) of the second one (P = 0.000002) (Fig. 3B).

Subsequently, we repeated the above protocol; however, in this case, 300 s after the initiation of the second tramadol "pulse," cells were preincubated with 5 μM capsazepine for 300 s, and the third 1 μM tramadol challenge was administered in the presence of capsazepine. Consistent with the above findings, the presence of the TRPV1 antagonist almost fully abrogated the effect of tramadol to induce $[Ca^{2+}]_i$ increase (Fig. 3A). Statistically, the amplitude of the third tramadol-induced $[Ca^{2+}]_i$ transients in the presence of capsazepine was only 12.7% ± 2.8% (mean ±

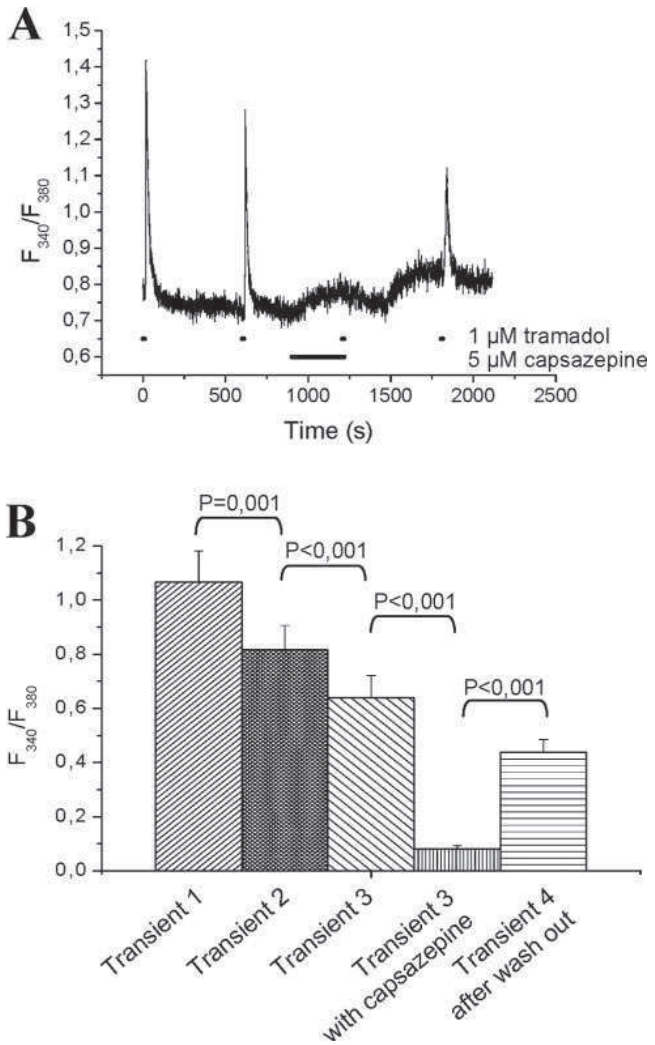

Figure 3. Effect of the TRPV1 antagonist capsazepine on the tramadol induced $[Ca^{2+}]_i$ increases in TRPV1-CHO cells. Cells growing on glass coverslips were loaded with 2 μM fura-2 AM and fluorescence ratio (F_{340}/F_{380}) values were recorded. (A) Cells were first challenged with two consecutive short (10 s) 1 μM tramadol "pulses" at 600 s intervals. Then, 300 s after the initiation of the second tramadol "pulse," cells were preincubated with 5 μM capsazepine for 300 s, and the third 1 μM tramadol challenge was administered in the presence of capsazepine. The fourth tramadol challenge was applied after washing out the antagonist. (B) Statistical analysis of F_{340}/F_{380} values upon repeated tramadol applications at 600 s intervals with or without capsazepine treatment. All values are expressed as the mean ± SEM of several determinations (n = 10). Significant differences (P values) were determined by t-test.

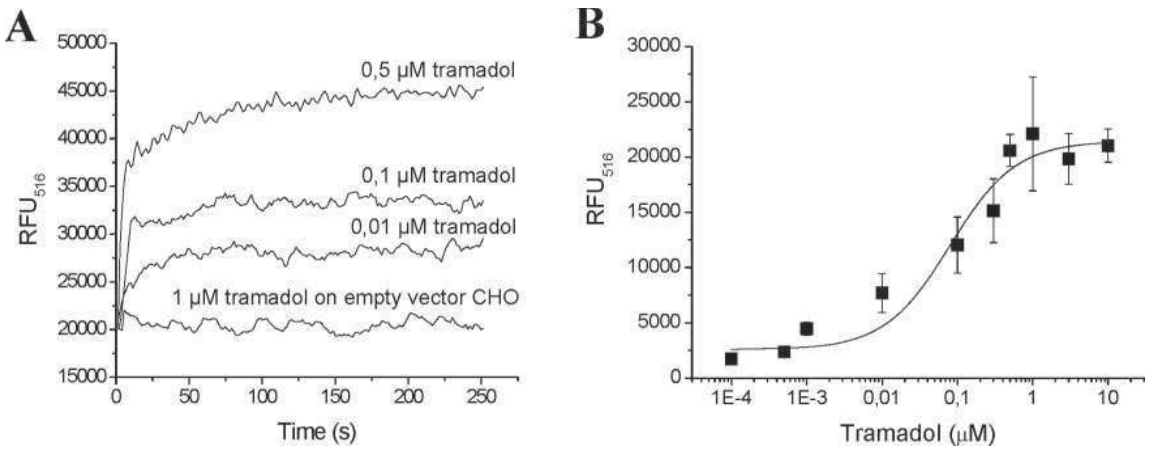

Figure 4. Concentration-dependence of tramadol to elevate $[Ca^{2+}]_i$ in TRPV1-CHO cells using FLIPR. (A) Cells were seeded into black walled clear-base 96-well plates at a density of 40,000 cells per well and were loaded with 2 μM fluo-4 AM. The plates were then placed into a FlexStation II^{384} to monitor cell fluorescence (lEX = 494 nM, lEM = 516 nM) before and after the addition of various concentrations of tramadol (the application time point were set to 0). Note the lack of effect of tramadol on empty vector expressing CHO cells. Results are representative of multiple determinations. (B) The theoretical curve was calculated by fitting the measured mean ± SEM values of four independent determinations to the Hill equation.

SEM, $n = 10$) ($P = 0.00008$) of those (third) increases, which were recorded in the lack of the TRPV1 antagonist (Fig. 3A and B). Finally, this inhibition of the tramadol-induced responses by capsazepine was reversible, since another tramadol application (600 s after the third one) again resulted in significantly ($P = 0.00003$) higher $[Ca^{2+}]_i$ transients than those evoked in the presence of the antagonist.

The Effect of Tramadol Is Concentration-Dependent

Finally, we investigated the concentration-dependence of tramadol on TRPV1-CHO cells. Because of the above marked tachyphylaxis, we were unable to use the single-cell Ca-imaging technique to record the effects of various tramadol concentrations on the very same cell. Therefore, the measurement of the dose–response curve of tramadol was performed using FLIPR. As seen in Figure 4A, tramadol (similar to the single-cell data shown above) did not alter the $[Ca^{2+}]_i$ of control (empty-vector expressing) CHO cell. In contrast, on TRPV1-CHO cells, it was able to increase $[Ca^{2+}]_i$ in a concentration-dependent fashion; mathematical analysis by fitting the measured values to the Hill equation resulted in an EC_{50} value of 0.08 ± 0.03 μM (mean ± SEM for four experiments) (Fig. 4B) (and 0.04 ± 0.01 μM for capsaicin, mean ± SEM for five experiments, data not shown).

DISCUSSION

In this study, we investigated the effect of an analgesic, tramadol, on the function of TRPV1. Using a heterologous expression system, we found that (1) tramadol, similar to capsaicin, significantly increased $[Ca^{2+}]_i$ of TRPV1-CHO cells in a concentration-dependent fashion; (2) its effect was reversibly prevented by the TRPV1 antagonist capsazepine; and (3) tramadol did not modify $[Ca^{2+}]_i$ in control (empty vector expressing) CHO cells. These findings strongly support the intriguing and novel concept that tramadol, surprisingly, acts as an agonist of TRPV1.

Interestingly, whereas repeated capsaicin application resulted in insignificant modification of the Ca-transients, tramadol was able to induce a marked tachyphylaxis. It was previously shown that different vanilloid agonists with different chemical features cause different patterns of calcium response (potency, maximal response, latency of response, variability of latency of response among individual cells, and tachyphylaxis) in CHO cells heterologously expressing TRPV1.[26] We propose, therefore, that differences in the effects of capsaicin and tramadol to induce tachyphylaxis are also due to the structural diversities of the two agents.

Previous studies have demonstrated that 50 mg single dose of tramadol (depending on IM or IV application routes) reaches 100–300 ng/mL (i.e., 0.3–1 μM) plasma levels.[27,28] It was important to observe that this plasma concentration corresponds well to the EC_{50} value of 0.08 ± 0.03 μM measured in our current study arguing for a potential *in vivo* (human) relevance of our findings (see also below).

As was detailed in the Introduction, tramadol (besides stimulating μ-opioid receptors) exerts a wide-array of inhibitory actions of numerous voltage- and ligand-gated neuronal channel populations, underlying its robust effect to mitigate pain. In light of these previous reports, our data presented in the current manuscript immediately invite a key question: How would the unexpected activation of the "pain-receptor" TRPV1 "fit" to the *in vivo* analgesic action "pattern" of this popular therapeutic drug? One straightforward explanation could be that the activation of TRPV1 by tramadol is rapidly followed by the desensitization of the sensory afferents (a phenomenon well characterized by vanilloid administration to nociceptive neurons[1,2,6]), which, in turn, would lead to the cessation of action potential firing, and hence pain sensation. This

idea may be supported by the fact that, in our system, tramadol induced a much stronger tachyphylaxis than capsaicin.

However, it is also well established that the activation of TRPV1 also results in the local release of various peptides (e.g., substance P, calcitonin gene-related peptide) from the sensory ending.[24,29,30] These neuropeptides, in turn, act on various neighboring cell types of the given tissue (e.g., mast cells, vessels, keratinocytes) and initiate numerous local regulatory mechanisms, such as vasodilation, immunomodulation, cytokine and mediator release, etc.[2,4,31] It is conceivable, therefore, that if tramadol (e.g., upon local application) stimulates TRPV1-expressing sensory afferents, the initiation of the "efferent" function of the nerve endings would result in such local responses.

As a support for this argument, in various human studies, local intradermal application of tramadol, besides inducing a local anesthetic effect similar to that of lidocaine, resulted in skin erythema, flare, and urticaria.[20–23] Of further importance, in certain studies, intradermal tramadol injection also initiated burning skin sensation and pain.[21,22] Likewise, when the local anesthetic effect of tramadol was investigated after short (1 min) venous retention of the drug, in 31% of the patients, transient burning pain sensation and skin erythema developed distally from the place of occlusion along the affected veins.[23] These *in vivo* results further suggest for that tramadol may indeed activate TRPV1.

Collectively, our presented findings, along with the above *in vitro* and *in vivo* data) suggest that tramadol, besides the aforementioned multiple targets, may indeed act as a "classical" agonist of TRPV1. Namely, tramadol may first excite sensory neurons (calcium influx and transient burning pain sensation), then initiate neuropeptide release (skin erythema and flare), and finally induce desensitization (tachyphylaxis) and analgesia. Hence, although further studies (e.g., using gene-deficient mice and freshly dissected sensory neurons endogenously expressing TRPV1) are to be performed to exactly define the role of TRPV1 in mediating the action of tramadol, the presented concept of "triple response" by tramadol may equally explain both the desired analgesic as well as the "unexpected" local side effects of the drug.

ACKNOWLEDGMENTS

The technical assistance of Ms. Ibolya Varga is gratefully appreciated. Tamás Bíró is the recipient of the János Bolyai Research Scholarship of the Hungarian Academy of Sciences. The authors declare no competing financial interests.

REFERENCES

1. Caterina MJ, Schumacher MA, Tominaga M, Rosen TA, Levine JD, Julius D. The capsaicin receptor: a heat-activated ion channel in the pain pathway. Nature 1997;389:816–24
2. Szallasi A, Blumberg PM. Vanilloid (capsaicin) receptors and mechanisms. Pharmacol Rev 1999;51:159–212
3. Hwang SW, Oh U. Direct activation of capsaicin receptors by products of lipoxygenases: endogenous capsaicin-like substances. Curr Opin Pharmacol 2002;2:235–42
4. Di Marzo V, Blumberg PM, Szallasi A. Endovanilloid signaling in pain. Curr Opin Neurobiol 2002;12:372–9
5. Tominaga M, Caterina MJ, Malmberg AB, Rosen TA, Gilbert H, Skinner K, Raumann BE, Basbaum AI, Julius D. The cloned capsaicin receptor integrates multiple pain-producing stimuli. Neuron 1998;21:531–43
6. Holzer P. Capsaicin: cellular targets, mechanism of action, and selectivity for thin sensory neurons. Pharmacol Rev 1991;43:143–201
7. Veronesi B, Oortgiesen M. The TRPV1 receptor: target of toxicants and therapeutics. Toxicol Sci 2006;89:1–3
8. Hirota K, Smart D, Lambert DG. The effects of local and intravenous anesthetics on recombinant rat VR1 vanilloid receptors. Anesth Analg 2003;96:1656–60
9. Komai H, McDowell TS. Differential effects of bupivacaine and tetracaine on capsaicin-induced currents in dorsal root ganglion neurons. Neurosci Lett 2005;380:21–5
10. Tsutsumi S, Tomioka A, Sudo M, Nakamura A, Shirakura K, Takagishi K, Kohama K. Propofol activates vanilloid receptor channels expressed in human embryonic kidney 293 cells. Neurosci Lett 2001;312:45–9
11. Gibson TP. Pharmacokinetics, efficacy, and safety of analgesia with a focus on tramadol HCl. Am J Med 1996;101:47–53
12. Pyati S, Gan TJ. Perioperative pain management. CNS Drugs 2007;21:185–211
13. Raffa RB, Friderichs E, Reimann W, Shank RP, Codd EE, Vaught JL. Opioid and nonopioid components independently contribute to the mechanism of action of tramadol, an 'atypical' opioid analgesic. J Pharmacol Exp Ther 1992;260:275–85
14. Dayer P, Desmeules J, Collart L. Pharmacology of tramadol. Drugs 1997;53:18–24
15. Berrocoso E, Mico JA, Ugedo L. In vivo effect of tramadol on locus coeruleus neurons is mediated by alpha2-adrenoceptors and modulated by serotonin. Neuropharmacology 2006;51:146–53
16. Ogata J, Minami K, Uezono Y, Okamoto T, Shiraishi M, Shigematsu A, Ueta Y. The inhibitory effects of tramadol on 5-hydroxytryptamine type 2C receptors expressed in Xenopus oocytes. Anesth Analg 2004;98:1401–6
17. Haeseler G, Foadi N, Ahrens J, Dengler R, Hecker H, Leuwer M. Tramadol, fentanyl and sufentanyl but not morphine block voltage-operated sodium channels. Pain 2006;126:234–44
18. Tsai TY, Tsai YC, Wu SN, Liu YC. Tramadol-induced blockade of delayed rectifier potassium current in NG108–15 neuronal cells. Eur J Pain 2006;10:597–601
19. Hara K, Minami K, Sata T. The effects of tramadol and its metabolite on glycine, gamma-aminobutyric acid, and *N*-methyl-D-aspartate receptors expressed in Xenopus oocytes. Anesth Analg 2005;100:1400–5
20. Pang WW, Mok MS, Chang DP, Huang MH. Local anesthetic effect of tramadol, metoclopramide, and lidocaine following intradermal injection. Reg Anesth Pain Med 1998;23:580–3
21. Acalovschi I, Cristea T, Margarit S, Gavrus R. Tramadol added to lidocaine for intravenous regional anesthesia. Anesth Analg 2001;92:209–14
22. Altunkaya H, Ozer Y, Kargi E, Babuccu O. Comparison of local anaesthetic effects of tramadol with prilocaine for minor surgical procedures. Br J Anaesth 2003;90:320–2
23. Pang WW, Huang PY, Chang DP, Huang MH. The peripheral analgesic effect of tramadol in reducing propofol injection pain: a comparison with lidocaine. Reg Anesth Pain Med 1999; 24:246–9
24. Szallasi A, Szabó T, Bíró T, Modarres S, Blumberg PM, Krause JE, Cortright DN, Appendino G. Resiniferatoxin-type phorboid vanilloids display capsaicin-like selectivity at native vanilloid receptors on rat DRG neurons and at the cloned vanilloid receptor VR1. Br J Pharmacol 1999;128:428–34
25. Lázár J, Szabó T, Kovács L, Blumberg PM, Bíró T. Distinct feature of recombinant rat vanilloid receptor-1 expressed in various expression systems. Cell Mol Life Sci 2003;60:2228–40
26. Tóth A, Wang Y, Kedei N, Tran R, Pearce LV, Kang SU, Jin MK, Choi HK, Lee J, Blumberg PM. Different vanilloid agonists cause different patterns of calcium response in CHO cells heterologously expressing rat TRPV1. Life Sci 2005;76:2921–32
27. Lintz W, Beier H, Gerloff J. Bioavailability of tramadol after i.m. injection in comparison to i.v. infusion. Int J Clin Pharmacol Ther 1999;37:175–83

28. Lintz W, Becker R, Gerloff J, Terlinden R. Pharmacokinetics of tramadol and bioavailability of enteral tramadol formulations. Fourth communication: drops (without ethanol). Arzneimittelforschung 2000;50:99–108
29. Holzer P. Local effector functions of capsaicin-sensitive sensory nerve endings: involvement of tachykinins, calcitonin gene-related peptide and other neuropeptides. Neuroscience 1988; 24:739–68
30. Okajima K, Harada N. Regulation of inflammatory responses by sensory neurons: molecular mechanism(s) and possible therapeutic applications. Curr Med Chem 2006;13:2241–51
31. Szolcsányi J. Forty years in capsaicin research for sensory pharmacology and physiology. Neuropeptides 2004;38: 377–84

IX.

The FASEB Journal • Research Communication

Inhibition of human hair follicle growth by endo- and exocannabinoids

Andrea Telek,[*,†,1] Tamás Bíró,[*,†,1,2] Enikő Bodó,[‡] Balázs I. Tóth,[*,2] István Borbíró,[*] George Kunos,[§] and Ralf Paus[‡]

[*]Department of Physiology and [†]Cell Physiology Research Group of the Hungarian Academy of Sciences, University of Debrecen, Medical and Health Science Center, Research Center for Molecular Medicine, Debrecen, Hungary; [‡]Department of Dermatology, University Hospital Schleswig-Holstein, Campus Lübeck, University of Lübeck, Lübeck, Germany; and [§]National Institute on Alcohol Abuse and Alcoholism, National Institutes of Health, Bethesda, Maryland, USA

ABSTRACT **Recent studies strongly suggest that the cannabinoid system is a key player in cell growth control. Since the organ-culture of human hair follicles (HF) offers an excellent, clinically relevant model for complex tissue interaction systems, we have asked whether the cannabinoid system plays a role in hair growth control. Here, we show that human scalp HF, intriguingly, are both targets and sources of endocannabinoids. Namely, the endocannabinoid N-arachidonoylethanolamide (anandamide, AEA) as well as the exocannabinnoid Δ (9)-tetrahydrocannabinol dose-dependently inhibited hair shaft elongation and the proliferation of hair matrix keratinocytes, and induced intraepithelial apoptosis and premature HF regression (catagen). These effects were inhibited by a selective antagonist of cannabinoid receptor-1 (CB1). In contrast to CB2, CB1 was expressed in a hair cycle-dependent manner in the human HF epithelium. Since we successfully identified the presence of endocannabinoids in human HF, our data strongly suggest that human HF exploit a CB1-mediated endocannabinoid signaling system for negatively regulating their own growth. Clinically, CB1 agonists may therefore help to manage unwanted hair growth, while CB1 antagonists might counteract hair loss. Finally, human HF organ culture offers an instructive, physiologically relevant new research tool for dissecting "nonclassical" effects of endocannabinoids and their receptor-mediated signaling in general.—Telek, A., Bíró, T., Bodó, E., Tóth, B. I., Borbíró, I., Kunos, G., Paus, R. Inhibition of human hair follicle growth by endo- and exocannabinoids. *FASEB J.* 21, 3534–3541 (2007)**

Key Words: cannabinoid receptor · proliferation · apoptosis · hair cycle

Δ^9-TETRAHYDROCANNABINOL (THC), the psychoactive component of marijuana, mimics the effects of numerous endogenous substances (collectively referred to as endocannabinoids) by binding to cannabinoid (CB) receptors (1–5). Centrally, these endogenous molecules are involved in regulating, *e.g.*, behavior and learning (1–3, 6–8), while their peripheral effects include the modulation of immune and cardiovascular functions (1–3, 9, 10) and the control of growth normal and transformed cells as well as cell death and survival (11–17). CB receptors reportedly are also found on human epidermal keratinocytes *in vitro*, with conflicting data as to which types (CB1, CB2) are actually expressed (18–20). Although activation of CB receptors may suppress growth, murine skin tumors (18) and human melanomas (16) and, furthermore, cannabinoids were suggested to modify *in vitro* proliferation and differentiation of transformed keratinocytes (19, 21), it is unclear whether CB receptors are functionally important in normal human skin physiology.

The organ culture of human scalp hair follicles (HF) in the growth stage of the hair cycle (anagen VI), which continue to grow rapidly after microdissection and produce hair shafts *in vitro* at almost the *in vivo*-speed seen on the human scalp (22), is ideally suited to follow-up the above reports of growth-modulatory effects of CB receptor ligands in the human system. Employing this assay, we had already shown, *e.g.*, that vanilloid receptor-1 (TRPV1) agonists (such as capsaicin) operate as potent inhibitors of human hair growth (23). Arguing, furthermore, that the HF is exquisitely sensitive to the effects of psychoemotional stress (24, 25); that THC is prominently incorporated into human hair shafts (26, 27); and that several psychotropic hormones have recently been recognized to modulate human hair growth (24, 28–32), we now have asked whether the endocannabinoid system is also involved in the control of human hair growth.

Since the cycling HF represents a prototypic, constantly remodeled epithelial-mesenchymal interaction system that switches between states of rapid epithelial proliferation (anagen), apoptosis-driven organ involution (catagen), and relative quiescence (telogen), the organ culture of human HF, which continues to un-

[1] These authors contributed equally to this work.

[2] Correspondence: Department of Physiology, University of Debrecen, Nagyerdei krt. 98. PO Box 22, 4032 Debrecen, Hungary. E-mail: biro@phys.dote.hu

doi: 10.1096/fj.06-7689com

0892-6638/07/0021-3534 © FASEB

dergo the anagen-catagen transformation *in vitro*, offers a highly instructive, easily accessible model for probing the effects of test agents on complex human tissue interaction systems (33, 34). Therefore, as an integral part of the ongoing exploration of the intriguing "nonclassical" neuro-endocrine role of the skin both under physiological and pathological conditions (35–39), the human HF organ culture promised to offer an ideal, physiologically and clinically relevant general model system for dissecting the as-yet-unclear functions of cannabinoids in the control of human cell growth and death *in situ*.

MATERIALS AND METHODS

Materials

AEA, 2-AG, AM-251, THC, and interferon-γ (IFNγ) were purchased from Sigma-Aldrich (Taufkirchen, Germany).

Isolation and maintenance of hair follicles

The study was approved by the Institutional Research Ethics Committees and adhered to Declaration of Helsinki guidelines. Human anagen HF (n=18–24 per group) were isolated from skin obtained from females undergoing face-lift surgery (23, 31). Isolated HF were maintained in Williams E medium (Biochrom, Cambridge, UK) supplemented with 2 mM L-glutamine (Invitrogen, Paisley, UK), 10 ng/ml hydrocortisone, 10 μg/ml insulin, and antibiotics (all from Sigma). Medium was changed every other day, whereas treatment with various cannabinoids was performed daily.

Measurement of hair shaft elongation

Length measurements were daily performed on individual HF using a light microscope with an eyepiece measuring graticule (23, 31).

Histology, histochemistry, quantitative histomorphometry

Cryostat sections (8 μm thick) of cultured HF were fixed in acetone, air-dried, and stained with hematoxylin-eosin (Sigma). Hair cycle stage (anagen, catagen) of each HF was assessed according to defined morphological criteria whereas melanin pigment was visualized by the Masson-Fontana histochemistry (23, 34).

Immunohistochemistry of CB receptors

For the detection of CB receptors on isolated HF, two complementary techniques, the tyramide-substrate amplification (TSA) and the alkaline phosphatase (AP) activity-based methods were used (23, 31). For the TSA technique, sections were first incubated by primary antibodies (1:400) against the N terminus of CB1 (H-150, sc-20754, Santa Cruz, Santa Cruz, CA, USA) or CB2 (Cat. No. 101550–1, Cayman Chemical, Ann Arbor, MI, USA). Samples were then labeled with biotinylated multilink swine anti-goat/mouse/rabbit IgG (1:200, DAKO, Glostrup, Denmark) and finally with streptavidine-horseradish peroxidase (TSA kit, Perkin Elmer, Boston, MA, USA) followed by an application of fluorescein-tyramide (1:50, TSA kit). Sections were counterstained by DAPI (1 μg/ml, Boehringer Mannheim, Mannheim, Germany). For the AP-based method, after staining with the appropriate CB-specific antibodies (1:40) and the biotinylated multilink swine anti-goat/mouse/rabbit IgG (1:200), sections were labeled by a streptavidin-AP conjugate (1% reagent mixture, Vector Laboratories, Burlingame, CA, USA). Immunoreactions were finally visualized using Fast Red (Sigma) and the sections were counterstained by hematoxylin (Sigma).

In both staining procedures, to further assess specificity of the immunostaining, primary labeling was also performed using goat C-terminus-specific antibodies: anti-CB1 (K-15, sc-10068, Santa Cruz) and anti-CB-2 (C-15, sc-10073, Santa Cruz). The application of these latter primary antibodies resulted in identical staining patterns (not shown). As negative controls, the appropriate primary antibodies were either omitted from the procedure or were preabsorbed with synthetic blocking peptides (purchased from Santa Cruz or Cayman). In addition, the specificity of CB receptor staining was also measured on tissues recognized to be CB1 (brain) or CB2 (spleen) positive (not show).

Image analysis

The intensity of fluorescence CB1-immunoreactivity in each section was measured at 5–10 previously defined reference regions of interest (ROI) of either the layers of distal ORS or the matrix keratinocytes at a 0–255 U/pixel intensity range using the Image Pro Plus 4.5.0 software (Media Cybernetics, Silver Spring, MD, USA), and the average of the CB1-specific immunosignal (mean±SE) was calculated (23). A similar approach was employed to define the melanin content of the bulb regions of individual HF, labeled by Masson-Fontana histochemistry.

Double immunolabeling of proliferating and apoptotic cells

To evaluate apoptotic cells in colocalization with a proliferation marker Ki-67, a Ki-67/TUNEL (terminal deoxynucleotidyl transferase biotin-dUTP nick end labeling) double-staining method was employed (23, 31). Cryostat sections were fixed in formalin/ethanol/acetic acid and labeled with a digoxigenin-deoxyUTP (ApopTag Fluorescein In Situ Apoptosis Detection Kit, Intergen, Purchase, NY, USA) in presence of terminal deoxynucleotidyl transferase (TdT), followed by incubation with a mouse anti-Ki-67 antiserum (DAKO). TUNEL+ cells were visualized by an antidigoxigenin FITC-conjugated antibody (ApopTag kit), whereas Ki-67 was detected by a rhodamine-labeled goat anti-mouse antibody (Jackson Immuno Research, West Grove, PA, USA). Finally, sections were counterstained by DAPI (1 μg/ml, Boehringer Mannheim). Negative controls were performed by omitting TdT and the Ki-67 antibody. The number of cells positive for Ki-67 and TUNEL immunoreactivity was counted per hair bulb and was normalized to the number of total (DAPI+) cells.

Quantitative "real-time" PCR (Q-PCR)

Q-PCR was performed on an ABI PRISM 7000 Sequence Detection System (Applied Biosystems, Foster City, CA, USA) using the 5′ nuclease assay (23, 31). Total RNA was isolated from pools of freshly dissected HFs (n=100–200) using TRIzol (Invitrogen) and 3 μg of total RNA were reverse-transcribed into cDNA by using 15 U of AMV reverse transcriptase (Promega, Madison, WI, USA) and 0.025 μg/μl random primers (Promega). PCR amplification was carried out by using the TaqMan primers and probes (Assay ID: Hs00275634_m1 for human CB1, Assay ID: Hs00361490_m1 for human CB2) using the TaqMan Universal PCR Master

Mix Protocol (Applied Biosystems). As internal controls, transcripts of glyceraldehyde 3-phosphate dehydrogenase (GAPDH) were determined (Assay ID: Hs99999905_m1 for human GAPDH). The amount of CB receptor-specific transcripts was normalized to those of GAPDH using the ΔΔCT method (23).

Determination of endocannabinoid levels

Freshly isolated HFs weighing ~50 mg were homogenized in 0.5 ml of an ice-cold solution of methanol: Tris buffer (50 mM, pH 8) 1:1 containing 7 ng of $^2H_4$-anandamide ($^2H_4$-AEA), synthesized as described in (40, 41). To each homogenate 2 ml of ice-cold chloroform:methanol 1:1 and 0.5 ml of 50 mM Tris buffer, pH 8, was added. The homogenate was centrifuged at 4°C (500 *g* for 2 min), and the chloroform phase was recovered and transferred to a borosilicate tube, and the water phase extracted two more times with ice-cold chloroform. The combined extract was evaporated to dryness at 32°C under a stream of nitrogen. The dried residue was reconstituted in 110 μl of chloroform, and 2 ml of ice-cold acetone was added. The precipitated proteins were removed by centrifugation (1800 *g*, 10 min) and the clear supernatant was removed and evaporated to dryness. The dry residues were reconstituted in 50 μl of ice-cold methanol, of which 35 μl was used for analysis by liquid chromatography/in line mass spectrometry, using an Agilent 1100 series LC-MSD, equipped with a thermostated autosampler and column compartment. Liquid chromatographic separation of endocannabinoids was achieved using a guard column (Discovery HS C18, 2 cm × 4.0 mm, 3 μm, 120A) and analytical column (Discovery HS C18, 7.5 cm × 4.6 mm, 3 μm) at 32°C with a mobile phase of methanol:water:acetic acid 85:15:0.1 (v/v/v) at a flow of 1 ml/min for 12 min followed by 8 min of methanol:acetic acid 100:0.1 (v/v). The MSD (model LS) was set for atmospheric pressure chemical ionization (APCI), positive polarity, and selected-ion-monitoring (SIM) to monitor ions m/z 348 for AEA, 352 for $^2H_4$-AEA, and 379 for 2-AG. The spray chamber settings: vaporizer 400°C, gas temperature 350°C, drying gas 5.0 l/min, and nitrogen, used as the nebulizing gas with a pressure of 60 psig. Calibration curves were produced using synthetic AEA and 2-AG (Cayman). The amounts of AEA and 2-AG in the samples were determined using inverse linear regression of standard curves. Values are expressed as fmol or pmol per mg wet tissue.

Statistical analysis

Statistical analysis was performed using a Mann-Whitney *U* test for unpaired samples (n=18–24 HFs per group) (23, 31).

RESULTS

AEA, unlike 2-AG, inhibits hair growth

First, microdissected, organ-cultured human scalp HF in the growth stage of the hair cycle (*i.e.*, anagen VI) (22, 23, 31) were stimulated with one of the best-characterized endocannabinoids, N-arachidonoylethanolamide (anandamide, AEA) (1–5, 42). AEA significantly (P<0.05) and dose-dependently inhibited hair shaft elongation (**Fig. 1*a***) and (as revealed by determining the number of Ki67 positive cells) hair matrix keratinocyte proliferation (Fig. 1*b*). In contrast, the endocannabinoid significantly (P<0.05) stimulated keratinocyte apoptosis in the epithelial hair bulb (as assessed by TUNEL labeling, Fig. 1*b*) as well as premature HF entry into apoptosis-driven organ involution (catagen) (Fig. 1*c*). It is worth noting, however, that AEA did not affect HF pigmentation (32, 33), since the melanin content of anagen VI HF remained unchanged (not shown).

We have also investigated the effect of the other main endocannabinoid, 2-arachidonoylglycerol (2-AG) (1–5, 42). Interestingly, 2-AG did not significantly alter human hair shaft elongation *in vitro* (Fig. 1*a*), HF proliferation, apoptosis, or catagen entry (not shown).

CB1, but not CB2, is expressed in the HF, and its level is regulated by the hair cycle

We then assessed whether HF express the molecular targets of cannabinoids (3, 5). By mutually complementary and confirmatory, independent immunohistochemical methods (**Fig. 2*a*, *b***), specific CB1 immunoreactivity (CB1-ir) was identified in the HF epithelium, primarily in outer root sheath (ORS) keratinocytes (but not on the fibroblasts of the HF dermal papilla). In addition, transcription of the CB1 gene in freshly isolated, microdissected human scalp HFs (more precisely: anagen VI hair bulbs) was demonstrated by quantitative RT-PCR (Fig. 2*d*). In contrast, of great importance, neither immunohistochemistry nor Q-PCR indicated the expression of CB2 in the HF (not shown).

Intriguingly, CB1 protein expression significantly increased on hair matrix (and, yet only marginally, on ORS) keratinocytes of cultured HF, which had been experimentally induced to undergo premature HF involution (catagen) phase by interferon-γ (IFNγ) treatment (23) (Fig. 2*b*, *c*). Moreover, we have also found that the intensity of CB1-ir was also up-regulated on AEA-treated catagen HF (not shown). These data show that normal human scalp HFs express CB1 (but not CB2) on the gene and protein level, and suggest that the intrafollicular CB1 expression is hair cycle-dependent.

Effects of AEA are mediated by CB1 but not by TRPV1

The above data also support the argument that the effects of AEA on the human scalp HF may be transmitted by CB1 receptors. Further in line with this hypothesis, we found that the specific CB1 antagonist AM-251 (1, 3, 5), which alone did not modify hair shaft elongation, completely abrogated the hair growth-inhibitory effect of AEA and normalized hair growth parameters to the vehicle control level (Fig. 1*a*). This finding corroborates the missing evidence of CB2 expression in human scalp HF on either the protein or gene level and suggests that the potent hair growth-inhibitory actions of the endocannabinoid AEA are most likely mediated by CB1.

However, previous reports have also documented that AEA may also activate TRPV1 and hence may act as

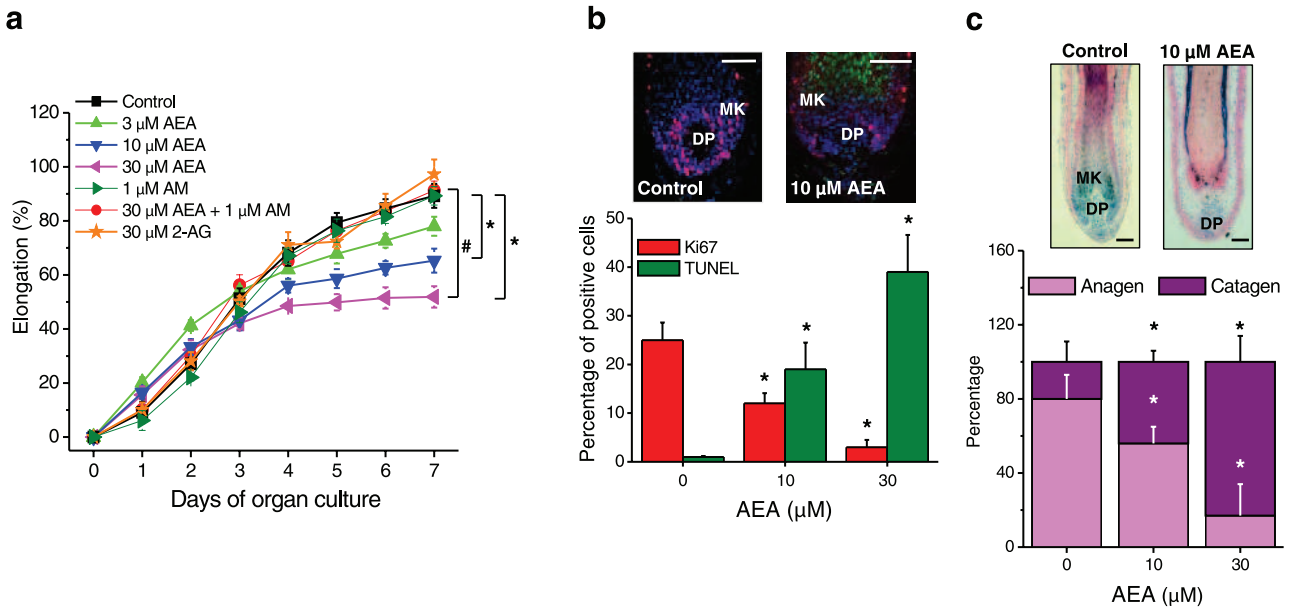

Figure 1. AEA inhibits hair shaft elongation and proliferation whereas it stimulates apoptosis of cultured human HF. *a)* Hair shaft elongation curves (mean±SE, 18–24 HF per group). $^{*}P < 0.05$ when compared to control; $^{\#}P < 0.05$ when values of the 30 μM AEA-treated group were compared to those of the 30 μM AEA + 1 μM AM-251 (AM) group. Note the lack of effect of 2-AG. *b)* Coimmunolabeling of proliferating (Ki-67+, red fluorescence) and apoptotic (TUNEL+, green fluorescence) cells, along with nuclei (DAPI, blue fluorescence). Statistical analysis of number of Ki-67+ and TUNEL+ cells as compared to the number of DAPI+ cells (mean±SE). *c)* Quantitative hair cycle histomorphometry on hematoxylin-eosin-stained sections. Percentage of HFs in anagen or catagen state (23, 33, 34) was determined (mean±SE). *b, c)* DP, dermal papilla, MK, matrix keratinocytes. Scale bars, 10 μm. $^{*}P < 0.05$ when compared to control.

an "endovanilloid" substance (3, 43, 44). In addition, we have previously shown that the human HF epithelium also expresses TRPV1 and that the specific activation of the TRPV1-coupled signaling by the exovanilloid capsaicin (a pungent ingredient of hot chili peppers) inhibits hair shaft elongation and proliferation, and induces apoptosis-driven catagen regression (23), very similar to the above action of AEA. Therefore, we also measured the possible role of TRPV1 in mediating the effects of AEA.

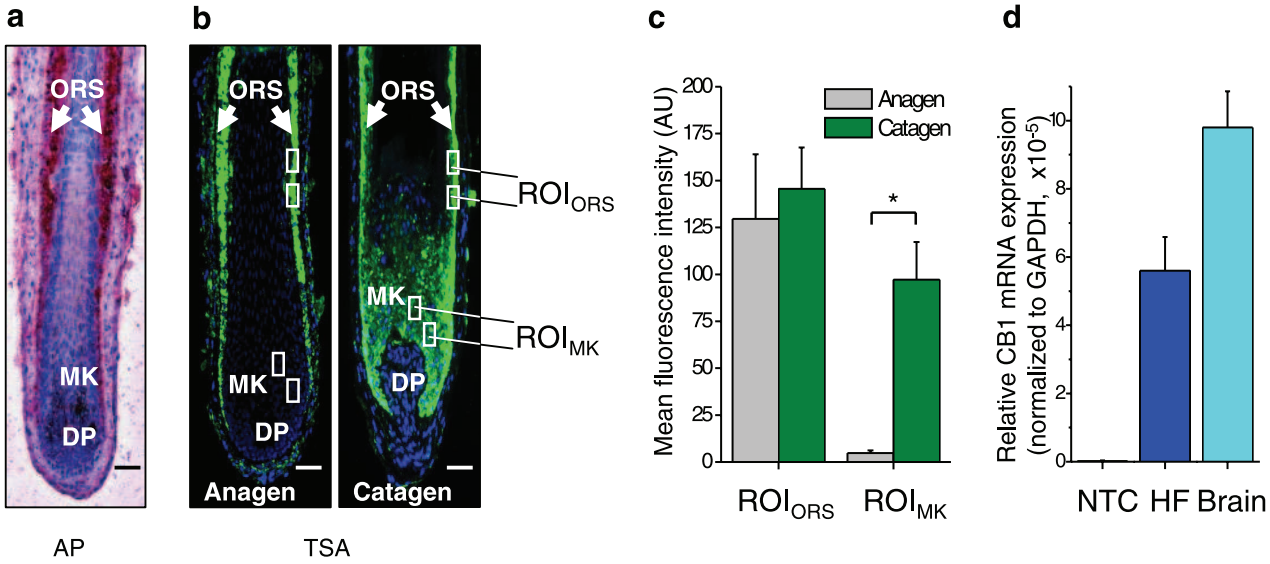

Figure 2. CB1 is expressed in the epithelium of the HF and is up-regulated in catagen. Immunodetection of CB1 using the alkaline phosphatase (AP) activity-based (*a*) and the tyramide-substrate amplification (TSA, *b*) methods. *b)* Expression of CB1 in anagen (no treatment) and catagen (1000 IU/ml IFNγ treatment for 5 days) HF. *c)* Statistical image analysis of CB1-specific fluorescence intensities in the outer root sheath (ORS) and matrix keratinocyte (MK) regions (mean±SE); 5–10 regions of interest (ROI, boxes in (*b*) per section, 18–24 HF per group. DP, dermal papilla. Scale bars, 10 μm. $^{*}P < 0.05$ when compared to control. *d)* Identification of CB1-specific mRNA transcripts in HF by quantitative RT-PCR. NTC, nontemplate control, Brain, positive control. Mean ± SE of quadruplicate determination.

As seen in **Fig. 3*a***, the TRPV1 antagonist iodoresiniferatoxin (I-RTX), which on its own did not modify "basal" hair growth (23), was unable to prevent the effect of AEA to inhibit hair shaft elongation suggesting the lack of involvement of TRPV1. Further corroborating this statement, we have also found that AEA and the TRPV1 agonist capsaicin exerted similar and, of great importance, additive effects to suppress hair growth (Fig. 3*a*), to inhibit the proliferation of HF matrix keratinocytes, and to induce intrafollicular apoptosis (Fig. 3*b*). Since the hair growth-inhibitory effect of capsaicin (confirming our previous results) (23) was fully abrogated by the TRPV1 antagonist I-RTX but not affected by the CB1 antagonist AM-251 (Fig. 3*a*), these findings strongly support the argument that the synergistic endocannabinoid and vanilloid systems operate independently to inhibit human hair growth and hence the effects of AEA are indeed exclusively mediated by CB1.

HF are sources of endocannabinoids

We were also interested in to define whether HF, besides responding to the action of cannabinoids and expressing CB1, also produce certain endocannabinoids. Therefore, in a pilot study, HF collected from two individuals, processed as described under Materials and Methods, and subjected to mass spectrometry to measure the presence of endocannabinoids. We showed for the first time that freshly dissected HF not only respond to but, intriguingly, also express such endocannabinoids as AEA and 2-AG. However, it was noteworthy to observe that whereas the level of AEA (6.6–11.2 fmol/mg tissue, range, $n=2$) was comparable to those of, *e.g.*, heart samples (~7.7 fmol/mg tissue) (9, 45), the level of 2-AG was much lower (0.2–0.3 pmol/mg tissue, range, $n=2$) than previously found in cardiac tissues (~3.5 pmol/mg tissue) (9, 45). Obviously, these initial, very preliminary data demand careful and systematic repetition using tissue extracts of many additional HF from several different individuals before definitive conclusions on the spectrum of endogenous cannibinoid receptor ligands can be drawn. In addition, these need to be integrated with information on the endocannabinoid content of healthy human skin and organ-cultured HF of various stages of HF cycling (*i.e.*, anagen, catagen).

THC also inhibits hair growth

THC, the key active ingredient in hashish and marijuana, is one of the best-investigated exocannabinoid (1–5) and is deposited at high levels in the hair shafts of human cannabis consumers (26, 27), *e.g.*, after inhalation or ingestion and of tumor patients treated with THC as an antiemetic, psychotropic agent. Therefore, we finally wished to investigate the effects of this prototypic exocannabinoid, which binds to both CB1 and CB2 (1–5), on human HF growth in organ-culture.

Almost identical to the actions of AEA reported above, THC significantly inhibited hair shaft elongation in a dose-dependent fashion, suppressed proliferation of HF keratinocytes, and induced both hair matrix

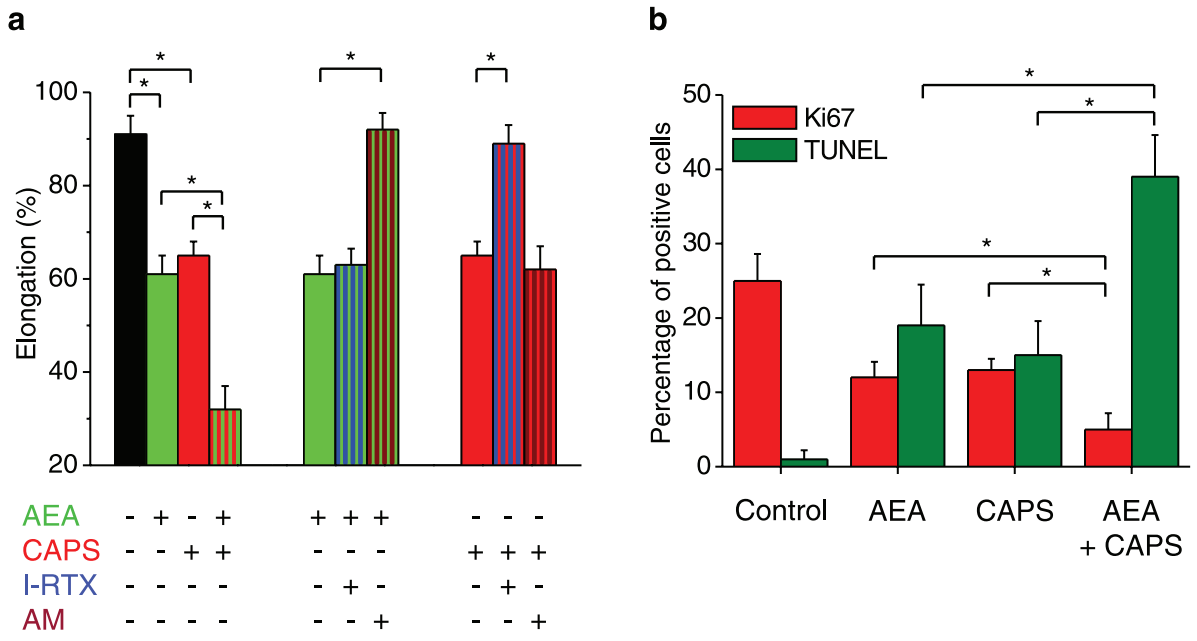

Figure 3. Effect of AEA to inhibit hair growth is mediated by CB1 but not by TRPV1. *a)* HF were treated with 10 μM AEA, 10 μM capsaicin (CAPS), 1 μM AM-251 (AM), and 50 nM I-RTX in the above combinations and hair shaft elongation was determined daily (mean±SE, 18–24 HF per group). Data represent elongation values at day 7 of organ-culture. *b)* HF (18–24 per group) were treated with 10 μM AEA, 10 μM CAPS, or their combination and, at day 7, coimmunolabeling of proliferating (Ki-67+) and apoptotic (TUNEL+) cells, along with nuclei (DAPI+), was performed. Data represent values of statistical analysis of number of Ki-67+ and TUNEL+ cells as compared to the number of DAPI+ cells (mean±SE). In both panels, asterisks mark significant ($P<0.05$) differences.

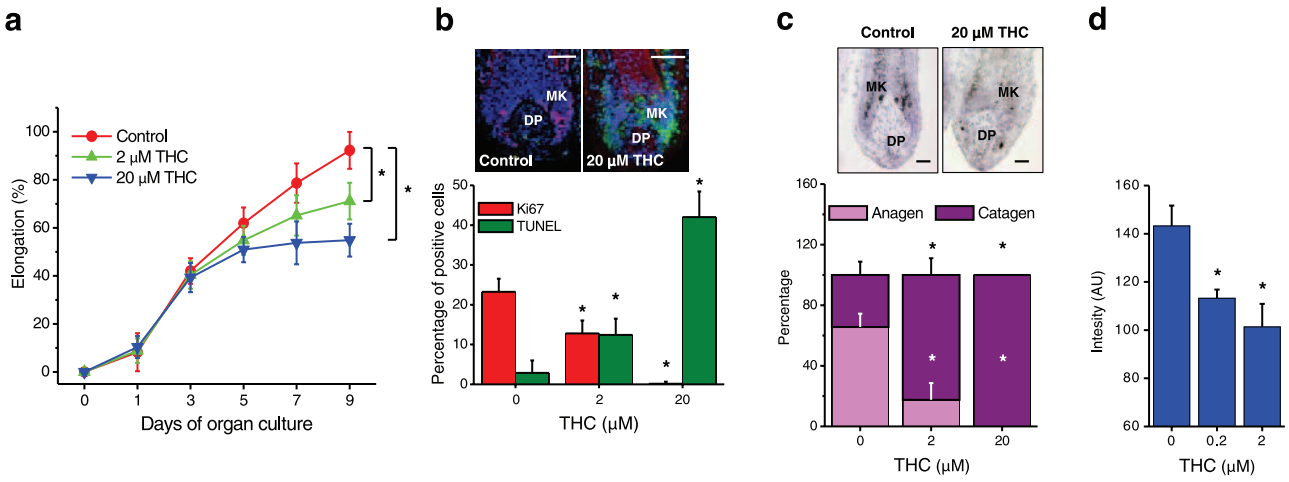

Figure 4. THC inhibits hair shaft elongation and proliferation, whereas it stimulates apoptosis of cultured human HF. *a)* Hair shaft elongation curves (mean±SE, 18–24 HFs per group). *$P < 0.05$ when compared to control (*b*) Coimmunolabeling of proliferating (Ki-67+, red fluorescence) and apoptotic (TUNEL+, green fluorescence) cells, along with nuclei (DAPI, blue fluorescence). Statistical analysis of number of Ki-67+ and TUNEL+ cells as compared with the number of DAPI+ cells (mean±SE). *c)* Quantitative hair cycle histomorphometry on hematoxylin-eosin-stained sections. Percentage of HF in anagen or catagen state (23, 33, 34) was determined (mean±SE). *b, c)* DP, dermal papilla, MK, matrix keratinocytes. Scale bars, 10 μm. *d)* Statistical image analysis of melanin content in the bulb region of those THC-treated HF which were not yet transformed to catagen (mean±SE); 5–10 regions of interest per section, 18–24 HF per group. *$P < 0.05$ when compared to control.

keratinocyte apoptosis and premature catagen development **(Fig. 4*a–c*)**. These data, therefore, suggest that exocannabinoids can mimic the hair growth-inhibitory effects of endocannabinoids.

We also determined the effect of THC on the melanin content of the HF. During this measurement, to differentiate the effect of the exocannabinoids from the well-known catagen-associated "shut-down" of follicular melanogenesis (33, 34, 46–48), the melanin content of only those THC-treated HF were defined, which were not yet transformed to catagen. Interestingly, as opposed to findings with AEA, we found that THC significantly and dose-dependently suppressed the melanin content of the HF (Fig. 4*d*), suggesting THC may also exert inhibitory effects on follicular melanogenesis *in situ* (independent of the normal, catagen-associated suppression of the melanin production of the HF) (33, 34, 46–48).

DISCUSSION

Exploration of cannabinoid functions in skin biology and pathology is an important, integral part of the ongoing exploration of the skin as a "nonclassical" neuro-endocrine organ. As a part of this quest, in this paper, we provide the first evidence that the prototypic endocannabinoid, AEA (which may even be produced within human HF), and the—notoriously abused—exocannabinoid, THC, both inhibit human hair shaft elongation and induce apoptosis-driven HF involution (catagen) *in vitro*. We show that these effects are most likely mediated via CB1 receptor-mediated signaling mechanism. Furthermore, we show that intrafollicular expression of the "targeted" CB1 is hair cycle-dependent and is up-regulated during catagen. Given that these effects were generated with intact components of a normal human miniorgan and under assay conditions that preserve *in vivo*-like key functions of this organ during the test period, our findings are both physiologically and clinically relevant. Furthermore, these data support the concept that human HF are both targets and sources of endocannabinoids, and exploit a physiologically relevant paracrine-autocrine endocannabinoid system for negatively regulating their own growth.

Since previous reports have extensively documented that AEA might exert its cellular actions via CB1, CB2, and/or TRPV1-coupled signaling mechanisms (1–5, 42–44), a central core of the current study was to identify the molecular target(s) of this endocannabinoid. Our results that *i)* the hair growth-inhibitory actions of AEA was fully abrogated by the CB1-specific antagonist AM-251; *ii)* the effects of AEA was not modified by the TRPV1 antagonist I-RTX; and *iii)* CB1 was successfully identified in the HF (both at the protein and mRNA levels), whereas CB2 was not found; suggest that (although TRPV1 is also functionally expressed in the HF) (23) AEA may exclusively act on CB1 to inhibit human hair growth and to modulate the hair cycle.

Experimental data with the coadministration of AEA and the TRPV1 agonist capsaicin, by showing that the similar effects of the two agents were additive (at least indirectly) further strengthened the above argument. However, these results (along with our presentation that the effect of capsaicin was not modified by the CB1 antagonist AM-251) also propose that the otherwise very intimately related (and often "overlapping") endocannabinoid and (endo)vanilloid systems (3, 43) synergistically yet, of importance, independently function to regulate various biological processes (elongation, pro-

liferation, apoptosis, cycling) of the human HF. This may also be further strengthened by our recent report showing that TRPV1 knockout mice (which possess an essentially unaltered endocannabinoid system) (49) exhibit a significant delay in the onset of the first spontaneous catagen during the morphogenesis of the HF (50). (Our currently running investigation of the morphogenesis and hair cycle of CB1 knockout mice will hopefully explore this interaction "the other way around").

Our findings that catagen development, *per se* (at least in organ-cultured human scalp HF), is already associated with a marked up-regulation of CB1 expression, suggests that, once catagen has been induced by either AEA or cannabinoid-independent mechanisms (such as, *e.g.*, IFNγ or on TRPV1 activation) (23), the HF substantially increases its susceptibility to (additional) stimulation by endocannabinoids *via* this receptor. This may then further accelerate the speed of catagen development, depending on the availability of endogenous agonists.

Our exciting pilot mass spectrometry data (which, as detailed above, demand further careful and systematic repetition using tissue extracts of many additional HF from several different individuals), which demonstrate the intrafollicular presence of substantial AEA levels in microdissected, rigorously washed human scalp HF, suggest that endogenous CB agonists may even be produced locally, *i.e.*, within the anagen hair bulb. However, it was surprising to observe that, unlike in most tissues (1–3, 42), the level of 2-AG was very low in the HF. This may reflect, *e.g.*, high intrafollicular levels of fatty acid amide hydrolase and monoacylglycerol lipase, which participate in the degradation of 2-AG (1–3, 42). Although further studies are to be performed to quantitatively define the expression of these molecules in the HF, the above hypothesis may, at least in part, explain our results that of the two major endocannabinoids (produced by the HF) only AEA was able to inhibit hair growth and that HF were unresponsive to 2-AG stimulation.

In our hands, the CB1 antagonist AM-251 alone did not modify hair shaft elongation which, at the first glance, might suggest that the endogenous cannabinoid tone does not affect hair growth. However, it is well documented that during certain pathological conditions (*e.g.*, inflammatory and autoimmune diseases), the level of numerous endocannabinoids (including AEA and 2-AG) and the expression profile of CB receptors are markedly altered (1–3, 51). Since inflammation as well as alterations in the activity of the immune system was shown to markedly contribute to the pathogenesis of several hair loss disorders (such as alopecia areata, effluvium) (52, 53), it might be hypothesized (and to be definitely measured in the near future) that endocannabinoid expression may, *e.g.*, be increased in such diseases. Therefore, our demonstration that the CB1 antagonist effectively abrogated the hair growth-inhibitory effects of AEA may be interpreted as a first, tentative proof-of-principle for a novel, CB1 *antagonist*-based adjuvant treatment option in the clinical management of certain human hair loss disorders.

Irrespective of their potential clinical implications and further intriguing applications (*e.g.*, future exploitation of the growth-inhibitory effect of CB *agonists* in the putative management of unwanted hair growth such as hirsutism), our results also show that human HF organ culture offers a very simple, yet highly instructive new research tool for exploring and dissecting "non-classical", growth- and apoptosis-modulatory effects of endo- and exocannabinoids and of receptor-mediated signaling in general under *physiologically relevant* conditions. Using microarray techniques (*cf.* 23, 32), this prototypic tissue interaction system can now even be exploited to identify novel target genes of CB-mediated signaling in the human system *in situ*. Certainly, the intriguing concept that human HF (at least on the scalp) may always (or hair cycle-dependently) more or less "stoned", and the challenge to selectively get the HF (rather than the central nervous system. . .) "high" in a clinically desired manner will surely excite patients, investigators, industry, regulatory institutions, the lay press, and politicians alike. FJ

This work was supported in part by Hungarian research grants (OTKA T049231, OTKA K063153, NKFP 1A/008/04) to T.B. and by a DFG grant (Pa 345/11–2) to R.P. The authors declare no competing financial interests.

REFERENCES

1. Di Marzo, V., Bifulco, M., De Petrocellis, L. (2004) The endocannabinoid system and its therapeutic exploitation. *Nat. Rev. Drug Discov.* **3,** 7712–7784
2. Piomelli, D. (2005) The endocannabinoid system: a drug discovery perspective. *Curr. Opin. Investig. Drugs* **6,** 672–679
3. Pacher, P., Batkai, S., and Kunos, G. (2006) The endocannabinoid system as an emerging target of pharmacotherapy. *Pharmacol. Rev.* **58,** 389–462
4. Di Marzo, V., and De Petrocellis, L. (2006) Plant, synthetic, and endogenous cannabinoids in medicine. *Annu. Rev. Med.* **57,** 553–574
5. Felder, C. C., Dickason-Chesterfield, A. K., and Moore, S. A. (2006) Cannabinoids biology: the search for new therapeutic targets. *Mol. Interv.* **6,** 149–161
6. De Vries, T. J., Shaham, Y., Homberg, J. R., Crombag, H., Schuurman, K., Dieben, J., Vanderschuren, L. J., and Schoffelmeer, A. N. (2001) A cannabinoid mechanism in relapse to cocaine seeking. *Nat. Med.* **7,** 1151–1154
7. Freund, T. F., Katona, I., and Piomelli, D. (2003) Role of endogenous cannabinoids in synaptic signaling. *Physiol. Rev.* **83,** 1017–1066
8. Jiang, W., Zhang, Y., Xiao, L., Van Cleemput, J., Ji, S. P., Bai, and G., Zhang, X. (2005) Cannabinoids promote embryonic and adult hippocampus neurogenesis and produce anxiolytic- and antidepressant-like effects. *J. Clin. Invest.* **115,** 3104–3416
9. Batkai, S., Jarai, Z., Wagner, J. A., Goparaju, S. K., Varga, K., Liu, J., Wang, L., Mirshahi, F., Khanolkar, A. D., Makriyannis, A., Urbaschek, R., Garcia, N. Jr., Sanyal, A. J., and Kunos, G. (2001) Endocannabinoids acting at vascular CB1 receptors mediate the vasodilated state in advanced liver cirrhosis. *Nat. Med.* **7,** 827–832
10. Croxford, J. L., Miller, S. D. (2003) Immunoregulation of a viral model of multiple sclerosis using the synthetic cannabinoid R+WIN55,212. *J. Clin. Invest.* **111,** 1231–1240
11. Galve-Roperh, I., Sanchez, C., Cortes, M. L., del Pulgar, T. G., Izquierdo, M., Guzman, M. (2000) Anti-tumoral action of cannabinoids: involvement of sustained ceramide accumulation

and extracellular signal-regulated kinase activation. *Nat. Med.* **6,** 313–319
12. Bifulco, M., Di Marzo, V. (2002) Targeting the endocannabinoid system in cancer therapy: a call for further research. *Nat. Med.* **8,** 547–550
13. Blazquez, C., Casanova, M. L., Planas, A., Del Pulgar, T. G., Villanueva, C., Fernandez-Acenero, M. J., Aragones, J., Huffman, J. W., Jorcano, J. L., and Guzman, M. (2003) Inhibition of tumor angiogenesis by cannabinoids. *FASEB J.* **17,** 529–531
14. Portella, G., Laezza, C., Laccetti, P., De Petrocellis, L., Di Marzo, V., and Bifulco, M. (2003) Inhibitory effects of cannabinoid CB1 receptor stimulation on tumor growth and metastatic spreading: actions on signals involved in angiogenesis and metastasis. *FASEB J.* **17,** 1771–1773
15. Bifulco, M., Laezza, C., Valenti, M., Ligresti, A., Portella, G., and DiMarzo, V. (2004) A new strategy to block tumor growth by inhibiting endocannabinoid inactivation. *FASEB J.* **18,** 1606–1608
16. Blazquez, C., Carracedo, A., Barrado, L., Real, P. J., Fernandez-Luna, J. L., Velasco, G., Malumbres, M., and Guzman, M. (2006) Cannabinoid receptors as novel targets for the treatment of melanoma. *FASEB J.* **20,** 2633–2635
17. Fernandez-Ruiz, J., Romero, J., Velasco, G., Tolon, R. M., Ramos, J. A., and Guzman, M. (2007) Cannabinoid CB(2) receptor: a new target for controlling neural cell survival? *Trends. Pharmacol. Sci.* **28,** 39–45
18. Casanova, M. L., Blazquez, C., Martinez-Palacio, J., Villanueva, C., Fernandez-Acenero, M. J., Huffman, J. W., Jorcano, J. L., and Guzman, M. (2003) Inhibition of skin tumor growth and angiogenesis in vivo by activation of cannabinoid receptors. *J. Clin. Invest.* **111,** 43–50
19. Maccarrone, M., Di Rienzo, M., Battista, N., Gasperi, V., Guerrieri, P., Rossi, A., and Finazzi-Agro, A. (2003) The endocannabinoid system in human keratinocytes. Evidence that anandamide inhibits epidermal differentiation through CB1 receptor-dependent inhibition of protein kinase C, activation protein-1, and transglutaminase. *J. Biol. Chem.* **278,** 33896–33903
20. Ständer, S., Schmelz, M., Metze, D., Luger, T. A., and Rukwied, R. (2005) Distribution of cannabinoid receptor 1 (CB1) and 2 (CB2) on sensory nerve fibers and adnexal structures in human skin. *J. Dermatol. Sci.* **38,** 177–188
21. Wilkinson, J. D., and Williamson, E. M. (2007) Cannabinoids inhibit human keratinocyte proliferation through a non-CB1/CB2 mechanism and have a potential therapeutic value in the treatment of psoriasis. *J. Dermatol. Sci.* **45,** 87–92
22. Philpott, M. P., Green, M. R., and Kealey, T. (1990) Human hair growth in vitro. *J. Cell Sci.* **3,** 463–471
23. Bodó, E., Bíró, T., Telek, A., Czifra, G., Griger, Z., Tóth, I. B., Mescalchin, A., Ito, T., Bettermann, A., Kovács, L., and Paus, R. (2005) A hot new twist to hair biology: involvement of vanilloid receptor-1 (VR1/TRPV1) signaling in human hair growth control. *Am. J. Pathol.* **166,** 985–998
24. Arck, P. C., Handjiski, B., Kuhlmei, A., Peters, E. M., Knackstedt, M., Peter, A., Hunt, S. P., Klapp, B. F., and Paus, R. (2005) Mast cell deficient and neurokinin-1 receptor knockout mice are protected from stress-induced hair growth inhibition. *J. Mol. Med.* **83,** 386–396
25. Peters, E. M., Arck, P. C., and Paus, R. (2006) Hair growth inhibition by psychoemotional stress: a mouse model for neural mechanisms in hair growth control. *Exp. Dermatol.* **15,** 1–13
26. Uhl, M., and Sachs, H. (2006) Cannabinoids in hair: strategy to prove marijuana/hashish consumption. *Forensic. Sci. Int.* **145,** 143–147
27. Skopp, G., Strohbeck-Kuehner, P., Mann, K., and Hermann, D. (2006) Deposition of cannabinoids in hair after long-term use of cannabis. *Forensic. Sci. Int.* [Epub ahead of print]
28. Paus, R., Theoharides, T. C., and Arck, P. C. (2006) Neuroimmunoendocrine circuitry of the 'brain-skin connection'. *Trends. Immunol.* **27,** 32–39
29. Botchkarev, V. A. (2003) Stress and the hair follicle: exploring the connections. *Am. J. Pathol.* **162,** 709–712
30. Arck, P. C., Handjiski, B., Peters, E. M., Peter, A. S., Hagen, E., Fischer, A., Klapp, B. F., and Paus, R. (2003) Stress inhibits hair growth in mice by induction of premature catagen development and deleterious perifollicular inflammatory events via neuropeptide substance P-dependent pathways. *Am. J. Pathol.* **162,** 803–814
31. Ito, N., Ito, T., Kromminga, A., Bettermann, A., Takigawa, M., Kees, F., Straub, R. H., and Paus, R. (2005) Human hair follicles display a functional equivalent of the hypothalamic-pituitary-adrenal axis and synthesize cortisol. *FASEB J.* **19,** 1332–1334
32. Foitzik, K., Krause, K., Conrad, F., Nakamura, M., Funk, W., and Paus, R. (2006) Human scalp hair follicles are both a target and a source of prolactin, which serves as an autocrine and/or paracrine promoter of apoptosis-driven hair follicle regression. *Am. J. Pathol.* **168,** 748–756
33. Paus, R., and Cotsarelis, G. (1999) The biology of hair follicles. *N. Engl. J. Med.* **341,** 491–497
34. Stenn, K. D., and Paus, R. (2001) Controls of hair follicle cycling. *Physiol. Rev.* **81,** 449–494
35. Slominski, A., and Wortsman, J. (2000) Neuroendocrinology of the skin. *Endocr. Rev.* **21,** 457–487
36. Slominski, A., Wortsman, J., Luger, T., Paus, R., and Solomon, S. (2000) Corticotropin releasing hormone and proopiomelanocortin involvement in the cutaneous response to stress. *Physiol. Rev.* **80,** 979–1020
37. Paus, R., Schmelz, M., Bíró, T., and Steinhoff, M. (2006) Frontiers in pruritus research: scratching the brain for more effective itch therapy. *J. Clin. Invest.* **116,** 1174–1186
38. Arck, P. C., Slominski, A., Theoharides, T. C., Peters, E. M., and Paus, R. (2006) Neuroimmunology of stress: skin takes center stage. *J. Invest. Dermatol.* **126,** 1697–1704
39. Slominski, A., Wortsman, J., Tuckey, R. C., and Paus, R. (2007) Differential expression of HPA axis homolog in the skin. *Mol. Cell Endocrinol.* **265,** 143–149
40. Giuffrida, A., Rodriguez de Fonseca, F., and Piomelli, D. (2000) Quantification of bioactive acylethanolamides in rat plasma by electrospray mass spectrometry. *Anal. Biochem.* **280,** 87–93
41. Batkai, S., Osei-Hyiaman, D., Pan, H., El-Assal, O., Rajesh, M., Mukhopadhyay, P., Hong, F., Harvey-White, J., Jafri, A., Hasko, G., Huffman, J. W., Gao, B., Kunos, G., and Pacher. P. (2007) Cannabinoid-2 receptor mediates protection against hepatic ischemia/reperfusion injury. *FASEB J.* [Epub ahead of print]
42. Kogan, N. M., and Mechoulam, R. (2006) The chemistry of endocannabinoids. *J. Endocrinol. Invest.* **29,** 3–14
43. Di Marzo, V., Blumberg, P. M., and Szallasi, A. (2002) Endovanilloid signaling in pain. *Curr. Opin. Neurobiol.* **12,** 372–379
44. Van Der Stelt, M., and Di Marzo, V. (2004) Endovanilloids. Putative endogenous ligands of transient receptor potential vanilloid 1 channels. *Eur. J. Biochem.* **271,** 1827–1834
45. Pacher, P., Batkai, S., Osei-Hyiaman, D., Offertaler, L., Liu, J., Harvey-White, J., Brassai, A., Jarai, Z., Cravatt, B. F., and Kunos, G. (2005) Hemodynamic profile, responsiveness to anandamide, and baroreflex sensitivity of mice lacking fatty acid amide hydrolase. *Am. J. Physiol. Heart. Circ. Physiol.* **289,** H533–541
46. Slominski, A., Paus, R., Plonka, P., Chakraborty, A., Maurer, M., Pruski, D., and Lukiewicz, S. (1994) Melanogenesis during the anagen-catagen-telogen transformation of the murine hair cycle. *J. Invest. Dermatol.* **102,** 862–869
47. Slominski, A., Tobin, D. J., Shibahara, S., and Wortsman, J. (2004) Melanin pigmentation in mammalian skin and its hormonal regulation. *Physiol. Rev.* **84,** 1155–1228
48. Slominski, A., Wortsman, J., Plonka, P. M., Schallreuter, K. U., Paus, R., and Tobin, D. J. (2005) Hair follicle pigmentation. *J. Invest. Dermatol.* **124,** 13–21
49. Pacher, P., Batkai, S., and Kunos, G. (2004) Haemodynamic profile and responsiveness to anandamide of TRPV1 receptor knock-out mice. *J. Physiol.* **558,** 647–657
50. Bíró, T., Bodó, E., Telek, A., Géczy, T., Tychsen, B., Kovács, L., and Paus, R. (2006) Hair cycle control by vanilloid receptor-1 (TRPV1): Evidence from TRPV1 knockout mice. *J. Invest. Dermatol.* **126,** 1909–1912
51. Carrier, E. J., Patel, S., and Hillard, C. J. (2005) Endocannabinoids in neuroimmunology and stress. *Curr. Drug. Targets CNS Neurol. Disord.* **4,** 657–665
52. Paus, R., Ito, N., Takigawa, M., and Ito, T. (2003) The hair follicle and immune privilege. *J. Investig. Dermatol. Symp. Proc.* **8,** 188–194
53. Paus, R., Nickoloff, B. J., Ito, T. (2005) A 'hairy' privilege. *Trends Immunol.* **26,** 32–40

Received for publication March 6, 2007.
Accepted for publication May 10, 2007.

X.

The FASEB Journal • Research Communication

Endocannabinoids enhance lipid synthesis and apoptosis of human sebocytes *via* cannabinoid receptor-2-mediated signaling

Nóra Dobrosi,* Balázs I. Tóth,* Georgina Nagy,† Anikó Dózsa,‡ Tamás Géczy,* László Nagy,‡ Christos C. Zouboulis,§,‖ Ralf Paus,¶,# László Kovács,* and Tamás Bíró*,1

*Department of Physiology, †Department of Dermatology, and ‡Department of Biochemistry and Molecular Biology, University of Debrecen, Medical and Health Science Center, Research Center for Molecular Medicine, Debrecen, Hungary; §Departments of Dermatology, Venereology, Allergology, and Immunology, Dessau Medical Center, Dessau, Germany; ‖Laboratory of Biogerontology, Dermato-Pharmacology, and Dermato-Endocrinology, Institute of Clinical Pharmacology and Toxicology, Charité, Universitaetsmedizin Berlin, Campus Benjamin Franklin, Berlin, Germany; ¶Department of Dermatology, University Hospital Schleswig-Holstein, University of Lübeck, Lübeck, Germany; and #School of Translational Medicine, University of Manchester, Manchester, UK

ABSTRACT **We had previously shown that both locally produced endocannabinoids and exocannabinoids, *via* cannabinoid receptor-1 (CB1), are powerful inhibitors of human hair growth. To further investigate the role of the cannabinoid system in pilosebaceous unit biology, we have explored in the current study whether and how endocannabinoids have an impact on human sebaceous gland biology, using human SZ95 sebocytes as cell culture model. Here, we provide the first evidence that SZ95 sebocytes express CB2 but not CB1. Also, prototypic endocannabinoids (arachidonoyl ethanolamide/anandamide, 2-arachidonoyl glycerol) are present in SZ95 sebocytes and dose-dependently induce lipid production and (chiefly apoptosis-driven) cell death. Endocannabinoids also up-regulate the expression of key genes involved in lipid synthesis (*e.g.*, PPAR transcription factors and some of their target genes). These actions are selectively mediated by CB2-coupled signaling involving the MAPK pathway, as revealed by specific agonists/antagonists and by RNA interference. Because cells with "silenced" CB2 exhibited significantly suppressed basal lipid production, our results collectively suggest that human sebocytes utilize a paracrine-autocrine, endogenously active, CB2-mediated endocannabinoid signaling system for positively regulating lipid production and cell death. CB2 antagonists or agonists therefore deserve to be explored in the management of skin disorders characterized by sebaceous gland dysfunctions (*e.g.*, acne vulgaris, seborrhea, dry skin).—Dobrosi, N., Tóth, B. I., Nagy, G., Dózsa, A., Géczy, T., Nagy, L., Zouboulis, C. C., Paus, R., Kovács, L., Bíró, T. Endocannabinoids enhance lipid synthesis and apoptosis of human sebocytes *via* cannabinoid receptor-2-mediated signaling. *FASEB J.* 22, 3685–3695 (2008)**

Key Words: cannabinoid receptor subtypes · human sebaceous gland-derived SZ95 sebocytes · acne vulgaris · signal transduction · peroxisome proliferator-activated receptor · gene expression

THE ENDOCANNABINOID SYSTEM (ECS), that is, endocannabinoids (such as arachidonoyl ethanolamide, AEA, and 2-arachidonoyl glycerol, 2-AG), specific cannabinoid receptors (CB1 and CB2), and enzymes involved in the synthesis and degradation of endocannabinoids, has emerged as a versatile modulatory system, implicated in a plethora of physiological and pathophysiological regulatory mechanisms (1–3). Classically, CB1-mediated effects were mostly described in the central nervous system and were shown to involve regulating *e.g.*, synaptic functions, memory, and motor learning (3–6). Peripherally, the ECS has become implicated in regulation of *e.g.*, immune and cardiovascular processes, apparently chiefly *via* CB2-coupled signaling (7–9).

Recent intriguing findings, however, have also identified the functional existence of various members of the ECS on numerous other, previously unappreciated cell and tissue types. Among these, we have been particularly interested in human and murine skin and related cutaneous phenomena. Elements of the ECS were extensively documented in epidermal keratinocytes (10–12). Moreover, cannabinoids were shown to suppress *in vitro* proliferation (and differentiation) of cultured epidermal keratinocytes (11, 13), similar to the effects of selective CB2 agonists on human coronary artery smooth muscle cells (14), as well as the *in vivo* growth of murine skin tumors (15) and human melanomas (16). In addition, using double CB1/CB2 gene-deficient mice, Karsak *et al.* (17) have elegantly demonstrated that endocannabinoids attenuate allergic contact dermatitis.

[1] Correspondence: Department of Physiology, University of Debrecen, Medical and Health Science Center, Research Center for Molecular Medicine, 4032 Debrecen, Nagyerdei krt. 98. PO Box 22, Hungary. E-mail: biro@phys.dote.hu

doi: 10.1096/fj.07-104877

We have recently identified a CB1-mediated mechanism for nonclassical, peripheral tissue activities of endocannabinoids and exocannabinoids in the human system (18). Namely, using organ-cultured human scalp hair follicles, we have shown that locally produced endocannabinoids (*via* CB1 that is expressed mainly on outer root sheath keratinocytes of the follicle) inhibit human hair growth and induce premature apoptosis-driven involution of this complex miniorgan (catagen).

Hair follicles most commonly are arranged in pilosebaceous units, which display another characteristic adnexal structure of mammalian skin, *i.e.*, the sebaceous gland (reviewed in refs. 19, 20). It is extensively documented that epithelial cells of the sebaceous gland, *i.e.*, sebocytes, play a central role in the regulation of cutaneous lipid homeostasis and that pathological malfunctions of these cells may result in such common cutaneous diseases as acne vulgaris (21–24).

Of importance, sebaceous gland cells reportedly also show CB receptor immunoreactivity *in situ* (12). However, apart from anecdotes about marijuana users often developing acne, direct evidence for the presence of functional ECS in sebaceous glands and a description of the potential effects of endocannabinoids on various biological processes of human sebocytes are lacking.

In the current study, we have therefore analyzed the presence and function of the ECS and related signaling mechanisms in human sebaceous gland-derived cells, using the SZ95 sebocyte cell line, one of the best-established human sebocyte cell culture models (25–27). Specifically, we intended to clarify which CB receptors are expressed by human sebocytes, and whether prototypic endocannabinoids (AEA, 2-AG) can be detected in SZ95 sebocytes. Furthermore, we have evaluated the effects of endocannabinoids on defined sebocyte functions (*e.g.*, lipid synthesis, cell growth and death, gene expression), using an array of cellular and molecular assays, and have defined the involvement of various intracellular signaling pathways in mediating the effects of endocannabinoids (by employing specific agonists, antagonists, and RNA interference).

Collectively, these studies provide the first evidence that human sebocytes selectively express functional CB2, contain key endocannabinoids, and utilize this endogenous cannabinoid signaling system for the autocrine and paracrine control of human sebocyte lipid production and death.

MATERIALS AND METHODS

Materials

AEA, 2-AG, arachidonyl-2-chloroethylamide (ACEA), AM-251, iodo-resiniferatoxin (I-RTX), and GF10203X were purchased from Sigma-Aldrich (Taufkirchen, Germany). JWH-015 and GW9662 were obtained from Cayman Chemical Company (Ann Arbor, MI, USA). PD098059 and wortmannin were obtained from Calbiochem (Nottingham, UK), and AM630 was from Tocris Bioscience (Ellisville, MO, USA).

Cell culturing

Human immortalized SZ95 sebocytes (25–27), were cultured in Sebomed® basal medium (Biochrom, Berlin, Germany) supplemented with 10% fetal bovine serum (Invitrogen, Paisley, UK), 1 mM $CaCl_2$, 5 ng/ml human recombinant epidermal growth factor (Sigma-Aldrich), 50 U/ml penicillin, and 50 μg/ml streptomycin (both from Biogal, Debrecen, Hungary).

Determination of endocannabinoid levels

The levels of endocannabinoids (AEA, 2-AG) were determined by liquid chromatography/in line mass spectrometry as described in our earlier reports (18, 28).

Immunocytochemistry

SZ95 sebocytes were fixed in acetone, permeabilized by 0.1% Triton-X-100 (Sigma-Aldrich) in phosphate-buffered saline (PBS), and then incubated with rabbit anti-CB1 or anti-CB2 primary antibodies (Cayman) for 60 min (dilution 1:200). Slides were then incubated with a goat anti-rabbit fluorescein-isothiocyanate (FITC) -conjugated secondary antibody (Vector Laboratories, Burlingame, CA, USA) (dilution 1:200), and nuclei were visualized using DAPI (Vector). Cells were examined on a Nikon Eclipse E600 fluorescent microscope (Nikon, Tokyo, Japan) (29).

Immunohistochemistry

The study was approved by the Institutional Research Ethics Committee and adhered to Declaration of Helsinki guidelines. Normal female trunk skin samples, obtained during plastic surgery, were fixed in 4% formalin and embedded in paraffin, and 4-μm-thick sections were obtained. After antigen retrieval and blocking of the endogenous peroxidase activity, tissue sections were incubated with the above CB1 and CB2 primary antibodies (Cayman) (dilution 1:150 for CB1, 1:200 for CB2). Sections were then incubated with the EnVision+ System Labeled polymer-HRP Anti-Rabbit (Dako, Glostrup, Denmark) with 3,3′-diaminobenzidine (DAB) visualization techniques. Tissue samples were finally counterstained with hematoxylin (Sigma-Aldrich) and mounted in aqueous mounting medium (Dako) (18, 29, 30).

In the course of the immunohistochemistry, numerous control experiments were performed. As "staining-negative" controls, the appropriate primary antibodies were either omitted from the procedure or were preabsorbed with synthetic blocking peptides (Cayman) (see **Fig. 1**). As "tissue-negative" controls, CB-labeling was performed on tissues not expressing CB1 (human mast cell line HMC-1) (31) or CB2 (HMC-1, human hair follicle) (18, 31). In addition, the specificity of CB receptor staining was also measured *1*) on tissues recognized to be CB1 (HaCaT epidermal keratinocytes, hair follicle) (10, 13, 18) or CB2 (HaCaT keratinocytes, human peripheral monocytes, spleen) positive (11, 18, 32) (data not shown); or *2*) by employing another set of antibodies against CB1 and CB2 (Santa Cruz Biotechnology, Santa Cruz, CA, USA). The application of these latter primary antibodies resulted in identical staining patterns (data not shown).

Western blot analysis

Western immunoblotting was performed as described in our earlier reports (29, 30, 33). In brief, cell lysates were subjected

to sodium dodecyl sulfate-polyacrylamide gel electrophoresis, transferred to BioBond nitrocellulose membranes (Whatman, Maidstone, England), and then probed with anti-CB1 or anti-CB2 receptor antibodies (1:200, Cayman); with a rabbit antibody against the mitogen-activated protein kinase (MAPK) Erk-1/2 (Santa Cruz); or a mouse antibody recognizing the phosphorylated form of Erk-1/2 (pErk-1/2, Santa Cruz) (1:1500 dilution in both cases). Horseradish peroxidase–polymer-conjugated, respective anti-rabbit or anti-mouse IgG antibodies (Envision labeling, DAKO) were used as secondary antibodies, and the immunoreactive bands were visualized by SuperSignal West Pico Chemiluminescent Substrate-enhanced chemiluminescence (Pierce, Rockford, IL, USA). Immunoblots were then subjected to densitometric analysis using an Intelligent Dark Box (Fuji, Tokyo, Japan) and the Image Pro Plus 4.5.0 software (Media Cybernetics, Silver Spring, MD, USA). To assess equal loading, membranes were stripped and then reprobed with a rabbit cytochrome-C (Cyt-C) antibody (Santa Cruz) followed by a similar visualization procedure as described above.

Reverse transcriptase-polymerase chain reaction (RT-PCR)

The expression of CB1 and CB2 receptor mRNA was determined by semiquantitative RT-PCR, as we have described before (18, 29, 30). In brief, isolated total RNA was reverse-transcribed into cDNA and then amplified on a GeneAmp PCR System 2400 DNA Thermal Cycler (Applied Biosystems, Foster City, CA, USA) using optimized thermal protocols. Primers were synthesized by Invitrogen (CB1, forward: CAAGCCCGCATGGACATTAGGTTA, CB1, reverse: TCCGAGTCCCCCATGCTGTTATC; CB2, forward: TCCCACTGATCCCCAATGACTACC, CB2, reverse: AGGATCTCGGGGCTTCTTCTTTTG; glyceraldehyde 3-phosphate dehydrogenase (GAPDH), forward: ATGGTGAAGGTCGGTGTGAAC, GAPDH, reverse: GCTGACAATCTTGAGGGAGT). PCR products were visualized on 1.5% agarose gel with ethidium bromide (0.5 mg/ml, Sigma-Aldrich) under UV, and the photographed bands were quantified by Image Pro Plus 4.5.0 software.

Quantitative real-time PCR

Quantitative PCR (Q-PCR) was performed on an ABI Prism 7000 sequence detection system (Applied Biosystems) using the 5′ nuclease assay, as detailed in our previous report (18, 29). To detect the expression of genes involved in the regulation of lipid synthesis (see also Table 1), the following TaqMan primers and probes were used: peroxisome proliferator-activated receptor (PPAR)α, forward: CATTACGGAGTCCACGCGT, PPARα, reverse: ACCAGCTTGAGTCGAATCGTT; PPARα, probe FAM-AGGCTGCAAGGGCTTCTTTCGGCG-TAMRA; PPARδ, forward: AGCATCCTCACCGGCAAAG, PPARδ, reverse: CCACAATGTCTCGATGTCGTG; PPARδ, probe FAM-CAGCCACACGGCGCCCTTTG-TAMRA; PPARγ, forward: GATGACAGCGACTTGGCAA, PPARγ, reverse: CTTCAATGGGCTTCACATTCA; PPARγ, probe FAM-CAAACCTGGGCGGTCTCCACTGAG-TAMRA; adipose differentiation-related protein (ADRP), forward: TGACTGGCAGTGTGGAGAAGA, ADRP, reverse: ATCATCCGACTCCCCAAGA; ADRP, probe FAM-TCTGTGGTCAGTGGCAGCATTAACACA-TAMRA; PPARγ-regulated angiopoietin-related protein (PGAR), forward: TCCGCAGGGACAAGAACTG, PGAR, reverse: CGGAAGTACTGGCCGTTGA; PGAR, probe FAM-TTGGAATGGCTGCAGGTGCCA-TAMRA; and a predesigned assay for cyclooxygenase-2 (COX-2) (Applied Biosystems, assay ID: Hs00153133_m1). As internal controls, transcripts of human cyclophilin-A (forward: ACGGCGAGCCCTTGG, reverse: TTTCTGCTGTCTTTGGGACCT; probe FAM-CGCGTCTCCTTTGAGCTGTTTGCA-TAMRA) were determined.

RNA interference (RNAi)

SZ95 sebocytes were seeded in 6-well culture plates in SeboMed medium lacking antibiotics. At 50–70% confluence, medium was replaced by serum-free OptiMEM (Invitrogen), and cells were transfected with various CB2-specific Stealth RNAi oligonucleotides (ID: HSS102085, HSS102086, HSS102087, Invitrogen) (40 nM) using Lipofectamine 2000 transfection reagent (Invitrogen). For controls, RNAi Negative Control Duplexes (Scrambled RNAi, Invitrogen) and CB1-specific Stealth RNAi oligonucleotides (ID: HSS102082) were employed. Three hours after transfection, medium was replaced by complete Sebomed® medium, and cells were allowed to recover for 24 h. The efficacy of siRNA-driven knockdown was daily evaluated by RT-PCR and Western blot analysis for 4 days (34).

Determination of intracellular lipids

For semiquantitative detection of sebaceous lipids, SZ95 sebocytes were cultured on glass coverslips and treated with several compounds (AEA, 2-AG) for 24–48 h. Cells were fixed in 4% paraformaldehyde (Sigma-Aldrich), washed in 60% isopropanol, and stained in Oil Red O solution (0.3% in isopropanol) (Sigma-Aldrich). Cells were counterstained with hematoxylin (Sigma-Aldrich) and were mounted in aqueous mounting medium (Dako) (35, 36).

For quantitative measurement, SZ95 sebocytes (15,000 cells/well) were cultured in 96-well black-well/clear-bottom plates (Greiner Bio One, Frickenhausen, Germany) in quadruplicates and were treated with compounds for 24–48 h. Supernatants were then discarded, and 100 μl of 1 μg/ml Nile red (Sigma-Aldrich) solution was added to each well. The emitted fluorescence was measured on a Molecular Devices FlexStation 384^{II} Fluorescence Image Microplate Reader (FLIPR, Molecular Devices, San Francisco, CA, USA). Results are presented as percentages of the relative fluorescence units (RFU) in comparison with the controls, using 485-nm excitation and 565-nm emission wavelengths for neutral lipids, and 540-nm excitation and 620-nm emission wavelengths for polar lipids (35–37).

Determination of viable cell number

The number of viable cells was determined by measuring the conversion of the tetrazolium salt MTT (Sigma-Aldrich) to formazan by mitochondrial dehydrogenases. Cells were plated in 96-well plates (15,000 cells/well) in quadruplicates and were cultured for 24–48 h. Cells were then incubated with 0.5 mg/ml MTT, and the concentration of formazan crystals (as an indicator of the viable cell number) was determined colorimetrically (A_{550}), according to our previous reports (29, 33, 34, 38).

Determination of apoptosis

Abolishment of mitochondrial membrane potential is one of the earliest markers of apoptosis (39). To assess the process, mitochondrial membrane potential of SZ95 sebocytes was determined using a MitoProbe $DilC_1(5)$ Assay Kit (Invitrogen). Cells (15,000 cells/well) were cultured in 96-well black-well/clear-bottom plates (Greiner Bio One) in quadruplicate and were treated with various compounds for 24–48 h. After removal of supernatants, cells were incubated with $DilC_1(5)$

working solution (30 μl/well), and the fluorescence of $DilC_1(5)$ was measured at 630-nm excitation and 670-nm emission wavelengths using FLIPR (36).

In addition, another hallmark of apoptosis (*i.e.*, membrane perturbation) was also assessed by flow cytometry according to our previous reports (29, 34, 36, 38). In brief, following treatment with various agents, SZ95 sebocytes were harvested and stained with an Annexin-V-FITC/propidium iodide (PI) apoptosis kit (Sigma-Aldrich) following the manufacturer's protocol. Fluorescence intensity was measured by a Coulter Epics XL (Beckman Coulter, Fullerton, CA, USA) flow cytometer.

Determination of necrosis/cytotoxicity

Necrotic cell death was first determined by measuring the glucose-6-phosphate-dehydrogenase (G6PD) release (G6PD Release Assay Kit, Invitrogen). The enzyme activity was detected by a 2-step enzymatic process that leads to the reduction of resazurin into red-fluorescent resorufin. SZ95 sebocytes (15,000 cells/well) were cultured in 96-well black-well/clear-bottom plates (Greiner Bio One) in quadruplicate and treated with various compounds for 24–48 h. A 2× reaction medium was then prepared according to the manufacturer's protocol and was added to the wells in 1:1 dilution. The fluorescence emission of resorufin was monitored by FLIPR at 545-nm excitation and 590-nm emission wavelengths (36).

The cytotoxic effects of cannabinoid treatment were also determined by Sytox Green staining (Invitrogen). The dye is able to penetrate (and then bind to the nucleic acids) only to necrotic cells with ruptured plasma membranes, whereas healthy cells with intact surface membranes show negligible Sytox Green staining. SZ95 sebocytes were cultured in 96-well black-well/clear-bottom plates (Greiner Bio One) and were treated with various compounds (AEA, 2-AG, JWH-015, ACEA) for 24–48 h. Supernatants were then discarded, and the cells were incubated with 1 μM Sytox Green solution. The fluorescence of Sytox Green was measured at 490-nm excitation and 520-nm emission wavelengths using FLIPR (36).

Statistical analysis

When applicable, data were analyzed using a 2-tailed unpaired t test, and values of $P < 0.05$ were regarded as significant. In addition, statistical differences were further verified using 1-way ANOVA with Bonferroni and Dunnett *post hoc* probes, resulting in similar results (data not shown).

RESULTS

Human sebaceous gland epithelium and human SZ95 sebocytes express CB receptors

First, we intended to identify the existence of CB receptors in human sebaceous gland *in situ* and on human SZ95 sebocytes. Similar to a previous report (12), *in situ*, both CB1- and CB2-like immunoreactivity was identified in the sebaceous gland epithelium of normal human scalp skin sections (**Fig. 1*A, B***). However, using mutually complementary and confirmatory immunocytochemistry and Western blot analysis on human SZ95 sebocytes, we were able to identify only the relatively high expression of CB2, whereas the appearance of CB1-like immunoreactivity, in all cases, was around the detection limit (Fig. 1*C–E*). In addition, supporting the above findings, transcription of the CB2 (but not of CB1) gene in SZ95 sebocytes was demonstrated by RT-PCR (Fig. 1*F*) and by real-time Q-PCR (not shown). For positive controls, human organ-cultured hair follicles (for CB1) (18) and human peripheral monocytes (for CB2) (32) (as well as other tissue and cell types listed in Materials and Methods, data not shown) were employed. Therefore, in striking contrast to human hair follicle epithelium *in situ* (18), human sebocytes express primarily, if not exclusively, CB2, at least *in vitro*.

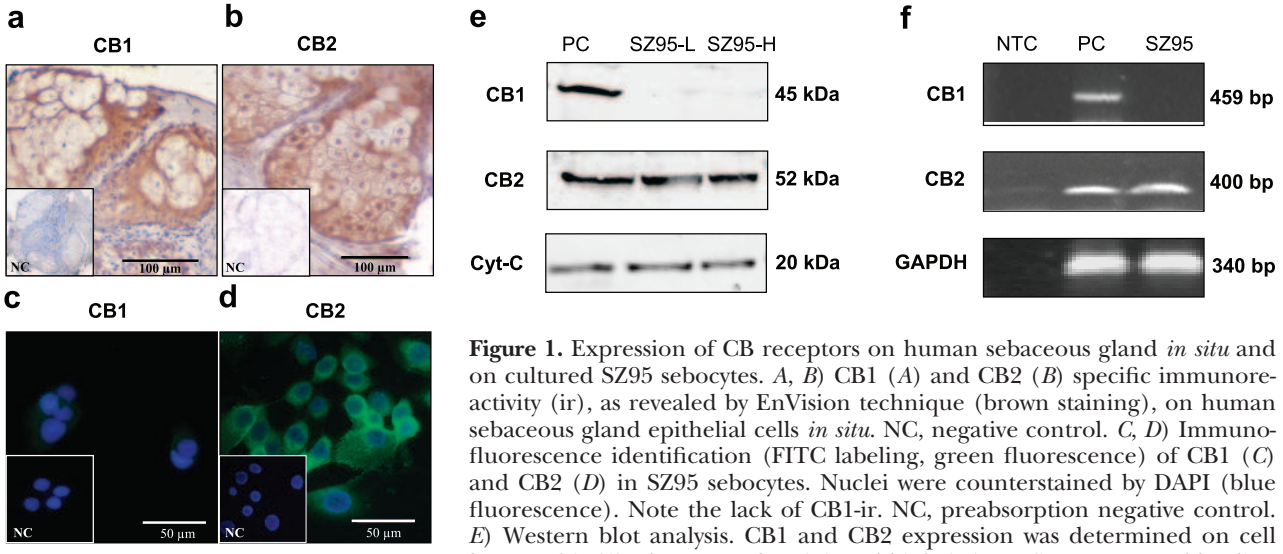

Figure 1. Expression of CB receptors on human sebaceous gland *in situ* and on cultured SZ95 sebocytes. *A*, *B*) CB1 (*A*) and CB2 (*B*) specific immunoreactivity (ir), as revealed by EnVision technique (brown staining), on human sebaceous gland epithelial cells *in situ*. NC, negative control. *C*, *D*) Immunofluorescence identification (FITC labeling, green fluorescence) of CB1 (*C*) and CB2 (*D*) in SZ95 sebocytes. Nuclei were counterstained by DAPI (blue fluorescence). Note the lack of CB1-ir. NC, preabsorption negative control. *E*) Western blot analysis. CB1 and CB2 expression was determined on cell lysates of SZ95 sebocytes at low (L) and high (H) confluences. Equal loading was assessed by determining expression of cytochrome C (Cyt-C). *F*) RT-PCR analysis of CB1 and CB2 mRNA transcripts. As an endogenous control, GAPDH expression was determined. NTC, nontemplate control. *E*, *F*) For positive controls (PC), human HaCaT keratinocytes (for CB1) and human monocytes (for CB2) were employed. In all cases, 3–5 additional experiments yielded similar results.

Human SZ95 sebocytes produce endocannabinoids

We also tested whether SZ95 sebocytes synthesize endocannabinoids. Using mass spectrometry, we were able to show that SZ95 sebocytes express both AEA (66.7±10 fmol/mg tissue) and 2-AG (6.2±1 pmol/mg tissue) (means±SE, n=4) at levels similar to those detected earlier in various skin samples; *e.g.*, ~50 fmol/mg tissue AEA in rat paw and mouse ear samples (17, 40) or 20–30 pmol/mg tissue 2-AG in mouse ear skin (17).

Endocannabinoids enhance lipid synthesis and induce apoptosis in SZ95 sebocytes

To further explore the functionality and the biological consequences of CB stimulation as well as possible auto- and paracrine-signaling events, we next investigated the effects of these endocannabinoids found in human SZ95 sebocytes on key functions of these cells. As revealed by Oil Red-O staining and quantitative Nile Red-based fluorescence assay, both AEA and 2-AG markedly (P<0.05) and dose dependently enhanced neutral lipid accumulation in SZ95 sebocytes (**Fig. 2*A*, *B***), reflecting stimulation of sebocyte differentiation (35).

By MTT assay, we also showed that stimulation with these endocannabinoids decreased sebocyte viability (Fig. 2*C*). To assess whether this effect was due to apoptosis and/or necrosis, first, flow cytometry analysis was performed. As seen in Fig. 2*D*, both AEA and 2-AG markedly (P<0.05) increased the number of Annexin-V-positive cells (reflecting phosphatidyl-serine translocation) (29, 34, 36, 38, 41), whereas the number of double Annexin-V- and PI-positive SZ95 sebocytes was only slightly elevated. This suggests that exogenously applied endocannabinoids primarily induce sebocyte apoptosis. In further support of this concept, in a series of quantitative fluorimetric assays, AEA (as well as 2-AG, data not shown) significantly decreased mitochondrial membrane potential (another hallmark of apoptosis) (36, 39) in a dose-dependent fashion (P<0.05), while

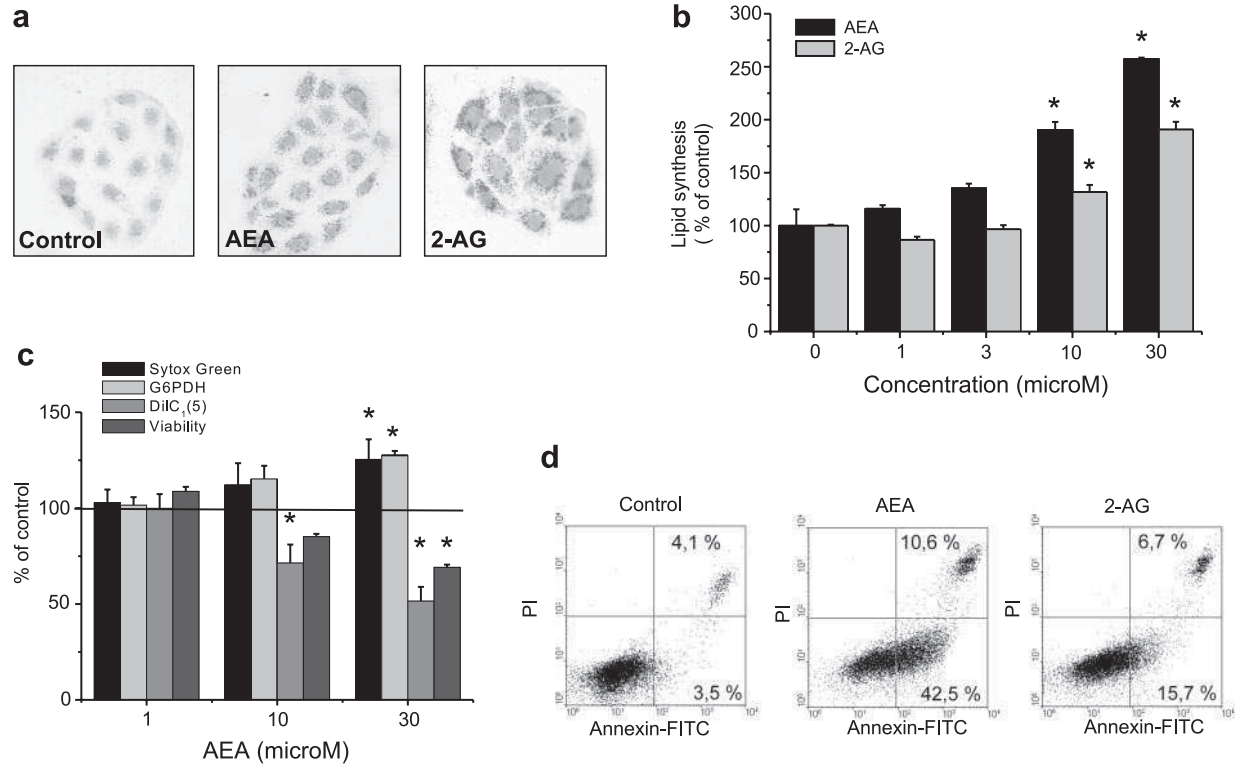

Figure 2. Endocannabinoids enhance lipid synthesis and induce cell death in SZ95 sebocytes. *A*) Semiquantitative detection of sebaceous lipids. SZ95 sebocytes were treated with vehicle or 30 μM AEA or 2-AG for 24 h, and lipids were labeled by Oil Red O solution (nuclei were counterstained with hematoxylin). *B*, *C*) Cells were cultured in 96-well plates in quadruplicates and were treated with various concentrations of AEA and 2-AG for 24–48 h. Graphs report quantitative measurement of intracellular neutral lipids as assessed by Nile red labeling followed by FLIPR measurement after 24 h (*B*) and quantitative determination of viable cell number and cell death (apoptosis, necrosis) after 48 h (*C*). Cell viability was assessed by a colorimetric MTT assay; necrotic cell death was measured by FLIPR-based G6PD release and Sytox Green assays; apoptotic cell death was investigated by a FLIPR-based $DilC_1(5)$ assay. Data (means±SE) are expressed as a percentage of the mean value (defined as 100%, solid line in *C*) of the vehicle-treated control group. * $P < 0.05$ *vs.* control. Three to 5 additional experiments yielded similar results. *D*) Measurement of apoptosis by flow cytometry. Control and endocannabinoid-treated (30 μM, 48 h) cells were harvested and stained with an Annexin-V-FITC and PI kit; fluorescence intensity values were detected by flow cytometry. Numbers represent percentages of cells exhibiting single Annexin-V-positive (apoptotic cells, lower right quadrant) and double Annexin-V- and PI-positive (necrotic cells, upper right quadrant) staining patterns. Two additional experiments yielded similar results.

only the highest concentration of AEA was able to moderately (yet significantly, $P<0.05$) increase Sytox Green accumulation and G6PD release, two complementary indicators of necrosis/cytotoxicity (Fig. 2*C*) (36).

The effects of AEA on human sebocytes are selectively mediated by CB2

We then investigated whether the cellular actions of AEA on SZ95 sebocytes were mediated by the CB receptors. As seen in **Fig. 3*A, B,*** the synthetic CB2-specific agonist JWH-015 (3, 7, 42)—but, notably, not the CB1-specific agonist ACEA (3, 7, 43)—mimicked the action of endocannabinoids to enhance lipid synthesis and to induce (chiefly apoptosis-driven) cell death. Moreover, the effects of AEA were prevented by the CB2-specific antagonist AM-630 (3, 7, 11, 28) (Fig. 3*C, D*) but not by the CB1-specific inhibitor AM-251 (3, 7, 18) (Fig. 3*C*). These data suggested that the sebocyte-modulatory effects of endocannabinoids are mediated by CB2 but not by CB1.

However, AEA, in various cellular systems, may also act on another receptor, *i.e.*, transient receptor potential vanilloid-1 (TRPV1, the capsaicin receptor) (3, 44, 45). Furthermore, we have recently described the functional existence of TRPV1-mediated signaling both in human organ-cultured hair follicles (29) and in SZ95 sebocytes (36). Therefore, to further dissect the exact cellular mechanisms of action of the endocannabinoid, we also measured the effect of the TRPV1 antagonist I-RTX (46) on the actions of AEA. As seen in Fig. 3*C*, I-RTX did not interfere with the ability of AEA to enhance lipid synthesis (and to induce cell death, data not shown).

Collectively, these functional data are in agreement with the apparent lack of CB1 expression in SZ95 sebocytes at either the protein or gene level (Fig. 1) and suggest that the cellular actions of endocannabinoids are mediated by CB2. To further assess the role of CB2, a series of RNAi experiments against the receptors was carried out (**Fig. 4*A, B***). Western blot and RT-PCR analysis revealed that the expression of CB2 was significantly knocked down by all 3 RNAi probes at day 2 after transfection and remained suppressed also on day 3. However, this phenomenon was reversible, because we observed a return of the immunosignals at day 4. Scrambled RNAi probes (Fig. 4*A*) or RNAi oligonucleotides against CB1 (data not shown) had no effect on the expression of CB2, indicating the specificity of the CB2 knockdown.

We then investigated the effects of AEA-treatment (24 h) on the lipid synthesis of RNAi-transfected SZ95 sebocytes on day 2. Similar to the effects of CB inhibitors, RNAi knockdown of CB2 resulted in the loss of effect of AEA in enhancing lipid synthesis. In contrast, treatment with the CB1-targeted RNAi did not affect the cellular action of AEA (Fig. 4*C*). Intriguingly, in SZ95 sebocytes with RNAi-mediated knockdown of CB2, we found markedly and significantly decreased basal lipid content as well (Fig. 4*C*). This strongly suggests that CB2-mediated signaling indeed plays an important endogenous role in the constitutive regulation of sebocyte lipid synthesis.

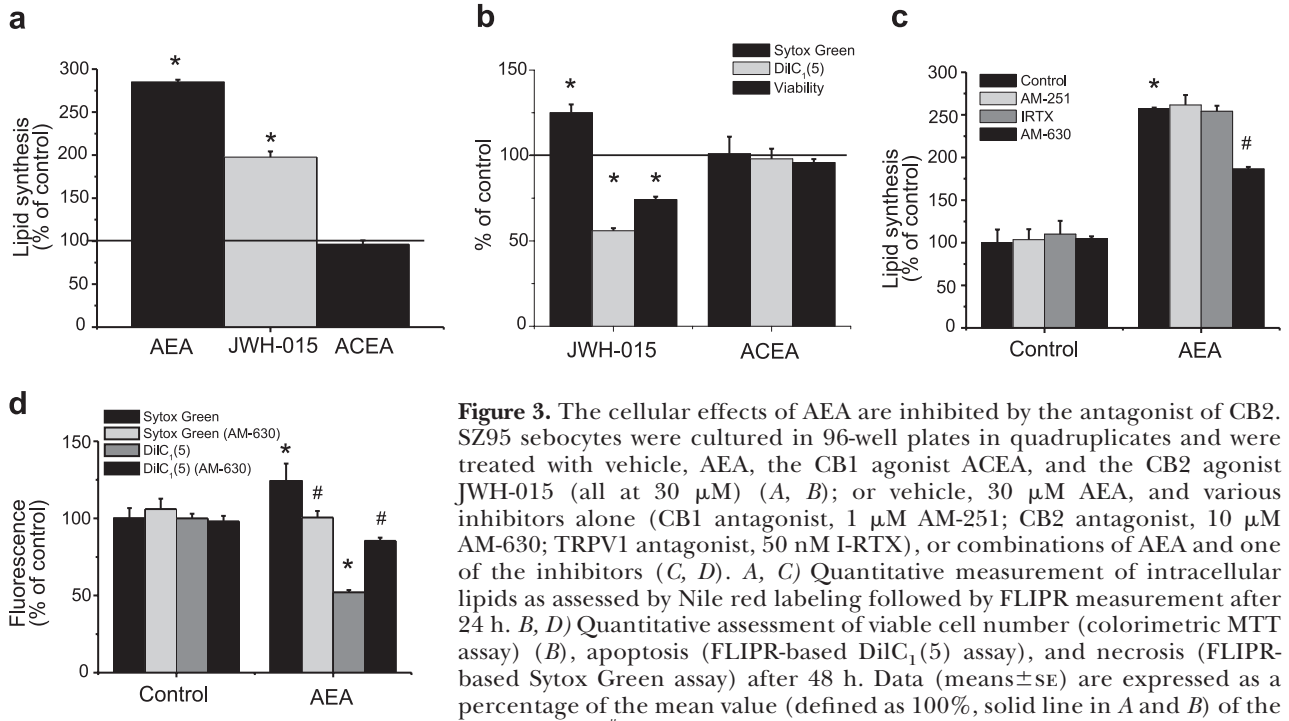

Figure 3. The cellular effects of AEA are inhibited by the antagonist of CB2. SZ95 sebocytes were cultured in 96-well plates in quadruplicates and were treated with vehicle, AEA, the CB1 agonist ACEA, and the CB2 agonist JWH-015 (all at 30 μM) (*A, B*); or vehicle, 30 μM AEA, and various inhibitors alone (CB1 antagonist, 1 μM AM-251; CB2 antagonist, 10 μM AM-630; TRPV1 antagonist, 50 nM I-RTX), or combinations of AEA and one of the inhibitors (*C, D*). *A, C)* Quantitative measurement of intracellular lipids as assessed by Nile red labeling followed by FLIPR measurement after 24 h. *B, D)* Quantitative assessment of viable cell number (colorimetric MTT assay) (*B*), apoptosis (FLIPR-based $DilC_1(5)$ assay), and necrosis (FLIPR-based Sytox Green assay) after 48 h. Data (means±SE) are expressed as a percentage of the mean value (defined as 100%, solid line in *A* and *B*) of the vehicle-treated control group. * $P < 0.05$ *vs.* control; # $P < 0.05$ *vs.* AEA without inhibitors. Three or 4 additional experiments yielded similar results.

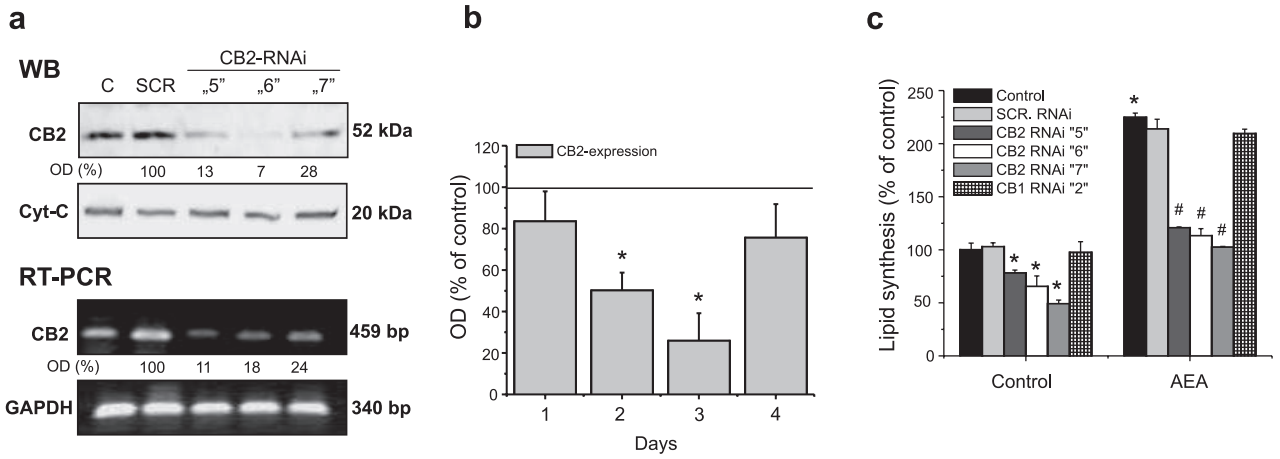

Figure 4. The cellular effects of AEA are prevented by RNAi-mediated knockdown of CB2. Various RNAi probes against CB2 (indicated by numbers) and CB1, as well as scrambled RNAi probe (SCR), were introduced to SZ95 sebocytes as described in Materials and Methods. To evaluate the efficacy of this intervention, at days 1–4 after transfection, cells were subjected to Western blot and RT-PCR analyses. *A*) Representative Western blot (WB) and RT-PCR results with CB2 at day 2 after transfection. As housekeeping molecules, expressions of cytochrome *c* (Cyt-C, Western blotting) and GAPDH (RT-PCR) were determined. In each case, amounts of CB2 were quantitated by densitometry (OD, optical density), normalized to those of the housekeeping molecule, and expressed as the percentage of the OD value of the SCR-treated group, regarded as 100%. Note that all CB2-specific RNAi probes employed markedly suppressed the expression of CB2 both at the protein and gene levels. C, transfection reagent-treated control group. *B*) Statistical analysis of Western blot data with CB2. OD values of CB2-specific immunosignals with RNAi probe 6 against CB2 were determined at days 1–4 after transfection in 3 independent experiments. Normalized OD values (to Cyt-C) in each group were then averaged and expressed as mean ± SE as the percentage of the averaged values of the respective SCR-treated groups, regarded as 100% (solid line). *C)* At day 2 after transfection, cells were seeded in 96-well plates and were treated with vehicle and 30 μM AEA for 24 h. Intracellular lipids were then quantitatively measured by Nile red labeling, followed by FLIPR measurement. Data (means±SE) are expressed as a percentage of the mean value (defined as 100%) of the vehicle-treated control group. * $P < 0.05$ *vs.* SCR; # $P < 0.05$ *vs.* AEA and SCR. Two additional experiments yielded similar results.

The CB2-mediated cellular signaling involves the MAPK pathway

On various cell types, CB receptor-mediated signaling, initiated by either endocannabinoids or exocannabinoids, recruits multiple intracellular pathway systems, such as protein kinase C (PKC), MAPK, or phosphatidyl-inositol-3-kinase (PI3K) (47–49). Therefore, we have also undertaken attempts to elucidate selected components of CB2-mediated intracellular signaling in human sebocytes.

As seen in **Fig. 5*A***, the enhancement of SZ95 lipid synthesis by AEA was not modified by the PKC inhibitor GF109203X (34, 38) or by the PI3K inhibitor wortmannin (48). In contrast, the MAPK inhibitor PD098059 (47) significantly ($P<0.05$) antagonized the effect of

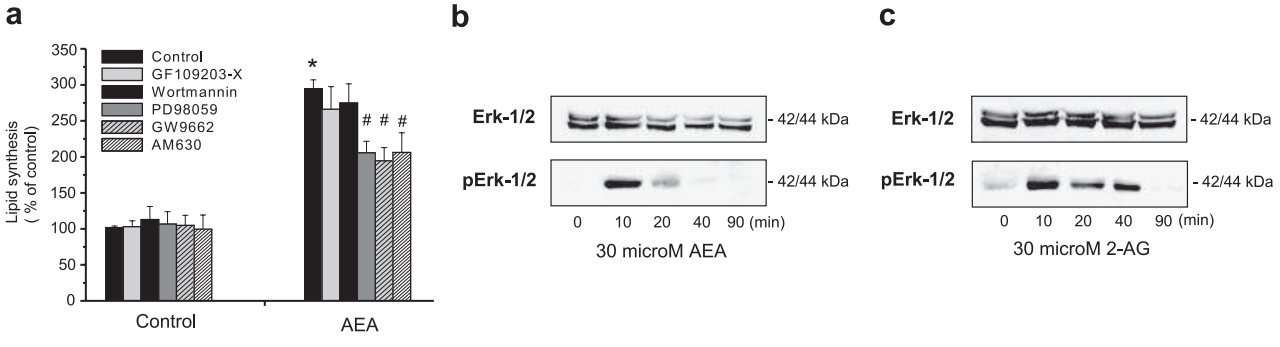

Figure 5. The CB2-mediated signaling induced by endocannabinoids involves the MAPK pathway. *A*) SZ95 sebocytes were cultured in 96-well plates in quadruplicates and were treated for 24 h with vehicle, 30 μM AEA, various inhibitors alone (CB2 antagonist, 10 μM AM-630; PKC antagonist, 100 nM GF109203X; MAPK inhibitor, 10 μM PD98059; PI3K inhibitor, 100 nM wortmannin; PPARγ inhibitor, 5 μM GW9662), or with combinations of AEA and one of the inhibitors. Intracellular lipids were then quantitatively determined with Nile red labeling, followed by FLIPR measurement. Data (means±SE) are expressed as a percentage of the mean value (defined as 100%) of the vehicle-treated control group. * $P < 0.05$ *vs.* vehicle; # $P < 0.05$ *vs.* AEA without inhibitors. Three additional experiments yielded similar results. *B, C*) Cells were treated with 30 μM AEA (*B*) or 30 μM 2-AG (*C*) for the times indicated, and then Western blotting was performed to reveal expressions of the MAPK Erk-1/2 and its phosphorylated form. Two additional experiments yielded similar results.

AEA, to an extent similar to that seen in the presence of the CB2 antagonist AM-630 (see Fig. 3*C*). This suggests an important involvement of the MAPK pathway in endocannabinoid-induced sebocyte lipid synthesis. This concept was further supported by the finding that both AEA and 2-AG induced a marked, transient phosphorylation of MAPK Erk-1/2, which indicated activation of the MAPK pathway (Fig. 5*B*, *C*).

Endocannabinoids upregulate expression of genes involved in the regulation of lipid synthesis

Members of the peroxisome proliferator-activated receptor (PPAR) nuclear transcription factor family are recognized as key regulators of lipid homeostasis in various cell types (50–53). Interestingly, recent reports directly link endocannabinoid signaling to certain PPARs (54, 55). Because the stimulation of lipid synthesis that we had demonstrated for endocannabinoids appears to be rather similar to that reported for selected PPAR ligands in SZ95 and SEB-1 sebocytes (37, 56, 57), we therefore investigated the effect of endocannabinoid treatment on the expression of PPAR isoforms in SZ95 sebocytes. As assessed by Q-PCR analysis (**Table 1**), both AEA and 2-AG significantly ($P<0.05$) up-regulated the expression of PPARδ and PPARγ, whereas PPARα gene expression was only increased in the 2-AG-treated group, at the 24-h time point.

Furthermore, both in human sebaceous glands and in cultured human SZ95 sebocytes, we have recently described (unpublished results) the expression pattern of recognized target genes (such as ADRP and PGAR), which are regulated or induced by PPARγ in macrophages, adipocytes, or dendritic cells (58–60). In addition, COX2 was also defined as PPARγ-induced target gene in SZ95 sebocytes (61). Hence, we finally also tested whether endocannabinoid treatment affects the expression of selected target genes. Intriguingly, both AEA and 2-AG dramatically elevated (*i.e.*, 10- to 15-fold increase at 24 h) the expression levels of all target genes investigated, further supporting the activation of PPARγ (Table 1). This idea was further strengthened by the observation that the effect of AEA to stimulate lipid accumulation in SZ95 sebocytes was significantly prevented by GW9662, a selective inhibitor of PPARγ (61) (Fig. 5*A*).

DISCUSSION

In an effort to explore the functional significance of the ECS in human skin physiology, in the current study, we have focused on the sebaceous compartment of its adnexal structures—an emerging, major neuroendocrine organ (19, 20, 23, 26). In this context, we provide here the first evidence that prototypic endocannabinoids (AEA, 2-AG) are produced by sebocytes, and show that these endocannabinoids (at physiologically relevant concentration) stimulate sebocyte lipid synthesis and apoptosis in a CB2-mediated manner. We also provide evidence suggesting that intrasebocyte signaling downstream of CB2 stimulation involves the MAPK pathway and various nuclear transcription factors well recognized in the regulation of lipid synthesis. Taken together, our data support the concept that human sebocytes are both sources and targets of endocannabinoids, where they function as constitutively active paracrine-autocrine positive regulators of sebaceous gland lipid homeostasis and negative regulators of sebocyte survival.

Previous reports have shown that endocannabinoids may exert their cellular actions *via* CB1, CB2, and, in the case of AEA, TRPV1 receptors (3, 18, 44, 45). Furthermore, we have recently described the functional existence of TRPV1 both in human sebaceous glands and in SZ95 sebocytes (36). Therefore, an important goal of our study was to identify the molecular targets of the endocannabinoids. Several lines of evidence indicate the endocannabinoids induce lipid synthesis and cell death in sebaceous cells exclusively *via* CB2 receptors. First, the cellular effects of endocannabinoids were abrogated by the CB2-specific antagonist AM-630 but not by TRPV1 or CB1 antagonists. Second, endocannabinoids were ineffective in sebocytes in which CB2 expression was selectively knocked down by RNAi. Third, the effects of endocannabinoids were mimicked by the synthetic CB2-specific agonist JWH-015 but not

TABLE 1. *Effect of endocannabinoid treatment on expression of selected genes in SZ95 sebocytes*

	AEA (fold change)		2-AG (fold change)	
Gene	12 h	24 h	12 h	24 h
PPARα	0.84 ± 0.12	0.96 ± 0.05	0.89 ± 0.08	1.44 ± 0.06*
PPARδ	1.67 ± 0.12*	2.07 ± 0.11*	1.33 ± 0.12*	2.28 ± 0.16*
PPARγ	1.00 ± 0.07	1.49 ± 0.01*	1.03 ± 0.08	2.22 ± 0.15*
COX2	2.06 ± 0.14*	6.93 ± 0.65*	1.59 ± 0.16*	2.45 ± 0.93*
ADRP	1.77 ± 0.07*	2.59 ± 0.22*	4.44 ± 0.45*	3.82 ± 0.34*
PGAR	9.95 ± 1.23*	11.6 ± 1.92*	16.0 ± 1.26*	13.4 ± 1.21*

SZ95 sebocytes were treated either with vehicle (control) or with 30 μM AEA or 2-AG for 12 or 24 h, and gene expression was determined by Q-PCR. Values were first normalized to gene expression levels of cyclophilin-A, and values of the endocannabinoid-treated samples were then normalized to the control (vehicle-treated), regarded as 1. Data are expressed as mean ± SE of 3 independent determinations performed in triplicate. * $P < 0.05$ *vs.* control.

by the CB1-specific agonist ACEA. Fourth, CB2 was successfully identified in SZ95 sebocytes (both at the protein and mRNA levels), whereas the expression of CB1 was uncertain.

We also intended to define the downstream signaling mechanisms activated by CB2. Among the multiple intracellular signal transduction systems (*e.g.*, PKC, MAPK, PI3K) known to be modulated by cannabinoids (47–49), we identified the MAPK pathway as a mediator of CB2-induced cellular actions of endocannabinoids in human sebocytes. We also show for the first time that CB2 activation in sebocytes also results in the induction PPAR isoforms and certain target genes (of PPARγ) involved in regulating lipid homeostasis in various cell types (50–53). This suggests that the ECS may modulate the lipogenic gene expression profile of the cells.

Our preclinical data in one of the best established human sebocyte cell culture systems encourage the systematic exploration now of whether CB2 antagonists or agonists can be exploited in the management of common skin disorders that are characterized by sebaceous gland dysfunctions (*e.g.*, acne vulgaris, seborrhea, dry skin, sebaceous gland-derived tumors). The observed enhancement of lipid synthesis induced by endocannabinoids strikingly resemble those seen in acne vulgaris, a common, multifactorial pilosebaceous inflammatory skin disease in which differentiation and hence lipid synthesis of sebocytes are pathologically increased (21, 23, 24). This, and the finding in CB2-silenced SZ95 sebocytes that both AEA-stimulated and *basal* lipid synthesis, were suppressed may be interpreted to indicate a role of enhanced CB2 signaling in acne pathogenesis. Proof-of-principle studies are now warranted to test the therapeutic value of CB2 blockade in the clinical management *e.g.*, of acne and seborrhea. Conversely, CB2 agonists deserve exploration as novel therapeutic tools for enhancing sebum production in excessively dry skin and/or for stimulating sebocyte apoptosis in sebaceous tumors.

CB1-mediated signaling inhibits human hair growth and induces apoptosis-driven regression in the hair follicle (18). Furthermore, it also suppresses differentiation of epidermal keratinocytes (10, 13). Moreover, both CB1 and CB2-coupled mechanisms have been reported to suppress murine (15) and human (16) skin tumor growth and to attenuate murine allergic contact dermatitis (17). Our current data suggest that the *endogenously active* ECS, which enhances sebocyte lipid synthesis and cell death selectively operates *via* CB2. This, in turn, suggests the existence of cell type-specific and receptor-selective regulatory endocannabinoid mechanisms in mammalian skin, which call for systematic further experimental dissection. Moreover, in view of growing insights into the importance of neuroendocrine cross-talks, *e.g.*, between cannabinoids/CBs and melanocortin receptors (63), and of the multiple neuroendocrine controls that human sebocytes are subject to (23, 24, 26), including melanocortin receptor-mediated ones (63), it also deserves to be dissected whether and how CB2-mediated signaling is regulated by other sebaceous neuroendocrine signals and/or modulates their production/activity.

In summary, we have shown the expression of functional CB2 receptors and of key endocannabinoids by human sebocytes, which may utilize this endogenous cannabinoid signaling system for the autocrine and paracrine control of sebocyte lipid production and death in a MAPK pathway-dependent manner. FJ

This work was supported in part by Hungarian research grants (OTKA T049231, OTKA K063153, ETT 480/2006, ETT 482/2006, RET 06/2004) to T.B., by a DFG grant (Pa 345/11–2) to R.P., and by the European Academy of Dermatology and Venereology (EADV) European Dermatology Research Award to C.C.Z. The authors declare no competing financial interests. T.B. is a recipient of the János Bolyai scholarship of the Hungarian Academy of Sciences.

REFERENCES

1. Di Marzo, V., Bifulco, M., and De Petrocellis, L. (2004) The endocannabinoid system and its therapeutic exploitation. *Nat. Rev. Drug Discov.* **3,** 7712–7784
2. Piomelli, D. (2005) The endocannabinoid system: a drug discovery perspective. *Curr. Opin. Investig. Drugs* **6,** 672–679
3. Pacher, P., Batkai, S., and Kunos, G. (2006) The endocannabinoid system as an emerging target of pharmacotherapy. *Pharmacol. Rev.* **58,** 389–462
4. Maldonado, R., and Rodríguez de Fonseca, F. (2002) Cannabinoid addiction: behavioral models and neural correlates. *J. Neurosci.* **22,** 3326–3331
5. Freund, T. F., Katona, I., and Piomelli, D. (2003) Role of endogenous cannabinoids in synaptic signaling. *Physiol. Rev.* **83,** 1017–1066
6. Maldonado, R., Valverde, O., and Berrendero, F. (2006) Involvement of the endocannabinoid system in drug addiction. *Trends Neurosci.* **29,** 225–232
7. Pacher, P., Bátkai, S., and Kunos, G. (2005) Cardiovascular pharmacology of cannabinoids. *Handb. Exp. Pharmacol.* **168,** 599–625
8. Storr, M. A., and Sharkey, K. A. (2007) The endocannabinoid system and gut-brain signalling. *Curr. Opin. Pharmacol.* **7,** 575–582
9. Wright, K. L., Duncan, M., and Sharkey, K. A. (2008) Cannabinoid CB2 receptors in the gastrointestinal tract: a regulatory system in states of inflammation. *Br. J. Pharmacol.* **153,** 263–270
10. Maccarrone, M., Di Rienzo, M., Battista, N., Gasperi, V., Guerrieri, P., Rossi, A., and Finazzi-Agrò, A. (2003) The endocannabinoid system in human keratinocytes. Evidence that anandamide inhibits epidermal differentiation through CB1 receptor-dependent inhibition of protein kinase C, activation protein-1, and transglutaminase. *J. Biol. Chem.* **278,** 33896–33903
11. Ibrahim, M. M., Porreca, F., Lai, J., Albrecht, P. J., Rice, F. L., Khodorova, A., Davar, G., Makriyannis, A., Vanderah, T. W., Mata, H. P., and Malan, T.P. Jr. (2005) CB2 cannabinoid receptor activation produces antinociception by stimulating peripheral release of endogenous opioids. *Proc. Natl. Acad. Sci. U. S. A.* **102,** 3093–3098
12. Ständer, S., Schmelz, M., Metze, D., Luger, T., and Rukwied, R. (2005) Distribution of cannabinoid receptor 1 (CB1) and 2 (CB2) on sensory nerve fibers and adnexal structures in human skin. *J. Dermatol. Sci.* **38,** 177–188
13. Paradisi, A., Pasquariello, N., Barcaroli, D., and Maccarrone, M. (2008) Anandamide regulates keratinocyte differentiation by inducing DNA methylation in a CB1 receptor-dependent manner. *J. Biol. Chem.* **283,** 6005–6012
14. Rajesh, M., Mukhopadhyay, P., Haskó, G., Huffman, J. W., Mackie, K., and Pacher, P. (2008) CB2 cannabinoid receptor agonists attenuate TNF-alpha-induced human vascular smooth muscle cell proliferation and migration. *Br. J. Pharmacol.* **153,** 347–357

15. Casanova, M. L., Blazquez, C., Martinez-Palacio, J., Villanueva, C., Fernandez-Acenero, M. J., Huffman, J. W., Jorcano, J. L., and Guzman, M. (2003) Inhibition of skin tumor growth and angiogenesis in vivo by activation of cannabinoid receptors. *J. Clin. Invest.* **111,** 43–50
16. Blazquez, C., Carracedo, A., Barrado, L., Real, P. J., Fernandez-Luna, J. L., Velasco, G., Malumbres, M., and Guzman, M. (2006) Cannabinoid receptors as novel targets for the treatment of melanoma. *FASEB J.* **20,** 2633–2635
17. Karsak, M., Gaffal, E., Date, R., Wang-Eckhardt, L., Rehnelt, J., Petrosino, S., Starowicz, K., Steuder, R., Schlicker, E., Cravatt, B., Mechoulam, R., Buettner, R., Werner, S., Di Marzo, V., Tüting, T., and Zimmer, A. (2007) Attenuation of allergic contact dermatitis through the endocannabinoid system. *Science* **316,** 1494–1497
18. Telek, A., Bíró, T., Bodó, E., Tóth, B. I., Borbíró, I., Kunos, G., and Paus, R. (2007) Inhibition of human hair follicle growth by endo- and exocannabinoids. *FASEB J.* **13,** 3534–3541
19. Paus, R., and Cotsarelis, G. (1999) The biology of hair follicles. *N. Engl. J. Med.* **341,** 491–497
20. Zouboulis, C. C. (2003) Sebaceous gland in human skin—the fantastic future of a skin appendage. *J. Invest. Dermatol.* **120,** xiv–xv
21. Zouboulis, C. C., Xia, L., Akamatsu, H., Seltmann, H., Fritsch, M., Hornemann, S., Rühl, R., Chen, W., Nau, H., and Orfanos, C. E. (1998) The human sebocyte culture model provides new insights into development and management of seborrhoea and acne. *Dermatology* **196,** 21–31
22. Toyoda, M., and Morohashi, M. (2001) Pathogenesis of acne. *Med. Electron Microsc.* **34,** 29–40
23. Zouboulis, C. C., and Böhm, M. (2004) Neuroendocrine regulation of sebocytes—a pathogenetic link between stress and acne. *Exp. Dermatol.* **13**(Suppl. 4), 31–35
24. Zouboulis, C. C., Eady, A., Philpott, M., Goldsmith, L. A., Orfanos, C., Cunliffe, W. C., and Rosenfield, R. (2005). What is the pathogenesis of acne? *Exp. Dermatol.* **14,** 143–152
25. Zouboulis, C. C., Seltmann, H., Neitzel, H., and Orfanos, C. E. (1999) Establishment and characterization of an immortalized human sebaceous gland cell line (SZ95). *J. Invest. Dermatol.* **113,** 1011–1020
26. Zouboulis, C. C., Seltmann, H., Hiroi, N., Chen, W., Young, M., Oeff, M., Scherbaum, W. A., Orfanos, C. E., McCann, S. M., and Bornstein, S. R. (2002) Corticotropin-releasing hormone: an autocrine hormone that promotes lipogenesis in human sebocytes. *Proc. Natl. Acad. Sci. U. S. A.* **99,** 7148–7153
27. Celso, C. L, Berta, M. A., Braun, K. M., Frye, M., Lyle, S., Zouboulis, C. C., and Watt, F. M. (2008) Characterisation of bipotential epidermal progenitors derived from human sebaceous gland: contrasting roles of c-Myc and beta-catenin. *Stem Cells* **26,** 1241–1252
28. Batkai, S., Osei-Hyiaman, D., Pan, H., El-Assal, O., Rajesh, M., Mukhopadhyay, P., Hong, F., Harvey-White, J., Jafri, A., Hasko, G., Huffman, J. W., Gao, B., Kunos, G., and Pacher. P. (2007) Cannabinoid-2 receptor mediates protection against hepatic ischemia/reperfusion injury. *FASEB J.* **21,** 1788–1800
29. Bodó, E., Bíró, T., Telek, A., Czifra, G., Griger, Z., Tóth, I. B., Mescalchin, A., Ito, T., Bettermann, A., Kovács, L., and Paus, R. (2005) A hot new twist to hair biology: involvement of vanilloid receptor-1 (VR1/TRPV1) signaling in human hair growth control. *Am. J. Pathol.* **166,** 985–998
30. Bodó, E., Kovács, I., Telek, A., Varga, A., Paus, R., Kovács, L., and Bíró, T. (2004) Vanilloid receptor-1 (VR1) is widely expressed on various epithelial and mesenchymal cell types of human skin. *J. Invest. Dermatol.* **123,** 410–413
31. Maccarrone, M., Fiorucci, L., Erba, F., Bari, M., Finazzi-Agrò, A., and Ascoli, F. (2000) Human mast cells take up and hydrolyze anandamide under the control of 5-lipoxygenase and do not express cannabinoid receptors. *FEBS Lett.* **468,** 176–180
32. Nong, L., Newton, C., Friedman, H., and Klein, T. W. (2001) CB1 and CB2 receptor mRNA expression in human peripheral blood mononuclear cells (PBMC) from various donor types. *Adv. Exp. Med. Biol.* **493,** 229–233
33. Bíró, T., Maurer, M., Modarres, S., Lewin, N. E., Brodie, C., Acs, G., Acs, P., Paus, R., and Blumberg, P. M. (1998) Characterization of functional vanilloid receptors expressed by mast cells. *Blood* **91,** 1332–1340
34. Griger, Z., Páyer, E., Kovács, I., Tóth, B. I., Kovács, L., Sipka, S., and Bíró, T. (2007) Protein kinase C-beta and -delta isoenzymes promote arachidonic acid production and proliferation of MonoMac-6 cells. *J. Mol. Med.* **85,** 1031–1042
35. Wróbel, A., Seltmann, H., Fimmel, S., Müller-Decker, K., Tsukada, M., Bogdanoff, B., Mandt, N., Blume-Peytavi, U., Orfanos, C. E., and Zouboulis, C. C. (2003) Differentiation and apoptosis in human immortalized sebocytes. *J. Invest. Dermatol.* **120,** 175–181
36. Tóth, I. B., Géczy, T., Czifra, G., Seltmann, H., Paus, R. Kovács L., Zouboulis C. C., and Bíró T. (2005) The vanilloid receptor 1 (TRPV1) is expressed and functionally active on human SZ95 sebocytes. *J. Invest. Dermatol.* **124**, A68
37. Alestas, T., Ganceviciene, R., Fimmel, S., Müller-Decker, K., and Zouboulis, C. C. (2006) Enzymes involved in the biosynthesis of leukotriene B4 and prostaglandin E2 are active in sebaceous glands. *J. Mol. Med.* **84,** 75–84
38. Papp, H., Czifra, G., Bodó, E., Lázár, J., Kovács, I., Aleksza, M., Juhász, I., Acs, P., Sipka, S., Kovács, L., Blumberg, P. M., and Bíró, T. (2004) Opposite roles of protein kinase C isoforms in proliferation, differentiation, apoptosis, and tumorigenicity of human HaCaT keratinocytes. *Cell. Mol. Life. Sci.* **61,** 1095–1105
39. Green, D.R., and Reed, J.C. (1998) Mitochondria and apoptosis. *Science* **281,** 1309–1312
40. Calignano, A., La Rana, G., Giuffrida, A., and Piomelli, D. (1998) Control of pain initiation by endogenous cannabinoids. *Nature* **394,** 277–281
41. Maccarrone, M., and Finazzi-Agró, A. (2003) The endocannabinoid system, anandamide and the regulation of mammalian cell apoptosis. *Cell Death Differ.* **10,** 946–955
42. Huffman, J. W. (2000) The search for selective ligands for the CB2 receptor. *Curr. Pharm. Des.* **6,** 1323–1337
43. Wagner, J. A., Abesser, M., Karcher, J., Laser, M., and Kunos, G. (2005) Coronary vasodilator effects of endogenous cannabinoids in vasopressin-preconstricted unpaced rat isolated hearts. *J. Cardiovasc. Pharmacol.* **46,** 348–355
44. Di Marzo, V., Blumberg, P. M., and Szallasi, A. (2002) Endovanilloid signaling in pain. *Curr. Opin. Neurobiol.* **12,** 372–379
45. Sharkey, K. A., Cristino, L., Oland, L. D., Van Sickle, M. D., Starowicz, K., Pittman, Q. J., Guglielmotti, V., Davison, J. S., and Di Marzo, V. (2007) Arvanil, anandamide and *N*-arachidonoyldopamine (NADA) inhibit emesis through cannabinoid CB1 and vanilloid TRPV1 receptors in the ferret. *Eur. J. Neurosci.* **25,** 2773–3782
46. Wahl, P., Foged, C., Tullin, S., and Thomsen, C. (2001) Iodoresiniferatoxin, a new potent vanilloid receptor antagonist. *Mol. Pharmacol.* **59,** 9–15
47. Derkinderen, P., Valjent, E., Toutant, M., Corvol, J. C., Enslen, H., Ledent, C., Trzaskos, J., Caboche, J., and Girault, J. A. (2003) Regulation of extracellular signal-regulated kinase by cannabinoids in hippocampus. *J. Neurosci.* **23,** 2371–2382
48. Ozaita, A., Puighermanal, E., and Maldonado, R. (2007) Regulation of PI3K/Akt/GSK-3 pathway by cannabinoids in the brain. *J. Neurochem.* **102,** 1105–1114
49. Vellani, V., Petrosino, S., De Petrocellis, L., Valenti, M., Prandini, M., Magherini, P.C., McNaughton, P.A., and Di Marzo, V. (2008) Functional lipidomics. Calcium-independent activation of endocannabinoid/endovanilloid lipid signalling in sensory neurons by protein kinases C and A and thrombin. [E-pub ahead of print] *Neuropharmacology.* doi:10.1016/j.neuropharm.2008.01.010
50. Desvergne, B., and Wahli, W. (1999) Peroxisome proliferator-activated receptors: nuclear control of metabolism. *Endocrin. Rev.* **20,** 649–688
51. Kersten, S., Desvergne, B., and Wahli, W. (2000) Roles of PPARs in health and disease. *Nature* **405,** 421–424
52. Chawla, A., Barak, Y., Nagy, L., Liao, D., Tontonoz, P., and Evans, R. M. (2001) PPAR-gamma dependent and independent effects on macrophage-gene expression in lipid metabolism and inflammation. *Nat. Med.* **7,** 48–52
53. Szatmari, I., Torocsik, D., Agostini, M., Nagy, T., Gurnell, M., Barta, E., Chatterjee, K., and Nagy, L. (2007) PPARgamma regulates the function of human dendritic cells primarily by altering lipid metabolism. *Blood* **110,** 3271–3280
54. Lenman, A., and Fowler, C. J. (2007) Interaction of ligands for the peroxisome proliferator-activated receptor gamma with the endocannabinoid system. *Br. J. Pharmacol.* **151,** 1343–1351

55. O'Sullivan, S. E. (2007) Cannabinoids go nuclear: evidence for activation of peroxisome proliferator-activated receptors. *Br. J. Pharmacol.* **152,** 576–582
56. Chen, W., Yang, C. C., Sheu, H. M., Seltmann, H., and Zouboulis, C. C. (2003) Expression of peroxisome proliferator-activated receptor and CCAAT/enhancer binding protein transcription factors in cultured human sebocytes. *J. Invest. Dermatol.* **121,** 441–447
57. Trivedi, N. R., Cong, Z., Nelson, A. M., Albert, A. J., Rosamilia, L. L., Sivarajah, S., Gilliland, K. L., Liu, W., Mauger, D. T., Gabbay, R. A., and Thiboutot, D. M. (2006) Peroxisome proliferator-activated receptors increase human sebum production. *J. Invest. Dermatol.* **126,** 2002–2009
58. Yoon, J. C., Chickering, T. W., Rosen, E. D., Dussault, B., Qin, Y., Soukas, A., Friedman, J. M., Holmes, W. E., and Spiegelman, B. M. (2000) Peroxisome proliferator-activated receptor gamma target gene encoding a novel angiopoietin-related protein associated with adipose differentiation. *Mol. Cell. Biol.* **20,** 5343–5349
59. Shappell, S. B., Gupta, R. A., Manning, S., Whitehead, R., Boeglin, W. E., Schneider, C., Case, T., Price, J., Jack, G. S., Wheeler, T. M., Matusik, R. J., Brash, A. R., and Dubois, R. N. 15S-Hydroxyeicosatetraenoic acid activates peroxisome proliferator-activated receptor gamma and inhibits proliferation in PC3 prostate carcinoma cells *Cancer Res.* **61,** 497–503, 2001
60. Vosper, H., Patel, L., Graham, T. L., Khoudoli, G. A., Hill, A., Macphee, C. H., Pinto, I., Smith, S. A., Suckling, K. E., Wolf, C. R., and Palmer, C. N. (2001) The peroxisome proliferator-activated receptor delta promotes lipid accumulation in human macrophages. *J. Biol. Chem.* **276,** 44258–44265
61. Zhang, Q., Seltmann, H., Zouboulis, C. C., and Konger, R. L. (2006) Involvement of PPARgamma in oxidative stress-mediated prostaglandin E(2) production in SZ95 human sebaceous gland cells. *J. Invest. Dermatol.* **126,** 42–48
62. Matias, I., Vergoni, A. V., Petrosino, S., Ottani, A., Pocai, A., Bertolini, A., and Di Marzo, V. (2008) Regulation of hypothalamic endocannabinoid levels by neuropeptides and hormones involved in food intake and metabolism: insulin and melanocortins. *Neuropharmacology* **54,** 206–212
63. Ganceviciene, R., Graziene, V., Böhm, M., and Zouboulis, C. C. (2007) Increased in situ expression of melanocortin-1 receptor in sebaceous glands of lesional skin of patients with acne vulgaris. *Exp. Dermatol.* **16,** 547–552

Received for publication April 4, 2008.
Accepted for publication June 5, 2008.

XI.

Acta Neuropathol (2000) 99 : 96–104

REGULAR PAPER

Judit Boczán · Sándor Boros · Ferenc Mechler
László Kovács · Tamás Bíró

Differential expressions of protein kinase C isozymes during proliferation and differentiation of human skeletal muscle cells in vitro

Received: 28 February 1999 / Revised, accepted: 24 June 1999

Abstract The mechanism of skeletal muscle regeneration in vivo can be well modeled in vitro by culturing skeletal muscle cells. In these cultures mononuclear satellite cells fuse to form polynuclear myotubes by proliferation and differentiation. The aim of this study was to determine how the different protein kinase C (PKC) isozymes were expressed during differentiation of human skeletal muscle in vitro. The expressions of desmin, used as a muscle-specific intermediate filament protein marker of differentiation, and of different PKC isozymes were detected by single and double immunohistochemical labeling, and by Western blot analysis. In skeletal muscle cells we could identify five PKC isozymes (PKCα, -γ, -η, -θ and -ζ). The expressions of PKCα and -ζ did not change significantly during differentiation; their levels of expression were high in the early immature cells and remained unchanged in later phases. In contrast, the expression levels of PKCγ and -η increased with differentiation. Furthermore, the cellular localization of PKCγ markedly altered during differentiation, with a perinuclear-nuclear to cytoplasmic translocation. The change in the level of expression of PKCθ during differentiation showed different pattern; its expression was high during the early phases, but a decreased immunostaining was detected in the matured, well-differentiated myotubes. We conclude, therefore, that cultured human skeletal muscle cells possess a characteristic PKC isozyme pattern, and that the different phases of differentiation are accompanied by different expression patterns of the various isozymes. These data suggest the possible functional and differential roles of PKC isozymes in human skeletal muscle differentiation.

Key words Skeletal muscle · Human · Differentiation · Protein kinase C · Isozymes

J. Boczán · S. Boros · L. Kovács · T. Bíró (✉)
Department of Physiology and Cell Physiology
Research Group of the Hungarian Academy of Sciences,
University Medical School of Debrecen, Nagyerdei krt. 98,
PO Box 22, H-4012 Debrecen, Hungary
e-mail: biro@phys.dote.hu,
Tel.: +36-52-416634, Fax: +36-52-432289

J. Boczán · F. Mechler
Department of Neurology,
University Medical School of Debrecen, Nagyerdei krt. 98,
PO Box 31, H-4012 Debrecen, Hungary

Introduction

Skeletal muscle cells possess a marked regeneration capacity [11]. During this process, which plays a central role in postnecrotic muscle reconstitution seen for example after muscle injury and in muscle dystrophies, the mononuclear satellite cells of the muscles proliferate and differentiate to form functional skeletal muscle fibers [6, 11]. The mechanism of muscular regeneration can be well modeled in vitro by culturing skeletal muscle cells [7, 31]. Satellite cells isolated enzymatically and mechanically from muscle biopsy specimens proliferate and fuse to form multinuclear myotubes (after the appropriate change of culture media), which eventually results in the development of matured, well-differentiated striated muscle cells [7, 31].

A variety of in vitro studies have been performed to follow the mechanism of muscle differentiation. Among the several muscle-specific candidates, the intermediate filament protein desmin has proven to be as one of the best markers of skeletal muscle differentiation since time-dependent changes in its expression level and staining pattern can be detected from the early stages of differentiation [2, 8, 33]. Furthermore, it has also been reported that proliferation and differentiation of satellite cells are under the control of several growth factors (e.g., insulin-like growth factor-1, prostaglandins, transforming growth factor-β; [11, 15]) and myogenic transcription factors (e.g., MyoD, MRF4, myf5, myogenin [6, 35]). The marked diversity in the intracellular signal transduction pathways influenced by these growth factors [15, 18] and, moreover, the very recent results claiming that the phosphorylation state of the transcription factors might affect muscle regeneration [21] suggest a complex regulation of the mus-

cle cell proliferation and differentiation by different kinase cascades [5].

Protein kinase C (PKC) comprises a family of serine/threonine kinases that play crucial roles in signal transduction and in the regulation of cellular proliferation and differentiation of several cell types [27–29]. At least 11 different isozymes of PKC have been isolated so far [16, 27], which can be grouped into four classes: PKCα, -βI, -βII, and -γ as calcium- and phorbol ester-dependent "conventional" PKC; PKCδ, -ε, -η, and -θ as calcium-independent and phorbol ester-responsive "novel" PKC; PKCζ and -λ as calcium-independent and phorbol ester-unresponsive "atypical" PKC; and PKCμ, a unique calcium-independent isoform.

Emerging evidence suggests important differences among PKC isozymes both in their regulation and in their biological roles. However, besides their functional diversity, they possess different patterns of tissue expression and subcellular localization, and they have different cofactor requirements [29]. Not only may some PKC isoforms be active for a given response whereas others are not, but different PKC isozymes may often have antagonistic effects on the same cellular event. Thus, PKCα was suggested to mediate phorbol 12-myristate 13-acetate (PMA)-induced cytostasis in K562 erythroleukemia cells, whereas PKCβII was involved in promoting proliferation [25]. Furthermore, in NIH 3T3 fibroblasts, PKCδ arrested cell growth, whereas PKCε had a stimulating effect on the same phenomenon [4, 24]. In C6 glioma cells [3] the expression levels of PKC isozymes markedly changed with cellular differentiation. These data suggest pivotal and differential regulatory roles of specific PKC isoforms in these processes.

PKC participates in the regulation of various cellular processes in different types of muscle. In cardiac muscle, the activation of PKC evoked a positive inotropic effect; furthermore, its pathognomic effect in the induction of cardiomyopathies was also implicated [30]. In smooth muscle cells, PKC has been described as an activator of the contractile machinery by phosphorylating several regulatory proteins such as calponin or caldesmon [26]. It has also been shown that the different PKC isoforms may differentially affect cellular responses; for example in A7r5 smooth muscle cells, the overexpression of PKCα decreased proliferation [34], whereas, in vascular smooth muscle cells, the overexpression of PKCβII, but not of PKCβI, increased cell doubling time [36].

Very little information is available, however, about the functional role of PKC in skeletal muscles. The modification of PKC activity altered insulin-dependent glucose transport [12] and vitamin D-induced calcium uptake [23]. Furthermore, treatments of avian skeletal muscle cells with vitamin D_3 and PMA modified the subcellular localization of PKC [22]. It was also shown that some phorbol esters, acting as activators of the enzyme, may down-regulate the transcription of gene sequences coding contractile proteins in terminally differentiated myotubes [38]. Nevertheless, the possible role of PKC (and especially of PKC isozymes) in such cellular processes as skeletal muscle proliferation, differentiation, or regeneration is basically unknown.

In this study we examined expression levels of different PKC isoforms during human skeletal muscle differentiation in vitro using desmin as a marker of the process. We report here that the levels of PKC isozymes alter as differentiation proceeds; thus, different stages of proliferation and differentiation are represented by different PKC isozyme patterns, suggesting different functional roles of PKC isoforms in human skeletal muscle differentiation in vitro.

Materials and methods

Cell culture

Satellite cells were obtained from muscle tissue waste of orthopedic surgery. The use of this material was approved by the Ethical Committee of the University Medical School of Debrecen. The procedure of growing myotubes closely followed the method of Sipos et al. [32]. Briefly, the biopsy material (23 biopsy samples were used to initiate cultures) was enzymatically dissociated at 37 °C in calcium/magnesium-free phosphate buffered saline solution (CMF-PBS) containing collagenase (250 U/ml, Type II, Sigma, St. Louis, Mo.) and bactotrypsin (3%, Difco, Detroit, Mich.). The reaction was stopped with Hanks' solution (136.75 mM NaCl, 5.36 mM KCl, 0.34 mM Na_2HPO_4, 0.44 mM KH_2PO_4, 0.81 mM $MgSO_4$, 1.26 mM $CaCl_2$, 5.56 mM glucose, 4.17 mM $NaHCO_3$, 10 mg/ml phenol red, pH 7.2) containing 10% fetal calf serum (FCS) (Sebak, Aidenbach, Germany). After filtrations and centrifugations (three times at 100 *g* for 10 min) the pellet was resuspended in Ham's F-12 (Sigma) growth medium containing 5% FCS and 5% horse serum (HS; Sebak), 2.5 mg/ml glucose, 0.3 mg/ml glutamate, 1.2 mg/ml $NaHCO_3$, 50 U/ml penicillin, 50 μg/ml streptomycin, 1.25 μg/ml fungizone (both from Biogal, Debrecen, Hungary), and kept at 5% CO_2 atmosphere on glass coverslips (Menzel-Glaser, Braunschweig, Germany) in petridishes (Nunc, Kamstrup, Denmark). After 3 days the culture medium was changed to Dulbecco's modified Eagle's medium (DMEM) (Sigma) containing 2% FCS and 2% HS to induce myoblast fusion and differentiation [32].

Western blot analysis

Cells were washed with ice-cold PBS, harvested in homogenization buffer (1% Triton X-100, 50 mM NaCl, 25 mM HEPES, 1 mM EDTA, 1 mM EGTA, 1 mM PMSF, 20 μM leupeptin, pH 7.4; all from Sigma) and disrupted by sonication on ice. The protein content of samples was measured by a modified amido black method [17]. Total cell lysates were mixed with SDS-PAGE sample buffer and boiled for 10 min at 100 °C. The samples were subjected to SDS-PAGE according to Laemmli [20] (8% gels were loaded with max. 20 μg protein per lane) and transferred to nitrocellulose membranes (Bio-Rad, Wien, Austria). Membranes were then blocked with 5% dry milk in PBS and probed with the appropriate antibody. All antibodies against PKC isozymes were developed in rabbits and were shown to react with human PKC isoforms; anti-PKCα, -η, and -ζ were from Sigma; anti-PKCγ, -δ and -ε from Gibco (Gaithersburg, Md.); anti-PKCβI and -βII from Biomol (Plymouth Meeting, USA); anti-PKCθ from Santa Cruz (Santa Cruz, Calif.). Monoclonal mouse antibody against the intermediate filament protein desmin (Dako, Glostrup, Denmark) was used to follow muscle differentiation. Peroxidase-conjugated goat anti-rabbit IgG (Bio-Rad) was used as secondary antibody in the cases of PKC isozymes and anti-mouse Vectastain ABC Kit (Vector, Burlingame, Calif.) in the case of desmin. Immunoreactive bands were finally visualized by ECL Western blotting detection kit (Amersham, Little Chalfont, UK).

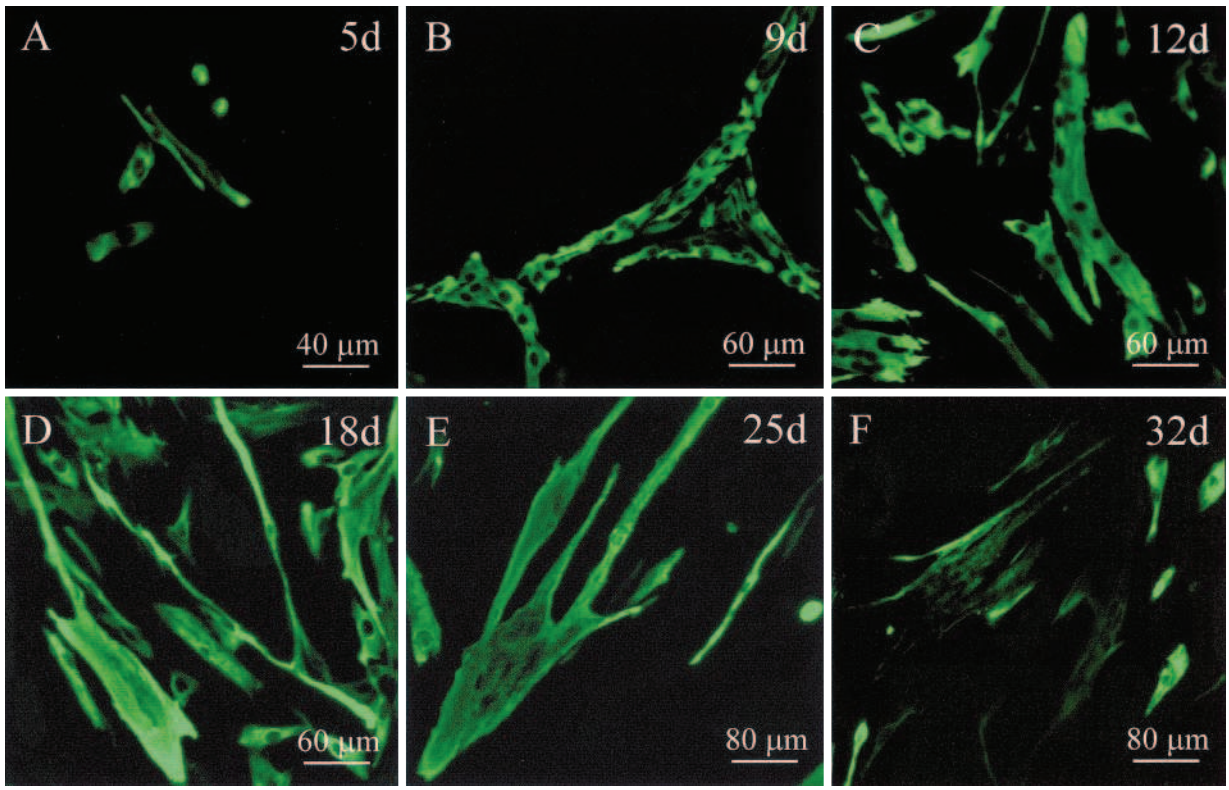

Fig. 1 A–F Immunohistochemical analysis of the expression of desmin in human skeletal muscle cells. Cells of different ages (*d* represents days) were fixed in acetone, solubilized by exposure to Triton X-100, and incubated with mouse anti-desmin antibody as described under Materials and methods. Immunofluorescence staining was employed using FITC-conjugated anti-mouse IgG. The figure is a representative of five individual experiments with similar results

Immunofluorescence analysis

Cultured myoblasts and myotubes were washed with PBS, fixed in acetone for 5 min at 4 °C, air dried, and blocked at room temperature for 30 min in blocking solution containing 0.6% Triton X-100 and 1% BSA. Cells were incubated with the appropriate rabbit anti-PKC antibody for 2 h (diluted 1 : 50 in blocking solution), and then with mouse anti-desmin antibody (1 : 100 in blocking solution) for 1 h. The samples were then incubated for 1 h with a biotin-conjugated goat anti-rabbit IgG (diluted 1 : 300 in PBS, Vector), and finally co-incubated with fluorescein isothiocyanate (FITC)-conjugated sheep anti-mouse IgG (diluted 1 : 50 in PBS, Amersham) and streptavidin-conjugated Texas Red (diluted 1 : 50 in PBS, Amersham) for an additional hour. The resulting green fluorescence of desmin and red fluorescence of PKC isozymes were studied by an Opton fluorescence microscope (Oberkochen, Germany).

Results

Desmin is an excellent marker of human skeletal muscle differentiation in vitro

Among the several markers regarded as good indicators of regeneration in skeletal muscle cells of other species [2, 8, 33], we investigated the expression of the 53-kDa muscle specific intermediate filament protein desmin during differentiation. Using immunohistochemistry we found that the expression level of desmin changed parallel with the time in culture (Fig. 1). The expression of desmin was negligible in the very young (1- to 2-day old) mononuclear satellite cells (data not shown). The intensity of staining then continuously and markedly increased during the proliferation phase (days 4–8; Fig. 1 A) and during the fusion of myoblasts (days 8–12; Fig. 1 B, C), and reached its maximum level between 12 and 20 days when young, immature myotubes appeared at their highest density (Fig. 1 C, D). Between days 24 and 29, the expression of desmin decreased slightly in the matured, multinuclear myotubes (Fig. 1 E). Finally, after 28–30 days (Fig. 1 F), the expression of desmin gradually decreased in the large myotubes (the staining remained significant only close to the sarcolemma), possibly due to the markedly increased

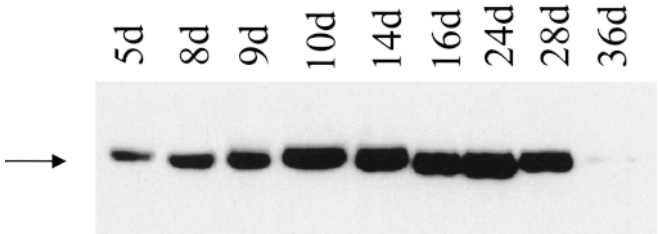

Fig. 2 Western blot analysis of the expression of desmin in human skeletal muscle cells. Cells of different ages (*d* represents days) were harvested, similar amounts of proteins were subjected to SDS-PAGE, and Western immunoblotting was performed using mouse anti-desmin antibody as described under Materials and methods. The figure is a representative of three individual experiments with similar results

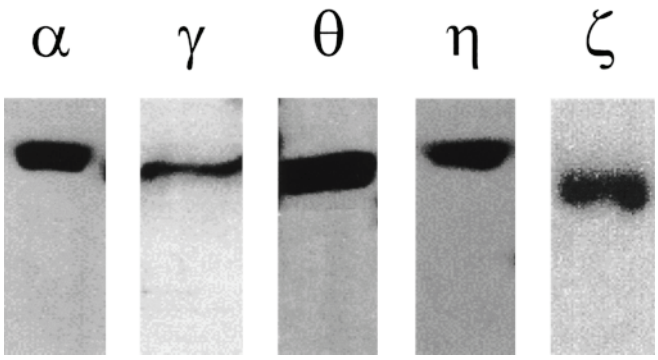

Fig. 3 Western blot analysis of the expression of different PKC isozymes in 15-day-old human skeletal muscle cells. Cells were harvested, similar amounts of proteins were subjected to SDS-PAGE, and Western immunoblotting was performed using different rabbit anti-PKC antibodies as described under Materials and methods. The figure illustrates one representative experiment of three sets of individual experiments for each PKC isoform

cell number and to the development of cell-to-cell contacts.

In parallel with the immunohistochemical analysis, we also examined the expression of desmin by Western blotting. By loading the same amounts of protein into each well (thus normalizing the intensity of the immunoreactive bands to cell protein), we found similar changes in the expression pattern of desmin (Fig. 2). Desmin production gradually increased during the phases of proliferation and myotube formation (up to days 10–12), and saturated with maximal intensity by days 12–18 of differentiation. Similar to the immunofluorescence data, a marked decrease of desmin production was observed after days 26–28. These data suggest that desmin is indeed an excellent marker of human skeletal muscle differentiation in vitro, at least up to day 25 of culture. For this reason, cell cultures older than 25 days were not used in further experiments.

Expressions of certain PKC isozymes (PKCγ, -η, and -θ) alter with differentiation

Using immunohistochemical analysis, we identified five PKC isozymes in cultured muscle cells (PKCα, -γ, -η, -ζ, and -θ) (Fig. 4–Fig. 8; see below). This observation was also confirmed by Western blot analysis of 15-day-old cultures (Fig. 3). On the other hand, we failed to detect any expressions of PKCβI, -βII, -δ and -ε by either method, although the presence of these isoforms was described in skeletal muscle cells of other species [9, 14, 37].

To achieve more information about the possible roles of PKC isozymes in differentiation, we investigated the co-expression of the desmin and the existing PKC isozymes using double immunohistochemical labeling (due to the limited protein content of the young cultures, we were unable to perform Western blot analysis). In young mononuclear satellite cells, PKCγ showed a nuclear-perinuclear patched staining which pattern did not alter during myotube formation and fusion (up to days 10–12; Fig. 4 A–C). With the appearance of immature, multinuclear myotubes, besides the nuclear-perinuclear patched stain-

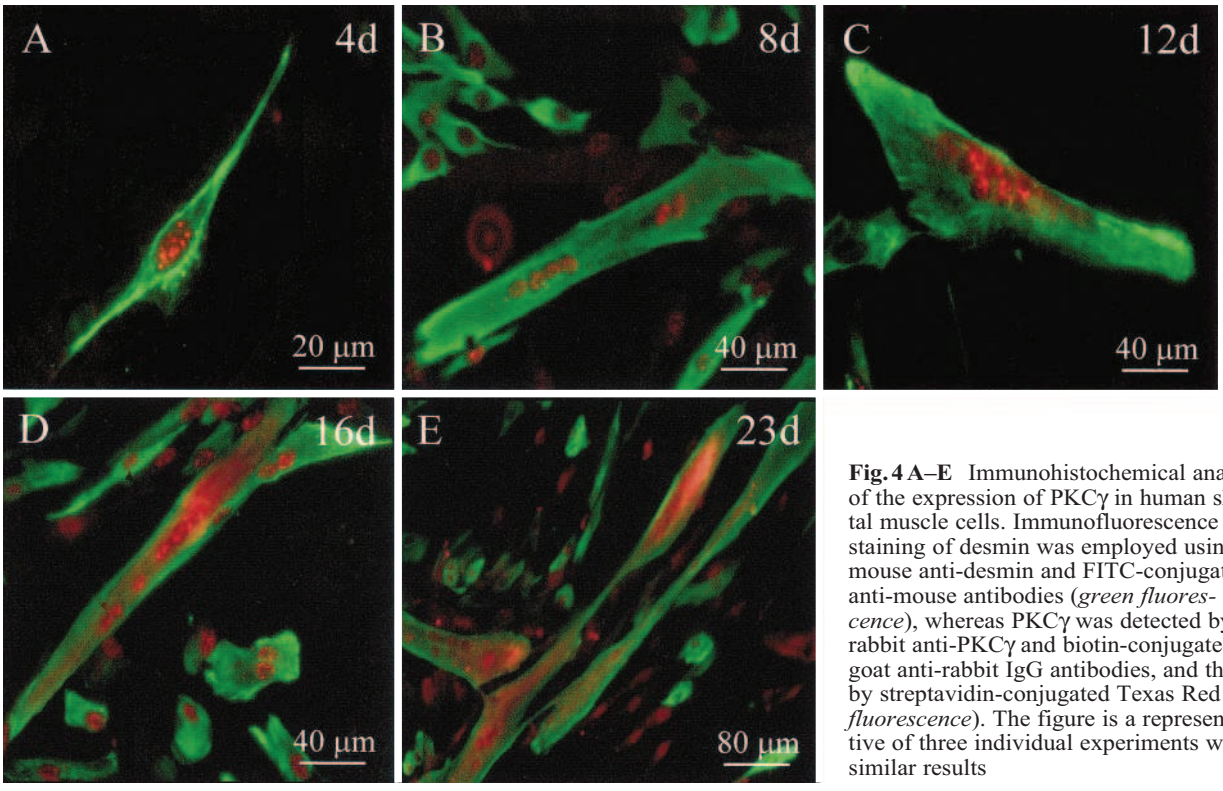

Fig. 4 A–E Immunohistochemical analysis of the expression of PKCγ in human skeletal muscle cells. Immunofluorescence staining of desmin was employed using mouse anti-desmin and FITC-conjugated anti-mouse antibodies (*green fluorescence*), whereas PKCγ was detected by rabbit anti-PKCγ and biotin-conjugated goat anti-rabbit IgG antibodies, and then by streptavidin-conjugated Texas Red (*red fluorescence*). The figure is a representative of three individual experiments with similar results

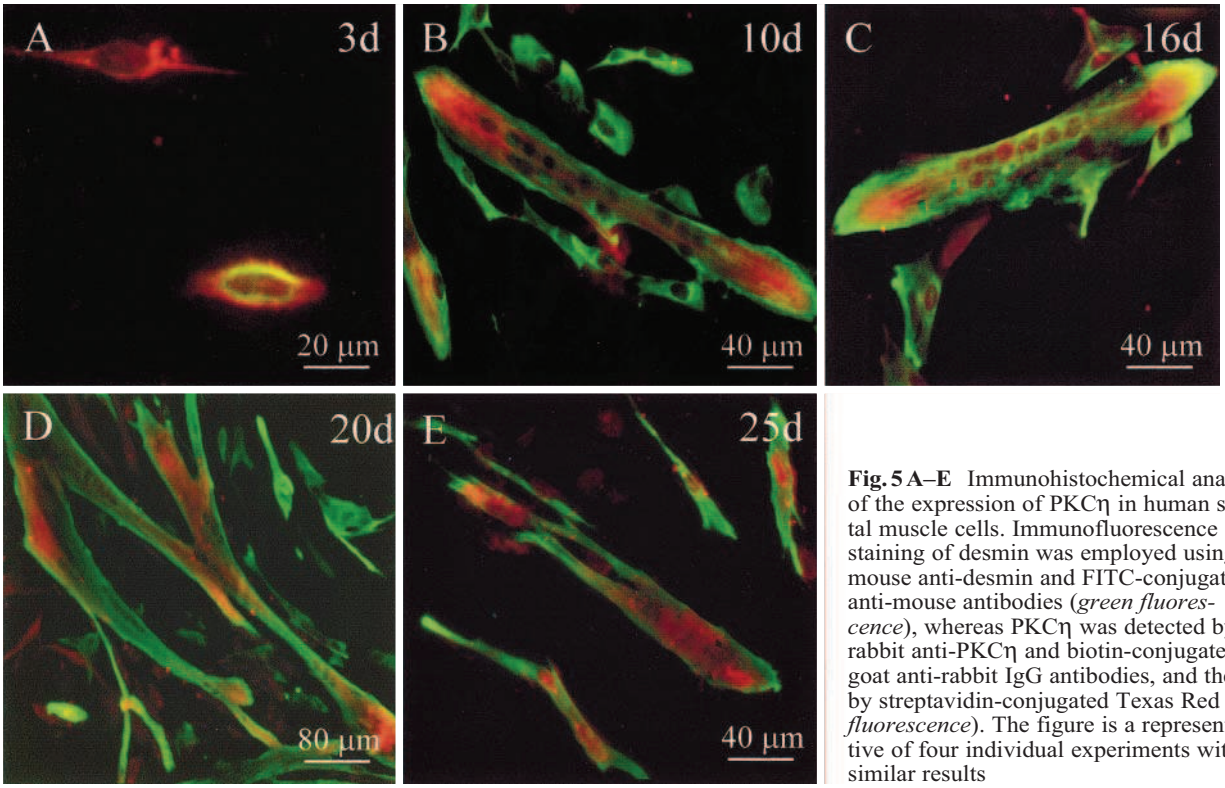

Fig. 5 A–E Immunohistochemical analysis of the expression of PKCη in human skeletal muscle cells. Immunofluorescence staining of desmin was employed using mouse anti-desmin and FITC-conjugated anti-mouse antibodies (*green fluorescence*), whereas PKCη was detected by rabbit anti-PKCη and biotin-conjugated goat anti-rabbit IgG antibodies, and then by streptavidin-conjugated Texas Red (*red fluorescence*). The figure is a representative of four individual experiments with similar results

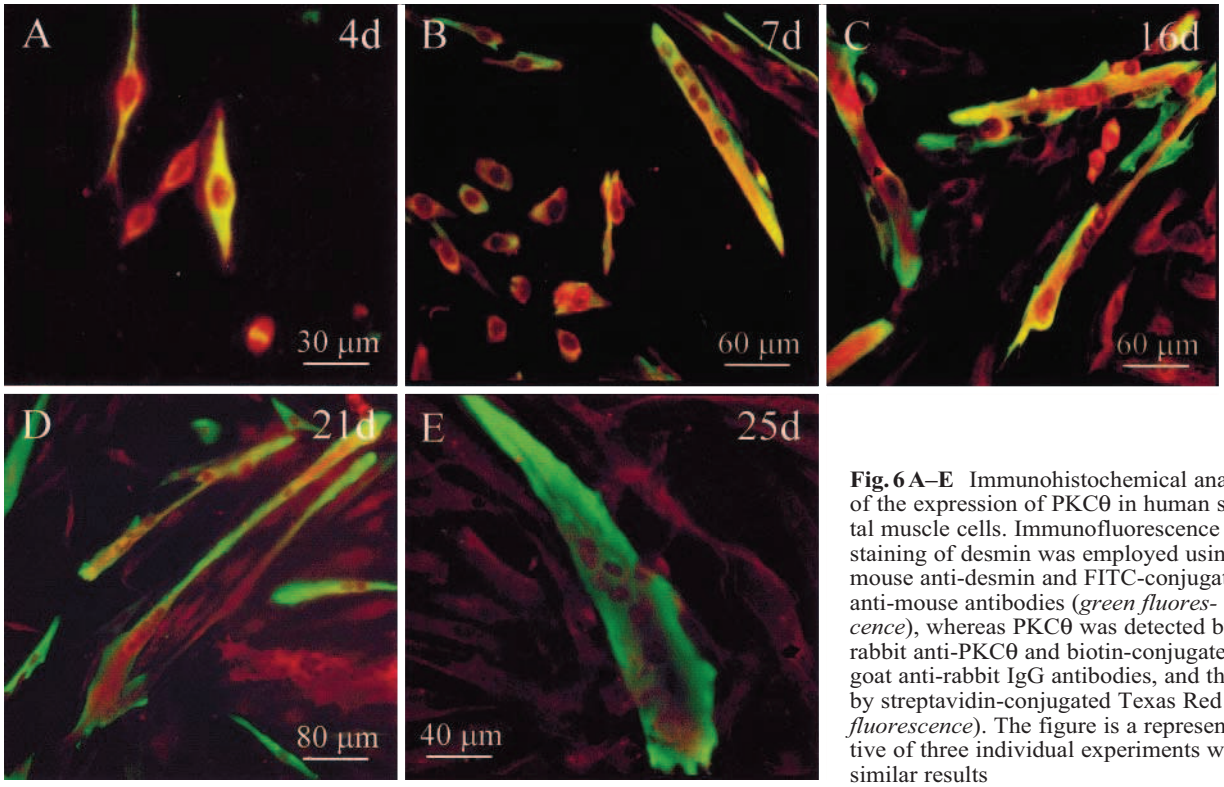

Fig. 6 A–E Immunohistochemical analysis of the expression of PKCθ in human skeletal muscle cells. Immunofluorescence staining of desmin was employed using mouse anti-desmin and FITC-conjugated anti-mouse antibodies (*green fluorescence*), whereas PKCθ was detected by rabbit anti-PKCθ and biotin-conjugated goat anti-rabbit IgG antibodies, and then by streptavidin-conjugated Texas Red (*red fluorescence*). The figure is a representative of three individual experiments with similar results

ing, faint cytoplasmic expression appeared (Fig. 4 D). In the older cultures (Fig. 4 E), the intensity of cytoplasmic staining markedly and consistently increased, particularly at the end of the myotubes where fusion activity was the most intensive. Furthermore, parallel with this increased cytoplasmic expression, the nuclear-perinuclear patched staining of PKCγ faded, representing an intracellular translocation of the enzyme.

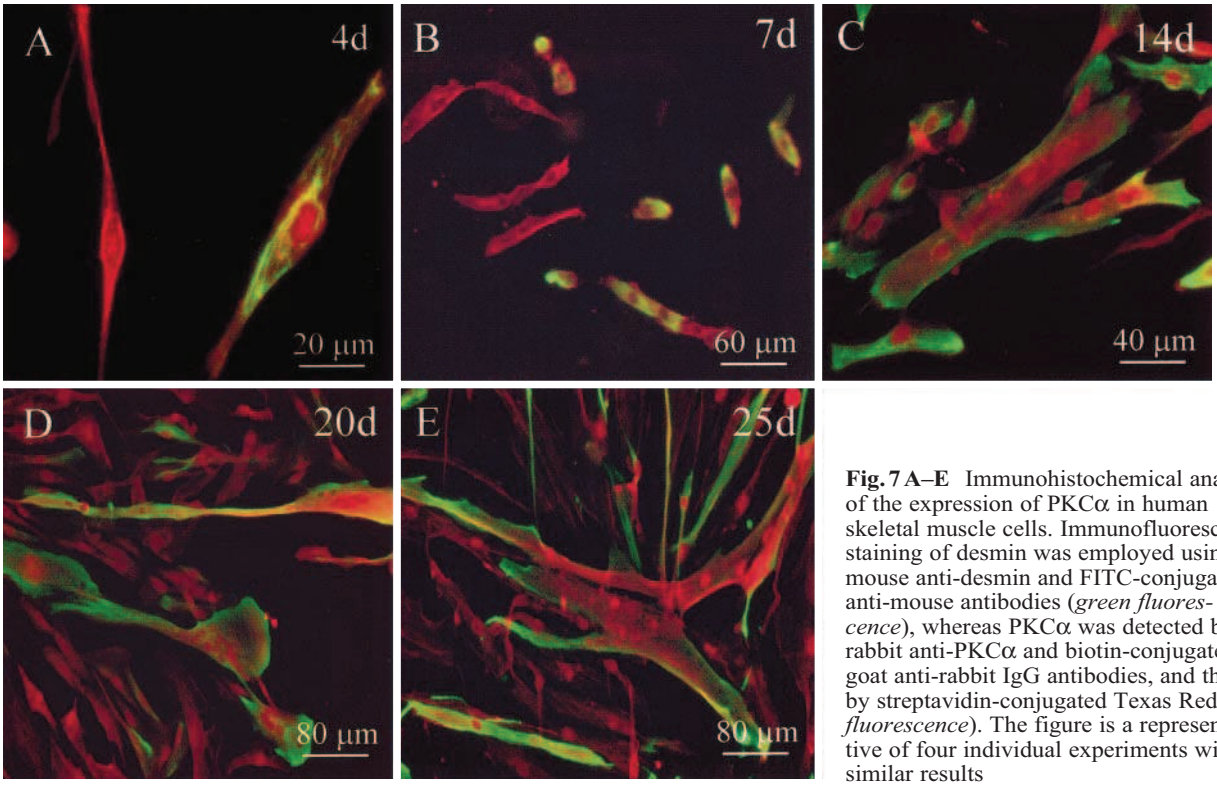

Fig. 7 A–E Immunohistochemical analysis of the expression of PKCα in human skeletal muscle cells. Immunofluorescence staining of desmin was employed using mouse anti-desmin and FITC-conjugated anti-mouse antibodies (*green fluorescence*), whereas PKCα was detected by rabbit anti-PKCα and biotin-conjugated goat anti-rabbit IgG antibodies, and then by streptavidin-conjugated Texas Red (*red fluorescence*). The figure is a representative of four individual experiments with similar results

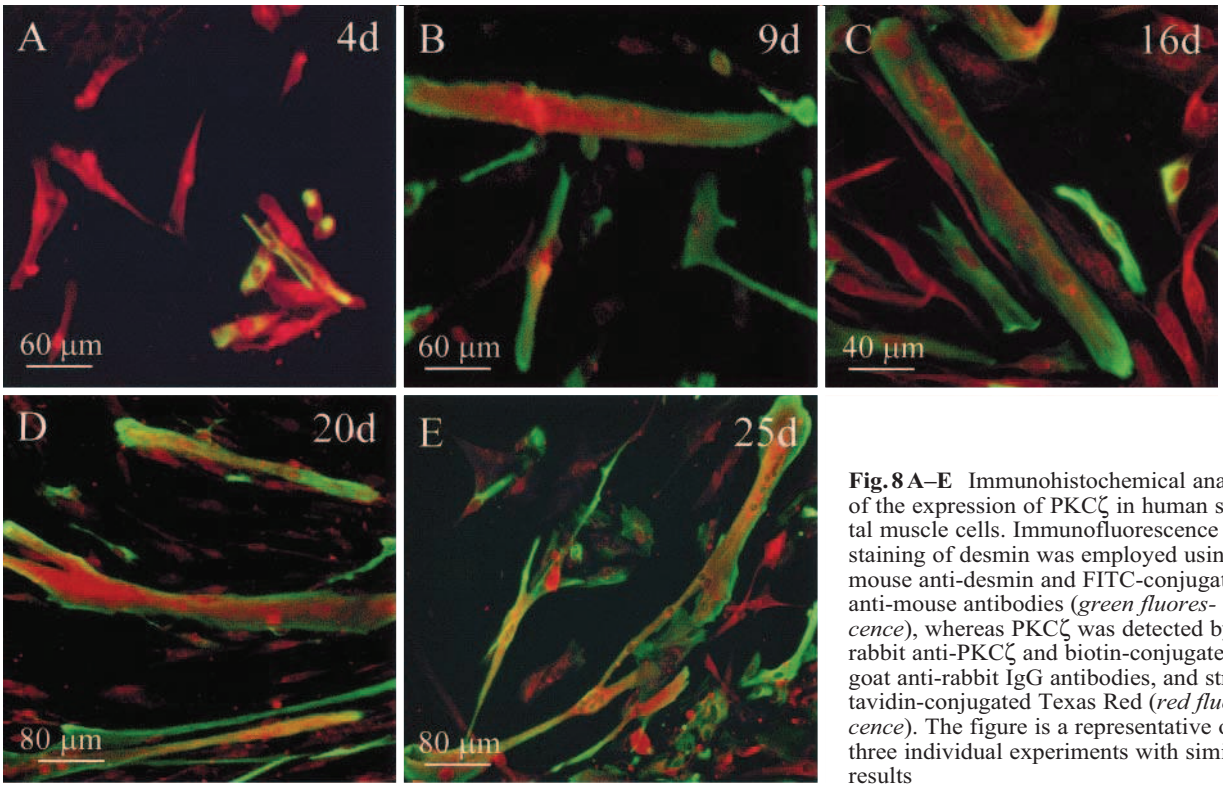

Fig. 8 A–E Immunohistochemical analysis of the expression of PKCζ in human skeletal muscle cells. Immunofluorescence staining of desmin was employed using mouse anti-desmin and FITC-conjugated anti-mouse antibodies (*green fluorescence*), whereas PKCζ was detected by rabbit anti-PKCζ and biotin-conjugated goat anti-rabbit IgG antibodies, and streptavidin-conjugated Texas Red (*red fluorescence*). The figure is a representative of three individual experiments with similar results

The changes in the expression levels of PKCη during muscle differentiation showed a tendency similar to that found in the case of PKCγ, although with the lack of intracellular translocation. Faint cytoplasmic staining appeared in 2- to 4-day-old mononuclear satellite cells (Fig. 5 A), which did not alter significantly in the proliferating phase (up to days 10–12; Fig. 5 B). The intensity of the expression, on the other hand, markedly increased with the appearance of the immature multinuclear myotubes, and then remained constantly high in the later phases of

differentiation (Fig. 5 C–E). Similar to that for PKCγ, maximal expression of PKCη was located in the cytoplasm of the fusion end of myotubes.

In contrast, the expression of PKCθ decreased with differentiation. A significant, intensive cytoplasmic expression was observed in young, mononuclear satellite cells (Fig. 6 A), which remained high during and after fusion (up to day 20); Fig. 6 B, C). However, after day 20–22, when the maturation of myotubes was accelerated, PKCθ staining decreased significantly (Fig. 6 D, E). As for PKCη, there was no measurable intracellular translocation of PKCθ during muscle differentiation.

Expressions of other PKC isozymes (PKCα and -ζ) do not alter with differentiation

The expression of PKCα reached significant levels in the cytoplasm of the young cells where only faint desmin spots represented initial proliferation and differentiation (Fig. 7 A, B). The relative expression level of this isozyme remained high during myotube formation and fusion, and did not alter with the appearance of the immature multinuclear myotubes (Fig. 7 C–E).

PKCζ showed a similar staining pattern; relatively high expression levels were detected in the cytoplasm of the young satellite cells even before desmin appeared (Fig. 8 A, B) and remained practically unchanged during the whole period of differentiation (Fig. 8 C, D). It was also of importance that neither of these isozymes showed intracellular translocation.

Discussion

In this study we have shown that human differentiating skeletal muscle cells possess characteristic patterns of PKC isozymes (α, γ, η, ζ, and θ). We have also demonstrated that expression levels of certain isoforms (PKCγ, -η and -θ) changed in parallel with the appearance of the differentiation marker desmin, whereas expression levels of other isozymes (PKCα and -ζ) remained relatively constant. These data suggest differential roles of PKC isozymes in human skeletal muscle differentiation in vitro.

In our experiments, during the process of differentiation, conventional calcium-dependent PKC isozymes (PKCα and -γ), novel calcium-independent PKC isozymes (PKCη and -θ), and the atypical (calcium- and phorbol-ester independent) PKCζ are expressed by cultured human skeletal muscle cells. This characteristic isoform pattern differed significantly from those described for rat or mouse skeletal muscle cells (PKCα, -δ, -ζ, -ε, -θ in rat skeletal muscles [9, 13, 14], but PKCα, -βI, -βII, -γ, -η, -ζ in mouse embryonic myoblasts [37]). Thus, our data provide further evidence that PKC isozymes of different groups exist within the same cell, and that the expression of the isozymes within the same tissue type possesses strong species dependence [19].

It is intriguing that differentiating human skeletal muscles cells lack PKCδ and -ε isozymes, which have been described as ubiquitously expressed in most tissue types [10, 27]. These PKC isozymes were generally regarded to be the major regulators of cellular proliferation and differentiation in several cell types (fibroblasts, glia cells, smooth muscles) [10, 27]; thus, their absence in cultured human skeletal muscle cells, which show intensive proliferation and differentiation is of great importance. Similarly, skeletal muscles from other mammalian species do not generally express these isozymes (except for adult rat muscles in which both PKCδ and -ε are expressed [9, 14]); hence, it seems that proliferation and differentiation are affected by other PKC isozymes in skeletal muscles.

Cultured human skeletal muscle cells, on the other hand, express PKCγ, an isozyme that was previously detected mainly in the nervous system [27, 28]. The search for this isozyme in muscle cells of different species indicates that it seems to be specific for human skeletal muscle since otherwise only mouse embryonic myoblasts were shown to express PKCγ [37]. Our skeletal muscle cultures did not contain neuronal elements; thus, the presence of PKCγ is not due to some "neuronal contamination" of the culture medium. Not only did the expression of PKCγ increase in parallel with time in culture (thus with differentiation), but there was a marked alteration in its cellular localization represented by perinuclear to cytoplasmic translocation. These data, which are in good agreement with previously published observations describing a decreased nuclear localization of PKCα but not of PKCδ during liver regeneration [1], and the differential modification of subcellular localizations of different PKC isoforms by vitamin D_3 in avian muscle cells [22] suggest that PKCγ may be a key factor in controlling differentiation.

One of the most important findings of our study is that different PKC isozymes possessed different expression patterns during different phases of differentiation. In the early, proliferative phase (before the fusion of satellite cells) the expressions of PKCα, -θ and -ζ is dominant, whereas the appearance of young, immature myotubes is accompanied by the additional elevation in the expression levels of PKCγ and -η (especially at the fusion ends of the myotubes). It seems, therefore, that in this intermediate phase of differentiation represented by the intensive fusion of myoblasts, all of the detected isozymes reached their maximal levels of expression, reflecting the possible roles of these isozymes in muscle differentiation. Finally, as differentiation proceeded, the expression of PKCθ decreased, whereas there were no measurable changes in the levels of other isozymes. Similar changes in the expression patterns of PKC isoforms were described during cellular proliferation and differentiation in C6 glioma cells [3] and during liver regeneration [1], which may suggest the pivotal roles of most of the existing PKC isozymes in the processes.

The changes in the expression patterns of PKC isozymes showed no correlation with the PKC group they belonged to. Patterns of early appearance and relatively

constant expression levels were shown by both the conventional PKCα and the atypical PKCζ. Furthermore, the expression of the conventional PKCγ and the novel PKCη were similar since they followed closely the progress of differentiation, whereas the expression of the novel PKCθ decreased with the time in culture. Hence, it seems that, besides calcium dependence, other factors may also regulate the activities of PKC isoforms during muscle differentiation.

Our data suggest that those isozymes (PKCγ, -η and -θ) whose expression levels changed during culturing may closely control muscular proliferation and differentiation, whereas isozymes with relatively constant expression levels (PKCα and -ζ) may provide continuous "background activity" for these processes. However, the functional roles of the different PKC isozymes in the process of in vitro proliferation and differentiation are yet to be understood.

Acknowledgement The authors are indebted to Ms. Ibolya Varga for helpful technical assistance, and to Profs. Róza Ádány and Margit Balázs for providing the technical background for the immunofluorescence analysis. This work was supported by Hungarian research grants: OTKA T16957, OTKA O23040, ETT 095/1996, FKFP 1289/1997, ETT 31/1998.

References

1. Allesanko A, Kahn WA, Westel WC, Hannun YZ (1992) Selective changes in protein kinase C isoenzymes in rat liver nuclei during liver regeneration. Biochem Biophys Res Commun 182 : 1333–1339
2. Bornemann A, Schmalbruch H (1992) Desmin and vimentin in regenerating muscles. Muscle Nerve 15 : 14–20
3. Brodie C, Kuperstein I, Ács P, Blumberg PM (1998) Differential role of specific PKC isoforms in the proliferation of glial cells and the expression of the astrocytic markers GFAP and glutamine synthetase. Mol Brain Res 56 : 108–117
4. Cacace AM, Guadagno SN, Krauss RS, Fabbro D, Weinstein IB (1993) The epsilon isoform of protein kinase C is an oncogene when overexpressed in rat fibroblasts. Oncogene 8 : 2095–2104
5. Cascade Lim RW, Zhu CY, Stringer B (1995) Differential regulation of primary response gene expression in skeletal muscle cells through multiple signal transduction pathways. Biochim Biophys Acta 1266 : 91–100
6. Chambers RL, McDermott JC (1996) Molecular basis of skeletal muscle regeneration. Can J Appl Physiol 21 : 155–184
7. Cossu G, Zani B, Colette M, Bouche M, Pacifici M, Molinaro M (1980) In vitro differentiation of satellite cells isolated from normal and dystrophic mammalian muscles. A comparison with embryonic myogenic cells. Cell Differ 9 : 357–368
8. Gard DL, Lazarides E (1980) The synthesis and distribution of desmin and vimentin during myogenesis in vitro. Cell 19 : 263–275
9. Given MB, Jie O, Zhao X, Giles TD, Greenberg SS (1998) Protein kinase C isozymes in skeletal muscles during the early stage of genetic and streptozotocin diabetes. Prog Soc Exp Biol Med 218 : 382–389
10. Goodnight J, Mischak H, Mushinski JF (1994) Selective involvement of protein kinase C isozymes in differentiation and neoplastic transformation. Adv Cancer Res 64 : 159–209
11. Grounds MD (1991) Towards understanding skeletal muscle regeneration. Pathol Res Pract 187 : 1–22
12. Henriksen EJ, Rodnick KJ, Holloszy JO (1989) Activation of glucose transport in skeletal muscle by phospholipase C and phorbol ester. Evaluation of the regulatory roles of protein kinase C and calcium. J Biol Chem 264 : 21 536–21 543
13. Hilgenberg L, Yearwood S, Milstein S, Miles K (1996) Neural influence on protein kinase C isoform expression in skeletal muscle. J Neurosci 16 : 4994–5003
14. Hong D, Huan J, Ou B, Yeh J, Saido TC, Cheeke PR, Forsberg NE (1995) Protein kinase C isoforms in muscle cells and their regulation by phorbol ester and calpain. Biochim Biophys Acta 1267 : 45–54
15. Husmann I, Soulet L, Gautron J, Martelly I, Barritault D (1996) Growth factors in skeletal muscle regeneration. Cytokine Growth Factor Rev 7 : 249–258
16. Jaken S (1996) Protein kinase isozymes and substrates. Curr Opin Cell Biol 8 : 18–173
17. Kaplan RS, Pedersen PL (1985) Determination of microgram quantities of protein in the presence of milligram levels of lipid with Amido Black 10B. Anal Biochem 150 : 97–104
18. Kramer IM (1996) Signal transduction through tyrosine protein kinases. In: Foreman JC, Johansen T (eds) Textbook of receptor pharmacology. CRC Press, New York, pp 255–274
19. Kuo JF (1994) Protein kinase C. Oxford University Press, New York
20. Laemmli UK (1970) Cleavage of structural proteins during the assembly of the head of bacteriophage T4. Nature 227 : 680–685
21. Liu LN, Dias P, Hougton PJ (1998) Modulation of Trh115 in MyoD positively regulates function in murine fibroblasts and human rhabdomyosarcoma cells. Cell Growth Differ 9 : 699–711
22. Marinissen MJ, Capiati D, Boland AR de (1998) 1,25$(OH)_2$-vitamin D_3 affects the subcellular distribution of protein kinase C isoenzymes in muscle cells. Cell Signal 10 : 91–100
23. Massheimer V, Boland AR de (1992) Modulation of 1,25-dihydroxivitamin D_3-dependent Ca^{2+} uptake in skeletal muscle by protein kinase C. Biochem J 281 : 349–352
24. Mischak H, Goodnight JA, Kolch W, Martiny-Baron GM, Schaechtle C, Kazanietz MG, Blumberg PM, Pierce JH, Mushinski JF (1993) Overexpression of protein kinase C-δ and -ε in NIH 3T3 cells induces opposite effects on growth, morphology, anchorage dependence, and tumorigenicity. J Biol Chem 268 : 6090–6096
25. Murray NR, Baumgardner GP, Burns DJ, Fields AP (1993) Protein kinase C isotypes in human erythroleukemia (K562) cell proliferation and differentiation. Evidence that beta II protein kinase C is required for proliferation. J Biol Chem 268 : 15847–15853
26. Nishikawa M, Hidaka H (1994) Protein kinase C in smooth muscle. In: Kuo JF (ed) Protein kinase C. Oxford University Press, New York, pp 236–248
27. Nishizuka Y (1988) The molecular heterogeneity of protein kinase C and its implication for cellular regulation. Nature 334 : 661–665
28. Nishizuka Y (1992) Intracellular signaling by hydrolysis of phospholipids and activation of protein kinase C. Science 258 : 607–614
29. Ohno S, Akita Y, Hata A, Osada S, Kubo K, Kohno Y, Akimoto K, Mizuno K, Saido T, Kuroki T, Suzuki K (1991) Structural and functional diversities of a family of signal transducing protein kinases, protein kinase C family; two distinct classes of PKC, conventional cPKC and novel nPKC. Adv Enzyme Regul 31 : 287–303
30. Pucéat M, Brown JH (1994) Protein kinase C in the heart. In: Kuo JF (ed) Protein kinase C. Oxford University Press, New York, pp 249–268
31. Schultz E, McCormick KM (1994) Skeletal muscle satellite cells. Rev Physiol Biochem Pharmacol 123 : 213–257
32. Sipos I, Harasztosi CS, Melzer W (1997) L-type calcium current activation in cultured human myotubes. J Muscle Res Cell Motil 18 : 353–367

33. Ven PFM van der, Schaart G, Jap PHK, Sengers RCA, Stadhouders AM, Ramaekers FCS (1992) Differentiation of human skeletal muscle cells in culture: maturation as indicated by titin and desmin striation. Cell Tissue Res 270 : 189–198
34. Wang S, Desai D, Wright G, Niles RM, Wright GL (1997) Effects of protein kinase Cα overexpression on A7r5 smooth muscle cell proliferation and differentiation. Exp Cell Res 236 : 117–126
35. Weintraub H (1993) The MyoD family and myogenesis: redundancy, networks, and thresholds. Cell 75 : 1241–1244
36. Yamamoto M, Acevedo-Duncan M, Chalfant CE, Patel NA, Watson JE, Cooper DR (1998) The roles of protein kinase C βI and βII in vascular smooth muscle cell proliferation. Exp Cell Res 240 : 349–358
37. Zapelli F, Willems D, Osada S, Ohno S, Wetsel WC, Molinaro M, Cossu G, Bouché M (1996) The inhibition of differentiation caused by TGFβ in fetal myoblasts is dependent upon selective expression of PKCθ: a possible molecular basis for myoblast diversification during limb histogenesis. Dev Biol 180 : 156–164
38. Zhu YY, Schwartz RJ, Crow MT (1991) Phorbol esters selectively downregulate contractile protein gene expression in terminally differentiated myotubes through transcriptional repression and message destabilization. J Cell Biol 115 : 745–754

XII.

Acta Neuropathol (2001) 102 : 55–62
DOI 10.1007/s004010000347

REGULAR PAPER

Judit Boczán · Tamás Bíró · Gabriella Czifra · József Lázár · Helga Papp
Helga Bárdos · Róza Ádány · Ferenc Mechler · László Kovács

Phorbol ester treatment inhibits proliferation and differentiation of cultured human skeletal muscle satellite cells by differentially acting on protein kinase C isoforms

Received: 4 July 2000 / Revised: 2 November 2000 / Accepted: 14 November 2000 / Published online: 21 June 2001

Abstract We have previously shown that cultured human skeletal muscle cells express five protein kinase C (PKC) isoforms (PKCα, -γ, -η, -θ, and -ζ) and that expression levels of various PKC isozymes differentially change during differentiation. In this study we investigated the effects of the PKC activator phorbol 12-myristate 13-acetate (PMA) on differentiation and on PKC isozymes of human skeletal muscle satellite cells. PMA inhibited the growth and fusion of cultured human myoblasts in a dose-dependent manner. In addition, prolonged treatment of cells with PMA suppressed the expression of the myogenic differentiation marker desmin showing similar dose-response characteristics. Furthermore, PMA also induced the intracellular translocation of PKCγ, -η, and -θ, whereas cellular localization of PKCα and -ζ were not altered. These changes in subcellular localization patterns were of great importance since only those PKC isoforms were translocated that possessed alterations in their expression levels during differentiation. Our findings, therefore, suggest that the PMA-induced inhibition of differentiation of human skeletal muscle cells is mediated by certain PKC isoforms. Moreover, these data strongly argue for differential and isozyme-specific roles of various PKC isoforms in these processes.

J. Boczán · T. Bíró (✉) · G. Czifra · J. Lázár · H. Papp · L. Kovács
Department of Physiology and Cell Physiology Research Group of the Hungarian Academy of Sciences,
University of Debrecen, Medical and Health Science Center, Medical School, Nagyerdei krt. 98. PO Box 22,
4012 Debrecen, Hungary
e-mail: biro@phys.dote.hu,
Tel.: +36-52-416634, Fax: +36-52-432289

J. Boczán · F. Mechler
Department of Neurology, University of Debrecen, Medical and Health Science Center, Medical School, Debrecen, Hungary

H. Bárdos · R. Ádány
Department of Preventive Medicine,
University of Debrecen, Medical and Health Science Center, Medical School, Debrecen, Hungary

Keywords Skeletal muscle · Human · Differentiation · Phorbol 12-myristate 13-acetate · Protein kinase C isozymes

Introduction

The various processes of in vivo human skeletal muscle regeneration (seen, for example, in post-traumatic or dystrophic muscle reconstitution [7, 13]) can be well modeled in vitro by culturing skeletal muscle cells [1, 8, 32]. In this model system, skeletal muscle satellite cells isolated enzymatically and mechanically from muscle biopsy specimens proliferate and fuse into multinuclear myotubes, which eventually results in the development of matured, well-differentiated striated myofibers [1, 8, 32].

The proliferation and differentiation of satellite cells are under the control of several growth factors [e.g., insulin-like growth factor-1, prostaglandins, transforming growth factor-β (TGF-β)] [13, 16] and myogenic transcription factors (e.g., MyoD, MRF4, myf5, myogenin) [7, 35]. The marked diversity in the intracellular signal transduction pathways influenced by these agents [16, 19], and, moreover, results claiming that the phosphorylation state of the transcription factors might affect muscle differentiation [22] suggest a complex regulation of the muscle cell proliferation and differentiation by different kinase cascades.

Protein kinase C (PKC) comprises a family of serine/threonine kinases that play pivotal roles in the regulation cellular proliferation and differentiation of numerous cell types [29, 30, 31]. To date, at least 11 different PKC isozymes have been identified [17, 29], which can be classified into the groups of the calcium- and phorbol ester-dependent "conventional" (PKCα, -βI, -βII, and -γ; cPKCs), the calcium-independent "novel" (PKCδ, -ε, -η, and -θ; nPKCs), and the calcium- and phorbol ester-independent "atypical" (PKCζ, -λ/ι, and -μ; aPKCs) isoforms. These isoforms possess a characteristic expression pattern in a given cell type, and isozyme-specifically regulate various cellular processes including proliferation and differentia-

tion [4, 31]. It was also postulated that not only may some PKC isoforms be active, whereas others are not, for a given response, but different PKC isozymes may often have antagonistic effects on the same cellular event. PKCα was, for example, suggested to mediate phorbol 12-myristate 13-acetate (PMA)-induced cytostasis in K-562 erythroleukaemia cells, whereas PKCβII was involved in inducing proliferation [27]. Furthermore, PKCδ arrested cell growth of NIH 3T3 fibroblasts, whereas PKCε had a stimulating effect on the same phenomenon [5, 26], suggesting pivotal and differential regulatory roles of specific PKC isoforms in these processes.

The regulatory roles of PKC have also been described in skeletal muscles. It has been shown that the modification of PKC activity by phorbol esters, such as PMA, stimulated insulin-dependent glucose transport [14, 33] and vitamin D-induced calcium uptake [24], and mimicked the effects of prostanoids in promoting myoblast fusion [9]. Treatments of skeletal muscle cells by vitamin D_3 modified the subcellular localization of PKC [23], also implicating functional role of PKC in mediating the effect of agents modifying skeletal muscle cellular functions. It has also been shown that phorbol esters might down-regulate the transcription of gene sequences coding contractile proteins in terminally differentiated myotubes [37], and, furthermore, that they abolish the up-regulation of myf5 gene expression (a muscle regulatory factor that is involved in the establishment of skeletal muscle precursor cells) by dexamethasone and anisomycin [28].

However, the role of PKC in cellular proliferation and differentiation of skeletal muscle cells is rather controversial and exerts marked species dependence. In primary cultures of rat satellite cells, treatment with highly specific PKC inhibitors or with PMA did not significantly alter myogenic differentiation [21]. In contrast, in cultured chick muscle cells, PMA modified the expressions of differentiation markers, selectively and reversibly inhibited the ongoing differentiation program [25], and blocked DNA synthesis [6]. Similar to these findings, in normal human skeletal muscle cells, PMA inhibited myogenesis but only in already fused myotubes [10, 11].

We have recently shown that cultured human skeletal muscle cells express five PKC isoforms (PKCα, -γ, -η, -θ, and -ζ) and that expression levels of different PKC isozymes differentially change during cellular proliferation and differentiation [1]. In the present study we examined the effect of PMA on human skeletal muscle proliferation and differentiation in vitro and, since there is no data available about the roles of different PKC isoforms in these processes in human skeletal muscle cells, the participation of existing PKC isoforms in the PMA-induced cellular events. We show here that prolonged PMA treatment led to the suppression of cellular proliferation and differentiation by differentially acting on certain PKC isoforms. PMA translocated PKCγ, -η and -θ to other cellular compartments, whereas cellular localization of PKCα and -ζ were not altered. These data strongly argue for different functional roles of PKC isoforms in the proliferation and differentiation of cultured human skeletal muscle cells.

Materials and methods

Antibodies

All antibodies against PKC isozymes were developed in rabbits and were shown to react with human PKC isoforms [1]; anti-PKCα, -η, and -ζ were from Sigma (St. Louis, Mo.); anti-PKCγ from Gibco (Gaithersburg, Md.); anti-PKCθ from Santa Cruz (Santa Cruz, Calif.). Monoclonal mouse antibody against the intermediate filament protein desmin (DAKO, Glostrup, Denmark) was used to follow muscle differentiation.

Cell culture and separation

Satellite cells were obtained from muscle tissue waste of orthopedic surgery. The use of this material was approved by the Ethical Committee of the University Medical School of Debrecen, Hungary. The technique of growing myotubes followed the method of Boczán et al. [1] with the introduction of a novel separation procedure using magnetic cell sorting (MACS; Miltényi Biotech, Bergisch Gladbach, Germany) to obtain fibroblast-free cultures. Briefly, the biopsy material (15 biopsy samples were used to initiate cultures) was enzymatically dissociated at 37°C in calcium/magnesium-free phosphate buffer saline solution (PBS) containing collagenase (250 U/ml, Type II, Sigma) and bactotrypsin (3%, Difco, Detroit, Mich.). The reaction was stopped with Hanks' solution (136.75 mM NaCl, 5.36 mM KCl, 0.34 mM Na_2HPO_4, 0.44 mM KH_2PO_4, 0.81 mM $MgSO_4$, 1.26 mM $CaCl_2$, 5.56 mM glucose, 4.17 mM $NaHCO_3$, 10 mg/ml phenol red, pH 7.2) containing 10% fetal calf serum (FCS) (Sebak, Aidenbach, Germany).

After filtration and centrifugation (3×, 100 *g*, 10 min), the pellet was washed twice in sterile PBS supplemented with 0.5% bovine serum albumin (BSA, Sigma), and resuspended in the same medium containing 20% anti-fibroblast MicroBeads (Miltényi Biotech). This labeling agent is a colloidal super-paramagnetic MicroBead conjugated to mouse anti-fibroblast monoclonal antibody recognizing a fibroblast-specific antigen. Cells were labeled in this solution for 30 min at room temperature in a dark room, then washed in PBS-BSA, and were subjected to a column, which was placed in the magnetic field of a MACS separator. The column was washed with 5 ml PBS-BSA and, since magnetically labeled fibroblasts were retained in the columns, fractions that ran through were collected. These fibroblast-free muscle cell suspensions were then resuspended in Ham's F-12 (Sigma) growth medium containing 5% FCS and 5% horse serum (HS, Sebak), 2.5 mg/ml glucose, 0.3 mg/ml glutamate, 1.2 mg/ml $NaHCO_3$, 50 U/ml penicillin, 50 μg/ml streptomycin, 1.25 μg/ml fungizone (both from Biogal, Debrecen, Hungary). Cells were cultured in a 5% CO_2 atmosphere on either glass coverslips (Menzel-Glaser, Braunschweig, Germany) in petri dishes or in 4-well multititer plates (Nunc, Kamstrup, Denmark). After 3 days, the culture medium was changed to Dulbecco's modified Eagle's medium (Sigma) containing 2% FCS and 2% HS to induce myoblast fusion and differentiation [1]. Fibroblasts were collected by washing the columns with 2 ml PBS-BSA after removing the column from the magnetic field. In control experiments, to determine the efficiency of separation, immunohistochemistry was performed on 14-day-old cultures initiated using either the non-separated total cell suspension or the separated muscle cell-enriched and fibroblast-rich fractions of the same biopsy. Cells were washed with PBS, fixed in acetone for 5 min at 4°C, air dried, and blocked at room temperature for 30 min in a blocking solution containing 0.6% Triton X-100 and 1% BSA. Cells were first incubated with the highly muscle cell-specific anti-desmin monoclonal antibody for 1 h (diluted 1:100 in blocking solution; DAKO) and then with a horseradish peroxidase-conjugated goat anti-mouse IgG (diluted 1:300 in PBS, Sigma) for 1 h. Immunoreactive signals were visualized by a standard diaminobenzidine method. As seen in Fig. 1, cultures initiated using separated, muscle-enriched fractions were practically free of fibroblasts, whereas significant numbers of fibroblasts were detected in non-separated cultures.

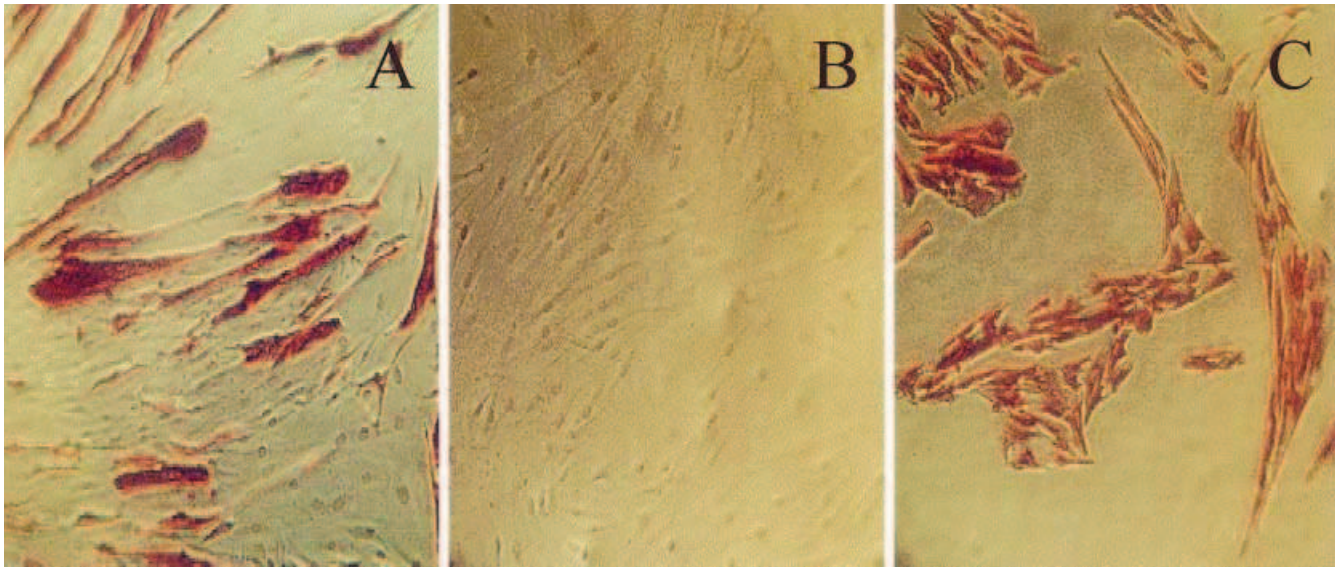

Fig. 1A–C Determination of efficiency of separation by immunohistochemistry. Cell cultures, using either the non-separated total cell suspension (**A**), or the fibroblast-rich (**B**) and muscle cell-enriched (**C**) fractions following separation of the same biopsy, were initiated. After 14 days in culture, cells were immunostained with mouse anti-desmin and horseradish peroxidase-conjugated goat anti-mouse antibodies, and visualized using diaminobenzidine; desmin-positive muscle cells possess a *brown* staining. Note that the separated, muscle cell-enriched cultures (**C**) lack practically any fibroblast contamination

Assessment of cellular growth and fusion

Cell cultures were treated daily from day 2 of culturing, for the time indicated, with either the vehicle dimethyl sulfoxide (DMSO, Sigma; less than 0.1%) or with different doses (0.1 nM–1 μM) of PMA. Supernatants were routinely tested for dead cells by a light microscope. Since counting of number of cells was uncertain, especially in the older cultures having much higher cell densities, growth curves were recorded by counting numbers of cell nuclei (5 independent visual fields per well) using an inverted phase contrast microscope and by averaging the values. The fusion of muscle cells was monitored morphologically and by calculating the fusion index of cultures. The fusion index was given as a ratio of the summed number of nuclei in myotubes (cell having two or more nuclei) and the total number of nuclei (including nuclei of mononuclear myoblasts and of myotubes). All data are expressed as mean ± SEM.

Western blot analysis

Cells were washed with ice-cold PBS, harvested in homogenization buffer (1% Triton X-100, 50 mM NaCl, 25 mM HEPES, 1 mM EDTA, 1 mM EGTA, 1 mM PMSF, 20 μM leupeptin, pH 7.4; all from Sigma) and disrupted by sonication on ice. Protein content of samples was measured by a modified Amido Black method [18]. Total cell lysates were mixed with SDS-PAGE sample buffer and boiled for 10 min at 100°C. The samples were subjected to SDS-PAGE according to Laemmli [20] (8% gels were loaded with max 10–20 μg protein/lane) and transferred to nitrocellulose membranes (Bio-Rad, Wien, Austria). Membranes were then blocked with 5% dry milk in PBS and probed with mouse anti-desmin antibody (DAKO) to follow muscle differentiation. An anti-mouse Vectastain ABC Kit (Vector, Burlingame, Calif.) containing anti-mouse secondary antibody (IgG) was then used to enhance specificity. Immunoreactive bands were finally visualized by an ECL Western blotting detection kit (Amersham, Little Chalfont, UK).

Immunohistochemistry and confocal microscopy

Control and PMA-treated muscle cells growing on glass coverslips were washed with PBS, fixed in acetone for 5 min at 4°C, air dried, and blocked at room temperature for 30 min in a blocking solution containing 0.6% Triton X-100 and 1% BSA. Cells were first incubated with the appropriate rabbit anti-PKC antibody for 2 h (diluted 1:50 in blocking solution) and then with a fluorescein isothiocyanate (FITC)-conjugated goat anti-rabbit IgG (diluted 1:160 in PBS, Sigma) for 1 h. Cells were visualized using a Zeiss MicroSystem Laser Scanning microscope (Oberkochen, Germany), and images were stored for further analysis.

Results

PMA inhibits growth and fusion of cultured human satellite cells, and decreases the expression of the muscle-specific differentiation marker desmin

To obtain information about how PMA treatment affects the events of in vitro skeletal muscle cell differentiation, we investigated the growth and fusion of satellite cells, and the expression of a muscle-specific differentiation marker desmin in the presence of the phorbol ester.

Human skeletal muscle cultures, growing in 4-well multititer plates, were treated daily with different concentrations of PMA (0.1 nM–1 μM) from day 2 of culturing for 1 week (further monitoring of cultures was obscured by the overgrow of cells preventing exact counting of nuclei). As seen in Fig. 2, PMA significantly decreased the number of cells (and of nuclei) per visual fields. Furthermore, in the PMA-treated cultures, only a few myotubes were observed, suggesting the inhibition of fusion as well (significant fusion activity was detected only in those cultures which were treated with low doses of PMA). Consistent with the fact that analysis of the cultures and the culturing media never revealed significant cytotoxicity upon PMA treatment (data not shown), these findings indicate that the effect of PMA was rather due to the inhibition of proliferation and not to cytotoxicity.

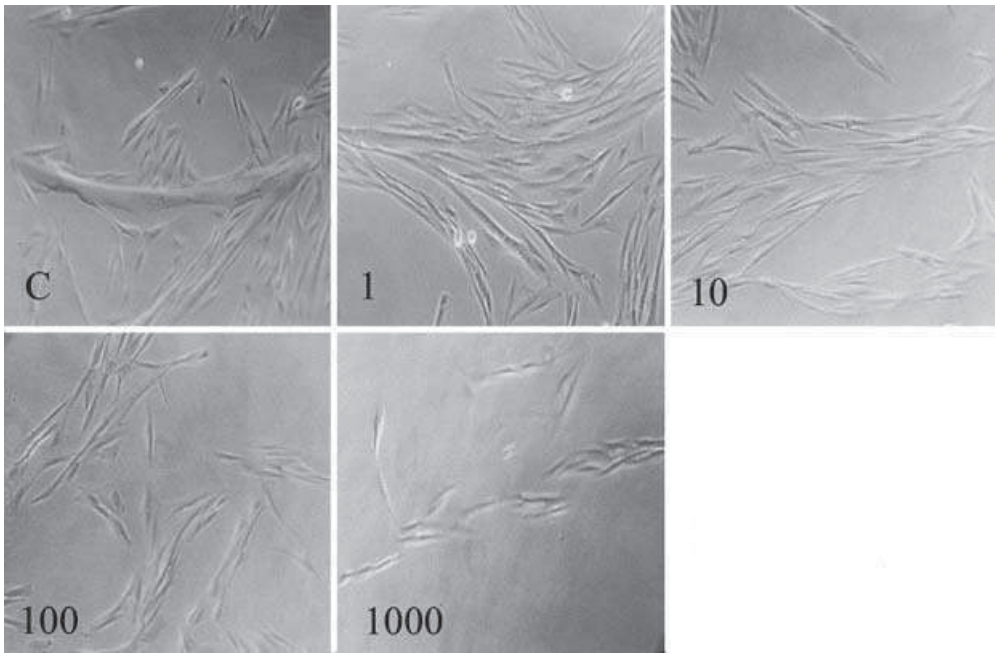

Fig. 2 Effect of PMA on growth of human cultured skeletal muscle cells. Cell cultures were treated daily from day 2 of culture with either DMSO (control, *C*) or with different doses (0.1–1000 nM) of PMA. Photomicrographs were taken at day 14 using an inverted phase contrast microscope. PMA decreased the number of cells per visual fields in a dose-dependent manner (*PMA* phorbol 12-myristate 13-acetate, *DMSO* dimethyl sulfoxide)

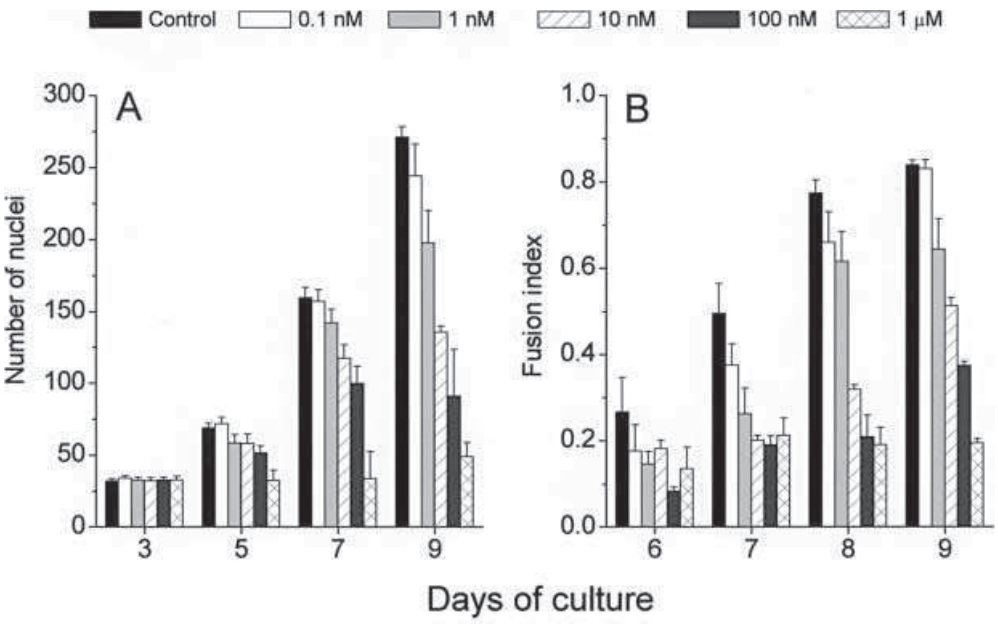

Fig. 3A, B Effect of PMA on the number of cell nuclei and on the fusion index of human cultured skeletal muscle cells. Cell cultures were treated daily from day 2 of culture with either DMSO (*Control*) or with different doses of PMA for 1 week. Counting of cell nuclei (**A**) and the calculation of fusion index (**B**) were performed daily. Values are expressed as mean ± SEM. Data are representative of three individual experiments with similar results. PMA inhibits both the proliferation and fusion of skeletal muscle satellite cells, showing similar dose-response characteristics

To quantitatively determine the inhibition of growth and fusion of muscle cells by PMA, growth curve analysis of cultures (by counting numbers of nuclei) and the calculation of the fusion index were performed. As seen in Fig. 3A, PMA inhibited the cellular growth in a dose- and time-dependent manner; significant inhibition was seen after 5–6 days of treatment, and 0.1–1 μM PMA were the most effective concentrations. As revealed by calculating the fusion index (Fig. 3B), PMA also suppressed the fusion of myoblasts (fusion started at day 5–6 in control cultures), showing a similar dose-response relationship.

To confirm that the PMA-induced inhibition of proliferation also results in the delay of maturation and differentiation, we also investigated the possible changes in the expression of the muscle-specific differentiation marker desmin (the intense appearance of which is regarded as a good indicator of skeletal muscle differentiation in vitro) [1, 2]. Similar to the previously described protocol, skeletal muscle cultures were treated daily with different concentrations of PMA from the day 2 of culturing. In this case, however, phorbol ester treatment was continued for 2 weeks since the expression of desmin has been described to have maximal levels in 12- to 16-day-old cultures [1]. As seen in Fig. 4 showing Western blot analysis of samples prepared at the end of this protocol, PMA decreased the expression of desmin in a dose-dependent manner, similar to that found in inhibiting cellular growth and fusion (desmin expression was hardly detected in the 1 μM PMA-treated

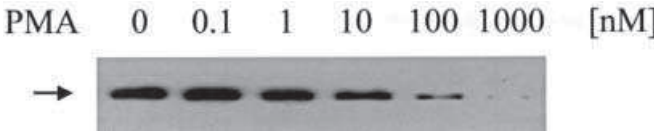

Fig. 4 Effect of PMA on the expression of the muscle-specific differentiation marker desmin. Cultures were treated with either DMSO (control, *C*) or with different concentrations of PMA from day 2 of culture for 2 weeks. Cells were then harvested, similar amounts of proteins were subjected to SDS-PAGE, and Western immunoblotting was performed using mouse anti-desmin antibody. Data are representative of three individual experiments with similar results. PMA decreases the expression of desmin in a dose-dependent fashion

cultures). We conclude that, since various PKC isoforms are differentially expressed during different stages of human skeletal muscle differentiation in vitro [1], and since PMA inhibited all of the examined events of this process, PKC might play a pivotal role in the regulation of skeletal muscle differentiation in vitro.

PMA translocates PKCγ, -η, and -θ but not PKCα and -ζ

In the second part of our study, we investigated the effect of the PMA treatment on the existing PKC isoforms. Since the activation of PKC can be characterized by a translocation between different intracellular compartments, and since PMA has been shown to induce translocation of the sensitive PKC isoforms in various cells types [17, 29, 30], we investigated the changes in subcellular localization of isoforms after PMA treatment. Cell cultures were treated with 1 μM PMA (or with the vehicle) from the day 2 of culture for 2 weeks, and then a confocal microscopy study was performed (following immunohistochemical labeling of PKCs) to monitor possible translocation. Since PMA treatment inhibited proliferation and fusion of cells, for better comparison, we also investigated the mononuclear myoblast or young myotubes (maximum 2–4 nuclei) in the control cultures. As seen in Fig. 5, PMA differentially affected the subcellular localization of various PKC isozymes without causing any significant down-regulation of the isoforms. PKCα exerted a rather homogeneous plasma and fairly intense nuclear membrane localization in the control cells, which was not affected significantly by PMA treatment. Similarly, the diffuse cytoplasmic staining and the intense nuclear-perinuclear accumulation of PKCζ were not modified by the phorbol ester (this latter finding was not unexpected since PKCζ is a phorbol ester-insensitive isoform).

In contrast, the subcellular localization of the other three isoforms was markedly changed by PMA (Fig. 5). PKCη, located mainly in the cytoplasm (and weakly in the nucleus) of control cells, was translocated to the perinuclear-nuclear membrane structures and also to the nucleus in the phorbol ester-treated cultures. Furthermore, PKCθ, which was stained mainly in the cytoplasm (and very faintly in the nucleus) in control cells, was translocated by PMA into the cell nucleus, resulting in a very intense patched nuclear staining, presumably labeling the nucleoli. Finally, PKCγ, located almost exclusively in the nucleus of mononuclear myoblasts in control cultures (only faint cytoplasmic signals were detected), was partially translocated into the cytoplasmic compartment; however, a significant nuclear staining also remained in the PMA-treated cells. These data indicate that prolonged PMA treatment differentially affected the localization of the PKC isozymes.

Discussion

In this report we show that the phorbol ester PMA inhibited the processes of proliferation, fusion, and the expression of the differentiation marker desmin in human skeletal muscle cells. In addition, this is the first demonstration that the PMA-induced cellular effects were accompanied by the differential translocation of certain PKC isoforms in these cells. Our data, therefore, strongly argue for the differential roles of PKC isozymes in human skeletal muscle differentiation in vitro.

In our experiments, PMA inhibited most of the events (proliferation, fusion, differentiation) of myogenic development of human skeletal muscle cells in vitro. These findings, at least in part, are similar to those described in the rare reports investigating human skeletal muscle differentiation. However, in contrast to the results of Fisher et al. [10, 11], we have observed significant inhibition of myogenesis by PMA even prior to fusion of the myoblasts. In addition, we have also shown that the PMA treatment suppressed the expression of the differentiation-specific marker desmin. These, rather minor, differences between our findings and Fisher's data may be due to the different culturing conditions used along the experiments (we employed a new separation procedure to obtain close to 95–100% fibroblast-free myogenic cell suspension). Nevertheless, our results that PMA inhibited differentiation of human skeletal muscle cells similarly to chick myoblasts [6, 25] but not to rat muscle cells [21] further strengthen the idea that the cellular effects of PMA on skeletal muscles cells (similarly to other cells types) [12, 26] exert marked species dependence.

One of the major novel findings of our experiments is that the PMA-induced inhibition of human skeletal muscle cells was accompanied by differential translocation of certain PKC isoforms within the cells. PMA caused subcellular changes in localization patterns of PKCγ, -η and -θ, whereas PKCα and -ζ were not translocated. It was also of great importance that the prolonged PMA treatment did not cause significant down-regulation of any of the PKC isozymes. Corresponding to our data, others have described differential modification of cellular localization and expression levels of existing PKC isoforms upon PMA treatment in skeletal muscle cells of other species. For example, in cultured rat muscles, prolonged PMA treatment selectively translocated PKCα, βII, and δ [3] and down-regulated PKCα and δ in the membrane compartment [15]. Furthermore, in L6 myogenic cell line, PMA down-regulated PKCα, δ and ε, but not the PKCμ and ι [34], whereas,

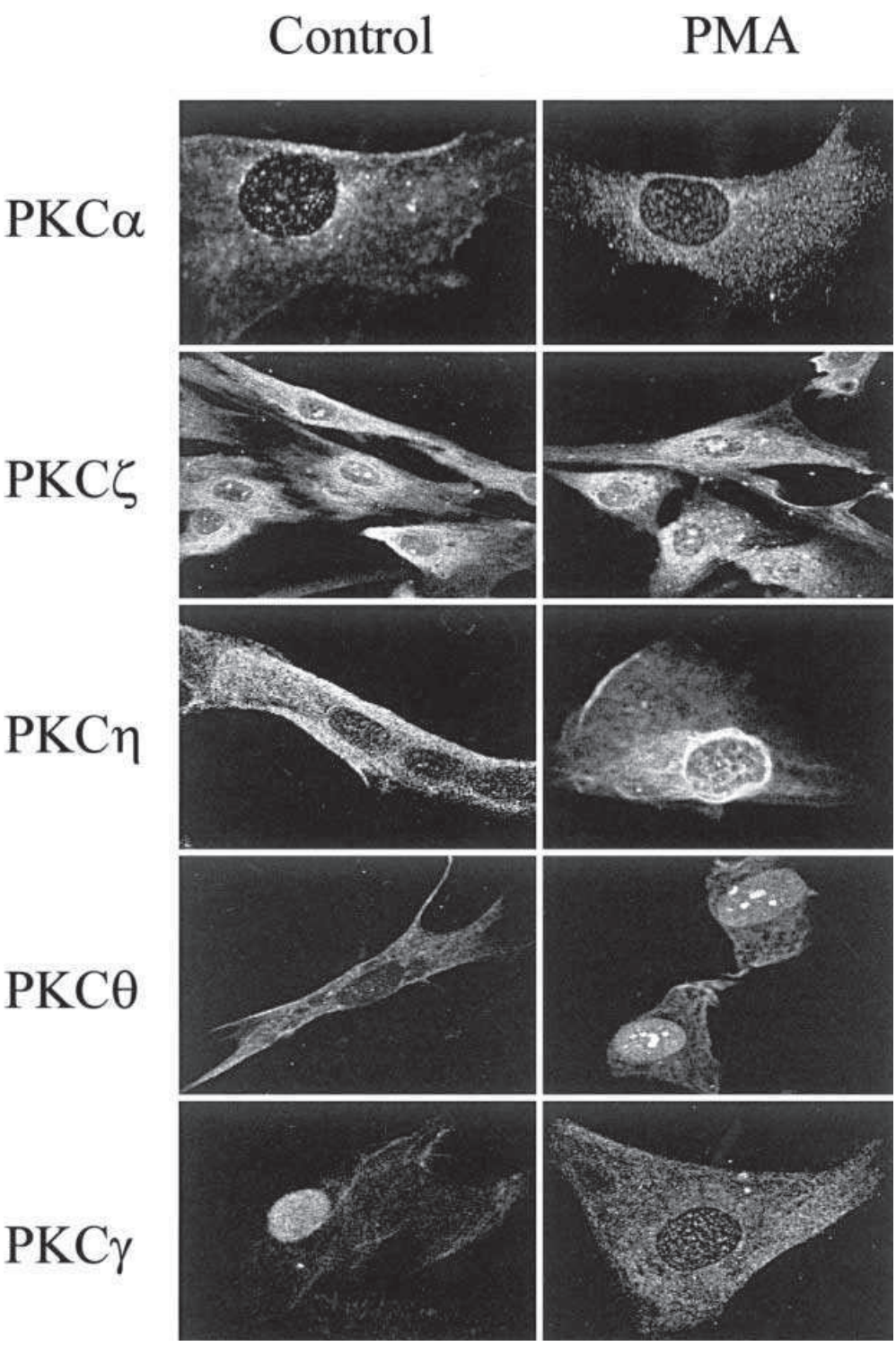

Fig. 5 Effect of PMA on subcellular localization of different PKC isoforms. Cell cultures were treated with either DMSO (*Control*) or with 1 μM PMA (*PMA*) for 2 weeks, and immunofluorescence staining of various PKC isoforms using rabbit anti-PKC and FITC-conjugated anti-rabbit antibodies was performed. Images were acquired by a laser scanning confocal microscope with strictly the same antibody staining and visualization procedure. PMA differentially translocates PKCη, -θ and -γ, whereas the subcellular localization of PKCα and -ζ are not modified by the phorbol ester

in chick myoblasts, it selectively down-regulated PKCα but not PKCβ, δ, ε, and ζ [6]. Similar to the differential sensitivity of PKC isoforms to PMA reported in other cell types [17], both our findings and these aforementioned data suggest that there is also a marked difference among phorbol ester-sensitive PKC isoforms (members of the "conventional" and "novel" groups) in responsiveness to PMA in skeletal muscle cells. For example, in our experiments, PMA induced the translocation of the "conventional" PKCγ but not of PKCα that also belongs to this group.

The lack of down-regulation of PKC isoforms during prolonged PMA treatment suggests that the inhibitory effect of PMA on human skeletal muscle differentiation was rather due to activation (hence translocation) and not to the decrease in cellular levels of certain isoforms (down-

regulation). Alternatively, the possibility that PMA first induced a fast down-regulation then (during its prolonged presence) the de novo re-synthesis of various PKC isoforms can not be excluded. However, our preliminary findings suggest (Bíró et al., unpublished observation) that there is no significant down-regulation of PKC isoforms upon short (1 day) PMA treatment of human skeletal muscle cells. The phenomenon of differential translocation without any down-regulation, therefore, argues for distinct cellular mechanisms and significance in regulating the two processes.

We have previously described [1] that, in human cultured skeletal muscle cells, the existing five PKC isoforms exerted differential expression patterns during cellular differentiation. There were no significant changes in the expressions of PKCα and -ζ during differentiation; however, the expressions of PKCγ and -η increased, whereas the expression of PKCθ decreased as differentiation proceeded. In this report we demonstrate that only those PKC isozymes were translocated upon PMA treatment that possessed alterations in levels of expression during differentiation in vitro. These data also strongly argues for the differential regulatory roles of the existing PKC isoforms in human skeletal muscle differentiation.

We have also found that the various PKC isoforms that were translocated upon PMA administration targeted different intracellular structures. PKCη was translocated from mainly the cytoplasm to the perinuclear-nuclear membrane structures and also, to a lesser extent, to the nucleus; PKCγ exerted a partial translocation from the cell nucleus to the cytoplasmic compartment; PKCθ moved from the cytoplasm to the cell nucleus and nucleoli. Since the proliferation and differentiation of skeletal muscle cells are under the strict control of myogenic transcription factors (e.g., MyoD, MRF4, myf5, myogenin) [7, 35], and since the phosphorylation state of the transcription factors might affect proliferation and differentiation of cultured muscle cells [22], it is of great significance that PMA inhibited the events of differentiation in parallel with targeting PKCη and -θ into the nucleus. Our data, therefore, suggest that these isozymes (in contrast to PKCα and -ζ that were not translocated by PMA) might negatively regulate the process of differentiation in human skeletal muscle cells. These findings are also in a good accord with the previously described fact that, in mouse myoblasts, the overexpression of PKCθ but not of PKCα and -ζ mediates the differentiation inhibitory effect of TGF-β [36].

There is an interesting phenomenon, however, in the case of PKCγ, suggesting an attractive hypothesis. As we have previously shown [1], this PKC isozyme (partially) translocates from the nuclear-perinuclear region to the cytoplasmic compartment in parallel with the development of differentiation (thus the appearance of matured multinuclear myotubes). Since PKCγ was the only PKC isoform that exerted such changes in subcellular localization during differentiation [1], this result argues for a role of the isoform in regulating the process. Our current presentation that PMA caused a very similar alteration in translocation pattern of PKCγ, therefore, would suggest that PMA is a positive regulator of human skeletal muscle differentiation. Since we found a significant and dose-dependent inhibition of all the examined events of differentiation by PMA, we can assume that the differentiation inhibitory effects of other PKC isoforms (presumably of PKCθ and -η) may have overcome the differentiation promoting effect of PKCγ. Naturally, another hypothesis, suggesting that the translocation of PKCγ during the differentiation [1] or upon PMA treatment rather reflects an inhibitory role of the isoform, can not be ruled out. Nevertheless, the exact, isozyme-specific roles of the various PKC isoforms in the above processes have yet to be investigated in detail.

In summary, we can conclude that the PMA-induced inhibition of the processes of human skeletal muscle differentiation is accompanied by the differential translocation of certain PKC isoforms. Our data, therefore, strongly argue for the differential and isozyme-specific roles of the various PKC isoforms in the regulation of human skeletal muscle differentiation.

Acknowledgements The authors are indebted to Ms. Ibolya Varga for helpful technical assistance. This work was supported by Hungarian Research Grants: OTKA T030246, OTKA O23040, AKP 98–75 3.2, ETT 31/1998, ETT 50/2000. Tamás Bíró is the recipient of the János Bolyai Research Scholarship of the Hungarian Academy of Sciences.

References

1. Boczán J, Boros S, Mechler F, Kovács L, Bíró T (2000) Differential expressions of protein kinase C isozymes during proliferation and differentiation of human skeletal muscle cells in vitro. Acta Neuropathol 99:96–104
2. Bornemann A, Schmalbruch H (1992) Desmin and vimentin in regenerating muscles. Muscle Nerve 15:14–20
3. Braiman L, Sheffi-Friedman L, Bak A, Tennenbaum T, Sampson SR (1999) Tyrosine phosphorylation of specific protein kinase C isoenzymes participates in insulin stimulation of glucose transport in primary cultures of rat skeletal muscle. Diabetes 48:1922–1999
4. Brodie C, Kuperstein I, Ács P, Blumberg PM (1998) Differential role of specific PKC isoforms in the proliferation of glial cells and the expression of the astrocytic markers GFAP and glutamine synthetase. Mol Brain Res 56:108–117
5. Cacace AM, Guadagno SN, Krauss RS, Fabbro D, Weinstein IB (1993) The epsilon isoform of protein kinase C is an oncogene when overexpressed in rat fibroblasts. Oncogene 8:2095–2104
6. Capiati DA, Limbozzi F, Tellez-Inon MT, Boland RL (1999) Evidence on the participation of protein kinase C alpha in the proliferation of cultured myoblasts. J Cell Biochem 74:292–300
7. Chambers RL, McDermott JC (1996) Molecular basis of skeletal muscle regeneration. Can J Appl Physiol 21:155–184
8. Cossu G, Zani B, Colette M, Bouche M, Pacifici M, Molinaro M (1980) In vitro differentiation of satellite cells isolated from normal and dystrophic mammalian muscles. A comparison with embryonic myogenic cells. Cell Differ 9:357–368
9. Farzaneh F, Entwistle A, Zalin RJ (1989) Protein kinase C mediates the hormonally regulated plasma membrane fusion of avian embryonic skeletal muscle. Exp Cell Res 181:298–304
10. Fisher PB, Miranda AF, Mufson RA, Weinstein LS, Fujiki H, Sugimura T, Weinstein IB (1982) Effects of teleocidin and the phorbol ester tumor promoters on cell transformation, differentiation, and phospholipid metabolism. Cancer Res 42:2829–2835

11. Fisher PB, Miranda AF, Babiss LE, Pestka S, Weinstein IB (1983) Opposing effects of interferon produced in bacteria and of tumor promoters on myogenesis in human myoblast cultures. Proc Natl Acad Sci USA 80:2961–2965
12. Goodnight J, Mischak H, Mushinski JF (1994) Selective involvement of protein kinase C isozymes in differentiation and neoplastic transformation. Adv Cancer Res 64:159–209
13. Grounds MD (1991) Towards understanding skeletal muscle regeneration. Pathol Res Pract 187:1–22
14. Henriksen EJ, Rodnick KJ, Holloszy JO (1989) Activation of glucose transport in skeletal muscle by phospholipase C and phorbol ester. Evaluation of the regulatory roles of protein kinase C and calcium. J Biol Chem 264:21536–21543
15. Hong DH, Huan J, Ou BR, Yeh JY, Saido TC, Cheeke PR, Forsberg NE (1995) Protein kinase C isoforms in muscle cells and their regulation by phorbol ester and calpain. Biochim Biophys Acta 1267:45–54
16. Husmann I, Soulet L, Gautron J, Martelly I, Barritault D (1996) Growth factors in skeletal muscle regeneration. Cytokine Growth Factor Rev 7:249–258
17. Jaken S (1996) Protein kinase isozymes and substrates. Curr Opin Cell Biol 8:168–173
18. Kaplan RS, Pedersen PL (1985) Determination of microgram quantities of protein in the presence of milligram levels of lipid with Amido Black 10B. Anal Biochem 150:97–104
19. Kramer IM (1996) Signal transduction through tyrosine protein kinases. In: Foreman JC, Johansen T (eds) Textbook of receptor pharmacology. CRC Press, New York, pp 255–274
20. Laemmli UK (1970) Cleavage of structural proteins during the assembly of the head of bacteriophage T4. Nature 227:680–685
21. Lagord C, Leibovitch MP, Carpentier G, Leibovitch SA, Martelly I (1996) The kinase inhibitor iso-H7 stimulates rat satellite cell differentiation through a non-protein kinase C pathway by increasing myogenin expression level. Cell Biol Toxicol 12:177–185
22. Liu LN, Dias P, Hougton PJ (1998) Modulation of Trh115 in MyoD positively regulates function in murine fibroblasts and human rhabdomyosarcoma cells. Cell Growth Differ 9:699–711
23. Marinissen MJ, Capiati D, Boland AR de (1998) 1, $25(OH)_2$-vitamin D_3 affects the subcellular distribution of protein kinase C isoenzymes in muscle cells. Cell Signal 10:91–100
24. Massheimer V, Boland AR de (1992) Modulation of 1, 25-dihydroxivitamin D_3-dependent Ca^{2+} uptake in skeletal muscle by protein kinase C. Biochem J 281:349–352
25. Mermelstein CS, Costa ML, Chagas Filho C, Moura Neto V (1996) Intermediate filament proteins in TPA-treated skeletal muscle cells in culture. J Muscle Res Cell Motil 17:199–206
26. Mischak H, Goodnight JA, Kolch W, Martiny-Baron GM, Schaechtle C, Kazanietz MG, Blumberg PM, Pierce JH, Mushinski JF (1993) Overexpression of protein kinase C-δ and -ε in NIH 3T3 cells induces opposite effects on growth, morphology, anchorage dependence, and tumorigenicity. J Biol Chem 268:6090–6096
27. Murray NR, Baumgardner GP, Burns DJ, Fields AP (1993) Protein kinase C isotypes in human erythroleukemia (K562) cell proliferation and differentiation. Evidence that beta II protein kinase C is required for proliferation. J Biol Chem 268: 15847–15853
28. Nimnual AS, Chang W, Chang NS, Ross AF, Gelman MS, Prives JM (1997) Identification of phosphorylation sites on AChR delta-subunit associated with dispersal of AChR clusters on the surface of muscle cells. J Cell Sci 110:2771–2779
29. Nishizuka Y (1988) The molecular heterogeneity of protein kinase C and its implication for cellular regulation. Nature 334:661–665
30. Nishizuka Y (1992) Intracellular signaling by hydrolysis of phospholipids and activation of protein kinase C. Science 258: 607–614
31. Ohno S, Akita Y, Hata A, Osada S, Kubo K, Kohno Y, Akimoto K, Mizuno K, Saido T, Kuroki T, Suzuki K (1991) Structural and functional diversities of a family of signal transducing protein kinases, protein kinase C family; two distinct classes of PKC, conventional cPKC and novel nPKC. Adv Enzyme Regul 31:287–303
32. Schultz E, McCormick KM (1994) Skeletal muscle satellite cells. Rev Physiol Biochem Pharmacol 123:213–257
33. Tanti JF, Rochet N, Gremeaux T, Van Obberghen E, Le Marchand-Brustel Y (1989) Insulin-stimulated glucose transport in muscle. Evidence for a protein kinase-C-dependent component which is unaltered in insulin-resistant mice. Biochem J 258: 141–146
34. Thompson MG, Mackie SC, Thom A, Palmer RM (1997) Regulation of phospholipase D in L6 skeletal muscle myoblasts. Role of protein kinase C and relationship to protein synthesis. J Biol Chem 272:10910–10916
35. Weintraub H (1993) The MyoD family and myogenesis: redundancy, networks, and thresholds. Cell 75:1241–1244
36. Zapelli F, Willems D, Osada S, Ohno S, Wetsel WC, Molinaro M, Cossu G, Bouché M (1996) The inhibition of differentiation caused by TGFβ in fetal myoblasts is dependent upon selective expression of PKCθ: a possible molecular basis for myoblast diversification during limb histogenesis. Dev Biol 130:156–164
37. Zhu YY, Schwartz RJ, Crow MT (1991) Phorbol esters selectively down-regulate contractile protein gene expression in terminally differentiated myotubes through transcriptional repression and message destabilization. J Cell Biol 115:745–754

XIII.

Available online at www.sciencedirect.com
SCIENCE DIRECT
Cellular Signalling 18 (2006) 1461 – 1472
CELLULAR SIGNALLING
www.elsevier.com/locate/cellsig

Insulin-like growth factor-I-coupled mitogenic signaling in primary cultured human skeletal muscle cells and in C2C12 myoblasts. A central role of protein kinase Cδ

Gabriella Czifra [a,b], István Balázs Tóth [a,b], Rita Marincsák [a], István Juhász [c], Ilona Kovács [d], Péter Ács [e], László Kovács [a,b], Peter M. Blumberg [e], Tamás Bíró [a,b,*]

[a] Department of Physiology, University of Debrecen, Medical and Health Science Center, Research Center for Molecular Medicine, Debrecen, Hungary
[b] Cell Physiology Research Group of the Hungarian Academy of Sciences, University of Debrecen, Medical and Health Science Center, Research Center for Molecular Medicine, Debrecen, Hungary
[c] Department of Dermatology, University of Debrecen, Medical and Health Science Center, Research Center for Molecular Medicine, Debrecen, Hungary
[d] Department of Pathology, Kenézy County Hospital, Debrecen, Hungary
[e] Molecular Mechanism of Tumor Promotion Section, Laboratory for Cellular Carcinogenesis and Tumor Promotion, National Cancer Institute, National Institutes of Health, Bethesda, MD, USA

Received 10 November 2005; received in revised form 21 November 2005; accepted 21 November 2005
Available online 3 January 2006

Abstract

In this study, we have investigated the effects of insulin-like growth factor-I (IGF-I) on cellular responses of primary human skeletal muscle cells and mouse C2C12 myoblasts. In human muscle, IGF-I stimulated proliferation and fusion of the cells and the expression of the differentiation marker desmin. These effects were completely inhibited by Rottlerin, the inhibitor of the protein kinase C (PKC)δ, but were not affected by the inhibition of the mitogen-activated protein kinase (MAPK) or the phosphatidylinositide 3-kinase (PI-3K) pathways. Furthermore, IGF-I initiated the selective translocation of PKCδ to the nucleus. In C2C12 myoblasts, the growth-promoting effects of IGF-I were abrogated by inhibition of PKCδ, but not by the inhibition of the PI-3K system. However, in contrast to the human data, the MAPK inhibitor PD098059 partially (yet significantly) also inhibited the action of IGF-I and, furthermore, IGF-I induced phosphorylation of the MAPK Erk-1/2. In addition, overexpression of constitutively active form of PKCδ in C2C12 cells fully mimicked, whereas overexpression of kinase inactive mutant of the isoform prevented the action of IGF-I. Finally, the inhibition of PKCδ suspended the IGF-I-induced phosphorylation of Erk-1/2 and, moreover, the inhibition of the MAPK pathway partially (yet significantly) inhibited the accelerated growth of C2C12 cells overexpressing PKCδ. Taken together, these results demonstrate a novel, central and exclusive involvement of PKCδ in mediating the action of IGF-I on human skeletal muscle cells, with an additional yet PKCδ-dependent contribution of the MAPK pathway on C2C12 myoblasts.

Keywords: Human skeletal muscle; C2C12 cells; Insulin-like growth factor-I (IGF-I); Protein kinase C (PKC); PKCδ; Mitogen-activated protein kinase (MAPK); Proliferation

1. Introduction

Insulin-like growth factor-I (IGF-I) acts as an autocrine, paracrine and endocrine regulator a cellular growth and development of skeletal muscle [1–3]. IGF-I, which is also produced by the skeletal muscle and satellite cells [4], for example stimulates gene expression, DNA and protein synthesis, different transport mechanisms, migration, proliferation and differentiation of cultured myogenic cells [2,5–9]. It was also documented that the expression of IGF-I is increased in satellite cells, myoblast, myotube and muscle fibers of atrophic skeletal muscles [10,11] suggesting that the growth factor may stimulate regenerative processes in the muscle [12,13]. This hypothesis was also strengthened by that the administration of

* Corresponding author. Department of Physiology, University of Debrecen, Medical and Health Science Center, Research Center for Molecular Medicine, Nagyerdei krt. 98. PO Box 22, H-4012 Debrecen, Hungary. Tel.: +36 52 416 634; fax: +36 52 432 289.
E-mail address: biro@phys.dote.hu (T. Bíró).

0898-6568/$ - see front matter © 2005 Elsevier Inc. All rights reserved.
doi:10.1016/j.cellsig.2005.11.007

recombinant human IGF-I or specific gene transfer therapies improved metabolism and function of impaired skeletal muscles of patients with muscle diseases [14–16].

It is generally accepted that IGF-I exerts its mitogenic cellular effects by acting on its one-transmembrane domain receptor, which bears tyrosine kinase activity [17]. It is also known that the binding of IGF-I to its receptor, after tyrosine (auto)phosphorylation of the receptor, results in the initiation of intracellular cascades of various kinase systems [18]. However, the interplay between the elements of these intracellular signaling pathways is very controversially described on skeletal muscle cell types of different species and under various experimental conditions. Namely, in mouse and rat skeletal muscle preparations (similarly to other cell types), the involvement of both the mitogen-activated protein kinase (MAPK) pathway and MAPK-independent signaling mechanisms, including the Akt/phosphatidylinositide 3-kinase (PI-3K) and the protein kinase C (PKC), were equally documented [5,6,19–21].

We, however, possess extremely limited data on the exact cellular signaling mechanism of IGF-I on human skeletal muscle cells [8]. Therefore, in this study, we measured the possible involvement of the MAPK, PI-3K and PKC systems in mediating the mitogenic effect of IGF-I on cultured primary human skeletal muscle cells. In addition, for comparison and to expand the technical repertoire with additional molecular biological methods, we repeated our experiment on the mouse C2C12 myoblast cell line that is very often used to study the effects of growth factors on skeletal muscles [5,6]. Our presented results strongly argue for the novel, central, and exclusive involvement of PKCδ in mediating the action of IGF-I on human skeletal muscle cells, with an additional yet PKCδ-dependent contribution of the MAPK pathway on C2C12 myoblasts.

2. Materials and methods

2.1. Materials

In this study, the following materials were used: IGF-I, GF10203X, Gö6976 and Rottlerin were from Sigma (St. Louis, MO, USA), whereas PD098059, U01216 and wortmannin were from Calbiochem (Nottingham, UK).

All antibodies against PKC isozymes were developed in rabbits and were shown to specifically react with the given PKC isoforms [22,23]: anti-PKCα, β, γ, η, ζ and λ/ι were from Sigma, whereas anti-PKCδ and θ from Santa Cruz Biotech (Santa Cruz, CA, USA). The specificity of anti-PKC antibodies was also tested by applying isoform-specific blocking peptides, which suspended the immunostaining in all cases (see Fig. 5). In addition, a monoclonal mouse antibody against the intermediate filament protein desmin (DAKO, Glostrup, Denmark) was used to follow muscle differentiation. Furthermore, a polyclonal rabbit antibody was used to detect the MAPK Erk-1/2 (42/44), whereas monoclonal mouse antibodies were employed to label the phosphorylated Erk-1/2 (pErk-1/2), the phosphorylated Tyr residues of proteins (pTyr) and cytochrome C (all from Santa Cruz Biotech).

2.2. Cell culture and separation

Human satellite cells were obtained from muscle tissue waste of orthopedic surgery and cultured according to our previously optimized and developed protocol. The procedure also included a magnetic separation procedure using Magnetic Cell Sorting (MACS; Miltényi Biotech, Bergisch Gladbach, Germany) to obtain fibroblast-free skeletal muscle cell cultures [22,23]. Briefly, the biopsy material (38 biopsy samples were used to initiate cultures during the course of our experiments) was enzymatically dissociated at 37 °C in calcium/magnesium-free phosphate buffer saline solution (PBS) containing collagenase (250 U/ml, Type II, Sigma) and bactotrypsin (3%, Difco, Detroit, MI, USA). The reaction was stopped with Hank's solution (in mM; 136.75 NaCl, 5.36 KCl, 0.34 Na_2HPO_4, 0.44 KH_2PO_4, 0.81 $MgSO_4$, 1.26 $CaCl_2$, 5.56 glucose, 4.17 $NaHCO_3$, 10 mg/ml phenol red, pH 7.2, all from Sigma) containing 10% fetal calf serum (FCS) (Invitrogen, Paisley, UK). After filtrations and centrifugations (3×, 100 g, 10 min), the pellet was washed twice in sterile PBS supplemented with 0.5% bovine serum albumin (BSA, Sigma), then was resuspended in the same medium containing 20% anti-fibroblast MicroBeads (Miltényi Biotech). This labeling agent is a colloidal super-paramagnetic MicroBead conjugated to a monoclonal mouse anti-fibroblast antibody recognizing a fibroblast-specific antigen. Cells were labeled in this solution for 30 min at room temperature, then washed in PBS-BSA and were subjected to a column, which was placed in the magnetic field of a MACS separator. The column was washed with 5 ml PBS-BSA and, since magnetically labeled fibroblasts were retained in the columns, fractions that ran through were collected. These fibroblast-free muscle cell suspensions were then resuspended in Ham's F-12 (Sigma) growth medium containing 5% FCS and 5% horse serum (HS, Invitrogen), 2.5 mg/ml glucose, 0.3 mg/ml glutamate, 1.2 mg/ml $NaHCO_3$, 50 U/ml penicillin, 50 μg/ml streptomycin and 1.25 μg/ml fungizone (all from Sigma). Cells were cultured at 5% CO_2 atmosphere on either 4-well multititer plates (Nunc, Kamstrup, Denmark) or on glass coverslips (Menzel-Glaser, Braunschweig, Germany) in Petri dishes for immunocytochemistry. After 3 days, the culture medium was changed to Dulbecco's Modified Eagle's Medium (DMEM) (Sigma) containing 2% FCS and 2% HS. As we have shown before, the separation procedure resulted in >95% fibroblast-free muscle-enriched cell suspension and cultures [23]. The use of this method was approved by the Ethical Committee of the University of Debrecen, Hungary and all patients gave written informed consent.

The mouse C2C12 myogenic skeletal muscle cell line was cultured in DMEM supplemented with 15% FCS and antibiotics, and were sub-cultured before reaching confluence to prevent high cell density-induced differentiation and myotube formation; therefore, C2C12 myoblasts were used throughout the study.

2.3. Assessment of cellular growth

In the case of human primary cultures, cells were treated daily from day 3 of culturing, for the time indicated, with either the vehicle dimethyl sulfoxide (DMSO, Sigma; less than 0.1%) or with different doses of agents. Supernatants were routinely tested for dead cells by a light microscope. Since counting of number of cells was uncertain, especially in the older cultures having much higher cell densities and multinuclear myotubes, growth curves were recorded by counting numbers of cell nuclei (five independent visual fields per well in duplicate culture disks) using an inverted phase contrast microscope and by averaging the values [23].

In the case of the C2C12 cell line, proliferation was measured by a colorimetric bromo-deoxyuridine (BrdU) assay kit (Boehringer Mannheim, Mannheim, Germany) [24]. In those BrdU assays where the effects of PKC acting agents were tested on cellular proliferation, cells were plated in 96-well multititer plates (5000 cells/well density, approximately 30% confluence) in quadruplicates and 4 h later were treated with different concentrations of the agents examined for the time indicated. Cells were then incubated with 10 μM BrdU for 4 h, and the cellular incorporation of BrdU (as the indicator of cellular proliferation) was determined colorimetrically (absorbance was measured at 450 nm) according to the manufacturer's protocol. When BrdU assays were employed to investigate growth properties of PKC transfectants, C2C12 cells were seeded at 1000 cells/well density and the BrdU incorporation was daily determined, as described above.

The fusion of muscle cells was monitored morphologically and by calculating the fusion index of cultures. The fusion index was given as a ratio of the summed number of nuclei in myotubes (cell having two or more nuclei) and the total number of nuclei (including nuclei of mononuclear myoblasts and of myotubes) [23].

In all cases, data are expressed as mean±S.E.M. Statistical analysis was performed by using the Student's *t*-test.

2.4. Western blot analysis

Cells were washed with ice-cold PBS, harvested in homogenization buffer (1% Triton X-100, 50 mM NaCl, 25 mM HEPES, 1 mM EDTA, 1 mM EGTA, 1 mM PMSF, 20 μM leupeptin, pH 7.4; all from Sigma) and disrupted by sonication on ice. Protein content of samples was measured by a modified Amido Black method [23,24]. Total cell lysates were mixed with SDS-PAGE sample buffer and boiled for 10 min at 100 °C. The samples were subjected to SDS-PAGE (8% gels were loaded with max. 10–20 μg protein per lane) and transferred to nitrocellulose membranes (Bio-Rad, Wien, Austria). Membranes were blocked with 5% dry milk in PBS and then first probed with primary antibodies and species-matched peroxidase-conjugated goat anti-rabbit or anti-mouse IgG secondary antibodies (BioRad). Immunoreactive bands were visualized by an ECL Western blotting detection kit (Amersham, Little Chalfont, England). When applicable, immunoblots were subjected to densitometric analysis using an Intelligent Dark Box (Fuji, Tokyo, Japan) and the Image Pro Plus 4.5.0 software (Media Cybernetics, Silver Spring, MD, USA), and then normalized densitometric values of the individual lanes of several independent experiments were determined. To assess equal loading, membranes were stripped in 200 ml of 50 mM Tris–HCl buffer (pH 7.5) containing 2% SDS and 0.1 β-mercaptoethanol (all from Sigma) at 65 °C for 1 h and were re-probed with a mouse anti-cytochrome *C* antibody (Santa Cruz Biotech) followed by a similar visualization procedure as described above.

2.5. Immunoprecipitation of PKCδ

Cells were washed several times with ice-cold PBS and scraped into 1 ml of radioimmunoprecipitation assay (RIPA) buffer containing 50 mM Tris–HCl, 1% NP-40, 0.25% Na-deoxycholate, 1 mM NaCl, 1 mM PMSF, 1 μg/ml leupeptin, 1 μg/ml aprotinin, 1 mM Na_2VO_4, 1 mM EDTA (all from Sigma), and were disrupted by sonication on ice. After mixing on an orbit shaker, the samples were incubated on ice for 15 min and then centrifuged in a microcentrifuge at 4 °C for 15 min at 15,000×*g*. The supernatant was removed, mixed with 100 μl of protein A/G Agarose (Sigma) and 5 μl of anti-PKCδ antibody (Santa Cruz Biotech), and then immunoprecipitation was performed by rotating the samples overnight at 4 °C. The samples were spun at 15,000×*g* at 4 °C for 5 min, the pellet was washed three times with RIPA buffer, and then resuspended in SDS-PAGE sample buffer and boiled for 10 min at 100 °C. All samples were subjected to Western blotting as described above.

2.6. Immunohistochemistry and confocal microscopy of PKC isoforms

Cells growing on glass coverslips were washed with PBS, fixed in acetone for 5 min at 4 °C, air dried and blocked at room temperature for 30 min in a blocking solution containing 0.6% Triton X-100 and 1% BSA (both from Sigma). Cells were first incubated with the appropriate rabbit anti-PKC antibodies for 2 h (diluted 1:50 in blocking solution) and then with a goat anti-rabbit fluorescein isothiocyanate (FITC)-conjugated secondary antibody (diluted 1:160 in PBS, Sigma) for 1 h. Immunosignals were visualized by a Zeiss Laser Scanning confocal microscope (Oberkochen, Germany) using the "z-stack mode" in which consecutive, 0.5–1 μm thick images were recorded along the full thickness of the immunostained cell. Usually, those images were analyzed in which all cellular compartments could be visualized (generally, the second image from the level of the coverslips).

2.7. Generation of PKC constructs

PKC constructs were engineered as described previously [25–27]. Briefly, the cDNA sequences of PKCδ and its kinase (dominant)-negative mutant (DN-PKCδ) were subcloned into a metallothionein promoter-driven eukaryotic expression vector (MTH) [28]. The vector sequence encodes a C-terminal PKCε-derived 12 amino acid tag (εMTH) and attaches it to the end of the PKC proteins. As we have previously shown [25,26], this epitope tag affects neither the localization nor the translocation of the given isoform.

2.8. Transfection of PKC isoforms

C2C12 cells were seeded in 6-well tissue culture dishes and at 60–70% confluence were transfected by either the empty pεMTH vector or by the vectors encoding the cDNA sequences of PKCδ or DN-PKCδ [25–27]. Transfections were performed using a Lipofectamine anionic detergent (Invitrogen) in serum-free OptiMEM (Invitrogen) solution using 2–4 μg cDNA according to the protocol suggested by the manufacturer. Cells were then selected in DMEM containing 750 μg/ml G418 (geneticin, Invitrogen) for 12–18 days, then single colonies were isolated. PKC overexpressing cells were cultured in supplemented DMEM containing 500 μg/ml G418. Experiments were routinely carried out on pools of transfected cells, but the results we confirmed on at least three other individual clones for each isoform. The efficacy of recombinant overexpression was monitored by Western blotting (see Fig. 7) and by measuring PKC-specific kinase activities according to as recently published by our laboratory [24].

3. Results

3.1. IGF-I stimulates proliferation, fusion and the expression of the differentiation marker desmin on primary human skeletal muscle cells

First, we quantitatively determined the effect of IGF-I on cellular proliferation of cultured human skeletal muscle cells. As revealed by daily counting of the number of nuclei, IGF-I (as expected [8,9]) markedly increased cellular proliferation of the cells in time- and dose-dependent manners (Fig. 1A), which effect started from day 5 (after 2 days of treatment), but most evidently could be recognized on days 6–8 (further counting was obscured by the overgrowth of the cultures).

Since proliferation of cultured human skeletal muscle cells is accompanied by the concomitant onset of differentiation program, exemplified by multinuclear myotube formation and the increased expressions of certain muscle-specific differentiation markers even in the well sub-confluent cultures [12,22,23], we also investigated the effect of IGF-I on the fusion of the myoblasts and the expression of the differentiation marker desmin [29]. As seen in Fig. 1B and C, IGF-I, besides increasing proliferation, elevated the number of multinuclear myotubes. In addition, as revealed by Western immunoblotting against desmin (Fig. 1D), IGF-I also increased the expression of the differentiation marker in a dose-dependent manner suggesting that the mitogenic effect of IGF-I was also accompanied by the onset of the maturation and differentiation program.

3.2. The action of IGF-I involves PKCδ but not the MAPK and PI3-K pathways on primary human skeletal muscle cells

As was described above, the cellular action of IGF-I, depending on the actual cell type, may involve the MAPK, PI3-K and/or PKC pathways [5,6,8,19–21]. Therefore, in the next phase of our experiments, we investigated the effects of PD098059 and U0126, inhibitors of the MAPK Erk-1/2 pathway; wortmannin, an inhibitor of the PI3-K; and GF109203X, a general PKC blocker [5,8,30] on the IGF-I evoked cellular response. As seen in Fig. 2A and B, the inhibition of the MAPK system by 20 μM PD098059 or 5 μM U0126 (not shown); or suppression of the activity of the PI3-K pathways by 100 nM wortmannin exerted insignificant effects on the

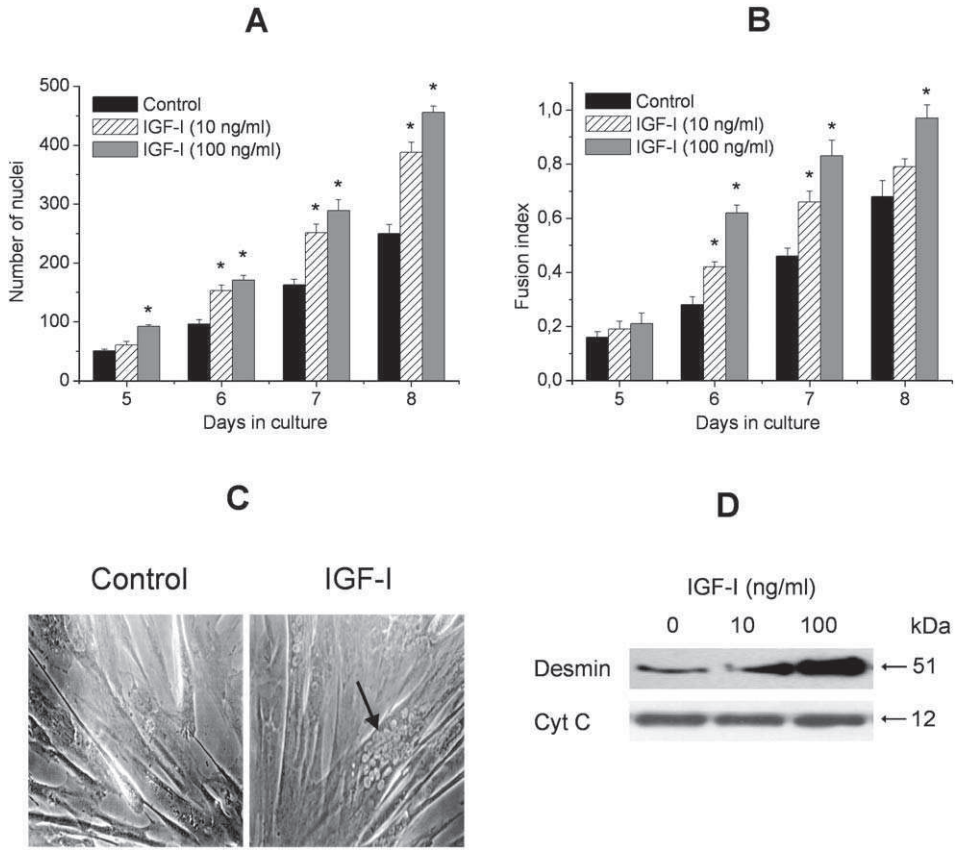

Fig. 1. Effect of IGF-I on proliferation, fusion and desmin expression of cultured primary human skeletal muscle cells. Cells were daily treated with different doses of IGF-I or DMSO (as control) from day 3 of culturing, and counting of the number of nuclei (A) and the calculation of the fusion index (B) were performed as described under Materials and methods. All values are expressed as mean±S.E.M. Asterisks mark significant ($p<0.05$) differences when compared to the daily-matched controls. (C) Photomicrographs of control and IGF-I-treated (100 ng/ml) cultured human skeletal muscle cells at day 8. The arrow indicates a large, multinucleated myotube in the treated cultures. (D) Cells were daily treated with different doses of IGF-I from day 3 of culturing until day 14. Cells were then harvested, similar amounts of proteins were subjected to SDS-PAGE, and Western immunoblotting was performed using a mouse anti-desmin antibody as described under Materials and methods. To assess equal loading, nitrocellulose membranes were stripped and re-probed with a mouse anti-cytochrome *C* antibody (Cyt *C*). The figure is a representative of three individual experiments with similar results.

cellular responses (i.e., increases in proliferation and differentiation) induced by IGF-I treatment. The lack of involvement of the MAPK Erk-1/2 was also supported by that IGF-I, unlike fibroblast growth factor (FGF, which was used as a positive control based on previously published data [5]), caused no measurable phosphorylation of Erk-1/2 (Fig. 2C) reflecting the lack of activation. As a marked contrast, inhibition of the PKC system by 1 μM GF109203X (which concentration alone did not affect the basal growth of the cells) completely prevented the mitogenic action of IGF-I and its effect to increase desmin expression (Fig. 2A and B).

These data strongly suggested the lack of involvement of the MAPK and the PI3-K systems but the central role of the PKC pathway in mediating the action of IGF-I in primary human skeletal muscle cells. As was previously shown by our laboratory [22,23,31] (and also confirmed in this study, Fig. 3), primary human skeletal muscle cells in culture express six PKC isoenzymes: the calcium-dependent "conventional" cPKCα and γ; the calcium-independent "novel" nPKCδ, θ and η; and the "atypical" aPKCζ (for classification of PKC isoforms, see [32]). Therefore, the above findings with GF109203X (which is an inhibitor of both the cPKC and nPKC isoenzymes) [30] suggested that one (or more) PKC isoform(s) might play central roles in mediating the cellular actions of IGF-I on the human skeletal muscle cells.

To clarify this issue, in the next experiments, we first measured the effect of Gö6976, the selective inhibitor of the cPKC isoforms (in our case, the PKCα and γ) [33], on the IGF-I-mediated responses. Using similar approaches, we could not detect any changes in the stimulatory effect of IGF-I on growth and differentiation in the presence of 200 nM Gö6976 (Fig. 2D and E), which data argued for the lack of involvement of PKCα and γ in the cellular action of IGF-I.

We then continued our experiments with the investigation of the nPKC isoforms. As seen in Fig. 2D and E, the specific inhibition of PKCδ by Rottlerin [34], used at as low concentration as 500 nM which concentration alone did not modify proliferation and the expression of desmin, completely inhibited the effects of IGF-I, identically to the action of GF10920X (Fig. 2A and B). These findings strongly implicated a pivotal role of nPKCδ in mediating the cellular effects of IGF-I on primary human cultured skeletal muscle cells.

It is generally accepted that the PKC isoenzymes, upon activation, translocate into another intracellular (usually

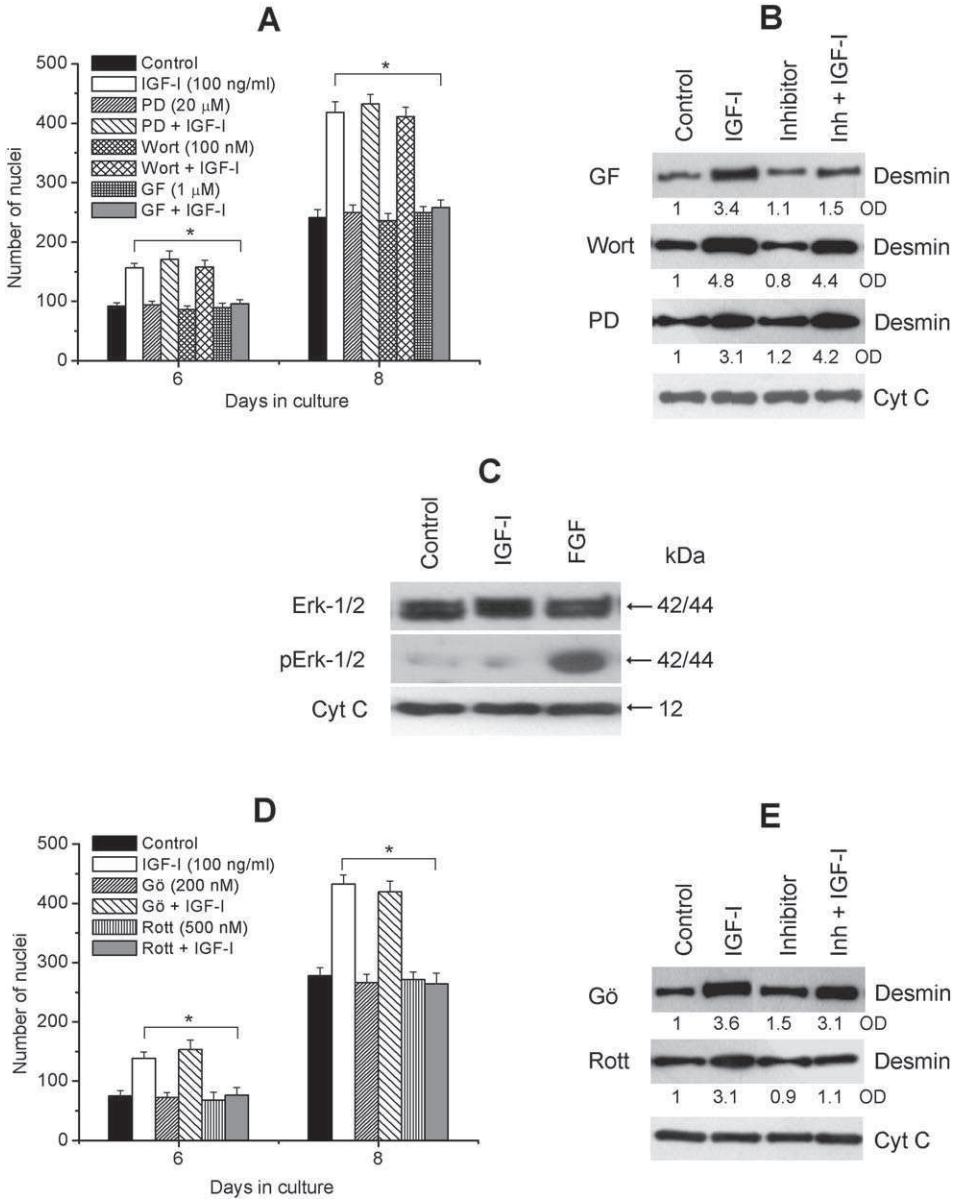

Fig. 2. Effect of the inhibition of the PKC, MAPK and PI-3K pathways on the actions of IGF-I on cultured primary human skeletal muscle cells. (A) From day 3 of culturing, cells were daily treated with 100 ng/ml IGF-I, or with various inhibitors such as 20 μM PD098059 (PD), 100 nM wortmannin (Wort), or 1 μM GF109203X (GF), or with the inhibitors and IGF-I together, then counting of the number of nuclei was performed. All values are expressed as mean±S.E.M. Asterisks mark significant ($p<0.05$) differences. (B) Cells were daily treated with the above combinations, then at day 14 cells were harvested, similar amounts of proteins were subjected to SDS-PAGE, and Western immunoblotting was performed against desmin. The amount of desmin in the different samples was quantitated by densitometry (optical density, OD) and expressed as relative numbers normalized to the OD value of immunoreactive bands of control groups without any treatment (regarded as OD 1). (C) At day 14 of culturing, cells were treated with 100 ng/ml of IGF-I or 10 ng/ml FGF for 30 min, then Western immunoblotting was performed using antibodies recognizing the MAPK Erk-1/2 or its phosphorylated form (pErk-1/2). (D) Cells were daily treated with 100 ng/ml IGF-I; or with various inhibitors such as 200 nM Gö6976 (Gö) or 500 nM Rottlerin (Rott); or with the inhibitors and IGF-I together, then counting of the number of nuclei was performed. All values are expressed as mean±S.E.M. Asterisks mark significant ($p<0.05$) differences. (E) Cells were daily treated with the above combinations, then, at day 14, Western immunoblotting was performed against desmin. The amount of desmin in the different samples was quantitated as described under point B. In the Western blot experiments (B, C, E), equal loading was assessed by determining the expression of cytochrome *C* (Cyt *C*). The Western blot data are representatives of at least three independent experiments for each inhibitor yielding similar results.

membrane) compartment [32,35]. In the next stage of our experiments, we, therefore, investigated the effect of IGF-I on the subcellular localization of the existing isoforms. As revealed by confocal microscopy, the application of 100 ng/ml IGF-I for 30 min did not modify the subcellular localization of PKCα, γ, η, θ and ζ (Fig. 3A). PKCα and η were found in the cytoplasm whereas PKCγ, θ and ζ in the cytoplasm and nucleus both in the control and IGF-I-treated cells. In contrast, we observed a marked subcellular translocation of PKCδ from the cytoplasm to the nucleus and to nuclear membrane upon IGF-I treatment (Fig. 3B). Consistent with the aforementioned findings with the specific PKCδ inhibitor Rottlerin (Fig. 2D and E), these observations further argued for the central role of this isoform in the cellular responses evoked by IGF-I.

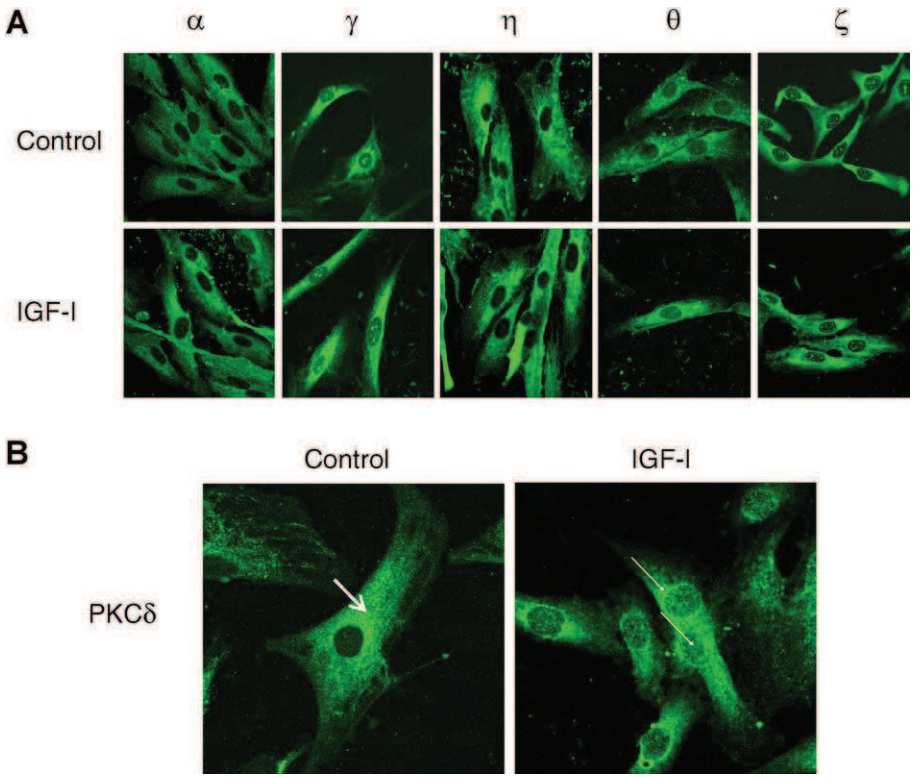

Fig. 3. Effect of IGF-I on the subcellular localization of the PKC isoforms in cultured primary human skeletal muscle cells. At day 7, cell cultures were treated with either DMSO (control) or with 100 ng/ml IGF-I for 30 min, then immunofluorescent staining of various PKC isoforms were employed using rabbit anti-PKC and FITC-conjugated, goat anti-rabbit antibodies. Images were acquired by a laser scanning confocal microscope using the "z-stack mode" with strictly the same antibody staining and visualization procedure (the second image from the level of the coverslips). (A) Lack of modification of subcellular localization of PKCα, γ, η, θ and ζ. (B) Translocation of PKCδ. In the control samples, PKCδ is mainly localized to the cytoplasm (opened arrow), whereas upon IGF-treatment, the isoform was translocated to the nucleus and to the nuclear membrane (solid arrows).

3.3. Besides the central involvement of PKCδ, the action of IGF-I is also mediated by the MAPK pathway on C2C12 myoblasts

In the next phase of our study, we repeated the above experiments on mouse C2C12 myoblasts. This cell line provided a fine tool, besides comparing our results on another skeletal muscle cell type, to expand the range of methods with additional biochemical and molecular biological techniques (applications of which were obscured by the very limited protein content and the lack of possibility for passaging of primary human cultures). BrdU proliferation ELISA assays revealed that IGF-I, very similarly to its action on human skeletal muscle cells, stimulated the cellular growth of C2C12 cells as well (Fig. 4A), which effect was paralleled by the formation of multinucleated myotubes in the sub-confluent cultures (Fig. 4B and C). In addition, the growth factor significantly elevated the expression of the differentiation marker desmin in the sub-confluent cultures (Fig. 4D), which, in the non-treated control cells, started to increase only with the onset of the high cell density-mediated differentiation program (data not shown).

Investigation of various putative signaling mechanisms in mediating the effect of IGF-I on C2C12 cells also revealed similar yet, of great importance, not identical data when compared to results with the primary human cultures. Namely, the mitogenic and differentiating actions of IGF-I on C2C12 myoblasts were completely antagonized by 1 μM GF109203X (an inhibitor of the PKC system) but were not affected by 100 nM wortmannin (blocker of the PI3-K pathway) (Fig. 5A and B). However, as a marked contrast to our data on the primary muscle cells, the presence of the MAP kinase inhibitor 20 μM PD098059 (which concentration alone negligibly affected the basal, IGF-I-independent growth of the cells) significantly, yet not completely (30–40% inhibition), prevented the effect of IGF-I (Fig. 5A and B). In addition, also in contrast to findings on primary human skeletal muscle cells (Fig. 2C), IGF-I treatment increased the phosphorylation levels of the MAPK Erk-1/2 (Fig. 6A) suggesting that the pathway was activated upon IGF-I application. These data demonstrated that, besides the PKC system, the MAP kinase pathway is also involved in the action of IGF-I on C2C12 myoblasts.

To clarify the roles of these two signaling mechanism, we first intended to identify that/those PKC isoenzyme(s) which might play a role in the IGF-I-mediated effects. Since previous findings only very superficially described the PKC isoform pattern of the C2C12 cell line [36], we first determined the expressions of the isoenzymes. As was revealed by Western blotting (and by RT-PCR and immunocytochemical methods, data not shown), C2C12 myoblasts possessed a very similar, but notably not an identical PKC isoform pattern to that of the primary human skeletal muscle cells. Namely, we were able to detect the expression of cPKCα and β, the nPKCδ, θ and η,

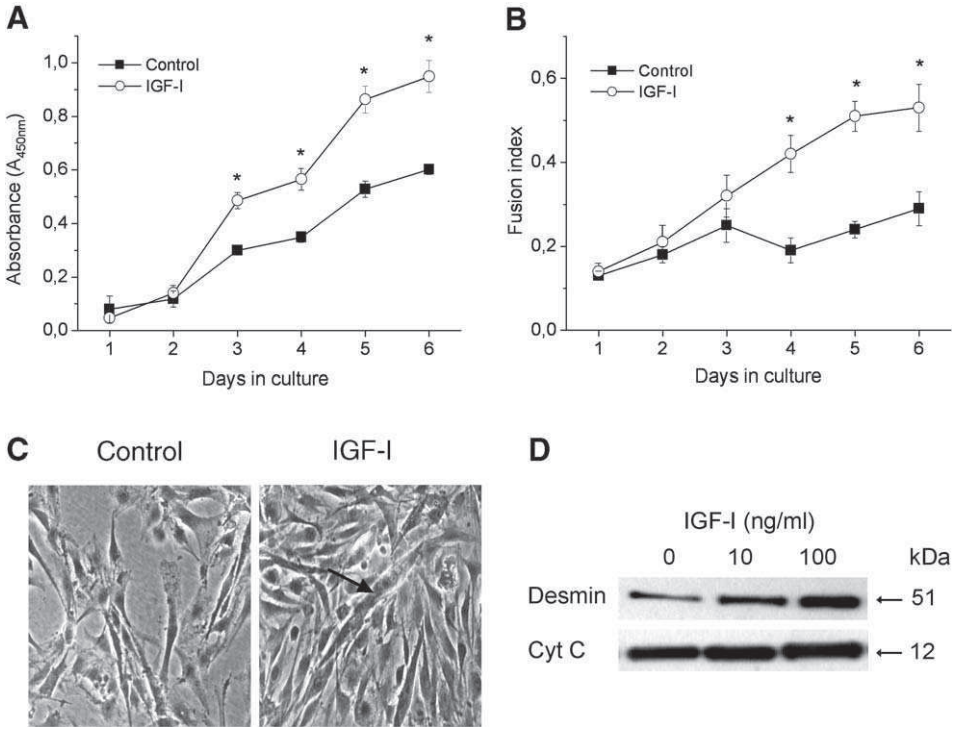

Fig. 4. Effects of IGF-I on proliferation, fusion and desmin expression of cultured C2C12 myoblasts. C2C12 myoblasts, growing in 96-well (A) or 12-well (B) microtiter plates, were daily treated with 100 ng/ml IGF-I or DMSO (as control) from day 1 of culturing, then the cellular proliferation (using BrdU assays, A) and the fusion index (B) were determined. In both cases, points represent the mean±S.E.M. of quadruplicate determinations in one representative experiment. At least three additional experiments yielded similar results. (C) Photomicrographs of control and IGF-I-treated (100 ng/ml) C2C12 cells at day 4 where the confluence of the control cultures was around 50–60%. The arrow indicates a large, multinucleated myotube in the treated cultures. (D) Cells were daily treated with different doses of IGF-I from day 1, then, at day 6 (at about 70–80% confluence), Western immunoblotting was performed to determine desmin and (after membrane stripping) cytochrome *C* (Cyt *C*) expressions. The figure is a representative of three individual experiments with similar results.

and the aPKCζ (Fig. 5C), but not of the cPKCγ, nPKCε and aPKCλ/ι (data not shown).

We then investigated the effects of various PKC (isoform) inhibitors on the IGF-I-induced cellular responses. As seen in Fig. 5B and D, identically to those found on the human muscle cells (Fig. 2D and E), 500 nM Rottlerin, the inhibitor of PKCδ, completely suspended the action of IGF-I (without affecting basal growth rate), whereas 200 nM Gö6976, the inhibitor of the cPKCs (in this case of PKCα and β), did not modify the cellular effects of the growth factor.

These data strongly argued for the central involvement of PKCδ in the above processes. To further test this hypothesis, the following multi-step biochemical and molecular biological approach was used. We first investigated whether IGF-I treatment affected the tyrosine-phosphorylation of PKCδ, a generally accepted phenomenon of activation [26,37]. As revealed by immunoprecipitation of PKCδ followed by Western blotting using a phosphotyrosine-specific antibody, the growth factor significantly elevated the tyrosine-phosphorylation level of PKCδ (Fig. 6B) with not measurable effects on the other PKCs (data not shown).

In addition, exploiting the ability of C2C12 myoblasts to be continuously passaged, we established such C2C12 cells, which stably overexpress a constitutively active recombinant PKCδ or a kinase (dominant) negative mutant of the isoform (DN-PKCδ) (for control, we used empty vector-transfected cells). We first examined the efficacy of recombinant overexpression. Cell lysates of pooled cultures and several transfected clones (data not shown) were subjected to Western blotting. Using an anti-PKCε antibody, which recognizes the ε-tag sequence of the recombinant, expressed PKCδ and DN-PKCδ (and, theoretically, the approximately 90 kDa endogenous PKCε which is not found in C2C12 myoblasts, see above), we were able to specifically detect the transfected enzymes (Fig. 7A). Furthermore, using an anti-PKCδ antibody, we found that the level of the recombinant proteins was approximately three- to four-fold higher than that of the endogenous PKCδ (Fig. 7A).

Using BrdU assays, we then compared the growth properties of control and overexpresser C2C12 cells. As seen in Fig. 7B, cells overexpressing PKCδ possessed a markedly accelerated proliferation rate when compared to the growth of control C2C12 cells. Actually, overexpression of PKCδ resulted in a very similar growth acceleration to that seen when control C2C12 cells were treated by IGF-I. In addition, IGF-I treatment of PKCδ overexpressers resulted in no further increase of proliferation, suggesting that the constitutive activation of nPKCδ mimicked the mitogenic effect of IGF-I on these cells.

The overexpression of DN-PKCδ resulted in opposite changes in the growth rate of the cells. Namely, the presence of the mutant isoform dramatically suppressed the proliferation of the cells when compared to the growth of the control myoblasts (Fig. 7B). In addition, IGF-I was unable to induce any

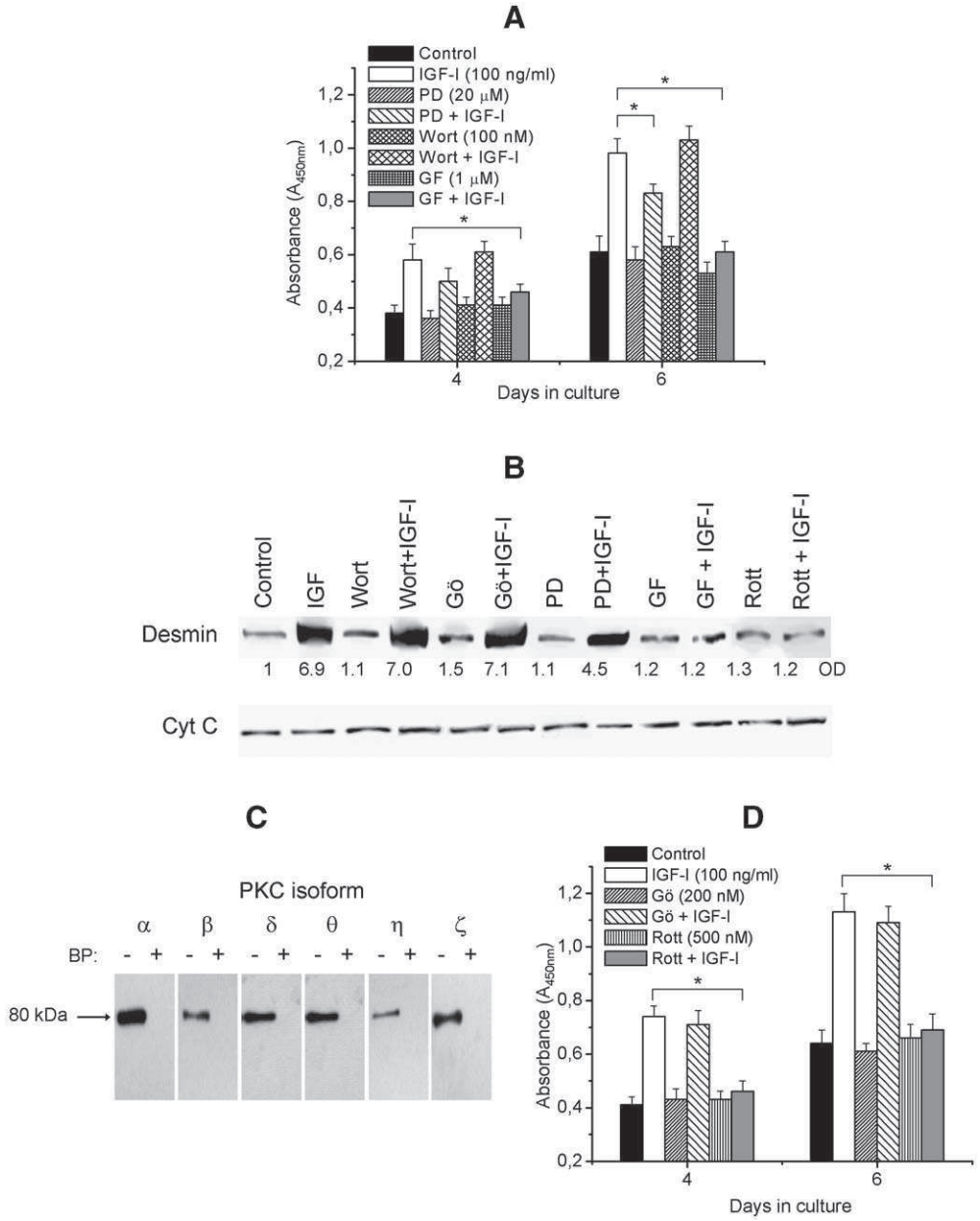

Fig. 5. Effect of the inhibition of the PKC, MAPK and PI-3K pathways on the actions of IGF-I on cultured C2C12 myoblasts. C2C12 cells were daily treated with 100 ng/ml IGF-I, or with various inhibitors such as 20 μM PD098059 (PD), 100 nM wortmannin (Wort) or 1 μM GF109203X (GF) (A, B); or with 200 nM Gö6976 (Gö) or 500 nM Rottlerin (Rott) (B, D); or with the inhibitors and IGF-I together, then quadruplicate BrdU assays were daily performed to assess cellular proliferation (A, D). All values are expressed as mean±S.E.M. Asterisks mark significant ($p<0.05$) differences. (B) Alternatively, cells were harvested at day 6 (at about 70–80% confluence) and Western immunoblotting was performed to determine desmin and (after membrane stripping) cytochrome *C* (Cyt *C*) expressions. The amount of desmin in the different samples was quantitated by densitometry (optical density, OD) and expressed as relative numbers normalized to the OD value of immunoreactive bands of control groups without any treatment (regarded as OD 1). Data are representatives of at least three independent experiments for each inhibitor yielding similar results. (C) Determination of the PKC isoform pattern of C2C12 cells at day 6 using Western blotting. To assess specificity of staining, samples were immunolabeled using appropriate primary antibodies with (+) or without (−) pre-absorption with the control blocking peptides (BP).

growth stimulation on these cells further arguing for that PKCδ is an obligatory element of the signaling pathway evoked by IGF-I.

3.4. PKCδ is an upstream regulator of the MAPK pathway in mediating the action of IGF-I on C2C12 myoblasts

The above results obtained with the overexpressers (i.e., PKCδ is a crucial mediator of the IGF-I signaling), along with those findings that Rottlerin (inhibitor of PKCδ) completely prevented the proliferative action of IGF-I whereas PD098059 (inhibitor of the MAPK pathway) only partially suspended the effect of IGF-I, argued for a possible relationship between PKCδ and the MAPK signaling. To investigate this hypothesis, we measured the effect of Rottlerin on the action of IGF-I to modify phosphorylation levels of PKCδ and the MAPK Erk-1/2. As was expected, the presence of 500 nM Rottlerin did not modify the effect of IGF-I to increase the

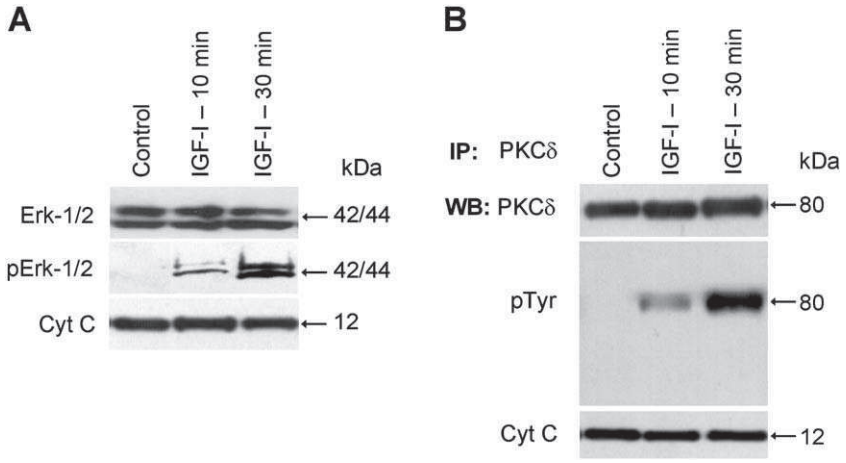

Fig. 6. Effects of IGF-I on the phosphorylation of the MAPK Erk-1/2 and on the tyrosine phosphorylation of PKCδ on cultured C2C12 myoblasts. (A) C2C12 cells were treated with 100 ng/ml IGF-I for 10 or 30 min and then Western blotting was performed to reveal expressions of the MAPK Erk-1/2, its phosphorylated form (pErk-1/2) and (to assess equal loading) cytochrome *C* (Cyt *C*). (B) C2C12 myoblasts were treated similarly, then immunoprecipitation (IP) was performed (as described under Materials and methods) using an anti-PKCδ antibody. Samples were then subjected to Western blotting (WB) using antibodies against phosphotyrosines (to determine the level of tyrosine phosphorylation of PKCδ), PKCδ (to determine the efficacy of immunoprecipitation) and cytochrome *C* (Cyt *C*, to further assess equal loading).

tyrosine phosphorylation of PKCδ (Fig. 8A). Of greatest importance, however, the specific PKCδ inhibitor significantly suppressed the IGF-I-induced phosphorylation of Erk-1/2 (Fig. 8B) suggesting that the effect of IGF-I to stimulate the phosphorylation of Erk-1/2 is PKCδ-dependent.

Finally, we investigated the effects of the two inhibitors on the proliferation of C2C12 myoblasts overexpressing the constitutively active PKCδ isoform. As seen in Fig. 8C, the accelerated proliferation of nPKCδ overexpressers was partially yet significantly (approximately by 35–40%) inhibited by 20 μM PD098059 very similarly to the effect of the inhibitor to suppress the mitogenic effect of IGF-I on control C2C12 cells (Fig. 5A and B). Furthermore, as was predictable, 500 nM Rottlerin exerted a complete inhibition of the increased growth of the PKCδ overexpressers, "back" to the level of the proliferation of the control C2C12 myoblast (Fig. 8C). These data strongly argue for the intimate relationship between PKCδ and the MAPK-coupled signaling and introduce PKCδ as an upstream activator of the MAPK pathway in mediating the cellular effects of IGF-I on C2C12 myoblasts.

4. Discussion

In this study, we investigated the effects of IGF-I on growth properties of cultured human skeletal muscle cells and C2C12 myoblasts and the participation of various signal

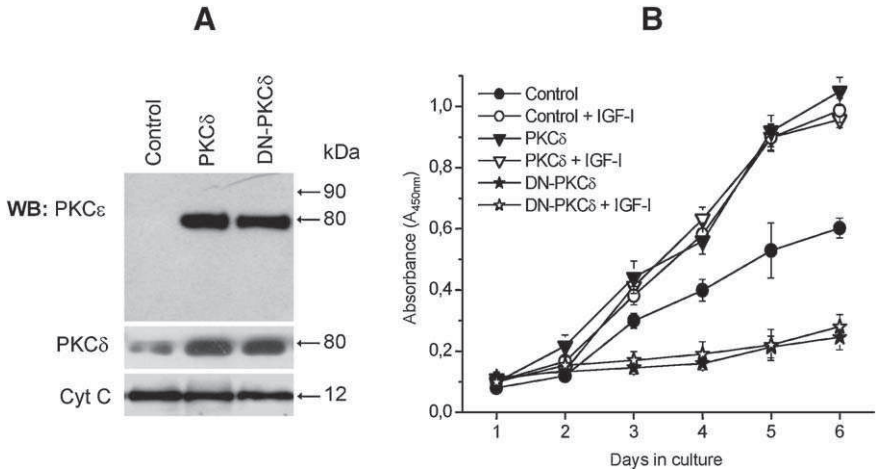

Fig. 7. Effect of the overexpression of the constitutively active and the kinase-negative mutant of PKCδ on control and IGF-I-induced growth of C2C12 myoblasts. (A) Determination of efficacy of overexpression. C2C12 cells stably overexpressing PKCδ, its kinase-negative mutant (DN-PKCδ) or the empty vector (Control) were harvested at day 6, and Western immunoblotting (WB) was performed using either an anti-PKCε antibody recognizing the ε-tag of the overexpressed PKCs; or with an anti-PKCδ antibody to determine the level of overexpression; or with an anti-cytochrome *C* (Cyt C) antibody to assess equal loading. (B) The above overexpresser cells were seeded at densities of 1000 cells/well in 96-well microtiter plates and were daily treated with 100 ng/ml IGF-I or vehicle. Cell proliferation was then daily determined using BrdU assays. Points represent the mean±S.E.M. of quadruplicate determinations in a representative experiment. Three additional experiments yielded identical results.

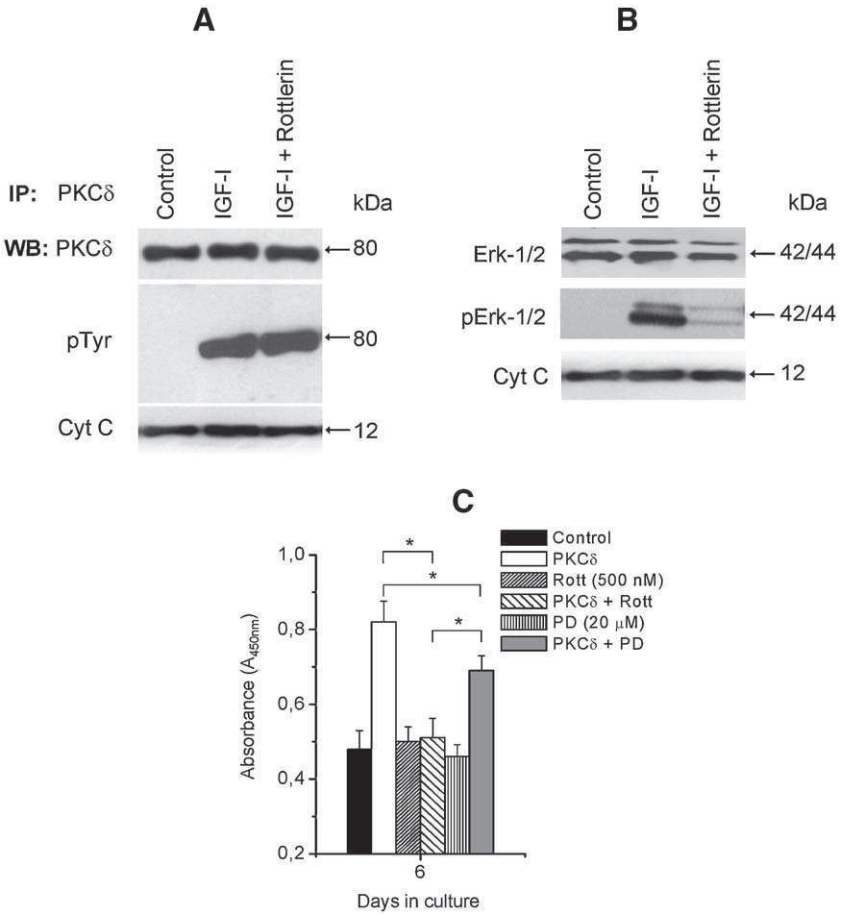

Fig. 8. Effect of various inhibitors on the phosphorylation of PKCδ and the MAPK Erk-1/2 and on the growth of C2C12 myoblasts overexpressing PKCδ. (A) C2C12 myoblasts were treated with vehicle, 100 ng/ml IGF or IGF-I plus 500 nM Rottlerin for 30 min, then immunoprecipitation (IP) was performed using an anti-PKCδ antibody. Samples were then subjected to Western blotting (WB) using antibodies against phosphotyrosines (to determine the level of tyrosine phosphorylation of PKCδ), PKCδ (to determine the efficacy of immunoprecipitation) and cytochrome *C* (Cyt *C*, to further assess equal loading). (B) C2C12 cells were treated similarly and then Western blotting was performed to reveal expressions of the MAPK Erk-1/2, its phosphorylated form (pErk-1/2) and cytochrome *C* (Cyt *C*). (C) C2C12 cells stably overexpressing PKCδ or the empty vector (control) were seeded at densities of 1000 cells/well in 96-well microtiter plates and daily treated with vehicle, 500 nM Rottlerin (Rott) or 20 μM PD098059. Cell proliferation was then daily determined (the figure shows data obtained at day 6) using BrdU assays. Points represent the mean±S.E.M. of quadruplicate determinations in a representative experiment. Asterisks mark significant ($p<0.05$) differences. Three additional experiments yielded identical results.

transduction systems in mediating the effect of the growth factor. Here we provide the first evidence that the action of IGF-I to stimulate proliferation and differentiation of human skeletal muscle cells (Fig. 1) is exclusively mediated by PKCδ but not by the other existing PKC isoforms or by the MAPK or the PI-3K pathways. This argument was supported by the following data: (1) the effect of IGF-I was completely inhibited by the PKCδ-specific inhibitor Rottlerin but not by the inhibitor of the "conventional" PKCα and γ isoforms or by inhibitors of the MAPK or the PI-3K pathways (Fig. 2); (2) IGF-I caused the selective translocation of PKCδ, presumably reflecting activation of the isoform (Fig. 3) [32,35]. Since such factors of myogenic proliferation and differentiation as myogenin and MyoD are under the strict, phosphorylation-mediated regulation, for example by the PKC system [38,39], the nuclear–perinuclear targeting of PKCδ by IGF-I may be a key step in initiating the mitogenic effect of the growth factor; (3) IGF-I did not stimulate the phosphorylation of the MAPK Erk-1/2 (Fig. 2).

According to our best knowledge, previously, only Foulstone et al. [8] have investigated the cellular signaling mechanism of IGF-I on human cultured skeletal muscle cells. In contrast to our findings, they have shown that both the MAPK and PI3-K pathways are involved in mediating the action of IGF-I. However, since (1) they used non-separated human myoblast of passages from 2 to 6 and cultivated them on gelatin, whereas we employed "strictly" fibroblast-free primary satellite cell cultures; (2) their cells were cultured in low serum (i.e., differentiating) media in which IGF-I was unable to promote myotube formation (in contrast to our data showing that IGF-I was an effective stimulator of fusion, see Fig. 1); (3) they did not measure at all the possible role of the PKC isoenzymes; the dissimilarities between their and our data are most probably due to the differences seen in the technical and culturing conditions.

Investigation of the IGF-I-coupled signaling on C2C12 myoblasts revealed similar, yet notably, not identical findings. We have shown that (1) the growth-promoting effect of IGF-I

was completely abrogated by the selective inhibition of PKCδ but not by the inhibitors of the cPKCs or the PI-3K system (Fig. 5); (2) IGF-I initiated the selective tyrosine phosphorylation of PKCδ, a putative sign of activation [32,35,37] (Fig. 6); (3) the recombinant overexpression of constitutively active form of PKCδ stimulated cellular growth and mimicked the proliferative action of IGF-I (Fig. 7); (4) the recombinant overexpression of kinase inactive form of PKCδ (DN-PKCδ) inhibited proliferation of C2C12 cells and completely prevented the development of the IGF-I-induced effects (Fig. 7). These data strongly argued for the central involvement of PKCδ in the development of IGF-I-specific mechanism in C2C12 cells as well.

However, on C2C12 myoblasts (as was previously suggested by Milasincic et al. [5]), we also found that the MAPK pathway is additionally involved in mediating the cellular action of IGF-I. This conclusion was supported by that the effect of IGF-I to promote cellular growth was partially (yet significantly) inhibited by the inhibitor of the MAPK (Fig. 5) and that IGF-I increased the activity-dependent phosphorylation of the MAPK Erk-1/2 (Fig. 6). Furthermore, since (1) the inhibition of PKCδ completely whereas that of the MAPK only partially prevented the mitogenic effect of IGF-I (Fig. 5); (2) the PKCδ inhibitor Rottlerin effectively inhibited the action of IGF-I to increase phosphorylation of Erk-1/2 (Fig. 8); (3) the accelerated growth of C2C12 myoblasts overexpressing PKCδ was partially inhibited by the MAPK inhibitor PD098059 (Fig. 8); our findings also indicated that the involvement of the MAPK system requires the preceding IGF-I-mediated activation of PKCδ, introducing the isoform as an "upstream" regulator of the MAPK pathway.

The role PKCδ (similarly to other PKC isoenzymes) was very often documented as a central signaling molecule coupled to tyrosine-kinase receptor activation by various growth factors. In keratinocytes, for example, PKCδ was shown to possess a cross-talk with the epidermal growth factor signaling pathway [40] and also mediated the proliferative effect of insulin [41], similarly to that seen on cultured rat muscle cells [42]. In addition, of great importance, this isoform functioned as a central element of the IGF-I-mediated cellular responses (such as migration and cell transformation) in fibroblasts and colonic epithelial cells [43,44]. In the frame of our current presentation, it appears, therefore, that PKCδ indeed plays a key role in mediating the IGF-I-coupled effect on numerous cell types, including skeletal muscle cells of various origins.

Finally, the experimental series presented in this report revealed another rather intriguing phenomenon. The PKCδ isoform was very often implicated in the regulation of cellular proliferation and differentiation of numerous cell types [45]. However, in most studies (for example, in human keratinocytes [24,31] and fibroblast [25,26,46]), the isoform was suggested to stimulate differentiation and to inhibit proliferation. Up to date, PKCδ was shown to stimulate proliferation (acting as a prosurvival factor) only in certain breast cancer cell lines [47]. Therefore, our current additional findings–i.e., overexpression of the constitutively active PKCδ stimulated whereas the kinase inactive DN-PKCδ mutant inhibited cellular growth of C2C12 myoblasts (along with our unpublished observations that nPKCδ overexpresser C2C12 cells, when injected to immunodeficient mice, initiated the development of large, malignantly transformed tumors, in contrast to control C2C12 myoblasts which induced benign tumors of much smaller size; Czifra et al., manuscript in preparation) (Fig. 7)–introduce nPKCδ as a novel significant player in skeletal muscle biology positively controlling cellular growth.

Acknowledgements

The technical assistance of Ms. Ibolya Varga is gratefully appreciated. This work was supported in part by Hungarian research grants: OTKA TS040773, OTKA T049231, NKFP 1A/008/04, RET 06/2004 and ETT 365/2003.

References

[1] G.R. Adams, J. Appl. Physiol. 93 (2002) 1159.
[2] D.J. Glass, Nat. Cell Biol. 5 (2003) 87.
[3] J.G. Tidball, J. Appl. Physiol. 98 (2005) 1900.
[4] A.A. Butler, S. Yakar, I.H. Gewolb, M. Karas, Y. Okubo, D. LeRoith, Comp. Biochem. Physiol., B. Biochem. Mol. Biol. 121 (1998) 19.
[5] D.J. Milasincic, M.R. Calera, S.R. Farmer, P.F. Pilch, Mol. Cell. Biol. 16 (1996) 5964.
[6] R.M. Palmer, M.G. Thompson, R.M. Knott, G.P. Campbell, A. Thom, K.S. Morrison, Biochim. Biophys. Acta 1355 (1997) 167.
[7] A. Zorzano, P. Kaliman, A. Guma, M. Palacin, Cell. Signal. 15 (2003) 141.
[8] E.J. Foulstone, C. Huser, A.L. Crown, J.M.P. Holly, C.E.H. Stewart, Exp. Cell Res. 294 (2004) 223.
[9] V. Jacquemin, D. Furling, A. Bigot, G.S. Butler-Brown, V. Mouly, Exp. Cell Res. 299 (2004) 148.
[10] K.A. Reardon, J. Davis, R.M. Kapsa, P. Choong, E. Byrne, Muscle Nerve 24 (2001) 893.
[11] S.W. Jones, R.J. Hill, P.A. Krasney, B. O'Conner, N. Peirce, P.L. Greenhaff, FASEB J. 18 (2004) 1025.
[12] M.D. Grounds, Pathol. Res. Pract. 187 (1991) 1.
[13] I. Husmann, L. Soulet, J. Gautron, I. Martelly, D. Barritault, Cytokine Growth Factor Rev. 7 (1996) 249.
[14] E. Vlachopapadopoulou, J.J. Zachwieja, J.M. Gertner, D. Manzione, D.M. Bier, D.E. Matthews, E. Slonim, J. Clin. Endocrinol. Metab. 80 (1995) 3715.
[15] D. Furling, A. Marette, J. Puymirat, Endocrinology 140 (1999) 4244.
[16] E.D. Rabinovsky, E. Gelir, S. Gelir, H. Lui, M. Kattash, F.J. DeMayo, S.M. Shenaq, R.J. Schwartz, FASEB J. 17 (2003) 53.
[17] J. Dupont, D. LeRoith, Horm. Res. 55 (2001) 22.
[18] I.M. Kramer, in: J.C. Foreman, T. Johansen T. (Eds.), Textbook of Receptor Pharmacology, CRC Press, NewYork, 1996, p. 255.
[19] T. Tsakiridis, E. Tsiani, P. Lekas, A. Bergman, V. Cherepanov, C. Whiteside, G.P. Downey, Biochem. Biophys. Res. Commun. 288 (2001) 205.
[20] S. Haq, H. Kilter, A. Michael, J. Tao, E. O'Leary, X.M. Sun, B. Walters, K. Bhattacharya, X. Chen, L. Cui, M. Andreucci, A. Rosenzweig, J.L. Guerrero, R. Patten, R. Liao, J. Molkentin, M. Picard, J.V. Bonventre, T. Force, Nat. Med. 9 (2003) 944.
[21] N. Tiffin, S. Adi, D. Stokoe, N.Y. Wu, S.M. Rosenthal, Endocrinology 145 (2004) 4991.
[22] J. Boczán, S. Boros, F. Mechler, L. Kovács, T. Bíró, Acta Neuropathol. 99 (2000) 96.
[23] J. Boczán, T. Bíró T, G. Czifra, J. Lázár, H. Papp, H. Bárdos, R. Ádány, F. Mechler, L. Kovács, Acta Neuropathol. 102 (2001) 55.
[24] H. Papp, G. Czifra, E. Bodó, J. Lázár, I. Kovács, M. Aleksza, I. Juhász, P. Ács, S. Sipka, L. Kovács, P.M. Blumberg, T. Bíró T., Cell Mol. Life Sci. 61 (2004) 1095.

[25] P. Ács, K. Bögi, A.M. Marquez, P.S. Lorenzo, T. Bíró, Z. Szállási, P.M. Blumberg, J. Biol. Chem. 272 (1997) 22148.
[26] P. Ács, Q.J. Wang, K. Bögi, A.M. Marquez, P.S. Lorenzo, T. Bíró, Z. Szállási, J.F. Mushinski, P.M. Blumberg, J. Biol. Chem. 272 (1997) 28793.
[27] L. Li, P.S. Lorenzo, K. Bögi, P.M. Blumberg, S.H. Yuspa, Mol. Cell. Biol. 19 (1999) 8547.
[28] Z. Oláh, C. Lehel, G. Jakab, W.B. Anderson, Anal. Biochem. 221 (1994) 94.
[29] A. Bornemann, H. Schmalbruch, Muscle Nerve 15 (1992) 14.
[30] D. Toullec, P. Pianetti, H. Coste, P. Bellevergue, T. Grand-Perret, M. Ajakane, V.B. Baudet, P. Boissin, E. Boursier, F. Loriolle, L. Duhamel, D. Charon, J. Kirilovsky, J. Biol. Chem. 266 (1991) 15771.
[31] T. Bíró, G. Czifra, E. Bodó, J. Lázár, I.B. Tóth, H. Papp, I. Kovács, I. Juhász, L. Kovács, J. Invest. Dermatol. 122 (2004) A21.
[32] Y. Nishizuka, Intracellular signaling by hydrolysis of phospholipids and activation of protein kinase C, Science 258 (1992) 607.
[33] G. Martiny-Baron, M.G. Kazanietz, H. Mischak, P.M. Blumberg, G. Kochs, H. Hug, D. Marme, C. Schachtele, J. Biol. Chem. 268 (1993) 9194.
[34] M. Gschwendt, H.J. Muller, K. Kielbassa, R. Zang, W. Kittstein, G. Rincke, F. Marks, Biochem. Biophys. Res. Commun. 199 (1994) 93.
[35] S. Jaken, Curr. Opin. Cell Biol. 8 (1996) 18.
[36] E. Meacci, V. Vasta, C. Donati, M. Farnararo, P. Bruni, FEBS Lett. 457 (1999) 184.
[37] M. Blass, I. Kronfeld, G. Kazimirsky, P.M. Blumberg, C. Brodie, Mol. Cell. Biol. 22 (2002) 182.
[38] L. Li, J. Zhou, G. James, R. Heller-Harrison, M.P. Czech, E.N. Olson, Cell 71 (1992) 1181.
[39] L.N. Liu, P. Dias, P.J. Houghton, Cell Growth Differ. 9 (1998) 699.
[40] M.F. Denning, A.A. Dlugosz, C. Cheng, P.J. Dempsey, R.J. Coffey, D.W. Threadgill, T. Magnuson, S.H. Yuspa, Exp. Dermatol. 9 (2000) 192.
[41] S. Shen, A. Alt, E. Wertheimer, M. Gartsbein, T. Kuroki, M. Ohba, L. Braiman, S.R. Sampson, T. Tennenbaum, Diabetes 50 (2001) 255.
[42] L. Braiman, A. Alt, T. Kuroki, M. Ohba, A. Bak, T. Tennenbaum, S.R. Sampson, Mol. Endocrinol. 15 (2001) 565.
[43] W. Li, Y.X. Jiang, J. Zhang, L. Soon, L. Flechner, V. Kapoor, J.H. Pierce, L.H. Wang, Mol. Cell. Biol. 18 (1998) 5888.
[44] F. Andre, V. Rigot, M. Remacle-Bonnet, J. Luis, G. Pommier, J. Marvaldi, Gastroenterology 116 (1999) 64.
[45] M. Gschwendt, Eur. J. Biochem. 259 (1999) 555.
[46] Z. Lu, A. Hornia, Y.W. Jiang, Q. Zang, S. Ohno, D.A. Foster, Mol. Cell. Biol. 17 (1997) 3418.
[47] M.A. McCracken, L.J. Miraglia, R.A. McKay, J.S. Strobl, Mol. Cancer Ther. 2 (2003) 273.

XIV.

Experimental Dermatology 2003: 12: 811–824
Blackwell Munksgaard . Printed in Denmark

EXPERIMENTAL DERMATOLOGY
ISSN 0906-6705

Protein kinase C isozymes regulate proliferation and high cell density-mediated differentiation in HaCaT keratinocytes

Papp H, Czifra G, Lázár J, Gönczi M, Csernoch L, Kovács L, Bíró T. Protein kinase C isozymes regulate proliferation and high cell density-mediated differentiation in HaCaT keratinocytes. Exp Dermatol 2003:12: 811–824. © Blackwell Munksgaard, 2003

Abstract: Protein kinase C (PKC) isoforms play pivotal roles in the regulation of differentiation of normal human epidermal keratinocytes (NHEK). In this study, we investigated the participation of the PKC system in the proliferation and high cell density-induced differentiation of the human immortalized keratinocyte line HaCaT. HaCaT keratinocytes possessed a characteristic PKC isoform pattern (PKCα, β, γ,δ,ε,η,θ,ζ), which altered during proliferation and differentiation. The GF109203X compound, a selective PKC inhibitor, suppressed the expressions of the late (granular cell) differentiation markers involucrin (INV) and filaggrin (FIL), and the terminal marker keratinocytes-specific transglutaminase-1 (TG), but did not affect the level of the early (spinous cell) marker keratin 10 (K10) and cellular proliferation. Phorbol 12-myristate 13-acetate (PMA), an activator of PKC, inhibited proliferation, elevated intracellular calcium concentration, decreased the expression of K10, and increased the expressions of INV, FIL, and TG. These data indicate that the endogenous activation of PKC regulates the expressions of the late differentiation markers, and that the exogenous activation of PKC by PMA results in the induction of terminal differentiation. Because the cellular effects of PMA were accompanied by differential down-regulations of the sensitive PKC isoforms in proliferating and differentiating cultures, our findings argue for the differential roles of the existing PKC isoforms in the regulation of cellular proliferation and high cell density-induced differentiation of HaCaT cells.

Helga Papp[1], Gabriella Czifra[1], József Lázár[1], Mónika Gönczi[1,2], László Csernoch[1,2], László Kovács[1,2] and Tamás Bíró[1,2]

[1]Department of Physiology and
[2]Cell Physiology Research Group of the Hungarian Academy of Sciences, University of Debrecen, Medical and Health Science Center, Medical Faculty, Hungary

Key words: human keratinocytes – HaCaT – differentiation – protein kinase C – isoenzymes

Tamás Bíró MD, PhD, Department of Physiology, Hungarian Academy of Sciences, University of Debrecen, Medical and Health Science Center, Medical Faculty, Hungary, H-4012 Debrecen, Nagyerdei krt. 98. PO Box 22
Tel.: +36 52 416 634
Fax: +36 52 432 289
e-mail: biro@phys.dote.hu

Accepted for publication 18 November 2002

Introduction

The epidermis, the most superficial layer of the skin, forms a major physical–chemical barrier to protect the organism against environmental factors. The structure and the function of the epidermis are maintained by a well-defined and -balanced program of proliferation and differentiation of the keratinocytes resulting in the basal, spinous, granular, and cornified layers (1). Once differentiation is initiated, the basal keratinocytes cease their proliferation and move toward the cornified layer. The process of differentiation can be investigated thoroughly by measuring the sequential appearance of various differentiation markers representing different stages of differentiation. Namely, keratins (K) 5 and 14 representing the basal layer will be exchanged to K1 and K10 in the spinous layer (1). Later, in the granular layer, these intracellular proteins will be shifted to involucrin (INV), filaggrin (FIL), and loricrin, which serve as substrates for the keratinocyte-specific transglutaminase-1 (TG) to form the chemically resistant cornified envelope structures in the terminally differentiated keratinocytes (2–4).

Protein kinase C (PKC) comprises a family of serine/threonine kinases that play central roles in the regulation of various cellular processes in

Abbreviations: NHEK: normal human epidermal keratinocytes; PKC: protein kinase C; PMA: phorbol 12-myristate 13-acetate; DMSO: dimethyl sulfoxide; SDS: sodium dodecyl sulfate; PAGE: polyacrylamide gel electrophoresis; K: keratin; DMEM: Dulbecco's modified eagle's minimal essential medium; FCS: fetal calf serum; BrdU: bromo-deoxyuridine; PBS: phosphate-buffered saline; BCA: bicinchoninic acid.

numerous cell types (5–7). Up to date, at least 11 different PKC isozymes have been identified (5,8), which can be classified into the groups of the calcium- and phorbol ester-dependent 'conventional' (PKCα, βI, βII, and γ; cPKCs), the calcium-independent 'novel' (PKCδ, ε, η, and θ; nPKCs), the calcium- and phorbol ester-independent 'atypical' (PKCζ, and λ/ι; aPKCs) isoforms, and the unique PKCμ. These isoforms possess a characteristic expression pattern in a given cell type, and isozyme-specifically regulate various cellular processes including proliferation and differentiation (4,6,9). It was also postulated that not only may some PKC isoforms be active whereas others not for a given response, but different PKC isozymes may often have antagonistic effects on the same cellular event (10–12) suggesting differential regulatory roles of specific PKC isoforms.

Emerging evidence suggest the pivotal role of PKC in the regulation of the proliferation and differentiation of keratinocytes. Both normal human epidermal keratinocytes (NHEK) and murine keratinocytes express several PKC isoforms. The existence of PKCα, δ, ε, η, and ζ is well documented (13–16); however, other PKC isoforms (namely PKCβ, γ, and μ) were also found in various keratinocytes (14,17,18). It was also shown that the PKC expression levels and the subcellular localization of certain isoforms (representing changes in their activities) altered with calcium- or high cell density-induced differentiation (15,16). In addition, the activation of PKC by phorbol 12-myristate 13-acetate (PMA) resulted in the inhibition of proliferation and the induction of terminal differentiation both in mouse (19–21) and NHEK (22–24). Furthermore, the inhibition of the PKC activity by selective inhibitors GF109203X and Ro 31-7549 compounds modified the expression of various differentiation markers (16) and stimulated cellular proliferation (25) and [^{3}H]-thymidine incorporation (26) suggesting that the endogenous (constitutive) activation of PKC may also regulate the processes. Very recently, isozyme-specific roles of PKC regulating cellular proliferation and differentiation of keratinocytes were also described. For example, PKCδ and η isoforms were shown to inhibit cellular growth and induce differentiation in NHEK when expressed using adenoviral vectors (27, 28) whereas PKCα was implicated in the regulation of differentiation of normal and neoplastic keratinocytes (29).

The HaCaT cell line was developed by a spontaneous transformation from unaffected keratinocytes of a patient suffering from melanoma (30). The cells are immortal but yet non-tumorgenic (30,31), express various differentiation markers (such as K1,K10,INV,FIL), and maintain their differentiation capacity (32). There is very little known, however, about the function of the PKC system in HaCaT keratinocytes. It was documented that the inhibition of PKC results in morphological changes of cultured cells and alteration in the expressions of certain differentiation markers (33), and, furthermore, that the changes in the expression of PKCδ is associated with the tumorgenic transformation of the cell line (34). However, there is no direct evidence available about the possible regulatory roles of the PKC isoforms in the proliferation and differentiation of HaCaT cells.

To address this issue, in this study, we examined the different PKC isoforms expressed in HaCaT cells, and, furthermore, the cellular effects of pharmacological modification of the PKC activity on the cellular function. We report here that the characteristic PKC isozyme pattern of HaCaT cells changes with alterations in the proliferation and differentiation status of the cells. We also demonstrate that the activation or inhibition of PKC by pharmacological agents modifies the proliferation and differentiation of HaCaT cells, very similarly (yet not identically) to that seen in NHEK (16,22–25).

Materials and methods

Cell culture

The human immortalized HaCaT keratinocyte cell line was a kind gift from Professor Norbert E. Fusenig (Division of Differentiation and Carcinogenesis, German Cancer Research Center, Heidelberg, Germany). Cells were cultured in (Sigma), 2 mM L-glutamine, 50 U/ml penicillin, 50 mg/ml streptomycin, 1.25 mg/ml fungizone (all from Biogal, Debrecen, Hungary) at 37°C in a 5% CO_2 atmosphere. Cell cultures were usually initiated at approximately 20% confluence (proliferating cells) in 25-cm^2 or 75-cm^2 tissue culture flasks, reached 100% confluence usually at day 6 of culturing, and started the high cell density-mediated differentiation (differentiating cells).

Determination of viable cell numbers

The number of viable cells was determined by measuring the conversion of the tetrazolium salt MTT to formazan (Sigma). Cells were plated in 96-well multititer plates (5000 cells/well density) in quadruplicates and were treated with different concentrations of the agents investigated for the time indicated. Cells were then incubated with 0.5 mg/ml MTT for 2 h, and the concentration of formazan crystal (as the indicator of number of viable cells) was determined colorimetrically according to the manufacturer's protocol. Data are expressed as mean ± SEM.

Determination of cellular proliferation

Proliferation was measured using a bromo-deoxyuridine (BrdU) assay kit (Boehringer Mannheim, Mannheim, Germany). Cells were plated in 96-well multititer plates (5000 cells/well density) in

quadruplicates and were treated with different concentrations of the agents examined for the time indicated. Cells were then incubated with 10 mM BrdU for 4 h, and the cellular incorporation of BrdU (as the indicator of cellular proliferation) was determined colorimetrically according to the manufacturer's protocol. Data are expressed as mean ± SEM.

Antibodies

All primary antibodies against PKC isoenzymes were developed in rabbits and were shown to react specifically with the given PKC isoforms (35,36). Anti-PKCα, β, ε, η, and ζ were from Sigma, whereas anti-PKCγ, δ, θ, and λ from Santa Cruz (Santa Cruz, CA, USA). Specificity of anti-PKC antibodies was also tested by applying isoform-specific blocking peptides, which suspended the immunostaining in all cases (data not shown). Monoclonal mouse antibodies against K10 (Sigma) and K17 (Novocastra, Benton Lane, Newcastle-upon-Tyne, UK), and against INV (Sigma), FIL (Biomedical Technologies, Inc., Stoughton, MA, USA), and TG (Biomedical Technologies, Inc.) were used as markers of keratinocyte differentiation.

Western blot analysis

Cells were washed with ice-cold phosphate-buffered saline (PBS), harvested in homogenization buffer [20 mM Tris–HCl, 5 mM EGTA, 1 mM 4-(2-aminoethyl)benzenesulfonyl fluoride, 20 mM leupeptin, pH 7.4; all from Sigma] and disrupted by sonication on ice. The protein content of samples was measured by a modified bicinchoninic acid (BCA) protein assay (Pierce, Rockford, IL, USA). Total cell lysates were mixed with SDS–PAGE sample buffer and boiled for 10 min at 100°C. The samples were subjected to sodium dodecyl sulfate–polyacrylamide gel electrophoresis (SDS-PAGE) according to Laemmli (37) (8% gels were loaded with 20–30 mg protein per lane) and transferred to nitrocellulose membranes (Bio-Rad, Wien, Austria). Membranes were then blocked with 5% dry milk in PBS and probed with the appropriate primary antibodies against the given PKC isoform or differentiation marker. Peroxidase-conjugated goat anti-rabbit and anti-mouse IgG antibodies (Bio-Rad) were used as secondary antibodies, and the immunoreactive bands were visualized by an ECL Western blotting detection kit (Amersham, Little Chalfont, UK) on light sensitive films (AGFA, Brussels, Belgium). The immunoblots were then subjected to densitometric analysis as described previously (38). Normalized densitometric values of the individual lanes in several independent experiments were then averaged and expressed as mean ± SEM.

Immunofluorescence analysis and confocal microscopy

Cultured HaCaT cells were washed with PBS, fixed in acetone for 5 min at 4°C, air dried, and blocked at room temperature for 30 min in blocking solution containing 0.6% Triton X-100 and 1% BSA. Cells were incubated with the appropriate rabbit anti-PKC antibodies for 2 h (diluted usually 1 : 50–100 in blocking solution). The samples were then incubated for 1 h with a biotin-conjugated goat anti-rabbit IgG (diluted 1 : 300 in PBS, Vector, Burlington, VA, USA) and Streptavidin-conjugated Texas Red (diluted 1 : 50 in PBS, Amersham) for an additional hour. The resulted red fluorescence of PKC isozymes was studied by either a Zeiss Opton fluorescence microscope or by a Zeiss MicroSystem Laser Scanning confocal microscope (Zeiss, Oberkochen, Germany).

Calcium imaging

Changes in intracellular calcium concentration ($[Ca^{2+}]_i$) were detected as described in our earlier report (39). In brief, a calcium sensitive probe was introduced into the intracellular space by incubating the keratinocytes with 5 μM fura-2 AM for 1 h at 37°C. Before each measurement, the cells were kept at room temperature (22–24°C) in normal Tyrode's solution (in mM; 137 NaCl, 5.4 KCl, 0.5 $MgCl_2$, 1.8 $CaCl_2$, 11.8 HEPES-NaOH, 1 g/l glucose, pH 7.4) for a half an hour to allow homogeneous distribution of the dye. The coverslips, containing the fura-2 loaded cells, were then placed on the stage of an inverted fluorescence microscope (Diaphot, Nikon, Tokyo, Japan). Excitation was altered between 340 and 380 nm using a dual wavelength monochromator (Deltascan, Photon Technology International, New Brunswick, NJ, USA). The emission was monitored at 510 nm with a photomultiplier at an acquisition rate of 10 Hz per ratio. Resting $[Ca^{2+}]_i$ levels were calculated according to the method of Grynkiewicz et al. (40) from the ratio ($R = F_{340}/F_{380}$) of the fluorescence intensities measured with excitation wavelength being 340 (F_{340}) and 380 nm (F_{380}) as described earlier (1) ($K_d = 76$ nM; Rmin = 0.42; Rmax = 8.6; $F_{380}[0]/F_{380}[Ca] = 15.3$). The resting $[Ca^{2+}]_i$ levels of usually 20 cells/coverslip were determined, and the values were then averaged and expressed as mean ± SEM. Statistical analysis was performed using a Student's *t*-test.

Results

The characteristic PKC isozyme pattern of HaCaT keratinocytes changes during proliferation and differentiation

We firstly determined the PKC isozyme pattern of HaCaT keratinocytes. Immunohistochemical analysis of cultures having approximately 80% confluence (Fig. 1) revealed that HaCaT cells express seven isoforms of PKC: the cPKCα and β; the nPKCδ, ε, η, and θ; and the aPKCζ. This expression pattern was also proven by parallel Western blotting (Fig. 2). In this case, the application of the above antibodies resulted in mostly individual immunostained bands (the exception was the anti-PKCα which also marked the catalytic subunit of the isoform). However, we were unable to detect any expression of PKCλ, whereas in the case of PKCγ, we very rarely obtained specific immunosignals (therefore, result with the PKCγ were not incorporated to this study) (data not shown).

We then measured whether the expression levels of surely expressed different isoforms alter during cellular proliferation and differentiation. Using the Western blot technique and by loading the same amounts of protein into each well (thus by normalizing the intensities of the immunoreactive bands to cell protein), we were able to detect differential changes in expression patterns of different PKC isoforms (Fig. 2). The expressions of certain isoforms (PKCα,β,η,θ, and ζ) did not alter significantly during the process of culturing. In contrast, the expression of PKCδ reached marked

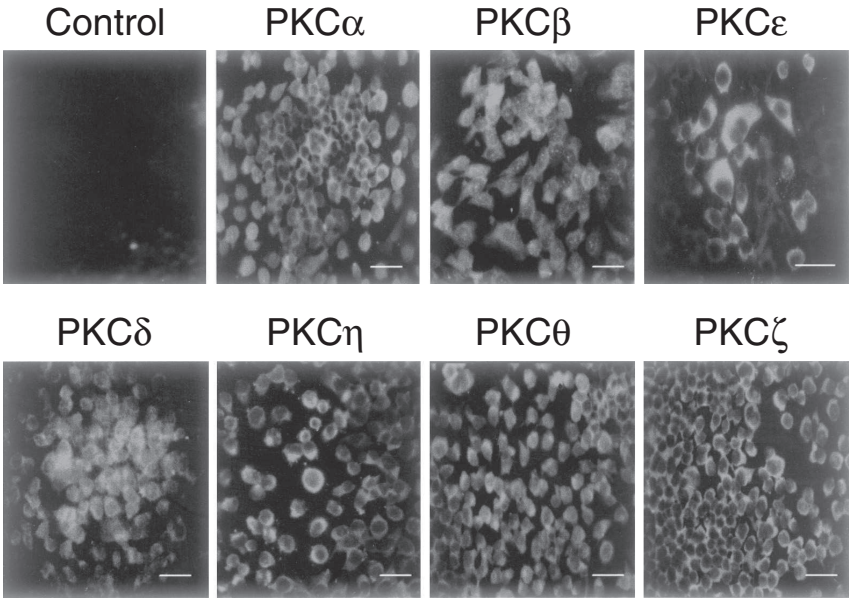

Figure 1. HaCaT keratinocytes possess a characteristic PKC isoform pattern. Cell cultures having approximately 80% confluence were fixed in acetone, solubilized by exposure to Triton X-100, and incubated with appropriate rabbit anti-PKC antibodies as described in Materials and methods. Immunofluorescent staining was employed using biotin-conjugated goat anti-rabbit IgG and Streptavidin-conjugated Texas Red. The first image from the left in the upper row (Control) represents an immunostaining without primary antibodies. The figure is a representative of at least four individual experiments for each isoform with similar results. Scale bars = 20 μm.

(and monotonously increasing) levels only in the differentiating cultures, whereas the expression of PKCε increased parallel with proliferation but, then, the isoform practically disappeared from the post-confluent cultures. These differential changes in the expressions of the existing isoforms were also proven by immunofluorescence staining (data not shown).

Lee et al. (16) have reported the translocation of PKCα from the cytoplasmic to the particulate compartment upon the induction of high cell density-mediated differentiation of NHEK, representing functional significance of the isoform in the process. Using confocal microscopy analyses on cells immunostained for the different PKC isozymes, we could not detect significant changes in subcellular localization of any of the isoforms in HaCaT cells (data not shown). Our findings therefore indicate that, in HaCaT cells, the induction of differentiation is accompanied by the changes in the expression pattern but not the subcellular localization of the various PKC isoforms.

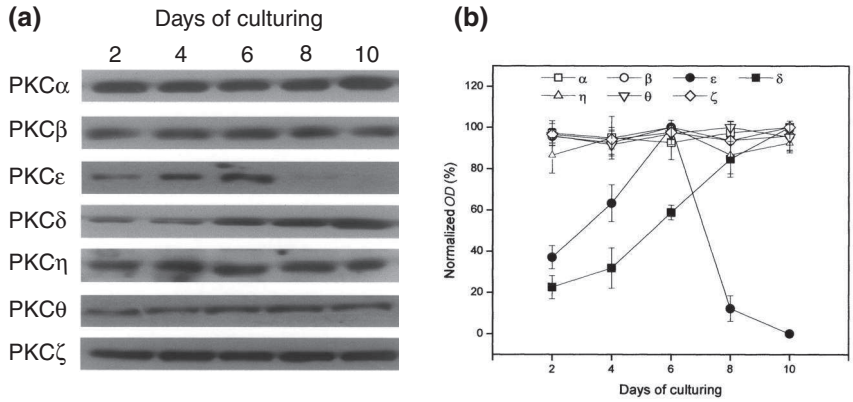

Figure 2. The PKC isoform pattern of HaCaT cells alters with proliferation and differentiation. (a) Cell cultures of different ages (cell reached confluence at day 6 of culturing) were harvested, similar amounts of proteins were subjected to SDS–PAGE, and Western immunoblotting was performed using rabbit anti-PKC antibodies as described in Materials and methods. (b) To demonstrate the tendencies of possible alterations, the amount of the given isoform at each day was quantitated by densitometry (optical density, *OD*), and expressed as the percentage of the maximal amount of the given isoform within the experiment (normalized *OD*). Points represent mean ± SEM of four independent experiments.

Inhibition of PKC modifies the expressions of keratinocyte differentiation markers but does not alter cellular proliferation and resting $[Ca^{2+}]_i$

In NHEK, during the process of differentiation, various differentiation markers are expressed representing different stages of differentiation (1–3). To follow the process in HaCaT cells, we investigated the expressions of the rather early (spinous cell) differentiation marker K10, of the rather late (granular cell) differentiation markers INV and FIL, of the terminal marker TG, and of the hyperproliferation-associated marker K17. Although the existence and expression patterns of all of these markers in HaCaT cells were carefully documented elsewhere (30,32), we first wished to test the alterations in their protein levels as a function of cell culturing time in our system, as well. As was expected, the expressions of the various differentiation markers differentially changed during culturing (Fig. 3a). The level of K10 reached its maximal value upon confluence and days 1–2 of post-confluence (a rather early marker), whereas the expressions of INV, FIL, and TG (rather late markers) were mostly dominant in the late post-confluent cultures (the level of the hyperproliferation-associated marker K17 did not change significantly during culturing). Furthermore, because the differentiation of NHEK is accompanied by an elevation in intracellular calcium concentration ($[Ca^{2+}]_i$) (41,42), we also employed functional calcium imaging to monitor the changes in $[Ca^{2+}]_i$ during culturing. As seen in Fig. 3(b), the $[Ca^{2+}]_i$ monotonously decreased with increasing proliferation tendency of the pre-confluent cells, whereas it gradually increased in the post-confluent (thus differentiating) cultures suggesting that the change in the levels of $[Ca^{2+}]_i$ is indeed a good indicator of differentiation in HaCaT cells as well.

We, then, intended to clarify whether the endogenous activation of PKC is required for regulating cellular proliferation and differentiation of HaCaT cells. We therefore employed the GF109203X compound which is a highly selective inhibitor of PKC competing with the ATP binding site of the 'conventional' and 'novel' isoforms (43, 44), and measured the changes in expressions of differentiation markers, cellular proliferation, and resting $[Ca^{2+}]_i$ of the cells.

To investigate the effect of the PKC inhibitor on the expressions of the differentiation markers, HaCaT cells having approximately 90% confluence were treated with different concentrations of the GF109203X compound for 5 days (until approximately the third day of post-confluence to initiate the high cell density-induced differentiation program), and then were subjected to Western blotting. As seen in Fig. 4(a,b), GF1209203X dose-dependently and differentially altered the expressions of the keratinocyte differentiation markers (greater than 1 μM doses were not applied due to cytotoxicity; see below). Whereas the expression of the spinous cell marker K10 was not modified significantly by the PKC inhibitor, the GF109203X compound markedly inhibited the expressions of the hyperproliferation-associated marker K17, the granular cell markers INV and

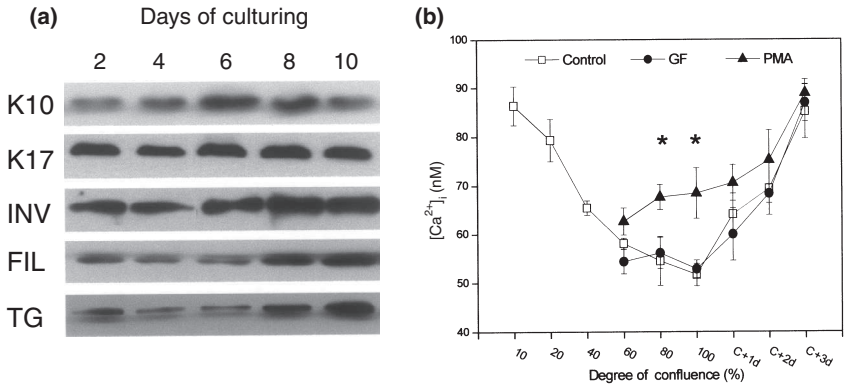

Figure 3. Changes in expressions of differentiation markers and in the resting $[Ca^{2+}]_i$ during proliferation and differentiation of HaCaT cells. (a) Cell cultures of different ages (cell reached confluence at day 6 of culturing) were harvested, similar amounts of proteins were subjected to SDS–PAGE, and Western immunoblotting was performed using mouse antibodies against the differentiation markers keratin 10 (K10), keratin 17 (K17), involucrin (INV), filaggrin (FIL), and keratinocyte-specific transglutaminase-1 (TG) as described in Materials and methods. (b) Control cell cultures (□) were cultured on glass coverslips from approximately 10% of confluence (C) to 3 days after reaching confluence (C + 3d). In parallel cultures, cells having 50–60% confluence were daily treated with either 1 μM GF109203X compound (●) or with 100 nM PMA (▲) up to 3 days of post-confluence. At the times indicated, cells were loaded with 5 μM fura 2-AM, and the resting intracellular calcium concentration ($[Ca^{2+}]_i$) of usually 20 cells/coverslip was determined as described in 'Materials and methods'. Points represent mean ± SEM values of 20 the determinations on each coverslip. Asterisks mark significant ($P < 0.05$) statistical differences between the PMA-treated and the daily matched control values.

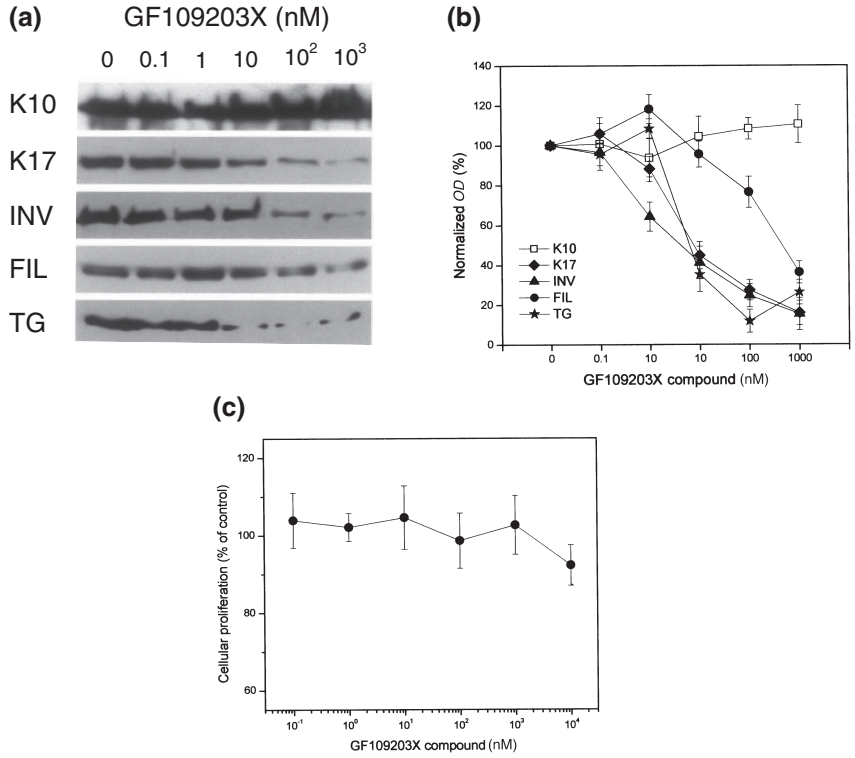

Figure 4. The inhibition of PKC by GF103203X modifies the expressions of keratinocyte differentiation markers but does not alter cellular proliferation in HaCaT cells. (a) HaCaT cells having approximately 90% confluence were treated with different concentrations of GF109203X compound for 5 days. Cells were then harvested, similar amounts of proteins were subjected to SDS–PAGE, and Western immunoblotting was performed using mouse antibodies against the differentiation markers keratin 10 (K10), keratin 17 (K17), involucrin (INV), filaggrin (FIL), and keratinocyte-specific transglutaminase-1 (TG) as described in 'Materials and methods'. (b) The amounts of the differentiation markers were quantitated by densitometry (optical density, *OD*), and expressed as the percentage of the control samples (normalized *OD*) treated with the vehicle DMSO only. Points represent mean ± SEM of three to four independent experiments. (c) HaCaT cells were seeded at 50–60% confluence in 96-well microtiter plates, treated with various concentrations of GF109203X compound for 3 days, then BrdU assays (●) were performed. Points represent mean ± SEM of quadruplicate determinations in one representative experiment. Two other experiments yielded similar results.

FIL, and the terminal marker TG in dose-dependent manners.

We have also investigated the potential endogenous role of PKC activation in the proliferation of HaCaT cells. In this case, cells were plated at approximately 50–60% confluence in 96-well microtiter plates, treated with various concentrations of the GF109203X compound for 3 days then a BrdU assay was performed to investigate cellular proliferation (these cultures reached 90–95% confluence during the protocol hence did not yet start the high cell density-induced differentiation program). As seen in Fig. 4(c), the GF109203X compound, in contrast to its effects on differentiation, did not significantly modify the cellular proliferation of HaCaT cells; only the 10 μM exerted minimal (less than 10%) inhibition. However, as revealed by parallel light microscopy control of the cultures (data not shown), this concentration caused rather cytotoxicity than inhibition of proliferation (the cells became round shaped and detached more intensively from the bottom of the flasks); therefore, this concentration was omitted from further experiments.

Similar findings were obtained in the case of the measurement of resting $[Ca^{2+}]_i$. Treatment of cells, seeded at 50–60% confluence, with 1 μM GF109203X compound for 6 consecutive days (the concentration that caused maximal alterations in the differentiation markers) did not significantly alter the resting $[Ca^{2+}]_i$ when compared with the daily matched control values (Fig. 3) suggesting that the modification of the expressions of the aforementioned differentiation markers was not related to changes in $[Ca^{2+}]_i$, another indicator of differentiation. Nevertheless, these data indicate that, in HaCaT keratinocytes, the endogenous activation of PKC is required mainly for the regulation of expressions of differentiation markers and not for the regulation of cellular proliferation and resting $[Ca^{2+}]_i$.

PMA inhibits cellular proliferation, increases $[Ca^{2+}]_i$, and alters the expressions of differentiation markers in HaCaT cells

In the next phase of our experiments, we investigated the effects of the well-known PKC activator PMA on the proliferation and differentiation of HaCaT cells. First, pre-confluent (approximately 50–60% confluence) proliferating cells in 96-well microtiter plates were treated with different concentrations of PMA for 3 days and then an MTT assay was performed. As seen in Fig. 5(a), PMA decreased viable cell numbers in a dose-dependent manner resulting in a 'U-shaped' dose–response curve. Because the effect of PMA to decrease viable cell numbers might be due to inhibition of proliferation or induction of cell death (apoptosis, necrosis), in parallel experiments (using strictly the same protocol), we investigated the effect of PMA on cellular proliferation using a BrdU assay. PMA inhibited the proliferation of the HaCaT cell showing very similar ('U-shaped') dose–response

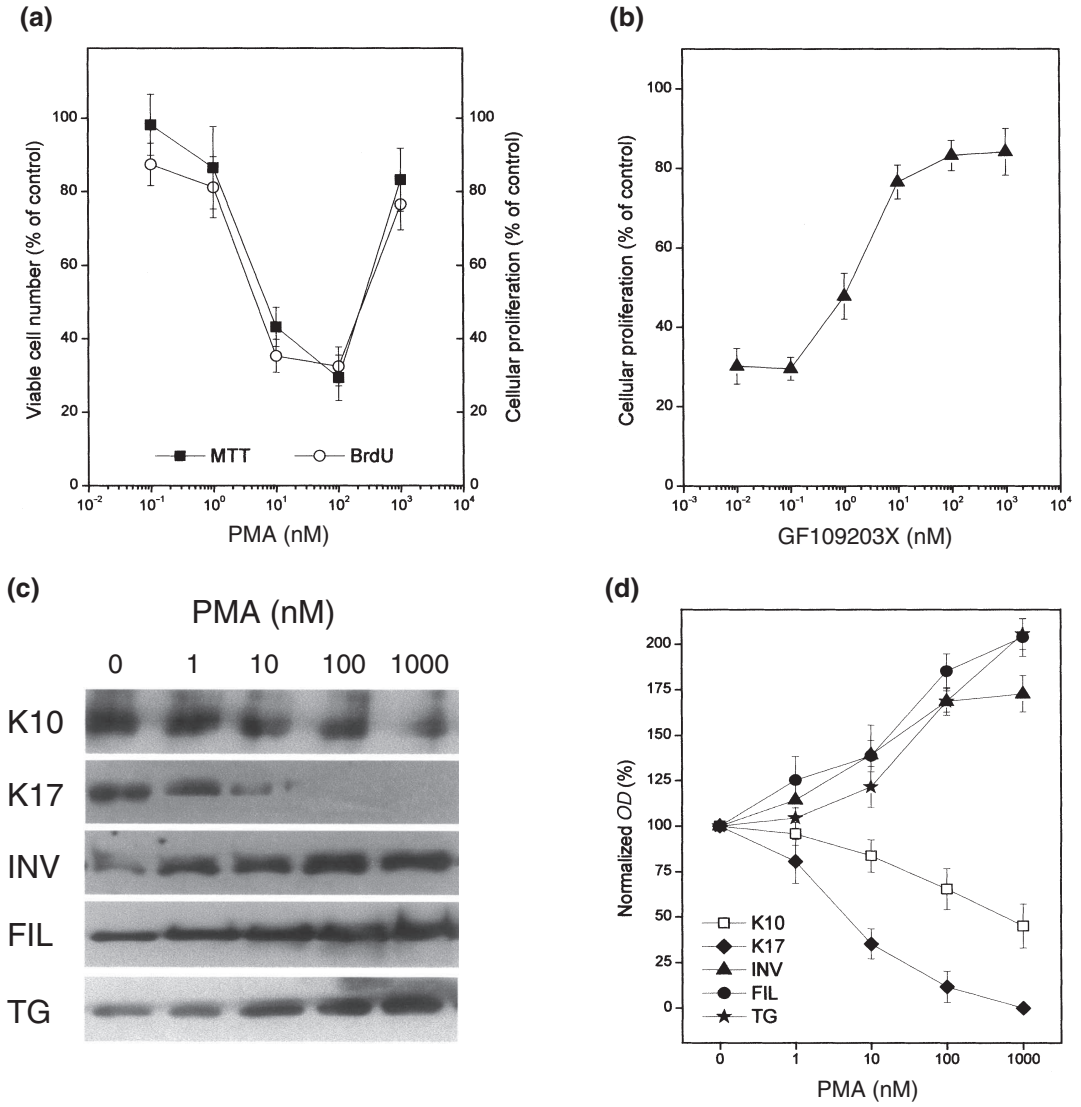

Figure 5. PMA inhibits proliferation and induces terminal differentiation in HaCaT cells. HaCaT cells were seeded at 50–60% confluence in 96-well microtiter plates, treated with various concentrations of PMA (a) or with various concentrations of GF109203X compound and 100 nM PMA (b) for 3 days, then either BrdU assays (● in a and ▲ in b) or MTT assays (■ in a) were performed. Points represent mean ± SEM of quadruplicate determinations in one representative experiment. Three to four other experiments yielded similar results. (c) HaCaT cells having approximately 90% confluence were treated with different concentrations of PMA for 5 days. Cells were then harvested, similar amounts of proteins were subjected to SDS–PAGE, and Western immunoblotting was performed using mouse antibodies against the differentiation markers keratin 10 (K10), keratin 17 (K17), involucrin (INV), filaggrin (FIL), and keratinocyte-specific transglutaminase-1 (TG) as described in 'Materials and methods'. (d) The amounts of the differentiation markers were quantitated by densitometry (optical density, *OD*), and expressed as the percentage of the control samples (normalized *OD*) treated with the vehicle DMSO only. Points represent mean ± SEM of three to four independent experiments.

characteristics to that found in the MTT assay (Fig. 5a) suggesting that the effect of PMA in decreasing viable cell numbers was mainly due to the inhibition of cellular proliferation and not due to cytotoxicity. This was also proven by the fact that the light microscopy examination of the cultures and lactate dehydrogenase release-based colorimetric cytotoxicity assays never revealed significant cell death with any of the PMA doses (data not shown).

Furthermore, we investigated whether the aforementioned effect of PMA on cellular proliferation was due to the specific action of the drug on the PKC. HaCaT cells were first pre-treated with different concentration of the GF109203X compound (up to 1 μM concentrations which did not cause any modification of proliferation; see Fig. 4c) for 1 h and then with 100 nM PMA (using the above protocol), which has proven to be the most efficient concentration in inhibiting cellular proliferation (Fig. 5a). As seen in Fig. 5(b), representing the results of BrdU assays, the GF109203X compound prevented the inhibitory effect of 100 nM PMA on cellular proliferation in a dose-dependent fashion suggesting the specific action of the phorbol ester on the PKC system.

We also determined the effect of PMA on the expression levels of the differentiation markers. In this case, HaCaT cells (seeded at approximately 90% confluence) were treated with different concentrations of PMA for 5 days (until approximately the third day of post-confluence), and then were subjected to Western blotting. As seen in Fig. 5(c,d), PMA differentially altered the expressions of the differentiation markers; whereas it inhibited the expressions of K10 and K17 (showing distinct dose–response relationships and different degrees of suppression), the levels of late-terminal markers INV, FIL, and TG were gradually and significantly increased by the phorbol ester. These results suggest that the PMA treatment caused a transition of HaCaT keratinocytes towards terminal differentiation in parallel by inhibiting early differentiation.

We also measured the possible changes in the resting $[Ca^{2+}]_i$ upon PMA treatment of the cultures. As seen in Fig. 3, treatment of cells seeded at 50–60% confluence with 100 nM PMA compound for 6 consecutive days resulted in a biphasic alteration in the resting $[Ca^{2+}]_i$ when compared with the daily matched control values. PMA increased the resting $[Ca^{2+}]_i$ in the pre-confluent cells; significant ($P < 0.05$) elevations were observed after the 1st (24% increase) and 2nd (32% increase) phorbol ester treatment. PMA, however, caused minor (less than 10%) or no elevations in resting $[Ca^{2+}]_i$ after reaching confluence. These data also argue that PMA initiates the terminal differentiation in HaCaT keratinocytes.

The PMA-induced cellular effects on proliferation and differentiation are differentially mediated by certain PKC isoforms

We also wished to identify those PKC isoforms that may mediate the cellular effects of PMA on proliferation and differentiation in HaCaT cells. It is generally accepted that the sensitive PKC isoforms first translocate then down-regulate upon the action of PMA in various cell types (7,8) including NHEK (14,24). Because translocation is a rather fast process (it occurs within minutes), we measured the down-regulation as an indicator of the prolonged action of PMA on cellular processes.

Proliferating (50–60% confluence) HaCaT cell cultures were treated with various concentrations of PMA for 3 days then Western blot analyses were performed to follow possible changes in the expression levels of the existing PKC isoforms. As seen Fig. 6(a), PMA differentially altered (down-regulated) the various PKC isoforms exerting distinct dose–response relationships. Actually, most of the sensitive isozymes (i.e. 'conventional' and 'novel' ones) but not the 'atypical' PKCζ possessed changes in their expressions, although the degrees of down-regulation were essentially different. There were isoforms (PKCα,β,ε, and θ) that completely (or almost completely) disappeared from the cells upon PMA treatment, although different phorbol ester concentrations were needed to cause down-regulation. In contrast, the down-regulation of PKCδ was significant (40–50%), although the isoform possessed marked expression levels in the PMA-treated cultures. Finally, we found very little (max. 20%) down-regulation of PKCη upon PMA treatment.

To identify those PKC isozymes that may mediate the effect of PMA on the differentiation markers, the determination of the PKC isoform content of the differentiating cells (seeded at approximately at 90% confluence and treated with PMA for 5 days) was also performed using Western blotting. Similarly to that found in proliferating cells, PMA differentially affected the expressions of the various PKC isoforms (Fig. 6b). However, it was of greatest importance that the PKC isoform population, which showed sensitivity to PMA in the differentiating HaCaT cells, was essentially different from that seen in the proliferating ones. PMA, in contrast to the

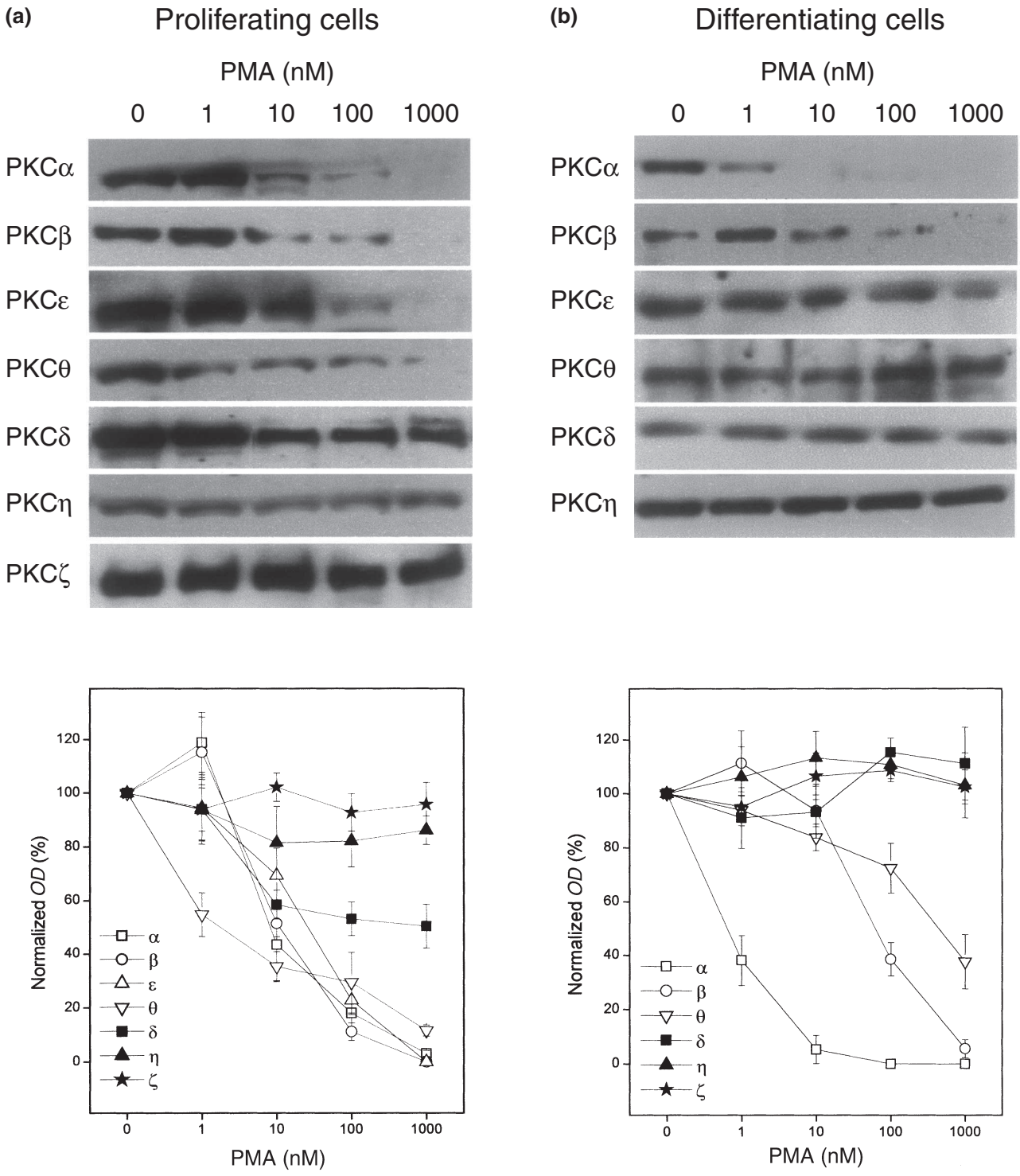

Figure 6. PMA differentially down-regulates the PKC isoforms in proliferating and differentiating HaCaT cells. Upper panels: HaCaT cell cultures having either 50–60% of confluence (proliferating cells) and treated with different concentrations of PMA for 3 days (a); or approximately 90% of confluence (differentiating cells) and treated with different concentrations of PMA for 5 days (b) were harvested, and similar amounts of proteins were subjected to SDS–PAGE. Western immunoblotting was then performed using rabbit antibodies against the various PKC isoforms as described in 'Materials and methods'. Lower panels: The amounts of the isoforms were quantitated by densitometry (optical density, *OD*), and expressed as the percentage of the control samples (normalized *OD*) treated with the vehicle DMSO only. Points represent mean ± SEM of three to four independent experiments for each isoform.

proliferating cells, did not cause any measurable down-regulation of PKCδ and η. Furthermore, although PKCα and θ were also down-regulated by PMA in the differentiating cells, the dose–response curves of PMA to induce down-regulation of these isoforms were different from those observed in the proliferating cultures also reflecting altered sensitivities of the isozymes. Namely, PKCα was more readily down-regulated by PMA in the differentiating cultures, whereas the expression of PKCθ decreased more in the proliferating cells upon PMA treatment. Finally, PMA, similarly to the proliferating cells, did not cause any down-regulation the phorbol ester-insensitive PKCζ, and, furthermore, PKCβ showed very similar sensitivities to the action of PMA in both cultures (as was shown before, the expression of PKCε was undetectable in the differentiating cultures; see Fig. 2). We can conclude therefore that a certain PKC isoform pattern participates in mediating the effect of PMA to induce terminal differentiation, which isozyme pattern is different from that seen in mediating the effect of the phorbol ester to inhibit cellular proliferation of HaCaT keratinocytes.

Discussion

Results obtained from our study suggest potential roles of the existing PKC isoforms in the regulation of proliferation and differentiation of human HaCaT keratinocytes. We have shown that HaCaT cells possess a characteristic PKC isoform pattern that alters with proliferation and differentiation and that the endogenous activation of PKC regulates the differentiation but not the proliferation and $[Ca^{2+}]_i$ of HaCaT cells. We have also presented that treatment of cells with the PKC activator PMA inhibited cellular growth and induced terminal differentiation by a spinous to granular transition of differentiation markers and by elevating $[Ca^{2+}]_i$. Because distinct PKC isoform populations were affected during the PMA-induced cellular responses in proliferating and differentiating cells, our findings strongly argue for the isozyme-specific, differential roles of the PKC isoforms in the processes.

In our hands, the HaCaT keratinocytes expressed several PKC isoforms: the cPKCα and β; the nPKCδ, ε, η, and θ; and the aPKCζ. This pattern of expression differed from that described by Geiges et al. (34) (the only extensive description in the literature about the PKC isozymes in HaCaT cells) as they documented the existence of PKCα, δ, ε, and ζ but not of PKCβ, θ, and η. Because we have shown the presence of the aforementioned isozymes using both Western blotting and immunofluorescence analyses; furthermore, as we used different antibodies than the Geiges's group; and, finally, as we recently confirmed the presence of these isoforms, using monoclonal antibodies (Bíró et al. unpublished observations), we believe that these differences are mainly due to technical dissimilarities.

It is generally accepted that NHEK express PKCα, δ, ε, η, and ζ, however, the existence of other PKC isoforms (namely PKCβ, γ, and μ) was also documented (14,17,18). Because the only isoform that has never been identified in NHEK but is expressed in HaCaT cells is PKCθ, we can conclude that the characteristic PKC isozyme pattern of HaCaT keratinocytes is similar to that of NHEK.

However, when we investigated the changes in the level of expressions and subcellular localization of the various PKC isoforms with proliferation and differentiation, some marked differences between NHEK and HaCaT cells were observed. In HaCaT cells, we found differential changes in the expression patterns of the isoforms during culturing: the expression of PKCδ increased with proliferation and differentiation whereas the expressions of PKCε showed a biphasic pattern: it increased in the proliferating and declined (disappeared) in the differentiating cultures (the expressions of the other isoforms were essentially the same during culturing). In NHEK *in vitro*, the expression levels of the existing PKCs did not change significantly during high cell density-induced differentiation (only the level of PKCα increased slightly) (16), although in NHEK *in vivo*, the PKCη was abundantly expressed only in the well-differentiated layers (45). Similarly, in NHEK and mouse keratinocytes induced to differentiate by elevating extracellular calcium concentration (15,46), and, furthermore, in differentiating keratinocytes of human reconstituted epidermis (47) marked changes in expression and activity of the PKC were observed during differentiation. A more prominent difference between HaCaT cells and NHEK was found when we examined the subcellular localization of the PKC isoforms during culturing. As was revealed by confocal microscopy, there were no measurable alterations in subcellular localization with any of the existing isoforms in HaCaT cells, which finding was in a marked contrast to those describing that, both in NHEK and mouse keratinocytes (15,16), certain PKC isozymes translocated upon differentiation. This difference may be due to the nature of the existing PKC isoforms in HaCaT cells (namely,

rather the PKC isozyme expression pattern than the localization alter with differentiation) or to the different experimental design to follow intracellular translocation (namely, we employed confocal microscopy after immunolabeling whereas others used subcellular fractionation and Western blotting).

The findings that different stages of proliferation and differentiation can be characterized by different PKC isozyme patterns suggested that these cellular mechanisms might be regulated by endogenous activation of PKC. Using the selective PKC inhibitor GF109203X compound, we were able to show that the expressions of the granular differentiation markers INV and FIL, and of the terminal marker TG are indeed dependent of the endogenous activation of PKC. Because the expression of the early (spinous cell) differentiation marker K10 was insignificantly affected by the PKC inhibitor, these findings indicate that, similarly to that in NHEK (16), the endogenous activation of PKC regulates spinous to granular transition in HaCaT keratinocytes induced to differentiate by confluence. In contrast, the GF109203X compound treatment (similarly to the effect of another selective PKC inhibitor, Ro 31-8220, on NHEK) (48) had practically no effect on resting $[Ca^{2+}]_i$, another marker of differentiation, suggesting that the endogenous activation of PKC may not be needed for all events of terminal differentiation in HaCaT cells. Similarly to this, the PKC inhibitor also did not modify cellular proliferation of HaCaT keratinocytes. Because others have reported even opposite (i.e. growth promoting) effects of the GF109203X compound in NHEK (25), we suppose that the lack of the effect of the PKC inhibitor to promote proliferation may be due to the already hyperproliferative state of the immortalized HaCaT cell line.

Another approach to investigate the role of PKC in HaCaT cell proliferation and differentiation was the analysis of the cellular effects of the PKC activator PMA. The phorbol ester, by specifically acting on sensitive PKC isoforms (see below), inhibited cellular growth, decreased the expression of the early (spinous cell) differentiation marker K10, and increased the expressions of all of the late-terminal differentiation markers examined. Furthermore, PMA treatment of the pre-confluent cultures (but not the already differentiating post-confluent ones) resulted in elevations in resting $[Ca^{2+}]_i$, also arguing for the induction of differentiation by the phorbol ester. These data therefore indicate that, identically with those described in NHEK (22–24), phorbol ester application leads to the induction of terminal differentiation in HaCaT keratinocytes as well, and, furthermore, that not only the endogenous but also the exogenous activation may induce similar cellular responses.

The chiefly opposite findings obtained using the PKC inhibitor GF109203X compound and PMA suggest that the phorbol ester exerted its cellular effect by first activating and then down-regulating certain sensitive PKC isoforms (see Fig. 6). Alternatively, the hypothesis that PMA treatment affected (activated and/or down-regulated) a distinct isoform population from that having an endogenous role in regulating HaCaT cell function also cannot be ruled out. Nevertheless, these speculations may explain those findings that, in contrast to the effect of PMA, the treatments of HaCaT cells by the PKC inhibitor did not modify the resting $[Ca^{2+}]_i$ levels, and that the expression of the hyperproliferation-associated marker K17 was equally decreased by both agents.

One of the major conclusions from our data is that the proliferation and high cell density-mediated differentiation appeared to be differentially regulated by certain PKC isoform populations. This statement is not only supported by the fact that different stages of differentiation could be characterized by different PKC isozyme patterns (see above), but also by those findings that PMA exerted its cellular effects on proliferating HaCaT cells (to inhibit proliferation) and on differentiating cells (to induce terminal differentiation) by differentially affecting the levels of various PKC isoforms (see Fig. 6). In the proliferating cells, PMA down-regulated practically all of the sensitive cPKC and nPKC isoforms (only PKCη showed a very little change upon the action of PMA) although the degrees of down-regulation and sensitivities of the various isoforms to PMA were usually different (as revealed by different dose–response curves). In the differentiating cells, however, PKCα, β, and θ were down-regulated by the phorbol ester (again, showing mostly different degrees and dose–response characteristics of down-regulation) whereas PKCδ and η were insignificantly modified by PMA. In addition, among those isoforms that were down-regulated both in the proliferating and differentiating cells by PMA, PKCα was more readily down-regulated in the differentiating cells whereas PKCθ showed more prominent down-regulation in the proliferating cells (PKCβ behaved similarly in both cultures). It appears therefore that (with the exception of PKCβ) the sensitivities of most of the PKC isoforms to the action of PMA altered with the onset of high cell density-mediated differentiation reflecting possible changes in their activities in regulating the process.

If we assume that the various PKC isozymes of a given cell may differentially and sometimes antagonistically act in regulating certain cellular processes (a phenomenon that does exist in several cells types) (10–12), the differential sensitivities of the PKCs to PMA may also explain the different dose–response relationships of PMA to inhibit proliferation and to modify the expressions of the differentiation markers. For example, in the proliferation experiments, the 'U-shaped' dose–response curve of PMA (i.e. 100 nM PMA was more effective than 1 μM PMA in inhibiting proliferation; see Fig. 5a) can be explained by the fact that the two different doses resulted in markedly different PKC isozyme patterns by differentially down-regulating the isoforms (see Fig. 6). Therefore, if the activity of a certain isoform that would inhibit proliferation was decreased and/or the activity of another that would promote cellular growth was increased by 1 μM PMA (and not by 100 nM PMA), the result would be a less pronounced growth inhibitory effect of the phorbol ester at the higher concentration.

In the framework of the previously discussed results, it may be premature to discuss possible isozyme-specific roles of the different PKCs in HaCaT cells not having exact, molecular biological data at hand. However, when we compared our findings to data found in the literature about NHEK (and very recently with HaCaT cells), a few striking similarities were observed, especially in the cases of PKCδ and η. These PKC isoforms, when over-expressed in NHEK using adenoviral vectors, were recently shown to inhibit cellular growth and induce differentiation (27,28), and PKCδ was described to promote apoptosis (28). It was also presented that PKCη localized almost exclusively in the most differentiated layers in healthy NHEK *in vivo* but also in the less differentiated layers of psoriatic epidermis (45), and that both isoforms were either down-regulated only in pre-confluent NHEK by PMA (47) or PKCη was not down-regulated at all (49). These previously described data were in a very good accord with our findings in HaCaT cells. PKCη present both in the proliferating and differentiating cultures (possible representing the hyperproliferative state of the HaCaT cells similarly to the psoriatic NHEK), showed minimal down-regulation upon the action of PMA in the pre-confluent cells, whereas it became resistant to the phorbol ester in the post-confluent cultures. In addition, the expression level of PKCδ gradually increased with differentiation, and also lost its sensitivity to PMA in the differentiating cultures. Consistent with previous results claiming that the tumorgenic transformation of HaCaT cells by ras-transfection resulted in the loss of PKCδ from the cells (34), and, furthermore, that the isoform-specific inhibition of PKCδ caused altered differentiation in HaCaT cells (50), our findings strongly argue for major regulatory roles of PKCδ and η in the differentiation of HaCaT keratinocytes as well. Naturally, the exact specific roles of these and the other existing isoforms are yet to be determined.

Acknowledgements

The authors are indebted to Ms. Ibolya Varga for helpful technical assistance, and to Professors Róza Ádány and Margit Balázs for providing the technical background of the immunofluorescent analysis. This work was supported by Hungarian research grants: OTKA T030246, OTKA F035036, ETT 50/2000, NKFP 00088/2001, OMFB 00200/2002. TB is a recipient of the György Békéssy Postdoctoral Scholarship of the Hungarian Ministry of Education.

References

1. Fuchs E. Epidermal differentiation: the bare essentials. J Cell Biol 1990: 111: 2807–2814.
2. Mehrel T, Hohl D, Rothnagel J A et al. Identification of a major keratinocyte cell envelope protein, loricrin. Cell 1990: 61: 1103–1112.
3. Schroder W T, Thacher S M, Stewart-Galetka S et al. Type I keratinocyte transglutaminase. expression in human skin and psoriasis. J Invest Dermatol 1992: 99: 27–34.
4. Goodnight J A, Mischak H, Mushinski J F. Selective involvement of protein kinase C isozymes in differentiation and neoplastic transformation. Adv Cancer Res 1994: 64: 159–209.
5. Nishizuka Y. The molecular heterogeneity of protein kinase C and its implication for cellular regulation. Nature 1988: 334: 661–665.
6. Ohno S, Akita Y, Hata A et al. Structural and functional diversities of a family of signal transducing protein kinases, protein kinase C family; two distinct classes of PKC, conventional cPKC and novel nPKC. Adv Enzyme Regul 1991: 31: 287–303.
7. Nishizuka Y. Intracellular signaling by hydrolysis of phospholipids and activation of protein kinase C. Science 1992: 258: 607–614.
8. Jaken S. Protein kinase isozymes and substrates. Curr Opin Cell Biol 1996: 8: 168–173.
9. Goodnight J A, Mischak H, Kolch W, Mushinski J F. Immunocytochemical localization of eight protein kinase C isozymes overexpressed in NIN 3T3 fibroblasts. Isoform-specific association with microfilaments, Golgi, endoplasmic reticulum, and nuclear and cell membranes. J Biol Chem 1995: 270: 9991–10001.
10. Mischak H, Goodnight J A, Kolch W et al. Overexpression of protein kinase C-δ and -ε in NIH 3T3 cells induces opposite effects on growth, morphology, anchorage dependence, and tumorigenicity. J Biol Chem 1993: 268: 6090–6096.
11. Murray N R, Baumgardner G P, Burns D J, Fields A P. Protein kinase C isotypes in human erythroleukemia (K562) cell proliferation and differentiation. Evidence that beta II protein kinase C is required for proliferation. J Biol Chem 1993: 268: 15847–15853.

12. Brodie C, Kuperstein I, Ács P, Blumberg P M. Differential role of specific PKC isoforms in the proliferation of glial cells and the expression of the astrocytic markers GFAP and glutamine synthetase. Mol Brain Res 1998: 56: 108–117.
13. Dlugosz A A, Mischak M, Mushinski J F, Yuspa S H. Transcripts encoding protein kinase C alpha, delta, epsilon, zeta, and eta are expressed in basal and differentiating mouse keratinocytes *in vitro* and exhibit quantitative changes in neoplastic cell. Mol Carcinog 1992: 5: 286–292.
14. Fischer S M, Lee M L, Maldve R E et al. Association of protein kinase C activation with ornithine decarboxylase in murine but not in human keratinocyte cultures. Mol Carcinog 1993: 7: 228–237.
15. Denning M F, Dlugosz A A, Williams E K, Szallasi Z, Blumberg P M, Yuspa S H. Specific protein kinase C isozymes mediate the induction of keratinocyte differentiation markers by calcium. Cell Growth Differ 1995: 6: 149–157.
16. Lee Y S, Yuspa Sh, Dlugosz A A. Differentiation of cultured human epidermal keratinocytes at high cell densities is mediated by endogenous activation of the protein kinase C pathway. J Invest Dermatol 1998: 111: 762–766.
17. Fisher G J, Tavakkol A, Leach K et al. Differential expression of protein kinase C isoenzymes in normal and psoriatic adult human skin: reduced expression of protein kinase C-betaII in psoriasis. J Invest Dermatol 1993: 101: 553–559.
18. Rennecke J, Johannes F J, Richter K H, Kittstein W, Marks F, Gschwendt M. Immunological demonstration of protein kinase C μ in murine tissues and various cell lines. Differential recognition of phosphorylated forms and lack of down-regulation upon 12-O-tetradecanoylphorbol-13-acetate treatment of cells. Eur J Biochem 1996: 242: 428–432.
19. Lichti U, Yuspa S H. Modulation of tissue and epidermal tranglutaminases in mouse epidermal cells after treatment with 12-O-tetradecanoylphorbol-13-acetate and/or retinoic acid *in vivo* and in culture. Cancer Res 1988: 48: 74–81.
20. Dlugosz A A, Yuspa S H. Coordinate changes in gene expression which mark the spinous to granular cell transition in epidermis are regulated by protein kinase C. J Cell Biol 1993: 120: 217–225.
21. Dlugosz A A, Yuspa S H. Protein kinase C regulates keratinocyte transglutaminase (TG_K) gene expression in cultured primary mouse epidermal keratinocytes induced to terminally differentiate by calcium. J Invest Dermatol 1994: 102: 409–414.
22. Liew F M, Yamanishi K. Regulation of transglutaminase 1 gene expression by 12-O-tetradecanoylphorbol-13-acetate, dexamethasone, and retinoic acid in culture human keratinocytes. Exp Cell Res 1992: 202: 310–315.
23. Matsui M S, Illarda I, Wang N, DeLeo V A. Protein kinase C agonist and antagonist effects in normal human epidermal keratinocytes. Exp Dermatol 1993: 2: 247–256.
24. Matsui M S, Wang N, DeLeo V A. Ultraviolet radiation B induces differentiation and protein kinase C in normal human epidermal keratinocytes. Photodermatol Photoimmunol Photomed 1996: 12: 103–108.
25. Le Panse R, Coulomb B, Mitev V, Bouchard B, Lebreton C, Dubertret L. Differential modulation of human fibroblast and keratinocyte growth by the protein kinase C inhibitor GF 109203X. Mol Pharmacol 1994: 46: 445–451.
26. Bollag W B, Ducote J, Harmon C S. Effects of the selective protein kinase C inhibitor, Ro 31-7549, on the proliferation of cultured mouse epidermal keratinocytes. J Invest Dermatol 1993: 100: 240–246.
27. Ohba M, Ishino K, Kashiwagi M et al. Induction of differentiation in normal human keratinocytes by adenovirus-mediated introduction of the η and δ isoforms of protein kinase C. Mol Cell Biol 1998: 18: 5199–5207.
28. Li L, Lorenzo P S, Bogi K, Blumberg P M, Yuspa S H. Protein kinase Cδ targets mitochondria, alters mitochondrial membrane potential, and induces apoptosis in normal and neoplastic keratinocytes when overexpressed by and adenoviral vector. Mol Cell Biol 1999: 19: 8547–8558.
29. Lee Y S, Dlugosz A A, McKay R, Dean N M, Yuspa S H. Definition by specific antisense oligonucleotides of a role for protein kinase Cα in expression of differentiation markers in normal and neoplastic mouse epidermal keratinocytes. Mol Carcinog 1997: 18: 44–53.
30. Boukamp P, Petrussevska R T, Breitkreutz D, Hornung J, Markham A, Fusenig N E. Normal keratinization in a spontaneously immortalized aneuploid human keratinocyte cell line. J Cell Biol 1998: 106: 761–771.
31. Boukamp P, Popp S, Altmeyer S et al. Sustained nontumorgenic phenotype correlates with largely stable chromosome content during long-term culture of the human keratinocyte line HaCaT. Genes Chromosomes Cancer 1997: 19: 201–214.
32. Ryle C M, Breitkreutz D, Startk H J et al. Density-dependent modulation with synthesis of keratins 1 and 10 in the human keratinocyte line HaCaT and in ras-transfected tumorgenic clones. Differentiation 1989: 40: 42–54.
33. Hegemann L, Wevers A, Bonnekoh B, Mahrle G. Changes of epidermal cell morphology and keratin expression induced by inhibitors of protein kinase C. J Dermatol Sci 1992: 3: 103–110.
34. Geiges D, Marks F, Gschwendt M. Loss of protein kinase Cδ from human HaCaT keratinocytes upon ras transfection is mediated by TGFα. Exp Cell Res 1995: 219: 299–303.
35. Boczán J, Bíró T, Czifra G et al. Phorbol ester treatment inhibits proliferation and differentiation of cultured human skeletal muscle satellite cells by differentially acting on protein kinase C isoforms. Acta Neuropathol 2001: 102: 55–62.
36. Boczán J, Boros S, Mechler F, Kovács L, Bíró T. Differential expressions of protein kinase C isozymes during proliferation and differentiation of human skeletal muscle cells in vitro. Acta Neuropathol 2000: 99: 96–104.
37. Laemmli UK. Cleavage of structural proteins during the assembly of the head of bacteriophage T4. Nature 1970: 227: 680–685.
38. Szallasi Z, Bogi K, Gohari S, Biro T, Acs P, Blumberg P M. Non-equivalent roles for the first and second zinc fingers of protein kinase Cδ. Effect of their mutation on phorbol ester-induced translocation in NIH 3T3 cells. J Biol Chem 1996: 271: 18299–18301.
39. Bíró T, Szabó I, Hunyadi J, Kovács L, Csernoch L. Distinct sub-populations in HaCaT cells as revealed by the characteristics of intracellular calcium release

induced by phosphoinositide-coupled agonists. Arch Dermatol Res 1998: 290: 270–276.
40. Grynkiewicz G, Poenie M, Tsien R Y. A new generation of Ca^{2+} indicators with greatly improved fluorescence properties. J Biol Chem 1985: 260: 3440–3350.
41. Hennings H, Michel D, Cheng C, Steinert P, Holbrook K, Yuspa S H. Calcium regulation or growth and differentiation of mouse epidermal cells in culture. Cell 1980: 19: 245–254.
42. Pillai S, Bikle D D. Adenosine triphosphate stimulates phosphoinositide metabolism, mobilizes intracellular calcium, and inhibits terminal differentiation of human epidermal keratinocytes. J Clin Invest 1992: 90: 43–51.
43. Toullec D, Pianetti P, Coste H et al. The bisindolylmaleimide GF 109203X is a potent and selective inhibitor of protein kinase C. J Biol Chem 1991: 266: 15771–15781.
44. Martiny-Baron G, Kazanietz M G, Mischak H et al. Selective inhibition of protein kinase C isozymes by the indolocarbazole Gö 6976. J Biol Chem 1993: 268: 9194–9197.
45. Koizumi H, Kohno Y, Osada S, Ohno S, Ohkawara A, Kuroki T. Differentiation-associated localization of nPKCη, a Ca^{++} independent protein kinase C, in normal human skin and skin diseases. J Invest Dermatol 1993: 101: 858–863.
46. Matsui M S, Chew S I, DeLeo V A. Protein kinase C in normal human epidermal keratinocytes during proliferation and calcium-induced differentiation. J Invest Dermatol 1992: 99: 565–571.
47. Gherzi R, Sparatore B, Patrone M, Sciutto A, Briata P. Protein kinase C mRNA levels and activity in reconstituted normal human epidermis: relationships to cell differentiation. Biochem Biophys Res Commun 1992: 184: 283–291.
48. Jones K T, Sharpe G R. Staurosporine, a non-specific PKC inhibitor, induces keratinocyte differentiation and raises intracellular calcium, but Ro 31-8220, a specific inhibitor, does not. J Cell Physiol 1994: 159: 324–330.
49. Murakami A, Chida K, Suzuki Y, Kikuchi H, Imajoh-Ohmi S, Kuroki T. Absence of down-regulation and translocation of the η isoform of protein kinase C in normal human keratinocytes. J Incest Dermatol 1996: 106: 790–794.
50. Dietrich C, Gumpert N, Heit I, Borchert-Stuhltrager M, Oesch F, Wieser R. Rottlerin induces a transformed phenotype in human keratinocytes. Biochem Biophys Res Commun 2001: 282: 575–579.

XV.

CMLS, Cell. Mol. Life Sci. 61 (2004) 1095–1105
1420-682X/04/091095-11
DOI 10.1007/s00018-004-4014-2

CMLS Cellular and Molecular Life Sciences

Research Article

Opposite roles of protein kinase C isoforms in proliferation, differentiation, apoptosis, and tumorigenicity of human HaCaT keratinocytes

H. Papp[a], G. Czifra[a,b], E. Bodó[a], J. Lázár[a], I. Kovács[e], M. Aleksza[c], I. Juhász[d], P. Ács[f], S. Sipka[c], L. Kovács[a,b], P. M. Blumberg[f] and T. Bíró[a,b,*]

[a] Department of Physiology
[b] Cell Physiology Research Group of the Hungarian Academy of Sciences, Fax: +36 52 432 289, e-mail: biro@phys.dote.hu
[c] 3rd Department of Internal Medicine
[d] Department of Dermatology, University of Debrecen, Medical and Health Science Center, Research Center for Molecular Medicine, Nagyerdei krt. 98, 4012 Debrecen, PO Box 22 (Hungary)
[e] Department of Pathology, Kenézy Hospital, Bartók B. u. 2-26, 4031 Debrecen (Hungary)
[f] Molecular Mechanism of Tumor Promotion Section, Laboratory for Cellular Carcinogenesis and Tumor Promotion, National Cancer Institute, National Institutes of Health, Building 37, 37 Convent Dr., MSC 4255, Bethesda, Maryland 20892 (USA)

Received 13 January 2004; received after revision 18 February 2004; accepted 25 February 2004

Abstract. We have previously shown that the protein kinase C (PKC) system plays a pivotal role in regulation of proliferation and differentiation of the human keratinocyte line HaCaT which is often used to assess processes of immortalization, transformation, and tumorigenesis in human skin. In this paper, using pharmacological and molecular biology approaches, we investigated the isoform-specific roles of certain PKC isoenzymes (conventional cPKCα and β; novel nPKCδ and ε) in the regulation of various keratinocyte functions. cPKCα and nPKCδ stimulated cellular differentiation and increased susceptibility of cells to actions of inducers of apoptosis, and they markedly inhibited cellular proliferation and tumor growth in immunodeficient mice. In marked contrast, cPKCβ and nPKCε increased both in vitro and in vivo growth of cells and inhibited differentiation and apoptosis. Our data present clear evidence for the specific, antagonistic roles of certain cPKC and nPKC isoforms in regulating the above processes in human HaCaT keratinocytes.

Key words. Human keratinocyte; HaCaT; protein kinase C; isoenzyme; recombinant overexpression; proliferation; differentiation; tumorigenesis.

Protein kinase C (PKC) comprises a family of serine/ threonine kinases that play crucial roles in the regulation of various cellular processes such as proliferation, differentiation, apoptosis, and tumorigenesis [1–4]. The members of the PKC family are the calcium- and phorbol ester-dependent 'conventional' isoforms (PKCα, βI, βII, and γ; cPKCs); the calcium-independent 'novel' isoforms (PKCδ, ε, η, and θ; nPKCs); and the calcium- and phorbol ester-independent 'atypical' (PKCζ and λ/ι; aPKCs) isoforms. These isoforms possess a characteristic expression pattern in a given cell type, and regulate in an isoenzyme-specific fashion various cellular processes including cell growth

* Corresponding author.

and death [4–6]. In addition, not only may some PKC isoforms be active whereas others not for a given response but different PKC isozymes may have antagonistic effects on the same cellular event [7–9], arguing for differential regulatory roles of specific PKC isoforms [4].

Emerging evidence suggests a pivotal role for PKC in the regulation of the proliferation and differentiation of normal human epidermal keratinocytes (NHEKs) as well as in the development of various skin tumors [10–13]. In addition, isoenzyme-specific roles of PKC in keratinocyte proliferation and differentiation have been described. For example, PKCα and δ were reported to be key components regulating the differentiation of NHEKs [10–15], and PKCε has been implicated in promoting skin tumor development in transgenic mice [12].

We have previously shown that immortalized HaCaT keratinocytes [16], which are very often used to model certain properties of NHEKs and to assess the processes of immortalization, transformation, and tumor progression in human skin [17, 18], possess a similar (although not identical) PKC system to that of NHEKs [19]. Namely, HaCaT cells express several PKC isoforms, the pattern of which alters with differentiation, and respond with cessation of proliferation and induction of differentiation upon the application of the PKC activator phorbol esters [19]. However, there are as yet little data available on the isoform-specific roles of the members of the PKC system in regulating HaCaT cells functions.

Exploiting the ability of HaCaT cells to be continuously passaged, in this study, in combination with the use of PKC inhibitors, we have constructed stable PKC transfectants of HaCaT cells and have investigated the possible roles of the PKC isozymes in regulating proliferation, differentiation, apoptosis, and the tumor induction properties of the cells. We report here that certain cPKC and nPKC isoforms play opposite roles in regulating the above processes, and that this antagonism could be seen even within members of the PKC sub-families.

Materials and methods

Antibodies

All primary antibodies against PKC isoenzymes were developed in rabbits and were shown to react specifically with the given PKC isoforms [19]. Anti-PKCα, β, and ε were from Sigma (St. Louis, Mo.), whereas anti-PKCδ was from Santa Cruz (Santa Cruz, Calif.). Specificities of anti-PKC antibodies were also tested by applying isoform-specific blocking peptides, which blocked the immunostaining in all cases (data not shown). Monoclonal mouse antibodies against involucrin (INV; Sigma), filaggrin (FIL; Biomedical Technologies, Stoughton, Mass.), and keratinocyte-specific transglutaminase-1 (TG; Biomedical Technologies) were used as markers of keratinocyte differentiation.

Generation of PKC constructs

PKC constructs were engineered as described previously [20, 21]. Briefly, the cDNA sequences of PKCα, β, δ, and ε were subcloned into a metallothionein promoter-driven eukaryotic expression vector (MTH) [22]. The vector sequence encodes a C-terminal PKCε-derived 12-amino-acid tag (εMTH) and attaches it to the end of the PKC proteins. As previously described [20], this epitope tag affects neither the localization nor the translocation of the given isoform.

Cell culture and transfection of cells

The human immortalized HaCaT keratinocyte cell line was a kind gift of Prof. N. E. Fusenig (Division of Differentiation and Carcinogenesis, German Cancer Research Center, Heidelberg, Germany). Cells were cultured in 25-cm^2 or 75-cm^2 tissue culture flasks (if not indicated otherwise) in Dulbecco's modified Eagle's medium (DMEM; Sigma) supplemented with 10% fetal calf serum (Sigma), 2 mM L-glutamine, 50 U/ml penicillin, 50 µg/ml streptomycin, 1.25 µg/ml fungizone (all from Biogal, Debrecen, Hungary) at 37°C in a 5% CO_2 atmosphere.

For transfection, HaCaT cells were seeded in 6-well tissue culture dishes and at 60–70% confluence were transfected by either the empty pεMTH vector (control cells) or by the vectors encoding the cDNA sequences of PKCα, β, δ, or ε [20, 21]. Transfections were performed using a lipofectamine anionic detergent (Invitrogen, Paisley, UK) in serum-free DMEM solution using 2–4 µg cDNA according to the protocol suggested by the manufacturer. Cells were selected in DMEM containing 750 µg/ml G418 (geneticin; Invitrogen) for 12–18 days. Then, single colonies were isolated. PKC-overexpressing cells were cultured in supplemented DMEM containing 500 µg/ml G418. Experiments were routinely carried out on pools of transfected cells, but the results were confirmed on at least three individual clones for each isoform. The efficacy of recombinant overexpression was monitored by Western blotting (see below and in fig. 2) using an anti-PKCε antibody (Sigma) which, beside recognizing the endogenously expressed PKCε (approximately 90 kDa), is able to detect the 'ε-tagged' transfected and overexpressed isoforms (approximately 80 kDa), resulting in double bands.

Determination of cellular proliferation

Proliferation was measured by a colorimetric bromodeoxyuridine (BrdU) assay kit (Boehringer Mannheim, Mannheim, Germany) and by analyzing standard growth curves. In those BrdU assays where the effects of PKC-acting agents were tested on cellular proliferation, cells were plated in 96-well multititer plates (5000 cells/well density) in quadruplicate, and 4 h later were treated with different concentrations of the agents and further incu-

bated for the time indicated. Cells were then incubated with 10 µM BrdU for 4 hours, and the cellular incorporation of BrdU (as the indicator of cellular proliferation) was determined colorimetrically according to the manufacturer's protocol. When BrdU assays were employed to investigate growth properties of PKC transfectants, cells were seeded at a density of 1000 cells/well and the BrdU incorporation was determined after the indicated days of culture, as described above.

To assess doubling times and maximal cell numbers of PKC overexpressers, 10^4 cells/well were plated in 12-well plates in triplicate in complete DMEM. Fresh medium was added every other day, and the cells in triplicate were harvested by trypsinization as indicated (usually on a daily basis) and counted using a hemocytometer. In determining the average doubling time, the 24-h time point was used as the starting point to avoid artifacts due to the initial lag period after plating [21]. The following equation was used to calculate doubling time: $\tau = D/\log_2(N/N_0)$ where τ is the doubling time, D is the number of days of culturing, N and N_0 are the number of cells at the end and the beginning of the experiments, respectively. To determine the maximal cell density, cells were grown in 12-well plates to confluence and kept post-confluent for 3 additional days with daily medium changes, and then counted as described above.

Western blot analysis

Cells were washed with ice-cold phosphate-buffered saline (PBS), harvested in homogenization buffer [20 mM TRIS-Cl, 5 mM EGTA, 1 mM 4-(2-aminoethyl)benzenesulfonyl fluoride, 20 µM leupeptin, pH 7.4; all from Sigma] and disrupted by sonication on ice [23]. The protein content of samples was measured by a modified BCA protein assay (Pierce, Rockford, Ill.). Total cell lysates were mixed with SDS-PAGE sample buffer and boiled for 10 min at 100 °C. The samples were subjected to SDS-PAGE according to Laemmli [24] (8% gels were loaded with 20–30 µg protein per lane) and transferred to nitrocellulose membranes (BioRad, Vienna, Austria). Membranes were then blocked with 5% dry milk in PBS and probed with the appropriate primary antibodies against the given PKC isoforms or differentiation markers. Peroxidase-conjugated goat anti-rabbit or anti-mouse IgG antibodies (BioRad) were used as secondary antibodies, and the immunoreactive bands were visualized by an ECL Western blotting detection kit (Amersham, Little Chalfont, U.K.) on light-sensitive films (AGFA, Brussels, Belgium). To assess equal loading, nitrocellulose membranes were stripped in 200 ml of 50 mM Tris-HCl buffer (pH 7.5) containing 2% SDS and 0.1 β-mercaptoethanol at 65 °C for 1 h and were reprobed with a mouse anti-cytochrome c antibody (Santa Cruz) followed by a similar visualization procedure as described above. When applicable, immunoblots were subjected to densitometric analysis as described previously [19] and normalized densitometric values of the individual lanes of several independent experiments were then determined.

PKC activity (kinase) assay

The PKC activity of transfected HaCaT cells was determined as described before [14, 20, 21]. Briefly, cells were lysed in the above lysis buffer, and the kinase activities of cell lysates (40 µg per reaction) were examined using histone III (H-III) or myosin light-chain kinase 20 (MLC20) as substrates (both from Sigma). The assay mixture contained 20 mM Tris (pH 7.5), 20 mM $MgCl_2$, 1 mM $CaCl_2$, 25 µM ATP, and 0.2 mg/ml substrate (all from Sigma), with 0.1 µCi of [γ-^{32}P]ATP (Amersham Biosciences, Freiburg, Germany) per assay. Data represent triplicate determinations.

Determination of apoptosis

Stable transfectants of HaCaT cells overexpressing the different PKC isoforms or the control empty vector were treated with vehicle, 10 µM 1α,25-dihydroxyvitamin D_3 [1α,25$(OH)_2D_3$] or 50 nM tumor necrosis factor α (TNFα) for 2 days. Cells were then collected by trypsinization and were incubated with 1 µl fluorescein isothiocyanate (FITC)-conjugated annexin V (Coulter-Immunotech, Hialeah, Fla.) for 10 min in the dark. Cells were then measured by a flow cytometer (Coulter EPICS XL-4) and the percentage of apoptotic cells compared to total cell number was determined.

Tumorigenicity in SCID mice

Cells overexpressing the various PKC isoforms (along with the control HaCaT cells) were grown in mass cultures, trypsinized and washed twice with PBS, and were then resuspended in culture medium at a density of $1-2 \times 10^6$ viable cells/200 µl. Severe combined immunodeficiency (SCID) mice were injected intradermally and observed over a period of 30 days (during this period, none of the animals showed lethal progression of tumor). Animals were finally euthanized and the averaged three-dimensional size and histological characteristics of the developed tumors (three to four animals for each group) were analyzed.

Histology and immunohistochemistry

The histological parameters were determined on formalin-fixed, paraffin-embedded, and hematoxylin-eosin (HE)-stained sections of the developed tumors. The averaged number of cell divisions was measured by counting the number of nuclei showing clear signs of mitosis in ten individual visual fields at high magnification using a light microscope, and results obtained in each tumor of the same group were then averaged and the mean values calculated.

In addition, to assess the number of proliferating cells, formalin-fixed, paraffin-embedded sections were immunostained against the nuclear marker Ki67 [25] using a streptavidine-biotin-complex (SABC) three-step immunohistochemical technique (DAKO, Hamburg, Germany). First, the inhibition of endogenous peroxidase activity was performed using 3% H_2O_2 in 100% methanol (both from Sigma). Then, non-specific binding was blocked by 1% bovine serum albumin (Sigma) in PBS buffer (pH 7.5). After testing various concentrations of the anti-Ki67 monoclonal mouse primary antibody (DAKO), an optimal 1:50 dilution was employed. The sections were then incubated in a humid chamber using a biotin-coupled anti-mouse secondary antibody (1:100; DAKO) followed by streptavidine conjugated with horseradish peroxidase (1:600; DAKO). To reveal the peroxidase activity, VIP SK-4600 (Vector, Burlingame, Calif.) was employed as a chromogen. The tissue samples were finally slightly counterstained with methyl green (DAKO) and mounted with Aquatex (Merck, Vienna, Austria). The averaged number of proliferating (Ki67-positive) cells was measured by counting the total number of Ki67-positive cells in ten individual visual fields at high magnification using a light microscope and the values were then normalized to the total number of cells measured in the fields.

Results

Effect of inhibition of PKC isoform activities on cellular proliferation and differentiation of HaCaT cells

Confirming our previous findings [19], we showed that the inhibition of endogenous PKC activity in HaCaT keratinocytes by a general PKC inhibitor GF109203X (inhibitor of the cPKC and nPKC isoenzymes) [26] suppressed the expression of the late differentiation markers INV, FIL, and TG, suggesting pivotal roles for the PKC

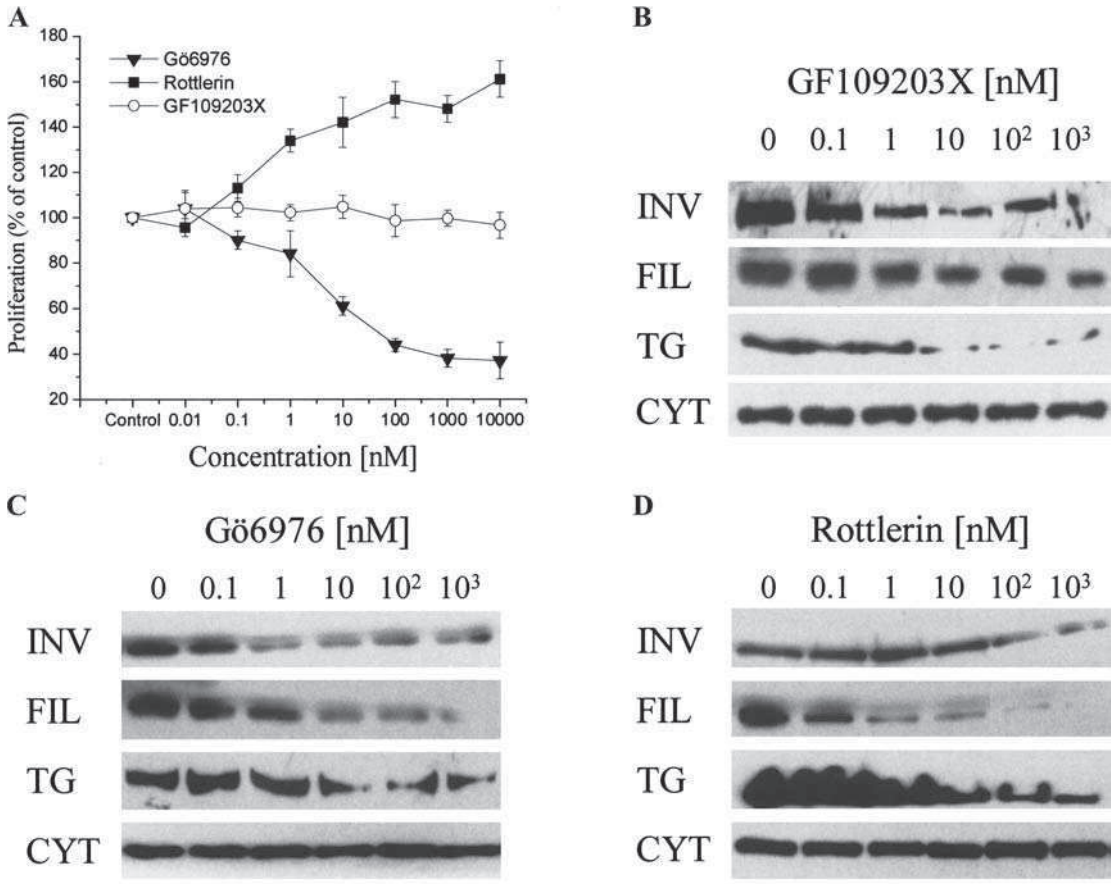

Figure 1. The inhibition of various PKC isoforms differentially modifies cellular proliferation and expression of keratinocyte differentiation markers in HaCaT cells. (*A*) HaCaT cells were seeded at densities of 5000 cells/well in 96-well microtiter plates, treated with various concentrations of PKC inhibitors for 2 days, and then BrdU assays were performed. Points represent the mean ± SE of quadruplicate determinations in one representative experiment. Two to three other experiments yielded similar results. (*B–D*) HaCaT cells were treated with different concentrations of GF109203X (*B*), Gö6976 (*C*), or rottlerin (*D*) for 3 days. Cells were then harvested, similar amounts of proteins were subjected to SDS-PAGE, and Western immunoblotting was performed using mouse antibodies against the differentiation markers INV, FIL, and keratinocyte-specific TG as described in Materials and methods. To assess equal loading, nitrocellulose membranes were stripped and reprobed with a mouse anti-cytochrome antibody (CYT). The figure is representative of two to three experiments yielding similar results.

system in regulating differentiation (fig. 1B). We also found that GF109203X (fig. 1A), in contrast to its dramatic effect on differentiation, did not modify the proliferation of these cells [19]. This latter result can be interpreted in (at least) two ways. First, these findings may suggest that the endogenous PKC activity does not contribute to the regulation of HaCaT cell proliferation. Alternatively, the inhibition of all of the existing cPKC and nPKC isoforms (we have previously shown that HaCaT keratinocytes express cPKCα and β, and nPKCδ, ε, η, and θ) [19] equally inhibited growth-promoting and growth-inhibiting PKC isoform activities, resulting in no net effect.

To test this latter hypothesis, we started to investigate the effects of other PKC inhibitors on HaCaT cell proliferation and differentiation. First, we employed the compound Gö6976, an inhibitor of the cPKC isoforms [27], i.e., cPKCα and β in HaCaT cells. As seen in figure 1A, in contrast to the effect of GF109203X, the inhibitor of the cPKC isoforms markedly inhibited the proliferation of the cells in a dose-dependent manner. Gö6976, however, induced a very similar pattern of changes in the expression of differentiation markers when compared to the effect of GF109203X (fig. 1B, C). Namely, the inhibitor decreased the expression of INV, FIL, and TG in a dose-dependent fashion as measured on Western blots. These results strongly argue for the positive roles of endogenous cPKC isoforms in the processes of proliferation and differentiation of HaCaT keratinocytes.

We then investigated the possible roles of the nPKC isoforms in these processes. Since commercially only the nPKCδ inhibitor rottlerin [28] was available, we measured the effects of this molecule on cellular functions of HaCaT keratinocytes. As seen in figure 1A, D, the inhibition of nPKCδ dose-dependently stimulated cellular proliferation whereas it inhibited the expression of the differentiation markers. Although confidence in the interpretation is limited because of possible effects of rottlerin on systems other than PKC, these findings at least suggested that endogenous nPKCδ activity is a positive regulator of differentiation whereas it functions as a negative modulator of proliferation.

Overexpression of certain cPKC and nPKC isoforms

The results with the inhibitors showed that certain isoforms might play important roles in the regulation of proliferation and differentiation of HaCaT keratinocytes. However, although GF109203X is widely used as a general PKC inhibitor, Gö6076 as an inhibitor of the classic PKCs, and rottlerin as a PKCδ inhibitor, none of these inhibitors is as specific and/or selective as was initially thought. For example, in some systems, GF109203X also blocks mitogen-activated protein kinase-activated protein kinase-1β and p70 S6 kinase [29], whereas rottlerin has been reported not to be selective for PKCδ [28]. Furthermore, the data could not differentiate, for example, between the putative isoform-specific roles of the cPKCα and β isoforms, and did not describe other nPKC isoform-specific functions. Therefore, using the previously introduced MTH vectors [20–23], we have stably transfected HaCaT keratinocytes with cPKCα and β and nPKCδ and ε. This latter isoform was chosen among the nPKC isoenzymes since its potential role in regulating cellular proliferation and differentiation has been extensively documented in several cell types including keratinocytes [5–7, 9, 12, 19, 30].

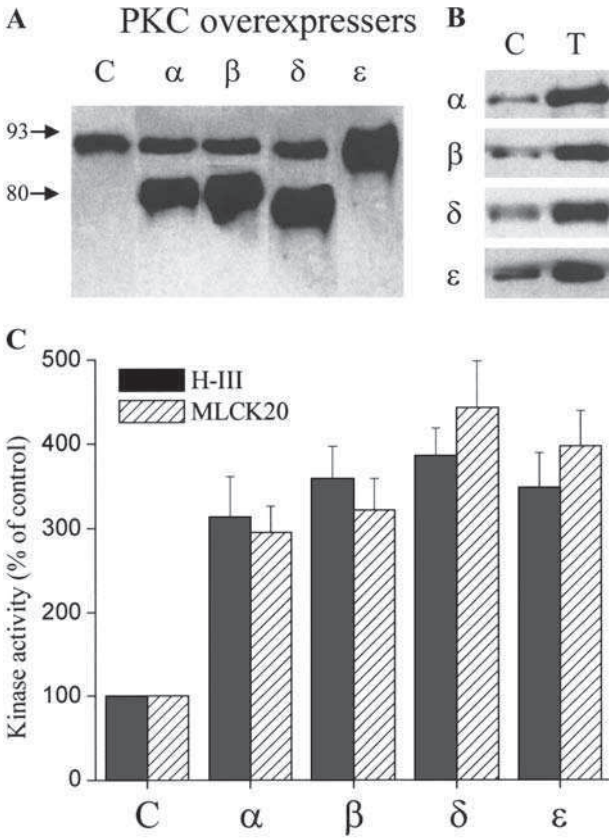

Figure 2. Overexpression of certain PKC isoforms in HaCaT cells. (*A*) Stable transfectants of HaCaT cells overexpressing the different PKC isoforms (Greek letters) or the empty vector (control, C) were harvested, similar amounts of proteins were subjected to SDS-PAGE, and Western immunoblotting was performed as described in Materials and methods. The membranes were then probed with an anti-PKCε antibody that recognizes both the endogenous nPKCε (approximately 90-kDa bands) and the ε-tag sequence of the recombinant, expressed PKC isoforms (approximately 80-kDa bands in the cases of the recombinant PKCα, β, and δ, and an approximately 90-kDa band in the case of the recombinant PKCε). (*B*) To detect the degree of overexpression, Western blot analysis was also performed on control (C) and PKC transfectant (T) HaCaT cells using isoform-specific antibodies that corresponded to the overexpressed recombinant PKC isoenzymes. (*C*) Cell lysates of overexpressors and control (empty vector-transfected, C) HaCaT cells were analyzed for kinase activity by measuring ^{32}P incorporation into H-III or myosin light-chain kinase 20 (MLCK20) substrates in triplicate determinations. The values are expressed as percent of control (mean ± SE). The figures are representative of three experiments for each isoenzyme yielding similar results.

We first examined the efficacy of recombinant overexpression. Cell lysates of pooled cultures (fig. 2) and several transfected clones (data not shown) were subjected to Western blotting. Using an anti-PKCε antibody, which recognizes both the endogenously present nPKCε (approximately 90-kDa bands) and the ε-tag sequence of the recombinant, expressed PKC isoforms (therefore, resulting in approximately 80-kDa bands in the cases of recombinant PKCα, β, and δ, and an approximately 90-kDa band in the case of recombinant PKCε), we were able to specifically detect the transfected isoenzymes (fig. 2A). Furthermore, using isoform-specific antibodies that corresponded to the overexpressed recombinant PKC isoenzymes, we found that the levels of the overexpressed PKCs (fig. 2B) were three- to seven-fold higher than those of the respective endogenous PKCs (data not shown). Finally, to establish that the overexpressed PKC isoforms were functionally active, we also measured kinase (PKC) activity on cell lysates. As seen in figure 2C, the cells expressing the recombinant PKC isoforms showed higher kinase activity, as assessed with both kinase substrates, compared with the control (empty vector-transfected) HaCaT cells.

Effects of overexpression of PKC isoforms on morphology of HaCaT cells

The overexpression of the PKC isoforms differentially affected the morphology of HaCaT keratinocytes. As seen in figure 3, the usual, characteristic cobblestone morphology of control (empty vector-transfected) HaCaT cells was dramatically changed by the overexpression of nPKCε; these cells exhibited a fibroblast-like, spindle-shaped phenotype. In addition, cells overexpressing cPKCβ also possessed elongated cell bodies (yet without processes) and formed denser islets during culture. The overexpression of PKCδ and α did not result in dramatic morphological changes; possibly, the nPKCδ-overexpressing HaCaT cells displayed a more cobblestone appearance.

Effects of overexpression of PKC isoforms on the proliferation and differentiation of HaCaT cells

We then investigated the effect of overexpression of the PKC isoforms on the proliferation of HaCaT keratinocytes. As revealed by BrdU assays (fig. 4A) and standard growth curve analyses (table 1), overexpression of the PKC isoforms markedly altered cell growth. Overexpression of cPKCα and nPKCδ decreased the proliferation of HaCaT cells. Conversely, keratinocytes overexpressing cPKCβ and nPKCε exhibited higher proliferation rates compared to the control (empty vector-transfected) cells.

The differences in proliferation were paralleled by the average doubling times and saturation densities of the cultures. Consistent with findings in the BrdU assays, cPKCα- and nPKCδ-overexpressing cells possessed prolonged doubling times and decreased saturation densities, while cells that overexpressed cPKCβ and nPKCε were characterized by markedly increased saturation densities and shortened doubling times (table 1).

To follow differentiation, we measured the expression of certain keratinocyte differentiation markers in the PKC-overexpressing cells. Since nPKCδ-overexpressing cells very often did not reach complete confluence and ceased

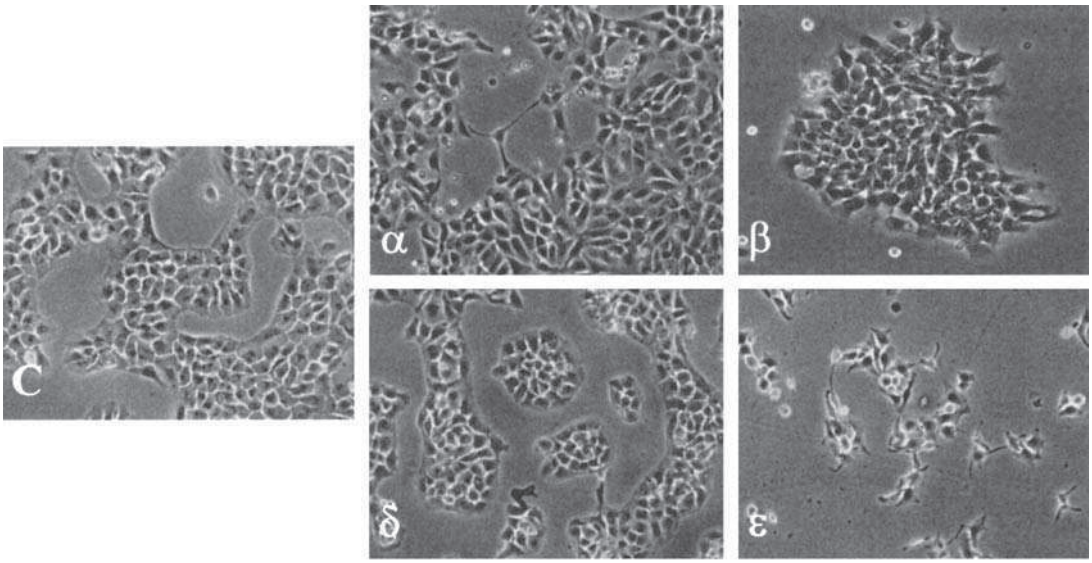

Figure 3. Overexpression of certain PKC isoforms alters morphology of HaCaT cells. Photomicrographs were taken using a phase contrast light microscope (magnification, × 200) on HaCaT cells stably overexpressing the PKC isoforms or the control empty vector (C). The figure is representative of three additional experiments with similar results.

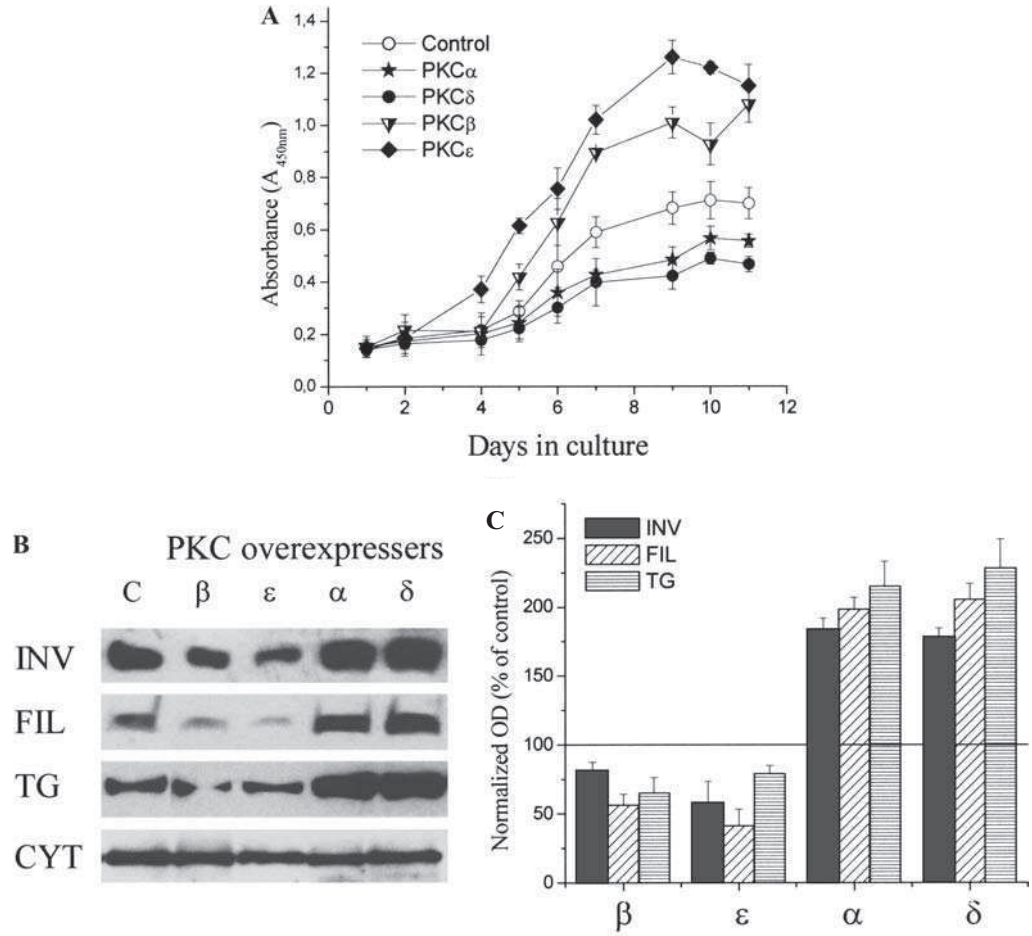

Figure 4. Overexpression of various PKC isoforms differentially alters cellular proliferation and expression of keratinocyte differentiation markers in HaCaT cells. (*A*) Control and PKC overexpresser HaCaT cells were seeded at densities of 1000 cells/well in 96-well microtiter plates and cell proliferation was determined after the indicated days of culture using BrdU assays as described in Materials and methods. Points represent the mean ± SE of quadruplicate determinations in one representative experiment for each isoform. At least three additional experiments for each PKC isoenzyme yielded similar results. (*B*) Stable transfectants of HaCaT cells overexpressing the different PKC isoforms or the control empty vector (C) were harvested, similar amounts of proteins were subjected to SDS-PAGE, and the Western immunoblotting was performed using mouse antibodies against the differentiation markers INV, FIL, and keratinocyte-specific TG as described in Materials and methods. To assess equal loading, nitrocellulose membranes were stripped and reprobed with a mouse anti-cytochrome antibody (CYT). The figure is representative of three experiments yielding similar results. (*C*) The amounts of the differentiation markers expressed in the PKC-overexpressing cells were quantitated by densitometry (optical density, OD), and expressed as the percentage of the OD value of immunoreactive bands of control cells (normalized OD). Bars represent the mean ± SE of three independent experiments.

Table 1. In vitro and in vivo growth analysis of HaCaT cells overexpressing various PKC isoforms.

Isoform	In vitro growth analysis		In vivo tumor growth analysis		
	doubling time (h)	saturation density (10^5 cells/cm^2)	averaged tumor size (mm)	number of cell division	percentage of Ki67-positive cells
Control	23.2 ± 2.5	1.4 ± 0.2	7 × 8 × 4.3	6.2 ± 1.0	25.2 ± 2.1
cPKCα	27.4 ± 3.2	1.0 ± 0.2	4.3 × 4 × 2.3	3.6 ± 0.5	13.2 ± 2.3
nPKCδ	30.5 ± 4.3	0.8 ± 0.1	4.6 × 4.3 × 2	4 ± 0.3	11.4 ± 3.1
cPKCβ	16.5 ± 3.3	2.1 ± 0.1	11 × 8.3 × 4.3	16 ± 1.2	34.9 ± 4.5
nPKCε	13.2 ± 3.9	2.8 ± 0.2	16 × 12 × 5.3	19.5 ± 2.8	41.4 ± 3.9

Various parameters were analyzed as described in Materials and methods. Data are expressed as the mean ± SE, except for averaged tumor size, where the three dimensional sizes of three to four tumors per group were averaged and the mean values are shown.

proliferating at about 80–90% of confluence (data not shown), reflecting a suppressed growth capacity, to obtain comparable data, all cell cultures were harvested at about 80–85% confluence, equal amounts of protein were subjected to SDS-PAGE, and the expression of various markers was investigated by Western blotting. As seen in figure 4B, C, in cells overexpressing cPKCα and nPKCδ isoenzymes, levels of the late-terminal differentiation markers increased, whereas in keratinocytes overexpressing the cPKCβ and nPKCε isoforms, the levels of the differentiation markers decreased compared to those of the control HaCaT cells.

Effects of overexpression of PKC isoforms on the apoptosis of HaCaT cells

Various PKC isoforms have been suggested to play pivotal roles in mediating apoptosis induced by various agents [4]. We therefore measured the effect of the known apoptosis inducers 1α,25(OH)$_2$D$_3$ and TNFα [31] on apoptosis in HaCaT cells overexpressing the various PKC isoenzymes. As determined by annexin V-based flow cytometry analysis (fig. 5), there were no major differences in the level of basal apoptosis for control and cPKCβ- and nPKCε-overexpressing HaCaT cells. In contrast, the basal apoptotic rates in the nPKCδ transfectants and, although to lesser extent, the cPKCα overexpressers were higher than in the control cells. In addition, the overexpression of PKCα and δ increased the susceptibility of cells to apoptosis induced by 10 µM 1α,25(OH)$_2$D$_3$ or 50 nM TNFα, whereas the PKCβ and ε overexpressers showed less sensitivity to the action of these agents than did the control cells.

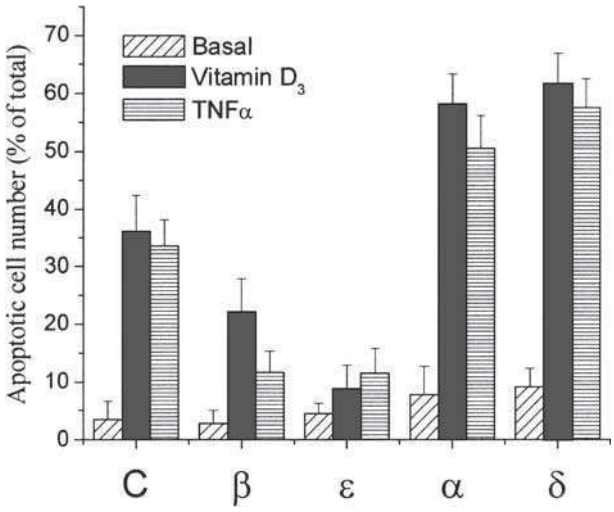

Figure 5. Overexpression of various PKC isoforms differentially alters apoptosis in HaCaT cells. Stable transfectants of HaCaT cells overexpressing the different PKC isoforms or the control empty vector (C) were treated with vehicle (Basal), 10 µM 1α,25 (OH)$_2$ D$_3$ (Vitamin D$_3$), or 50 nM TNFα for 2 days and then apoptosis was determined using an annexin V-based flow cytometry assay as described in Materials and methods. Data are expressed as the percentage of apoptotic cells compared to total cell number and represent the mean ± SE of three independent experiments.

Effects of overexpression of PKC isoforms on tumorigenicity in SCID mice

Finally, we investigated the behavior of PKC overexpressing cells in assays for tumor formation and in vivo growth. SCID mice (three to four in each group) were injected with a cell suspensions of HaCaT cells ($1-2 \times 10^6$ viable cells/200 µl) overexpressing different PKC isoforms and, after 30 days, tumors which had developed were characterized. As revealed on HE-stained sections, control HaCaT cells formed basal cell-enriched tumors with expansive growth properties at the periphery and with intense maturation and differentiation (formation of keratin islets, dyskeratotic cells, sometimes cyst formation) at the center of the tumor (fig. 6). The relative sizes of the proliferating and differentiating fields were approximately the same. The injection of HaCaT cells overexpressing the various PKC isoforms generally did not change the major histological characteristics of the tumors. In other words, all tumors maintained the expansive (i.e., non-infiltrative, benign) growth characteristics and histological features of peripheral proliferation and central differentiation. However, of greatest importance, we found marked differences in the average size of the tumors, the number of dividing cells, and the relative ratio of the proliferating and differentiating parts on the histological sections. Overexpression of nPKCε and cPKCβ resulted in increased tumor growth, as reflected by the markedly increased tumor sizes and number of dividing cells (table 1). Moreover, the relative ratio of the proliferating to the differentiating parts also increased in these tumors (more than 70% of the histological section was dominated by the proliferating part in the nPKCε- and cPKCβ-overexpressing HaCaT cell-induced tumors). In contrast, tumors initiated by cPKCα and nPKCδ overexpressers possessed suppressed averaged tumor sizes, decreased numbers of mitoses, and an increased dominance of the differentiating part (more than 70% of the tumor histological picture) (fig. 6 and table 1).

These differential features of PKC-overexpressing cells in tumorigenesis were also proven by analyzing the number of Ki67-positive cells in the tumors. As seen in table 1, in tumors induced by nPKCε- and cPKCβ-overexpressing cells, the number of Ki67-positive (proliferating) cells increased whereas in tumors induced by cPKCα and nPKCδ transfectants, the number decreased compared to that of the control cells.

Discussion

Previous experimental findings from our laboratory [19], in good accordance with a wide array of data in the liter-

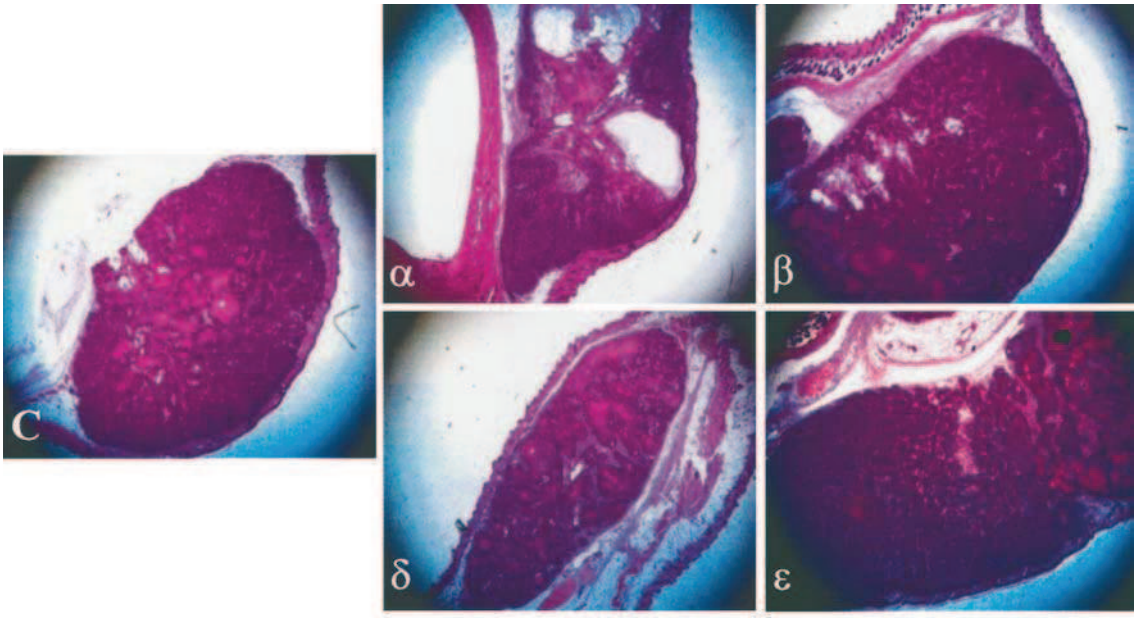

Figure 6. Cells overexpressing certain PKC isoforms induce different tumors in SCID mice. Stable transfectants of HaCaT cells overexpressing the different PKC isoforms or the control empty vector (C) at $1-2 \times 10^6$ viable cells/200 µl density were injected intradermally into SCID mice. After 30 days, animals were euthanized, the developed tumors were excised and HE staining was performed on formalin-fixed paraffin-embedded sections. Original magnification, × 20.

ature [10–15], unambiguously argued for the central role of the PKC system in regulation of numerous keratinocyte-specific cellular processes. Moreover, in the case of NHEKs, isoform-specific functions of certain isozymes (e.g., cPKCα and nPKCδ and η) were also described. With respect to the HaCaT cells, however, we possessed very little information about the exact role of the PKC system and, more importantly, of the individual isoforms in the cellular mechanisms. In the present paper, using combined pharmacological and molecular biological approaches, we report that among the several PKC isoenzymes expressed in HaCaT cells [19], certain members of the cPKC and nPKC sub-families possess opposite roles in regulating proliferation, differentiation, apoptosis, and tumorigenesis.

A key issue in the interpretation of our findings was the relevance of our data obtained with HaCaT keratinocytes for complete NHEKs. The cPKCα isoform, one of the most studied PKC isoforms in keratinocyte biology, was shown to play a central role in the calcium- and high cell density-induced terminal differentiation program in mouse and human keratinocytes [10–13, 15, 30]. This isoform was also shown to be rapidly and markedly down-regulated by phorbol esters both in NHEKs [10] and HaCaT cells [19], which was regarded as a key signal in mediating the action of the above agents to induce terminal differentiation. In our current experiments, we furthermore showed that the overexpression of cPKCα promoted differentiation and apoptosis but inhibited proliferation and tumor growth (figs 4–6). These findings strongly argue that, similar to its behavior in NHEKs, cPKCα may play a central role in the positive regulation of differentiation and negative regulation of growth of HaCaT keratinocytes.

Comparison of data obtained with cells overexpressing cPKCα (i.e., stimulation of apoptosis and differentiation, inhibition of growth) with those obtained using Gö6976, the inhibitor of the cPKC isoforms (i.e., inhibition of both proliferation and differentiation; fig. 1) suggested that cPKCβ (another cPKC isoform in HaCaT cells that was presumably also inhibited by Gö6976) may oppositely regulate the above processes. Indeed, the proliferation and tumorigenic activity of cells overexpressing cPKCβ was markedly increased whereas their differentiation and apoptotic tendencies were suppressed when compared to the control HaCaT cells (figs 4–6). These findings were in good accord with previous data stating that the expression of cPKCβ is altered in psoriasis where the sophisticated balance of keratinocyte proliferation and differentiation is impaired [32].

Data obtained using the compound Gö6976 highlight another important feature of the antagonistic roles of isoforms belonging to the conventional group of the PKC family. If cPKCα stimulates differentiation and inhibits growth and, conversely, cPKCβ stimulates proliferation and inhibits differentiation, the inhibitory effect of Gö6976 (the inhibitor of both cPKCα and β) on both proliferation and differentiation (fig. 1) could only be explained by the stimulatory actions of the two isoenzymes (i.e., cPKCα on differentiation and apoptosis, cPKCβ on

proliferation and tumorigenicity) being more effective than their inhibitory actions on the other responses. Nevertheless, our data clearly present the opposite roles of cPKC isoforms possessing similar activation mechanisms in regulating various cellular processes in HaCaT keratinocytes.

During the investigation of the novel PKC isoenzymes, a strikingly similar phenomenon was observed. The nPKCε has been extensively documented as a key positive regulator of cellular proliferation in various cell types [4, 5, 7, 9]. Overexpression of nPKCε was also shown to lead to pathological proliferation (hyperproliferative transformation) and down-regulation or overexpression of the dominant negative mutant of the enzyme results in inhibition of proliferation and induction of differentiation [5, 7, 9]. In addition, very recently, the promoting role of nPKCε in skin tumor formation in transgenic mice was also reported [12]. Since we have previously shown that, as in NHEK cells [30], nPKCε is almost exclusively expressed in the proliferating but not in the differentiating HaCaT cells [19], our current results that the growth rate and tumorigenicity of cells overexpressing nPKCε dramatically increased whereas the differentiation and apoptotic capacities decreased (figs 4–6) unambiguously argue for the positive regulatory role of this isoform in in vitro and in vivo growth of HaCaT keratinocytes as well.

Opposite findings were obtained regarding nPKCδ (figs 1, 4–6); i. e., this isoform functioned as a positive regulator of differentiation and apoptosis with a parallel inhibitory action on cellular and tumor growth. We have previously shown that the expression level of nPKCδ was remarkably elevated in differentiating HaCaT keratinocytes [19]. In addition, several groups have reported that the activation or overexpression of nPKCδ in keratinocytes inhibited proliferation, initiated the differentiation program [14], and mediated the apoptotic effect of several inducers both in NHEK [14, 33, 34] and HaCaT [35] cells. In addition, malignant transformation of HaCaT keratinocytes by Ha-ras overexpression was shown to result in the disappearance of nPKCδ from the cells [36] and treatment of control HaCaT cells by rottlerin induced an altered (proliferating) phenotype [37]. Consistent with these literature data, our findings further argue for the positive and central role of nPKCδ in the initiation and development of differentiation and apoptosis.

Finally, we should note that, to the best of our knowledge, this is the first demonstration of the tumor-inducing properties of HaCaT cells in SCID mice. In contrast to data obtained in nude mice, where control HaCaT cells formed characteristic cystic granules (which regressed after a few weeks) [16, 18], HaCaT keratinocytes induced expansively growing benign tumors in SCID animals which were histologically very similar to those developed by injecting benign ras-transfected HaCaT cells into nude mice [17, 18]. These data argue that, similar to the growth properties of other tumorigenic cell types [38–40], the tumor-inducing capabilities of HaCaT cells are more profound in SCID mice than in nude mice. Nevertheless, since the overexpression of none of the PKC isoforms (not even of cPKCβ or nPKCε) resulted in malignant transformation (in contrast to malignant ras transfection) [17, 18], although certain PKC isoforms stimulate in vitro and in vivo growth of HaCaT keratinocytes, their constitutive presence alone is apparently not enough for malignant transformation of the cells.

In summary, we can conclude that the isoform-specific roles of certain cPKC and nPKC isoforms enrolled in this study in the regulation of in vitro and in vivo growth, differentiation, and apoptosis of human HaCaT keratinocytes are very similar to those previously described in NHEKs, supporting the relevance of our findings for complete normal human epidermal cells.

Acknowledgement. This work was supported by Hungarian research grants: OTKA F035036, OTKA T037531, OTKA TS040773, NKFP 00088/2001, OMFB 00200/2002, ETT 365/2003. T. Bíró is a recipient of the György Békésy Postdoctoral Scholarship of the Hungarian Ministry of Education.

1 Nishizuka Y. (1988) The molecular heterogeneity of protein kinase C and its implication for cellular regulation. Nature **334:** 661–665
2 Ohno S., Akita Y., Hata A., Osada S., Kubo K., Kohno Y. et al. (1991) Structural and functional diversities of a family of signal transducing protein kinases, protein kinase C family; two distinct classes of PKC, conventional cPKC and novel nPKC. Adv. Enzyme Regul. **31:** 287–303
3 Nishizuka Y. (1992) Intracellular signaling by hydrolysis of phospholipids and activation of protein kinase C. Science **258:** 607–614
4 Gutcher I., Webb P. R. and Anderson N. G. (2003) The isoform-specific regulation of apoptosis by protein kinase C. Cell. Mol. Life Sci. **60:** 1061–1070
5 Goodnight J. A., Mischak H. and Mushinski J. F. (1994) Selective involvement of protein kinase C isozymes in differentiation and neoplastic transformation. Adv. Cancer Res. **64:** 159–209
6 Goodnight J. A., Mischak H., Kolch W. and Mushinski J. F. (1995) Immunocytochemical localization of eight protein kinase C isozymes overexpressed in NIN 3T3 fibroblasts: isoform-specific association with microfilaments, Golgi, endoplasmic reticulum, and nuclear and cell membranes. J. Biol. Chem. **270:** 9991–10001
7 Mischak H., Goodnight J. A., Kolch W., Martiny-Baron G. M., Schaechtle C., Kazanietz M. G. et al. (1993) Overexpression of protein kinase C-δ and -ε in NIH 3T3 cells induces opposite effects on growth, morphology, anchorage dependence, and tumorigenicity. J. Biol. Chem. **268:** 6090–6096
8 Murray N. R., Baumgardner G. P., Burns D. J. and Fields A. P. (1993) Protein kinase C isotypes in human erythroleukemia (K562) cell proliferation and differentiation: evidence that beta II protein kinase C is required for proliferation. J. Biol. Chem. **268:** 15847–15853
9 Brodie C., Kuperstein I., Ács P. and Blumberg P. M. (1998) Differential role of specific PKC isoforms in the proliferation of glial cells and the expression of the astrocytic markers GFAP and glutamine synthetase. Mol. Brain Res. **56:** 108–117
10 Lee Y. S., Yuspa S. H. and Dlugosz A. A. (1998) Differentiation of cultured human epidermal keratinocytes at high cell densi-

ties is mediated by endogenous activation of the protein kinase C pathway. J. Invest. Dermatol. **111:** 762–766
11 Bikle D. D., Ng D., Tu C. L., Oda Y. and Xie Z. (2001) Calcium- and vitamin D-regulated keratinocyte differentiation. Mol. Cell. Endocrinol. **177:** 161–171
12 Jansen A. P., Dreckschmidt N. E., Verwiebe E. D., Wheeler D. L., Oberley T. D. and Verma A. K. (2001) Regulation of the induction of epidermal ornithine decarboxylase and hyperplasia to the different skin tumor-promotion susceptibilities of protein kinase C alpha, -delta, and -epsilon transgenic mice. Int. J. Cancer. **93:** 635–643
13 Neill G. W., Ghali L. R., Green J. L., Ikram M. S., Philpott M. P. and Quinn A. G. (2003) Loss of protein kinase C alpha expression may enhance the tumorigenic potential of Gli1 basal cell carcinoma. Cancer Res. **63:** 4692–4697
14 Li L., Lorenzo P. S., Bogi K., Blumberg P. M. and Yuspa S. H. (1999) Protein kinase Cδ targets mitochondria, alters mitochondrial membrane potential, and induces apoptosis in normal and neoplastic keratinocytes when overexpressed by an adenoviral vector. Mol. Cell. Biol. **19:** 8547–8558
15 Lee Y. S., Dlugosz A. A., McKay R., Dean N. M. and Yuspa S. H. (1997) Definition by specific antisense oligonucleotides of a role for protein kinase Cα in expression of differentiation markers in normal and neoplastic mouse epidermal keratinocytes. Mol. Carcinog. **18:** 44–53
16 Boukamp P., Petrussevska R. T., Breitkreutz D., Hornung J., Markham A. and Fusenig N. E. (1988) Normal keratinization in a spontaneously immortalized aneuploid human keratinocyte cell line. J. Cell Biol. **106:** 761–771
17 Breitkreutz D., Boukamp P., Ryle C. M., Stark H.-J., Roop D. R. and Fusenig N. E. (1991) Epidermal morphogenesis and keratin expression in c-Ha-ras-tranfected tumorgenic clones of the human HaCaT cell line. Cancer Res. **51:** 4402–4409
18 Fusenig N. E. and Boukamp P. (1998) Multiple stages and genetic alterations in immortalization, malignant transformation, and tumor progression of human skin keratinocytes. Mol. Carcinog. **23:** 144–158
19 Papp H., Czifra G., Lázár J., Boczán J., Gönczi M., Csernoch L. et al. (2003) Protein kinase C isozymes regulate proliferation and high cell density-mediated differentiation of HaCaT keratinocytes. Exp. Dermatol. **12:** 811–824
20 Ács P., Bögi K., Marquez A. M., Lorenzo P. S., Bíró T., Szállási Z. et al. (1997) The catalytic domain of protein kinase C chimeras modulates the affinity and targeting of phorbol ester induced translocation. J. Biol. Chem. **272:** 22148–22153
21 Ács P., Wang Q. J., Bögi K., Marquez A. M., Lorenzo P. S., Bíró T. et al. (1997) Both the catalytic and regulatory domains of protein kinase C chimeras modulate the proliferation properties of NIH 3T3 cells. J. Biol. Chem. **272:** 28793–28799
22 Oláh Z., Lehel C., Jakab G. and Anderson W. B. (1994) A cloning and epsilon-epitope-tagging insert for the expression of polymerase chain reaction-generated cDNA fragments in *Escherichia coli* and mammalian cells. Anal. Biochem. **221:** 94–102
23 Lázár J., Szabó T., Kovács L., Blumberg P. M. and Bíró T. (2003) Distinct features of recombinant vanilloid receptor-1 expressed in various expression systems. Cell. Mol. Life Sci. **60:** 2228–2240
24 Laemmli U. K. (1970) Cleavage of structural proteins during the assembly of the head of bacteriophage T4. Nature **227:** 680–685
25 Rose D. S. C., Maddox P. H. and Brown D. C (1994) Which proliferation markers for routine immunohistology? A comparison of five antibodies. J. Clin. Pathol. **47:** 1010–1014
26 Toullec D., Pianetti P., Coste H., Bellevergue P., Grand-Perret T., Ajakane M. et al. (1991) The bisindolylmaleimide GF 109203X is a potent and selective inhibitor of protein kinase C. J. Biol. Chem. **266:** 15771–15781
27 Martiny-Baron G., Kazanietz M. G., Mischak H., Blumberg P. M., Kochs G., Hug H. et al. (1993) Selective inhibition of protein kinase C isozymes by the indolocarbazole Gö 6976. J. Biol. Chem. **268:** 9194–9197
28 Gschwendt M., Müller H.-J., Kialbassa K., Zang R., Kittstein W, Rincke G. et al. (1994) Rottlerin, a novel protein kinase inhibitor. Biochem. Biophys. Res. Commun. **199:** 93–98
29 Alessi D. R. (1997) The protein kinase C inhibitors Ro 318220 and GF 109203X are equally potent inhibitors of MAPKAP kinase-1β and p70 S6 kinase. FEBS Lett. **402:** 121–123
30 Zang L. C., Ng D. C. and Bikle D. D. (2003) Role of protein kinase α in calcium induced keratinocyte differentiation: defective regulation in squamous cell carcinoma. J. Cell. Physiol. **195:** 249–259
31 Müller-Wieprecht V., Riebeling C., Stooss A., Orfanos C. E. and Geilen C. C. (2000) Bcl-2 transfected HaCaT keratinocytes resist apoptotic signals of ceramides, tumor necrosis factor α and 1α,25-dihydroxyvitamin D_3. Arch. Dermatol. Res. **292:** 455–462
32 Fisher G. J., Tavakkol A., Leach K., Burns D., Basta P., Loomis C. et al. (1993) Differential expression of protein kinase C isoenzymes in normal and psoriatic adult human skin: reduced expression of protein kinase C-betaII in psoriasis. J. Invest. Dermatol. **101:** 553–559
33 Denning M. F., Wang Y., Nickoloff B. J. and Wrone-Smith T. (1998) Protein kinase Cdelta is activated by caspase-dependent proteolysis during ultraviolet radiation-induced apoptosis of human keratinocytes. J. Biol. Chem. **273:** 29995–30002
34 Denning M. F., Wang Y., Tibudan S., Alkan S., Nickoloff B. J. and Qin J. Z. (2002) Caspase activation and disruption of mitochondrial membrane potential during UV radiation-induced apoptosis of human keratinocytes requires activation of protein kinase C. Cell Death Differ. **9:** 40–52
35 Fukunaga M., Oka M., Ichihashi M., Yamamoto T., Matsuzaki H. and Kikkawa U. (2001) UV-induced tyrosine phosphorylation of PKC delta and promotion of apoptosis in the HaCaT cell line. Biochem. Biophys. Res. Commun. **289:** 573–579
36 Geiges D., Marks F. and Gschwendt M. (1995) Loss of protein kinase Cδ from human HaCaT keratinocytes upon ras transfection is mediated by TGFα. Exp. Cell. Res. **219:** 299–303
37 Dietrich C., Gumpert N., Heit I., Borchert-Stuchltrager M., Oesch F. and Wieser R. (2001) Rottlerin induces a transformed phenotype in human keratinocytes. Biochem. Biophys. Res. Commun. **282:** 575–579
38 Xie X., Brunner N., Jensen G., Albrectsen J., Gotthardsen B. and Rygaard J. (1992) Comparative studies between nude and scid mice on the growth and metastatic behavior of xenografted human tumors. Clin. Exp. Metastasis **10:** 201–210
39 Taghian A., Budach W., Zietman A., Freeman J., Gioioso D. and Suit H. D. (1993) Quantitative comparison between the transplantability of human and murine tumors into the brain of NCr/Sed-nu/nu nude and severe combined immunodeficient mice. Cancer Res. **53:** 5018–5021
40 Kubota T., Yamaguchi H., Watanabe M., Yamamoto T., Takahara T., Takeuchi T. et al. (1993) Growth of human tumor xenografts in nude mice and mice with severe combined immunodeficiency (SCID). Surg. Today **23:** 375–377

XVI.

J Mol Med (2007) 85:1031–1042
DOI 10.1007/s00109-007-0209-y

ORIGINAL ARTICLE

Protein kinase C-β and -δ isoenzymes promote arachidonic acid production and proliferation of MonoMac-6 cells

Zoltán Griger · Edit Páyer · Ildikó Kovács · Balázs I. Tóth · László Kovács · Sándor Sipka · Tamás Bíró

Received: 28 November 2006 / Revised: 8 February 2007 / Accepted: 30 March 2007 / Published online: 5 June 2007

Abstract In this study, we investigated the putative roles of certain protein kinase C (PKC) isoenzymes in the regulation of proliferation and arachidonic acid (AA) release in the human monocytoid MonoMac-6 cell line. Experiments employing specific PKC inhibitors and molecular biological methods (RNA-interference, recombinant overexpression) revealed that the two dominantly expressed isozymes, i.e., the "conventional" cPKCβ and the "novel" nPKCδ, promote AA production and cellular proliferation. In addition, using different phospholipase A_2 (PLA_2) inhibitors, we were able to show that the calcium-independent $iPLA_2$ as well as diacylglycerol lipase (but not the cytosolic PLA_2) function as "downstream" targets of cPKCβ and nPKCδ. In addition, we have also found that, among the other existing PKC isoforms, cPKCα plays a minor inhibitory role, whereas nPKCε and aPKCζ apparently do not regulate these cellular processes. In conclusion, in this paper we provide the first evidence that certain PKC isoforms play pivotal, specific, and (at least partly) antagonistic roles in the regulation of AA production and cellular proliferation of human monocytoid MonoMac-6 cells.

Keywords Protein kinase C · Isoenzymes · MonoMac6 cells · Arachidonic acid release · Proliferation

Z. Griger · E. Páyer · B. I. Tóth · L. Kovács · T. Bíró
Department of Physiology, University of Debrecen,
Research Center for Molecular Medicine,
Medical and Health Science Center,
Nagyerdei krt. 98.,
4032 Debrecen, Hungary

B. I. Tóth · L. Kovács · T. Bíró (✉)
Cell Physiology Research Group of the Hungarian Academy of Sciences, University of Debrecen,
Research Center for Molecular Medicine,
Medical and Health Science Center,
Debrecen, Hungary
e-mail: biro@phys.dote.hu

Z. Griger · I. Kovács · S. Sipka
IIIrd Department of Internal Medicine, University of Debrecen,
Research Center for Molecular Medicine,
Medical and Health Science Center,
Debrecen, Hungary

ZOLTÁN GRIGER graduated at the University of Debrecen, Medical and Health Science Center, Debrecen, Hungary. He is working on his Ph.D. in the Department of Physiology. He is presently a Resident fellow in the IIIrd Department of Internal Medicine, Division of Immunology. His research interests include intracellular signal transduction processes in monocytic and lymphocytic cell lines, and in polysystemic immunological diseases.

TAMÁS BÍRÓ received his Ph.D. in Physiology and Neurobiology from the University of Debrecen, Medical and Health Science Center, Debrecen, Hungary. He is presently an Associate Professor of Physiology and Chief of the Laboratory for Cellular and Molecular Physiology at the Department of Physiology (University of Debrecen). His research interests include investigation of surface membrane channels, receptors, and intracellular kinase systems and related signaling mechanisms.

Introduction

Protein kinase C (PKC) comprises a family of serine threonine kinases that play key roles in the regulation of various cellular functions [1]. Up to date, at least 11 different PKC isoenzymes have been identified, which can be classified into the groups of the calcium- and phorbol ester-dependent "conventional" cPKCs (PKCα, βI, βII, and γ), the calcium-independent "novel" nPKCs (PKCδ, ε, η, and θ), the calcium- and phorbol ester-independent "atypical" aPKCs (PKCζ and λ/ι), and the unique PKCμ [2, 3]. These isoforms, possessing characteristic tissue and cellular distribution, specifically regulate various cellular functions such as proliferation, differentiation, cytokine production, mediator release, and receptor-mediated signal transduction [1, 4]. For example, we have previously shown that cPKCα inhibited in vitro and, of great importance, in vivo proliferation of human keratinocytes, whereas cPKCβ effectively stimulated growth of the cells [4].

It was also shown that the different PKC isoforms very often play central roles in the proliferation, differentiation, and apoptotic processes in human mononuclear cells such as monocytes, macrophages, and lymphocytes [5–7]. Moreover, the involvement of the PKC system was also documented in mediating such biological actions of leukocytes as degranulation, chemotaxis, adherence, superoxide formation, phagocytosis, and arachidonic acid (AA) production and liberation [8–11]. For example, Di Marzo et al. [12] have reported that the activation of PKC, by phosphorylating components of the receptor-G_i-protein complex, switches the coupling of dopamine receptor-2 from inhibition of adenylyl cyclase toward facilitation of AA release [12]. However, the exact function of the PKC isoforms in the generation of AA is not fully recognized.

Moreover, it is also of current debate how various physiological and pathological stimuli can differentially activate the various isoforms of the PKC system. For example, Manicassamy et al. [13] have found that nPKCθ is required for enhancing the survival of activated $CD4^+$ T cells by up-regulating Bcl-x_L (by inhibition of apoptosis via a caspase- and mitochondria-dependent pathway) after T cell receptor (TCR) stimulation. Similar to nPKCθ-deficient primary $CD4^+$ T cells, small interfering RNA-mediated knock-down of nPKCθ in Jurkat cells also resulted in apoptosis upon TCR stimulation [13]. In addition, the crucial facilitating role of nPKCθ was also suggested in the proliferation of human T lymphocytes upon mitogen and interleukin-2 exposure [14]. Furthermore, it is also known that the activation of PKC is required for the ultimate activation of the transcription factor NF-κB and hence for the adaptive immune response in lymphocytes [15]. However, the connection between the PKC activation and NF-κB is not clarified yet. In B cells, however, Martin et al. found that the loss of aPKCζ selectively impairs signaling through the B cell receptor, resulting in inhibition of cell proliferation and survival, impairment in the activation of ERK, and inhibition of transcription of NF-κB-dependent genes [16]. In contrast, only very limited data is available about the possible functions of PKC isoforms in the proliferation of human peripheral monocytes [5].

Recent studies of our laboratories also suggested the participation of distinct PKC isozymes in the development of certain pathological alterations seen in mononuclear cell-related diseases. Namely, we have previously shown that, in monocytes of patients with newly diagnosed systemic lupus erythematosus (SLE; i.e., receiving no steroid therapy), the expression levels of nPKCδ and ε was dramatically suppressed when compared to healthy control monocytes [17]. We have also presented that, in these diseased cells, the AA release was decreased compared to monocytes of healthy individuals [18]. Furthermore, we also found that corticosteroid treatment of patients with SLE resulted in a marked elevation ("normalization") of the levels of nPKCδ and ε, in parallel with the improvement in the clinical status and number of biochemical parameter, including, of great importance, AA production [17].

As the above findings strongly argued for that there might be an intimate connection between the certain PKC isoforms and the proliferation and AA production of monocytes (a phenomenon that is already documented, for example, in macrophages and related cell lines [7, 8, 10]), in the current study, using combined pharmacological and molecular biological approaches, we intended to investigate the isoform-specific roles of various PKC isoforms in the human monocytic cell line MonoMac-6. This model system was specifically chosen, as we have previously characterized the PKC isozyme pattern of these cells [17], and furthermore, as there is no data in the literature about the involvement of the PKC system regarding the proliferation and AA production. Based on our results, in this paper, we provide the first evidence that certain PKC isoforms play pivotal, specific, and (at least partly) antagonistic roles in the regulation of cellular proliferation and AA production of human monocytoid MonoMac-6 cells.

Materials and methods

Cell culture

MonoMac-6 cells were cultured under lipopolysaccharide-free conditions in Roswell Park Memorial Institute (RPMI)-1640 medium containing 10% fetal bovine serum, 2 mM L-glutamine, 1 mM sodium pyruvate, 0.1 mM nonessential amino acids, 200 U/ml penicillin, 200 μg/ml streptomycin (all from Sigma, St Louis, MO, USA).

Transient transfection of PKC isoforms

Cells were transfected using the Amaxa Nucleofection technology (Amaxa, Cologne, Germany). Cells were resuspended in solution from nucleofector kit V, also available as part of the Amaxa cell optimization kit, following the Amaxa guidelines for cell line transfection (see Amaxa literature for further details about this kit). Briefly, 100 μl of 3.5×10^6 cell suspension mixed with 4-μg enhanced green fluorescent protein (eGFP)-conjugated complimentary DNA (cDNA) vectors (encoding the sequence of various PKC isoforms as well as the empty vector, all from Clontech, Mountain View, CA, USA) was transferred to the provided cuvette and nucleofected with an Amaxa nucleofector apparatus (Amaxa). Cells were transfected using the U-01 pulse protocol and were immediately transferred into 12-well plates containing 37°C pre-warmed culture medium. After transfection, cells were cultured from 2 to 48 h, and then, the efficacy of overexpression was analyzed by fluorescent microscopy, flow cytometry, and Western blotting.

Flow cytometry

To assess the transfection efficiency of eGFP-conjugated PKC constructs and also of possible changes of cell viability, MonoMac-6 cells (4, 24, and 48 h after transfection) were subjected to flow cytometry analysis (Coulter Epics XL, Beckman Coulter, Fullerton, CA, USA). The transfection efficacy was measured by determining fluorescence intensity values, whereas living and dead cells were identified by forward and side scatter parameters.

RNA-interference (siRNA)

Cells were seeded in 6-well culture plates in RPMI media containing serum, but lacking antibiotics. At 40–50% confluence, cells were transfected with small interfering RNA (siRNA) probes against PKCs or with fluorescein-labeled control siRNA (Santa Cruz, Santa Cruz, CA, USA) previously mixed (and incubated at room temperature for 25 min) with a transfection medium also containing the transfection reagent (both provided by Santa Cruz for use in siRNA transfection protocols). The efficacy of siRNA-driven "knock-down" of the PKCs was daily evaluated by Western blotting for 4 days.

Western blot analysis

Cells were washed with ice-cold phosphate-buffered saline (PBS), harvested in homogenization buffer [20 mM Tris–HCl, 5 mM ethylene glycol tetraacetic acid, 1 mM 4-(2-aminoethyl)benzenesulfonyl fluoride, 20 mM leupeptin, pH 7.4; all from Sigma], and disrupted by sonication on ice. The protein content of samples was measured by a modified bicinchoninic acid protein assay (Pierce, Rockford, IL, USA). Total cell lysates were mixed with sodium dodecyl sulfate-polyacrylamide gel electrophoresis (SDS-PAGE) sample buffer and boiled for 10 min at 100°C. The samples were subjected to SDS-PAGE (8% gels were loaded with 20- to 30-mg protein per lane) and transferred to nitrocellulose membranes (Bio-Rad, Wien, Austria) [4]. Membranes were then blocked with 5% dry milk in PBS and probed with the appropriate primary antibodies against the given PKC isoform; anti-PKCα, ε, and ζ were from Sigma, whereas anti-PKCβ_I, γ, δ, θ, and λ from Santa Cruz. Peroxidase-conjugated goat anti-rabbit immunoglobulin G antibodies (Bio-Rad) were used as secondary antibodies, and the immunoreactive bands were visualized by an enhanced chemiluminescence Western blotting detection kit (Amersham, Little Chalfont, UK). Immunoblots were subjected to densitometric analysis using an Intelligent Dark Box (Fuji, Tokyo, Japan) and the Image Pro Plus 4.5.0 software (Media Cybernetics, Silver Spring, MD, USA), and then normalized densitometric values of the individual lanes of several independent experiments were determined and expressed as mean±SEM. To assess equal loading, membranes were stripped in 200 ml of 50 mM Tris–HCl buffer (pH 7.5) containing 2% SDS and 0.1 β-mercaptoethanol (all from Sigma) at 65°C for 1 h and were re-probed with a mouse β-actin antibody (Sigma) followed by a similar visualization procedure as described above.

Quantitative "real-time" PCR

Quantitative polymerase chain reaction (Q-PCR) was carried out on an ABI PRISM 7000 Sequence Detection System (Applied Biosystems, Foster City, CA, USA) by using the 5′ nuclease assay. Total RNA was isolated using TRIzol (Invitrogen). One microgram of total RNA were then reverse transcribed into cDNA by using 15 units of avian myeloblastosis virus reverse transcriptase (Promega, Madison, WI, USA) and 0.025 μg/μl random primers (Promega). PCR amplification was carried out by using the TaqMan primers and probes (Assay ID: Hs00176973_m1 for PKCα; Assay ID: Hs00176998_m1 for PKCβ1; Assay ID: Hs00178914_m1 for PKCδ; Assay ID: Hs00178455_m1 for PKCε and Assay ID: Hs00177051_m1 for PKCζ) using the TaqMan Universal PCR Master Mix Protocol (Applied Biosystems). As internal controls, transcripts of glyceraldehyde 3-phosphate dehydrogenase (GAPDH) were determined (Assay ID: Hs99999905_m1 for human GAPDH).

Determination of cellular proliferation

The proliferation of the cells was determined by measuring the conversion of the methylthiazol tetrazolium (MTT) salt

to formazan (Sigma). Cells were plated in 96-well multititer plates (5×10^5/ml density) in quadruplicates and were treated with different concentrations of the reagents for the time indicated (see respective figures). Cells were then incubated with 0.5 mg/ml MTT for 3 h, and the concentration of formazan crystal (as the indicator of number of viable cells) was determined colorimetrically according to the manufacturer's protocol. Data are expressed as mean±SEM.

AA release

Cells at 10^5 cells/ml densities were preincubated with [^{3}H] AA (Amersham, Little Chalfont, UK) in CO_2 incubator at 37°C for 20 h. After extensive washing, the cells were further incubated with either culturing medium (basal production of AA) or with various agents investigated for 4 h, and the released [^{3}H]AA was determined by scintillation counting. Each value was calculated as the average of triplicates of cultured cells and at least four individual experiments were performed.

Statistical analysis

When applicable, data were analyzed using a two-tailed unpaired *t*-test, and $P<0.05$ values were regarded as significant differences.

Results

Using flow cytometry, we have previously shown that MonoMac-6 cells possess functionally active PKC system [17]. Namely, they express the cPKCα and β, nPKCδ and ε, and aPKCζ; interestingly, we were unable to detect any expression of nPKCη—an isoform that does exist in human peripheral monocytes [17]—and other PKC isoforms (cPKCγ, nPKCθ, aPKCλ/ι, or PKCμ). In this study, these results were confirmed by Western blotting and Q-PCR (Fig. 1a and b). Using the latter technique, we were also able to show that the relative expression levels of various PKC isoforms in MonoMac-6 cells are different. Namely, certain PKC isoforms possessed relatively high (nPKCδ>>>>cPKCβ>aPKCζ), whereas others low (cPKCα>nPKCε) expression levels normalized to the endogenous control GAPDH (Fig. 1b).

We then intended to determine the potential roles of the PKC system in the regulation of cellular functions of MonoMac-6 cells. As seen in Fig. 1c, application of the general PKC activator phorbol 12-myristate 13-acetate (PMA; for 2 days) resulted in a significant and dose-dependent decrease in the proliferation of cells. In parallel, as was assessed by Western blotting (Fig. 1a), expressions of cPKCβ and nPKCδ were suppressed (possibly due to down-regulation of the isoforms) by 100 nM PMA (as well as 10 nM PMA, data not shown), whereas the cellular levels of cPKCα and aPKCζ were not changed. Interestingly, the expression of nPKCε increased upon the phorbol ester treatment. These finding argued for that the affected (i.e., down- and up-regulated PKCs) might mediate the growth-inhibitory effect of PMA.

Moreover, confirming our previous data [17], we also found that the administration of PMA induced a remarkable increase in the AA release (Fig. 1d), which also suggested the involvement of the PKC pathway. To further determine the participation of the existing PKCs in the effect of PMA, certain PKC inhibitors were investigated. As seen in Fig. 1d, the cPKC inhibitor (in our case, the inhibitor of the cPKCα and β) Gö6976 [19] as well as Rottlerin (a selective inhibitor of the nPKCδ [20]) significantly prevented the effect of the phorbol ester to induce AA release.

The above data strongly suggested an important role of certain PKC isoforms in modulation of cellular proliferation and AA release. The participation of numerous isoforms in the effect of PMA, however, resulted in a very complex phenomenon and did not permit to define the exact isoform-specific regulatory roles of the PKCs in the cellular processes. Therefore, to further dissect the mechanism, we then modified the endogenous activity of the existing isoenzymes and measured the effect of such interventions on the "basal" proliferation and AA release of the cells. Incubation of MonoMac-6 cells with a cPKC inhibitor Gö6976 remarkably impeded cellular division in a dose-dependent fashion (Fig. 2a). Similarly, the inhibition of the nPKCδ by Rottlerin also dose-dependently suppressed cellular proliferation (Fig. 2b). It was important to observe, however, that neither Rottlerin nor Gö6976 was able to affect the basal AA release when applied alone (Fig. 2c). Notably, using Trypan-blue staining and glucose-6-phosphate-dehydrogenase release cytotoxicity assay, we observed insignificant cell death, even at the highest concentrations applied (data not shown). This was in good accord with previous findings in the literature [19, 20] demonstrating the lack of cytotoxic effects of Gö-6976 and Rottlerin at the concentrations applied in the current study.

Recent findings about the limitation of the specificity and selectivity of the above inhibitors [21–24] and, moreover, the lack of efficient inhibitors for nPKCε and aPKCζ, however, forced us to further investigate the roles of the isoenzymes using various molecular biological techniques. Along these lines, we transiently overexpressed the isoforms in a GFP-tagged fusion protein format. The high efficacy of recombinant overexpression (measured 24 h after transfection) was monitored by fluorescence microscopy (Fig. 3) and flow cytometry, which the latter technique resulted in an average >80% cell survival rate

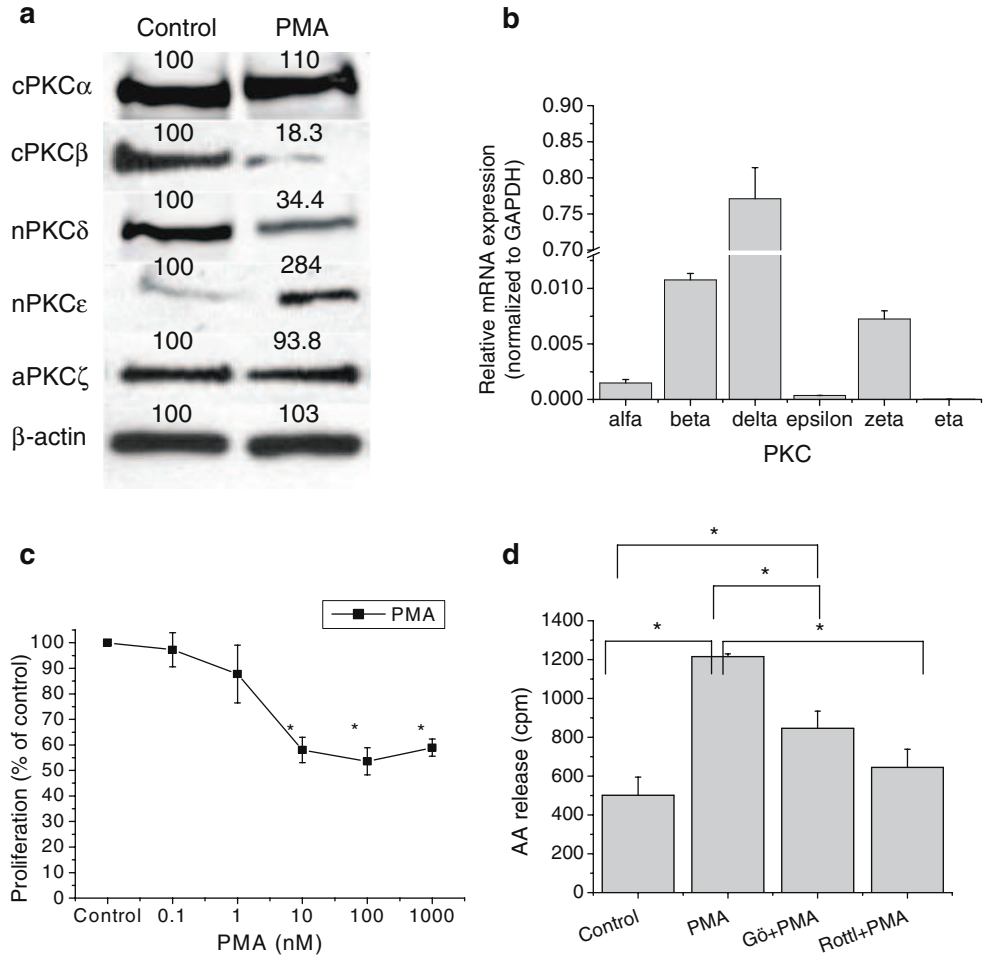

Fig. 1 The PKC isoforms pattern of MonoMac6 cells and the effect of PMA treatment. **a** Cells were treated with 100 nM PMA for 2 days and (along with control cells) were subjected to Western immunoblotting using anti-PKC antibodies. The amounts of the individual PKC isoforms were quantitated by densitometry and expressed as the percentage of the value of immunoreactive bands of control cells regarded as 100%. The figure is a representative of several determinations for each isoform. **b** Q-PCR analysis of the expression of various PKC isoforms in MonoMac-6 cells. Data were normalized to the expression of the internal control GAPDH of the same sample. **c** Cells were seeded at densities of 50,000 cells/well in96-well microtiter plates, treated with various concentration of PMA for 2 days, and cell proliferation was determined using MTT assays. *Points* represent the mean±SEM of quadruplicate determinations in one representative experiment and expressed as a percentage of the control (non-treated) group regarded as 100%. Three additional experiments yielded similar results. *Asterisks* represent significant ($P<0.05$) changes compared to control **d** Cells at 10^5 cells/ml densities were treated with culturing medium (*Control*), 100 nM PMA, and 5 μM calcium ionophore A23187 (*PMA*), PMA+A23187 and 20 nM Gö6976 (*Gö+PMA*), or PMA+A23187 and 100 nM Rottlerin (*Rott+PMA*) for 4 h, and the release of AA was determined in triplicate. Data were expressed as mean±SEM. *Asterisks* represent significant ($P<0.05$) changes

and >70% transfection efficiency (data not shown). In addition, Western blot analysis also revealed the successful overexpression of the isoforms (Fig. 3, insets).

We then measured the effect of PKC isoform overexpression on the AA release of the cells. First, we measured the effect of the transfection itself on potential cell death and AA leakage of the cells. As seen in Fig. 4a, transient transfection of the empty eGFP vector resulted in similar basal and PMA-induced AA release to those of the control (i.e., non-transfected) cells suggesting that the transfection procedure did not alter the responsiveness of the cells.

As seen in Fig. 4b, e, and f, the overexpression of cPKCα, nPKCε, or aPKCζ did not affect the basal AA release. In contrast to these findings, the overexpression of cPKCβ or nPKCδ significantly elevated the basal AA release (Fig. 4c and d). However, it was intriguing to observe that the overexpression of cPKCα (unlike any of the other four isoforms) significantly affected the PMA-induced AA release; namely, it inhibited the effect of the phorbol ester (Fig. 4b).

It is generally accepted that different phospholipase A_2 (PLA_2) enzymes that play key roles in cellular synthesis of AA [25, 26]—such as the cytosolic phospholipase A_2

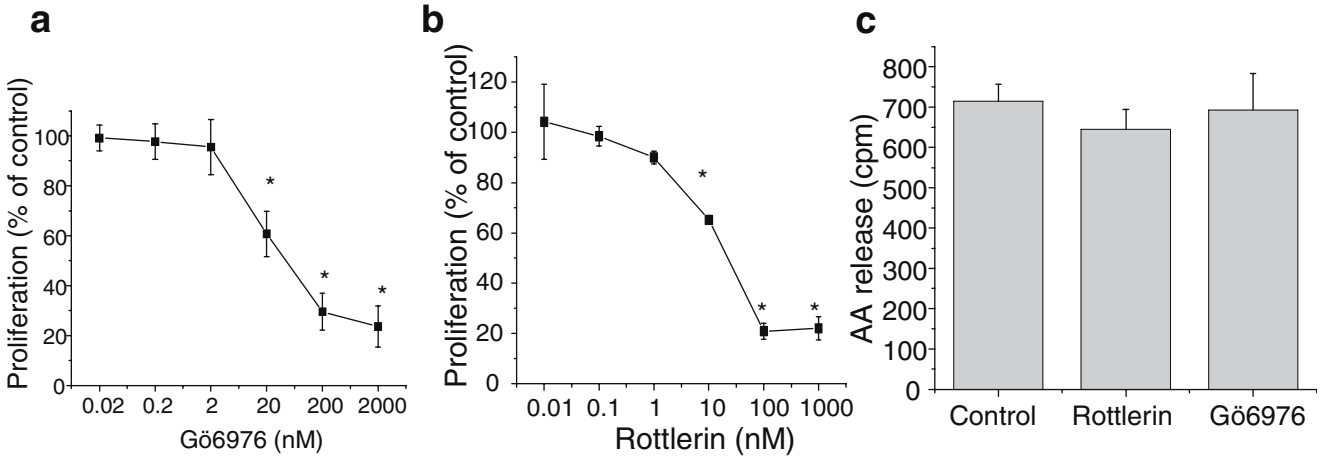

Fig. 2 Effects of different PKC inhibitors on proliferation and AA release of MonoMac-6 cells. Cells were seeded at densities of 50,000 cells/well in 96-well microtiter plates, treated with various concentration of Gö6976 (**a**) or Rottlerin (**b**) for 2 days, and cell proliferation was determined using MTT assays. *Points* represent the mean±SEM of quadruplicate determinations in one representative experiment and expressed as a percentage of the control (non-treated) group regarded as 100%. Three additional experiments yielded similar results. **c** Cells were treated with culturing medium (*Control*), 100 nM Rottlerin (*Rottlerin*), or 20 nM Gö6976 (*Gö6976*) for 4 h, and the release of AA was determined in triplicate. Data were expressed as mean±SEM. *In all panels*, *asterisks* represent significant ($P<0.05$) changes compared to control

($cPLA_2$), the calcium-independent phospholipase A_2 ($iPLA_2$), and diacylglycerol (DAG) lipase—might be the "down-stream" targets of various PKCs [8, 27–29]. Therefore, to further evaluate the putative molecular mechanism coupled to the cPKCβ- and nPKCδ-mediated signaling, we aimed to determine the effects of the inhibitors [30–32] of these enzymes on the basal AA release of control (eGFP transfected) MonoMac-6 cells and on the elevated basal AA production of the cPKCβ and nPKCδ transfectants. In control cells, application of the $cPLA_2$ inhibitor AACOCF3 did not modify the basal AA release. In contrast, incubating the cells with the $iPLA_2$ inhibitor PACOCF3 or the DAG lipase inhibitor RHC-80267 significantly decreased the basal AA production of the cells (Fig. 5a). Importantly, similar phenomena were observed in the cases of the two overexpressers (Fig. 5b and c). Namely, the $iPLA_2$ and the DAG lipase inhibitors significantly inhibited the elevated basal AA release of the cPKCβ and nPKCδ transfectants, whereas the $cPLA_2$ inhibitor was ineffective.

Unfortunately, the transient overexpression method did not permit the parallel investigation of the alteration in the proliferation rate of the cells, as (within 48 h), on the one hand, the majority (>50%) of the cells fairly rapidly died (most likely because of membrane injury induced by Nucleofection), and on the other, we observed a significant decrease in the number of GFP-fusion protein-expressing cells in the cultures (data not shown). Therefore, we employed another molecular biological approach (namely, the RNA-interference technique) to reveal the specific, endogenous roles of the above three isoforms (i.e., cPKCα and β, and nPKCδ) in the regulation of the proliferation of the cells.

Western blot analysis revealed (Fig. 6a–d) that the expressions of all three PKC isoforms investigated were significantly "knocked down" by distinct siRNA probes at day 2. However, these phenomena were reversible, as we observed a "return" of the immunosignals at day 4. Importantly, in analogy to data obtained with the various PKC inhibitors (see Fig. 2a and b), the "knock-down" of nPKCδ and cPKCβ partially (yet significantly at day 2) suppressed the proliferation rate of the cells (Fig. 6e) in which the effects were mostly "diminished" by day 4 (in parallel to the reappearance of the given PKC isoenzyme in the cells). It was also intriguing to observe that, at day 2, the sum of growth inhibition of nPKCδ and cPKCβ "knock-downs" exactly matched the effect of 10–1,000 nM PMA (added alone for 2 days) to inhibit proliferation (see also in Fig. 1c). Conversely, the siRNA-induced down-regulation of cPKCα slightly elevated the growth rate of the cells. Taken together, these results strongly argue that cPKCβ and δ promote, whereas cPKCα rather inhibits, proliferation of MonoMac-6 cells.

Discussion

In this study, using combined pharmacological and molecular biological approaches, we provide the first evidence that certain PKC isozymes of the existing isoforms specifically, differentially, and (most probably) antagonistically regulate the proliferation and AA release of the monocytoid cell line MonoMac-6.

According to best of our knowledge, this is the first demonstration that the nPKCδ (which is, by far, the

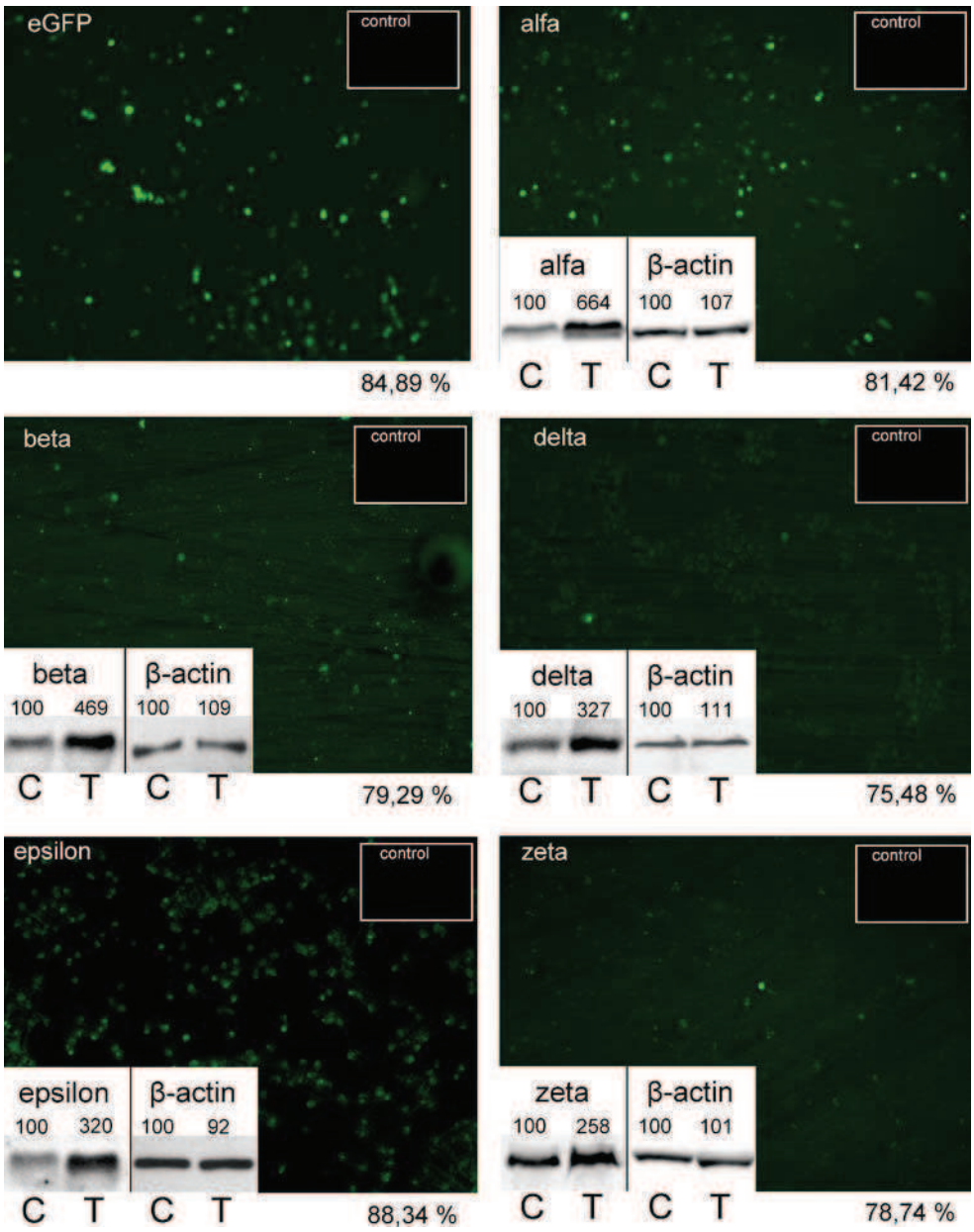

Fig. 3 Transfection efficacy of transiently overexpressed GFP-tagged PKC isoforms and the empty eGFP vector. Cells were transfected with eGFP-tagged empty or PKC-containing vectors as described under "Materials and methods," and fluorescence images were taken 24 h after transfection. *In all images*, *insets in the top right corners* show control cultures where the transfection medium lacked the vectors. Twenty-four hours after transfection, control (*C*) and transfected (*T*) cells were harvested and subjected to Western immunoblotting using anti-PKC antibodies (*insets in the bottom left corners*). The amounts of the individual PKC isoforms were quantitated by densitometry and expressed as the percentage of the value of immunoreactive bands of control cells regarded as 100%

dominant PKC isoform in MonoMac-6 cells, Fig. 1b) acts as a positive regulator of both the proliferation and the AA release in human monocytoid cells. This argument is supported by numerous lines of evidence: (1) The isoform was remarkably down-regulated (hence, possessed lower expression levels) upon PMA treatment in parallel with the growth inhibitory action of the phorbol ester (Fig. 1a and c); (2) pharmacological inhibition of endogenous activity of nPKCδ suppressed proliferation (Fig. 2b); (3) the selective inhibitor of the isozyme inhibited PMA-induced AA release (Fig. 1d); (4) siRNA-driven "knock-down" of the isoform significantly inhibited the proliferation of the cells (Fig. 6e). It should be noted, however, that the nPKCδ inhibitor did not modify the basal AA production (Fig. 2c) suggesting that, in contrast to its role in the regulation of proliferation, the endogenous basal (yet fairly high) expression and activity of the isoform most probably does not participate in the processes of basal AA production. On the contrary, it appears that, when nPKCδ was recombinantly overexpressed (hence, possessed an even more increased activity), it significantly elevated the basal AA production of the cells (Fig. 4d) suggesting that, upon exogenous activation, the isoform may mediate the action of agents to promote AA production.

Strikingly similar results were obtained when investigating the function of another highly expressed isozyme, cPKCβ (a previously more extensively studied isoform) in MonoMac-6 cell functions. Namely, the isoenzyme was also down regulated during PMA-induced growth inhibition (Fig. 1a and c), whereas inhibition of its endogenous

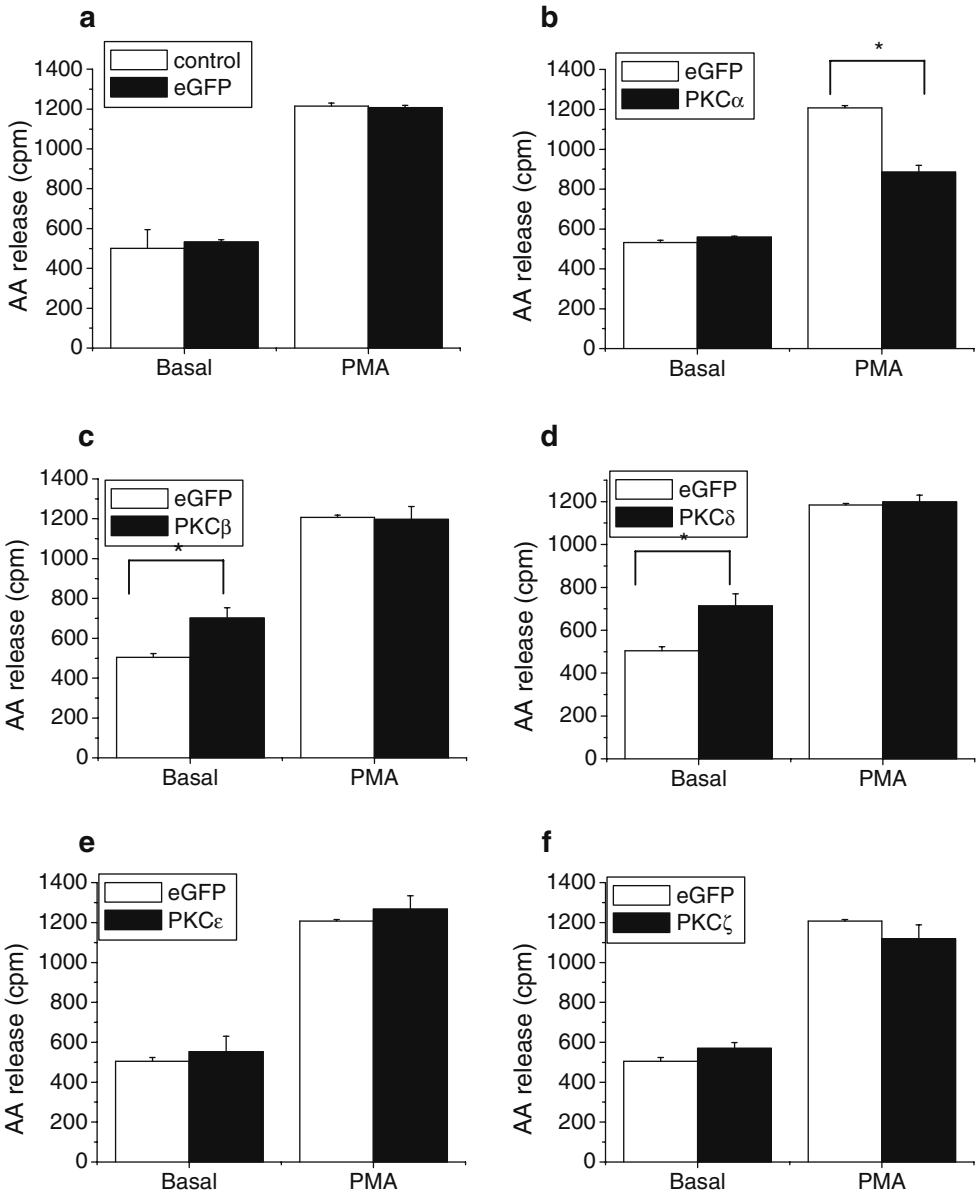

Fig. 4 AA release in PKC-transfected MonoMac-6 cells. Cells were transfected with eGFP-tagged empty or PKC-containing vectors as described under "Materials and methods" and, after 24 h, were seeded at 10^5 cells/ml densities to 12-well plates. The transfected cells, along with cells treated with the transfection medium lacking the vectors (*control*), were treated with culturing medium (*Basal*) or with 100 nM PMA and 5 μM calcium ionophore A23187 (*PMA*) for 4 h, and the release of AA was determined in triplicate. Data were expressed as mean±SEM. *Asterisks* represent significant ($P<0.05$) changes

activity (Fig. 2a) or suppression of its expression level by siRNA (Fig. 6e) significantly inhibited proliferation of the cells. These data are in good accord with previous studies showing that stable transfection of human myeloid THP-1 cell line with antisense-PKCβ reduced proliferation [5] and that the recombinant overexpression of this isoform enhanced proliferation of the human erythroleukemia cells K562 [33].

With respect to AA production, the overexpression of cPKCβ also resulted in a significant elevation of the basal AA release of the cells (Fig. 4c), whereas inhibition of cPKCβ by Gö6976 significantly prevented the action of PMA to stimulate AA production (Fig. 1d). This was in line with previous demonstrations that PKCβ mediated the effect of PMA to stimulate AA production in murine RAW 264.7 macrophages [28]. In addition, also similar to the function of nPKCδ, suppression of the endogenous cPKCβ activity did not modify the basal AA production (Fig. 2c). Finally, it was also important to observe that increased AA release in cells overexpressing cPKCβ and nPKCδ (similarly to control cells) was fully abrogated by the inhibitor of the iPLA$_2$ enzyme in which findings identify this "downstream" molecule as a potential target of these PKC isozymes (Fig. 5). Experiments with the DAG lipase inhibitor RHC-80267 revealed that this enzyme may be also activated by cPKCβ and nPKCδ. However, experiments with newly developed, more specific inhibitors [34, 35] would further strengthen this hypothesis. In summary, these results strongly argue for the positive role of cPKCβ and nPKCδ in the regulation of proliferation and AA release of the monocytoid MonoMac-6 cells.

Experimental data with cPKCα, however, suggested that this isoform (which possessed a very low expression level

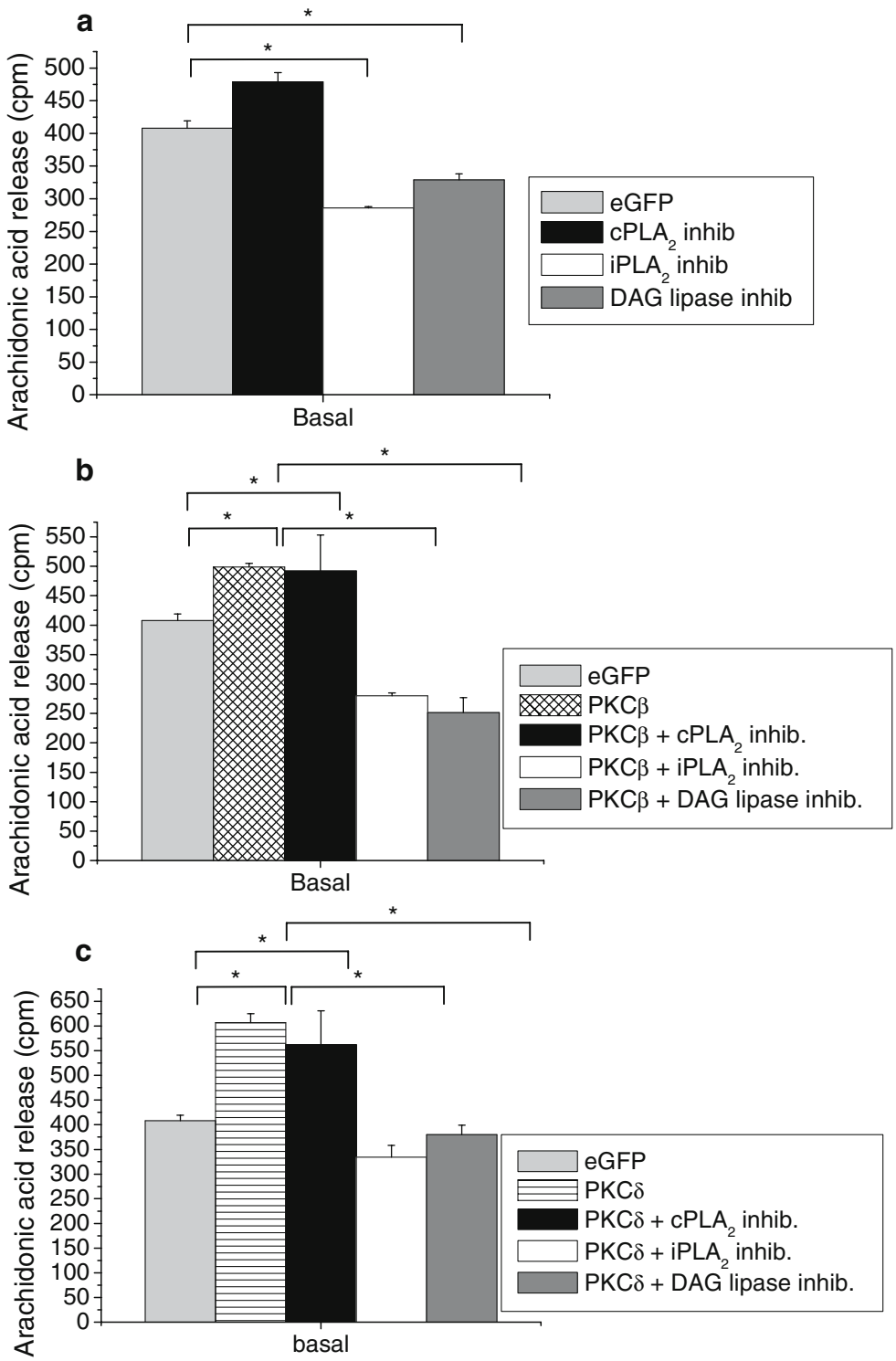

Fig. 5 Effects of inhibitors of various AA producing enzymes on the AA release. Cells transfected with the empty eGFP vector (*eGFP*) as well as cPKCβ or nPKCδ were treated with the $cPLA_2$ inhibitor AACOCF3 (100 ìM), the $iPLA_2$ inhibitor PACOCF3 (10 μM), or the DAG lipase inhibitor RHC-80267 (10 μM) for 4 h, and the basal release of AA was determined in triplicate. Data were expressed as mean±SEM. *Asterisks* represent significant ($P<0.05$) changes

in the cells, Fig. 1b) plays a minor yet (most probably) opposite role in the regulation the MonoMac-6 cell processes when compared to the actions of cPKCβ and nPKCδ. The only significant finding with this isoform was that its overexpression efficiently prevented the effect of PMA to stimulate the AA production of the cells (Fig. 4b). Interestingly, even when overexpressed, it did not affect at all the basal AA release (Fig. 4b) suggesting the lack of involvement of this isoforms in the regulation of the process. Moreover, we observed only a slightly increased growth rate of those cells in which cPKCα was "knocked down" using siRNA (Fig. 6e), which may suggest the negative role of this isoform in regulating proliferation of the cells. This hypothesis is also supported by previous data

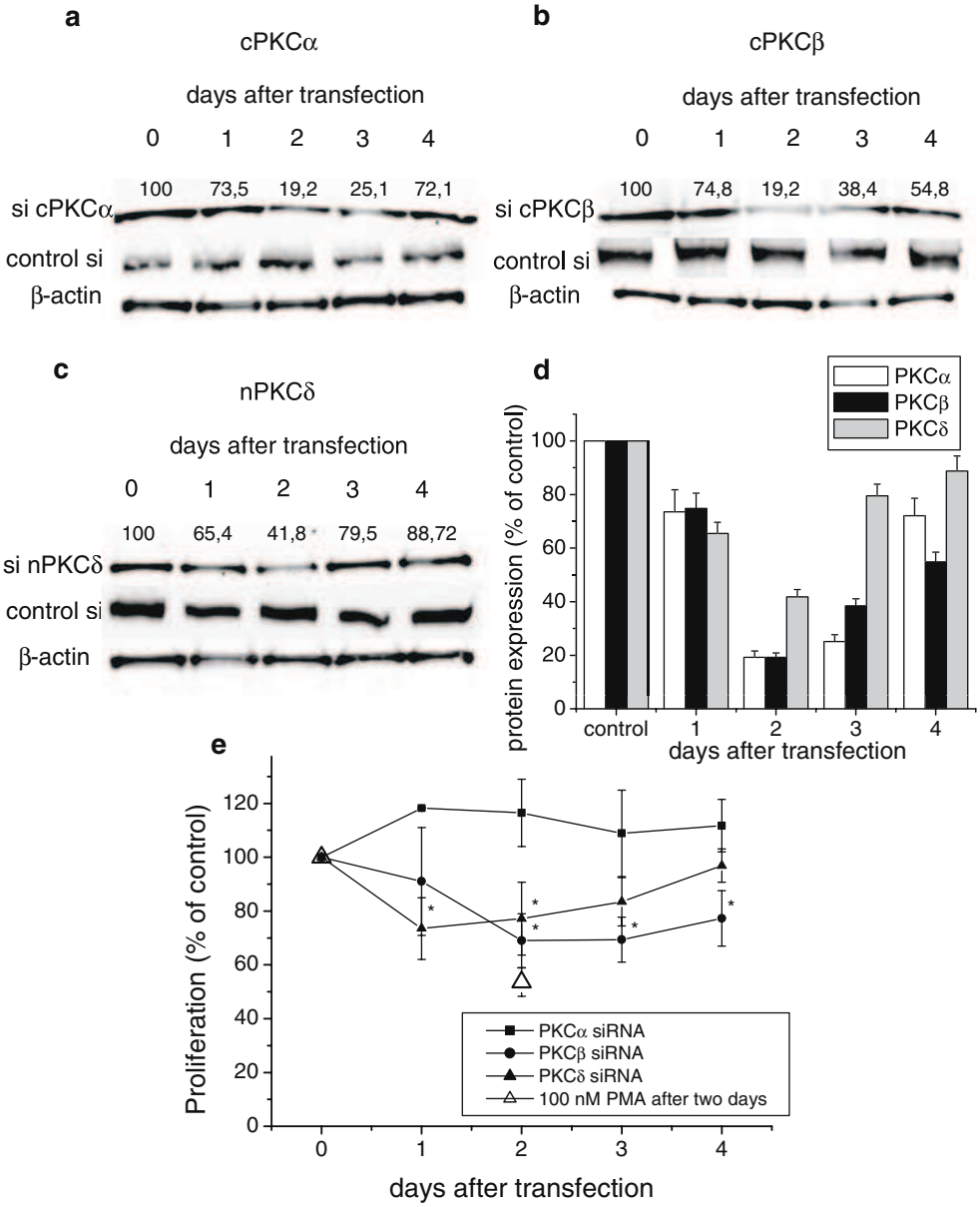

Fig. 6 siRNA-driven "knock-down" of various PKC isoforms and its effect on the proliferation of MonoMac-6 cells. **a**–**c** Various siRNA probes against cPKCα and β and nPKCδ (as well as the control siRNA) were introduced to the cells as described under "Materials and methods." To evaluate the efficacy of this intervention, cells were then subjected to Western immunoblotting using anti-PKC antibodies (*upper two lanes*). As controls, the expression of β-actin was also determined (*lower lanes*). *Numbers* represent densitometry values as *described under* (***d***). **d** In each case, the amounts of the individual PKC isoforms were quantitated by densitometry, normalized to those of β-actin, and expressed as the percentage of the value obtained at day 0 regarded as 100%. **e** Transfectant cells were seeded at densities of 50,000 cells/well in 96-well microtiter plates, and the cell proliferation was daily determined using MTT assays. *Points* represent the mean±SEM of quadruplicate determinations in one representative experiment and expressed as a percentage of the proliferation of the daily-matched, control siRNA-transfected group regarded as 100%. Three additional experiments yielded similar results. *Asterisks* represent significant ($P<0.05$) changes compared to these control groups

showing that antisense-PKCα enhanced the proliferation of human myeloid THP-1 cell line [5], that PKCα overexpressers human K562 erythroleukemia cells possessed a much slower growth rate than control cells [28], and that, in the 32D mouse myeloid progenitor cell line, cPKCα participated in the TPA-induced myeloid differentiation [36]. Finally, the very low endogenous expression level and, hence, the relatively minor (negative) role of cPKCα in the regulation of proliferation of MonoMac-6 cells may also explain the "unexpected" growth-inhibitory effect of cPKC inhibitor Gö6976 (Fig. 2a), which most probably, exerted its inhibitory action on the growth-promoting cPKCβ possessing >seven-fold higher expression level than cPKCα (Fig. 1b).

In our hands, the nPKCε and aPKCζ did not seem to participate in the above cellular processes of the cells. Firstly, transient overexpression of these isozymes did not affect the basal or PMA-induced AA release of the cells (Fig. 4e and f). Moreover, as expected, PMA treatment did not influence the protein expression of aPKCζ (Fig. 1a). Interestingly, the level of nPKCε seemed to double after PMA administration (Fig. 1a); however, as the endogenous level of this isoform was by far the lowest (e.g., less than 1/20 of cPKCβ as revealed by Q-PCR, Fig. 1b), we think that this alteration in the protein expression has negligible role, especially when compared to the effect of PMA to down-regulate cPKCβ or nPKCδ.

Finally, our results may even have clinical implications. As we have previously shown, the diseased monocytes from freshly diagnosed SLE patients possessed impaired AA production as well as low nPKCδ and ε levels [17, 18].

Of great importance, we have moreover documented that the clinically effective corticosteroid treatment of the patients in vivo or the isolated monocytes in vitro "normalized" both the AA release and the expressions of the two isoforms (at both protein and mRNA levels) suggesting that the pathological levels of nPKCδ and/or ε might be responsible for the decreased AA production in SLE monocytes [17]. In addition, our previous results also suggested that the "normalization" of the AA production in the monocytes by corticosteroid treatment of SLE patients was due to the "reactivation" of the $iPLA_2$-dependent pathway [18]. Therefore, our current presentation that, in the monocytoid MonoMac-6 cell line, (1) the overexpression of nPKCδ markedly increased AA production, whereas that of nPKCε did not modify the process (Fig. 4d and e), and (2) the effect of nPKCδ overexpression to elevate AA release could be completely reversed by the inhibition of the $iPLA_2$ enzyme (Fig. 5c), invite an attractive hypothesis that the selective activation of nPKCδ may be a fine tool in the therapeutic management of SLE-related alterations of monocyte functions. In addition, in such monocytoid cells where cPKCα is more abundant that in MonoMac-6 cells (for example, in monocytes from SLE patients; [17]), an alternative approach could be a selective inhibition of (the, most probably, growth inhibitory) cPKCα.

Acknowledgments This work was supported by Hungarian Research grants: OTKA T37531, OTKA T049231, OTKA K63153, NKFP 1A/008/04, RET 06/2004. The authors declare no competing financial interests.

References

1. Nishizuka Y (1988) The molecular heterogenity of protein kinase C, and it's implication for cellular regulation. Nature 334:661–665
2. Jaken S (1996) Protein kinase C isoenzymes and substrates. Curr Opin Cell Biol 8:168–173
3. Wilkinson SE, Nixon JS (1998) T-cell signal transduction and the role of protein kinase C. Cell Mol Life Sci 54:1122–1144
4. Papp H, Czifra G, Bodó E, Lázár J, Kovács I, Aleksza M, Juhász I, Ács P, Sipka S, Kovács L, Blumberg PM, Bíró T (2004) Opposite roles of protein kinase C isoforms in proliferation, differentiation, apoptosis, and tumorigenicity of human HaCaT keratinocytes. Cell Mol Life Sci 61:1095–1105
5. Dieter P, Schwende H (2000) Protein kinase C-α and -β play antagonistic roles in the differentiation process of THP-1 cells. Cell Signal 12:297–302
6. Sodhi A, Sedhi G (2005) Role of protein kinase Cδ in UV-B-induced apoptosis of macrophages in vitro. Cell Signal 17:377–383
7. Silberman DM, Zorrilla-Zubilete M, Cremaschi GA, Genaro AM (2005) Protein kinase C-dependent NF-κB activation is altered in T cells by chronic stress. Cell Mol Life Sci 62:1744–1754
8. Akiba S, Ohno S. Chiba M, Kume K, Hayama M, Sato T (2002) Protein kinase Cα-dependent increase in Ca^{2+}-independent phospholipase A_2 in membranes and arachidonic acid liberation in zymosan-stimulated macrophage-like P388D1 cells. Biochem Pharmacol 63:1969–1977
9. Hii CS, Huang ZH, Bilney A, Costabile M, Murray AW, Rathjen DA, Der CJ, Ferrante A (1998) Stimulation of p38 phosphorylation and activity by arachidonic acid in HeLa cells, HL60 promyelocytic leukemic cells, and human neutrophils. Evidence for cell type-specific activation of mitogen-activated protein kinases. J Biol Chem 273:19277–19282
10. Todt JC, Hu B, Punturieri A, Sonstein J, Polak T, Curtis JL (2002) Activation of protein kinase CβII by the stereo-specific phosphatidylserine receptor is required for phagocytosis of apoptotic thymocytes by resident murine tissue macrophages. J Biol Chem 277:35906–35914
11. Haeggstrom JZ, Wetterholm A (2002) Enzymes and receptors in the leukotriene cascade. Cell Mol Life Sci 59:742–753
12. Di Marzo V, Vial D, Sokoloff P, Schwartz JC, Piomelli D (1993) Selection of alternative G-mediated signaling pathways at the dopamine D2 receptor by protein kinase C. J Neurosci 11:4846–4853
13. Manicassamy S, Gupta S, Huang Z, Sun Z (2006) Protein kinase C-θ-mediated signals enhance $CD4^+$ T cell survival by up-regulating Bcl-x_L. J Immunol 176(11):6709–6716
14. Meller N, Elitzur Y, Isakov N (1999) Protein kinase C-θ (PKCθ) distribution analysis in hematopoietic cells: proliferating T cells exhibit high proportions of PKCθ in the particulate fraction. Cell Immunol 193(2):185–193
15. Lucas PC, McAllister-Lucas LM, Nunez G (2004) NF-κB signaling in lymphocytes: a new cast of characters. J Cell Sci 117(Pt 1):31–39
16. Martin P, Duran A, Minguet S, Gaspar ML, Diaz-Meco MT, Rennert P, Leitges M, Moscat J (2002) Role of ζPKC in B-cell signaling and function. EMBO J 21(15):4049–4057
17. Bíró T, Griger Z, Kiss E, Papp H, Aleksza M, Kovacs I, Zeher M, Bodolay E, Csepany T, Szucs K, Gergely P, Kovacs L, Szegedi G, Sipka S (2004) Abnormal cell-specific expressions of certain protein kinase C isoenzymes in peripheral mononuclear cells of patients with systemic lupus erythematosus: effect of corticosteroid application. Scand J Immunol 60:421–428
18. Sipka S, Szántó S, Szűcs K, Kovács I, Kiss E, Antal-Szalmás P, Lakos G, Aleksza M, Illés Á, Gergely P, Szegedi G (2001) Decreased arachidonic acid release in peripheral blood monocytes of patients with systemic lupus erythematosus. J Rheumatol 28:2012–2017
19. Martiny-Baron G, Kazanietz MG, Mischak H, Blumberg PM, Kochs G, Hug H, Marme D, Schachtele C (1993) Selective inhibition of protein kinase C isozymes by the indolocarbazole Gö 6976. J Biol Chem 268:9194–9197
20. Gschwendt M, Müller HJ, Kialbassa K, Zang R, Kittstein W, Rincke G, Marks F (1994) Rottlerin, a novel protein kinase inhibitor. Biochem Biophys Res Commun 199:93–98
21. Davies SP, Reddy H, Caivano M, Cohen P (2000) Specificity and mechanism of action of some commonly used protein kinase inhibitors. Biochem J 351:95–105
22. Soltoff SP (2001) Rottlerin is a mitochondrial uncoupler that decreases cellular ATP levels and indirectly blocks protein kinase C6 tyrosine phosphorylation. J Biol Chem 276:37986–37992
23. Kayali AG, Austin DA, Webster NJ (2002) Rottlerin inhibits insulin-stimulated glucose transport in 3T3-L1 adipocytes by uncoupling mitochondrial oxidative phosphorylation. Endocrinology 143:3884–3896
24. Tapia JA, Jensen RT, Garcia-Marin LJ (2006) Rottlerin inhibits stimulated enzymatic secretion and several intracellular signaling transduction pathways in pancreatic acinar cells by a non-PKC-δ-dependent mechanism. Biochim Biophys Acta 1763:25–38
25. Smith WL, DeWitt DL, Garavito RM (2000) Cyclooxygenases: structural, cellular, and molecular biology. Annu Rev Biochem 69:145–182

26. Balsinde J, Winstead MV, Dennis EA (2002) Phospholipase A_2 regulation of arachidonic acid mobilization. FEBS Lett 531:2–6
27. Karimi K, Lennartz MR (1995) Protein kinase C activation precedes arachidonic acid release during IgG-mediated phagocytosis. J Immunol 155:5786–5794
28. Lin WW, Chen BC (1998) Distinct PKC isoforms mediate the activation of cPLA2 and adenylyl cyclase by phorbol ester in RAW264.7 macrophages. Br J Pharmacol 125:1601–1609
29. Guidarelli A, Cerioni L, Tommasini I, Brune B, Cantoni O (2005) A downstream role for protein kinase Cα in the cytosolic phospholipase A_2-dependent protective signalling mediated by peroxynitrite in U937 cells. Biochem Pharmacol 69:1275–1286
30. Martel MA, Patenaude C, Menard C, Alaux S, Cummings BS, Massicotte G (2006) A novel role for calcium-independent phospholipase A in α-amino-3-hydroxy-5-methylisoxazole-propionate receptor regulation during long-term potentiation. Eur J Neurosci 23:505–513
31. Ackermann EJ, Conde-Frieboes K, Dennis EA (1995) Inhibition of macrophage Ca^{2+}-independent phospholipase A_2 by bromoenol lactone and trifluoromethyl ketones. J Biol Chem 270:445–450
32. Lin WW, Chang SH, Wu ML (1998) Lipoxygenase metabolites as mediators of UTP-induced intracellular acidification in mouse RAW 264.7 macrophages. Mol Pharmacol 53:313–321
33. Murray NR, Baumgardner GP, Burns DJ, Fields AP (1993) Protein kinase C isotypes in human erythroleukaemia (K562) cell proliferation and differentiation. Evidence that βII protein kinase C is required for proliferation. J Biol Chem 268:15847–15853
34. Bisogno T, Howell F, Williams G, Minassi A, Cascio MG, Ligresti A, Matias I, Schiano-Moriello A, Paul P, Williams EJ, Gangadharan U, Hobbs C, Di Marzo V, Doherty P (2003) Cloning of the first sn1-DAG lipases points to the spatial and temporal regulation of endocannabinoid signaling in the brain. J Cell Biol 163(3):463–468
35. Bisogno T, Cascio MG, Saha B, Mahadevan A, Urbani P, Minassi A, Appendino G, Saturnino C, Martin B, Razdan R, Di Marzo V (2006) Development of the first potent and specific inhibitors of endocannabinoid biosynthesis. Biochim Biophys Acta 1761 (2):205–212
36. Mischak H, Pierce JH, Goodnight J, Kazanietz MG, Blumberg PM, Mushinski JF (1993) Phorbol ester-induced myeloid differentiation is mediated by protein kinase C-α and -δ and not by protein kinase C-βII, -ε, -ζ, and -η. J Biol Chem 268:20110–20115

XVII.

Oral Diseases (2009) 15, 328–335. doi:10.1111/j.1601-0825.2009.01526.x

http://www.blackwellmunksgaard.com

ORIGINAL ARTICLE

Increased expression of TRPV1 in squamous cell carcinoma of the human tongue

R Marincsák[1,2], BI Tóth[1], G Czifra[1], I Márton[2], P Rédl[2], I Tar[2], L Tóth[3], L Kovács[1], T Bíró[1]

[1]*Department of Physiology,* [2]*Faculty of Dentistry and* [3]*Department of Pathology, University of Debrecen, Medical and Health Science Centre, Research Centre for Molecular Medicine, Debrecen, Hungary*

OBJECTIVES: Recent reports have unambiguously identified the presence and the growth-modulatory role of transient receptor potential vanilloid-1 (TRPV1), a central integrator of pain sensation, on numerous non-neuronal cell types and, of great importance, in certain malignancies. In this study, we have investigated the molecular expression of TRPV1 in the human tongue and its high-incidence malignant (squamous cell carcinoma, SCC) and premalignant (leukoplakia) conditions.

METHODS: Immunohistochemistry, Western blotting and quantitative 'real-time' Q-PCR were performed to define the expression of TRPV1.

RESULTS: A weak and sparse TRPV1-specific immunoreactivity was identified in the basal layers of the healthy human tongue epithelium. By contrast, we observed a dramatically elevated TRPV1-immunoreactivity in all layers of the epithelium both in precancerous and malignant samples. Furthermore, statistical analysis revealed that the marked overexpression of TRPV1 found in all grades of SCC showed no correlation with the degree of malignancy of the tumours. Finally, the molecular expression of TRPV1 was also identified in an SCC-derived cell line and was shown to be increased in parallel with the accelerated growth of the cells.

CONCLUSION: Collectively, our findings identify TRPV1 as a novel, promising target molecule in the supportive treatment and diagnosis of human tongue SCC.
Oral Diseases (2009) **15**, 328–335

Keywords: transient receptor potential vanilloid-1 (TRPV1); human tongue epithelium; human tongue squamous cell carcinoma; leukoplakia; overexpression

Correspondence: Tamás Bíró, MD, PhD, Department of Physiology, University of Debrecen, Medical and Health Science Centre, Research Centre for Molecular Medicine, 4032 Debrecen, Nagyerdei krt. 98. PO Box 22, Hungary. Tel: +36 52 416 634, Fax: +36 52 432 289, E-mail: biro@phys.dote.hu
Received 6 January 2009; revised 18 February 2009; accepted 22 February 2009

Introduction

Transient receptor potential vanilloid-1 (TRPV1), a member of the large TRP channel family, is a non-selective calcium-permeable cation channel which was originally described on nociceptive sensory afferents as a central integrator of pain sensation (Caterina *et al*, 1997; Tominaga *et al*, 1998). Indeed, TRPV1 can be activated by numerous exogenous and endogenous agents such as capsaicin (alkaloid of hot chilli peppers), resiniferatoxin (pungent compound isolated from *Euphorbia resinifera*), heat, low pH, inflammatory mediators, etc (Di Marzo *et al*, 2002; Ugawa *et al*, 2002). The activation of TRPV1 results in depolarization of the sensory afferents, firing of action potentials and hence the onset of pain sensation (Moran *et al*, 2004).

Recent reports, however, have unambiguously identified the presence of TRPV1 on numerous non-neuronal cell types as well. We and others have found that functional TRPV1 is expressed, for example, on various epithelial cells such as human skin keratinocytes (Denda *et al*, 2001; Inoue *et al*, 2002; Southall *et al*, 2003; Bodó *et al*, 2004, 2005), bronchial epithelium (Veronesi *et al*, 1999), urothelium (Birder *et al*, 2001; Lazzeri *et al*, 2004), cells of the gastrointestinal tract (Geppetti and Trevisani, 2004; Faussone-Pellegrini *et al*, 2005) as well as on mast cells (Bíró *et al*, 1998a), glial cells (Bíró *et al*, 1998b), etc. Moreover, it was also shown that the activation of TRPV1 on these cells may result in changes e.g. in proliferation, apoptosis, differentiation and/or cytokine release (Bíró *et al*, 1998a; Veronesi *et al*, 1999; Birder *et al*, 2001; Bodó *et al*, 2004; Lazzeri *et al*, 2004).

In relation to these mostly *in vitro* functional data on regulation of cell growth, it is also of great importance that TRPV1 is expressed at various levels in certain malignancies (Prevarskaya *et al*, 2007). For example, elevated TRPV1 expression was identified in carcinomas of the human prostate (Sanchez *et al*, 2005), colon (Domotor *et al*, 2005), pancreas (Hartel *et al*, 2006), or urinary bladder (Lazzeri *et al*, 2005). Moreover, certain

data also indicate that the level of TRPV1 may alter in relation to the degree of malignancy; e.g. positive (prostate cancer) (Sanchez *et al*, 2005) or negative [bladder carcinoma (Lazzeri *et al*, 2005), glioma (Amantini *et al*, 2007)] correlations were equally found with increasing grades of the respective tumours.

Although sparse reports indicate that dietary capsaicin may inhibit tongue carcinogenesis in rats, intriguingly, we lack data on the existence of the 'capsaicin receptor' TRPV1 on structures of the oral cavity which comprise the primary 'target' of the regularly consumed TRPV1 agonist capsaicin (Tanaka *et al*, 2002). Therefore, in this study, by focusing on the human tongue, we investigated the expression of the molecule in the epithelial cells of the organ. Moreover, we also defined the putative alterations in the level of TRPV1 in human squamous cell carcinoma (SCC) of the tongue which comprises one of the highest incidence malignancies of the oral cavity (indeed, it accounts for 20–50% of all oral cavity neoplasias with a 5-year mortality rate of approximately 50% and a poor survival index that has not changed significantly in the past half-century) (Byers *et al*, 1998; Nagler *et al*, 2007; Molina *et al*, 2008).

Methods

Human tissues

The study was approved by the Institutional Research Ethics Committee and written consent was obtained from all patients (Table 1). Seven normal adult (healthy) tongue epithelial tissue samples were obtained for routine diagnosis. The control patients had no history of pre- or malignant oral mucosal lesions. Eight epithelial leukoplakia lesions and 18 tongue SCC samples were involved in the study and were verified by histopathological evaluations by expert pathologists. Neither the leukoplakia patients nor the SCC patients had the previous or contemporary oral malignancies.

Human tissue sample preparation

In general, the fresh tissue specimens were divided into two parts (Varga *et al*, 2004). One part of the samples was fixed in 4% paraformaldehyde, embedded in paraffin and processed for histopathology grading and for immunohistochemistry (see below). The second part was frozen in liquid nitrogen and to collect tissue parts containing epithelial tissue-enriched samples (and, therefore, free of non-epithelial tissues such as muscle or connective tissue, which may contain TRPV1) (Miyamoto *et al*, 2005; Cavuoto *et al*, 2007), the samples were serially cut using a cryomicrotome starting from the surface of the tumour until the lamina propria was reached (This was verified by serial haematoxylin–eosin stained sections as described in our earlier reports) (Varga *et al*, 2004). The sections were then collected on ice and were processed for either quantitative 'real-time' PCR (Q-PCR) or Western blot analysis (see below). Unfortunately, the volume of the leukoplakia specimens was so limited that we could perform only immunohistochemistry on these samples.

Table 1 Histopathological and clinical information about studied samples

Histopathological diagnosis	*Case ID no.*	*Age, year (mean, range)*	*Sex (men/women)*
Normal tissue	1–7	56 (51–60)	4/3
Leukoplakia	8–15	48 (42–59)	5/3
Well-differentiated SCC (grade 1)	16–22	53 (42–60)	4/3
Moderately differentiated SCC (grade 2)	23–31	61 (49–69)	6/3
Poorly differentiated SCC (grade 3)	32–33	58	2/0

SCC, human tongue squamous cell carcinoma.

Immunohistochemistry

The expression of TRPV1 was determined using horseradish-peroxidase (HRP) based method using diaminobenzidine (DAB) as a chromogene. In brief, paraffin-embedded sections (5 μm), after antigen retrieval (in citrate-buffer, pH 6.0, at 750 W in microwave oven for 10 min), were first incubated with a primary rabbit anti-TRPV1 antibody which recognizes the C-terminus of TRPV1 (1:1000; Sigma-Aldrich, St Louis, MO, USA). Sections were then incubated with a goat anti-rabbit HRP-polymer-conjugated secondary antibody (EnVision kit; DAKO, Glostrup, Denmark). Immunoreactions were finally visualized using DAB-substrate (EnVision kit DAKO) and the sections were counterstained by haematoxylin (Sigma-Aldrich).

To assess specificity of the immunostaining, primary labelling was also performed using another set of antibodies (both from Santa Cruz, Santa Cruz, CA, USA); i.e. rabbit anti-TRPV1 *vs* the N-terminus of TRPV1 (H-150, sc-20813, 1:50 dilution) and goat C-terminus-specific anti-TRPV1 (D-20, sc-12502, 1:50 dilution). The application of these latter primary antibodies resulted in identical staining patterns (data not shown). In addition, for negative controls of the labelling procedure, antibodies were either omitted from the procedure or were preabsorbed by control blocking peptides provided (along with appropriate protocols) by the manufacturers. For positive controls, human skin (Bodó *et al*, 2004, 2005) and prostate tissues (Sanchez *et al*, 2005) were employed (data not shown).

Image analysis

Immunohistochemical images were captured and digitalized using an RT Spot Colour CCD camera (Diagnostic Instruments Inc., Sterling Heights, MI, USA) integrated on a Nikon Eclipse 600 fluorescence and light microscope (Nikon, Tokyo, Japan). Digitalized images were then analysed using Image Pro Plus 4.5 (Media Cybernetics, Bethesda, MD, USA) image analysis software as detailed in our previous reports (Bodó *et al*, 2004, 2005). The intensity of TRPV1-ir was measured at 10 randomly placed, equally areas of interest (AOI) and the average of immunopositive pixels of the 10 AOI (expressed as mean ± s.e.m.) was determined (Bodó *et al*, 2005).

Cell culturing

The CAL27 cell line (Gioanni *et al*, 1988), derived from human tongue SCC, was purchased from LGC Promochem (Wesel, Germany). Cells were cultured in Dulbecco's Modified Eagle's Medium (Sigma-Aldrich) supplemented with 10% foetal bovine serum (Invitrogen, Paisley, UK), 2 mM Glutamine (Sigma-Aldrich), 50 U ml^{-1} penicillin and 50 μg ml^{-1} streptomycin (both from Biogal, Debrecen, Hungary). Medium was changed every other day and cells were subcultured at 80% confluence.

Immunocytochemistry

CAL27 cells growing on glass cover slips were washed with phosphate-buffered saline, fixed in acetone for 5 min at 4°C, air dried and blocked at room temperature for 30 min in a blocking solution containing 0.6% Triton X-100 and 1% bovine serum albumin (all from Sigma-Aldrich). Cells were first incubated with the appropriate rabbit anti-TRPV1 antibody for 1 h (1:1000; Sigma-Aldrich) and then with a fluorescein isothiocyanate (FITC)-conjugated goat anti-rabbit IgG (1:300; Vector, Burlingame, CA, USA) for 1 h. Cell nuclei were counterstained by 4,6-diamidino-2-phenylindole (DAPI) (Vector). Confocal microscopy images were acquired using a Zeiss LSM 510 microscope (Oberkochen, Germany) and images were stored for further analysis (Varga *et al*, 2004; Czifra *et al*, 2006).

Western blotting

Tissues and cells were homogenized in lysis buffer (20 mM Tris-Cl, pH 7.4, 5 mM EGTA, 1 mM 4-(2-aminoethyl)benzenesulfonyl fluoride, 20 μM leupeptin, all from Sigma-Aldrich) and the protein content of samples was measured by a modified BCA protein assay (Pierce, Rockford, IL, USA). The samples were subjected to SDS-PAGE (8% gels were loaded with 120 μg protein per lane), transferred to nitrocellulose membranes (BioRad, Vienna, Austria), and then probed with the above primary anti-TRPV1 antibody (1:1000, Sigma-Aldrich). HRP-conjugated secondary antibodies (EnVision; DAKO) were then employed and the immunoreactive bands were visualized by enhanced chemiluminescence (Pierce). To assess equal loading (and to obtain an endogenous control), membranes were stripped in 200 ml of 50 mM Tris-HCl buffer (pH 7.5) containing 2% SDS and 0.1 β-mercaptoethanol (all from Sigma-Aldrich) at 65°C for 1 h and were re-probed with a β-actin antibody (1:100; Santa Cruz) followed by a similar visualization procedure as described above. To quantitatively assess the immunosignals, immunoblots were finally subjected to densitometric analysis using an Intelligent Dark Box (Fuji, Tokyo, Japan) and the Image Pro Plus 4.5.0 software (Media Cybernetics). The values of the densitometric analysis in several independent experiments were normalized to the average of the immunosignal of the controls and expressed as mean $\pm$ s.e.m. (Varga *et al*, 2004; Czifra *et al*, 2006).

Quantitative 'real-time' Q-PCR

The Q-PCR was carried out on an ABI PRISM 7000 Sequence Detection System (Applied Biosystems, Foster City, CA, USA) by using the 5′ nuclease assay according to our previous reports (Bodó *et al*, 2005; Griger *et al*, 2007). Briefly, frozen tissues were pulverized under liquid N_2 and total RNA was isolated using TRIzol (Invitrogen). Three micrograms of total RNA were then reverse transcribed into cDNA by using 15 units of AMV reverse transcriptase (Promega, Madison, WI, USA) and 0.025 μg μl^{-1} random primers (Promega). PCR amplification was carried out by using the TaqMan primers and probes (Assay ID: Hs00218912_m1 for human TRPV1) using the TaqMan Universal PCR Master Mix Protocol (Applied Biosystems). As internal controls, transcripts of glyceraldehyde 3-phosphate dehydrogenase (GAPDH) were determined (Assay ID: Hs99999905_m1 for human GAPDH), and the amount of TRPV1 transcripts were normalized to those of GAPDH using the $\Delta\Delta$CT method.

Statistical analysis

Statistical analysis was carried out using SPSS software version 13.0 (SPSS Inc., Chicago, IL, USA). For statistical analysis, a two-tailed un-paired *t*-test was employed and $P < 0.05$ values were regarded as significant differences.

Results

Using immunohistochemistry, a minor TRPV1-specific (see negative controls in Figure 1a⁄xi,a⁄xii) immunoreactivity (ir) was identified on epithelial cells of healthy (control) human tongue. On the ventral surface of the tongue, this faint immunosignal was exclusively localized to the most upper layers of the stratum (str.) superficiale (Figure 1a⁄i,a⁄ii). However, on the specialized epithelium of the dorsal surface of the tongue, mostly intracellular TRPV1-ir (with characteristic granular pattern) was found in the basal epithelial cells of the str. basale (Figure 1a⁄iii,a⁄iv). By contrast, neither the cells of the lamina propria nor of the submucosa showed immunoreaction.

Intriguingly, the epithelium of the premalignant leukoplakia samples exhibited an intense and characteristics TRPV1-ir when compared with the healthy tissues (Figure 1a⁄v,a⁄vi). On all cells of the str. basale and str. spinosum, TRPV1-ir was clearly localized to the cell membrane. Furthermore, this immunopositivity was also identified on degenerated cells of the str. superficiale as well as on the hyper-orthokeratotic surface.

On human SCC samples, on tumour epithelial cells infiltrating the submucosa, we observed a markedly increased TRPV1-ir when compared with the controls (Figure 1a⁄vii,a⁄viii). It was also evident that besides the weak surface membrane-localized immunosignals, the dominant TRPV1-specific staining pattern (i.e. intracellular⁄granular localization) highly resembled to those found on cells on the str. spinosum in the control tissues.

Investigation of the epithelium surrounding the tumour invasion revealed another intriguing phenomenon. Namely, on this thickened epithelium which still possesses the characteristic morphological appearance of that of the 'healthy' tissues, TRPV1-ir was also dramatically increased (when compared with the controls) on all layers

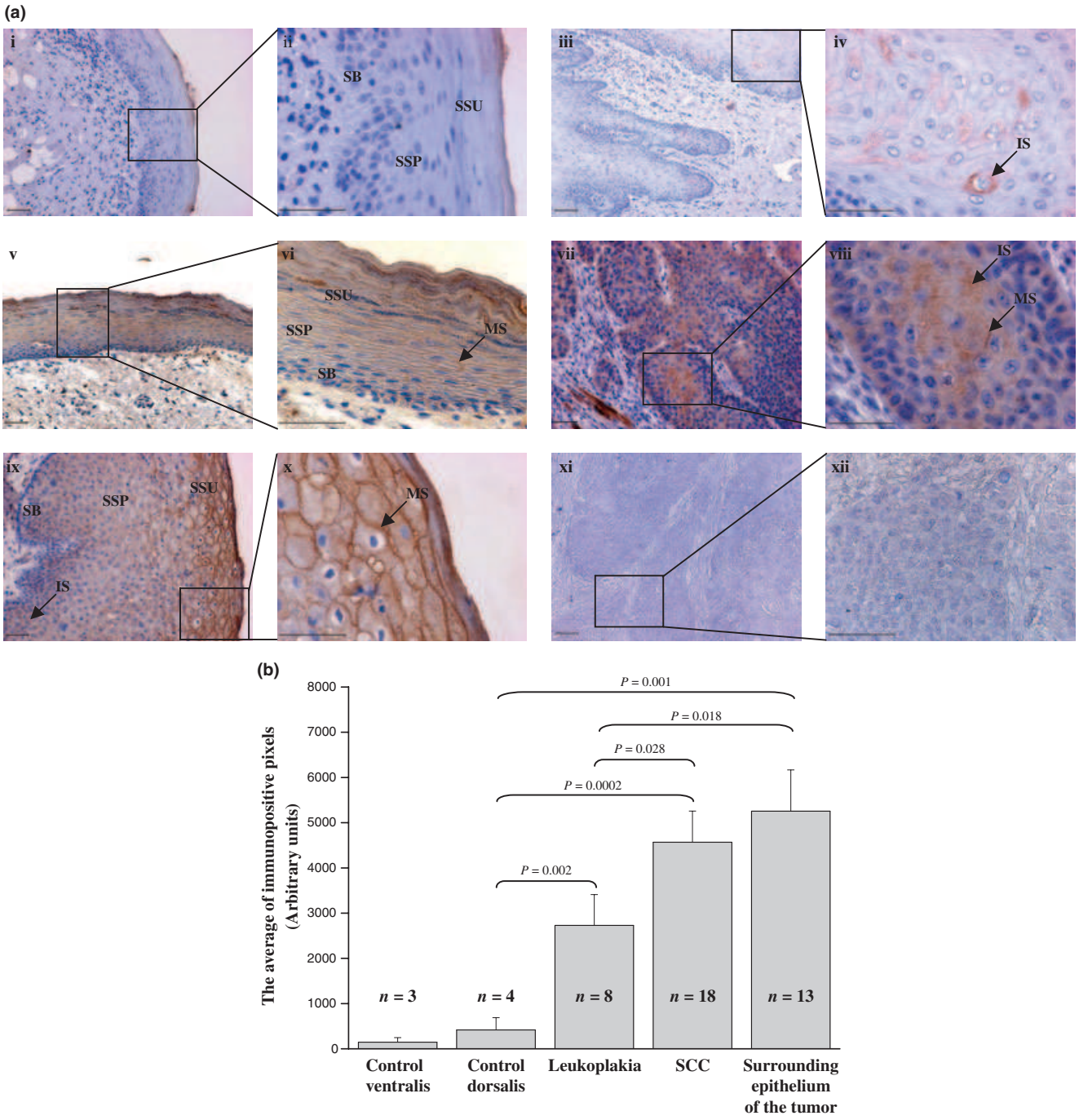

Figure 1 *Localization of transient receptor potential vanilloid-1 (TRPV1) in healthy, premalignant (leukoplakia) and squamous carcinoma of the human tongue*. (**a**) TRPV1-specific immunoreactivity (ir) with diaminobenzidine as a chromogene (brown staining) on healthy and diseased human tongue samples. Nuclei were counterstained by haematoxylin. Ventral (i, ii) and dorsal (iii, iv) surfaces of the healthy tongue. (v, vi) Leukoplakia. (vii, viii) Squamous cell carcinoma; tumour epithelial cell invasion of the submucosa. (ix, x) Epithelium surrounding the tumour invasion. (xi, xii) Preabsorption negative control on tumour sections. Scale bars, 50 μm. MS, membrane staining, IS, intracellular staining, SB, str. basale, SSP, str. spinosum, SSU, str. superficiale. (**b**) Digitalized images obtained on numerous samples (*n* values) were analysed using Image Pro Plus 4.5 image analysis software (see Methods). The intensity of TRPV1-ir was measured at 10 randomly placed, equal areas of interest (AOI) and the average (expressed as mean ± s.e.m.) of immunopositive pixels of the 10 AOI was defined. *P* values were determined using two-tailed un-paired *t*-test

of the epithelium (Figure 1a/ix,a/x). Basal cells of the str. basale and str. spinosum, similar to described above, exhibited intracellular/granular staining pattern. However, TRPV1-ir was rather localized to the cell membrane on cells of the more apical (str. spinosum and superficiale) layers. Moreover, the intensity of TRPV1-ir gradually increased towards the surface and reached in maximal values in the upper layers of the str. superficiale.

The intensity of immunosignals was then quantitated by image analysis software (as detailed under Methods). Comparison of the average intensity values revealed that TRPV1-ir was markedly and significantly higher in

sections from leukoplakia ($P = 0.002$), at the site of SCC invasion ($P = 0.0002$) and on the superficial epithelium surrounding the tumours ($P = 0.001$) when compared with those of the dorsal epithelium of the control samples (which exhibited the strongest immunosignals on the healthy tongue, Figure 1a/iii,a/iv). In addition, mutual comparison of the diseased samples also defined significant differences between TRPV1-ir values of the precancerous leukoplakia and the SCC samples ($P = 0.028$) and of the epithelium surrounding the tumours ($P = 0.018$) (Figure 1b).

Although these results clearly indicated the overexpression of TRPV1 in human tongue SCC, because of the rather semi-quantitative nature of the above technique, we also investigated the level of TRPV1 in SCC samples using Western blot (followed by quantitative densitometry analysis) and Q-PCR techniques. These two complementary techniques concordantly revealed that the expression of the TRPV1-specific mRNA transcripts and protein, yet exhibiting marked inter-individual variations, was higher in all tumour samples investigated (Figure 2a,b). Statistical analysis of densitometry and Q-PCR values of all SCC samples indicated that this elevation was significantly different in the grade 1 ($P = 0.005$ for Western blot, $P = 0.0002$ for Q-PCR) and grade 2 ($P = 0.003$ for Western blot, $P = 0.001$ for Q-PCR) SCC groups, when compared with the controls (Figure 2c). Although (at least) a similar increase in TRPV1 expression was also identified in grade 3 tumour samples, the low number of the available tumour samples ($n = 2$) made it impossible to perform statistical analysis. Of further importance, we found statistically insignificant differences when respective values of the tumour samples with various grades were mutually compared with one another (Figure 2c).

Finally, we investigated the expression of TRPV1 at the cellular levels using the human SCC-derived cells line CAL27. As assessed by immunocytochemistry followed by confocal microscopy analysis, TRPV1-ir was localized both to the surface membrane and in the cytoplasm of the cells (Figure 3a), similar to tumour cells *in situ* (see Figure 1a/vii,a/viii). In addition, quantitative Western blot and Q-PCR analyses also revealed that the expression of TRPV1 (both at the protein and mRNA levels) significantly and, of importance, gradually increased in parallel to the accelerated growth rate (hence the confluence) of the cell cultures (Figure 3b,c).

Discussion

Dietary capsaicin primarily acts on cells of the gastrointestinal tract. The previous studies have clearly identified the existence the 'capsaicin receptor' TRPV1 on parietal cells of the human stomach (Faussone-Pellegrini *et al*, 2005) and on certain epithelial cell types of this organ system (Ward *et al*, 2003; Geppetti and Trevisani, 2004; Domotor *et al*, 2005). However, to our best knowledge, our current study provides the first evidence that TRPV1 is expressed (both at the mRNA and protein levels) on the primary 'target' of capsaicin, i.e. on epithelial cells of the human tongue.

Mutually complementary immunohistochemical, Western blot and Q-PCR analyses have also shown that the relatively low level of TRPV1 expression

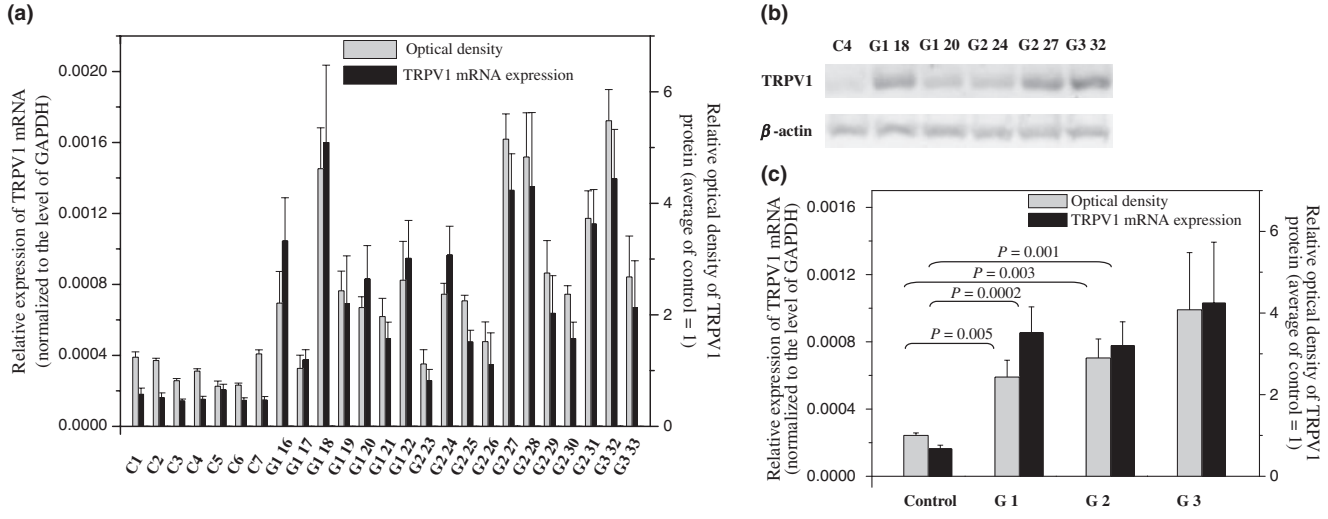

Figure 2 *Expression of transient receptor potential vanilloid-1 (TRPV1) is increased in squamous carcinoma of the human tongue*. (**a**) Epithelial tissues of normal tongue (control, C) and squamous carcinomas of the human tongue with various tumour grades (G1–G3) were collected, processed as described under Methods and subjected to Western blot (followed by densitometry analysis) and Q-PCR to determine TRPV1 expression. During Western blot, the amount of TRPV1 was quantitated using densitometry in triplicates and normalized to those of β-actin. Panels represent mean ± s.e.m. values compared with the average of the control samples (C1–C7) defined as 1. During Q-PCR, data of TRPV1 expression (obtained in three triplicate determinations of each sample) were normalized to the level of glyceraldehyde 3-phosphate dehydrogenase (GAPDH) of the same sample and are expressed as mean ± s.e.m. (**b**) Representative Western blot data of several determinations yielding similar results of control (sample no. 4) and on squamous carcinomas with grade (G) 1 (samples no. 18, 20), G2 (samples no. 24, 27) and G3 (sample no. 32). Equal loading was assessed by determining the expression of β-actin. (**c**) Statistical analysis of Western blot and Q-PCR data presented in panel A. *P* values were determined using two-tailed un-paired *t*-test

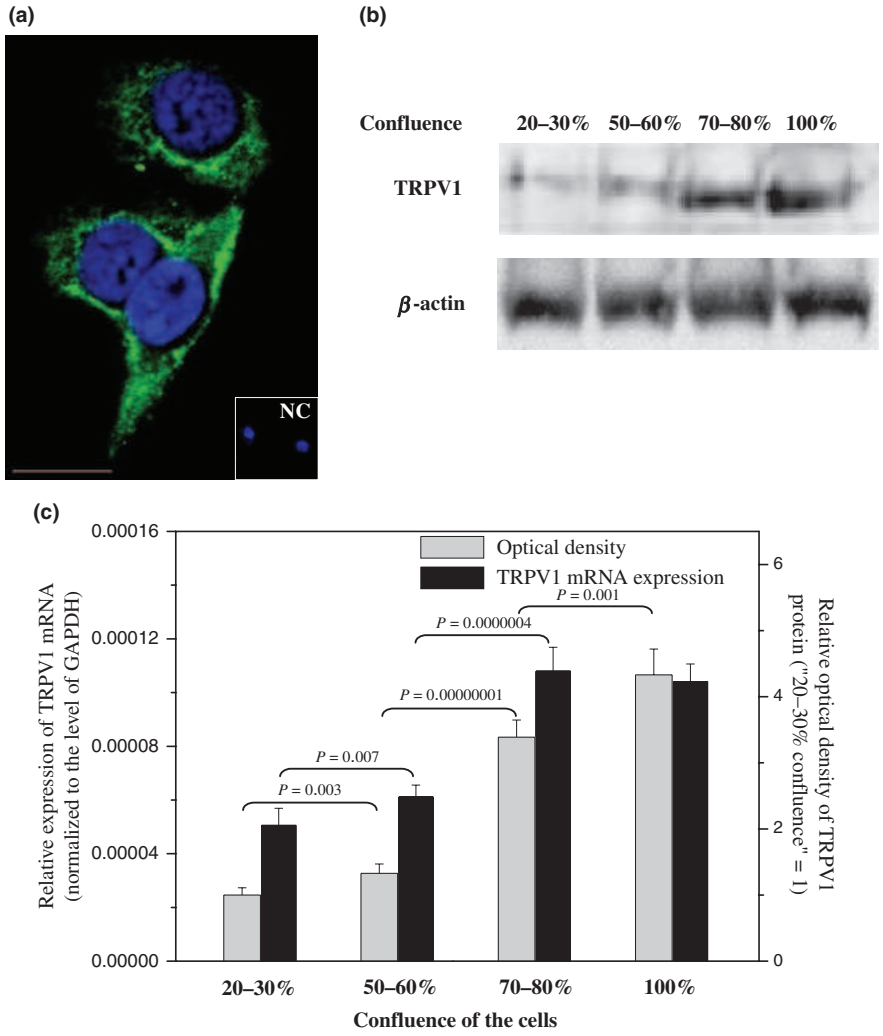

Figure 3 *Transient receptor potential vanilloid-1 (TRPV1) is expressed on cultured human tongue squamous carcinoma-derived CAL27 cells and its level alters in parallel to the proliferation of the cells.* (**a**) TRPV1 immunoreactivity on CAL27 cells (green fluorescence), as visualized by confocal microscopy. Nuclei were counterstained by 4,6-diamidino-2-phenylindole (DAPI) (blue fluorescence). Inset, preabsorption negative control (NC). Scale bar, 10 μm. (**b**) Western blot analysis of TRPV1 expression on cell lysates of CAL27 cells harvested at various confluences. Equal loading was assessed by determining the expression of β-actin. (**c**) Statistical analysis of Western blot and Q-PCR analysis performed on CAL27 cells harvested at various confluences. During Western blot, in each sample, the amount of TRPV1 was quantitated by densitometry and normalized to those of β-actin; optical density value of the '20–30% confluence' sample was defined as 1. During Q-PCR, data of TRPV1 expression were normalized to the level of glyceraldehyde 3-phosphate dehydrogenase (GAPDH) of the same sample and are expressed as mean ± s.e.m. of three independent determinations. Three additional experiments yielded similar results. *P* values were determined using two-tailed un-paired *t*-test

(localized mostly to the basal layers of the epithelium in healthy tongue tissues) was markedly increased in all grades of human tongue SCC samples. These intriguing data suggested that TRPV1 – similarly to findings on other epithelial cells such as human skin keratinocytes (Denda *et al*, 2001; Inoue *et al*, 2002; Southall *et al*, 2003; Bodó *et al*, 2004, 2005), bronchial epithelium (Veronesi *et al*, 1999) and urothelium (Birder *et al*, 2001; Lazzeri *et al*, 2004) – may participate in the growth control of the cells. This idea was further supported by showing that the expression of TRPV1 gradually increased with the accelerated growth rate of the human tongue SCC-derived cell line CAL27. Although further (both *in vitro* and *in vivo*) studies are invited to clarify the growth-modulatory role of TRPV1 (similar to the work of Tanaka *et al* (2002) suggesting that dietary capsaicin may inhibit tongue carcinogenesis in rats), our findings identify TRPV1 as a novel, promising target molecule in the putative supportive treatment of human tongue SCC.

Intriguingly, the above evaluations have also revealed that the elevated TRPV1 expression in SCC tissues of all grades did not correlate with the degree of malignancy of the tumours. It appears therefore, that in contrast to findings on prostate (Sanchez *et al*, 2005) carcinomas as well as on gliomas (Amantini *et al*, 2007) where definite correlations were described, TRPV1 may not serve as a prognostic factor in the clinics of human tongue SCC.

Nonetheless, several lines of evidence demonstrate that TRPV1 may rather act as a novel diagnostic molecule in human tongue transformation. For example, in the current study, we also present that TRPV1 is highly overexpressed already in the grade 1 (low malignancy) SCC group. Moreover, of further importance, markedly elevated levels of TRPV1 were identified in the precancerous leukoplakia samples and also in the 'healthy' epithelium surrounding the tumour invasion. These data suggest that the overexpression of the molecule may be a relatively early step in the process of tumour genesis; hence, determination of TRPV1 levels may hold out a promise for the benefits of early diagnosis.

Finally, we have also observed that – similar to other neuronal and non-neuronal cell types such as e.g. sensory neurons (Eun *et al*, 2001), mast cells (Turner *et al*, 2003), various skin cells (Bodó *et al*, 2004, 2005), hepatoblastoma cells (Vriens *et al*, 2004; Waning *et al*, 2007), – the specific TRPV1-ir was not restricted to the

plasma membrane of the cells but intracytoplasmic staining patterns were also found. Moreover, here we also show that the subcellular localization pattern of the receptor is markedly different in the various diseased samples; e.g. mostly intracytoplasmic staining in the healthy epithelium and in the submucosal SCC islets whereas prominent surface membrane TRPV1-ir in the leukoplakia samples, in the more superficial layers of the SCCs and in the epithelium surrounding the SCC (see Figure 1). Although further studies are invited to define the exact functional role of the intracellular TRPV1 in SCC-derived cells, these data demonstrate that TRPV1 may have a central role in the transformation of the epithelium of the human tongue leading to unwanted growth. This hypothesis is supported by the previous findings showing that the intracellularly localized TRPV1 indeed functions as Ca-release channel and hence may act as a key regulator of cell morphology, viability and migration (Vriens *et al*, 2004; Han *et al*, 2007; Nilius *et al*, 2007; Waning *et al*, 2007).

Collectively, our current findings identify TRPV1 as a novel, promising target molecule in the supportive treatment and diagnosis human tongue SCC.

Acknowledgements

This work was supported in part by Hungarian Research grants: OTKA 49231, OTKA 63153, ETT 480/2006, ETT 482/2006, RET 06/2004. Tamás Bíró is the recipient of the János Bolyai Research Scholarship of the Hungarian Academy of Sciences.

Conflict of interest

The authors declare no competing financial interests.

Author contributions

Rita Marincsák and Tamás Bíró contributed to the research design. Rita Marincsák, Balázs I. Tóth , Gabriella Czifra contributed to the acquisition and analysis of data. Rita Marincsák and Tamás Bíró contributed to the interpretation of data. Pál Rédl and Ildikó Tar contributed to the collection of the human samples and László Tóth contributed to the hystopathological analysis of these samples. Rita Marincsák and Tamás Bíró contributed in drafting the paper. Ildikó Márton and László Kovács worked on the critical revision of the paper.

References

Amantini C, Mosca M, Nabissi M *et al* (2007). Capsaicin-induced apoptosis of glioma cells is mediated by TRPV1 vanilloid receptor and requires p38 MAPK activation. *J Neurochem* **102:** 977–990.

Birder LA, Kanai AJ, de Groat WC *et al* (2001). Vanilloid receptor expression suggests a sensory role for urinary bladder epithelial cells. *Proc Natl Acad Sci USA* **98:** 13396–13401.

Bíró T, Maurer M, Modarres S *et al* (1998a). Characterization of functional vanilloid receptors expressed by mast cells. *Blood* **91:** 1332–1340.

Bíró T, Brodie C, Modarres S, Lewin NE, Ács P, Blumberg PM (1998b). Specific vanilloid responses in C6 rat glioma cells. *Brain Res Mol Brain Res* **56:** 89–98.

Bodó E, Kovács I, Telek A *et al* (2004). Vanilloid receptor-1 is widely expressed on various epithelial and mesenchymal cell types of human skin. *J Invest Dermatol* **123:** 410–413.

Bodó E, Bíró T, Telek A *et al* (2005). A ''hot'' new twist to hair biology: Involvement of vanilloid receptor-1 (VR1/TRPV1) signaling in human hair growth control. *Am J Pathol* **166:** 985–998.

Byers RM, El-Naggar AK, Lee YY *et al* (1998). Can we detect or predict the presence of occult nodal metastases in patients with squamous carcinoma of the oral tongue? *Head Neck* **20:** 138–144.

Caterina MJ, Schumacher MA, Tominaga M, Rosen TA, Levine JD, Julius D (1997). The capsaicin receptor: a heat-activated ion channel in the pain pathway. *Nature* **389:** 816–824.

Cavuoto P, McAinch AJ, Hatzinikolas G, Janovská A, Game P, Wittart GA (2007). The expression of receptors for endocannabinoids in human and rodent skeletal muscle. *Biochem Biophys Res Commun* **364:** 105–110.

Czifra G, Tóth IB, Marincsák R *et al* (2006). Insulin-like growth factor-I-coupled mitogenic signaling in primary cultured human skeletal muscle cells and in C2C12 myoblasts. A central role of protein kinase Cdelta. *Cell Signal* **18:** 1461–1472.

Denda M, Fuziwara S, Inoue K *et al* (2001). Immunoreactivity of TRPV1 on epidermal keratinocyte of human skin. *Biochem Biophys Res Commun* **285:** 1250–1252.

Di Marzo V, Blumberg PM, Szallasi A (2002). Endovanilloid signaling in pain. *Curr Opin Neurobiol* **12:** 372–379.

Domotor A, Peidl Z, Vincze A *et al* (2005). Immunohistochemical distribution of vanilloid receptor, calcitonin-gene related peptide and substance P in gastrointestinal mucosa of patients with different gastrointestinal disorders. *Inflammopharmacol* **13:** 161–177.

Eun SY, Jung SJ, Park YK, Kwak J, Kim SJ, Kim J (2001). Effects of capsaicin on Ca^{2+} release from the intracellular Ca^{2+} stores in the dorsal root ganglion cells of adult rats. *Biochem Biophys Res Commun* **285:** 1114–1120.

Faussone-Pellegrini MS, Taddei A, Bizzoco E, Lazzeri M, Vannucchi MG, Bechi P (2005). Distribution of the vanilloid (capsaicin) receptor type 1 in the human stomach. *Histochem Cell Biol* **124:** 61–68.

Geppetti P, Trevisani M (2004). Activation and sensitisation of the vanilloid receptor: role in gastrointestinal inflammation and function. *Br J Pharmacol* **141:** 1313–1320.

Gioanni J, Fischel JL, Lambert JC *et al* (1988). Two new human tumour cell lines derived from squamous cell carcinomas of the tongue: establishment, characterization and response to cytotoxic treatment. *Eur J Cancer Clin Oncol* **24:** 1445–1455.

Griger Z, Páyer E, Kovács I *et al* (2007). Protein kinase C-beta and -delta isoenzymes promote arachidonic acid production and proliferation of MonoMac-6 cells. *J Mol Med* **85:** 1031–1042.

Han P, McDonald HA, Bianchi BR *et al* (2007). Capsaicin causes protein synthesis inhibition and microtubule disassembly through TRPV1 activities both on the plasma membrane and intracellular membranes. *Biochem Pharmacol* **73:** 1635–1645.

Hartel M, di Mola FF, Selvaggi F *et al* (2006). Vanilloids in pancreatic cancer: potential for chemotherapy and pain management. *Gut* **55:** 519–528.

Inoue K, Koizumi S, Fuziwara S, Denda S, Inoue K, Denda M (2002). Functional vanilloid receptors in cultured normal human epidermal keratinocytes. *Biochem Biophys Res Commun* **291:** 124–129.

Lazzeri M, Vannucchi MG, Zardo C *et al* (2004). Immunohistochemical evidence of vanilloid receptor 1 in normal human urinary bladder. *Eur Urol* **46:** 792–798.

Lazzeri M, Vannucchi MG, Spinelli M *et al* (2005). Transient receptor potential vanilloid type 1 (TRPV1) expression changes from normal urothelium to transitional cell carcinoma of human bladder. *Eur Urol* **48:** 691–698.

Miyamoto R, Tokuda M, Sakuta T, Nagaoka S, Torii M (2005). Expression and characterization of vanilloid receptor subtype 1 in human dental pulp cell cultures. *J Endod* **31:** 652–658.

Molina FD, Bertollo EM, Assis CM *et al* (2008). Apoptosis in tongue squamous cell carcinoma and its correlation with clinically occult cervical metastasis. *Micron* **38:** 910–914.

Moran MM, Xu H, Clapham DE (2004). TRP ion channels in the nervous system. *Curr Opin Neurobiol* **14:** 362–369.

Nagler R, Ben-Izhak O, Cohen-Kaplan V *et al* (2007). Heparanase up-regulation in tongue cancer: tissue and saliva analysis. *Cancer* **110:** 2732–2739.

Nilius B, Owsianik G, Voets T, Peters JA (2007). Transient receptor potential cation channels in disease. *Physiol Rev* **87:** 165–217.

Prevarskaya N, Zhang L, Barritt G (2007). TRP channels in cancer. *Biochim Biophys Acta* **1772:** 937–946.

Sanchez MG, Sanchez AM, Collado B *et al* (2005). Expression of the transient receptor potential vanilloid 1 (TRPV1) in LNCaP and PC-3 prostate cancer cells and in human prostate tissue. *Eur J Pharmacol* **515:** 20–27.

Southall MD, Li T, Gharibova LS, Pei Y, Nicol GD, Travers JB (2003). Activation of epidermal vanilloid receptor-1 induces release of proinflammatory mediators in human keratinocytes. *J Pharmacol Exp Ther* **30:** 217–222.

Tanaka T, Kohno H, Sakata K *et al* (2002). Modifying effects of dietary capsaicin and rotenone on 4-nitroquinoline 1-oxide-induced rat tongue carcinogenesis. *Carcinogenesis* **23:** 1361–1367.

Tominaga M, Caterina MJ, Malmberg AB *et al* (1998). The cloned capsaicin receptor integrates multiple pain-producing stimuli. *Neuron* **21:** 531–543.

Turner H, Fleig A, Stokes A, Kinet JP, Penner R (2003). Discrimination of intracellular calcium store subcompartments using TRPV1 (transient receptor potential channel, vanilloid subfamily member 1) release channel activity. *Biochem J* **371:** 341–350.

Ugawa S, Ueda T, Ishida Y, Nishigaki M, Shibata Y, Shimada S (2002). Amiloride-blockable acid-sensing ion channels are leading acid sensors expressed in human nociceptors. *J Clin Invest* **110:** 1185–1190.

Varga A, Czifra G, Tállai B *et al* (2004). Tumour grade-dependent alterations in the protein kinase C isoform pattern in urinary bladder carcinomas. *Eur Urol* **46:** 462–465.

Veronesi B, Oortgiesen M, Carter JD, Devlin RB (1999). Particulate matter initiates inflammatory cytokine release by activation of capsaicin and acid receptors in a human bronchial epithelial cell line. *Toxicol Appl Pharmacol* **154:** 106–115.

Vriens J, Janssens A, Prenen J, Nilius B, Wondergem R (2004). TRPV channels and modulation by hepatocyte growth factor/scatter factor in human hepatoblastoma (HepG2) cells. *Cell Calcium* **36:** 19–28.

Waning J, Vriens J, Owsianik G *et al* (2007). A novel function of capsaicin-sensitive TRPV1 channels: involvement in cell migration. *Cell Calcium* **42:** 17–25.

Ward SM, Bayguinov J, Won KJ, Grundy D, Berthoud HR (2003). Distribution of the vanilloid receptor (VR1) in the gastrointestinal tract. *J Comp Neurol* **465:** 121–135.

XVIII.

J Cancer Res Clin Oncol (2009) 135:507–514
DOI 10.1007/s00432-008-0482-3

ORIGINAL PAPER

Increased expressions of cannabinoid receptor-1 and transient receptor potential vanilloid-1 in human prostate carcinoma

Gabriella Czifra · Attila Varga · Katalin Nyeste · Rita Marincsák · Balázs I. Tóth · Ilona Kovács · László Kovács · Tamás Bíró

Received: 16 May 2008 / Accepted: 10 September 2008 / Published online: 1 October 2008

Abstract
Purpose Recently, functional cannabinoid receptor-1 (CB1) and vanilloid receptor-1 (TRPV1) have been described in human prostate and prostate cancer-derived cell lines where the activation of the receptors resulted in inhibition of cellular growth. We, however, lack the description of the expression of these molecules in human prostate cancer (PCC) and in benign prostate hyperplasia (BPH).
Methods Therefore, immunohistochemistry, Western blotting, and quantitative "real-time Q-PCR were performed to define the expressions of CB1 and TRPV1 in healthy and diseased prostate tissues.
Results CB1 was identified in epithelial and smooth muscle cells types of the human prostate, whereas TRPV1 was exclusively localized to the mucosal cells. We also found that the expression of CB1 and TRPV1 (both at the protein and mRNA levels) were significantly up-regulated in PCC. However, while the increased expression of TRPV1 showed a proper correlation with increasing PCC tumor grades, such phenomenon was not observed with CB1. In addition, we also measured markedly elevated CB1 levels in BPH tissues whilst the expression of TRPV1 was not altered when compared to healthy control prostate.
Conclusions Our findings strongly argue for that (1) the CB1 and TRPV1 molecules as well as their ligands may indeed possess a promising future role in the treatment of PCC; (2) TRPV1 may also serve as a prognostic factor in PCC; and (3) CB1 may act as a potential target molecule in the therapeutic management of BPH.

Keywords Benign prostate hyperplasia · Cannabinoid receptor-1 (CB1) · Human prostate carcinoma · Transient receptor potential vanilloid-1 (TRPV1)

G. Czifra · K. Nyeste · R. Marincsák · B. I. Tóth · L. Kovács · T. Bíró (✉)
Department of Physiology, Medical and Health Science Center, Research Center for Molecular Medicine, University of Debrecen, Nagyerdei krt 98, 4032 Debrecen, Hungary
e-mail: biro@phys.dote.hu

A. Varga
Department of Urology, Medical and Health Science Center, Research Center for Molecular Medicine, University of Debrecen, Nagyerdei krt 98, 4032 Debrecen, Hungary

I. Kovács
Department of Pathology, Kenézy Hospital, Bartók B. u. 2-26, 4043 Debrecen, Hungary

Introduction

Although the metabotropic, G-protein coupled cannabinoid receptor-1 (CB1) and the ligand-gated, calcium-permeable ion channel transient receptor potential vanilloid subtype-1 (TRPV1) possess markedly distinct structural properties, they share a wide array of common features both in localization and function. Namely, these receptors were originally described on specific neuronal structures and were implicated in the regulation of behavior, learning, and memory (for CB1), and in pain and temperature sensation (for TRPV1) (Caterina and Julius 2001; De Petrocellis et al. 2004; Pacher et al. 2005). In addition, they can be activated by numerous exogenous (e.g., Δ^9-tetrahydrocannabinol for CB1, capsaicin for TRPV1) and endogenous (endocannabinoids, endovanilloids) substances, among which various fatty acid and arachidonic acid derivatives (e.g., anandamide) may equally act on both receptors (Caterina and Julius 2001; De Petrocellis et al. 2004; Pacher et al. 2005). Moreover, it was also postulated that the CB1- and TRPV1-coupled

signaling mechanisms very often interact, hence resulting in a complex, bi-directional regulatory relationship (Caterina and Julius 2001; De Petrocellis et al. 2004; Di Marzo et al. 2004; Paus et al. 2006).

Of great importance, other studies also revealed that CB1 and TRPV1 are additionally expressed on numerous non-neuronal cell types such as, e.g., keratinocytes, hair follicle cells, uroepithelium, and smooth muscle cells (Lazzeri et al. 2004; Bodó et al. 2005; Pacher et al. 2005; Paus et al. 2006). On these cells, it was suggested that the two receptors and their endogenous ligands play key roles in the regulation of such processes as, e.g., proliferation, differentiation, apoptosis, and cytokine production (Lazzeri et al. 2004; Bodó et al. 2005; Pacher et al. 2005; Paus et al. 2006).

The functional role of the cannabinoid and vanilloid systems in the regulation of cell proliferation and death was also described in human prostate cancer (PCC) derived cell lines. Namely, it was shown that exogenous or endogenous cannabinoid and vanilloid ligands induced in vitro growth-inhibition and (apoptotic or necrotic) cell death of the PCC cell lines expressing CB1 and TRPV1 (Nithipatikom et al. 2004; Sarfaraz et al. 2005; Sanchez et al. 2005, 2006; Mori et al. 2006). Furthermore, recent reports presented that vanilloids in vivo effectively prevented the growth or induced the regression of xenograft tumors induced by PCC-derived cell lines (Sanchez et al. 2006; Mori et al. 2006), similar to the action of cannabinoids on skin tumors (Casanova et al. 2003).

These elegant studies strongly suggested that CB1 and TRPV1 might function as putative target molecules in the management of the most prevalent male malignancy PCC. However, although the in situ expression of both receptors was described in healthy prostate tissue (and, for TRPV1, in samples from benign prostate hyperplasia [BPH] patients) (Galiegue et al. 1995; Ruiz-Llorente et al. 2003; Sanchez et al. 2005; Stein et al. 2004), we lack the exact quantitative determination of putative alterations in the expression levels of CB1 and TRPV1 in certain human hyperproliferative prostate diseases. Therefore, in the current study, we determined the mRNA and protein levels of CB1 and TRPV1 in healthy (control) human prostate, in PCC tissues of various tumor grades, and (for further comparison in another prostate disease) in samples obtained from BPH patients.

Methods

Human prostate tissues

The study was approved by the Institutional Research Ethics Committee and written consent was obtained from all patients. The study involved 35 cases of PCC (8 cases of G1, 10 cases of G2, 8 cases of G3, and 9 cases of G4 grades) removed by prostatectomy, 12 samples of BPH removed by transurethral resection, and 9 samples of normal (healthy) prostate obtained from transplantation donors. In each case, the tissues were divided into three parts according to our previous report (Varga et al. 2004). One part of the samples was fixed in 4% paraformaldehyde, embedded in paraffin, and processed for pathohistological grading (using the Gleason system) and immunohistochemistry (see below). The other two parts were quick-frozen either in RNA Later (Invitrogen, Paisley, UK) or in lysis buffer (see below) in liquid N_2 and processed for either Q-PCR or Western blot analysis, respectively (see below).

Immunohistochemistry

Initially, the expression of TRPV1 and CB1 was determined by an alkaline phosphatase (AP)-based method following our previously optimized protocol (Bodó et al. 2004, 2005). In brief, paraffin-embedded sections (5 μm), after antigen retrieval (in citrate-buffer, pH 6.0, at 750 W in microwave oven for 10 min), were first incubated with primary rabbit antibodies (both from Santa Cruz, Santa Cruz, CA, USA): anti-CB1 versus the N-terminus of CB1 (H-150, sc-20754, 1:50 dilution); anti-TRPV1 versus the N-terminus of TRPV1 (H-150, sc-20813, 1:50 dilution). In addition experiments, to further assess specificity of the immunostaining, primary labeling was performed using goat C-terminus-specific antibodies: anti-CB1 (K-15, sc-10068, 1:50 dilution) and anti-TRPV1 (D-20, sc-12502, 1:50 dilution). The application of these latter primary antibodies resulted in identical staining patterns (data not shown). After staining with the primary antibodies, sections were incubated with biotinylated anti-goat or anti-rabbit IgG (1:200) (Vector Laboratories, Burlingame, CA, USA) and then by a streptavidin–AP conjugate (1% reagent mixture (Vector). Immunoreactions were finally visualized using AP-substrate in Tris–HCl buffer (pH 8.2–8.5) (Vector) and the sections were counterstained by hematoxylin (Sigma, St. Louis, MO, USA). For negative controls of the labeling procedure, antibodies were pre-absorbed by control blocking peptides provided (along with appropriate protocols) by the manufacturer (Santa Cruz). For positive controls, human organ-cultured hair follicle and full-thickness skin sections (according to our previous reports, Bodó et al. 2004, 2005; Telek et al. 2007) were employed (data not shown).

When double fluorescence labeling of CB1 was performed (Bodó et al. 2005; Telek et al. 2007), sections were first stained with either of the above anti-CB1 antibodies and then by another set of (mouse) primary antibodies (both from DAKO, Glostrup, Denmark) versus either the epithelial

cell marker cytokeratin-7 (CK7, 1:50 dilution) or the smooth muscle marker α-actin (SMA, 1:100 dilution). Subsequently, tissues were incubated with species-matched (i.e., anti-rabbit or -goat) fluorescein isothiocyanate (FITC)-coupled secondary antibodies (1:300 dilution) (Vector) to visualize CB1 and finally by anti-mouse Texas red-conjugated secondary antibodies (1:300 dilution) (Vector) to label CK-7 or SMA.

Quantitative "real-time" Q-PCR

Q-PCR was carried out on an ABI PRISM 7000 Sequence Detection System (Applied Biosystems, Foster City, CA, USA) using the 5′ nuclease assay as described in our earlier reports (Bodó et al. 2004, 2005; Telek et al. 2007; Griger et al. 2007). Briefly, frozen prostate tissues were pulverized under liquid N_2 and total RNA was isolated using TRIzol (Invitrogen). Three micrograms of total RNA were then reverse transcribed into cDNA using 15 units of AMV reverse transcriptase (Promega, Madison, WI, USA) and 0.025 μg/μl random primers (Promega). PCR amplification was carried out using the TaqMan primers and probes (Assay ID: Hs00218912_m1 for human TRPV1; Assay ID: Hs00275634_m1 for human CB1) using the TaqMan Universal PCR Master Mix Protocol (Applied Biosystems). As internal controls, transcripts of glyceraldehyde 3-phosphate dehydrogenase (GAPDH) and human *β*-actin were determined (Assay ID: Hs99999905_m1 for human GAPDH; Assay ID: Hs99999903_m1 for human *β*-actin), and the amount of CB1 or TRPV1 transcripts were normalized to those of controls using the ΔΔCT method.

Western blotting

Tissues were homogenized in lysis buffer (20 mM TRIS–Cl, pH 7.4, 5 mM EGTA, 1 mM 4-(2-aminoethyl)benzenesulfonyl fluoride, 20 μM leupeptin, all from Sigma) and the protein content of samples was measured by a modified BCA protein assay (Pierce, Rockford, IL, USA) as described in our previous reports (Varga et al. 2004; Bodó et al. 2004, 2005; Telek et al. 2007; Griger et al. 2007). The samples were subjected to SDS-PAGE (8% gels were loaded with 20–30 μg protein per lane), transferred on to nitrocellulose membranes (BioRad, Vienna, Austria), and then probed with the above primary anti-TRPV1 or anti-CB1 antibodies (1:100). HRP-conjugated secondary antibodies (1:1000, BioRad) were then employed, and the immunoreactive bands were visualized by enhanced chemiluminescence (Pierce). To assess equal loading (and to obtain an endogenous control), membranes were stripped in 200 ml of 50 mM TRIS–HCl buffer (pH 7.5) containing 2% SDS and 0.1 *β*-mercaptoethanol (all from Sigma) at 65°C for 1 h and were re-probed with a mouse cytochrome-C antibody (Sigma) followed by a similar visualization procedure as described above. To quantitatively assess the immunosignal, immunoblots were finally subjected to densitometric analysis using an Intelligent Dark Box (Fuji, Tokyo, Japan) and the Image Pro Plus 4.5.0 software (Media Cybernetics, Silver Spring, MD, USA). To obtain normalized data, values of CB1 and TRPV1 in several independent experiments were normalized to the immunosignal of cytochrome-C and expressed as mean ± SEM. For statistical analysis, a two-tailed un-paired *t* test was employed and P values <0.05 were regarded as significant differences.

Results

Using AP-based immunohistochemistry, confirming previous findings (Ruiz-Llorente et al. 2003; Sanchez et al. 2005), specific CB1 and TRPV1 immunoreactivities (ir) were identified in situ on (healthy) control human prostate (Fig. 1). We, however, also found that while the TRPV1-ir was clearly restricted to the epithelial cells, the CB1-specific signals (besides the previously described epithelial cells) (Ruiz-Llorente et al. 2003) were also localized to the stroma.

To identify those cells types that express CB1, double fluorescence immunolabeling was performed. As seen in Fig. 2, in healthy prostate samples, CB1 was expressed both in the CK7 positive epithelial cells and in the SMA expressing smooth muscle elements as well.

We then started to investigate the expressions of the two receptors in various hyperproliferative diseases of the human prostate. In BPH samples, the TRPV1-ir showed a similar localization pattern (i.e., epithelial cells) and intensity to that of the healthy control samples (Fig. 1). However, we observed a dramatically increased expression of CB1, both in the epithelial and smooth muscle cells in BPH (Figs. 1, 2). Similarly, we found that the level of CB1 was also increased in samples from PCC patients, especially in the epithelial cells (Figs. 1, 2). Of great importance, we were furthermore able to detect a remarkably elevated TRPV1 expression in the epithelial cells of PCC samples when compared to either the healthy or the BPH sections (Fig. 1).

Although the above immunohistochemical determination strongly suggested that the level of CB1 increased both in BPH and PCC, whereas that of TRPV1 elevated in PCC the semi-quantitative nature of this technique did not permit exact, quantitative determination of the expressions of the molecules. Therefore, in the next phase of our experiments, we further analyzed CB1 and TRPV1 expression using Western blotting and Q-PCR. In addition, to measure a putative relationship between the expressions of the receptors

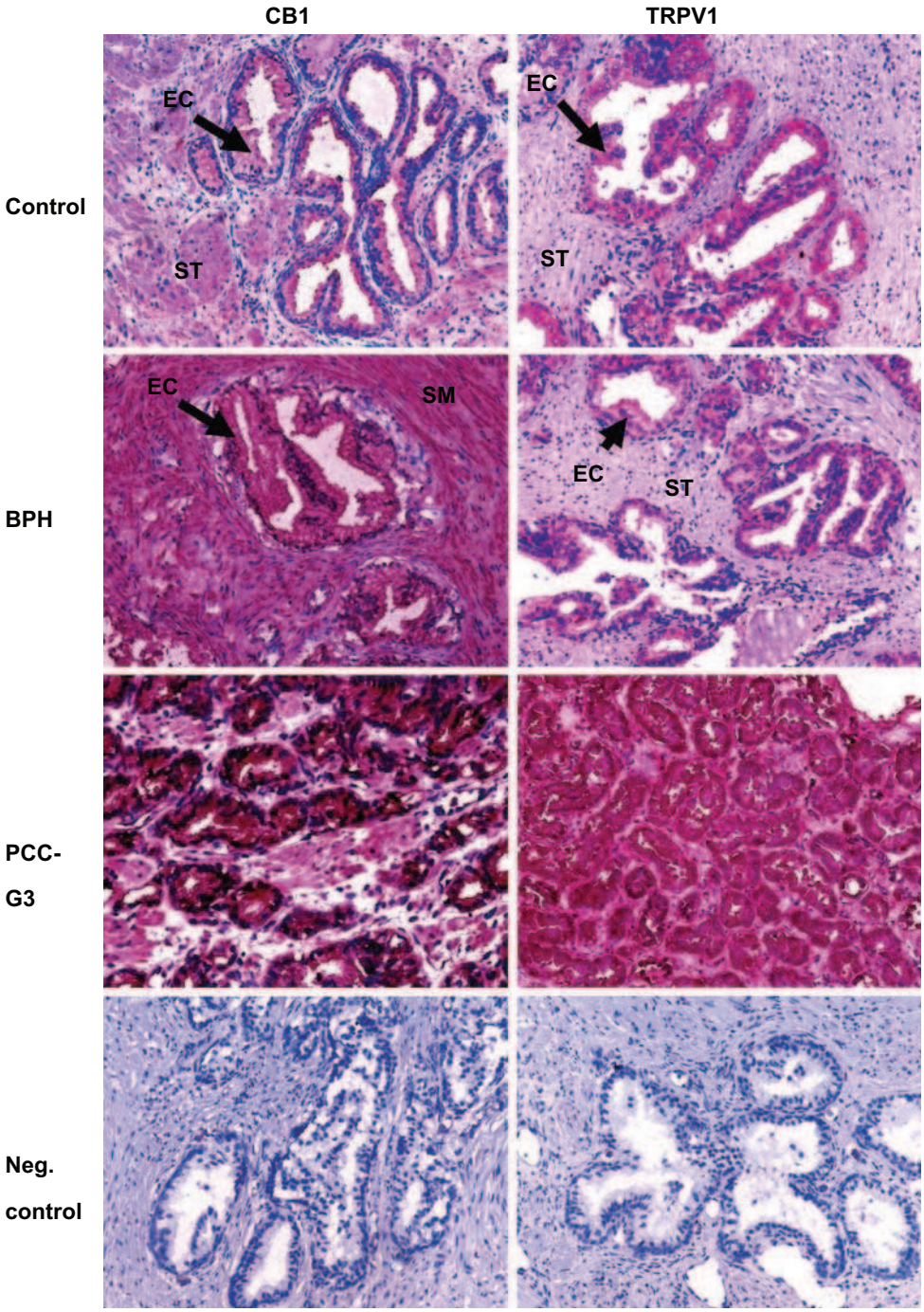

Fig. 1 Expression of *CB1* and *TRPV1* in healthy (*control*) human prostate tissue, in *BPH*, and in *PCC*. *CB1* and TRPV1 immunoreactivity on healthy prostate (*control*) and diseased prostate tissues, as revealed by alkaline phosphatase method. Representative of data obtained on 12 *BPH* and 8 *G3 PCC* tissues. *Negative control* was obtained by pre-absorbing the antibodies with appropriate blocking peptides. Magnification, ×200

(which apparently are up-regulated in PCC) and the degree of malignancy, we also employed PCC tissues of various tumor grades.

Both Western blot (followed by quantitative densitometry analyses of numerous samples) and Q-PCR analyses revealed that the expressions of CB1 protein and specific mRNA transcripts were indeed remarkably and significantly increased in BPH (when compared to healthy control) (Fig. 3a–c). In addition, we also identified significantly (yet not that markedly) elevated CB1 levels in the PCC samples of all grades investigated (Fig. 3a–c). Interestingly, however, no correlation was observed between the degree of CB1 expression and the increasing tumor grades. Namely, when values of the groups of various tumor grades were statistically compared to one another, the only significant difference was found between the G1 and G2 PCC groups, but only when measured by immunoblotting (Fig. 3b, c).

The investigation of TRPV1 expression revealed that, in contrast to data obtained with CB1, the levels of TRPV1

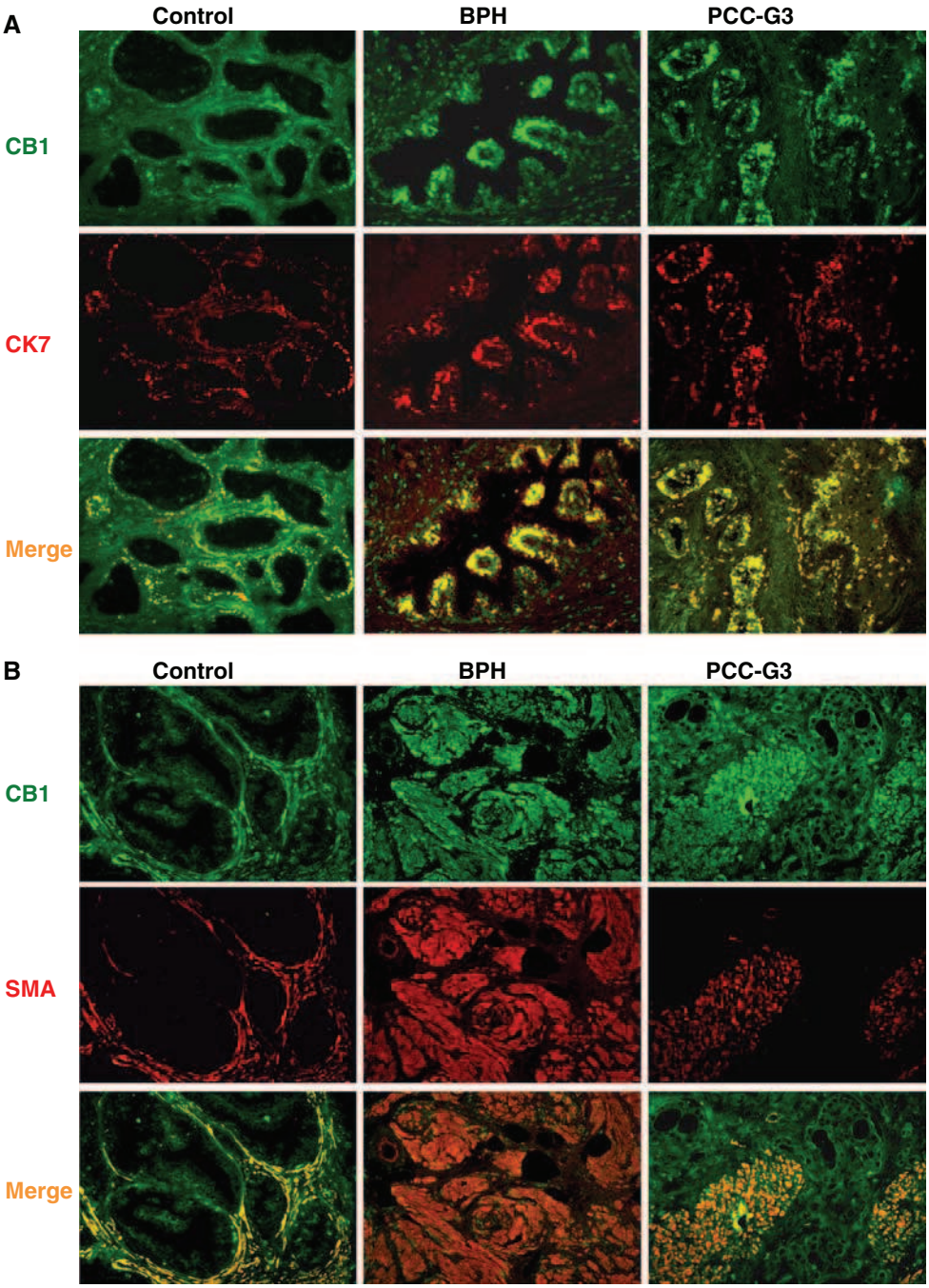

Fig. 2 Cell-specific expression of *CB1* in healthy (*control*) human prostate tissue, in *BPH*, and in *PCC*. Double immunofluorescence labeling of CB1 (FITC, *green*) and epithelial cytokeratin-7 (**a** *CK7*, *Texas red*) or smooth muscle α-actin (**b** *SMA*, *Texas red*) on healthy prostate (*control*) and diseased prostate tissues. Representative of data obtained on 12 *BPH* and 8 *G3 PCC* tissues. Magnification, ×200

protein and mRNA were not increased in BPH tissues (Fig. 3a, d, e). Similarly, the expression of the receptor was not altered in the G1 (low malignancy) PCC samples. As a marked contrast, however, we were able to detect significantly elevated TRPV1 mRNA and protein levels in PCC samples of G2–G4 grades (Fig. 3d, e). In addition, the statistical analysis showed that, as opposed to findings with CB1, the expression of TRPV1 (both the protein and mRNA levels) in almost all cases increased in parallel and gradually with the degree of malignancy, i.e., with increasing PCC grades (Fig. 3d, e) (the only statistically insignificant difference was found between the mRNA values of G2 and G3 samples, yet the G3 samples showed increasing tendencies of TRPV1 expression).

Discussion

The novel results presented in this paper provide the first evidence that CB1 is significantly elevated in human PCC tissues (mostly in the epithelial elements) when compared to normal healthy prostate. These findings are in perfect

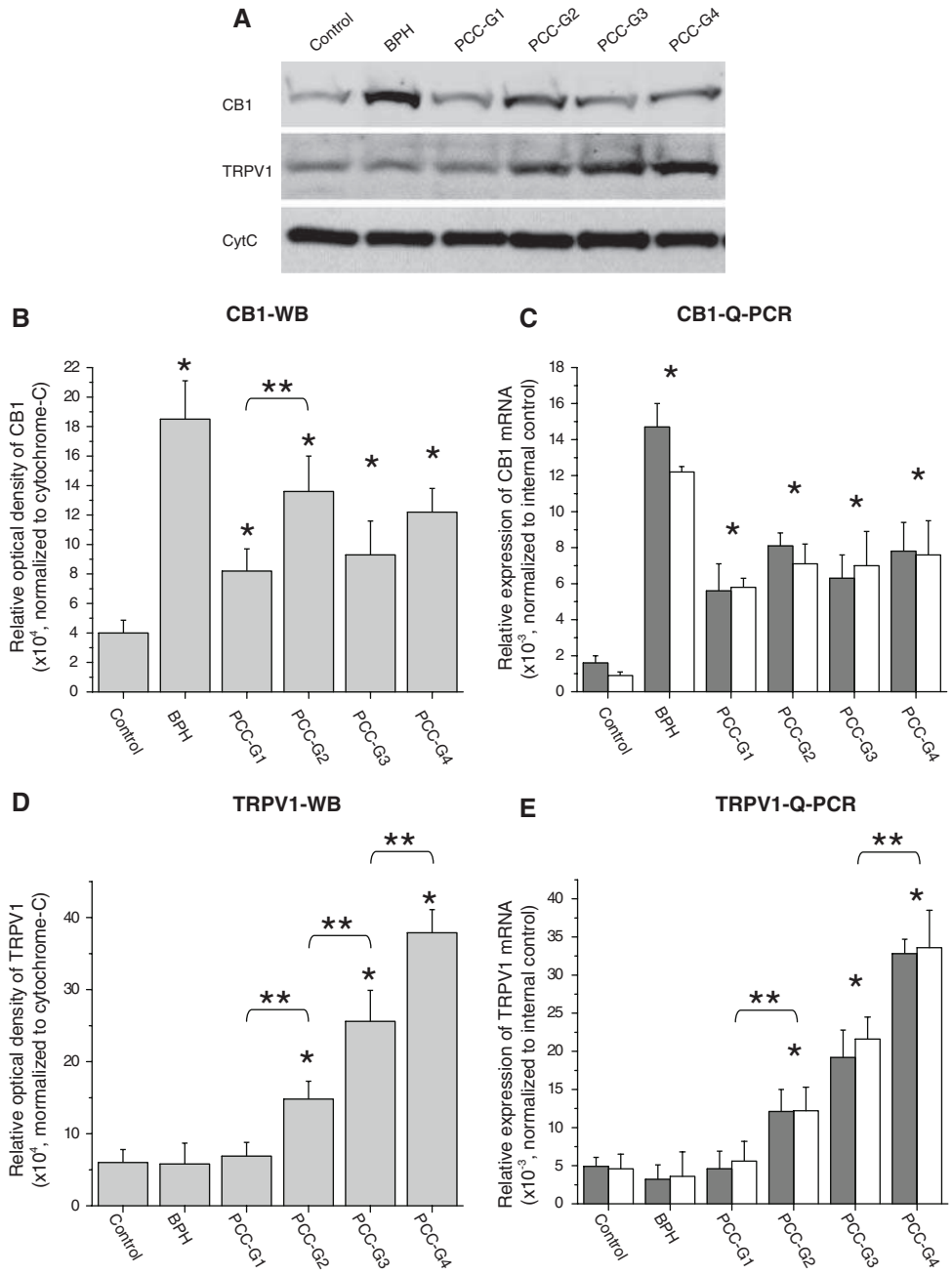

Fig. 3 Quantitative expression of *CB1* and *TRPV1* in healthy (*control*) human prostate tissue, in *BPH*, and in *PCC*. **a** Representative Western blot data of 9 normal (healthy) prostate, 8 *G1-PCC*, 10 *G2-PCC*, 8 *G3-PCC*, 9 *G4-PCC*, and 12 *BPH* tissue samples. **b**, **d** Densitometry analysis of Western blot experiments carried out on the above prostate samples in duplicates. The amount of CB1 (**b**) and TRPV1 (**d**) protein levels in a given tissue was quantitated by densitometry and normalized to the optical density values of cytochrome C of the same sample. Normalized values were then averaged within the same (healthy, diseased) group. **c**, **e** Q-PCR analysis of the above prostate samples. The amount of CB1- (**c**) and TRPV1-specific (**e**) mRNA transcript was determined in triplicates and then normalized to those of GAPDH (*gray* columns) and *β*-actin (*white columns*). Normalized values were then averaged within the same (healthy, diseased) group. In all panels, points represent the mean ± SEM of normalized values of numerous samples in each group. *Mark significant ($P \leq 0.05$) differences compared to the healthy control, whereas ** indicate significant ($P \leq 0.05$) differences between the groups indicated

line with previous data presenting that (1) the expression of the receptor was higher in human PCC-derived epithelial cell lines than in cell cultures initiated from non-malignant human prostate tissues (Sarfaraz et al. 2005); and (2) numerous cannabinoids were shown to induce cells death of these CB1-overexpressing PCC-derived cell lines (Nithipatikom et al. 2004; Sarfaraz et al. 2005). Therefore, although further studies (e.g., on xenograft tumors induced by PCC-derived cell lines in immunodeficient mice) are to be performed to reveal the in vivo potential of cannabinoid compounds on tumor growth, our results further argue for that CB1 may indeed act as a clinically exploitable target molecule in the treatment of PCC.

Interestingly, however, our experiments have also shown that the elevated CB1 expression PCC tissues of all grades did not correlate with the degree of malignancy of the tumors. These data may suggest that (in contrast to human hepatocellular carcinoma where the expression of CB1 well correlated with the clinical outcome of the disease) (Xu et al. 2006) the CB1 level may not serve as a prognostic factor in PCC.

Another intriguing novel finding of our study was that, similar to CB1, the level of TRPV1 was also increased in PCC. There were, however, two important differences when compared the expression patterns of the two receptors. First, the expression of CB1, unlike that of TRPV1, was

significantly elevated even in G1 PCC samples. Second, as a marked contrast to data with CB1, the degree of elevation of TRPV1 in PCC showed clear correlation with increasing degrees of malignancy of the samples. It appears, therefore, that TRPV1 may "join" the group of other calcium-permeable TRP channels (such as TRPV6 and TRPM8), which are now recognized as prognostic tumor markers of PCC (Fixemer et al. 2003; Zhang and Barritt 2006).

Interestingly, previous studies on another human urogenital tract tumor, i.e., urinary bladder carcinomas, revealed exactly opposite findings. Namely, Lazzeri et al. (2005) have shown that the expression of TRPV1 (which was also found in the epithelial cells) (Lazzeri et al. 2004) gradually decreased with increasing tumor grades. The explanation of this contradiction is unknown yet, for the potential therapeutic targeting of TRPV1 to be definitely determined.

Similarly, the another novel result of our study that CB1 (but, notably, not TRPV1) is highly overexpressed in BPH tissues, also invite further in vivo and in vitro studies to clarify the putative role of the receptor to control the benign (yet, from a clinical point-of-view, "to be treated") unwanted growth of the tissue.

Taken together, our presented results strongly argue for that (1) the CB1 and TRPV1 molecules as well as their ligands may indeed possess a promising, future role in the treatment of PCC; (2) TRPV1 may serve as a prognostic factor in PCC; and (3) CB1 may act as a potential target molecule in the therapeutic management of BPH.

Acknowledgments This work was supported by Hungarian research grants: OTKA 63153, OTKA 49231, ETT 480/2006, ETT 482/2006, RET 06/2004. The authors state no competing financial interest. T.B. is a recipient of the János Bolyai research scholarship of the Hungarian Academy of Sciences.

References

Bodó E, Kovács I, Telek A, Varga A, Paus R, Kovács L et al (2004) Vanilloid receptor-1 is widely expressed on various epithelial and mesenchymal cell types of human skin. J Invest Dermatol 123:410–413. doi:10.1111/j.0022-202X.2004.23209.x

Bodó E, Bíró T, Telek A, Czifra G, Griger Z, Tóth IB et al (2005) A "hot" new twist to hair biology: Involvement of vanilloid receptor-1 (VR1/TRPV1) signaling in human hair growth control. Am J Pathol 166:985–998

Casanova ML, Blazquez C, Martinez-Palacio J, Villanueva C, Fernandez-Acenero MJ, Huffman JW et al (2003) Inhibition of skin tumor growth and angiogenesis in vivo by activation of cannabinoid receptors. J Clin Invest 111:43–50

Caterina MJ, Julius D (2001) The vanilloid receptor: a molecular gateway to the pain pathway. Annu Rev Neurosci 24:487–517. doi:10.1146/annurev.neuro.24.1.487

De Petrocellis L, Cascio MG, Di Marzo V (2004) The endocannabinoid system: a general view and latest additions. Br J Pharmacol 141:765–774. doi:10.1038/sj.bjp.0705666

Di Marzo V, Bifulco M, De Petrocellis L (2004) The endocannabinoid system and its therapeutic exploitation. Nat Rev Drug Discov 3:7712–7784. doi:10.1038/nrd1495

Fixemer T, Wissenbach U, Flockerzi V, Bonkhoff H (2003) Expression of the Ca2+-selective cation channel TRPV6 in human prostate cancer: a novel prognostic marker for tumor progression. Oncogene 22:7858–7861. doi:10.1038/sj.onc.1206895

Galiegue S, Mary S, Marchand J, Dussossoy D, Carriere D, Carayon P et al (1995) Expression of central and peripheral cannabinoid receptors in human immune tissues and leukocyte subpopulations. Eur J Biochem 232:54–61. doi:10.1111/j.1432-1033.1995.tb20780.x

Griger Z, Páyer E, Kovács I, Tóth IB, Kovács L, Sipka S et al (2007) Protein kinase Cβ and δ isoenzymes promote arachidonic acid production and proliferation of MonoMac-6 cells. J Mol Med 85:1031–1042. doi:10.1007/s00109-007-0209-y

Lazzeri M, Vannucchi MG, Zardo C, Spinelli M, Beneforti P, Turini D et al (2004) Immunohistochemical evidence of vanilloid receptor 1 in normal human urinary bladder. Eur Urol 46:792–798. doi:10.1016/j.eururo.2004.08.007

Lazzeri M, Vannucchi MG, Spinelli M, Bizzoco E, Beneforti P, Turini D et al (2005) Transient receptor potential vanilloid type 1 (TRPV1) expression changes from normal urothelium to transitional cell carcinoma of human bladder. Eur Urol 48:691–698. doi:10.1016/j.eururo.2005.05.018

Mori A, Lehmann S, O'Kelly J, Kumagai T, Desmond JC, Pervan M et al (2006) Capsaicin, a component of red peppers, inhibits the growth of androgen-independent, p53 mutant prostate cancer cells. Cancer Res 66:3222–3229. doi:10.1158/0008-5472.CAN-05-0087

Nithipatikom K, Endsley MP, Isbell MA, Falck JR, Iwamoto Y, Hillard CJ et al (2004) 2-Arachidonoylglycerol: a novel inhibitor of androgen-independent prostate cancer cell invasion. Cancer Res 64:8826–8830. doi:10.1158/0008-5472.CAN-04-3136

Pacher P, Batkai S, Kunos G (2005) Cardiovascular pharmacology of cannabinoids. Handb Exp Pharmacol 168:599–625. doi:10.1007/3-540-26573-2_20

Paus R, Schmelz M, Bíró T, Steinhoff M (2006) Frontiers in pruritus research: scratching the brain for more effective itch therapy. J Clin Invest 116:1174–1186. doi:10.1172/JCI28553

Ruiz-Llorente L, Sanchez MG, Carmena MJ, Prieto JC, Sanchez-Chapado M, Izquierdo A et al (2003) Expression of functionally active cannabinoid receptor CB1 in the human prostate gland. Prostate 54:95–102. doi:10.1002/pros.10165

Sanchez MG, Sanchez AM, Collado B, Malagarie-Cazenave S, Olea N, Carmena MJ et al (2005) Expression of the transient receptor potential vanilloid 1 (TRPV1) in LNCaP and PC-3 prostate cancer cells and in human prostate tissue. Eur J Pharmacol 515:20–27. doi:10.1016/j.ejphar.2005.04.010

Sanchez AM, Sanchez MG, Malagarie-Cazenave S, Olea N, Diaz-Laviada I (2006) Induction of apoptosis in prostate tumor PC-3 cells and inhibition of xenograft prostate tumor growth by the vanilloid capsaicin. Apoptosis 11:89–99. doi:10.1007/s10495-005-3275-z

Sarfaraz S, Afaq F, Adhami VM, Mukhtar H (2005) Cannabinoid receptor as a novel target for the treatment of prostate cancer. Cancer Res 65:1635–1641. doi:10.1158/0008-5472.CAN-04-3410

Stein RJ, Santos S, Nagatomi J, Hayashi Y, Minnery BS, Xavier M et al (2004) Cool (TRPM8) and hot (TRPV1) receptors in the bladder and male genital tract. J Urol 712:1175–1178. doi:10.1097/01.ju.0000134880.55119.cf

Telek A, Bíró T, Bodó E, Tóth IB, Borbíró I, Kovács L et al (2007) Inhibition of human hair follicle growth by endo- and exocannabinoids. FASEB J 21:3534–3541. doi:10.1096/fj.06-7689com

Varga A, Czifra G, Tállai B, Németh T, Kovács I, Kovács L et al (2004) Tumor grade-dependent alterations in the protein kinase C isoform pattern in urinary bladder carcinomas. Eur Urol 46:462–465

Xu X, Liu Y, Huang S, Liu G, Xie C, Zhou J et al (2006) Overexpression of cannabinoid receptors CB1 and CB2 correlates with improved prognosis of patients with hepatocellular carcinoma. Cancer Genet Cytogenet 171:31–38. doi:10.1016/j.cancergencyto.2006.06.014

Zhang L, Barritt GJ (2006) TRPM8 in prostate cancer cells: a potential diagnostic and prognostic marker with a secretory function? Endocr Relat Cancer 13:27–38. doi:10.1677/erc.1.01093

XIX.

European Urology

European Urology 46 (2004) 462–465

Tumor Grade-Dependent Alterations in the Protein Kinase C Isoform Pattern in Urinary Bladder Carcinomas

Attila Varga[a,1], Gabriella Czifra[b,1], Béla Tállai[a], Tamás Németh[c], Ilona Kovács[d], László Kovács[b], Tamás Bíró[b,*]

[a]*Department of Urology, University of Debrecen, Debrecen, Hungary*
[b]*Department of Physiology and Cell Physiology Research Group of the Hungarian Academy of Sciences, Nagyerdei krt. 98, PO Box 22, 4012 Debrecen, Hungary*
[c]*Department of Pathology, University of Debrecen, Debrecen, Hungary*
[d]*Medical and Health Science Center, Research Center for Molecular Medicine, Kenézy University Hospital, Debrecen, Hungary*

Accepted 20 April 2004

Available online 31 May 2004

Abstract

Objectives: Members of the protein kinase C (PKC) isoenzyme family play central role in the tumorigenesis of several tissues. In this study our goal was to determine the possible alterations in the protein kinase C (PKC) isoform pattern in relation with the different tumor grade in human urinary bladder carcinomas.

Methods: Western blot analysis, followed by quantitative densitometry, was performed to define the expression of PKC isoforms in the epithelial tissue of human urinary bladder carcinomas with various tumor grades and in control samples.

Results: The human urinary bladder epithelium expressed five PKC isoforms (PKCα, β, δ, ε, ζ), the levels of which differentially altered as a function of tumor grade. Namely, whereas the expressions of PKCβ and δ decreased with increasing grade of the carcinomas, the levels of PKCα, ε, and ζ showed opposite patterns of changes.

Conclusions: These grade-dependent alterations in the PKC isoform pattern strongly argue for the central yet antagonistic roles of certain members of the PKC system in malignant transformation of human urinary bladder epithelium.

Keywords: Protein kinase C; Isoenzymes; Urinary bladder carcinoma; Tumorigenesis

1. Introduction

Protein kinase C (PKC) comprises a family of serine/threonine kinases that play central roles in the regulation of various cellular processes such as proliferation and tumorigenesis [1]. The members of the PKC family are the calcium- and phorbol ester-dependent ''conventional'' (cPKCα, βI, βII, and γ), the calcium-independent ''novel'' (nPKCδ, ε, η, and θ), the calcium- and phorbol ester-independent ''atypical'' (aPKCζ and λ/ι) isoforms and the unique PKCμ [2]. These isoforms possess a characteristic expression pattern in a given cell type, and regulate in an isoenzyme-specific, and very often antagonistic, fashion various cellular processes including cell growth, cell death and transformation [3]. For example, nPKCδ was suggested to promote cellular differentiation whereas, in contrast, PKCε of the same novel family was suggested as a key stimulator of in vitro and in vivo (tumor) growth of numerous cell types [3,4].

Numerous reports have shown alterations in the PKC isoform pattern in parallel with the onset of cellular transformation leading to transformed phenotype in several tissues including e.g., fibroblasts [4], skin cells [5,6], breast epithelium [7], uterus [8], and prostate [9], suggesting the role of the PKC system in the

* Corresponding author. Tel. +36-52-416-634; Fax: +36-52-432-289.
E-mail address: biro@phys.dote.hu (T. Bíró).
[1] Attila Varga and Gabriella Czifra equally contributed to this work.

0302-2838/$ – see front matter © 2004 Elsevier B.V. All rights reserved.
doi:10.1016/j.eururo.2004.04.014

pathogenesis and progression of various tumors. However, up to date, only very few data have implicated the significance of the PKC system in the urinary bladder tumors [10,11]. Therefore, in the current study, our goal was to define the possible alterations in the PKC isoform pattern of all three groups in relation with the different tumor grade in human urinary bladder carcinomas.

2. Materials and methods

The study involved 23 cases (17 men, 6 women) of transitional cell carcinoma of the bladder removed by transurethral resection (17 cases), partial bladder resection (4 cases), or cystectomy (2 cases), and 6 samples of normal bladder obtained during prostatectomy. The removed samples were divided into two parts. One was processed to obtain formalin-fixed, paraffin-embedded sections and to perform routine haematoxylin-eosin staining-based grading [12] and staging according to the TNM system [13]. Based on the histological diagnosis, 9 cases were of G1 grade (1 pTa, 8 pT1), 8 cases were of G2 grade (4 pT1, 3 pT2, 1 pT3b), and 6 cases were of G3 grade (2 pT2, 4 pT3b). The second part was frozen in liquid nitrogen and, to collect tissue parts containing epithelial tissue-enriched samples (and, therefore, free of non-epithelial tissues such as smooth muscle that may contain a different PKC isoform pattern from that of the epithelial cell types [1,2]), these frozen samples were serially cut using a cryomicrotome starting from the surface of the tumor until the lamina propria was reached (this was verified by serial haematoxylin-eosin stained sections). The sections were then collected on ice and were processed in a lysis buffer containing protease inhibitors as described previously [14]. Vigorously equal amounts (20–30 μg) of protein were subjected to SDS-PAGE and then transferred to nitrocellulose membranes (BioRad, Vienna, Austria). Membranes were first probed with appropriate anti-PKC antibodies (1:500–1:1000 dilutions in milk) then with a peroxidase-conjugated goat secondary antibody (IgG, 1:1000 dilution, BioRad). Polyclonal (rabbit) antibodies against PKCα, β, γ, δ, ε, η, and ζ (Sigma, St. Louis, MO, USA) and against PKCθ, λ/ι, and μ (Santa Cruz, Santa Cruz, CA, USA) were used as primary antibodies. Specificity of antibodies was measured using appropriate blocking peptides, which in all cases effectively suspended the immunosignal (data not shown). Immunoreactive bands were finally visualized by an enhanced chemiluminescence (ECL) detection kit (Amersham, Little Chalfont, UK) and were subjected to quantitative densitometry analyses using a GelDoc system (BioRad) [15]. For statistical analysis, the Student t test was used. Data were expressed as mean ± SEM and p values of less than 0.05 were regarded as significant differences. The study was approved by the Institutional Research Ethics Committee.

3. Results

Western blot analysis revealed that samples from both the normal and diseased urinary bladder epithelium expressed five PKC isoforms; the cPKCα and β, the nPKCδ and ε, and the aPKCζ (Fig. 1A). The other PKC isoforms (cPKCγ, nPKCη and θ, aPKCλ/ι, PKCμ) were not detected (data not shown). Of great importance, however, in the tumor samples of various grades we found marked yet differential alterations in the levels of the existing isoforms. As measured by quantitative densitometry analyses of the immunoblots (Fig. 1B), in the G1 tumors, only the expression of aPKCζ increased significantly (when compared to the values of the normal bladder tissues) whereas the levels of other isoforms remained unchanged. In contrast, the expressions of all PKC isoform in G2 and/or G3 carcinomas significantly differed from the healthy control values. The levels of cPKCβ and nPKCδ were

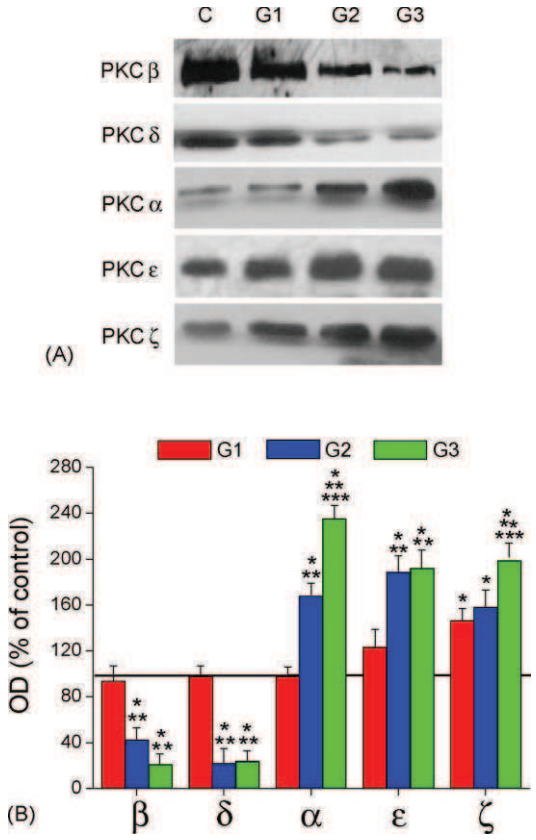

Fig. 1. Alterations in the PKC isoform patterns in urinary bladder carcinomas of various tumor grades. Epithelial tissues of normal urinary bladder (control, C) and transitional carcinomas with various tumor grades (G) were collected, processed in protease inhibitor containing lysis buffer, and vigorously equal amounts of protein were subjected to SDS-PAGE to perform Western blot analysis of the PKC isoforms as described under "Materials and methods". (A) Representative Western blot data of several determinations yielding similar results. (B) The amounts of the expressed PKC isoenzymes were quantitated by densitometry (optical density; OD), and values obtained with the tumor samples were expressed as the percentage of the control samples (normalized OD), regarded as 100% (solid line). Points represent mean ± SEM of several independent experiments for each antigen. The * represents significant ($p < 0.05$) differences of OD values of any tumor sample compared to control. The ** represents significant ($p < 0.05$) differences between the OD values of the G2 or G3 tumors compared to that of the G1 samples. The *** represents significant ($p < 0.05$) differences between the OD values of the G3 tumors compared to that of the G2 samples.

markedly suppressed in the G2 and G3 samples when compared to the control (or to the G1 tumors, $p < 0.05$ in all cases) yet the expressions did not differ between the G2 and G3 groups. However, the levels of the other three isoforms significantly elevated with increasing tumor grades, with only minor differences in the expression patterns. For example, the expression of cPKCα (and, at least tendency-wise, of aPKCζ) gradually increased with increasing tumor grades whereas the level nPKCε was equally high in the G2 and G3 carcinomas.

4. Discussion

In this study we provide clear evidence that expressions of the existing five PKC isoforms differentially alter as a function of tumor grade of human urinary bladder carcinomas. Whereas the expressions of PKCβ and δ decreased with increasing grade of the tumors, the levels of PKCα, ε, and ζ showed opposite patterns of changes. These findings, similarly to numerous other tissues [3–9], strongly argue for a potential central role of the PKC system in the tumorigenesis in the human urinary bladder epithelium as well. In addition, the opposite changes seen in the levels of the isoforms also highlight that the individual isoenzymes act antagonistically in the above process. In this context, it was also of great importance that the opposite behavior could also be seen even within the members of the PKC subfamilies. Namely, the levels of calcium-dependent ''conventional'' cPKCα and β, similarly to that of the calcium-independent ''novel'' nPKCδ and ε, altered in opposite manners. Therefore, it appears that the differential expression pattern changes in relation with the altered tumor grade cannot be merely ascribed to different activation mechanism of the given isoforms.

According to our knowledge, only the group of Sampson [10,11] has carried our similar studies to define the PKC expression in urinary bladder tumors. Besides striking similarities (i.e., decrease in the levels of cPKCβ and nPKCδ and increase in expression of aPKCζ with increasing tumor grade), our experiments also resulted in markedly different data. In contrast to their results, we observed marked and consistent alterations in the expressions of cPKCα and of nPKCε (this latter isoform was not enrolled to their study), although we were unable to detect nPKCη in our samples. Besides the putative technical, antibody, and geographic differences, these dissimilarities might be attributed to two other factors. The first one is that, in their study, most of the G1 and G2 tumors possessed stage pTa whereas our samples of these grades were mostly of pT1 and pT2 stage. In addition, they carried out their Western analysis of crude tumor extracts whilst we collected exclusively epithelial tissues to avoid mixture with mesenchymal tissues that may possess different PKC isoform pattern. Nevertheless, both their previous presentation and our current findings unambiguously argue for the importance of the PKC family in the tumorigenesis of bladder epithelium.

Acknowledgements

This work was supported by Hungarian research grants: OTKA F035036, OTKA T037531, OTKA TS040773, NKFP 00088/2001, OMFB 00200/2002, ETT 365/2003. Tamás Bíró is a recipient of the György Békésy Postdoctoral Scholarship.

References

[1] Nishizuka Y. The molecular heterogeneity of protein kinase C and its implication for cellular regulation. Nature 1988;334:661–5.
[2] Ohno S, Akita Y, Hata A, Osada S, Kubo K, Konno Y, et al. Structural and functional diversities of a family of signal transducing protein kinases, protein kinase C family; two distinct classes of PKC, conventional cPKC and novel nPKC. Adv Enzyme Regul 1991;31:287–303.
[3] Goodnight JA, Mischak H, Mushinski JF. Selective involvement of protein kinase C isozymes in differentiation and neoplastic transformation. Adv Cancer Res 1994;64:159–209.
[4] Mischak H, Goodnight JA, Kolch W, Martiny-Baron GM, Schaechtle C, Kazanietz MG, et al. Overexpression of protein kinase C-δ and -ε in NIH 3T3 cells induces opposite effects on growth, morphology, anchorage dependence, and tumorigenicity. J Biol Chem 1993; 268:6090–6.
[5] Neill GW, Ghali LR, Green JL, Ikram MS, Philpott MP, Quinn AG. Loss of protein kinase Calpha expression may enhance the tumorigenic potential of Gli1 in basal cell carcinoma. Cancer Res 2003;63:4692–7.
[6] Selzer E, Okamoto I, Lucas T, Kodym R, Pehamberger H, Jansen B. Protein kinase C isoforms in normal and transformed cells of the melanocytic lineage. Melanoma Res 2002;12:201–9.
[7] Franz MG, Norman JG, Fabri PJ, Gower Jr WR. Differentiation of pancreatic ductal carcinoma cells associated with selective expression of protein kinase C isoforms. Ann Surg Oncol 1996;3:564–9.
[8] Bamberger AM, Bamberger CM, Wald M, Kratzmeier M, Schulte HM. Protein kinase C (PKC) isoenzyme expression pattern as an indicator of proliferative activity in uterine tumor cells. Mol Cell Endocrinol 1996;123:81–8.
[9] Koren R, Meir DB, Langzam L, Dekel Y, Konichezky M, Baniel J, et al. Expression of protein kinase C isoenzymes in benign hyperplasia and carcinoma of prostate. Oncol Rep 2004; 11:321–6.

[10] Langzam L, Koren R, Gal R, Kugel V, Paz A, Farkas A, et al. Patterns of protein kinase C isoenzyme expression in transitional cell carcinoma of bladder. Relation to degree of malignancy. Am J Clin Pathol 2001;116:377–85.

[11] Koren R, Langzam L, Paz A, Livne PM, Gal R, Sampson SR. Protein kinase C (PKC) isoenzymes immunohistochemistry in lymph node revealing solution-fixed, paraffin embedded bladder tumors. Appl Immunohistochem Mol Morphol 2000;8:166–71.

[12] Mostofi FK, Sobin LH, Torlani H. Histological typing of urinary bladder tumors. In International classification of tumours. Vol. 10. Geneva: World Health Organization; 1973.

[13] Silverberg SG, DeLellis RA, Frable WJ. Principles and Practice of Surgical Pathology, ed. 3, New York: Churchill Livingstone; 1997. p. 2191–5.

[14] Lázár J, Szabó T, Kovács L, Blumberg PM, Bíró T. Distinct features of recombinant vanilloid receptor-1 expressed in various expression systems. Cell Mol Life Sci 2003;60:2228–40.

[15] Papp H, Czifra G, Lázár J, Boczán J, Gönczi M, Csernoch L, et al. Protein kinase C isozymes regulate proliferation and high cell density-mediated differentiation of HaCaT keratinocytes. Exp Dermatol 2003;12:811–24.

XX.

Abnormal Cell-Specific Expressions of Certain Protein Kinase C Isoenzymes in Peripheral Mononuclear Cells of Patients with Systemic Lupus Erythematosus: Effect of Corticosteroid Application

T. Bíró*, Z. Griger*, E. Kiss†, H. Papp*, M. Alekszа†, I. Kovács†, M. Zeher†, E. Bodolay†, T. Csépány‡, K. Szûcs§, P. Gergely§, L. Kovács*, G. Szegedi¶ & S. Sipka†

Abstract

We have studied the expressions of various protein kinase C (PKC) isoenzymes in T cells and monocytes from patients with systemic lupus erythematosus (SLE), in comparison to those of healthy controls and patients with other immunological disorders. As measured by Western blotting, the levels of PKCβ, δ, η, ε, θ and ζ (but not of PKCα) significantly decreased in T cells of SLE patients. In monocytes, however, we observed marked suppressions only in the expressions of PKCδ, ε and ζ but not in the expressions of other PKC isoforms. *In vivo* corticosteroid application, as well as *in vitro* steroid treatment of monocytes, elevated the expressions of most isoforms close to normal values; however, the decreased levels of PKCθ and ζ were not affected by steroid application. These alterations were characteristic to SLE because we could not detect any changes in the PKC levels in mononuclear cells of primary Sjögren's syndrome and mixed connective tissue disease patients. These results suggest that impaired PKC isoenzyme pattern may exist in the T cells and monocytes of SLE patients. Furthermore, the clinically efficient glucocorticoid application in SLE can increase the expression of some members of PKC system.

*Department of Physiology and Cell Physiology Research Group of the Hungarian Academy of Sciences; †III Department of Internal Medicine; ‡Department of Neurology, University of Debrecen, Medical and Health Science Center, Research Center for Molecular Medicine; §Department of Medical Chemistry; and ¶Autoimmune Disease Research Group of the Hungarian Academy of Sciences, Debrecen, Hungary

Received 21 January 2004; Accepted in revised form 26 May 2004

Correspondence to: Dr S. Sipka, MD, PhD, DSc, III Department of Internal Medicine, University of Debrecen, Medical and Health Science Center, Medical School, H-4004 Debrecen, Hungary. E-mail: sipka@iiibel.dote.hu

Introduction

Systemic lupus erythematosus (SLE) is an autoimmune disease characterized by altered cellular and humoral immune responses leading to pathological autoantibody production. In the pathomechanism of the disease, a complex multicellular dysfunction of monocytes/macrophages and T lymphocytes is involved [1]. The abnormal signalling events in lupus T cells are chiefly manifested at the level of signal transduction, and include pathological protein kinase A cascade events [2], abnormal transcription activities [3] and defective T-cell receptor ζ chain expression [4–6]. The SLE-specific modifications in monocyte functions can be characterized by decreased chemotaxis, phagocytic activity, altered productions of various cytokines and costimulatory molecules [7, 8]. In addition, our laboratory has recently described a decreased release of arachidonic acid (AA) in monocytes of SLE patients [9].

Protein kinase C (PKC) comprises a family of serine/threonine kinases that play key roles in the regulation of various cellular processes [10]. Up to date, 11 different PKC isoenzymes have been identified, which can be classified into the groups of the calcium- and phorbol ester-dependent 'conventional' (PKCα, βI, βII and γ; cPKCs), the calcium-independent 'novel' (PKCδ, ε, η and θ; nPKCs), the calcium- and phorbol ester-independent 'atypical' (PKCζ and λ/ι; aPKCs) isoforms and the unique PKCμ. These isoforms specifically regulate various cellular functions such as proliferation, cytokine production and receptor-mediated signal transduction [10]. PKC has been shown to play key roles in numerous T-cell and monocyte functions as well. In T cells, PKC isoforms regulate, for example, the transcription activity of NF-κB, interleukin (IL) 2 promoter activation and the proliferation and maturation of the cells [11–15]. Similarly, the pivotal roles of various members of the PKC family in regulation

of monocyte-specific mediator production, stimuli-induced oxidative respiratory burst and phagocytic activities were also demonstrated [16–18].

There is little known, however, about the PKC systems in mononuclear cells of SLE patients. Although the very few reports described a decreased intrinsic PKC activity in T cells [19], there is no data available about possible alterations in the PKC system in the defective monocytes of SLE patients, and, furthermore, about the isoform-specific alteration in mononuclear cells in SLE. It seemed to be straightforward, therefore, to measure quantitatively the expressions of the existing PKC isoenzymes in T cells and monocytes of patients with SLE, in comparison with the PKC profiles of healthy controls and patients with other immunological disorders. Furthermore, because corticosteroids were connected to some PKC-dependent signal transduction processes [20, 21], we also investigated the effect of steroid therapy on the PKC isoform levels and disease status. We report here for the first time that T cells and monocytes possess differential, cell- and isoform-specific suppression in the levels of certain PKC isoforms which alterations might explain the impaired immunological functions of these cells. In addition, we also present that some (but not all) of the isoform defects could be reversed and improved by glucocorticosteroid treatment, in parallel to the improvement of the disease-related symptoms.

Patients and methods

Patients. The SLE study population consisted of 22 patients, 20 women and 2 men, average of age 36 years, range 21–58 years. They all fulfilled at least four of the American College of Rheumatology classification criteria [22]. The actual activity of the disease was scored according to the SLE Disease Activity Index (SLEDAI). Patients with SLEDAI > 3.0 were regarded as clinically active subjects. The mean SLEDAI rating was 3.6, range 0–20. The average duration of disease was 5.1 years, range 2–20. Eleven patients were free of any glucocorticosteroid (their averaged SLEDAI was 0.9), whereas 11 patients received 2–40 mg/day corticosteroid treatment (their averaged SLEDAI was 6.6) One woman (26 years old) with freshly diagnosed active SLE (SLEDAI: 20) was tested before the treatment with pulse dose of glucocorticosteroid (4×500 mg methylprednisolone/day, 1×250 mg i.v., then 64 mg/day for a month) and also 8 days later. Patients with lupus nephritis were not enrolled in this study. Either anti ds-DNA or anti-Sm or both characteristic antibodies could be detected in this group of SLE patients. All the nine patients with primary Sjögren's syndrome were women; the average of their age was 60.3 years, range 51–73 years, and the average of the duration of the disease was 10.2 years, range 4–19 years. Anti-SS-A antibody positivity was 6/9, whereas anti-SS-B occurred in 4/9 cases. They all were treated according to the scheme of 8 mg methylprednisolone/48 h. All the six patients with mixed connective tissue disease (MCTD) were women; the average of their age was 48.6 years (range 38–56 years). The average of the duration of disease was 16.7 years (range 8–19 years). All the patients were positive for anti-U1 ribonuclear protein antibodies. Two of them were without any steroid and cytostatic treatments, two took 4 mg/day of steroid and two were treated by 8 mg/48 h of methylprednisolone + 100 mg of Cytoxan/day. As controls, the peripheral blood samples of 21 healthy Caucasian subjects (12 women, 9 men, average age 41 years, range 21–56 years) were studied. Approval was given through the Institutional Review Board, and informed consent was obtained from all patients.

Preparation of purified T-cell and monocyte populations. A Dynal magnetic-bead cell separation technique was used to obtain purified cell suspensions [9]. The average monocyte purity was >85% whereas the average of T-cell purity was >95%, as was assessed by flow cytometry analysis of specific surface markers.

Cell culturing. Peripheral monocytes and MonoMac6 cells were cultured under lipopolysaccharide-free conditions in RPMI-1640 media containing 10% fetal bovine serum, 2 mM L-glutamine, 1 mM sodium pyruvate, 0.1 mM nonessential amino acids, 200 U/ml penicillin and 200 μg/ml streptomycin (all from Sigma, St. Louis, MO, USA).

Western blotting. Control and diseased cell suspensions, as well as MonoMac6 cells, were processed in a lysis buffer containing protease inhibitors as described previously [23], and vigorously equal amounts (20–30 μg) of protein were subjected to SDS-PAGE and then transferred to nitrocellulose membranes (Bio-Rad, Vienna, Austria). Membranes were blocked with 5% dry milk and were first probed with appropriate anti-PKC antibodies (1 : 500–1 : 1000 dilutions in milk) then with a peroxidase-conjugated goat secondary antibody (IgG, 1 : 1000 dilution, Bio-Rad) to enhance specificity. Polyclonal (rabbit) antibodies against PKCα, β, γ, δ, ε, η and ζ (Sigma) and against PKCθ (Santa Cruz, CA, USA) were used as primary antibodies throughout the experiments. However, to assure antibody specificity, appropriate blocking peptides and another set of primary monoclonal (mouse) antibodies against the same PKC isoforms (Transduction Laboratories, Lexington, KY, USA) were also employed. Except for polyclonal anti-PKCα antibody, which stained the holoenzyme and the catalytic subunit resulting in double immunosignals, single and specific bands were obtained with both sets of antibody (data not shown). Immunoreactive bands were finally visualized by an enhanced chemiluminescence Western blotting detection kit (Amersham, Little Chalfont, England) on light sensitive films (AGFA, Brussels, Belgium) and were subjected to quantitative densitometric analyses using a GelDoc system (Bio-Rad).

Flow cytometry analysis. Peripheral monocytes and MonoMac6 cells were fixed by 1% paraformaldehyde

and permeabilized by saponin (Sigma). The intracellular PKC isoenzymes were first labelled using the above polyclonal (rabbit) primary antibodies then with a FITC-conjugated goat antirabbit (IgG) secondary antibody (Vector, Burlingame, USA). After fixation, cells were analyzed by a flow cytometer (Coulter EPICS XL-4, USA) and, after isotype control calibration, the percentage of cells expressing the FITC-labelled PKC isoforms was determined.

Real-time quantitative-polymerase chain reaction (Q-PCR). Q-PCR was carried out on an ABI PRISM 7000 Sequence Detection System (Applied Biosystems, Foster City, CA, USA) by using the 5′ nuclease assay. Total RNA was isolated from the cells using TRIzol (Invitrogen, Paisley, UK) following the manufacturer's procedure. Three micrograms of total RNA were then reverse transcribed into cDNA by using 15 units of AMV reverse transcriptase (Promega, Madison, WI, USA) and 0.025 μg/ml random primers (Promega). PCR amplification was carried out by using TaqMan primers and probes (assay ID: Hs00176973_m1 for PKCα, Hs00176998_m1 for PKCβ, Hs00178914_m1 for PKCδ, Hs00178455_m1 for PKCε, Hs00178933_m1 for PKCη and Hs00177051_m1 for PKCζ) following the procedure of the manufacture (TaqMan Universal PCR Master Mix Protocol, Applied Biosystems). As an internal control, transcripts of glyceraldehyde 3-phosphate dehydrogenase (GAPDH) were determined (Assay ID: Hs99999905_m1).

Measurement of AA release. MonoMac6 cells (10^5/ml) were preincubated with [^{3}H]AA (Amersham, UK) at 37 °C for 20 h [9]. After extensive washing, cells were further incubated in the culturing medium for additional 4 h and the released [^{3}H]AA to the medium was regarded as the basal production of AA. The determination of the PKC-dependent AA release was performed by the administration of 100 nM phorbol 12-myristate 13-acetate (PMA) (Sigma) with or without a calcium ionophore (A23187, 5 μM, Sigma) for 4 h. Each value was calculated as the average of triplicates of cultured cells.

Statistical analysis. The quantitative optical density results obtained from the Western analysis were normalized to the daily matched control data, then these normalized values were averaged and the mean ± SEM values were calculated. Statistical comparison of data was performed using Student's *t*-test. *P*-values less than 0.05 were considered significant.

Results

Alterations in the expressions of PKC isoforms in T cells of SLE patients without and with steroid treatments

The possible alterations in the PKC isoform pattern in the different T-cell populations using Western blot analysis were determined. We could detect seven PKC isoforms (PKCα, β, δ, ε, η, θ and ζ) in T-cell suspensions of both healthy controls and SLE patients (PKCγ was not detected in the T cells). Then we tried to select various groups among the SLE patients to be able to define whether the status of the disease (active, inactive) or the applied therapy (e.g. corticosteroid) affected the PKC isoform levels.

The PKC isoform expression pattern in the T cells of SLE patients with no steroid therapy ($n = 11$) differed remarkably from that of the healthy controls ($n = 21$) (Fig. 1A) (Table 1). Whereas the levels of PKCα showed no measurable changes, there were marked and significant (but variable) decreases in the expressions of PKCβ, δ, ε and θ, and a moderate, yet significant, suppression in the level of PKCζ (Table 1). Comparison of these data to those obtained with T cells of SLE patients receiving steroid treatment ($n = 10$) revealed that the expressions of PKCβ, δ, ε and η but not of PKCθ and ζ were partially or almost completely normalized in this group (Fig. 1A) (Table 1). These PKC isoenzyme alterations seemed to be characteristic of SLE because we could not detect any significant changes in the expressions of the PKC isoforms in T cells of SS ($n = 9$) and MCTD ($n = 6$) patients (Fig. 1A) (Table 1).

When the Western blot data were compared on patients with active or inactive disease status to the isoform levels of healthy volunteers, no correlation was observed (data not shown).

Alterations in the expressions of PKC isoforms in monocytes of SLE patients without and with steroid treatments

We measured the PKC isoform pattern in monocyte populations of patients with SLE using also Western blotting. As a striking difference compared to the T-cell data, we found that the expressions of several existing isoforms (PKCα, β and η) were similar in the monocytes of steroid-free SLE patients to the healthy controls (Fig. 1B) (Table 2). In contrast, the levels of PKCε and δ markedly whereas the expression of PKCζ moderately yet significantly decreased in the diseased monocytes (PKCθ and γ were not present in these cells). Similarly to the T-cell results, in the monocytes of SLE patients who received corticosteroid therapy, the expressions of some isoforms returned differentially to the levels of controls. Namely, whereas the expressions of PKCδ and ε markedly and significantly increased (compared to the steroid-free group), the level of PKCζ remained lower than seen in monocytes of healthy volunteers. These alterations also were characteristic of SLE because we could not measure any significant change in the PKC pattern of monocytes of patients with SS (Fig. 1B) (Table 2). In addition, similarly to the T-cell findings, comparing the results found in the monocytes of patients with active or inactive SLE, there was no difference between them and the isoform levels of the healthy volunteers (data not shown).

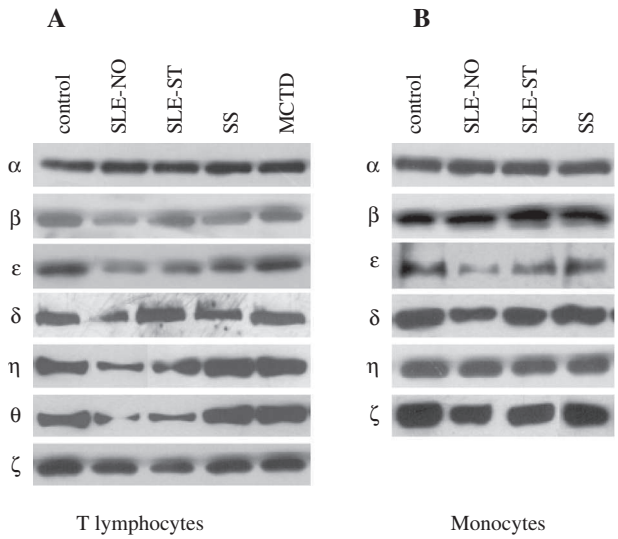

Figure 1 Alterations in the protein kinase C (PKC) isoform patterns in mononuclear cells of patients with systemic lupus erythematosus. Purified T lymphocytes (A) and monocytes (B) from healthy volunteers (control), patients with systemic lupus erythematosus without (SLE-NO) and with (SLE-ST) steroid therapy, and with Sjögren's syndrome (SS) and mixed connective tissue disease (MCTD) were processed in protease inhibitor containing lysis buffer, and vigorously equal amounts of protein were subjected to SDS-PAGE and then transferred to nitrocellulose membranes. Membranes were first probed with appropriate polyclonal (rabbit) anti-PKC antibodies (Greek letters) then with a peroxidase conjugated antirabbit goat secondary antibody (IgG). Immunoreactive bands were visualized by an enhanced chemiluminescence (ECL) Western blotting detection kit on light sensitive films. Figure shows a representative result of several determinations.

Effect of in vitro steroid treatment on PKC isoform levels

To support the clinical observations regarding steroid treatment and the PKC levels, isolated monocytes from healthy volunteers ($n = 3$) were *in vitro* treated for 2 days with 10 μM hydrocortisone, total RNA was isolated, and the levels of mRNA transcripts of PKC isoforms were determined by quantitative real-time Q-PCR. As seen in Fig. 2A, steroid application selectively and significantly up-regulated the level of nPKCε (when compared to the nontreated cells) whereas the expressions of the other isoforms were not affected.

In addition, we were able to perform a similar *in vitro* study on peripheral isolated monocytes of a freshly diagnosed SLE patient (free of any treatment). As seen in Fig. 2B, *in vitro* corticosteroid application, identically to the above Western blot data (Fig. 1B), markedly increased the transcript levels of nPKCδ and ε (but not of the other isoforms) compared to the expressions seen in the nontreated monocytes. These data indicate that, similarly to the *in vivo* effects (Fig. 1), *in vitro* corticosteroid application also increases the expressions of certain PKC isoforms.

Investigation of PKC isoforms, the effect of steroid application and the PKC-dependent AA release in MonoMac6 monocytoid cells

Because SLE is accompanied by severe monocytopenia, obscuring thorough investigation of various functional phenomena, and, in addition, because freshly diagnosed (i.e. nontreated) SLE cases are very rarely found, we performed additional functional assays on the human monocytoid cell line MonoMac6. As revealed by Western blotting and flow cytometry (Fig. 3), these cells possessed a very similar (yet not identical) PKC isoform pattern to that seen in human peripheral monocytes (Fig. 1B). Namely, they expressed cPKCα and β; nPKCδ and ε; and aPKCζ but only hardly detectable levels of PKCη (data not shown).

Table 1 Protein kinase C (PKC) isoform patterns in T cells of systemic lupus erythematosus (SLE), Sjögren's syndrome (SS) and mixed connective tissue disease (MCTD) patients as measured by densitometry of Western blots

	SLE			
Isoform	Without steroid	With steroid	SS	MCTD
PKCα	102 ± 6	108 ± 11	103 ± 8	101 ± 8
PKCβ	58 ± 8*	91 ± 12†	110 ± 6	106 ± 6
PKCε	32 ± 13*	75 ± 9†	108 ± 5	110 ± 7
PKCδ	49 ± 7*	83 ± 12†	102 ± 7	104 ± 4
PKCη	42 ± 10*	78 ± 9†	93 ± 4	91 ± 8
PKCθ	21 ± 6*	19 ± 8‡	102 ± 3	101 ± 10
PKCζ	72 ± 8*	76 ± 12‡	97 ± 8	99 ± 4

Optical density values of immunoreactive bands of Western blots were determined on healthy and diseased cells. The values of the diseased samples ($n \geq 4$ for each isoform in both SLE groups; $n \geq 3$ in the SS and MCTD groups) were then normalized to those of the daily matched control, healthy subjects ($n \geq 5$ for each isoform), and the normalized data of all patients having the same disorder were averaged. All data are expressed as mean ± SEM of percentage values of control determinations (regarded as 100%).
*Significant ($P < 0.05$) decreases compared to control.
†Significant ($P < 0.05$).
‡Insignificant changes (increases) in the SLE group with steroid treatment compared to the SLE group without steroid application.

Table 2 Protein kinase C (PKC) isoform patterns in monocytes of systemic lupus erythematosus (SLE), Sjögren's syndrome (SS) and mixed connective tissue disease (MCTD) patients as measured by densitometry of Western blots

	SLE		
Isoform	Without steroid	With steroid	SS
PKCα	102 ± 3	101 ± 4	103 ± 8
PKCβ	96 ± 6	105 ± 8	108 ± 6
PKCε	25 ± 9*	63 ± 11†	97 ± 8
PKCδ	51 ± 6*	85 ± 5†	110 ± 5
PKCη	105 ± 7	96 ± 7	102 ± 7
PKCθ	Not measurable		
PKCζ	69 ± 8*	73 ± 13‡	103 ± 8

Optical density values of immunoreactive bands of Western blots were determined on healthy and diseased cells. The values of the diseased samples ($n \geq 4$ for each isoform in both SLE groups; $n \geq 3$ in the SS group) were then normalized to those of the daily matched control, healthy subjects ($n \geq 5$ for each isoform), and the normalized data of all patients having the same disorder were averaged. All data are expressed as mean ± SEM of percentage values of control determinations (regarded as 100%).

*Significant ($P < 0.05$) decreases compared to control.

†Represents significant ($P < 0.05$).

‡Insignificant changes (increases) in the SLE group with steroid treatment compared to the SLE group without steroid application.

Of great importance, however, flow cytometry analysis revealed that the expression of nPKCε was significantly less in the MonoMac6 cells than in the healthy monocytes (the levels of the other isoforms were essentially the same) (Fig. 3A). Actually, the suppressed level of nPKCε was very similar to that found in the SLE monocytes (Fig. 1B) (Table 2). Moreover, also similarly to the peripheral monocytes (Fig. 2), *in vitro* hydrocortisone treatment (10 μM for 1 or 2 days) selectively increased both the mRNA transcript (Fig. 3B) and protein (Fig. 3C) levels of nPKCε.

These findings strongly argued that the MonoMac6 cell line may serve as a fine tool to model the PKC alterations seen in SLE monocytes. To test this hypothesis, we performed an additional functional assay to measure PKC-dependent AA release of the cells. We found that the PKC activator PMA (100 nM) was able to increase AA release from MonoMac6 cells exclusively when a calcium ionophore (A23187, 5 μM) was also present in the medium. This finding was in good accord with our previous data [9] that the PKC dependent AA release was decreased in the SLE monocytes compared to control, and that this impairment was mostly seen when the PKC activator PMA was applied alone (i.e. without a calcium ionophore to increase intracellular calcium concentration). These data strongly suggest that the suppressed calcium-independent nPKC levels (presumably nPKCε) may contribute to the decreased AA release in SLE monocytes. Finally, these data indicate the MonoMac6 cell line may indeed act as a suitable model to investigate the functional changes

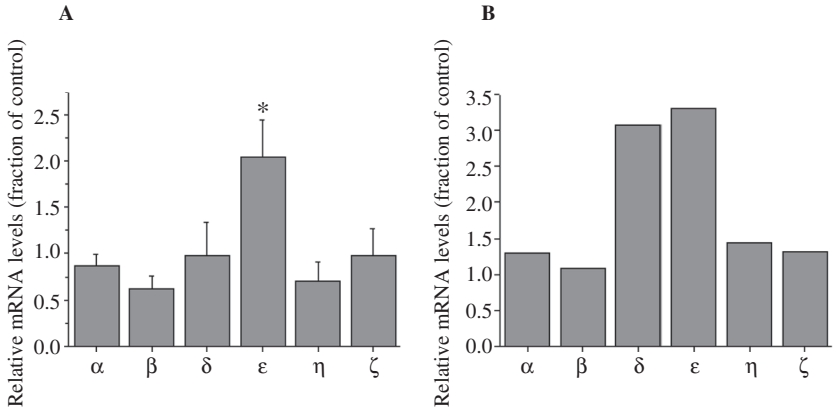

Figure 2 Effect of *in vitro* corticosteroid treatment of protein kinase C (PKC) isoform expression in control and SLE monocytes. Monocytes from three healthy volunteers (A) and one SLE patient (B) were *in vitro* treated for 2 days with vehicle (control) or 10 μM hydrocortisone, then total RNA was isolated and the levels of mRNA transcripts of PKC isoforms were determined in triplicate by real time quantitative polymerase chain reaction (Q-PCR) as described under *Patients and methods*. Absolute values were normalized to transcripts of glyceraldehyde 3-phosphate dehydrogenase (GAPDH) and the values obtained with the steroid-treated groups are shown as the fraction of the control groups. In panel A, the mean ± SEM values of three independent experiments are shown. Asterisk represents significant ($P < 0.05$) changes compared to control.

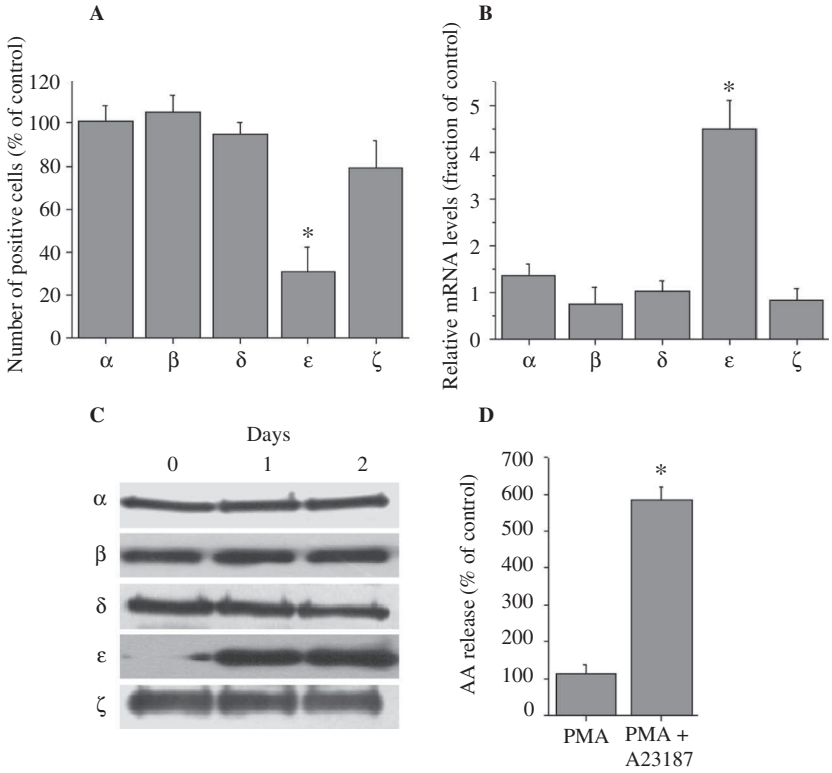

Figure 3 Protein kinase C (PKC) isoform expression, *in vitro* corticosteroid treatment and PKC-dependent arachidonic acid release in MonoMac6 cells. (A) MonoMac6 cells and healthy isolated monocytes (control) were fixed, permeabilized and PKC isoenzymes were labeled using polyclonal primary antibodies and a FITC-conjugated goat antirabbit secondary antibody. Flow cytometry analysis was then performed to determine the number of positive cells, and values obtained with the MonoMac6 cells were expressed as mean ± SEM of percentage values of control (healthy monocytes) determinations (regarded as 100%). (B) MonoMac6 cells were *in vitro* treated for 2 days with vehicle (control) or 10 μM hydrocortisone, the total RNA was isolated and the levels of mRNA transcripts of PKC isoforms were determined in triplicate by real time quantitative polymerase chain reaction (Q-PCR) as described under *Patients and methods*. Absolute values were normalized to transcripts of glyceraldehyde 3-phosphate dehydrogenase (GAPDH) and the values obtained with the steroid-treated groups are shown as the fraction of the control groups (mean ± SEM of three independent experiments). (C) MonoMac6 cells were *in vitro* treated with 10 μM hydrocortisone for the time indicated, then cell lysates were subjected to SDS-PAGE, and the expressions of PKC isoforms were determined by Western blotting as described under Patients and Methods. (D) MonoMac6 cells were treated with culturing medium (control), 100 nM PMA alone (PMA) or with 100 nM PMA and 5 μM calcium ionophore A23187 (PMA + A23187) for 4 h, and the release of arachidonic acid (AA) was determined in triplicate as described under *Patients and methods*. Data of three independent experiments were expressed as mean ± SEM of percentage values of control (medium-treated) samples (regarded as 100%). Asterisks represent significant ($P < 0.05$) changes compared to control.

related to steroid treatment and the PKC isoforms in SLE monocytes.

Discussion

In the T-cell function, the central roles of several PKC isoforms have been extensively documented. For example, PKCθ has been shown to play a crucial role in gene transcription regulation, T-cell activation, T-cell receptor ζ chain expression, and, similarly to PKCβ and δ, the regulation of production of IL-2 and its receptor [6, 13–15]. In addition, PKCβ was suggested as a key element of proper T-cell locomotion [24], whereas PKCζ was described to maintain the integrity of actin cytoskeleton and to mediate IL-induced T-cell proliferation [12]. Therefore, in the framework of these data and the central position of the PKC system in the signal transduction cascades [10], our current demonstration that levels of these PKC isoforms were significantly suppressed in T lymphocytes of SLE patients (Table 1) may, at least partly, explain the previously documented complex abnormalities of T cells in SLE [1, 4, 25].

Similarly to the T-cell findings, PKCα, β, δ, η, ε and ζ were all shown to play critical roles in various monocyte functions [16–18]. Our current presentation that, in contrast to the T-cell data, dramatic cell-specific decreases were found only in the levels of PKCε and δ with minimal suppression of PKCζ in the monocytes of SLE patients (Table 2), is the first description of monocyte-specific PKC abnormalities in this disease. Therefore, we can only assume that the decrease in the levels of PKCε and δ (and possibly of PKCζ) may also contribute to the

impaired (and chiefly PKC-dependent) monocyte functions seen in SLE [7]. Because participation of the PKC system (mostly of PKCε) is required for the induction of mitogen-activated protein kinase phosphatase−1 in lipopolysaccharide stimulated macrophages [26] and for the defense against bacterial infection [27], the decreased expressions of these enzymes may be one of the factors explaining the defect of phagocytic function in SLE.

This hypothesis about the central role of the calcium-independent PKC isoforms in monocyte functions is also supported by our earlier findings [9] and our current demonstration (Fig. 3). Namely, under calcium-free conditions, the PKC activator PMA was much less effective in inducing AA production in monocytes of SLE patients (than in healthy monocytes) and in the MonoMac6 cell line which possessed an SLE-like suppression in the level of PKCε. Finally, the marked suppression of the level of PKCε and δ isoforms described as key regulators of proliferation and differentiation of various cell types [10, 28], may also explain some of the SLE-related proliferation defects of peripheral mononuclear cells [1].

Another major finding of our work was that the suppressed levels of most (but, very importantly, not all) of the PKC isoforms could be improved by both *in vivo* (Tables 1 and 2) and *in vitro* (Fig. 2) corticosteroid treatment (similarly to the phenomenon seen in the MonoMac6 cell line, Fig. 3). It seems therefore that the decreased expression of some of the PKC isoenzymes in SLE cells is a transient state, and it can be reversed and repaired by corticosteroids. This was also supported by that recently we could carry out a preliminary study on samples of a young patient who appeared at our ambulance in the severe acute phase of SLE (SLEDAI 20) still at the first time being never treated before. The influence of steroid pulse therapy resulted in profound elevations in the levels of her impaired PKC isoenzymes (mostly of PKCε and δ), circulating IL-2, IL-4, and a slight decrease in the amount of circulating IFNγ in parallel with the improved disease status (SLEDAI 10). It should be emphasized, however, that there were also isoforms (PKCθ and, to a lesser extent, PKCζ), the expressions of which could not be modified by steroid (Tables 1 and 2) (Figs 2 and 3), arguing for different isoform-specific actions and limitations of steroid therapy on the PKC levels in SLE, and suggesting the need for further elucidation of the exact mechanism of steroid action on the PKCs.

Moreover, our findings might have further clinical implications. First, our demonstration that the presented alterations in the PKC levels are characteristic to SLE (because mononuclear cells of SS and MCTD patients possessed very similar PKC isoform patterns to the control cell populations) (Tables 1 and 2) suggests that the determination of PKC profile in polysystemic autoimmune diseases might serve as a fine tool, in addition to other biochemical and immunological markers (e.g. antibody profile, cytokine levels) [29–31], to further differentiate between such diseases. Second, our results that even a relatively short steroid therapy can strongly affect the numerous PKC-related signalling pathways of SLE cells argue for a very careful selection of appropriate patient groups for the investigations on SLE patients during their comparisons to subjects of other autoimmune diseases.

Acknowledgments

This work was supported by Hungarian Research grants: OTKA T030246, OTKA F035036, OTKA T37531, ETT 50/2000, ETT 566/2000, NKFP 88/2001, OMFB 200/2002. Tamás Bíró is a recipient of the György Békésy Postdoctoral Scholarship of the Hungarian Ministry of Education.

References

1 Tsokos GC, Wong HK, Enyedy EJ, Nambiar MP. Immune cell signaling in lupus. Curr Opin Rheumatol 2000;12:355–63.
2 Khan IU, Laxminarayana D, Kammer GM. Protein kinase A RIβ subunit deficiency in lupus T lymphocytes: bypassing a block in RIβ translation reconstitutes protein kinase A activity and augments IL-2 production. J Immunol 2001;166:7600–5.
3 Herndon TM, Juang Y-T, Solomou EE, Rothwell SW, Gourley MF, Tsokos GC. Direct transfer of p65 into T lymphocytes from systemic lupus erythematosus patients leads to increased levels of interleukin-2 promoter activity. Clin Immunol 2002;103:145–53.
4 Nambiar MP, Enyedy EJ, Warke GV *et al.* T cell signaling abnormalities in systemic lupus erythematosus are associated with increased mutations/polymorphisms and splice variants of T cell receptor ζ chain messenger RNA. Arthritis Rheum 2001;44:1336–50.
5 Enyedy EJ, Nambiar M, Liossis S-N, Dennis G, Kammer GM, Tsokos GS. Fcε receptor type I γ chain replaces the deficient T cell receptor ζ chain in T cells of patients with systemic lupus erythematosus. Arthritis Rheum 2001;44:1114–21.
6 Tsokos GC, Nambiar MP, Juang YT. Activation of the Ets transcription factor Elf-1 requires phosphorylation and glycosylation: defective expression of activated Elf-1 is involved in the decreased TCR zeta chain gene expression in patients with systemic lupus erythematosus. Ann N Y Acad Sci 2003;987:240–5.
7 Steinbach F, Henke F, Krause B, Thiele B, Burmester GR, Hiepe F. Monocytes from systemic lupus erythematosus patients are severely altered in phenotype and lineage flexibility. Ann Rheum Dis 2000;59:283–8.
8 Katsiari CG, Liossis S-N, Souliotis VL, Dimopoulos M, Manoussakis MN, Sfikakis PP. Aberrant expression of the costimulatory molecule CD40 ligand on monocytes from patients with systemic lupus erythematosus. Clin Immunol 2002;103:54–62.
9 Sipka S, Szántó S, Szûcs K *et al.* Decreased arachidonic acid release in peripheral blood monocytes of patients with systemic lupus erythematosus. J Rheumatol 2001;28:2012–7.
10 Nishizuka Y. The molecular heterogeneity of protein kinase C and its implication for cellular regulation. Nature 1988;334:661–5.
11 Goodnight JA, Mischak H, Mushinski JF. Selective involvement of protein kinase C isozymes in differentiation and neoplastic transformation. Adv Cancer Res 1994;64:159–209.
12 Gomez J, de Aragon AM, Bonay P *et al.* Physical association and functional relationship between protein kinase C zeta and the actin cytoskeleton. Eur J Immunol 1995;25:2673–8.

13 Szamel M, Appel A, Schwinzer R, Resch K. Different protein kinase C isoenzymes regulate IL-2 receptor expression or IL-2 synthesis in human lymphocytes stimulated via the TCR. J Immunol 1998;160:2207–14.
14 Bi K, Tanaka Y, Coudronniere N *et al.* Antigen-induced translocation of PKC-theta to membrane rafts is required for T cell activation. Nat Immunol 2001;2:556–63.
15 Long A, Kelleher D, Lynch S, Volkov Y. Cutting edge: protein kinase Cβ expression is critical for export of IL-2 from T cells. J Immunol 2001;167:636–40.
16 Zheng L, Zomerdijk TP, Aarnoudse C, van Furth R, Nibbering PH. Role of protein kinase C isoenzymes in Fc gamma receptor-mediated intracellular killing of Staphylococcus aureus by human monocytes. J Immunol 1995;155:776–84.
17 Kontny E, Ziokowska M, Ryzewska A, Maslinski W. Protein kinase C-dependent pathway is critical for the production of pro-inflammatory cytokines (TNF-alpha, IL-1beta, IL-6). Cytokine 1999;11:839–48.
18 Herrera-Velit P, Knutson KL, Reiner NE. Phosphatidylinositol 3-kinase-dependent activation of protein kinase Cζ in bacterial lipopolysaccharide-treated human monocytes. J Biol Chem 1997;272:16445–52.
19 Tada Y, Nagasawa K, Yamauchi Y, Tsukamoto H, Niho Y. A defect in the protein kinase C system I T cells from patients with systemic lupus erythematosus. Clin Immunol Immunopathol 1991;60:220–31.
20 Dwivedi Y, Pandey GN. Administration of dexamethasone up-regulates protein kinase C activity and the expression of the gamma and epsilon protein kinase C isozymes in the rat brain. J Neurochem 1999;72:380–7.
21 Kajita K, Ishizuka T, Miura A *et al.* Glucocorticoid-induced insulin resistance associates with activation of protein kinase C isoforms. Cell Signal 2001;13:169–75.
22 Hochberg M. Updating the American College of Rheumatology revised criteria for the classification of systemic lupus erythematosus. Arthitis Rheum 1997;40:1725–34.
23 Boczán J, Boros S, Mechler F, Kovács L, Bíró T. Differential expressions of protein kinase C isozymes during proliferation and differentiation of human skeletal muscle cells *in vitro*. Acta Neuropathol 2000;99:96–104.
24 Volkov Y, Long A, McGrath S, Ni Eidhin D, Kelleher D. Crucial importance of PKC-β(I) in LFA-I-mediated locomotion of activated T cells. Nature Immunol 2001;2:508–14.
25 Kammer GM, Perl A, Richardson BC, Tsokos GC. Abnormal T cell signal transduction in systemic lupus erythematosus. Arthritis Rheum 2002;46:1139–54.
26 Vallador AF, Xaus J, Comalada M, Soler C, Celada A. Protein kinase Cε is required for the induction of mitogen-activated protein kinase phosphatase-1 in lipopolysaccharide-stimulated macrophages. J Immunol 2000;164:29–37.
27 Castrillo A, Pennington DJ, Otto F, Parker PJ, Owen MJ, Bosca L. Protein kinase Cε is required for macrophage activation and defense against bacterial infection. J Exp Med 2001;194:1231–42.
28 Miyamoto A, Nakayama K, Imaki H *et al.* Increased proliferation of B cells and auto-immunity in mice lacking protein kinase Cdelta. Nature 2002;416:965–9.
29 Smolen JS, Steiner G. Mixed connective tissue disease. To be or not to be? Arthritis Rheum 1998;41:768–77.
30 Sugimoto K, Morimoto S, Kaneko H *et al.* Decreased IL-4 producing CD4+ T cells in patients with active systemic lupus erythematosus – relation to IL-12R expression. Autoimmunity 2002;35:381–7.
31 Bodolay E, Aleksza M, Antal-Szalmás P *et al.* Serum cytokine levels and type 1 and type 2 intracellular T cell cytokine profiles in mixed connective tissue disease. J Rheumatol 2002;29:2136–42.

XXI.

Frontiers in pruritus research: scratching the brain for more effective itch therapy

Ralf Paus,[1] Martin Schmelz,[2] Tamás Bíró,[3] and Martin Steinhoff[4]

[1]Department of Dermatology and Allergy, University of Lübeck, Lubeck, Germany. [2]Department of Anesthesiology and Critical Care Medicine, Faculty of Clinical Medicine Mannheim, University of Heidelberg, Mannheim, Germany. [3]Department of Physiology, University of Debrecen, Medical and Health Science Center, Research Center for Molecular Medicine, Debrecen, Hungary. [4]Department of Dermatology, IZKF Münster, Ludwig Boltzmann-Institute for Immunobiology of the Skin, University Hospital Münster, Munster, Germany.

This Review highlights selected frontiers in pruritus research and focuses on recently attained insights into the neurophysiological, neuroimmunological, and neuroendocrine mechanisms underlying skin-derived itch (pruritogenic pruritus), which may affect future antipruritic strategies. Special attention is paid to newly identified itch-specific neuronal pathways in the spinothalamic tract that are distinct from pain pathways and to CNS regions that process peripheral pruritogenic stimuli. In addition, the relation between itch and pain is discussed, with emphasis on how the intimate contacts between these closely related yet distinct sensory phenomena may be exploited therapeutically. Furthermore, newly identified or unduly neglected intracutaneous itch mediators (e.g., endovanilloids, proteases, cannabinoids, opioids, neurotrophins, and cytokines) and relevant receptors (e.g., vanilloid receptor channels and proteinase-activated, cannabinoid, opioid, cytokine, and new histamine receptors) are discussed. In summarizing promising new avenues for managing itch more effectively, we advocate therapeutic approaches that strive for the combination of peripherally active antiinflammatory agents with drugs that counteract chronic central itch sensitization.

The study of pruritus in a nutshell

Itching (pruritus) is perhaps the most common symptom associated with numerous skin diseases and can be a lead symptom of extracutaneous disease (e.g., malignancy, infection, and metabolic disorders) (1, S1). However, despite approximately a century of pruritus research (2, S2, S3), there is no generally accepted therapy for the treatment of itch, and many mysteries, misconceptions, and controversies still haunt this rather neglected, yet clinically important and scientifically fascinating, niche in the life sciences (3, 4, 5).

It is the brain that itches, not the skin

Pruritus causes the desire to scratch the skin and is experienced as a sensation arising in the skin. However, like all other skin sensations, itch, strictly speaking, is an extracutaneous event — a product of CNS activities. The intense itch we feel after an insect bite, in a patch of atopic eczema, during an episode of food-induced urticaria, or in association with diabetes, uremia, or scabies mite infection (S1) represents a neuronal projection of a centrally formed sensation into defined regions of the integument (localized pruritus) or into large territories of our body surface (generalized pruritus).

Interestingly, our individual reception of and emotional response to itch strongly depends on its exact quality: while a tickling sensation usually is experienced as pleasurable, persistent itch is an annoying or even torturous sensation (S4). While one is tempted to interpret this as indicating a distinct molecular and/or structural basis of these different itch qualities, it has proven excruciatingly difficult to identify their molecular, structural, and neurophysiological differences (ref. 1; see below).

As pruritus can arise from localized or systemic, peripheral or central stimuli, it is useful to differentiate between its different types. One recent classification system suggests distinctions be made among neurogenic (arising from neurophysiological dysfunction, e.g., due to cholestasis or psychotropic medication), neuropathic (due to a primary neurological disorder), psychiatric (e.g., parasitophobia), and pruritogenic pruritus (arising from skin diseases) (3, 6). This Review discusses only the latter, most frequent type of pruritus, which requires the involvement and activity of cutaneous sensory neurons that transmit the "itchy" signals via dorsal root ganglia and the spinal cord to the CNS.

Current concepts of itch pathways underlying pruritogenic pruritus and of CNS regions involved in itch processing are summarized in Figure 1. More plainly speaking, when one senses the difficult-to-control desire to fight itching by self-inflicted painful stimuli, the impression that one's *skin* itches is nothing but a sensory illusion created by the brain. Thus the CNS-controlled, itch-alleviating motoric activity that unfolds in response to pruritus directly "talks back" to our CNS, almost as if we were scratching the brain itself.

Scratching highlights the close relation of pain and itch

Both pain and itch can be reduced by soft rubbing, which activates fast-conducting, low-threshold nerve fibers (7). However, the most characteristic response to itching is the scratch reflex: a more or less voluntary, often subconscious motoric activity to counteract the itch by slightly painful stimuli. This itch reduction is based on a spinal antagonism between pain- and itch-processing neurons (8). This illustrates a therapeutically exploitable, key concept in contemporary pruritus research: itch appears to be under tonic inhibitory control of pain-related signals (1, 4, 5, 8, 9). Indeed, itch and pain share the use of many neurophysiological tools and processing centers and induce similar autonomous skin reactions. Also, chronic pain and central sensitization to itch appear to be neurophysiologically closely related phenomena (4).

Nonstandard abbreviations used: ACh, acetylcholine; CB, cannabinoid receptor; CGRP, calcitonin gene–related peptide; NGF, nerve growth factor; PAR, proteinase-activated receptor; SP, substance P; TRP, transient receptor potential; TRPV, TRP vanilloid-type.

Conflict of interest: The authors have declared that no conflict of interest exists.

Citation for this article: *J. Clin. Invest.* **116**:1174–1185 (2006). doi:10.1172/JCI28553.

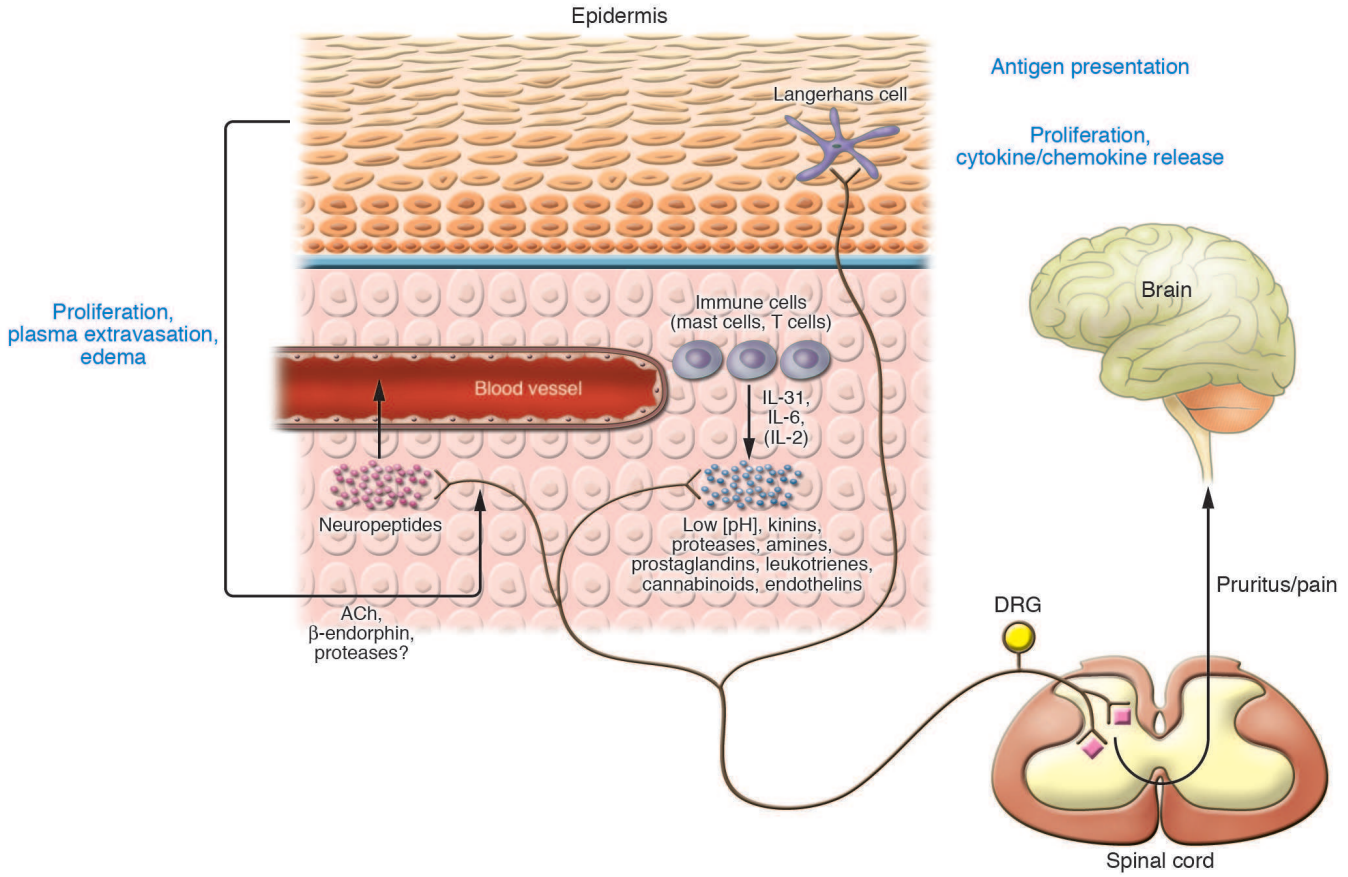

Figure 1
Table 2 and neurophysiological pathways activated during pruritus (pruritogenic itch). Exogenous or endogenous mediators stimulate specific subtypes of peripheral nerve endings of primary afferent neurons (pruriceptors). High-affinity receptors for pruritogenic mediators transmit the stimulus via intracellular signaling from the periphery to the dorsal root ganglia (DRG) and the spinal cord. Within the spinal cord, itch signals can be modulated (see *It is the brain that itches, not the skin*). From lamina I, a specific area within the dorsal horn of the spinal cord, the signal is transmitted to the CNS after crossing to the contralateral side (see Figure 3). Activation of specific areas in the CNS results in the perception of itch, leading to discomfort and a scratch response. Additionally, the associated peripheral axon reflex may lead to the release of mast cell–stimulating neuropeptides (e.g., SP), thereby amplifying pruritus via release of histamine, tryptase, and TNF-α, for example (see Table 1). This figure does not consider the interaction between pain and itch fibers on the spinal cord level (see *The enigmatic neurophysiology of itch is becoming increasingly understood*). Figure modified with permission from *The Journal of Investigative Dermatology* (5).

Itch and pain serve different purposes

Yet itch is clearly distinct from pain with respect to the subjective sensation, the inducing stimuli, and the reflex patterns. In contrast to pain-related withdrawal reflexes, itching stimuli provoke the characteristic scratching reflex. This close connection suggests that the neuronal apparatus for itch has developed as a nocifensive system for removal of irritating objects and agents assaulting the skin and thereby the body's integrity (e.g., parasites, insects, sharp objects, irritants, and allergens). While the withdrawal reflex is an adequate response to external noxious stimuli, scratching makes good sense for noxious agents that have successfully passed the epidermal barrier and have already invaded the skin. Here, withdrawal would be useless. Instead, localizing the injured site by scratching and subjecting it to closer examination in order to detect any exogenous danger is required. Thus having skin capable of inducing the symptom of itch may have afforded a substantial selective advantage during evolution.

The sensation of itch and nociception are distinct entities

Results from early psychophysical studies on itch and pain "spots" (S5) invited the interpretation that itch is a kind of low-intensity pain. However, we now know that the sensation of itch and nociception cannot be equated with each other. In fact, the once-popular theories that itch is based on a specific pattern of action potentials running through pain pathways or that itch results from the combination of other primary sensory signals have now fallen out of favor (3, 10). Likewise the confirmation of the long-denied existence of central itch-specific neuronal pathways in the human and feline systems supports the concept that the sensation of itch and nociception represent distinct sensory systems (9, 11). Nevertheless, it remains perhaps the most central, and as yet unmet, challenge of neurophysiological pruritus research to fully unravel the biological commonalities *and* differences between itch and pain. In any case, the systematic, comparative exploration of the mechanisms underlying pain and itch sensations has already proven to be a constant source of innovation and stimulation for investigators who study pruritus.

Table 1
"The itching army" — selected pruritogens, their sources, and functions

Pruritogenic stimuli	Receptors	Sources, receptors expressed by	Comments	Selected references
ACh	Nicotinergic (nAChR) and muscarinergic (mAChR) ACh receptors	Autonomic cholinergic nerves, keratinocytes, lymphocytes, melanocytes, dermal fibroblasts, ECs	Mediates itch in AD patients. mAChR3 is probably involved in itch.	(35, 111, S19)
CGRP	CGRP receptors	Sensory nerve fibers	Expression on central terminals; sensitization of nerve endings. Increased pain transmission; prolongation of itch latency following SP injection (inhibitory effect on itching). Involved in itchy skin diseases.	(59)
CRH and POMC	CRH-R1 and -R2	For CRH-R1, keratinocytes, mast cells; for CRH-R2, BM mast cells	Release of histamine, cytokines, TNF-α, VEGF from mast cells. CRH-like immunoreactivity on sensory nerves (rat).	(72, 112)
Cytokines	Cytokine receptors (e.g., IL-1, IL-31)	Leukocytes, keratinocytes, ECs, nerves	T cells release IL-31 during inflammation and activate monocytes and keratinocytes via the IL-31 receptor (IL-31R). IL-31R is upregulated in AD and prurigo.	(10, 113, S20)
Endocannabinoids	CBs (CB1, CB2)	Nerves, immune cells, keratinocytes, hair follicles	Antipruritic in the periphery.	(99, 100)
ETs	ET receptors (ET_A, ET_B)	Endothelium, mast cells	Burning itch; degraded by chymase via ET_A receptor activation.	(S21, S22)
Endovanilloids[A]	Activation of TRPV1. Sensitization of TRPV1 via activation of specific receptors.	TRPV1 expressed on sensory neurons, mast cells, epidermal and hair follicle keratinocytes, Langerhans cells, smooth muscle, and sebocytes	Short-term TRPV1 activation: pain and itch induction, depletes neuropeptides from sensory neurons. Long-term antipruritic effect of TRPV1 agonists (e.g., capsaicin): suspend interplay between sensory neurons and mast cells. Affects epidermal and hair follicle proliferation, differentiation, apoptosis, and cytokine release. Increased expression in epidermal keratinocytes of prurigo nodularis patients.	(3, 4, 83, 84, 87, 90, 92)
Histamine	Histamine receptors (H1R–H4R)	Sensory nerve fibers	In humans, histamine induces itch by stimulating specific sensory fibers, whereas H1 (and H2, less so) antagonists reduce itch in numerous clinical trials. In mice, H3 antagonists induce scratching behavior, whereas H1 and H4 antagonists effectively suppress pruritus.	(1, 11, 27, S23, S24)
Kallikreins, proteases	Partly by PARs, tryptic enzymes	Keratinocytes, ECs, mast cells, platelets	Massive itch behavior in mice overexpressing epidermal kallikrein-7. Potential role of other kallikreins. Chymase degrades pruritic and antipruritic peptides. Tryptase induces inflammation and itch by a neurogenic mechanism via PAR_2. Microbial proteases may induce itch and inflammation via PAR_2.	(60, 64, 114, S25, S26)
Kinins	Bradykinin receptors (B1R, B2R)	ECs, immunocytes	Bradykinin induces pain rather than pruritus. B2R antagonists reduce itch.	(S27)
Leukotriene B4	Leukotriene receptors	Sensory nerve fibers, keratinocytes	Leukotriene B4 induces itch and is also involved in the SP- and nociceptin-mediated induction of itch.	(S28, S29)
NKA and SP	Tachykinin (NK) receptors (NKRs)	Sensory nerve fibers	NKA: Upregulation of keratinocyte NGF expression. SP: low (physiologically relevant) concentrations: priming of mast cells; release of TNF-α, histamine, leukotriene B4, and prostaglandins from mast cells (agents involved in pruritus and burning).	(115, S30–S33)
NGF, BDNF, NTs	Specific receptors: TrkA (NGF), TrkB (NT-4, BDNF), TrkC (NT-3)	Keratinocytes, mast cells, fibroblasts, eosinophils	NGF levels enhanced in AD; induces tryptase release from mast cells. Inducible by histamine. TrkA enhanced in karatinocytes during inflammation. NT-4 enhanced in AD, induces sprouting of sensory nerves. BDNF increases eosinophil chemotaxis levels in AD, inhibits apoptosis. NTs sensitize receptive nerve endings and upregulate neuronal neuropeptides and TRPV1.	(25, S34–S36)

Opioids	μ-, κ-, δ-Opioid receptors (partly receptor-independent cell activation)	Nerves, keratinocytes	Antipruritic effect of μ-opioid antagonists (central effect) and κ-opioid agonists (spinal cord level). Opioid agonists do not provoke itch upon injection or intradermal application. μ-Opioid receptor upregulation in AD.	(9, 55, 116, 117, S37)
PACAP and VIP	VPAC receptors	Autonomic and sensory nerve fibers, lymphocytes, dermal ECs, Merkel cells	PACAP: involved in flush, vasodilatation, pain, neurodegeneration; pruritus(?); induces release of histamine from mast cells. VIP: histamine release from mast cells, allodynia (no allodynia in AD) intensifies ACh-induced itch in AD patients.	(59, S38, S39)
Prostaglandins	Prostanoid (P) receptors	Sensory nerve fibers, keratinocytes	Prostaglandin E2 induces itch in humans but not in mice. Prostaglandin D2 reduces IgE-mediated scratching in mice.	(118, S28, S40)

Stimuli are listed alphabetically. [A]Endovanilloids include heat, acidosis, eicosanoids, histamine, bradykinin, extracellular ATP, prostaglandins, and various neutrophins. AD, atopic dermatitis; BDNF, brain-derived neurotrophic factor; CRH, corticotropin-releasing hormone; ET, endothelin; NK, neurokinin; NT, neurotrophin; PACAP, pituitary adenylate cyclase–activating polypeptide; POMC, pro-opiomelanocortin; VIP, vasoactive intestinal polypeptide; VPAC, VIP/PACAP receptor.

There are many more peripheral itch–inducing stimuli than histamine

A bewilderingly wide range of peripheral itch–inducing stimuli generated within or administered to the skin can trigger pruritus. The key message here is that the chorus of itch-inducing agents (Table 1) contains many more protagonists than the usual suspect, histamine. This includes several that are not yet widely appreciated as pruritic compounds or itch-relevant receptors (e.g., proteases, leukotrienes, ion channels, cytokines). The role of histamine, in contrast, is overestimated: small doses of histamine that fail to produce itch are still sufficient to produce edema and erythema upon intracutaneous injection, and nonsedative antagonists of the histamine receptors H1 and/or H2 have often been proven to be of low or no efficacy as antipruritic drugs (refs. 12–15; although others claim efficacy, refs. 16, 17), while other pruritogens (e.g., pH changes, opioids, proteases, cytokines, acetylcholine [ACh], and neurotrophins in atopic dermatitis patients; see Figure 1 and Table 1) are often more powerful itch inducers than histamine.

In addition, the dominant role of intracutaneous inflammation in itch pathogenesis, and the vicious cycles of neurogenic inflammation (18, 19) upregulating and perpetuating chronic itch, must be taken into account (see *Itch is modulated by painful and nonpainful stimuli: role of opioid receptors*). Also, the skin excels in extensive innervation of nonneuronal cells (e.g., keratinocytes, Merkel cells, and Langerhans cells in the epidermis and mast cells in the dermis), adding to the complexity of the signaling loops that have to be considered when investigating the pathogenesis of itch (4). Neurotrophins such as nerve growth factor (NGF) — copiously produced by, for example, the skin epithelium in order to direct and control sensory skin innervation (20), which is thought to be involved in the pathogenesis of prototypic pruritic dermatoses such as prurigo nodularis and atopic dermatitis (21–23) and whose therapeutic administration is pruritogenic (24) — nicely exemplify the complexity of itch pathogenesis and the cascades of itch-promoting events that render pruritus such a difficult-to-manage clinical problem. Upregulation of intracutaneous neurotrophin production and/or the expression of cognate receptors by inflammatory stimuli (e.g., in the context of atopic dermatitis) increases sensory innervation, lowers the itch threshold, upregulates the expression and/or sensitization of other receptor systems involved in itch pathogenesis (e.g., vanilloid receptors), upregulates the production of other pruritogenic agents (e.g., substance P [SP]), and perpetuates inflammation (e.g., by inducing mast cell degranulation and by forcing the affected individual to engage in a crescendo of scratching activity that further promotes skin inflammation; refs. 4, 19, 20, 25, 26).

Recently, however, additional histamine receptors have been discovered, and at least one of them — H4R — operates as an "itch receptor" in mice (27). This finding sheds new light on an old itch suspect and may explain why H1R antagonists are not efficient in certain pruritic skin diseases. This example also nicely illustrates why the study of pruritus has proven to be a field of endless fascination and discovery for clinicians, psychologists, pharmacologists, neurobiologists, endocrinologists, and neuroimmunologists alike.

General limitations of an effective antipruritic therapy

Evidently we need to engage in a lot of scratching our own brains until we can offer our itching patients more efficient, more individually tailored, safer, and better-tolerated itch management. Considerable progress has been achieved in the development of animal models for itch by changing from acute injection models to a disease-related approach (e.g., ref. 28). Nevertheless, specific animal models for many clinical itch conditions are still missing. Also the objective, reproducible quantification of itch is a much more tricky and treacherous art than one may suspect. Simple psychophysics using visual analog scales is still the gold standard, but it may best be combined with objective behavioral measurements using digital accelerometers or piezoelectronic devices (29). Thus far there are no sound indications that itch-specific genes exist. Finally, we face the lack of well-tolerated, easily administered, nonsedative compounds that selectively target dominant CNS "itch centers" — which probably do not exist anyway (see *The enigmatic neurophysiology of itch is becoming increasingly understood*).

Irrespective of these formidable limitations, it is rewarding, exciting, and important to scout for therapeutically promising frontiers in pruritus research — defining and redefining along the way the many intriguing open questions that just make you itch for more satisfactory answers.

The enigmatic neurophysiology of itch is becoming increasingly understood

The neurophysiological basis for the itch sensation was unclear for decades. Several competing theories coexisted until itch-selective neurons were found in humans, which explained the histamine-induced itch sensation (11). Slowly conducting C-fibers that trans-

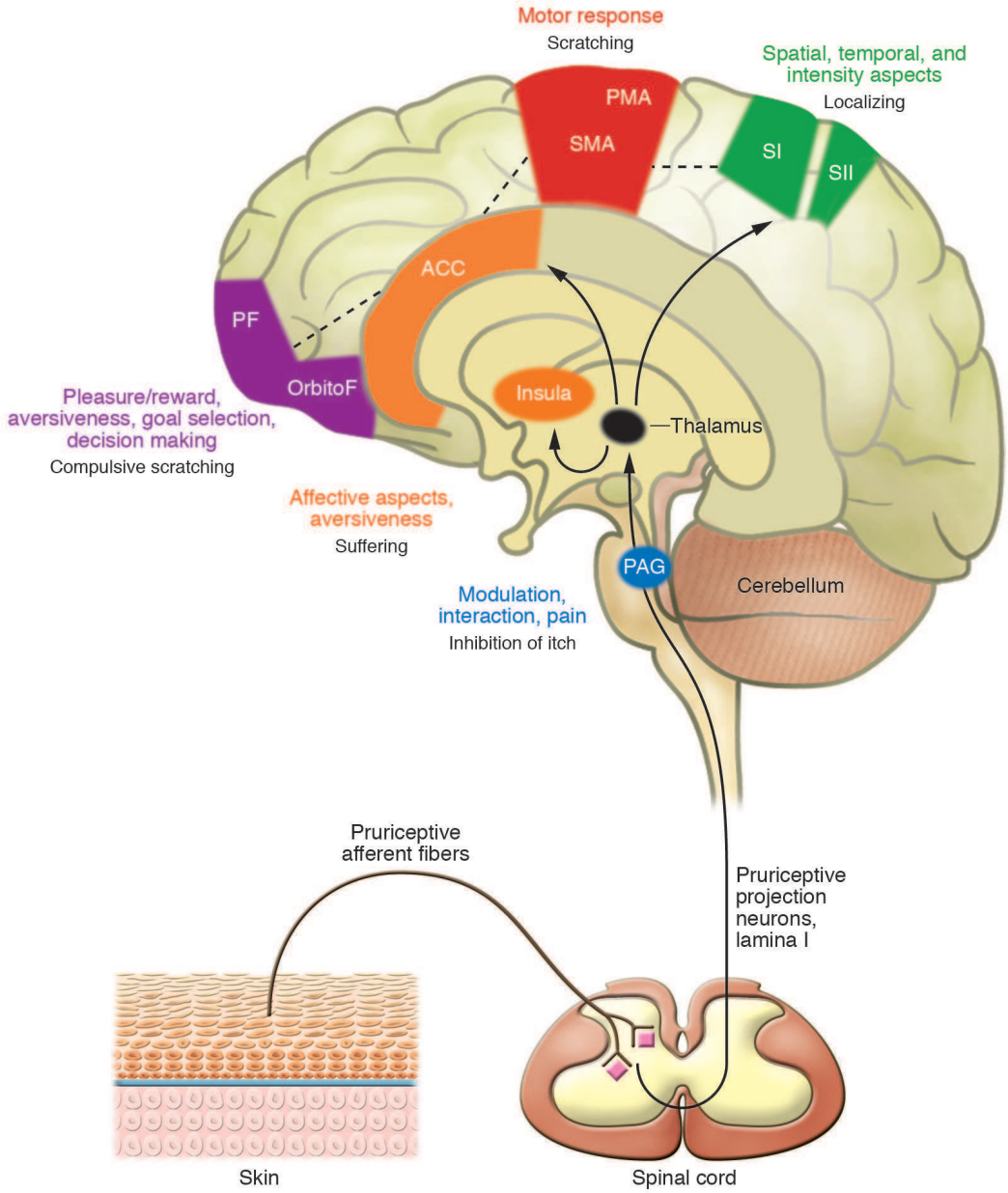

Figure 2
Central processing of pruritus. Pruriceptive primary afferent nerve fibers from the skin activate spinal neurons in lamina I of the dorsal horn, which project to the thalamus. Direct excitatory connections from the thalamus include anterior cingulate cortex (ACC), insular cortex (Insula), and primary and secondary somatosensory cortices (SI, SII). The putative function of brain areas activated in central imaging studies of itch are summarized. SMA, supplementary motor area; PMA, premotor area; PF, prefrontal cortex; OrbitoF, orbitofrontal cortex; PAG, periaqueductal gray.

duce itch signals have been discovered among the group of mechanoinsensitive C-afferents in healthy subjects and itch patients (30), suggesting a specific pathway for itch. In contrast, the most common type of C-fibers, mechano-heat–sensitive polymodal nociceptors, do not show prolonged activation by histamine and are related to pain processing (31, 32). The histamine-sensitive itch fibers, also known as pruriceptors, are characterized by a particularly low conduction velocity, large innervation territories, mechanical unresponsiveness, high transcutaneous electrical thresholds, and generation of an axon reflex erythema (11, 32–35). However, this histamine-sensitive fiber class cannot account for all aspects of pruritus, particularly the mechanically evoked classification. Thus other classes of primary afferents must be involved in the histamine-independent generation of pruritus (36). This diversity of primary afferent "itch fibers" would nicely fit to the different submodalities of pruritus ("itch quality") observed in patients (37, 38, S6).

The concept that dedicated pruritogenic neurons exist has been extended by recordings in the cat spinal cord. These results have demonstrated the existence of a specialized class of mechanically insensitive, histamine-sensitive dorsal horn neurons projecting to the thalamus (9). Thus the combination of dedicated peripheral and central neurons with a unique response pattern to pruritogenic

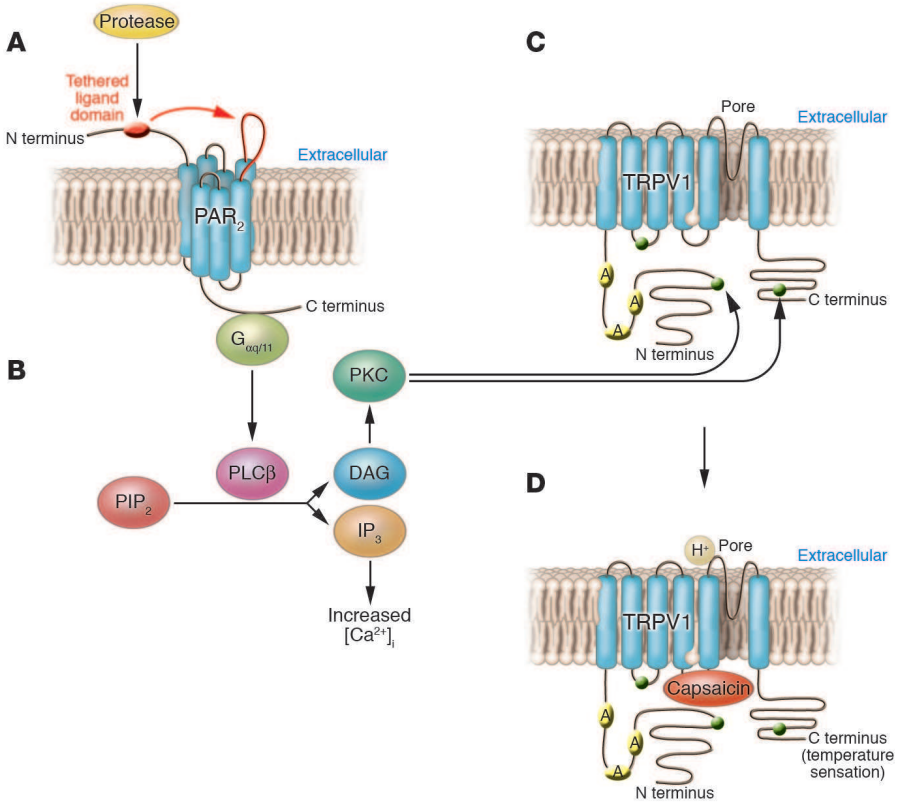

Figure 3
Pruritogenic receptors interact synergistically, thereby amplifying itch or pain. (**A**) Activation of PAR_2 leads to binding of G proteins ($G_{\alpha q/11}$), followed by (**B**) stimulation of the intracellular PKC pathway and mobilization of intracellular [Ca^{2+}] via phopholipase Cβ (PLCβ), diacylglycerol (DAG), and inositol triphosphate (IP_3). PIP_2, phosphatidylinositol 4,5-biphosphate. This results in (**C**) sensitization of TRPV1 by phosphorylation of the intracellular C terminus (heterologous sensitization). Sensitization of TRPV1 leads to (**D**) a lowered threshold for capsaicin binding or temperature, i.e., stimulation of TRPV1. This mechanism affects release of neuropeptides (activation of mast cell degranulation) from nerve terminals of sensory nerves as well as stimulation of activation potentials (transmission of pain and pruritus to the spinal cord).

mediators and anatomically distinct projections to the thalamus provides the basis for a specialized neuronal itch pathway.

Interestingly, these projection neurons do not exhibit spontaneous activity as the pain-processing projection neurons do. This lack of spontaneous activity may be due to active inhibition exerted by pain-processing neurons (8). Suppressing this inhibition might therefore provoke itch by a pure spinal mechanism — without any activation of primary afferent neurons from the skin (as seen in neuropathic and neurogenic pruritus). Thus one important challenge for more effective itch management will be to develop drugs that selectively upregulate the spinal inhibition of itch signals arriving from the skin.

The itch-selective spinal neurons form a distinct pathway projecting from lamina I of the spinal cord to the ventrocaudal part of the nucleus medialis, which projects to the anterior cingulate and dorsal insular cortex (9, 39) (Figure 2). The supraspinal processing of itch and its corresponding scratch response in humans have recently been investigated by functional PET (fPET) and functional MRI (fMRI). Here induction of itch by histamine application *coactivates* the anterior cingulate and insular cortex, premotor and supplementary motor areas, cerebellum, primary somatosensory cortex, and thalamus (40–42). As done earlier for pain sensation, particular aspects of the itch sensation have been correlated with the activation of certain brain areas: spatial and temporal aspects may be processed in the primary somatosensory cortex, planning of the scratch response in the premotor and supplementary motor cortices, and affective and motivational aspects in the anterior cingulate (38, 43) and insular cortex (Figure 2). All these brain areas are also involved in pain processing (44). Thus differences between pain and itch processing likely do not result from activation of distinct brain centers, but reflect a different activation pattern of basically identical centers. For example, itch processing may be characterized by weaker activation of primary and secondary somatosensory cortices but relatively stronger activation of ipsilateral motor areas and anterior cingulate compared with pain sensation.

When the modulation of itch by painful cold stimuli was examined by fPET, the periaqueductal gray matter was activated only when painful and itching stimuli were applied simultaneously (42). This activation was combined with reduced activity in the anterior cingulate, dorsolateral prefrontal cortex, and parietal cortex. This suggests that the periaqueductal gray, which is known for its role in endogenous pain inhibition, might also be involved in the central inhibition of itch by pain (Figure 2).

Studies with fMRI have largely confirmed activations that had been revealed by earlier PET results. However, they also found strong activation of prefrontal and orbitofrontal cortices (45, S7). These frontal brain areas are involved in reward systems and decision making but also in hedonic experiences (46); their activation might contribute to the compulsive component and thereby further increase the multidimensionality of the itch sensation.

Given the complex activation pattern and the broad overlap of pain processing, a clear anatomical target for centrally acting antipruritic therapy is lacking. Also, identification of pharmacological targets will require more specific imaging techniques, such as ligand-PET. This already has been successfully used to localize receptor density and to verify genetic differences in occupancy of opioid receptors (47). Though this has increased our understanding of how acute experimental itch is processed, central imaging has not yet identified critical anatomic or pharmacologic targets in clinical pruritus. Therefore, imaging studies in itch patients are urgently required, although as one can learn from the pain field, such studies are much more complex and difficult to interpret than the simplistic experimental setting using itch models in healthy volunteers.

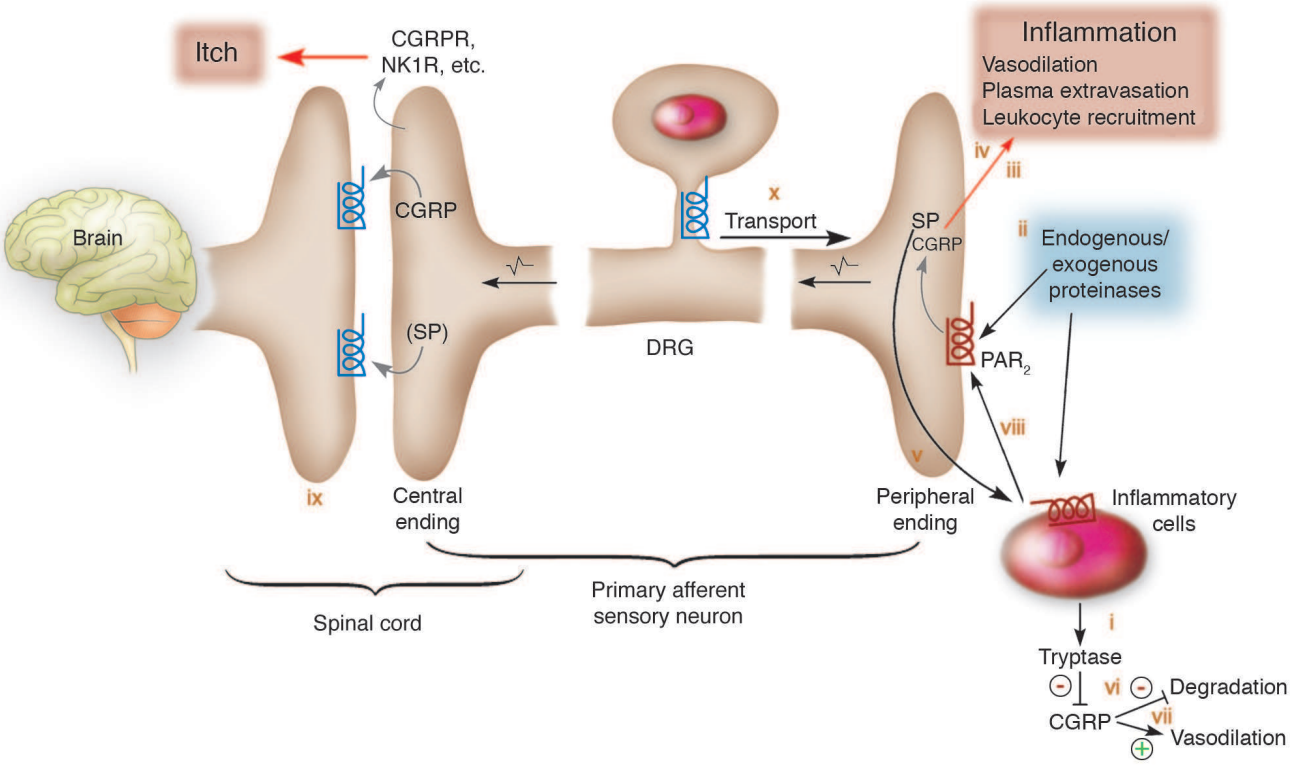

Figure 4
PARs play a key role in pruritus during neurogenic inflammation. (i) Tryptase released from degranulated mast cells activates PAR_2 at the plasma membrane of sensory nerve endings. (ii) Activation of PAR_2 by tryptase, trypsins, kallikreins, or probably exogenous proteinases (bacteria, house dust mite) stimulates the release of calcitonin gene–related peptide (CGRP) and tachykinins, e.g., SP, from sensory nerve endings. (iii) CGRP interacts with the $CGRP_1$ receptor to induce arteriolar dilation and hyperaemia. (iv) SP interacts with the neurokinin-1 receptor (NK1R) on endothelial cells of postcapillary venules to cause gap formation and plasma extravasation. Hyperaemia and plasma extravasation cause edema during inflammation. (v) SP may stimulate degranulation of mast cells, providing a positive-feedback mechanism. (vi) Tryptase degrades CGRP and terminates its effects. (vii) CGRP inhibits SP degradation by neutral endopeptidase and also enhances SP release, thereby amplifying its effects. (viii) Mediators from mast cells and other inflammatory cells stimulate the release of vasoactive peptides from sensory nerves and also sensitize nerves. (ix) At the spinal cord level, PAR_2-induced intracellular Ca^{2+} mobilization leads to release of CGRP (and SP) from central nerve endings, thereby activating CGRP receptor (CGRPR) and NK1R to transit itch responses to the central nervous system. (x) During inflammation, PAR_2 may be peripherally transported, thereby increasing receptor density and stimulation. Figure modified with permission from *Nature Medicine* (64, 125).

Itch is modulated by painful and nonpainful stimuli: role of opioid receptors

It is common experience that the itch sensation can be reduced by scratching. The inhibition of itch by painful stimuli has been experimentally demonstrated by use of various painful thermal, mechanical, and chemical stimuli (S8). Painful electrical stimulation reduced histamine-induced itch for hours in an area spanning 10 centimeters beyond the site of stimulus, suggesting a central mode of action (48). Recent results suggest that noxious heat stimuli and scratching produce a stronger itch inhibition than do noxious cold stimuli (49).

On the contrary, analgesia may reduce the inhibition of itch by pain, thus enhancing pruritus (50). This phenomenon is particularly relevant to spinally administered μ-opioid receptor agonists, which induce segmental analgesia often combined with segmental pruritus (31). Conversely, μ-opioid antagonists have antipruritic effects in experimentally induced itch (S9) and also in patients with cholestatic itch. Remarkably, in some cholestatic patients treated with naloxone, the reduction of itch is accompanied by the induction of pain (51) and withdrawal-like reactions (52). This suggests an upregulation of endogenous opioids in these patients.

In contrast to strong analgesic and pruritic spinal effects of μ-opioids, an inhibition of both pain and itch — albeit weaker — is observed in the periphery (46, 53, 54). The role of nonneuronal opioid receptors and the secondary release of endogenous opioids (see *Additional TRP channels are interesting targets in pruritus management*) for the modulation of pruritus is as yet unclear. For example, it has been speculated that internalization of the μ-opiate receptor in the epidermis of patients with atopic dermatitis may lead to the availability of free opioid ligands, which then induce chronic pruritogenic signals via altered unmyelinated nerve C-fibers (4, 55).

Chronic skin inflammation causes peripheral sensitization to itch

It has been known for decades that acute or chronic skin inflammation lowers the threshold for pruritic stimuli and thus causes peripheral itch sensitization (56, S2). The complex mechanisms underlying these phenomena (wheal, flare, edema) are becoming better understood. During inflammation, several cells release mediators that potentially bind to and activate high-affinity receptors on sensory neurons. Upon stimulation, mast cells release his-

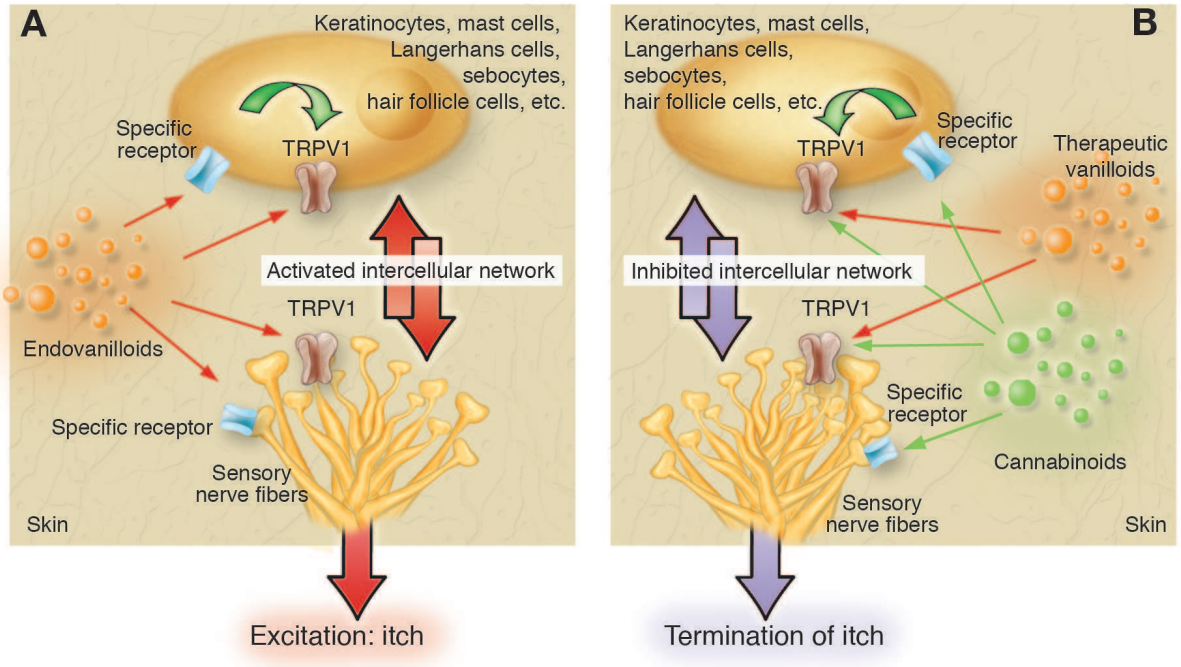

Figure 5
The putative role of TRPV1 signaling in the pathogenesis and therapy of itch. (**A**) Pruritogenic endovanilloids either directly or indirectly (via their own cognate receptors) activate and/or sensitize TRPV1 expressed on sensory neurons and nonneuronal cell types, which augments the bidirectional intercellular network to initiate itch. (**B**) Repeatedly applied topical vanilloids (such as capsaicin) may desensitize neuronal and nonneuronal TRPV1–mediated signaling so as to counteract the pruritogenic intercellular network and hence terminate itch. Note that certain cannabinoids (via acting either on specific CB receptors or directly on TRPV1) may augment the efficacy of vanilloid therapy.

tamine, tryptase, TNF-α, prostaglandins, and/or leukotrienes; keratinocytes release ACh, proteases, or β-endorphin; endothelial cells release kinins and protease-IV; and T cells release IL-2, IL-6, or IL-31, among others (Figure 1 and Table 1) (18, 19).

Peripheral sensory nerve endings express an armada of receptors that are involved in both inflammation and itch (Figure 1 and Table 1). Thus prolonged stimulation of itch receptors in the inflammatory environment may cause peripheral sensitization to itch. So far, less is known about the communication among the different neuronal receptors. For example, neuronal receptors such as transient receptor potential (TRP) vanilloid-type 1 (TRPV1) and proteinase-activated receptor 2 (PAR_2) may potentiate pain or pruritus by transactivation (Figure 3) (refs. 57, 58; reviewed in refs. 59–63, S10). Thus one wonders whether inhibitors of TRPV1 and/or PAR_2 (see *Proteinase-activated receptors play a key role in pruritus during neurogenic inflammation*) alleviate inflammation-associated (pruritogenic) itch.

Proteinase-activated receptors play a key role in pruritus during neurogenic inflammation

In fact, we have learned that proteases are more than just "scissors of destruction"; rather, they are representative of a group of mediators that communicate with nerves, thereby modulating inflammation, pain, *and* pruritus (64, 65). Similar to histamine or prostaglandins, certain proteases act as signaling molecules by activating PARs (66, S11). Proteases from plants (e.g., pollen), mites (e.g., house dust mite), or inflammatory cells (e.g., mast cell tryptase) can induce pruritus and/or inflammation (Figure 4; reviewed in ref. 60). PAR_2, which can be activated by tryptase during inflammation or hypersensitivity, mediates neurogenic inflammation reflected by edema, plasma extravasation, and recruitment of leukocytes (64, 67). Interestingly, tryptase and PAR_2 are upregulated on sensory nerves during atopic dermatitis, and PAR_2 agonists induce pruritus in these patients, suggesting that PAR_2 — similar to histamine receptors — is a receptor for "itchy" proteases (68). It is unknown whether PAR_1 and PAR_4 are also involved in the itch pathway and under which circumstances proteases may induce pain, inflammation, or pruritus. From first indications, it seems to be a matter of protease concentration (69). Since PAR_2 is not only expressed in peripheral neurons but also in the spinal cord and brain, protease inhibitors and antagonists of PAR_2 may be important tools for the treatment of itch with or without acute or chronic inflammation.

Chronic skin inflammation may cause central itch sensitization

Recent findings shed new light on the role of chronic inflammatory stimuli in pruritus with special regard to central sensitization of itch fibers. Activity in pruriceptors not only provokes itch but additionally facilitates spinal itch processing, resulting in touch- or brush-evoked pruritus around an itching site (itchy skin) (S2, S12). It requires ongoing activity in primary afferents and is most probably elicited by low-threshold mechanoreceptors (A-β fibers) (S12, S13). Moreover, even normally painful stimuli can be misinterpreted as itch in a chronic itch condition when applied directly to pruritic skin lesions (48, 56).

Ongoing activity of pruriceptors, which presumably underlies central sensitization for itch, has already been confirmed microneurographically in a patient with chronic pruritus (30). In addition, lasting activation of pruriceptors by histamine has been shown to experimentally induce central sensitization for itch in

Table 2
Frontiers in itch research and possible therapeutic consequences

Frontier	Possible therapeutic consequence	Selected references
Similar spinal or supraspinal sensitization processes in chronic pain and itch	Antipruritic treatment with typical analgesics for neuropathic pain (e.g., gabapentin, antidepressants)	(119, S41)
Similar peripheral sensitization processes in inflammatory pain and itch (e.g., NGF)	Anti-NGF treatment for inflammatory pain and itch	(120, S42)
Effects of proteases in pain and itch; role of PAR_2	Serine protease inhibitors or antagonists of PAR_2 for treatment of inflammatory itch and pain	(64, 114)
Understanding the complexity of the CNS when processing itch	Identifying new central targets in the itch pathway	(41, 42)
Understanding the role of the epidermis in itch sensation	Antipruritic treatment using modifiers of keratinocyte function and epidermal barrier dysfunction	(121, 122)
Role of neuronal cytokine receptors in itch sensation	Antipruritic therapy using specific cytokine suppressors	(113, S20)
Role of TRPV1 in the pathogenesis of itch	Antipruritic treatment using natural TRPV1 agonists such as modified forms of capsaicin or resiniferatoxin	(4, 83)
Role of TRP channels in itch	Antipruritic treatment using thermal therapy	(123, 124)

healthy volunteers (56). Thus there is emerging evidence for a role of central sensitization in itch modulation during chronic pruritus. As there are many mediators and mechanisms that are potentially algogenic in inflamed skin (70), many of them could provoke itch in a sensitized patient.

Psychoemotional stress triggers or enhances itch

Clinically, it has long been appreciated that both acute stress (stressful life events) and chronic psychoemotional stress can trigger or enhance pruritus (18, 19, 71). Recent insights into the neuroendocrinology and neuroimmunology of stress responses have improved our understanding of why this may happen. Stress responses are known to be learned, to involve cortical centers, and to activate the hypothalamus-pituitary-adrenal axis (72, 73). Since stress responses can be reprogrammed (e.g., by behavioral and neuropharmacological/neuroendocrine therapy), deeper knowledge of the mechanisms underlying central itch control may lead to novel, innovative, psychosomatic, or neuropharmacological approaches for behavioral itch therapy. There is much to be learned about stress-induced itch from stress-related analgesia (74). Independent of direct effects of stress hormones (e.g., adrenocorticotropin-releasing hormone, cortisol, noradrenaline), the activation of endogenous pain–inhibitory systems, part of which are naloxone sensitive (75), should directly enhance itch processing by reducing its inhibition.

Moreover, the experience of increased itch upon stressful events would also lead to conditioning of itch and thereby aggravate and perpetuate stress-induced itch. For example, a close relationship between itch and psychological factors has been demonstrated in hand dermatoses, especially in patients who were convinced that stress was a major trigger of their disease (76).

The important role of learning processes in the development of chronic pain has been recognized (77) and resulted in the development of successful operant behavioral treatment regimens (S14) for chronic pain patients. Although there is evidence for clinically relevant learning effects in chronic itch (S15), the formation and reprogramming of itch memory has not yet been systematically explored.

Endovanilloids and the TRPV1 ion channel are promising targets for antipruritic therapy

A novel putative mechanism in the pathogenesis of itch has recently emerged. Certain itch mediators — such as eicosanoids, histamine, bradykinin, ATP, and various neurotrophins (78–81) — can be collectively coined as having endovanilloid functions (82). These agents, along with other potentially pruritogenic stimuli such as mild heat (>43°C) and acidosis, either directly or indirectly activate and/or sensitize TRPV1 (78, 83, 84).

TRPV1 belongs to the superfamily of TRP channels, which is composed of 6 groups of molecules: the canonical (TRPC), the vanilloid (TRPV), the melastatin (TRPM), the polycystin (TRPP), the mucolipin (TRPML), and the ankyrin transmembrane protein 1 (TRPA) subfamilies. In general, these molecules act as nonselective calcium-permeable sensory transduction channels detecting, for example, temperature and osmotic/mechanical changes (reviewed in ref. 85).

TRPV1 was originally described as appearing on nociceptive sensory neurons (83) as a central integrator of various pain-inducing stimuli. Besides endovanilloid-induced activation (Figures 3 and 5), TRPV1 can be effectively activated by capsaicin, the pungent ingredient of hot chili peppers. TRPV1 activation first excites (84), then desensitizes, the sensory afferents — an effect that establishes the basis for the therapeutic application of vanilloids to mitigate pain and itch (3, S16). Vanilloid administration results in a depletion of neuropeptides (such as SP) in the C-fibers, which suspends the interplay between skin sensory neurons and mast cells (Figure 1) (3, 6, 10). Indeed, topical capsaicin suppresses histamine-induced itch (86) and is increasingly used in the therapy of pruritus in numerous skin diseases (reviewed in refs. 3, 6, 87).

A new itchy twist has recently propelled TRPV1 research beyond its confinement to sensory physiology: functional TRPV1 channels are now recognized to be expressed by numerous nonneuronal cell types, including human epidermal and hair follicle keratinocytes, dermal mast cells, and dendritic cells (88–90). TRPV1 activation — besides markedly affecting keratinocyte proliferation, differentiation, and apoptosis — results in the release of pruritogenic cytokine mediators from these nonneuronal cells (91, 92).

These findings invite researchers to postulate that, besides activating their own cognate receptors (Table 1), the endovanilloid itch mediators also activate and/or sensitize TRPV1 expressed on itch-specific sensory neurons (to fire action potentials) and many other skin cells (to upregulate the release of pruritogenic substances; Figure 5A) (4). In consequence, repeatedly applied topical capsaicin, or other therapeutically promising vanilloids, may desensitize neuronal and nonneuronal TRPV1-mediated signaling so as to counteract pruritogenic intercellular signaling (Figure 5B). In fact, TRPV1 expression is dramatically increased in lesional epidermal keratinocytes of prurigo nodularis patients (90), and topical capsaicin is effective in this intensely pruritic disease characterized by vicious cycles of neurogenic inflammation and neurotrophin-induced nerve sprouting (3, 93, S1).

The most notorious clinical limitation of capsaicin application is the burning sensation. Therefore, better TRPV1 agonists that cause only a minor excitation but are still potent desensitizers are needed. A chief candidate is resiniferatoxin (S17), which is 3 times more potent as a desensitizer (i.e., to treat pain and itch) than as an excitatory agent (i.e., to cause pain) (S16). Alternatively, TRPV1 antagonists (such as capsazepine or iodo-resiniferatoxin; S16) deserve more attention as potential antipruritic agents.

Are endocannabinoids involved in itch pathogenesis?

The cannabinoid system (94) provides another putative itch frontier. Cannabinoid receptor 1 (CB1) and TRPV1 show marked colocalization in sensory neurons (94). Moreover, CB1 agonists effectively suppress histamine-induced pruritus (95), suggesting the involvement of CB1 signaling in the initiation of itch. Furthermore, under inflammatory conditions (96) cannabinoids also activate the TRPV1 pathway and thereby switch their neuronal effect from inhibition (97) to excitation and sensitization (Figure 3) (98). Finally, since CBs, just like TRPV1, are also expressed by nonneuronal human skin cells (99, 100), CBs may be involved in the neuronal/nonneuronal cellular network of pruritogenic stimuli arising in skin. Thus coadministration of a TRPV1 agonist with a CB1 agonist would be expected to serve as a potent antipruritic regimen (Figure 5B). In addition, this would prevent the acute burning sensation initiated by capsaicin, since CB agonists (e.g., anandamide and HU210) prevent the excitation induced by capsaicin (101, 102).

Additional TRP channels are interesting targets in pruritus management

The fact that cold generally alleviates itch while increasing temperature tends to aggravate it (3, S1) draws our attention to other members of the TRPV subfamily (TRPV2, TRPV3, and TRPV4). These channels operate as cellular temperature sensors, since all are activated by differential temperatures (103–105). TRPV3 shows a very similar neuronal expression pattern to that of TRPV1, and TRPV3 subunits may form heteromultimeric structures by interacting with TRPV1 monomers (105). Therefore, TRPV3 may act as signal cotransducer and/or regulator of TRPV1-mediated pain and itch.

Most intriguingly, quite like TRPV1, functional TRPV2, TRPV3, and TRPV4 channels are highly expressed by epidermal keratinocytes and mast cells (104, 106–108). Moreover, TRPV4 is activated by such lipid peroxidation products as eicosanoids, which function as TRPV1-activating pruritogenic substances (109). Physical and thermal activation of TRPV2 causes mast cells to degranulate, which depends on protein kinase A–related signaling (107) — one of the chief mechanisms in initiating pain- and itch-inducing TRPV1 sensitization (81).

Finally, TRPM8 receptors deserve to be mentioned. Expressed by C-type sensory neurons, they serve as thermosensors for coolness and cold (i.e., 8°C to –28°C). TRPM8 is also activated by chemicals — menthol, menthol analogs, and icilin (S18) — that produce sensations of cold (110). Menthol has a long tradition in topical anti-itch therapy (albeit with moderate success; ref. S1), and in an animal model of scratching provoked by a magnesium-deficient diet, topical icilin significantly reduced excoriations in hairless rats (4). In short, all of these receptors warrant systematic exploration of their nonthermosensor, itch-related signaling roles.

Conclusion and perspectives

This exploration of recent frontiers in pruritus research reveals that we still lack a single, universally effective pharmacological handle on combating itch and that, due to the inherent neurophysiological and neuroimmunological complexity of itch pathophysiology, it would be naive to expect that such a one-shot cure of itch will become available any time soon. However, the complexity of the interactions between the central and peripheral nervous system and the skin in producing this symptom notwithstanding, a broad but concrete spectrum of molecular targets for effective itch intervention has moved into view. If these "hot spot" molecules, both in the CNS and peripheral nervous system, are further explored systematically, we undoubtedly will move much closer to developing more effective therapeutic combination strategies for pruritus management.

In particular, it has become apparent that timely combination approaches that target both the peripheral production of inflammation-induced itch signals and the peripherally incited vicious cycles that perpetuate itch and cause spinal and central sensitization to itch are needed. Thus the combination of peripherally active antiinflammatory agents with drugs that counteract chronic central itch sensitization is a particularly sensible approach beyond the antihistamine horizon. Table 2 concludes this excursion by summarizing some of our current personal favorites among the "itch frontiers," which we expect to pave the way for the development of innovative and more effective approaches to itch management in the future.

Acknowledgments

The authors gratefully acknowledge the administrative assistance of C. Mess and C. Moormann in putting the finishing touches to this Review and the support of Deutsche Forschungsgemeinschaft (Pa 345/11-2 to R. Paus; STE 1014/2-1 and IZKF Stei2/027/06 to M. Steinhoff; and KGF 107 to M. Schmelz) and Hungarian Scientific Research Fund (OKTA K63153 to Tamás Bíró), which have aided the writing of this Review.

Note: References S1–S42 are available online with this article; doi:10.1172/JCI28553DS1.

Address correspondence to: Ralf Paus, Department of Dermatology, University Hospital Schleswig-Holstein, Campus Lübeck, University of Lübeck, D-23538 Lübeck, Germany. Phone: 49-451-500-2543; Fax: 49-451-500-5161; E-mail: ralf.paus@uk-sh.de.

Martin Schmelz and Tamás Bíró contributed equally to this work.

1. Greaves, M.W., and Khalifa, N. 2004. Itch: more than skin deep. *Int. Arch. Allergy Immunol.* **135**:166–172.
2. Graham, D.T., Goodell, H., and Wolff, H.G. 1951. Neural mechanisms involved in itch, itchy skin, and tickle sensations. *J. Clin. Invest.* **30**:37–49.
3. Yosipovitch, G., Greaves, M.W., and Schmelz, M. 2003. Itch. *Lancet.* **361**:690–694.
4. Biro, T., et al. 2005. How best to fight that nasty itch - from new insights into the neuroimmunological, neuroendocrine, and neurophysiological bases of pruritus to novel therapeutic approaches. *Exp. Dermatol.* **14**:225–240.
5. Steinhoff, M., et al. 2006. Neurophysiological, neuroimmunological and neuroendocrine basis of pruritus. *J. Invest. Dermatol.* In press.
6. Twycross, R., et al. 2003. Itch: scratching more than the surface. *QJM.* **96**:7–26.
7. Bromm, B., Scharein, E., and Vahle-Hinz, C. 2000. Cortex areas involved in the processing of normal and altered pain. *Prog. Brain Res.* **129**:289–302.
8. Schmelz, M. 2001. A neural pathway for itch. *Nat. Neurosci.* **4**:9–10.
9. Andrew, D., and Craig, A.D. 2001. Spinothalamic lamina I neurons selectively sensitive to histamine: a central neural pathway for itch. *Nat. Neurosci.* **4**:72–77.
10. Stander, S., and Steinhoff, M. 2002. Pathophysiology of pruritus in atopic dermatitis: an overview. *Exp. Dermatol.* **11**:12–24.
11. Schmelz, M., Schmidt, R., Bickel, A., Handwerker, H.O., and Torebjork, H.E. 1997. Specific C-receptors for itch in human skin. *J. Neurosci.* **17**:8003–8008.
12. Klein, P.A., and Clark, R.A. 1999. An evidence-based review of the efficacy of antihistamines in relieving pruritus in atopic dermatitis. *Arch. Dermatol.* **135**:1522–1525.
13. Munday, J., et al. 2002. Chlorpheniramine is no more effective than placebo in relieving the symptoms of childhood atopic dermatitis with a nocturnal itching and scratching component. *Dermatology.* **205**:40–45.
14. Rukwied, R., Lischetzki, G., McGlone, F., Heyer, G., and Schmelz, M. 2000. Mast cell mediators other than histamine induce pruritus in atopic dermatitis patients: a dermal microdialysis study. *Br. J. Dermatol.* **142**:1114–1120.
15. Hanifin, J.M. 1990. The role of antihistamines in atopic dermatitis. *J. Allergy Clin. Immunol.* **86**:666–669.
16. Imaizumi, A., Kawakami, T., Murakami, F., Soma, Y., and Mizoguchi, M. 2003. Effective treatment of pruritus in atopic dermatitis using H1 antihistamines (second-generation antihistamines): changes in blood histamine and tryptase levels. *J. Dermatol. Sci.* **33**:23–29.
17. Monroe, E.W. 1992. Relative efficacy and safety of loratadine, hydroxyzine, and placebo in chronic idiopathic urticaria and atopic dermatitis. *Clin. Ther.* **14**:17–21.
18. Arck, P.C., Slominski, A., Theoharides, T.C., Peters, E.M.J., and Paus, R. 2006. Neuroimmunology of stress: skin takes center stage. *J. Invest. Dermatol.* 126. In press.
19. Paus, R., Theoharides, T.C., and Arck, P.C. 2006. Neuroimmunoendocrine circuitry of the 'brain-skin connection'. *Trends Immunol.* **27**:32–39.
20. Botchkarev, N.V., et al. 2006. Neurotrophins in skin biology. *J. Invest. Dermatol.* **2**:31–36.
21. Lee, M.R., and Shumack, S. 2005. Prurigo nodularis: a review. *Australas. J. Dermatol.* **46**:211–218; quiz 219–220.
22. Johansson, O., Liang, Y., and Emtestam, L. 2002. Increased nerve growth factor- and tyrosine kinase A-like immunoreactivities in prurigo nodularis skin -- an exploration of the cause of neurohyperplasia. *Arch. Dermatol. Res.* **293**:614–619.
23. Tanaka, A., and Matsuda, H. 2005. Expression of nerve growth factor in itchy skins of atopic NC/NgaTnd mice. *J. Vet. Med. Sci.* **67**:915–919.
24. Aloe, L. 2004. Rita Levi-Montalcini: the discovery of nerve growth factor and modern neurobiology. *Trends Cell Biol.* **14**:395–399.
25. Groneberg, D.A., et al. 2005. Gene expression and regulation of nerve growth factor in atopic dermatitis mast cells and the human mast cell line-1. *J. Neuroimmunol.* **161**:87–92.
26. Toyoda, M., et al. 2002. Nerve growth factor and substance P are useful plasma markers of disease activity in atopic dermatitis. *Br. J. Dermatol.* **147**:71–79.
27. Bell, J.K., McQueen, D.S., and Rees, J.L. 2004. Involvement of histamine H4 and H1 receptors in scratching induced by histamine receptor agonists in Balb C mice. *Br. J. Pharmacol.* **142**:374–380.
28. Seike, M., Ikeda, M., Kodama, H., Terui, T., and Ohtsu, H. 2005. Inhibition of scratching behavior caused by contact dermatitis in histidine decarboxylase gene knockout mice. *Exp. Dermatol.* **14**:169–175.
29. Rees, J., and Murray, C.S. 2005. Itching for progress. *Clin. Exp. Dermatol.* **30**:471–473.
30. Schmelz, M., et al. 2003. Active "itch fibers" in chronic pruritus. *Neurology.* **61**:564–566.
31. Andrew, D., Schmelz, M., and Ballantyne, J.C. 2003. Itch – mechanisms and mediators. In *Progress in pain research and management*. J.O. Dostrovsky, D.B. Carr, and M. Koltzenburg, editors. ISAP Press. Seattle, Washington, USA. 213–226.
32. Schmelz, M., et al. 2003. Chemical response pattern of different classes of C-nociceptors to pruritogens and algogens. *J. Neurophysiol.* **89**:2441–2448.
33. Weidner, C., et al. 1999. Functional attributes discriminating mechanoinsensitive and mechanoresponsive C nociceptors in human skin. *J. Neurosci.* **19**:10184–10190.
34. Schmidt, R., Schmelz, M., Weidner, C., Handwerker, H.O., and Torebjork, H.E. 2002. Innervation territories of mechanoinsensitive C nociceptors in human skin. *J. Neurophysiol.* **88**:1859–1866.
35. Schmelz, M., et al. 2000. Which nerve fibers mediate the axon reflex flare in human skin? *Neuroreport.* **11**:645–648.
36. Ikoma, A., Handwerker, H., Miyachi, Y., and Schmelz, M. 2005. Electrically evoked itch in humans. *Pain.* **113**:148–154.
37. Darsow, U., et al. 2001. New aspects of itch pathophysiology: component analysis of atopic itch using the 'Eppendorf Itch Questionnaire'. *Int. Arch. Allergy Immunol.* **124**:326–331.
38. Darsow, U., et al. 2000. Processing of histamine-induced itch in the human cerebral cortex: a correlation analysis with dermal reactions. *J. Invest. Dermatol.* **115**:1029–1033.
39. Craig, A.D. 2002. How do you feel? Interoception: the sense of the physiological condition of the body. *Nat. Rev. Neurosci.* **3**:655–666.
40. Hsieh, J.C., et al. 1994. Urge to scratch represented in the human cerebral cortex during itch. *J. Neurophysiol.* **72**:3004–3008.
41. Drzezga, A., et al. 2001. Central activation by histamine-induced itch: analogies to pain processing: a correlational analysis of O-15 H2O positron emission tomography studies. *Pain.* **92**:295–305.
42. Mochizuki, H., et al. 2003. Imaging of central itch modulation in the human brain using positron emission tomography. *Pain.* **105**:339–346.
43. Vogt, B.A., Vogt, L., and Laureys, S. 2006. Cytology and functionally correlated circuits of human posterior cingulate areas. *Neuroimage.* **29**:452–466.
44. Apkarian, A.V., Bushnell, M.C., Treede, R.D., and Zubieta, J.K. 2005. Human brain mechanisms of pain perception and regulation in health and disease. *Eur. J. Pain.* **9**:463–484.
45. Walter, B., et al. 2005. Brain activation by histamine prick test-induced itch. *J. Invest. Dermatol.* **125**:380–382.
46. Kringelbach, M.L. 2005. The human orbitofrontal cortex: linking reward to hedonic experience. *Nat. Rev. Neurosci.* **6**:691–702.
47. Zubieta, J.K., et al. 2003. COMT val158met genotype affects mu-opioid neurotransmitter responses to a pain stressor. *Science.* **299**:1240–1243.
48. Nilsson, H.J., Levinsson, A., and Schouenborg, J. 1997. Cutaneous field stimulation (CFS): a new powerful method to combat itch. *Pain.* **71**:49–55.
49. Yosipovitch, G., Fast, K., and Bernhard, J.D. 2005. Noxious heat and scratching decrease histamine-induced itch and skin blood flow. *J. Invest. Dermatol.* **125**:1268–1272.
50. Atanassoff, P.G., et al. 1999. Enhancement of experimental pruritus and mechanically evoked dysesthesiae with local anesthesia. *Somatosens. Mot. Res.* **16**:291–298.
51. McRae, C.A., et al. 2003. Pain as a complication of use of opiate antagonists for symptom control in cholestasis. *Gastroenterology.* **125**:591–596.
52. Jones, E.A., Neuberger, J., and Bergasa, N.V. 2002. Opiate antagonist therapy for the pruritus of cholestasis: the avoidance of opioid withdrawal-like reactions. *QJM.* **95**:547–552.
53. Stein, C., Schafer, M., and Machelska, H. 2003. Attacking pain at its source: new perspectives on opioids. *Nat. Med.* **9**:1003–1008.
54. DeHaven-Hudkins, D.L., et al. 2002. Antipruritic and antihyperalgesic actions of loperamide and analogs. *Life Sci.* **71**:2787–2796.
55. Bigliardi-Qi, M., Lipp, B., Sumanovski, L.T., Buechner, S.A., and Bigliardi, P.L. 2005. Changes of epidermal mu-opiate receptor expression and nerve endings in chronic atopic dermatitis. *Dermatology.* **210**:91–99.
56. Ikoma, A., et al. 2003. Neuronal sensitization for histamine-induced itch in lesional skin of patients with atopic dermatitis. *Arch. Dermatol.* **139**:1455–1458.
57. Amadesi, S., et al. 2004. Protease-activated receptor 2 sensitizes the capsaicin receptor transient receptor potential vanilloid receptor 1 to induce hyperalgesia. *J. Neurosci.* **24**:4300–4312.
58. Moormann, C., et al. 2006. Functional characterization and expression analysis of the proteinase-activated receptor-2 in human cutaneous mast cells. *J. Invest. Dermatol.* **126**:746–755.
59. Steinhoff, M., et al. 2003. Modern aspects of cutaneous neurogenic inflammation. *Arch. Dermatol.* **139**:1479–1488.
60. Steinhoff, M., et al. 2005. Proteinase-activated receptors: transducers of proteinase-mediated signaling in inflammation and immune response. *Endocr. Rev.* **26**:1–43.
61. Vergnolle, N., Ferazzini, M., D'Andrea, M.R., Buddenkotte, J., and Steinhoff, M. 2003. Proteinase-activated receptors: novel signals for peripheral nerves. *Trends Neurosci.* **26**:496–500.
62. Szolcsanyi, J. 2004. Forty years in capsaicin research for sensory pharmacology and physiology. *Neuropeptides.* **38**:377–384.
63. Grassberger, M., Steinhoff, M., Schneider, D., and Luger, T.A. 2004. Pimecrolimus -- an anti-inflammatory drug targeting the skin. *Exp. Dermatol.* **13**:721–730.
64. Steinhoff, M., et al. 2000. Agonists of proteinase-activated receptor 2 induce inflammation by a neurogenic mechanism. *Nat. Med.* **6**:151–158.
65. Vergnolle, N., et al. 2001. Proteinase-activated receptor-2 and hyperalgesia: a novel pain pathway. *Nat. Med.* **7**:821–826.
66. Ossovskaya, V.S., and Bunnett, N.W. 2004. Protease-activated receptors: contribution to physiology and disease. *Physiol. Rev.* **84**:579–621.
67. Su, X., Camerer, E., Hamilton, J.R., Coughlin, S.R., and Matthay, M.A. 2005. Protease-activated receptor-2 activation induces acute lung inflammation by neuropeptide-dependent mechanisms. *J. Immunol.* **175**:2598–2605.

68. Shelley, W.B., and Arthur, R.P. 1955. Mucunain, the active pruritogenic proteinase of cowhage. *Science.* **122**:469–470.
69. Obreja, O., Rukwied, R., Steinhoff, M., and Schmelz, M. 2006. Neurogenic components of trypsin- and thrombin-induced inflammation in rat skin, in vivo. *Exp. Dermatol.* **15**:58–65.
70. Steen, K.H., Steen, A.E., and Reeh, P.W. 1995. A dominant role of acid pH in inflammatory excitation and sensitization of nociceptors in rat skin, in vitro. *J. Neurosci.* **15**:3982–3989.
71. Gieler, U., Kupfer, J., Niemeier, V., and Brosig, B. 2003. Psyche and skin: what's new? *J. Eur. Acad. Dermatol. Venereol.* **17**:128–130.
72. Slominski, A., and Wortsman, J. 2000. Neuroendocrinology of the skin. *Endocr. Rev.* **21**:457–487.
73. McEwen, B., and Lasley, E.N. 2004. *The end of stress as we know it*. Dana Press. Washington, DC, USA. 239 pp.
74. Willer, J.C., Dehen, H., and Cambier, J. 1981. Stress-induced analgesia in humans: endogenous opioids and naloxone-reversible depression of pain reflexes. *Science.* **212**:689–691.
75. Vaughan, C.W. 2005. Stressed-out endogenous cannabinoids relieve pain. *Trends Pharmacol. Sci.* **27**:69–71.
76. Niemeier, V., Nippesen, M., Kupfer, J., Schill, W.B., and Gieler, U. 2002. Psychological factors associated with hand dermatoses: which subgroup needs additional psychological care? *Br. J. Dermatol.* **146**:1031–1037.
77. Flor, H., Knost, B., and Birbaumer, N. 2002. The role of operant conditioning in chronic pain: an experimental investigation. *Pain.* **95**:111–118.
78. Hwang, S.W., et al. 2000. Direct activation of capsaicin receptors by products of lipoxygenases: endogenous capsaicin-like substances. *Proc. Natl. Acad. Sci. U. S. A.* **97**:6155–6160.
79. Chuang, H.H., et al. 2001. Bradykinin and nerve growth factor release the capsaicin receptor from PtdIns(4,5)P2-mediated inhibition. *Nature.* **411**:957–962.
80. Shin, J., et al. 2002. Bradykinin-12-lipoxygenase-VR1 signaling pathway for inflammatory hyperalgesia. *Proc. Natl. Acad. Sci. U. S. A.* **99**:10150–10155.
81. Mohapatra, D.P., and Nau, C. 2003. Desensitization of capsaicin-activated currents in the vanilloid receptor TRPV1 is decreased by the cyclic AMP-dependent protein kinase pathway. *J. Biol. Chem.* **278**:50080–50090.
82. Di Marzo, V., Blumberg, P.M., and Szallasi, A. 2002. Endovanilloid signaling in pain. *Curr. Opin. Neurobiol.* **12**:372–379.
83. Caterina, M.J., et al. 1997. The capsaicin receptor: a heat-activated ion channel in the pain pathway. *Nature.* **389**:816–824.
84. Caterina, M.J., and Julius, D. 2001. The vanilloid receptor: a molecular gateway to the pain pathway. *Annu. Rev. Neurosci.* **24**:487–517.
85. Clapham, D.E. 2003. TRP channels as cellular sensors. *Nature.* **426**:517–524.
86. Weisshaar, E., Heyer, G., Forster, C., and Handwerker, H.O. 1998. Effect of topical capsaicin on the cutaneous reactions and itching to histamine in atopic eczema compared to healthy skin. *Arch. Dermatol. Res.* **290**:306–311.
87. Biro, T., Acs, G., Acs, P., Modarres, S., and Blumberg, P.M. 1997. Recent advances in understanding of vanilloid receptors: a therapeutic target for treatment of pain and inflammation in skin. *J. Investig. Dermatol. Symp. Proc.* **2**:56–60.
88. Inoue, K., Koizumi, S., Fuziwara, S., Denda, S., and Denda, M. 2002. Functional vanilloid receptors in cultured normal human epidermal keratinocytes. *Biochem. Biophys. Res. Commun.* **291**:124–129.
89. Bodo, E., et al. 2004. Vanilloid receptor-1 (VR1) is widely expressed on various epithelial and mesenchymal cell types of human skin. *J. Invest. Dermatol.* **123**:410–413.
90. Stander, S., et al. 2004. Expression of vanilloid receptor subtype 1 in cutaneous sensory nerve fibers, mast cells, and epithelial cells of appendage structures. *Exp. Dermatol.* **13**:129–139.
91. Southall, M.D., et al. 2003. Activation of epidermal vanilloid receptor-1 induces release of proinflammatory mediators in human keratinocytes. *J. Pharmacol. Exp. Ther.* **304**:217–222.
92. Bodo, E., et al. 2005. A hot new twist to hair biology: involvement of vanilloid receptor-1 (VR1/TRPV1) signaling in human hair growth control. *Am. J. Pathol.* **166**:985–998.
93. Stander, S., Luger, T., and Metze, D. 2001. Treatment of prurigo nodularis with topical capsaicin. *J. Am. Acad. Dermatol.* **44**:471–478.
94. Klein, T.W. 2005. Cannabinoid-based drugs as anti-inflammatory therapeutics. *Nat. Rev. Immunol.* **5**:400–411.
95. Dvorak, M., Watkinson, A., McGlone, F., and Rukwied, R. 2003. Histamine induced responses are attenuated by a cannabinoid receptor agonist in human skin. *Inflamm. Res.* **52**:238–245.
96. Singh, M.E., McGregor, I.S., and Mallet, P.E. 2005. Repeated exposure to Delta(9)-tetrahydrocannabinol alters heroin-induced locomotor sensitisation and Fos-immunoreactivity. *Neuropharmacology.* **49**:1189–1200.
97. Akerman, S., Kaube, H., and Goadsby, P.J. 2004. Anandamide acts as a vasodilator of dural blood vessels in vivo by activating TRPV1 receptors. *Br. J. Pharmacol.* **142**:1354–1360.
98. van der Stelt, M., et al. 2005. Anandamide acts as an intracellular messenger amplifying Ca(2+) influx via TRPV1 channels. *EMBO J.* **24**:3517–3518.
99. Maccarrone, M., et al. 2003. The endocannabinoid system in human keratinocytes. Evidence that anandamide inhibits epidermal differentiation through CB1 receptor-dependent inhibition of protein kinase C, activation protein-1, and transglutaminase. *J. Biol. Chem.* **278**:33896–33903.
100. Stander, S., Schmelz, M., Metze, D., Luger, T., and Rukwied, R. 2005. Distribution of cannabinoid receptor 1 (CB1) and 2 (CB2) on sensory nerve fibers and adnexal structures in human skin. *J. Dermatol. Sci.* **38**:177–188.
101. Richardson, J.D., Kilo, S., and Hargreaves, K.M. 1998. Cannabinoids reduce hyperalgesia and inflammation via interaction with peripheral CB1 receptors. *Pain.* **75**:111–119.
102. Rukwied, R., Watkinson, A., McGlone, F., and Dvorak, M. 2003. Cannabinoid agonists attenuate capsaicin-induced responses in human skin. *Pain.* **102**:283–288.
103. Caterina, M.J., Rosen, T.A., Tominaga, M., Brake, A.J., and Julius, D. 1999. A capsaicin-receptor homologue with a high threshold for noxious heat. *Nature.* **398**:436–441.
104. Peier, A.M., et al. 2002. A heat-sensitive TRP channel expressed in keratinocytes. *Science.* **296**:2046–2049.
105. Smith, G.D., et al. 2002. TRPV3 is a temperature-sensitive vanilloid receptor-like protein. *Nature.* **418**:186–190.
106. Chung, M.K., Lee, H., Mizuno, A., Suzuki, M., and Caterina, M.J. 2004. TRPV3 and TRPV4 mediate warmth-evoked currents in primary mouse keratinocytes. *J. Biol. Chem.* **279**:21569–21575.
107. Stokes, A.J., Shimoda, L.M., Koblan-Huberson, M., Adra, C.N., and Turner, H. 2004. A TRPV2-PKA signaling module for transduction of physical stimuli in mast cells. *J. Exp. Med.* **200**:137–147.
108. Moqrich, A., et al. 2005. Impaired thermosensation in mice lacking TRPV3, a heat and camphor sensor in the skin. *Science.* **307**:1468–1472.
109. Watanabe, H., et al. 2003. Anandamide and arachidonic acid use epoxyeicosatrienoic acids to activate TRPV4 channels. *Nature.* **424**:434–438.
110. McKemy, D.D., Neuhausser, W.M., and Julius, D. 2002. Identification of a cold receptor reveals a general role for TRP channels in thermosensation. *Nature.* **416**:52–58.
111. Schmelz, M., Schmid, R., Handwerker, H.O., and Torebjork, H.E. 2000. Encoding of burning pain from capsaicin-treated human skin in two categories of unmyelinated nerve fibres. *Brain.* **123**:560–571.
112. Slominski, A.T., et al. 1999. Cutaneous expression of CRH and CRH-R. Is there a "skin stress response system?" *Ann. N. Y. Acad. Sci.* **885**:287–311.
113. Sonkoly, E., et al. 2006. IL-31: a new link between T cells and pruritus in atopic skin inflammation. *J. Allergy Clin. Immunol.* **117**:411–417.
114. Steinhoff, M., et al. 2003. Proteinase-activated receptor-2 mediates itch: a novel pathway for pruritus in human skin. *J. Neurosci.* **23**:6176–6180.
115. Roosterman, D., Cottrell, G.S., Schmidlin, F., Steinhoff, M., and Bunnett, N.W. 2004. Recycling and resensitization of the neurokinin 1 receptor. Influence of agonist concentration and Rab GTPases. *J. Biol. Chem.* **279**:30670–30679.
116. Stander, S., et al. 2003. Neurophysiology of pruritus: cutaneous elicitation of itch. *Arch. Dermatol.* **139**:1463–1470.
117. Blunk, J.A., et al. 2004. Opioid-induced mast cell activation and vascular responses is not mediated by mu-opioid receptors: an in vivo microdialysis study in human skin. *Anesth. Analg.* **98**:364–370, table of contents.
118. Neisius, U., Olsson, R., Rukwied, R., Lischetzki, G., and Schmelz, M. 2002. Prostaglandin E2 induces vasodilation and pruritus, but no protein extravasation in atopic dermatitis and controls. *J. Am. Acad. Dermatol.* **47**:28–32.
119. Yesudian, P.D., and Wilson, N.J. 2005. Efficacy of gabapentin in the management of pruritus of unknown origin. *Arch. Dermatol.* **141**:1507–1509.
120. Horiuchi, Y., Bae, S., and Katayama, I. 2005. Nerve growth factor (NGF) and epidermal nerve fibers in atopic dermatitis model NC/Nga mice. *J. Dermatol. Sci.* **39**:56–58.
121. Ashida, Y., Denda, M., and Hirao, T. 2001. Histamine H1 and H2 receptor antagonists accelerate skin barrier repair and prevent epidermal hyperplasia induced by barrier disruption in a dry environment. *J. Invest. Dermatol.* **116**:261–265.
122. Miyamoto, T., Nojima, H., Shinkado, T., Nakahashi, T., and Kuraishi, Y. 2002. Itch-associated response induced by experimental dry skin in mice. *Jpn. J. Pharmacol.* **88**:285–292.
123. Peier, A.M., et al. 2002. A TRP channel that senses cold stimuli and menthol. *Cell.* **108**:705–715.
124. Xu, H., et al. 2002. TRPV3 is a calcium-permeable temperature-sensitive cation channel. *Nature.* **418**:181–186.
125. Brain, S.D. 2000. New feelings about the role of sensory nerves in inflammation. *Nat. Med.* **6**:134–135.

XXII.

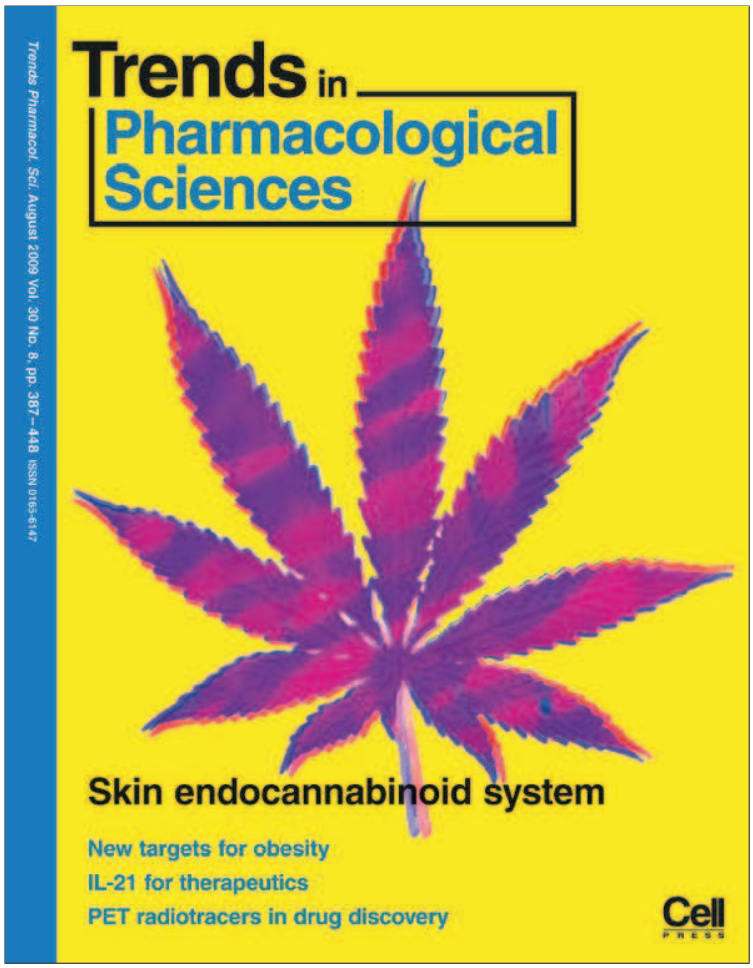

Review

Cell PRESS

The endocannabinoid system of the skin in health and disease: novel perspectives and therapeutic opportunities

Tamás Bíró[1], Balázs I. Tóth[1], György Haskó[2], Ralf Paus[3,4] and Pál Pacher[5]

[1] Department of Physiology, University of Debrecen, Research Center for Molecular Medicine, Debrecen 4032, Hungary
[2] University of Medicine and Dentistry, Department of Surgery, New Jersey Medical School, Newark, NJ 07103, USA
[3] Department of Dermatology, University Hospital Schleswig-Holstein, University of Lübeck, Lübeck 23538, Germany
[4] School of Translational Medicine, University of Manchester, Manchester, M13 9PL, UK
[5] Section on Oxidative Stress Tissue Injury, Laboratory of Physiological Studies, National Institutes of Health/NIAAA, Rockville, MD 20892-9413, USA

The newly discovered endocannabinoid system (ECS; comprising the endogenous lipid mediators endocannabinoids present in virtually all tissues, their G-protein-coupled cannabinoid receptors, biosynthetic pathways and metabolizing enzymes) has been implicated in multiple regulatory functions both in health and disease. Recent studies have intriguingly suggested the existence of a functional ECS in the skin and implicated it in various biological processes (e.g. proliferation, growth, differentiation, apoptosis and cytokine, mediator or hormone production of various cell types of the skin and appendages, such as the hair follicle and sebaceous gland). It seems that the main physiological function of the cutaneous ECS is to constitutively control the proper and well-balanced proliferation, differentiation and survival, as well as immune competence and/or tolerance, of skin cells. The disruption of this delicate balance might facilitate the development of multiple pathological conditions and diseases of the skin (e.g. acne, seborrhea, allergic dermatitis, itch and pain, psoriasis, hair growth disorders, systemic sclerosis and cancer).

The skin as an emerging neuro-immuno-endocrine organ

The skin and its appendages establish a 'passive' physico-chemical barrier against constant environmental

Glossary

Acne vulgaris (or acne): a common, multi-etiological skin condition characterized by increased sebum production and inflammation of the sebaceous glands; acne can be induced and/or aggravated, for example, by stress, endocrine conditions (adolescence), immune/inflammatory factors, bacterial infection of the skin, diet, and so on.
a (*N*-arachidonoylethanolamine) and 2-AG (2-arachidonoylglycerol): the two most studied endocannabinoids, which exert biological effects similar to marijuana via activation of two main cannabinoid receptors.
Alopecia: a type of pathological hair loss affecting mostly the scalp; most common forms of alopecia: universalis, areata, androgenetic.
Cannabinoid receptors: G-protein-coupled receptors that bind to and mediate the effects of cannabinoids.
Cannabinoids: as a broader definition, cannabinoids refer to a group of substances that are structurally related to Δ^9-tetrahydrocannabinol (THC), that bind to cannabinoid receptors, or that modulate the activity of the endocannabinoid system. Cannabinoids can be divided to various classes: 'phytocannabinoids' occuring in the cannabis plant; 'endogenous cannabinoids' produced in the body; and 'synthetic cannabinoids' chemically synthesized in a laboratory to target cannabinoid receptors and/or enzymes involved in the production or metabolism of endocannabinoids.
Dermatitis: a universal term describing inflammation of the skin; as most skin diseases, dermatitis can be induced by various factors such as, for example, allergens (allergic dermatitis), infections, eczema (atopic dermatitis), external compounds (contact dermatitis) and so on.
Effluvium (or telogen effluvium): a form of alopecia characterized by diffuse hair shedding.
Endocannabinoid system (ECS): it includes endocannabinoids, the enzymes involved in the biosynthesis or metabolism, and their two G-protein-coupled cannabinoid receptors, CB_1 and CB_2, which are present in virtually all tissues.
Endocannabinoids: bioactive lipid mediators produced in virtually all cell types and organs of the body, which exert biological effects similar to those of marijuana. The most extensively studied endocannabinoids are AEA and 2-AG.
Hair cycle: a life-long regeneration program of the hair follicles controlled by various factors; the hair cycle can be divided to three major phases: anagen (growth), catagen (regression or involution) and telogen (resting or quiescence).
Hirsutisms: is excessive and increased hair growth (especially in women) on body regions where the occurrence of hair normally is minimal or absent.
Orthodromic, antidromic: in a neuron, an orthodromic impulse (i.e. an action potential) runs along an axon in its normal direction, that is, away from the soma towards the axon ending. An antidromic impulse in an axon refers to conduction of the action potentials opposite to the normal, orthodromic direction (i.e. from the axon terminal to the soma).
Phytocannabinoids: cannabinoids that are isolated from the plant *Cannabis sativa*; the most known phytocannabinoid is THC and cannabidiol.
Pilosebaceous unit: consists of the hair shaft, the hair follicle, the sebaceous gland and the erector pili muscle, which causes the hair to stand up when it contracts.
Psoriasis: is a chronic, autoimmune skin disease that is characterized by epidermal hyperproliferation and skin inflammation.
Seborrhea (or seborrhoeic dermatitis): an inflammatory skin condition that particularly affects the sebaceous-gland-enriched areas of the skin; similar to acne, multiple factors are listed in its etiology.
Sebum: a lipid-enriched, oily exocrine product of the sebaceous glands; sebum has various function such as waterproof-barrier formation, anti-microbial activity, transport, thermoregulation and so on.
Systemic sclerosis (scleroderma): a chronic autoimmune disease characterized by diffuse fibrosis (accumulation of connective tissue), degenerative changes, and vascular abnormalities in the skin, joints and internal organs.
THC: the main active ingredient of the plant *Cannabis sativa*, which predominantly exerts its physiological effects via two main G-protein-coupled cannabinoid receptors.
TRPV1: transient receptor potential cation channel, subfamily V, member 1; also referred as vanilloid receptor 1 (VR1).

Corresponding authors: Bíró, T. (biro@phys.dote.hu); Pacher, P. (pacher@mail.nih.gov).

0165-6147/$ – see front matter doi:10.1016/j.tips.2009.05.004 Available online 14 July 2009

Box 1. Introduction to skin biology

The skin is the largest organ of the integumentary system (the organ system that protects the body from damage) and is composed of multiple layers and cell types:

Epidermis: made of keratinocytes (which provide waterproofing and serve as a barrier to infection), Merkel cells (which function as mechanoreceptors for the sensation of touch and pressure), melanocytes (whose activity of melanogenesis defines skin color) and Langerhans cells (which function as professional antigen-presenting cells of the skin immune system). In addition, sensory nerve endings (recognizing e.g. touch, pressure, temperature as well as pain and itch) might also reach the lower layers of the epidermis.

Dermis: a dense connective tissue composed of collagen, elastic and reticular fibers produced mainly by dermal fibroblasts. In addition, the dermis is supplied by blood and lymphatic vessels and is highly innervated by both sensory afferent as well as motor efferent (which participate e.g. in vasoregulation) nerve fibers establishing a dense neuronal network. Of further importance, the dermis is the 'home' of the skin appendages such as the hair follicles as well as the sebaceous and sweat glands.

Hypodermis (or subcutis): made of adipocytes, fibroblasts and macrophages (part of the skin immune system). In addition, the subcutis is well supplied by vessels and nerve fibers.

The skin layers and cell types form a complex, multicellular communications network, the proper function of which establish the physiological skin homeostasis. Selected functions of the skin involve:

Barrier functions: waterproof anatomical protection barrier against, for example, physical environmental challenges (e.g. UV, temperature), microbial invasion, allergens, chemical irritants and so on.

Sensory functions: sensation of heat and cold, touch, pressure, vibration as well as pain and itch (related to tissue injury); release of neuropeptides that regulate local vasoregulatory, immune-inflammatory and trophic functions.

Motor functions: vasoregulation (dilation or constriction of blood vessels) and piloerection.

Transport functions: transport of respiratory gases and nutrients between skin layers as well as from/to the skin surface; absorption of topically applied medications.

Exocrine functions: production and release (to the skin surface) of sweat and sebum, which exocrine products participate, for example, in thermoregulation, physical barrier formation, anti-microbial activity and so on.

Thermoregulatory functions: insulation by the subcuticular adipose tissue (actually, skin contains 50% of body fat); large cutaneous blood supply that enables precise control of direct heat losing mechanisms (i.e. radiation, convection and conduction); vasoregulation (vasodilation promotes heat loss whereas vasoconstriction preserves body heat); evaporation (both insensible via skin pores and sensible via sweating); piloerection to further support insulation.

Endocrine functions: synthesis of a wide-array of hormones (e.g. vitamin D, steroids and peptide hormones) in multiple cutaneous cells; functional expression of hormone receptors as well as enzymes involved in the synthesis and metabolism of hormones; immune and inflammatory functions (a wide array of cutaneous immune-competent cells); synthesis and release of pro- and anti-inflammatory mediators (e.g. cytokines, chemokines and trophic factors) in almost all skin populations; anti-microbial activity of the sebum.

Regenerative functions: well-orchestrated and balanced proliferation, differentiation, survival and death 'programs' of the cutaneous cells and appendage structures, which enable life-long regeneration and regeneration of the skin; stem cell supply; wound healing.

challenges. However, a plethora of recent research has defined that the skin and its adnexal components (i.e. hair follicles, sebaceous and sweat glands) also function as 'active' neuro-immuno-endocrine organs [1] with (i) well-defined neuronal networks and related functions; (ii) a wide-array of constantly remodeling non-neuronal cells and 'mini-organs' (i.e. hair follicle, sebaceous gland); (iii) orchestrated immunological machinery for inflammatory and immunological mechanisms; (iv) the synthesis and release of numerous growth factors, vasoactive substances and hormones (Box 1).

For the delicate execution of cutaneous neuro-immuno-endocrine functions, the aforementioned components establish a complex, multicellular communication network [2,3]. For example, activation of sensory neurons by various stimuli not only induces the antidromic (see Glossary) transmission of signals to the central nervous system but also results in the orthodromic release of certain neuropeptides (such as substance P and calcitonin-gene-related peptide) from the sensory afferents [4,5]. By contrast, these neuropeptides might then act on cutaneous non-neuronal cell types and exert local immuno-endocrine effects. Indeed, almost all skin cell populations (including those of the pilosebaceous unit) are capable of producing and releasing pro- and/or anti-inflammatory mediators that, by acting on neighboring cell types, can then fine-tune the overall immune response of the skin [1,3,5]. Similarly, production of numerous hormones by multiple cell types in the skin can exert local (paracrine or autocrine) regulation of cellular metabolism and functions of other cutaneous cell populations [1–5]. It is also important to note that the 'passive' (physico-chemical barrier) and 'active' (neuro-immuno-endocrine) functions of the skin and its appendages are strongly dependent on life-long regeneration and rejuvenation of cutaneous non-neuronal cells and mini-organs. These functions are defined by the well-orchestrated, delicate balance of cellular and organ proliferation and growth, survival and death, and regulated by a multitude of soluble mediators (e.g. growth and trophic factors, cytokines and chemokines) released from the skin cells [1–5].

Collectively, proper execution of the aforementioned mechanisms and the plasticity and pleiotropic nature of the cutaneous cells establish a solid base for physiological human skin homeostasis. Moreover, an appropriate equilibrium of cutaneous functions also enables the skin to protect the human body from constant environmental 'stressor' challenges such as microbial invasion, allergens, UV exposure and chemical irritation, among others. It is no wonder, therefore, that pathological alterations of cutaneous growth control and immuno-endocrine functions could lead to the development of multiple prevalent clinical conditions such as hyperproliferative skin diseases (e.g. psoriasis, tumors), hair growth disorders (e.g. alopecia, effluvium, hirsutism), acne vulgaris and atopic dermatitis [1–7].

In this article, the physiological regulatory function of the endocannabinoid system (ECS) in proliferation, differentiation, apoptosis and cytokine, mediator and hormone production of various cell types of the skin and appendages (e.g. hair follicle, sebaceous gland) are highlighted (Figure 1), and evidence on the putative involvement of the ECS in certain pathological conditions of the skin, such as allergic dermatitis, cutaneous itch and pain, and

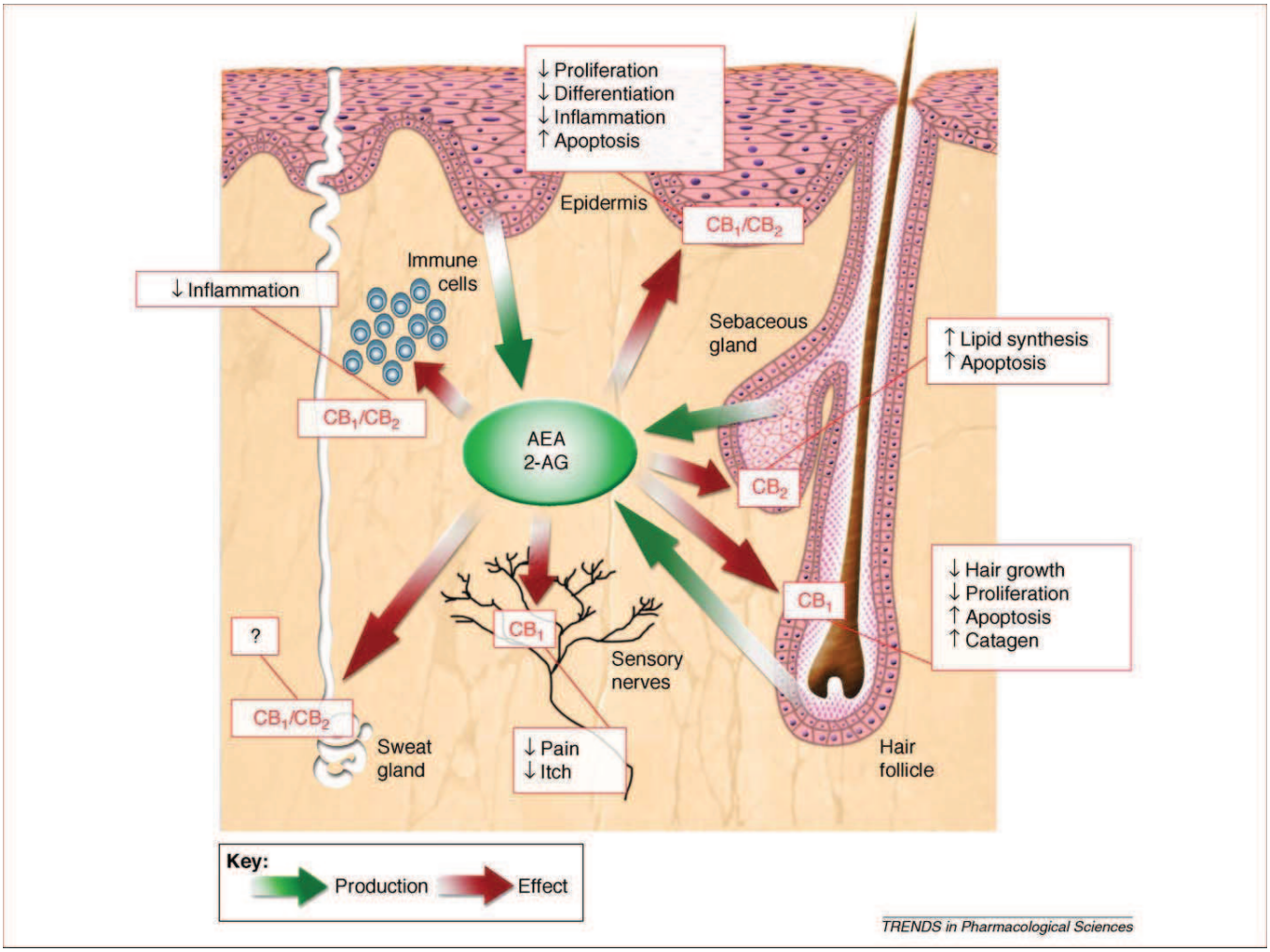

Figure 1. Functions of the cutaneous ECS. Prototypic endocannabinoids such as anandamide (*N*-arachidonoylethanolamine; AEA) and 2-arachidonoylglycerol (2-AG) are produced locally in various cellular compartments of the skin (i.e. epidermis, sebaceous gland, hair follicle) (green arrows). These endocannabinoids, via binding to cannabinoid receptor subtypes 1 and/or 2 (CB_1/CB_2), constitutively control the proper and well-balanced cutaneous functions (e.g. sensation, growth, survival, immune competence and/or tolerance) (red arrows). For example, activation of CB_1 and CB_2 on epidermal keratinocytes by locally produced endocannabinoids results in the suppression of cellular proliferation, differentiation and the release of inflammatory mediators as well as the induction of apoptosis. Likewise, endocannabinoids, via CB_1/CB_2, inhibit inflammatory responses of resident and infiltrating immune cells. Furthermore, activation of CB_1 in the hair follicle by AEA attenuates hair shaft elongation and intrafollicular proliferation, whereas it stimulates apoptosis and the development of catagen regression. On another member of the pilosebaceous unit (i.e. on the sebaceous gland-derived sebocytes), locally released endocannabinoids markedly enhance lipid production and apoptosis via CB_2. Finally, skin-derived endocannabinoids inhibit various sensory phenomena (e.g. pain and itch) via CB_1 expressed on sensory afferent nerves.

neoplastic cell growth, are discussed. Future preclinical and clinical research directions and strategies to therapeutically target ECS for the management of various skin diseases are also envisioned.

The ECS and the skin

Identification of the main cannabinoid receptors (CB_1 and CB_2), their endogenous lipid ligands (endocannabinoids), biosynthetic pathways and metabolizing enzymes (collectively termed the ECS) [8–10], coupled with the discovery and/or rational design of numerous exogenous ligands for CB receptors [11], has triggered an exponential growth in studies exploring the continuously growing regulatory functions of this newly discovered physiological system both in health and disease [12–14].

Excitingly, modulating the activity of the ECS has turned out to hold tremendous therapeutic potential for a multitude of diseases and pathological conditions affecting humans [13,15,16], ranging from inflammatory [17], neurodegenerative [18–20], gastrointestinal [21,22], liver [23,24], cardiovascular disorders [25,26] and obesity [27,28], to ischemia/reperfusion injury [29], cancer [30] and pain [31].

The most extensively studied endocannabinoids are anandamide (*N*-arachidonoylethanolamine, AEA) and 2-arachidonoylglycerol (2-AG) [8,32]. Multiple pathways are involved in synthesis and cellular uptake of these lipid mediators; these are described in several excellent recent reviews [10,33,34] and beyond the scope of this article. The most common degradation pathways for AEA and 2-AG are the fatty acid amid hydrolase (FAAH) and monoacylglycerol lipase (MAGL) enzymes [10]. Endocannabinoids, similar to Δ^9-tetrahydrocannabinol (THC; the main active ingredient of the plant *Cannabis sativa*), predominantly exert their physiological effects via two main G-protein-coupled cannabinoid receptors; however,

Table 1. Functions of the cutaneous ECS

Experimental system	Main findings	Pharmacological tools employed	Notes	Refs
***In vitro* cell and organ cultures**				
Human epidermal keratinocytes (NHEK, HaCaT)	CB_1 and CB_2 are expressed NAPE-PLD, AMT/EMT and FAAH are expressed AEA is produced AEA inhibits proliferation and induces apoptosis via CB_1 Synthetic cannabinoids do not affect proliferation AEA inhibits differentiation via CB_1	AEA, NADA: endocannabinoids WIN-55 212–2: mixed CB_1/CB_2 agonist JWH-133: selective CB_2 agonist SR141716A: selective CB_1 antagonist/inverse agonist SR144528: selective CB_2 antagonist/inverse agonist	CB_1 and CB_2 are expressed on human and mouse skin cell populations *in situ*	[36–45]
Human and murine transformed (tumorigenic) epidermal keratinocytes	Human: phyto- and synthetic cannabinoids inhibit proliferation (CB_1/CB_2 independent) Murine: synthetic cannabinoids inhibit proliferation and induce apoptosis via CB_1 and CB_2	HU210, WIN-55 212–2: mixed CB_1/CB_2 agonists JWH-015, JWH-133, BML-190: selective CB_2 agonists THC, cannabidiol, cannabinol and cannabigerol: phytocannabinoids SR141716A: selective CB_1 antagonist/inverse agonist SR144528: selective CB_2 antagonist/inverse agonist	Murine skin produces AEA and 2-AG, which express NAPE-PLD, AMT/EMT and FAAH	[36,47,53]
Human organ-cultured hair follicles	CB_1 is expressed AEA and 2-AG are produced AEA (unlike 2-AG) and THC inhibit hair shaft elongation and proliferation, and induce intraepithelial apoptosis and catagen regression via CB_1	AEA, 2-AG: endocannabinoids, mixed CB_1/CB_2 agonists THC: phytocannabinoid, mixed CB_1/CB_2 agonists AM-251: selective CB_1 antagonist/inverse agonist	CB_1 and CB_2 are expressed on human hair follicle *in situ*	[36,37,41]
Human sebaceous-gland-derived SZ95 sebocytes	CB_2 is expressed AEA and 2-AG are produced AEA and 2-AG stimulate lipid/sebum production and apoptosis via CB_2	AEA, 2-AG: mixed CB_1/CB_2 agonists ACEA: selective CB_1 agonists JWH-015: selective CB_2 agonists AM-251: selective CB_1 antagonist/inverse agonist AM-630: selective CB_2 antagonist/inverse agonist	CB_1 and CB_2 are expressed on human sebaceous gland *in situ*	[36,37,42]
***In vivo* animal models**				
Tumor induction in mice	Synthetic CB_1/CB_2 agonists inhibit tumor growth, angiogenesis and metastasis, and induce apoptosis in non-melanoma tumors and melanomas	THC: phytocannabinoid WIN-55 212–2: mixed CB_1/CB_2 agonist JWH-133: selective CB_2 agonist SR141716A: selective CB_1 antagonist/inverse agonist SR144528, AM-630: selective CB_2 antagonists/inverse agonist	Skin tumors (basal and squamous cell carcinomas, melanoma) express CB_1 and CB_2	[36,39]
Cutaneous contact allergic dermatitis	$CB_{1/2}$ double knockout mice display exacerbated allergic skin inflammation FAAH-deficient display reduced allergic response in the skin Locally administered CB antagonists exacerbate allergic inflammation Synthetic CB agonists and THC suppress inflammation	THC: phytocannabinoid HU210: mixed CB_1/CB_2 agonist HU308: selective CB_2 agonist SR141716A: selective CB_1 antagonist/inverse agonist SR144528: selective CB_2 antagonist/inverse agonist	Skin levels of endocannabinoids increase in contact dermatitis	[40]
IgE-induced cutaneous anaphylaxis	Synthetic CB agonists and PEA suppress inflammation	WIN-55 212–2, HU-210, CP 55 940: mixed CB_1/CB_2 agonists JWH-133: selective CB_2 agonist SR141716A, AM-281: selective CB_1 antagonists/inverse agonist SR144528, AM-630: selective CB_2 antagonists/inverse agonist		[57]
Acute and chronic contact dermatitis	CB_2 antagonist attenuates inflammation	2-AG: endocannabinoid, mixed CB_1/CB_2 agonists AM-251: selective CB_1 antagonist/inverse agonist SR144528: selective CB_2 antagonists/inverse agonist	Skin level of 2-AG increases in contact dermatitis	[61]
Allergic contact dermatitis	CB_2 knockout mice display suppressed allergic skin inflammation Orally administered CB_2 antagonist attenuates inflammation	2-AG: endocannabinoid, mixed CB_1/CB_2 agonists HU308: selective CB_2 agonist SR144528, JTE-907: selective CB_2 antagonists/inverse agonists		[62,63]

Table 1 (*Continued*)

Experimental system	Main findings	Pharmacological tools employed	Notes	Refs
UV-induced skin carcinogenesis and inflammation	$CB_{1/2}$ double knockout mice display attenuated UVB-induced skin carcinogenesis and inflammation	WIN-55 212–2: mixed CB_1/CB_2 agonist		[55]
Bleomycin-induced dermal fibrosis	CB_2 knockout mice display increased dermal fibrosis and inflammation	AM-630: selective CB_2 antagonists/inverse agonist	Leukocyte expression of CB_2 critically influences experimental fibrosis	[64]
	CB_2 antagonist increased, agonist decreased the fibrosis and inflammation	JWH-133: selective CB_2 agonist		

Abbreviations: 2-AG, 2-arachidonoylglycerol; AEA, arachidonoylethanolamide; AMT/EMT, anadamide/endocannabinoid membrane transporter; $CB_{1/2}$, type-1 and -2 cannabinoid receptor; FAAH, fatty acid amide hydrolase; IgE, immunoglobulin E; NADA, *N*-arachidonoyldopamine; NAPE, *N*-acylphosphatidylethanolamines; NAPE-PLD, NAPE-hydrolyzing phospholipase D; NHEK, normal human epidermal keratinocytes; PEA, *N*-palmitoylethanolamine; THC, Δ^9-tetrahydrocannabinol; UV, ultraviolet.

numerous additional signaling mechanisms and receptor systems (e.g. transient receptor potential cation channel, subfamily V, member 1; TRPV1) might also be involved [35]. Initially, the CB_1-mediated effects were described centrally and CB_1 receptors were thought to be restricted to the central nervous system, whereas CB_2 was first identified at the periphery in immune cells. Excitingly, findings over the past decade have clearly demonstrated that functional ECS is present almost in all peripheral organ systems [13–15].

Indeed, components of the ECS have also been discovered in the skin recently (Figure 1). Both CB_1 and CB_2 immunoreactivities were observed on numerous human and murine skin cell populations *in situ* such as on cutaneous nerve fibers, mast cells, epidermal keratinocytes and cells of the adnexal tissues [36–42]. Similarly, both CB_1 and CB_2 have been identified (at protein and mRNA levels) on cultured human primary (NHEK) and HaCaT keratinocytes [43–45]. Interestingly, in organ-cultured human hair follicles, exclusive expression of CB_1 was described [41], whereas CB_2 expression (unlike CB_1) was found on human sebaceous gland-derived SZ95 sebocytes [42]. AEA and 2-AG were detected in rodent skin [40,46], as well as in human organ-cultured hair follicles [41] and SZ95 sebocytes [42]. AEA, along with its transporter (AMT/EMT), synthetic and metabolizing enzymes (NAPE-PLD and FAAH) were also identified in cultured NHEK and HaCaT keratinocytes [43], and in murine epidermal cells/skin [40,47]. TRPV1, as key peripheral integrator of various sensory phenomena (e.g. pain, heat, itch), was originally described on nociceptive sensory neurons as a molecular target for capsaicin, the pungent vanilloid ingredient of hot chili peppers [48]. More recently, similar to $CB_{1/2}$, TRPV1 was also found on numerous non-neuronal cells types including human skin epidermal keratinocytes, dermal mast cells, Langerhans cells, sebocytes, sweat gland epithelium and various keratinocyte populations of the hair follicle [49–52]. TRPV1 might have important roles in skin health and in certain skin disorders, especially in ones associated with inflammation, pain and itch (e.g. in various types of dermatitis) [3–5,7]. However, the involvement of TRPV1-coupled signaling in the cellular actions of AEA on cell growth, differentiation, proliferation and survival might exert marked cell-type specificity in the skin, and depending on the cell type it can be synergistic, antagonistic or independent from the $CB_{1/2}$ receptor stimulation [41,42,45,51,52]. The discussion of these complex effects is beyond the scope of this brief synopsis.

Role of the cutaneous ECS in skin growth control, survival and differentiation

Recent intriguing data suggest that the cutaneous ECS is fully functional (Figure 1). Indeed, as described later, the ECS has been implicated in the regulation of skin cell proliferation, survival and differentiation, the delicate balance of which is a key determinant of proper cutaneous homeostasis. Furthermore, fine-tuning of the endocannabinoid tone appears to be a key factor in modulating cutaneous growth and differentiation (Table 1).

Epidermis

Both phytocannabinoids and synthetic CB agonists inhibited proliferation of cultured transformed (HPV-16 E6/E7) human epidermal keratinocytes; yet, these effects were CB_1- and CB_2-independent [53]. On tumorigenic transformed murine keratinocytes (PDV.C57 and HaCa4), by contrast, the growth-inhibitory actions of synthetic CB agonists were prevented by both CB_1 and CB_2 antagonists [36]. It is also noteworthy that, on these latter mouse keratinocytes, the growth-inhibitory action of the cannabinoids was accompanied by CB_1- and CB_2-dependent apoptosis [36]. Interestingly, synthetic CB_1 and CB_2 agonists were ineffective in modulating cellular growth of both cultured NHEKs and non-tumorigenic human (HaCaT) and murine (MCA3D) keratinocytes [36].

By contrast, a recent study found that AEA markedly inhibited cellular growth and induced dose- and CB_1-dependent apoptosis in human HaCaT keratinocytes [45]. Consistently with this report, the ECS also regulates human epidermal differentiation, probably via CB_1-dependent mechanisms. Maccarrone *et al.* [43] have elegantly demonstrated that AEA, locally produced in the cells, inhibited the differentiation of cultured NHEK and HaCaT keratinocytes, as evidenced by the transcriptional downregulation of keratin 1, keratin 5, involucrin and transglutaminase-5 [44] and suppression of the formation of cornified envelopes. They have also shown that these effects were mediated by increasing DNA methylation through mitogen-activated protein kinase (MAPK)-dependent pathways (p38, p42/44) triggered by CB_1 activation [44]. Involvement of CB_1 in the regulation of epidermal differentiation is also suggested by the differential *in situ* expression of CB_1 in the human epidermis, being higher in the more differentiated (granular and spinous) layers [36,37].

Skin appendages

The pilosebaceous unit of the human skin, comprising the intimately localized hair follicle (HF) and the sebaceous gland (SG), can be regarded as the 'brain' of the skin because it controls a wide-array of the biological functions of this organ (from stem-cell supply through immunomodulation to cytokine production) [1–3]. Recent studies have suggested that the ECS might also have a regulatory role in the human pilosebaceous unit. Both human organ-cultured HFs and human SG-derived SZ95 sebocytes have been reported to produce AEA and 2-AG [41,42]. Furthermore, AEA and THC (but not 2-AG) dose-dependently inhibited hair shaft elongation and the proliferation of hair matrix keratinocytes. Cannabinoids also induced intraepithelial apoptosis and premature HF regression (characteristic signs of catagen transformation in the HF), processes that could be inhibited by a selective CB_1 antagonist. Because CB_1, unlike CB_2, is expressed in a hair-cycle-dependent manner in the human HF epithelium, these data support the idea that human HFs exploit a CB_1-mediated endocannabinoid signaling system that might act as an autocrine–paracrine negative regulator of human hair growth. Consistently with this idea, a recent study has demonstrated that CB_1 receptor antagonists do, indeed, induce hair growth in mice [54].

Interestingly, differential CB_2-dependent regulation by endocannabinoids has been observed in human immortalized SZ95 sebocytes [42]. In accordance with these findings, SZ95 sebocytes predominantly express CB_2, suggesting that CB_2 is largely expressed in undifferentiated epithelial cells of the human SG *in situ* [37,42]. Both AEA and 2-AG enhanced lipid production and induced (chiefly apoptosis-driven) cell death, hallmarks of sebocyte differentiation and hence a model of holocrine sebum production [42] via CB_2-coupled signaling involving the MAPK pathway. Moreover, endocannabinoids also upregulated the expression of key genes involved in lipid synthesis (e.g. peroxisome proliferator-activated receptor [PPAR] transcription factors and some of their target genes). Because cells with 'silenced' CB_2 exhibited significantly suppressed basal lipid production, these results collectively suggest that human sebocytes utilize an autocrine–paracrine, endogenously (and probably constitutively) active, CB_2-mediated endocannabinoid signaling system for positively regulating lipid production and cell death.

Skin tumorigenesis

Accumulating recent evidence also implicates the ECS in the regulation of growth of skin cells *in vivo*. Casanova *et al.* [36] have demonstrated that various human skin tumors (e.g. basal cell carcinoma, squamous cell carcinoma) express both CB_1 and CB_2. Local administration of synthetic CB_1 and CB_2 agonists induced growth inhibition of malignant skin tumors generated by intradermal inoculation of tumorigenic PDV.C57 mouse keratinocytes into nude mice. This growth inhibition was accompanied by enhanced intra-tumor apoptosis and impaired tumor vascularization (altered blood vessel morphology, decreased expression of pro-angiogenic factors such as VEGF, placental growth factor and angiopoietin 2). Consistently, cannabinoids were also reported to inhibit the *in vivo* growth of melanomas that express CB_1 and CB_2 by decreasing growth, proliferation, angiogenesis and metastasis formation, while increasing apoptosis [39]. By contrast, a recent study of Zheng *et al.* [55] suggested that CB receptors and the related signaling pathways might be involved in the promotion of *in vivo* skin carcinogenesis. Using CB_1/CB_2 double gene-deficient mice, Zheng *et al.* [55] demonstrated that an absence of CB_1 and CB_2 receptors resulted in a marked decrease in UVB-induced skin carcinogenesis. They also found that a marked attenuation of UVB-induced activation of MAPKs and nuclear factor-κB was also associated with CB_1 and CB_2 deficiency.

Collectively, these studies suggest that the cutaneous ECS, as in other organs, might act to tonically modulate cell growth, proliferation and death [30,56] (Figure 1).

Role of the cutaneous ECS in allergic, inflammatory and fibrotic functions

Since the original discovery of the CB_2 receptors in immune cells, much evidence using various CB receptor agonists and antagonists or compounds that enhance the levels of endocannabinoids by decreasing their metabolism suggest that the ECS has numerous important immune modulatory effects (e.g. suppression of production of various cytokines, chemokines, arachidonic acid-derived pro-inflammatory metabolites and nitric oxide) during inflammation [17]. Although some controversies do exist in the field, it is generally recognized that the ECS exerts protective functions in large number of acute and chronic inflammatory diseases [13,17].

A recent study by Karsak *et al.* [40] has suggested that the ECS exerts a protective role in allergic inflammation of the skin. Using an animal model for cutaneous contact (allergic) hypersensitivity, Karsak *et al.* [40] elegantly demonstrated that the skin level of endocannabinoids was increased in contact dermatitis. They also found that mice lacking both CB_1 and CB_2 (or treated with antagonists of these receptors) displayed exacerbated allergic inflammatory response. The existence of the ECS-mediated protection was also supported by a reduced allergic response in the skin of FAAH-deficient mice, which have increased levels of the endocannabinoid AEA. Moreover, the skin inflammation was suppressed by locally administered THC [40]. Similarly, in a murine model of passive IgE-induced cutaneous anaphylaxis, both synthetic non-selective CB agonists and saturated *N*-acylethanolamine derivatives (homologues of *N*-palmitoyl ethanolamine, PEA) exerted marked anti-inflammatory properties *in vivo* [57]. Notably, PEA does not act directly at CB_1, CB_2 or TRPV1, but it can markedly augment the effects of AEA at these receptors [58,59] as well as directly activate PPARα [60].

By contrast, using different animal models for acute and chronic contact dermatitis, Oka *et al.* [61] reported elevated 2-AG levels in the diseased skin. The symptoms of skin inflammation were markedly attenuated by CB_2 (but not CB_1) antagonists [61]. Likewise, others using different animal models (Table 1) to induce allergic contact dermatitis reported a decrease in the cutaneous inflammation of

CB_2-deficient mice [62], and similar suppression of the inflammatory response by orally administered CB_2 antagonists was also observed [62,63]. Consistently, Zheng *et al.* [55], using CB_1/CB_2 double gene-deficient mice, recently reported that CB receptors are involved not only in the promotion of *in vivo* skin carcinogenesis (see earlier) but also in the UVB-induced cutaneous inflammatory processes. The reasons for the conflicting data on the role of CB_1 and CB_2 in cutaneous allergic responses and tumorigenesis are not clear, but they could, in part, be explained by the differences in the experimental models used (Table 1) and by an emerging scenario, according to which in some physiological functions 'too much' endocannabinoid tone can be as bad as 'too little', and both 'enhancers' and 'reducers' might be useful for the same type of disorder depending on its phase or exact cause [14]. The use of CB_1 and/or CB_2 antagonists, which are also inverse agonists [11] (Table 1), might further complicate the interpretation of some of these findings.

In a recent study Akhmetshina *et al.* [64] have demonstrated that CB_2 knockout mice or controls treated with CB_2 antagonist were more sensitive to bleomycin-induced dermal fibrosis compared with wild types and exhibited increased dermal thickness and leukocyte counts in the lesional skin. The phenotype of knockouts was mimicked by transplantation of knockout bone marrow into control mice, whereas CB_2 knockouts transplanted with bone marrow from wide-type mice did not display an increased sensitivity to bleomycin-induced fibrosis, indicating that leukocyte expression of CB_2 critically influences experimental fibrosis [64]. Decreased dermal fibrosis and inflammation was observed upon treatment with the CB_2 agonist, suggesting a potential therapeutic utility of selective CB_2 agonists for the treatment of early inflammatory stages of systemic sclerosis.

Role of the ECS in cutaneous sensory functions: pain and itch

The ECS has a crucial role in central and peripheral processing, and in the control of such skin-derived sensory phenomena as pain and itch. Synthetic CB agonists and/or endocannabinoids exert potent analgesic effects in both humans and animals by activation of CB_1 and/or CB_2 and possibly other receptors (e.g. TRPV1) at sensory nerve terminals and/or inflammatory cells. However, the detailed discussion of these effects is beyond the scope of this article and we would like to refer readers to overviews on this subject [31,65–67].

Perspectives in the ECS-targeted management of skin diseases

The aforementioned preclinical data encourage one to systematically explore whether ECS-modulating drugs can be exploited in the management of common skin disorders. However, the pleiotropic nature and strong cell-type dependence of the cutaneous ECS-mediated functions will require careful judgment for patient selection and indications. In this section, we review preliminary data and discuss the possible applications of ECS-targeted therapies (Figure 2; Table 2).

Psoriasis and skin tumors: aiming to increase ECS tone

Data showing that the cutaneous ECS tonically inhibits cell growth and angiogenesis and induces apoptosis in most of the skin cell types, and that both human non-melanoma and melanoma tumors express considerable amounts of CB_1 and CB_2 [36,39,41,42,45,53], now warrant proof-of-principle studies to test the therapeutic value of cannabinoid agonists in the clinical management of hyperproliferative skin disease (e.g. psoriasis, which is characterized by a highly accelerated turnover of epidermal keratinocyte proliferation) and skin tumors of various cutaneous cell origins. Furthermore, these interventions (as detailed later) might also suppress skin inflammation seen in psoriasis.

Hair growth disorders: aiming to increase or decrease ECS tone

The novel concept that human HFs are both targets and sources of endocannabinoids, which, via CB_1 establish an autocrine–paracrine system for negatively regulating hair growth, invites careful investigation of the growth-inhibitory effects of CB_1 agonists in the putative management of unwanted hair growth such as hirsutism. Likewise, future exploitation of CB_1-antagonist-based adjuvant treatment options in the clinical management of alopecia areata and effluvium is also of potential interest.

Acne and seborrhea

Acne and seborrhea, the most common dermatological diseases, are characterized by highly elevated lipid (sebum) production of the SGs. In light of the aforementioned data that CB_2 activation in the SG by locally produced endocannabinoids markedly enhances lipid synthesis [42], it is envisaged that those agents that suppress the local production of endocannabinoids (NAPE-PLD and/or DAGL inhibitors) in the diseased SG and/or inhibit CB_2 on the sebocytes (CB_2 antagonists) might have

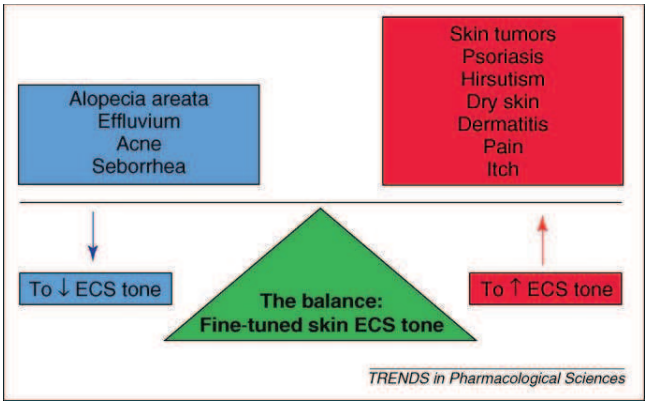

Figure 2. ECS-targeted approaches in skin diseases. Modulations of the fine-tuned tone of the cutaneous endocannabinoid system (ECS) could have therapeutic values in the management of a large variety of human skin diseases. For example, suppression of the skin ECS tone (using e.g. CB antagonists and/or agents that attenuate the local production of endocannabinoids) could be used in the therapy of certain hair growth (e.g. forms of alopecia, effluvium) and sebaceous gland disorders (e.g. acne, seborrhea). Conversely, augmentation of the tone of the cutaneous ECS (using e.g. CB agonists and/or agents that stimulate the local production of endocannabinoids) could be beneficial in the treatment of various benign and malignant skin tumors, hyperproliferative skin diseases (e.g. psoriasis), excessive hair growth (e.g. hirsutism), different forms of dermatitis, dry skin conditions and sensory phenomena (e.g. pain, itch).

Table 2. Possible ECS-targeted approaches in skin diseases

Disease	Target cell population	Target receptor	Possible approach	Expected effects
Skin tumors	Transformed skin cell	CB_1 and CB_2	CB agonists or agents that increase ECS tone	Suppression of growth, angiogenesis and metastasis; induction of apoptosis
Psoriasis	Keratinocyte, immune cell	CB_1 and CB_2	CB agonists or agents that increase ECS tone	Suppression of keratinocyte proliferation and inflammation
Unwanted hair growth (e.g. hirsutism)	Hair follicle epithelium	CB_1	CB_1 agonists or agents that increase ECS tone	Suppression of hair growth, induction of intrafollicular apoptosis and catagen regression
Alopecia areata, effluvium	Hair follicle epithelium	CB_1	CB_1 antagonists or agents that decrease ECS tone	Stimulation of hair shaft elongation; suppression of intrafollicular apoptosis and catagen regression; induction of anagen
Acne, seborrhea	Sebaceous gland epithelium	CB_2	CB_2 antagonists or agents that decrease ECS tone	Inhibition of sebum/lipid production in the sebaceous gland
Dry skin	Sebaceous gland epithelium	CB_2	CB_2 agonists or agents that increase ECS tone	Stimulation of sebum/lipid production in the sebaceous gland
Dermatitis	Infiltrating immune cell, keratinocyte, sebocyte	CB_1 and CB_2	CB agonists or agents that increase ECS tone	Suppression of immune/inflammatory processes
Systemic sclerosis (scleroderma)	Infiltrating immune cells, fibroblasts	CB_2	CB_2 agonists or agents that increase ECS tone	Suppression of immune/inflammatory processes and fibrosis
Pain	Sensory neuron, keratinocyte, other skin cells	CB_1 and CB_2	CB agonists or agents that increase ECS tone	Suppression of release a algogenic substances; inhibition of transmission of signals in the nervous system
Itch	Sensory neurons, keratinocyte, sebocyte, other skin cells	CB_1 and CB_2	CB agonists or agents that increase ECS tone	Suppression of release a pruritogenic substances; inhibition of transmission of signals in the nervous system

$CB_{1/2}$, type-1 and -2 cannabinoid receptor; ECS, endocannabinoid system.

therapeutic values. Furthermore, transdermal penetration of cannabinoids is well established [68,69], raising the possibility that these agents could be efficiently applied topically to the skin in the form of a cream.

Dry skin and related conditions

Conversely, applications of formulations containing cannabinoids that stimulate CB_2 (CB2 agonists) in the SG, and/or augment the local production of endocannabinoids and/or inhibit their degradation (FAAH and/or MAGL inhibitors) in the SG might act as novel therapeutic tools in excessively dry skin by enhancing fat production in the SG (and, hence, might attract the interest of the cosmetics industry). It is important to note, however, that ideally these topical medications should contain such phyto- and/or synthetic ECS-acting substances that, on absorption to the blood, do not penetrate the brain and hence do not exert psychoactive effects. It is also noteworthy that skin dryness is a leading cause of and/or accompanied by other skin diseases and symptoms such as itching and dermatitis. Therefore, such cannabinoid-containing creams could also be beneficial under these conditions.

With respect to the possible treatment of itching, it is most promising that Stander *et al.* [65] have reported that topically applied emollient cream containing PEA markedly (>86%) reduced itching associated with dry skin. Therefore, it can be hypothesized that the fat-production-promoting actions of cannabinoids might, at least in part, contribute to the beneficial effects seen in these patients.

Dermatitis

Topical formulations that contain cannabinoid ligands (or that enhance the cutaneous ECS tone) could have therapeutic values in skin inflammations. Indeed, recently, a new drug containing PEA has been approved by the FDA for the treatment of dermatitis [70]. Moreover, a recent pilot study on 20 pediatric patients suffering from atopic dermatitis aimed to assess the efficacy and safety of the twice daily application of a topical emulsion containing 2% adelmidrol, a PEA analog. Excitingly, this study showed an 80% increase in symptom resolution [70,71].

Systemic sclerosis

A recent experimental study has suggested that CB_2 agonists could represent a promising approach for the treatment of early inflammatory stages of systemic sclerosis (scleroderma) [64].

Pain and itch

As detailed elsewhere, various cannabinoid agonists in addition to agents that increase the cutaneous levels of endocannabinoids have been effectively used in various models of pain and itch [13,31,65–67].

Conclusions and future directions in experimental and clinical research

Collectively, it seems that the main physiological function of the cutaneous ECS is to constitutively control the proper and well-balanced proliferation, differentiation and survival, as well as immune competence and/or tolerance, of skin cells. Pathological alterations in the activity of the fine-tuned cutaneous ECS might promote or lead to the development of certain skin diseases. Therefore, it is envisaged (this is also strongly supported by pilot studies) that the targeted manipulation of the ECS (aiming to normalize the unwanted skin cell growth, sebum production and skin inflammation) might be beneficial in a multitude of human skin diseases. However, to predict the real therapeutic potential and translate the exciting preclinical observations discussed earlier into clinical practice, numerous important questions should carefully be addressed (Box 2).

Box 2. Outstanding questions

- Are all members of the ECS functionally expressed in the human skin and appendages?
- How do various endogenous mechanisms (e.g. hormones, cytokines) that were shown to be involved in the control of human skin homeostasis regulate the activity of ECS?
- Is there any crosstalk between the ECS and the endovanilloid system in the human skin?
- Is there any alteration in the expression levels and patterns of elements of the ECS in various human skin diseases?

Nevertheless, targeting the cutaneous ECS for therapeutic gain remains an intriguing and provocative possibility warranting future studies.

Acknowledgements

This publication was supported by Intramural Research Program of the National Institutes of Health/National Institute on Alcohol Abuse and Alcoholism (www.nih.gov; www.niaaa.nih.gov; to P.P.) and by the Hungarian Scientific Research Fund (www.otka.hu; OTKA 63153 to T.B.).

References

1 Roosterman, D. *et al.* (2006) Neuronal control of skin function: the skin as a neuroimmunoendocrine organ. *Physiol. Rev.* 86, 1309–1379
2 Paus, R. *et al.* (2006) Frontiers in pruritus research: scratching the brain for more effective itch therapy. *J. Clin. Invest.* 116, 1174–1186
3 Paus, R. *et al.* (2006) Neuroimmunoendocrine circuitry of the 'brain-skin connection'. *Trends Immunol.* 27, 32–39
4 Ansel, J.C. *et al.* (1997) Interactions of the skin and nervous system. *J. Investig. Dermatol. Symp. Proc.* 2, 23–26
5 Luger, T.A. (2002) Neuromediators–a crucial component of the skin immune system. *J. Dermatol. Sci.* 30, 87–93
6 Steinhoff, M. *et al.* (2005) Proteinase-activated receptors: transducers of proteinase-mediated signaling in inflammation and immune response. *Endocr. Rev.* 26, 1–43
7 Steinhoff, M. *et al.* (2006) Neurophysiological, neuroimmunological, and neuroendocrine basis of pruritus. *J. Invest. Dermatol.* 126, 1705–1718
8 Mechoulam, R. *et al.* (1998) Endocannabinoids. *Eur. J. Pharmacol* 359, 1–18
9 Howlett, A.C. *et al.* (2002) International Union of Pharmacology. XXVII. Classification of cannabinoid receptors. *Pharmacol. Rev.* 54, 161–202
10 Di Marzo, V. (2008) Endocannabinoids: synthesis and degradation. *Rev. Physiol. Biochem. Pharmacol.* 160, 1–24
11 Pertwee, R.G. (2005) Pharmacological actions of cannabinoids. *Handb. Exp. Pharmacol.* 1–51
12 Mackie, K. (2006) Cannabinoid receptors as therapeutic targets. *Annu. Rev. Pharmacol. Toxicol.* 46, 101–122
13 Pacher, P. *et al.* (2006) The endocannabinoid system as an emerging target of pharmacotherapy. *Pharmacol. Rev.* 58, 389–462
14 Di Marzo, V. (2008) Targeting the endocannabinoid system: to enhance or reduce? *Nat. Rev. Drug Discov.* 7, 438–455
15 Pertwee, R.G. (2005) The therapeutic potential of drugs that target cannabinoid receptors or modulate the tissue levels or actions of endocannabinoids. *AAPS J.* 7, E625–E654
16 Pertwee, R.G. (2009) Emerging strategies for exploiting cannabinoid receptor agonists as medicines. *Br. J. Pharmacol.* 156, 397–411
17 Klein, T.W. (2005) Cannabinoid-based drugs as anti-inflammatory therapeutics. *Nat. Rev. Immunol.* 5, 400–411
18 Mechoulam, R. *et al.* (2002) Endocannabinoids and neuroprotection. *Sci. STKE* 2002, RE5
19 Centonze, D. *et al.* (2007) The endocannabinoid system in targeting inflammatory neurodegenerative diseases. *Trends Pharmacol. Sci.* 28, 180–187
20 Baker, D. and Pryce, G. (2008) The endocannabinoid system and multiple sclerosis. *Curr. Pharm. Des.* 14, 2326–2336
21 Izzo, A.A. and Camilleri, M. (2008) Emerging role of cannabinoids in gastrointestinal and liver diseases: basic and clinical aspects. *Gut* 57, 1140–1155
22 Wright, K.L. *et al.* (2008) Cannabinoid CB2 receptors in the gastrointestinal tract: a regulatory system in states of inflammation. *Br. J. Pharmacol.* 153, 263–270
23 Mallat, A. and Lotersztajn, S. (2008) Endocannabinoids and liver disease. I. Endocannabinoids and their receptors in the liver. *Am. J. Physiol. Gastrointest. Liver Physiol.* 294, G9–G12
24 Pacher, P. and Gao, B. (2008) Endocannabinoids and liver disease. III. Endocannabinoid effects on immune cells: implications for inflammatory liver diseases. *Am. J. Physiol. Gastrointest. Liver Physiol.* 294, G850–G854
25 Mach, F. *et al.* (2008) Cannabinoid receptors in acute and chronic complications of atherosclerosis. *Br. J. Pharmacol.* 153, 290–298
26 Pacher, P. *et al.* (2008) Modulation of the endocannabinoid system in cardiovascular disease: therapeutic potential and limitations. *Hypertension* 52, 601–607
27 Di Marzo, V. (2008) The endocannabinoid system in obesity and type 2 diabetes. *Diabetologia* 51, 1356–1367
28 Engeli, S. (2008) Dysregulation of the endocannabinoid system in obesity. *J. Neuroendocrinol.* 20 (Suppl. 1), 110–115
29 Pacher, P. and Hasko, G. (2008) Endocannabinoids and cannabinoid receptors in ischaemia-reperfusion injury and preconditioning. *Br. J. Pharmacol.* 153, 252–262
30 Guzman, M. (2003) Cannabinoids: potential anticancer agents. *Nat. Rev. Cancer* 3, 745–755
31 Walker, J.M. and Hohmann, A.G. (2005) Cannabinoid mechanisms of pain suppression. *Handb. Exp. Pharmacol.* 509–554
32 Mechoulam, R. and Hanus, L. (2000) A historical overview of chemical research on cannabinoids. *Chem. Phys. Lipids* 108, 1–13
33 Ahn, K. *et al.* (2008) Enzymatic pathways that regulate endocannabinoid signaling in the nervous system. *Chem. Rev.* 108, 1687–1707
34 Liu, J. *et al.* (2008) Multiple pathways involved in the biosynthesis of anandamide. *Neuropharmacology* 54, 1–7
35 Howlett, A.C. (2005) Cannabinoid receptor signaling. *Handb. Exp. Pharmacol.* 53–79
36 Casanova, M.L. *et al.* (2003) Inhibition of skin tumor growth and angiogenesis *in vivo* by activation of cannabinoid receptors. *J. Clin. Invest.* 111, 43–50
37 Stander, S. *et al.* (2005) Distribution of cannabinoid receptor 1 (CB1) and 2 (CB2) on sensory nerve fibers and adnexal structures in human skin. *J. Dermatol. Sci.* 38, 177–188
38 Ibrahim, M.M. *et al.* (2005) CB2 cannabinoid receptor activation produces antinociception by stimulating peripheral release of endogenous opioids. *Proc. Natl. Acad. Sci. U. S. A.* 102, 3093–3098
39 Blazquez, C. *et al.* (2006) Cannabinoid receptors as novel targets for the treatment of melanoma. *FASEB J.* 20, 2633–2635
40 Karsak, M. *et al.* (2007) Attenuation of allergic contact dermatitis through the endocannabinoid system. *Science* 316, 1494–1497
41 Telek, A. *et al.* (2007) Inhibition of human hair follicle growth by endo- and exocannabinoids. *FASEB J.* 21, 3534–3541
42 Dobrosi, N. *et al.* (2008) Endocannabinoids enhance lipid synthesis and apoptosis of human sebocytes via cannabinoid receptor-2-mediated signaling. *FASEB J.* 22, 3685–3695
43 Maccarrone, M. *et al.* (2003) The endocannabinoid system in human keratinocytes. Evidence that anandamide inhibits epidermal differentiation through CB1 receptor-dependent inhibition of protein kinase C, activation protein-1, and transglutaminase. *J. Biol. Chem.* 278, 33896–33903
44 Paradisi, A. *et al.* (2008) Anandamide regulates keratinocyte differentiation by inducing DNA methylation in a CB1 receptor-dependent manner. *J. Biol. Chem.* 283, 6005–6012
45 Biro, T. *et al.* (2006) The endocannabinoid/endovanilloid anandamide regulates proliferation and apoptosis of human keratinocytes via novel signaling interactions between vanilloid receptor-1 (TRPV1) and cannabinoid receptor-1 (CB1). *J. Invest. Dermatol.* 126, 95
46 Calignano, A. *et al.* (1998) Control of pain initiation by endogenous cannabinoids. *Nature* 394, 277–281
47 Berdyshev, E.V. *et al.* (2000) Stress-induced generation of N-acylethanolamines in mouse epidermal JB6 P+ cells. *Biochem. J.* 346, 369–374
48 Szallasi, A. and Blumberg, P.M. (1999) Vanilloid (Capsaicin) receptors and mechanisms. *Pharmacol. Rev.* 51, 159–212

49 Stander, S. *et al.* (2004) Expression of vanilloid receptor subtype 1 in cutaneous sensory nerve fibers, mast cells, and epithelial cells of appendage structures. *Exp. Dermatol.* 13, 129–139
50 Denda, M. *et al.* (2001) Immunoreactivity of VR1 on epidermal keratinocyte of human skin. *Biochem. Biophys. Res. Commun.* 285, 1250–1252
51 Bodo, E. *et al.* (2005) A hot new twist to hair biology: involvement of vanilloid receptor-1 (VR1/TRPV1) signaling in human hair growth control. *Am. J. Pathol.* 166, 985–998
52 Toth, B.I. *et al.* (2009) Transient receptor potential vanilloid-1 signaling inhibits differentiation and activation of human dendritic cells. *FEBS Lett.* 583, 1619–1624
53 Wilkinson, J.D. and Williamson, E.M. (2007) Cannabinoids inhibit human keratinocyte proliferation through a non-CB1/CB2 mechanism and have a potential therapeutic value in the treatment of psoriasis. *J. Dermatol. Sci.* 45, 87–92
54 Srivastava, B.K. *et al.* (2009) Hair growth stimulator property of thienyl substituted pyrazole carboxamide derivatives as a cb1 receptor antagonist with *in vivo* antiobesity effect. *Bioorg. Med. Chem. Lett.* 19, 2546–2550
55 Zheng, D. *et al.* (2008) The cannabinoid receptors are required for ultraviolet-induced inflammation and skin cancer development. *Cancer Res.* 68, 3992–3998
56 Sarfaraz, S. *et al.* (2008) Cannabinoids for cancer treatment: progress and promise. *Cancer Res.* 68, 339–342
57 Dalle Carbonare, M. *et al.* (2008) A saturated *N*-acylethanolamine other than *N*-palmitoyl ethanolamine with anti-inflammatory properties: a neglected story. *J. Neuroendocrinol.* 20 (Suppl. 1), 26–34
58 Di Marzo, V. *et al.* (2001) Palmitoylethanolamide inhibits the expression of fatty acid amide hydrolase and enhances the anti-proliferative effect of anandamide in human breast cancer cells. *Biochem. J.* 358, 249–255
59 Costa, B. *et al.* (2008) The endogenous fatty acid amide, palmitoylethanolamide, has anti-allodynic and anti-hyperalgesic effects in a murine model of neuropathic pain: involvement of CB_1, TRPV1 and PPARgamma receptors and neurotrophic factors. *Pain* (in press)
60 LoVerme, J. *et al.* (2005) The search for the palmitoylethanolamide receptor. *Life Sci.* 77, 1685–1698
61 Oka, S. *et al.* (2006) Involvement of the cannabinoid CB2 receptor and its endogenous ligand 2-arachidonoylglycerol in oxazolone-induced contact dermatitis in mice. *J. Immunol.* 177, 8796–8805
62 Ueda, Y. *et al.* (2007) Involvement of cannabinoid CB2 receptors in the IgE-mediated triphasic cutaneous reaction in mice. *Life Sci.* 80, 414–419
63 Ueda, Y. *et al.* (2005) Involvement of cannabinoid CB_2 receptor-mediated response and efficacy of cannabinoid CB(2) receptor inverse agonist, JTE-907, in cutaneous inflammation in mice. *Eur. J. Pharmacol.* 520, 164–171
64 Akhmetshina, A. *et al.* (2009) The cannabinoid receptor CB2 exerts antifibrotic effects in experimental dermal fibrosis. *Arthritis Rheum.* 60, 1129–1136
65 Stander, S. *et al.* (2006) *Hautarzt* 57, 801–807
66 Ashton, J.C. and Milligan, E.D. (2008) Cannabinoids for the treatment of neuropathic pain: clinical evidence. *Curr. Opin. Investig. Drugs* 9, 65–75
67 Jhaveri, M.D. *et al.* (2007) Endocannabinoid metabolism and uptake: novel targets for neuropathic and inflammatory pain. *Br. J. Pharmacol.* 152, 624–632
68 Valiveti, S. *et al.* (2004) Transdermal delivery of the synthetic cannabinoid WIN 55,212-2: *in vitro/in vivo* correlation. *Pharm. Res.* 21, 1137–1145
69 Lodzki, M. *et al.* (2003) Cannabidiol-transdermal delivery and anti-inflammatory effect in a murine model. *J. Control. Release* 93, 377–387
70 Pulvirenti, N. *et al.* (2007) Topical adelmidrol 2% emulsion, a novel aliamide, in the treatment of mild atopic dermatitis in pediatric subjects: a pilot study. *Acta Dermatovenerol. Croat.* 15, 80–83
71 Lambert, D.M. (2007) Allergic contact dermatitis and the endocannabinoid system: from mechanisms to skin care. *ChemMedChem* 2, 1701–1702